Human and environmental change at North Atlantic coastal settlements, ca. AD 900-1700: a chronological perspective



Jamie Kathleen Anderson

Hertford College

University of Oxford

A thesis submitted for the degree of

Doctor of Philosophy

Trinity 2017

This thesis is dedicated to
my parents, Patricia and Robert Anderson.

Acknowledgements

Thank you to my supervisors, Dr David Griffiths and Professor Mark Pollard, and to all of the people who shared information with me, answered my questions, and in general helped me along my way. They are too numerous to name, so I will just name the one who did the most, Victoria Cullen.

Abstract

How environmental change affects human settlement is a research question that is becoming increasingly important to us in the twenty-first century. The North Atlantic, from ca. AD 900-1800, is currently one of the most well-studied regions and times for answering this research question. Norse exploration of the North Atlantic and subsequent colonisation and settlement – both short- and long-term – of the various islands there has been interpreted as a narrative of adaptation to new and changing environmental conditions. Although there is a relative wealth of archaeological and environmental data from the region, chronology remains an area needing further study. This thesis synthesises a wide range of scientific chronological data – constructing new chronologies for two small-scale landscapes in case studies from Iceland and Orkney, and then using Bayesian modelling to derive new analyses from published dating information throughout the region – in order to work towards a cohesive narrative of North Atlantic settlement and adaptation that includes scientific chronologies.

Contents

1 Introduction **1**

1.1 Research Questions 4

1.2 Research Design 5

1.3 Thesis Structure 6

2 The Medieval and Late Medieval North Atlantic **7**

2.1 Setting the scene: the North Atlantic ca. AD 900-1800 7

2.1.1 Phase definitions 8

2.2 Climate impact research and the North Atlantic 9

2.2.1 Orkney: the transition into the wider European social and economic sphere 12

2.2.2 Iceland: from the end of the Freestate through the 'Dark Ages' 17

2.2.3 Transition from the Medieval Warm Period into the Little Ice Age 22

2.3 Previous archaeological research throughout the North Atlantic . . . 25

2.4 Theoretical frameworks for conceptualizing human/environment interaction in the North Atlantic ca. AD 800-1800 27

2.5 Using chronology to understand archaeological landscapes within regional frameworks of cultural and environmental change 32

3 Archaeological and Environmental Chronologies in the North Atlantic **33**

3.1 Tephrochronology 33

3.2 Tephra and distal microtephra deposition in the landscape 35

3.2.1 Transport pathways of tephra 37

3.2.2 Terrestrial deposits 38

3.2.3 Lacustrine deposits 41

3.2.4 Other records of tephra fall 43

3.3 Icelandic tephra-producing eruptions from the last 2000 years 43
3.3.1 Askja 50
3.3.2 Eyjafjöll 50
3.3.3 Grímsvötn 50
3.3.4 Hekla 51
3.3.5 Katla 52
3.3.6 Öræfajökull 53
3.3.7 Snæfellsjökull 54
3.3.8 Torfajökull 54
3.3.9 Veiðivötn/Bárdarbunga 55
3.3.10 Distal tephras from unknown systems/eruptions 55
3.4 Distal deposition in the North Atlantic 56
3.4.1 Previous tephra finds in Vestfirðir 57
3.4.2 Previous microtephra finds in Orkney 58
3.5 Other chronological methods 59
3.5.1 AMS radiocarbon and OSL 59
3.6 'Chronometric Hygiene' 62
3.6.1 Bayesian modelling and OxCal: statistical methods for refining chronological information 63
3.7 Conclusions 64

4 Study Locations **66**
4.1 Selection of case studies 66
4.2 Vestfirðir (the West Fjords), Iceland 69
4.2.1 The Vatnsfjörður archaeological landscape 72
4.2.2 Sveinhúsavatn (Svein's House Lake) 80
4.2.3 Vatnsfjörður Homefield 82
4.2.4 Kaldalonsjökull 86
4.3 Mainland, Orkney, Scotland 90
4.3.1 The Birsay-Skaill Landscape Project 90
4.3.2 East Mound samples 96
4.3.3 Spretta Meadow and Hobbister A and B samples 96
4.4 Summary 99

5 Experimental procedures and methods **100**
5.1 Sampling for distal tephra from archaeological and environmental sites 100
5.2 Laboratory procedures for the extraction of tephra and microtephra . 101

5.3 Wavelength Dispersive Spectrometry – Electron Probe MicroAnalysis (WDS-EPMA) . . . 103
5.3.1 Potential analytical problems . . . 106
5.3.1.1 Sample preparation errors . . . 106
5.3.1.2 Alkali mobilization . . . 106
5.3.1.3 Low totals . . . 107
5.3.1.4 Sample shape/microlites . . . 108
5.4 Data processing and statistical methods . . . 110
5.4.1 Filtering data . . . 111
5.4.2 Visual assessment of data . . . 111
5.4.3 Sources for correlation and the creation of a database of proximal data . . . 112
5.4.4 Correlating sample layers with known geochemistry . . . 112
5.4.5 Statistical transformations of data . . . 114
5.4.6 Chronostratigraphies and OxCal . . . 115
5.5 Integrating scientific results with archaeological interpretations . . . 117
5.6 Summary . . . 118

6 Field and laboratory results 120
6.1 On-site sampling . . . 120
6.1.1 Iceland . . . 120
6.1.1.1 Sveinhúsavatn samples . . . 120
6.1.1.2 Vatnsfjörður Homefield samples . . . 121
6.1.1.3 Vatnsfjörður visible tephra layer samples . . . 123
6.1.1.4 Kaldalonsjökull . . . 128
6.1.2 Orkney . . . 129
6.1.2.1 East Mound samples . . . 129
6.1.2.2 Hobbister A and B and Spretta Meadow samples . . . 130
6.2 Tephrostratigraphies . . . 132
6.2.1 The results of initial microtephra extraction . . . 132
6.2.1.1 Iceland . . . 133
6.2.1.2 Orkney . . . 140
6.2.1.3 Summary . . . 144
6.2.1.4 Layers targeted for WDS-EPMA . . . 144
6.3 WDS-EPMA data: Major and minor element composition of samples 146
6.3.1 Iceland . . . 146

6.3.1.1 Sveinhúsavatn . . . 146
6.3.1.2 Homefield . . . 150
6.3.1.3 Kaldalonsjökull . . . 155
6.3.1.4 Vatnsfjörður archaeological site . . . 159
6.3.2 Orkney . . . 164
6.3.2.1 Hobbister . . . 164
6.4 Summary . . . 166

7 Interpretation: The chronology of Vatnsfjörður 168
7.1 Vatnsfjörður archaeological site . . . 169
7.1.1 Correlating distal layers with proximal glass chemistry . . . 169
7.1.1.1 OxT-5163 . . . 171
7.1.1.2 OxT-5165 . . . 173
7.1.1.3 OxT-5166 . . . 175
7.1.1.4 OxT-7094 . . . 176
7.1.1.5 OxT-7095 . . . 177
7.1.1.6 OxT-7097 . . . 177
7.1.1.7 OxT-7098 . . . 177
7.1.1.8 OxT-7099 . . . 178
7.1.1.9 Conclusions . . . 178
7.2 Hekla 1693 in the Vatnsfjörður archaeological site . . . 181
7.2.1 Area 14 . . . 182
7.2.2 Area 32 . . . 183
7.2.3 Group 8562 . . . 185
7.2.4 Group 10515 . . . 187
7.2.5 Area 40 . . . 190
7.2.6 Area 45 . . . 191
7.2.7 Tephra from Hekla 1693 and the interpretation of the Vatnsfjörður excavations . . . 191
7.3 Homefield . . . 195
7.4 Correlating distal layers with proximal glass chemistry . . . 195
7.4.1 OxT-4672 . . . 195
7.4.2 OxT-4674 . . . 197
7.4.3 OxT-4675 . . . 198
7.4.4 OxT-4676 . . . 199
7.4.5 OxT-4677 . . . 200

7.4.5.1 OxT-4679 and OxT-4680 . . . 201
7.4.5.2 OxT-4681 . . . 203
7.4.6 Conclusions . . . 204
7.5 Kaldalonsjökull . . . 205
7.5.1 Correlating distal layers with proximal glass chemistry . . . 205
7.5.1.1 OxT-5133 . . . 205
7.5.1.2 OxT-5135 . . . 205
7.5.1.3 OxT-5136 . . . 206
7.5.1.4 OxT-5142 . . . 207
7.5.1.5 OxT-5148 . . . 208
7.5.1.6 OxT-5149 and OxT-5150 . . . 208
7.5.1.7 Conclusions . . . 209
7.5.2 Homefield and Kaldalonsjökull chronologies . . . 209
7.5.3 Integrating the chronology of the Homefield with its pollen record 215
7.6 Sveinhúsavatn . . . 219
7.6.1 Correlating distal layers with proximal glass chemistry . . . 219
7.6.1.1 OxT-4308 . . . 219
7.6.1.2 OxT-4309 . . . 219
7.6.1.3 OxT-4310 . . . 222
7.6.1.4 OxT-4685 . . . 222
7.6.1.5 Conclusions . . . 223
7.6.2 Sveinhúsavatn chronology . . . 225
7.6.3 The importance of the bay/lake transition to the farm at Vatnsfjörður . . . 227
7.7 Linking records across Vatnsfjörður . . . 232
7.8 Connecting Vatnsfjörður to Icelandic archaeology . . . 234
7.9 Summary . . . 242

8 Interpretation: The chronology of the East Mound, Bay of Skaill 244
8.1 Bayesian Modelling and the East Mound . . . 245
8.2 Correlating distal layers with proximal glass chemistry . . . 249
8.2.1 Hobbister B correlation . . . 250
8.2.1.1 Hekla 1510, Hekla 1947, and the British Isles . . . 250
8.3 Linking the East Mound to Hobbister B . . . 256
8.4 Developing a combined archaeological and environmental chronology for the Bay of Skaill . . . 259

8.5 Summary 265

9 The Chronology of the North Atlantic ca. AD 900-1800 268

9.1 Modelling dates from the North Atlantic islands 268
9.1.1 Orkney 269
9.1.2 Shetland 269
9.1.3 Western Isles 271
9.1.4 The Faroe Islands 273
9.1.5 Iceland 273
9.1.6 Greenland 276
9.1.7 North America (Vinland) 276
9.2 Modelling Regional Change in Shetland, the Western Isles, and the Faroe Islands 281
9.2.1 Correcting for the Marine Reservoir Effect 281
9.2.2 Calibration Curve 282
9.2.3 Modelled Calendar Ages for Relative Phases 283
9.2.3.1 Shetland 283
9.2.3.2 Western Isles 288
9.2.3.3 The Faroe Islands 290
9.3 The Chronology of Conversion 296
9.3.1 Orkney: Religious Conversion Modelled Part I 296
9.3.2 Iceland: Religious Conversion Modelled Part II 304
9.3.3 Conversion Chronology - Orkney and Iceland 312
9.4 Greenland - Timing of Settlement, Landscape Use, and Abandonment 314
9.5 Modelling *landnám* 325
9.6 Conclusions 328

10 Conclusions and Future Research 330

10.1 Summary of qualitative results 330
10.2 Summary of main interpretation 331
10.3 Chronology as a tool for understanding the interaction between the human past and palaeoclimate 335
10.4 Future research 337
10.5 Final thoughts 340

Bibliography 342

A ***Unfiltered WDS-EPMA data*** **390**

B ***Filtered WDS-EPMA data*** **441**

C ***Database of known geochemistry*** **459**

D ***R code*** **494**

E ***East Mound radiocarbon, OSL, and stratigraphic diagrams*** **496**

F ***Orkney, Highlands, and Western Isles Published Chronological Information*** **510**

G ***Linear Interpolation Code*** **515**

List of Figures

2.1 Map of Orkney 13
2.2 Map of Iceland 17

3.1 Volcanoes near Vestfirðir. 36
3.2 TAS plot. 46

4.1 Landscape case studies. 67
4.2 Vestfirðir map. 70
4.3 Satellite view of Vatnsfjörður. 74
4.4 Layout of Vatnsfjörður excavations. 75
4.5 Photo of Vatnsfjörður site. 77
4.6 Example of turf wall construction. 78
4.7 Kaldalonsjökull location. 87
4.8 Orkney locations. 91
4.9 Orkney geology. 92
4.10 Bay of Skaill map. 93
4.11 Plan view of the East Mound. 95

5.1 Microtephra extraction method. 102
5.2 Steps for preparing samples for WDS-EPMA. 104
5.3 Different types of microtephra shards. 109
5.4 Example entry into OxCal 116
5.5 Example table output of model 116
5.6 Example plot output of model 117

6.1 Photograph of Sveinhúsavatn core. 121
6.2 Sediment log of Sveinhúsavatn core. 122
6.3 Sediment log of Homefield core. 122
6.4 Plan of the Viking Age area with sample locations marked. 124

6.5 Aerial view of Farm Mound area with sample locations marked. . . . 125
6.6 Location of Area 40 and Test Trench 45 126
6.7 Visible tephra layer from the Vatnsfjörður site. 127
6.8 Sediment log of Kaldalonsjökull core. 129
6.9 Locations of areas discussed in East Mound excavation. 130
6.10 Stratigraphy of SG08 Section 8 (from Area 1), #1. 130
6.11 Stratigraphy of SG08 Section 8 (from Area 1), #2. 131
6.12 Stratigraphy of SG08 Section 38 (from Area 2). 131
6.13 Stratigraphy of SG08, Unit #175 (from the metalworking area). . . . 131
6.14 Stratigraphy of SG08, Unit #176 (from the metalworking area). . . . 131
6.15 Different colours of individual microtephra shards. 133
6.16 Tephrostratigraphy for Sveinhúsavatn. 134
6.17 Tephrostratigraphy for the Homefield core. 136
6.18 Tephrostratigraphy for Kaldalonsjökull. 139
6.19 Tephrostratigraphy for Hobbister A. 140
6.20 Tephrostratigraphy for Hobbister B. 141
6.21 Tephrostratigraphy for the top 10 cm of Hobbister B. 142
6.22 Tephrostratigraphy for Spretta Meadow. 143
6.23 Photograph by the author of microtephra shards 149

7.1 Isopach maps for Katla 1721, Hekla 1300, Hekla 1693, and Hekla 1766 170
7.2 Published glass chemistry of Katla 1721, Hekla 1300, Hekla 1693, and Hekla 1766 172
7.3 Correlation of OxT-5163. 173
7.4 Comparison of OxT-5165 analyses 174
7.5 Correlation of OxT-5166. 175
7.6 Correlation of OxT-7094. 176
7.7 Correlation of OxT-7095. 177
7.8 Correlation of OxT-7097. 178
7.9 Correlation of OxT-7098. 179
7.10 Correlation of OxT-7099. 180
7.11 Stratigraphic profile of Area 14. 182
7.12 Stratigraphic profile of northwestern side of Area 32. 184
7.13 Stratigraphy of Group 8562 in the Farm Mound. 185
7.14 Aerial photograph of Room 8562 186
7.15 Stratigraphy of group 10515. 187

7.16 Group 10515 photographed from above before the removal of layers . 188
7.17 Group 10515 photographed from above after the removal of layers . . 188
7.18 Photograph of Group 10515, facing north 189
7.19 Stratigraphy of test trench Area 45. 192
7.20 OxT-4672 correlation 196
7.21 OxT-4674 correlation 197
7.22 OxT-4675 correlation 198
7.23 OxT-4676 correlation 199
7.24 OxT-4677 correlation. 201
7.25 Second OxT-4677 correlation. 202
7.26 OxT-4679 and OxT-4680 correlation. 203
7.27 OxT-4681 compared to *Landnám* tephra 204
7.28 OxT-5133 correlation. 206
7.29 OxT-5135 correlation. 207
7.30 OxT-5142 correlation. 208
7.31 OxT-5148 correlation. 209
7.32 Tephra layers found in both the Homefield core and the Kaldalonsjökull core. 211
7.33 Comparison of proximal and distal data from Hekla 1766 213
7.34 Comparison of proximal and distal data from Hekla 1693 214
7.35 Pollen and spore percentage data for Vatnsfjörður wet meadow site, alongside charcoal concentration onsite. 217
7.36 Correlation of OxT-4308 220
7.37 Correlation of OxT-4309 221
7.38 Correlation of OxT-4310 223
7.39 Correlation of OxT-4685 224
7.40 Foram counts with tephrostratigraphy of Sveinhúsavatn core 226
7.41 Transitional phases of Sveinhúsavatn 228
7.42 The deposition rate for sediment in the lake 229
7.43 Tephra isochrons in Vatnsfjörður landscape 233
7.44 Timeline of selected environmental and archaeological records from Iceland. 236
7.45 Map of Iceland 237

8.1 Results of the East Mound model. 248
8.2 Correlation bi-plots for Hobbister B 0-7.5 cm. 251

8.3 Correlation bi-plots for Hobbister B 0-7.5 cm. 252
8.4 Hobbister B deposition model with Hekla 1510 (green) and Hekla 1947 (blue). 258
8.5 Location of all places named in Table F.1. 261
8.6 Timeline of Orcadian archaeological and environmental events. 262

9.1 Location of dated sites from Orkney. 270
9.2 Location of dated sites from Shetland. 272
9.3 Location of dated sites from the Western Isles. 274
9.4 Location of dated sites from the Faroe Islands. 275
9.5 Locations of dated sites from Iceland. 277
9.6 Location of radiocarbon dates from Greenland's Western Settlement. 278
9.7 Location of radiocarbon dates from Greenland's Eastern Settlement. . 279
9.8 Location of radiocarbon dates from Greenland's Middle Settlement. . 280
9.9 Model of all (non-eliminated) dates from Shetland. 284
9.10 Model of Old Scatness. 287
9.11 Model of dates from the Western Isles. 291
9.12 Faroe Islands model part A. 293
9.13 Faroe Islands model part B. 294
9.14 Excerpt of dates from the Faroe Islands model on the calibration curve. 295
9.15 Results of overlapping phases model for Orkney conversion. 300
9.16 Model of the dates from Scar as a single phase (Bronk Ramsey 2009; Reimer et al. 2013; OxCal v.4.3). N = 3, A = 112. 301
9.17 Contiguous model of dates from Orkney conversion period (Bronk Ramsey 2009; Reimer et al. 2013; OxCal v.4.3). N = 58, A = 120.5. . 303
9.18 Boxplot comparing the δ^{13}C results from pagan burials and Christian burials. 306
9.19 Results of the contiguous Icelandic conversions model. 309
9.20 Results of the overlapping Icelandic burials model. 311
9.21 Western Settlement model. 317
9.22 Middle Settlement model. 319
9.23 Eastern Settlement model part A. 321
9.24 Eastern Settlement model part B. 322
9.25 Eastern Settlement model part B. 323
9.26 Map comparing modelled dates for *landnám*. 327

1 | Introduction

Scientific chronologies are a relatively recent development in archaeology, and they have revolutionised the way that archaeologists, and the public, interpret the past. Radiocarbon dating, tephrochronology, optically stimulated luminescence, and more provide options for putting a nearly-exact date to past events that, prior to the 1950s, could only be understood in relative terms. The development of Bayesian modelling for archaeological chronologies in the 1990s and 2000s created a powerful tool to refine those dates and link them together based on their stratigraphy and phasing. These advancements allow archaeologists to explore the past with an accuracy and precision that, although it can seem commonplace today, is truly a marvel in the context of all previous understandings of the human and environmental past.

One way to explore the past through chronology is to ask, how do cultures respond to environmental change over time? Seeking answers to this question have increasingly entered our global consciousness, with their urgency growing in just the (admittedly many) years it has taken me to write this thesis. Researchers in many fields, including anthropology, geography, and environmental studies (e.g. McGovern et al. 1988; Buckland et al. 1997; Bonsall et al. 2002; Blinman 2008) are conducting studies into past and present environmental change, but this is a topic that archaeologists are uniquely able to interpret. Mitchell (2008: 1095-1096) writes, 'Archaeologists are in a privileged position to understand and make sense of the impact of climate change on human populations' due to the archaeologist's ability to see ecological circumstances for human populations over long time periods as well as understand that, outside of modern, industrial Western culture, the vast majority of human history has taken place in a setting highly exposed to the natural environment. However, before archaeologists can create coherent and factually supported narratives, several issues of methodology and interpretation must be addressed.

The most crucial of these issues today is the task of developing accurate and precise chronologies that can link multiple records in time. Despite the advancements de-

scribed above, much work remains. In a recent paper suggesting a potential agenda for future research integrating palaeoclimatic and environmental data with records of human change, Caseldine and Turney (2010: 90) write that, 'Chronology and dating techniques are a principal area in need of further research before we can accurately draw conclusions about palaeoclimate and the human past...'. Studies that seek to tie human movement to environmental changes (and in some cases vice versa) must show the correlative relationships between the two systems in order to draw out causation. Without accurate and precise chronologies for both archaeological and environmental records, and demonstrable links between the records, these relationships will remain general, inconclusive, and based on guesswork.

In this thesis, I address these issues by using a variety of chronological methods to investigate the relationship between humans and the natural environment in the North Atlantic. First, I present two case studies: the Vatnsfjörður landscape project in the Vestfirðir (West Fjords) region of Iceland, and the East Mound at the Birsay-Skaill Landscape Project in Orkney, Scotland. Members of the Norse cultural zone created farmsteads in both landscapes sometime in the tenth century; Vatnsfjörður was continuously farmed until 1906, while the longhouse at the East Mound was occupied for only a brief period of time, with what evidence there is for farmstead resettlement located far away from the mound.

After these case studies, I expand the focus of the thesis to the wider North Atlantic region during this period. The coastal North Atlantic during the last twelve hundred years is an ideal location to study the interaction of humans and the environment for four reasons. First, coastal settlements face a number of challenges due to climatic and environmental change, including but not limited to sea-level fluctuation, violent storms, sea ice, erosion (often anthropogenic), and temperature changes affecting marine resources. Second, in the islands of the North Atlantic, coastal settlements are often located in marginal environments. Marginal environments are defined as those that are, 'sensitive to even modest changes in biophysical, social, and economic conditions' (Smit et al. 1991: 333). Marginal environments have become major places for research into the impacts of environmental change over time due to their fragility; they respond more quickly and more dramatically than more robust environments would. As a result, environmental changes have a higher chance of being evident in archaeological and environmental records. All studied areas are located in high latitudes, often in areas that have shown great susceptibility to climatic changes in the last one thousand years (e.g. McKinsey et al. 2005; Morocco et al. 2007; Ogilvie

1990; Ogilvie and Jonsson 2001; Sommerville et al. 2007). Third, the Norse settlement period took place during the temperate years of the MWP (Medieval Warm Period), but the period that followed was the LIA (Little Ice Age), which was marked by colder and less predictable weather, meaning that these settlements were occupied during a time of known climatic change. Finally, the shared Norse heritage of the North Atlantic islands in this period means that the coastal farmstead settlers at the studied locations would have approached environmental change with similar cultural expectations, practices, and knowledge-bases. The two case studies thus provide an opportunity to understand how people who were likely to have similar reactions responded to coastal environmental change.

Chronology, especially aided by Bayesian modelling, is able to be the link between records, to draw out the sequence of events and test possible relationships between them. Our ability as archaeologists to create accurate and precise chronologies continues to develop, and throughout this thesis, I discuss specific avenues for future studies. We are still learning, through the trial and error of research, both the methods for creating chronologies and the limits of our ability to analyse the chronologies we create. For example, although the techniques of AMS radiocarbon dating are well understood and most AMS radiocarbon dates, especially for the time period under consideration here, are considered reliable,[1] the use of Bayesian modelling to refine bodies of dates continues to be a major focus of research (e.g., Blockley et al. 2004; Bayliss et al. 2007; Andr 2010; Blaauw 2012). Regional landscape studies like the ones presented here using Bayesian modelling are still rare (but see Whittle et al. 2011).

Tephrochronology, meanwhile - especially in its distal and micro- incarnations - is a research method still very much in its infancy. Thoughtful analyses of data that seek to understand the processes behind tephra deposition (e.g., Davies et al. 2007; Swindles et al. 2013; Shapley and Finney 2015) and work towards establishing datasets about geochemistry and ashfall coverage for future tephra research (e.g., Meara 2011; Rea et al. 2012; Kawabata et al. 2015) continue to push the field towards a future when it can offer more definitive results in more depositional scenarios and more locations. Results that may seem modest or even negative in their outcome can contribute to understanding where tephra has and has not fallen as well as how the landscape has changed since the initial depositional event. The thesis situates itself firmly within those analyses that approach the challenges of the dating methods used.

[1] See Chapter 9 for a more thorough discussion of this.

1.1 Research Questions

This thesis asks three main research questions:

1. How can scientific chronologies, in their current state, be used to understand the relationship between records of environmental and archaeological change?
2. How did environmental change, both anthropogenic and natural, affect human life at coastal settlements in the North Atlantic?
3. How can better chronologies help us understand regional social change like colonisation and religious conversion?

Caseldine and Turney's (2010) statement emphasises the need for better chronologies to understand the links between archaeological and palaeoclimatic and environmental records. That is undisputed. It is unclear if significant methodological advances in chronology building will have any serious impact on researchers' ability to understand the connections between such complex systems as human/environment interaction. In some cases - such as current research into the MRE (marine reservoir effect) and FRE (freshwater reservoir effect) for radiocarbon dates from Iceland (e.g., Ascough et al. 2011) - there continues to be a need for methodological advancement. Although archaeologists and environmental scientists currently have at their disposal a variety of well-understood methods that can provide accurate and precise chronologies, many of those records rely upon the vagaries of sample material availability (radiocarbon dating) or the possibility of a volcanic eruption coinciding with a major event (tephrochronology). Therefore this thesis assesses, using these two case studies and then statistical modelling of published dates throughout the region, whether it is methodological advancements that are necessary to build better links between archaeological and palaeoclimatic records or whether chronology building will continue to be a problem for these types of studies even as the science behind it advances.

North Atlantic coastal farmsteads and their surrounding landscapes from this period arguably have not been well studied using scientifically-derived chronologies, as is discussed in Chapter 2 Chapter 9. This is particularly true of the Vestfirðir region, which has seen almost no excavation, and the Scottish Isles, where coastal locations have been excavated but have had very few scientific dates associated with them (with exceptions, e.g., Griffiths forthcoming). In addition to querying how chronology-building fits into making the link between human and environmental records, this thesis also investigates the development of coastal farmsteads and the environmental

challenges and opportunities that life at those locations presented to settlers from the Norse and later periods.

Finally, this thesis contributes new information about late-Holocene Icelandic distal tephras. Geographically, the two areas that have new tephra data from this thesis - Vestfirðir, Iceland, and Mainland Orkney, Scotland - have seen very little tephrochronological research, especially for terrestrial tephras from the past 2000 years. The mapping of tephra fall and stratigraphy contributes to the overall goals of tephrochronological research (Dugmore et al. 2011: 10).

1.2 Research Design

After choosing the two case studies, I conducted fieldwork in both landscapes. I brought tephrochronological samples to the lab for extraction and geochemical characterization of any microtephras in the sediment. Where possible, these were then correlated with published data on tephras proximal to volcanic sources. Icelandic records from the late ninth century AD have chronicled, often to the day and even sometimes to the hour, when volcanic eruptions occurred (e.g., Þorarinsson 1967). This record, combined with fifty years of research into tephras and tephrochronology in Iceland, means that correlations can be made for many distal layers. In some cases a tephra layer can only be correlated to a volcanic system rather than a single eruption, or not to any known tephras at all. These data are still useful for future studies in the same areas that may identify similar tephras.

Once all chronological information about each case study had been gathered (either through tephra identification or collecting radiocarbon and OSL dates) then the information was used to create the most accurate, precise, and statistically robust chronologies possible. In the case of the East Mound, I created a Bayesian model for the archaeological site. Developments at the archaeological excavations and within their local environments were then synchronised temporally. From there, these chronologies were interpreted for evidence of how coastal settlements might have been affected by temporally linked environmental change. These interpretations were then extended to the respective wider regions of the case studies. The results of the case studies were then compared.

Finally, in order to move beyond the localised case studies into understanding the chronology of the region, I collected currently published (as of mid-2017) chronological

data from the study area into a database. I then developed several Bayesian models to answer questions about cultural and environmental change across the region. This was done to test the applications of Bayesian modelling for large-scale, regional datasets.

1.3 Thesis Structure

The thesis is divided into ten chapters. Following this introduction, the second chapter, 'The Medieval and Late Medieval North Atlantic', reviews current published literature to set the archaeological stage for the research presented in the thesis, and then reviews current publications combining archaeological and environmental research in the studied place and time. The third chapter, 'Archaeological and Environmental Chronologies in the North Atlantic', provides a review of current studies and developments in tephrochronology, emphasising ash dispersion and depositional processes which might affect tephrostratigraphies. The chapter also describes the major volcanic systems of Iceland and characterises the dominant glass chemistry of tephra from their eruptions. Then it briefly describes other chronological methods (radiocarbon and OSL) and Bayesian modelling. The fourth chapter is an in-depth introduction to the two case studies. The fifth chapter, 'Experimental Procedures and Methods', describes the field techniques, laboratory procedures, analytical methods, and finally the archaeological theory that shaped the research in this thesis. This includes a description of the process for extracting microtephra samples from sediment cores as well as methods for interpreting the WDS-EPMA (wavelength dispersive spectroscopy-electron probe micro-analyzer) data that form a majority of the results presented in the thesis. The sixth chapter presents the results of the laboratory portion of the research: the tephrostratigraphies and results of WDS-EPMA on the microtephra samples. Chapters seven and eight focus on a critical assessment and interpretation of these results, from correlating the described microtephra layers with known proximal volcanic events to describing the age models and interpretations of those that resulted from the research. Chapter nine moves beyond the case studies to incorporate the chronology of the entire region through a database of published dates and Bayesian modelling of key research questions. Chapter ten summarises the conclusions and provides suggestions for future research.

2 | The Medieval and Late Medieval North Atlantic

The North Atlantic ca. AD 900-1800 was a dynamic landscape and seascape undergoing rapid and near-constant human and environmental change. Norse colonisers faced the challenges of colonisation and settlement of various islands as they moved east to west across the ocean. On each island, environmental changes both within and beyond their control – from local erosion to hemisphere-wide temperature fluctuations – demanded community responses. In this chapter, I introduce the study area and review critically the current state of research in studies describing human/environmental interaction in the region.

2.1 Setting the scene: the North Atlantic ca. AD 900-1800

The Norse colonisation of the North Atlantic took place from the eighth to the eleventh centuries. It was part of a wider movement, as many people left their Scandinavian homelands and travelled west, south, and east across Europe, Russia, and North America. The reasons for this 'Viking diaspora' as Barrett (2008) has termed it have been debated for many years. Recent explanations include: technological advances in sea-faring technology; population pressure within Scandinavia from enhanced agriculture in the favourable growing conditions of the Medieval Warm Period; political or religious motives; the influence of strong individuals desiring to move beyond their homeland; economic booms and the subsequent creation of trading centres (*wics*) in the kingdoms and polities to the south as irresistible raiding targets; expansion of demand in Europe for a slave trade; and a lack of familial opportunities at home due to female infanticide creating a cutthroat marriage market within Scandinavia (Wormald 1982; Myhre 1993; Hill and Cowie 2001; Skre 2001; Halsall 2003;

Hodges 2006; Barrett 2008). Whatever factor or combination of factors spurred this outward movement, Norse settlers had established settlements on all the major islands of the North Atlantic within two centuries. In the British Isles, they either integrated with or replaced the previous population, with most Norse settlers concentrated in modern-day Scotland, northern and eastern England, and Ireland, where agricultural economies had been present since the Neolithic (Barrett et al. 2000). Further north and west, in the Faroe Islands, Iceland, Greenland, and possibly Newfoundland, the Norse entered into 'pristine' landscapes – there were no agricultural societies present, and, in Iceland and the Faroe Islands, very few if any people (e.g., Church et al. 2013). By the 1260s, both Orkney and Iceland were part of the North Atlantic Kingdom of Norway, which extended from Norway and also included Greenland, the Faroe Islands, and Shetland.

These islands were connected by shared governance, culture, and, one can assume, a sense of geographic and, in more remote areas, environmental marginality. Hunter et al. (2007: 515) write, 'Islands are fragile economic units, vulnerable to population change or even extinction through disease, migration, invasion, climatic instability, or even cultural influence'. Defining how each community – and the individual settlements within them – fared in the transition from the warm, agriculturally-favourable climate of the Medieval Warm Period to the more variable, colder weather of the Little Ice Age illuminates how island societies, and the local communities that comprise them, respond to environmental change.

2.1.1 Phase definitions

The period studied in this thesis spans 1000 years and crosses the boundaries of many historical phases, several of which are overlapping and/or are called different things by different researchers. Therefore some phases may have multiple names, or may apply only to one geographical location. In general, these are:

1. *Landnám*: the first generation of Norse settlers in any area; e.g., *landnám* in Iceland is generally dated to ca. AD 870, whereas in Greenland it is dated to sometime in the late tenth century (Schofield et al. 2008) and in the Faroe Islands to ca. AD 800 (Arge 1991; Arge et al. 2005).

2. Settlement period or Norse colonisation period: varies from island to island, but in general is from ca. AD 800 - AD 1000. The end of the period is traditionally AD 1000, which is the date given by some historical sources for the Norse

conversion to Christianity in a number of locations (e.g., Vésteinsson 2000). However, for Orkney and Shetland this is often just called the Viking period, and lasts until AD 1100.

3. Medieval period: This period spans ca. AD 1000-1250 or 1300; its end is often marked as the beginning of the LIA.
4. Late Norse Period: From ca. AD 1000-1500.
5. Late medieval period: From ca. AD 1250 or 1300 until ca. AD 1550.
6. Dark Ages (Iceland only): In Icelandic historiography, this spans ca. AD 1400-1800 (Hastrup 1990; Hastrup 1992; Karlsson 2000).
7. Early modern period: This spans roughly from ca. AD 1550-1800.

These phase definitions apply across the research presented in this thesis, although there is obviously some overlap between time periods and therefore phase names should be treated strictly as a rough categorisation.

2.2 Climate impact research and the North Atlantic

The intersection of society and the natural environment, sometimes known as cultural ecology or climate impact research, became a popular research topic in the second half of the twentieth century. Prior to that, most archaeological and historical interpretations portrayed human civilization as either uncoupled from surrounding environments or affected only by catastrophic environmental changes. Researchers such as Julian Steward, writing about indigenous peoples in the high desert of North America; Karl Butzer, writing about Africa; and H. H. Lamb, writing mostly about Europe, were some of the first researchers to explore these concepts (e.g., Butzer 1971; Lamb 1977; Steward 1977; Lamb 1982). In the North Atlantic, Lamb's work can be distinguished from that of previous researchers by the explicit connections he drew between specific climatic events and specific moments in human history. His *Climate: Present, Past and Future* (1977) and *Climate, History, and the Modern World* (1982) highlight the interdisciplinary nature of research into human/environment interactions. Lamb brings together different strands of data, from history, geography, and the natural sciences, to present as complete a record as was possible at the time of writing of past climate change such as the MWP and LIA and its influence on the history of human civilization.

Jared Diamond's (2005) popular science book *Collapse* presented these ideas to the public by describing a number of societies, prehistoric, historic, and modern, whose cultural and economic continuity in the face of new or changing environmental conditions led, he argues, to their downfall. It is not revolutionary to say that the way that academic thought has evolved on the topic of past human and environment interaction mirrors changing thought outside the academy about the relationship between globalised human civilization and planet Earth in the late twentieth and early twenty-first centuries. Many scholars and popular authors see the first images of the earth from space as the beginning of the modern environmental movement, and it is therefore not surprising that academic thought on the topic has followed closely behind it (Jones et al. 2001). The human relationship to changing environmental conditions – whether anthropogenic or similar to those that have fluctuated throughout the past several million years of human evolution – has now moved beyond the academy and into popular and political discourse.

Academic thought inevitably has moved towards a more nuanced understanding of the interplay between climate and society. This move has taken place to a large extent in the past two decades, as researchers began to publish about the Norse Greenland colony (e.g., McGovern et al. 1988; McGovern 1990; Buckland et al. 1996; Barlow et al. 1997). The results of their investigations opened the floodgates to scholarship set in a variety of cultures, time periods, and locations (e.g., Buckland et al. 1997; Nicoll 2004; Benson et al. 2006). Discussions about the negotiation between environmental change and societal constraints on responding to it currently dominate, as many of the examples discussed later in this chapter demonstrate.

The North Atlantic, particularly during the age of Norse colonisation and subsequent contraction, has emerged in the past two decades as a major research area for scholars studying human/environment interaction. The North Atlantic cultural zone, from approximately AD 800, experienced climate change in marginal landscapes, with a variety of outcomes for human settlements. This cultural zone has at its core a group of islands that were colonised by the Norse: the British Isles including Orkney, Shetland, and the Western Isles; the Faroe Islands; Iceland; and Greenland (McGovern et al. 1988; Amorosi et al. 1997; Edwards et al. 2004).[1] These are often considered in the context of the wider Scandinavian expansion that took place from the eighth

[1]L'Anse aux Meadows, the Norse settlement in Newfoundland, is also sometimes included in this group, but it seems to have been occupied for only a short period of time and to have been more of a impermanent seasonal camp rather than a settlement (Wallace 2003).

century to ca. AD 1000. After the expansion period, the colonies on those islands remained in the northern European economic and cultural sphere for centuries.

Norse colonisation took settlers of European descent into a wide variety of environmental conditions, all to varying degrees different from their Scandinavian homelands.[2] In the northern British Isles, Norse settlers encountered places that had been inhabited by Europeans for thousands of years. In Iceland, they entered an empty landscape where they were probably the first environmentally-significant human inhabitants; in the Faroe Islands, it is unclear if they were the first inhabitants or not, but they seem to have been the first to make a significant human impact (Ahronson 2000; Church et al. 2005; Ahronson 2007; Church et al. 2013). Finally, they entered areas inhabited by non-Europeans practising hunter gatherer lifestyles in Greenland and North America. At each of these places, Norse settlers had to adapt their methods for exploiting the landscape to fit both environmental conditions and economic demand. For trans-Atlantic Norse culture as a whole, the result was the development of an integrated North Atlantic economy that brought together resources from several different zones and traded them throughout the area and to more exotic locales beyond (Roesdahl 1987; Barrett et al. 2000; Barrett et al. 2004). For individual colonies and regions within colonies, the outcomes of these adaptations were varied, leading to degrees of 'success' and 'failure' within the wider economic, social, and physical landscape (e.g., Buckland et al. 1996; Amorosi et al. 1997; McGovern et al. 2007; Schofield et al. 2008). This is discussed further in Section 2.4.

Coinciding with, and perhaps contributing to, the Norse expansion was the MWP[3] when North Atlantic environmental and archaeological records indicate that the climate was relatively warm and therefore conducive to agriculture at high latitudes (e.g., Patterson et al. 2010). This lasted from ca. AD 800-1300. Following the MWP was the LIA, a period when climate in the North Atlantic became colder as well as more varied. This took place approximately from AD 1300-1900.[4] The LIA coincides with decreasing agricultural viability across the North Atlantic. These environmental conditions are discussed more in Section 2.1.

Both the MWP and the LIA have come under scrutiny in the past few decades, as many different climate-proxy models have either proven or disproven their existence. However the current consensus is that, for the North Atlantic region, the MWP and

[2]The Kingdom of Denmark also played a large role in this expansion, but it was Norwegians who populated Orkney and Iceland.

[3]Also sometimes known as the Medieval Climate Optimum.

[4]Dates for both the MWP and the LIA are subject to local differences.

LIA are verifiable climatic phenomena at a broad scale (IPCC 2007). Past climates are understood through the use of climate proxy data; commonly used climate proxies are pollen, glacial ice cores, and dendrochronological records, but there are many others. The selection of climate proxies requires care, as numerous studies have shown that even large-scale climate proxies like the Greenland ice cores have a strong regional bias and may not reflect climate conditions as close as a few hundred miles from their coring location (Dawson et al. 2003; Dugmore et al. 2007a). However, various climate studies and models have broadly confirmed Lamb's (1982) conclusions: in the North Atlantic, both at the regional and local scale, there was a warm-cool-warm cycle during the last 1200 years (Helama et al. 2009). Based on our current understanding of climate, the NAO (North Atlantic Oscillation) may have been in a positive phase during the MWP, including a shift north for the Gulf Stream, while the opposite may have been true during the LIA, with subsequent warming and cooling effects on the North Atlantic climate (Stenseth et al. 2003; Mann 2007). The positive and negative phases of the NAO have been correlated to respectively warmer and colder climatic conditions in the North Atlantic (Visbeck et al. 2001).

Therefore, Norse North Atlantic expansion and subsequent contraction took place with the backdrop – or perhaps main player – of climate change. Individual islands and even settlement sites also faced local environmental changes that shaped how the landscape was used. For example, in coastal northwestern Iceland, sea ice blocking access to the coastal waters was a legitimate concern in colder years (Ogilvie 1990), whereas that was not the case in Orkney. Broadly, it is unsurprising that the places settled by the Norse had dramatically different fates: while the Norse abandoned North America and Greenland, Iceland and the Faroe Islands starved for a time, whereas Orkney and Shetland achieved a measure of success accompanied by integration into the global economy. Norse cultural responses coupled with local environmental change, both different in each colony, must have played large roles in determining their fates.

2.2.1 Orkney: the transition into the wider European social and economic sphere

Around the end of the first millennium AD, the political and cultural situation in Orkney changed. Norse settlers replaced the Pictish that had dominated the islands and Northern Scotland for several centuries (Ritchie 1994). The nature of this cultural

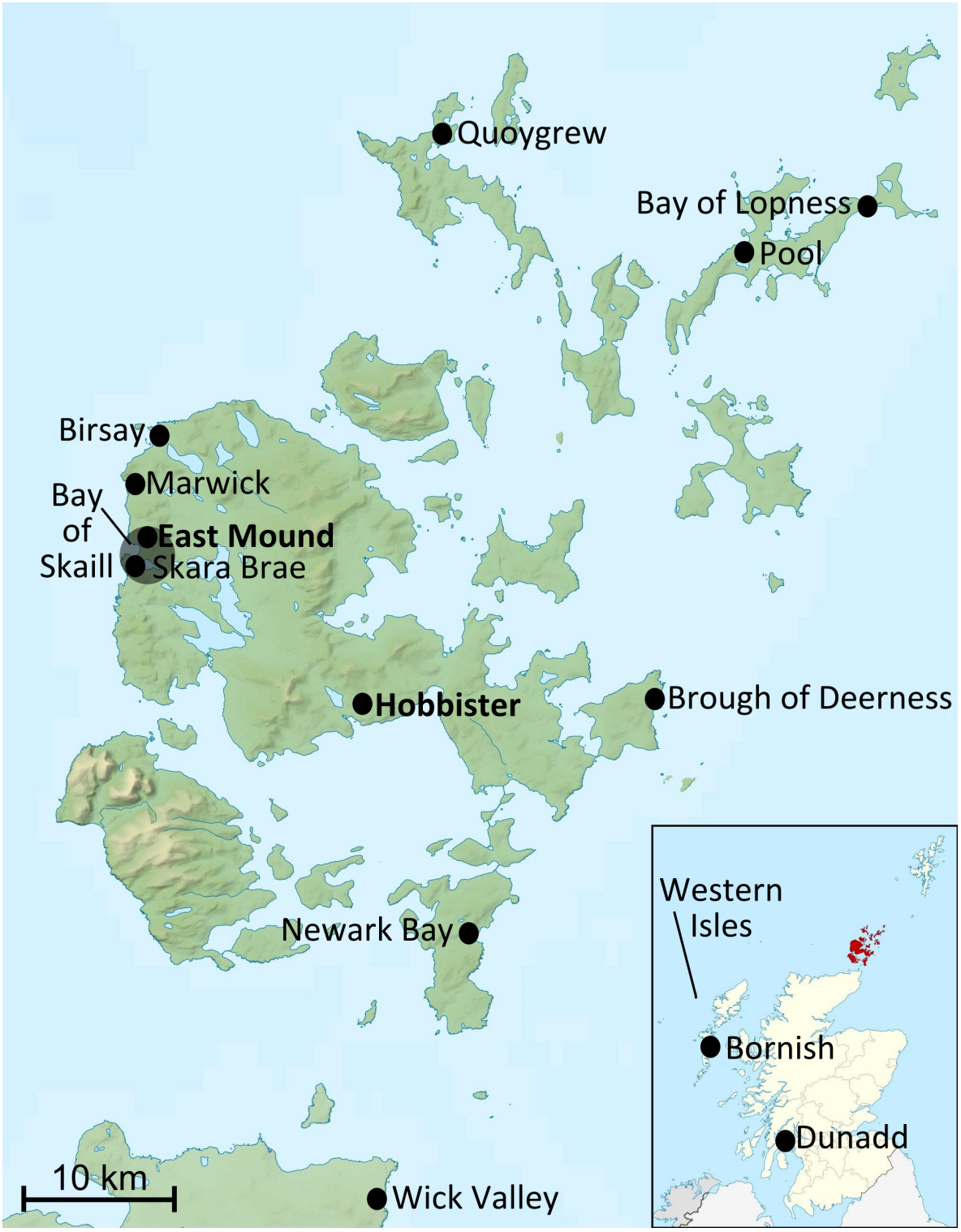


Figure 2.1: A map of Orkney showing major locations mentioned in the text below as well at the location of the landscape project at the Bay of Skaill(map base from Wikimedia 2015).

change is not known, but it seems likely that it was very localised. For example, Buteux (1997) sees a degree of continuity in the archaeological evidence between the Pict and Norse phases at Pool, Skaill Deerness[5], and the Brough of Birsay, whereas documentary sources stress the violence of the Norse incursion throughout the British Isles. Hunter (2007: 147) sees this process occurring in phases: first, the Northern Isles were a transitional staging ground for Norse exploratory forays further south; next, they were colonised by settlers from Norway; finally, they became an official part of the Kingdom of Norway with the establishment of the Earldom of Orkney at the end of the ninth century. This final phase was accompanied by the integration of Orkney into the European trading market, as well as the consolidation of settlements (*ibid.*). However, the majority of known evidence is about elite centres like the Brough of Birsay and the Brough of Deerness (Morris 1989; Morris 1996; Buteux 1997), to the exclusion of smaller farmsteads.

The social structure during this period of Orkney remains elusive. The major written source, the *Orkneyinga Saga*, is largely a record of feuding elites and its creation dates to several centuries later than the events it purports to depict. Archaeological evidence reveals that some farms were clearly more powerful than others, but how powerful and for how long is unclear. For example, the progression of phases at Birsay Bay, a major multi-period site, has not been unambiguously tied into the chronological record for the rest of Orkney (Morris 1989; 1996). The general pattern of elite settlements on Orkney - similar to northern mainland Scotland (Caithness) and Jarlshof on Shetland - was the development of an early farmstead into a small, multi-farm community centred around a church (Hamilton 1956; Roesdahl 1987; Morris et al. 1996). However, at other settlements, like Pool (Hunter 2007), Westness (Kaland 1993), and Buckquoy (Ritchie 1977), in Orkney and Underhoull in northern Scotland (Small 1966), farmsteads seem to have remained as individual farms rather than nucleated settlements. Hunter (2007: 144) suggests that, as was the case at Pool, even these individual farms became part of the wider Norse economy - the farm there, while seemingly independent, was producing an excess of cereal crops that Hunter theorises were for either export or taxation purposes. This was accompanied by evidence of dairying, and Hunter ultimately concludes that the farm at Pool may have produced dairy goods for themselves and other farms in the area. Likewise, Cant (1984: 173) sees Norse and medieval Orkney as a tightly-knit, well-organised society. He envisions a society where a progression of earls held control with a base at

[5]Not to be confused with the Bay of Skaill.

the large settlement of Birsay, and smaller, regional centres were controlled by local nobles who had status and influence over the neighbouring population.

Beyond small scale, local trade within Orkney, these farmers also may have grown flax for export (Bond and Hunter 1987). Kaland (1982) suggests that grain may have been exported from Orkney to Iceland and in return the Orcadians received tar, timber, and maybe boats, while Shaw (1980) documents that seventeenth century Orkney was a major exporter of grain to both Shetland and Norway, and had been for some time. The result of trade within the Kingdom of Norway and internationally was Orkney's integration with the wider European economy and society. Buteux (1997: 268) sees the construction of St Magnus Cathedral in Kirkwall in the 12th century as proof that Orkney had passed from the Viking world of the *Orkneyinga Saga* and into the world of European markets as envisioned by Barrett (2004).

The role of marine resources, and particularly cod, in Orcadian trade during this time period has been studied more extensively than grain exportation. In part, this focus is the product of the relatively recent development of stable isotope research into past human diets and its emphasis on discerning percentages of marine versus terrestrial food sources. For example, human remains from a cemetery in Newark Bay, Orkney, showed an increase in marine consumption, particularly among males, into the late medieval period, although the results of the study must be considered preliminary due to its small sample size (Richards et al. 2006). Zooarchaeological evidence for an increase in marine resource exploitation has also been found from the Norse period onward at Buckquoy, Jarlshof, and Underhoull (Hunter 2007: 144). However, McGovern (1990) and Fenton (1997) maintain that the average Orcadian farmer was primarily an agriculturalist who supplemented his crops with seasonal fishing. How the exploitation of marine resources related to the growing of grain – whether the farmers were, like in Iceland, seasonal fishermen – is unclear.

Therefore, our current understanding of Orkney from Norse settlement to its transition into the later medieval economy is composed of competing theories. Were they fishermen or agriculturalists? Did they export goods or grow just enough for themselves? Are the patterns at the large, elite currently-excavated sites indicative of wider trends or outliers in a landscape mostly composed of small-time farmers/fishermen? Very few of these excavations have precise or accurate dated material. With stronger chronologies, it could become clearer if these activities took place simultaneously or not. Correlating events could give a better picture of the rapidity with which change occurred and if there were geographical patterns occurring – such as a group in one

area, perhaps under the influence of a powerful individual landowner, engaging in more collective farming practices.

Not all excavations at Orkney suffer from a lack of dated evidence. For example, Simpson (1997) has studied Marwick Bay in the west of Mainland, Orkney from the late Norse period until the late nineteenth century. His study examines soil formation and relict soil properties and he concludes that common lands around Marwick Bay were carefully managed. People chose areas to exploit based upon the cultural landscape – and, although there was some degradation in the form of erosion or overgrazing, land use was not static and adapted over time to meet the challenges presented by that degradation. Community organization was crucial: by the 1300s, the parish Bailie Court regulated movement of livestock and oversaw the maintenance of turf dykes, and this local regulation continued into the modern era (*ibid*: 375).

Elsewhere in Orkney, the farm at Quoygrew, Westray, has been studied during the transition from the Viking to medieval period, using geoarchaeology and soil micromorphology to focus on the relationship between agriculture and fishing. This is considered as part of the integration of 'peripheral' North Atlantic polities – Iceland, Shetland, Orkney – into new state structures within Europe (Barrett et al. 2000; Simpson et al. 2005: 355). The study by Simpson et al. uses the record of domestic debris accumulations at the site, in conjunction with radiocarbon dates, to define the changing fortunes for agricultural and fishing economies at the local level. They found that fishing at Quoygrew advanced into a larger market early – as the Viking period ended, and the medieval period began in Orkney – to satisfy demand for the large continental market, while cereal production remained small, with exports directed to Iceland and northern Norway (2005: 374).[6] The importance of cultural memory to understanding landscape change at this scale is highlighted by the authors when they write, 'At a local level, economic transition and intensification were dependent upon earlier settlement and on the wide-ranging and complex cultural knowledge that local people had of their local environment' (*ibid.*).



Figure 2.2: A map of Iceland showing major locations mentioned in the text as well at the location of the landscape project at Vatnsfjörður.

2.2.2 Iceland: from the end of the Freestate through the 'Dark Ages'

Archaeological studies form the basis for the current understanding of Iceland during the settlement and medieval periods. The sagas purport to describe the settlement period but, because they were written down much later than *landnám*, they are not considered to be reliable sources for documenting ways of life in this period. Excavations of landscapes and individual settlements have contributed to the understanding that Iceland from shortly after the settlement period until at least the thirteenth century and probably beyond for most places was composed of what Vésteinsson (2006) has termed 'communities of dispersed settlements' and what Juliusson (2010) describes as similar to manorial demesnes elsewhere in Europe. These dispersed settlements slowly grew together in many locations but during the centuries to come a system of tenancy took root that ultimately displaced a large proportion of the

[6]Simpson et al. draw their evidence for these cereal exports from *Islendinga Saga* and *Bandamanna Saga*.

Icelandic population (Bolender 2006).

After the AD 1262 demise of the Freestate (also known as the Commonwealth), Iceland lost its independence and was ruled by the Norwegian and then Danish crowns. The period afterwards, particularly after the first plague epidemic of 1402, is often called 'Iceland's Dark Ages'. Karlsson (2000) provides the only complete surveys of Icelandic history written in English, from which much of what is written below is drawn. The rich literary tradition of the Icelanders, so prolific during the twelfth and thirteenth centuries, fell away after the end of the Freestate and until ca. 1700 there are long periods from which very few historical sources survive, particularly the 1400s (Karlsson 1996). The intervening centuries were marked by plague, famine, and the occasional volcanic eruption like that of the Lakí fissure in 1783 that devastated farmland, livestock, and led to more famine. Notably, the only part of Iceland spared the second major plague epidemic, in 1495, was Vestfirðir (Karlsson 1996: 267). Iceland's shores were raided by pirates as well as English and Spanish sailors intent upon cashing in on its lucrative fishing grounds. Initially, Denmark's control, so many miles away, was sporadic and Iceland was largely left to fend for itself during these periods of hardship. In the seventeenth century, Danish control became stronger, as the King of Denmark imposed a trading monopoly on Iceland in an attempt to control the highly lucrative cod trade.

The eighteenth century was the final century of the era known as the 'Dark Ages' of Icelandic history. The majority of Icelanders were tenant farmers, and because they had to move between farms from year to year, there was little incentive for individuals to make improvements and so many farm buildings fell into disrepair (Edvardsson et al. 2004; Bolender 2006). At the same time, however, saga literature began to be rediscovered and studied both in Iceland and further abroad, particularly in Denmark. From a demographic standpoint, the most important event was the Móðuharðindin, the 'Mist Hardships' or 'Mist Famine', which followed the eruption of the Lakí fissure in 1783. The destruction of farmland and subsequent death of livestock caused a famine that killed 20-25% of the Icelandic population over the next two years (Vasey 1991).

The general overview of Icelandic history across these centuries serves as a background to the local and regional events that archaeologists study. However, most excavations in Iceland have focused on the Saga times, from *landnám* to the end of the Freestate (Friðriksson 1994) with a few notable exceptions (e.g., Sveinbjarnardóttir 1992; Dugmore et al. 2007a). Sveinbjarnardóttir (1992), in her comprehensive

archaeological survey of farms in Iceland, found that most of the areas of Iceland that she studied experienced decline and abandonment from ca. AD 1300 through the sixteenth century, when her survey stops. The counterpoint to that decline comes from the Snaefellsnes peninsula, where coastal fisheries grew during that time period. She attributes the decline elsewhere to the climate, plagues, and volcanic disasters that crippled the country, but also notes that in many cases these events led only to a temporary abandonment followed by resettlement. She stresses the importance of social and economic changes, such as the rise of fishing as a major export, to driving the evolution of settlements in Iceland.

One of the few researchers to have studied this period in Icelandic history is Hastrup (1990; 1992). In her anthropological studies of Icelandic society from 1400-1800, she stresses that the end of the Freestate and the first plague outbreak in 1402 transformed it. To her, the period from 1400-1800 was one of a 'disintegrating social system in which only a minority were "free" in the old sense of being landowners, in which kinship no longer mattered for the rank and file, and in which mass death from starvation was recurrent' (1992: 106). She offers as support the loss of technological skill in agriculture that led to recurrent shortages of labour and thus of food. However, she also acknowledges that the change from the MWP to the LIA had serious consequences for agriculture in Iceland. She uses place-name and literary evidence to show that, in the period of settlement, it was common to grow grain throughout Iceland. She then cites Þórarinsson (1956: 15-16), who believes that grain growing was abandoned in the northern and eastern parts of the island by the end of the 12th century. By 1350, only barley was a viable crop in Iceland, and that was confined to a few places in the south (Hastrup 1990: 58).

Like Sveinbjarnardóttir (1992), Hastrup does find one area of the Icelandic socio-economic situation that fares well during this period, and that is fishing. She notes that fishing became such a lucrative and important part of the Icelandic economy that the 13th century law book *Grágás* had to specify that no one could hold a house without some livestock (meaning rely solely upon fishing) without the rest of the *hreppur* (community) consenting to it. From this time period until the twentieth century, it was common for farm-owners to send their workers to fishing stations on the coast for at least part of the winter. Farmers might also collectively own a fishing boat. This was common throughout Iceland, but the most successful fishing areas were the northwest, Snæfellsnes and Vestfirðir. Beginning in the fourteenth century, Hastrup states that fish became such an important trade item that these

areas were wealthier than other parts of the country for several centuries (1992: 174). She argues, however, that fishing occupied a liminal space in Icelandic society, which, in her opinion, was nostalgic for the period of *landnám* and the sagas. Therefore, Icelandic society celebrated the farming lifestyle of its ancestors even though the land itself could no longer support the population on farming alone (1990: 82-83). Unfortunately, Hastrup does not address those areas in the northwest of the country where fishing was creating success.

In Iceland, recent archaeological research has focused on two different strands: first, discovering which resources were important and how the use of those resources changed over time, particularly using zooarchaeology (e.g., McGovern et al. 2006; Harrison et al. 2008; Hambrecht 2009); and second, discovering the impact of Norse settlement on the previously unpopulated landscape (e.g., Dugmore et al. 2000; Buckland and Panagiotakopulu 2005; Mairs et al. 2006).

One of the largest of these studies has been on the Mývatn district in northern Iceland, where the 'Landscapes of Settlement' project (McGovern et al. 2007) has documented the settlement of that area, particularly with regards to faunal analysis, from the *landnám* period until the thirteenth century. This has specifically focused on the use of marine resources, and also documents the high-status longhouse and settlement at Hofstaðir in comparison to other nearby farms (Friðriksson et al. 2004).

The high-status farm at Reykholt, Borgarfjörður, in western Iceland, was a major political and religious centre during the medieval period. It was excavated in the late 1990s with a focus on how the environmental record may have influenced its prosperity (Sveinbjarnardóttir et al. 2007). Findings there indicate that there is no link between climatic change and both the growing of cereal crops and the deforestation of birch in the area; instead, both of those environmental changes seem linked to choices made by wealthy landowners there such as labour availability, the price of cereal crops, and a need for fuel (*ibid.*: 203-204).

A study of medieval farm abandonment for five farms in Þórsmörk, South Iceland, asks whether or not the climatic changes of the Little Ice Age resulted in the farms' abandonment, or whether other forces were at work (Dugmore et al. 2006). The authors note that environmental change may be irrelevant to farm abandonment in many archaeological cases, as what appears in the archaeological record as an 'abandoned frontier' may in fact be the result of changes in settlement patterns unrelated to environmental change (Vésteinsson 1998; Dugmore et al. 2006: 336). In this

study, Dugmore et al. note the importance of timing archaeological and environmental change closely, to ascertain if environmental changes occurred prior to settlement abandonment (2006: 336). From soil profiles, they find that environmental impacts did occur in the period leading up to the abandonment of the Þórsmörk farms. The authors theorise that this was caused by the settlers seeing a 'false analogy' between the climates of southern Iceland and Scandinavia and the northern British Isles, in terms of landscape appearance and some plant species; as a result, they mistook the landscapes for having a similar ecology, when in fact, Scandinavia and the British Isles had that appearance because of centuries of deforestation and the creation of 'cultural steppe' landscapes, whereas Icelandic landscapes were not deforested; they were incapable of supporting much tree growth at all. As a result, the two types of landscapes had different carrying capacities for livestock, and, as Iceland was closer to the edge of agricultural limits, it was more sensitive to change (Dugmore et al. 2006: 340-341). Their ultimate findings are that the abandonments at Þórsmörk occurred because of political manoeuvring by the Church, to shift resource management around the landscape, but that the impetus for this manoeuvring was soil erosion and woodland changes as a result of poor landscape management (*ibid.*: 344). They conclude that the combination of social policy and evolving environmental conditions overcame the settlement's ability to survive.

A similar but much geographically larger study of landscape change comes from Eyjafjallahreppur, south Iceland, a region that extends from below sea-level coastal lowlands to an upland frontier. Sveinbjarnardóttir et al. (2006) studied thirty-eight landholdings from the ninth through the seventeenth centuries, and used documentary sources to date their settlement and abandonment. The authors conclude that the pace of change in the landscape increased during the LIA, and suggest that this may be caused by either climatic changes or cultural changes relating to the amount of land required for marriage in an area where the landscape could not sustain subdivided farms. However, the dating methodology used in this study is very imprecise and so changes in the archaeological record cannot be correlated to specific environmental events.

Prior to the Vatnsfjörður excavation, very little archaeological or historical studies had focused on Vestfirðir. Edvardsson et al. (2004: 37) is one of the few published sources for the area. They provide a counterpoint to Hastrup in their description of the eighteenth century. They note that although outsiders had come to the country with Enlightenment ideals about how to improve agricultural conditions, these would

have been pointless in the face of the social and environmental conditions that the majority of agriculturalists in the northwest faced. Tenant farming meant that methods like intensive manuring or better hay storage would have given benefits to the next tenants or resulted in greater profit to landlords and therefore raised rents, so farmers had little incentive to do so. Meanwhile, because of its geography, Vestfirðir faced worse environmental conditions than much of the rest of the country,[7] and so there was little land for pasture (e.g., Hjort et al. 1985). Instead, Edvardsson et al. write, northwestern farmers most likely put effort into exploiting the abundant natural resources of the area – not just fishing, but also stranded marine mammals and driftwood (2004: 37). The extent to which this happened is unclear, but zooarchaeological evidence suggests that cod fishing played a major role in the northwestern economy (e.g., Perdikaris et al. 2005).

Accompanying all of the turmoil and social malaise in Iceland after the demise of the Freestate was the impact of changing climate. The warm years that had accompanied Iceland's settlement passed away, and, from ca. 1300, the Icelanders faced several centuries of increased sea ice, colder winters, and unpredictable weather.

2.2.3 Transition from the Medieval Warm Period into the Little Ice Age

The archaeological effects of the MWP and LIA specifically in Orkney have not yet been studied in enough detail to understand their impact. Whatever the timeline and breakdown of labour, the rise of the fishing industry in Shetland and Orkney seems to have led to modest prosperity and population stability and perhaps even heightened success as the climate cooled at the beginning of the period (Amorosi et al. 1997: 498). Although Hunter (2003) argues that the LIA did not impact northern Britain in the same way that it did in Greenland and other, more northerly Norse colonies, the major Orcadian farm at Skaill, Deerness, declined after the 12th century (Buteux 1997). Meanwhile, Oram and Adderley (2008) propose a climate-triggered crisis among the agrarian society in Highland Scotland ca. 1300-1400. Although no evidence for that has yet been found in Orkney, it seems likely that any crisis in Highland Scotland would also have affected Orkney's interconnected economy. In general, however, it seems that the advent of the cod trade brought success to Orkney.

[7] This is discussed more in Chapter 4.

The archipelago's rising prosperity and integration into the European market is in strong contrast to the LIA's impact on Iceland, as is discussed in Section 2.2.2.

Cultural evidence for climate change in this period has been used as a climate proxy, drawing on the Icelandic written record. Ogilvie (1990) writes that perhaps the most compelling argument for the existence of the MWP is that people went to the effort to settle Iceland. Recent temperature proxies from the northwestern Iceland marine shelf have found that the area began to experience high temperatures from ca. AD 800 (Andrews et al. 2009). This matches well with evidence from the sagas, which describe a favourable climate during the period of settlement (ca. AD 870-900) that allowed for large farms and successful crops (Ogilvie 1990; Patterson et al. 2010). There was less drift ice during the period from AD 200 to ca. 1100, with an increase in sea ice beginning ca. 1250 (Andrews et al. 2009). This research has formed the basis for understanding the impact of the MWP in Iceland.

In lower latitudes, the MWP also may have had a significant effect. Barrett and Richards (2004) argue that warmer sea temperatures drove more cod north into the cooler waters off Norway and the Northern Isles and led to an increase in fishing production around AD 1000. This in turn led to marine-fishing intensification for the Scottish Isles and their integration into the wider North Atlantic economic sphere. Isotopic study on limpet shells from Viking age to medieval archaeological midden deposits in Quoygrew, Orkney, found that there was a wide seasonal range of temperatures compared to the modern day during the MWP, with notably warmer summers and colder winters than in current conditions (Mobilia 2009). However, this study was limited in scope and, as stated above, there is very little information directly from Orkney for the MWP. In general though, the MWP seems to have been a series of warmer-than-average years across the North Atlantic region with occasional downturns (Patterson et al. 2010).

The LIA, meanwhile, seems to have been a period of climatic variability: not a period of unbroken cold, but instead one of fluctuation, warm in some years but with overall difficult and cold seasons (Kirkbride and Dugmore 2006; Geirsdóttir et al. 2009a; Helama et al. 2009). During this time, total icepack and glacial size grew across the northern hemisphere, despite some warm years and even decades (Massé et al. 2008). It was this unpredictability that would have presented the most difficulty to communities relying upon cultural knowledge about weather and annual climate cycles. Historical accounts and oral traditions from and about the period emphasise the unpredictability of weather patterns and seasonal changes time and again (e.g.,

Ogilvie and Jonsson 2001; McKinzey et al. 2005). These studies are important from an archaeological perspective because they provide accounts – in some cases firsthand – of how rapidly fluctuating environmental conditions affected, and continue to affect, human lives. For example, the importance of climatic predictability to economic activities as well as the maintenance of cultural traditions is apparent from these records of human response to climatic change. Ogilvie's (1990) study of Icelandic written sources – historical records and the sagas – from the *landnám* onward reveal that, at least as recorded by medieval Icelanders, the LIA was not consistently cold, but prone to unpredictable downturns for which the people were unprepared. An entry typical of these annals is one from 1374: 'Winter and spring so severe that no one remembered the like. In the north there was no growth of grass. The sea ice lay right up to St Bartholomew's Day (24 August/1 September). No ship came to Iceland [that year] as they all had to turn back to Norway' (Ogilvie 1990: 244). The change in climate was unlike anything that had previously been experienced by the Icelanders; this had major ramifications for an agricultural community that relied upon cultural knowledge about past seasonality to plan its food production.

As elsewhere in the North Atlantic, the pattern that the LIA took in Iceland has been recognised as a series of climatic fluctuations, rather than a consistent period of cold. The earliest study of climate oscillations in Iceland was Þórarinsson (1969), who combined archaeological, historical, and geological sources to make his argument. Various climate proxies published during the intervening years have developed this picture further. There is some disagreement among models, in part because of how much human settlement has altered soils and vegetation used as climate proxies (Gudmundsson 1997: 88). However, in general there is agreement with Geirsdóttir et al. (2009a), who have found that Iceland's transition into the Little Ice Age occurred in two steps, with initial summer cooling taking place from AD 1250-1300 and then staying that way, followed by a more severe drop in summer temperatures beginining in AD 1450-1500. Some of the most severe years of the LIA were the late 1600s and late 1700s, although the latter was exacerbated by widespread famine and poor weather caused by the Lakí eruption (Grattan and Pyatt 1994; Ogilvie and Jonsson 2001; Stothers 1996; Vasey 1991).

As in Iceland, climatic variability marked the Little Ice Age in Orkney. There was a strong increase in storm activity (Morocco et al. 2007; Sommerville et al. 2007). There may have been lying snowfields on higher elevations throughout Scotland and the Scottish Isles (Morocco et al. 2007). An LIA increase in storminess, combined

with anthropogenic factors, may have contributed to serious erosion, particularly in upland regions (Ballantyne 1991). Also related to storminess, stratigraphy in the Bay of Skaill is characterised by periodic thick deposits of wind-blown sand. Large storms stripped so much sand from the bay that the Neolithic settlement at Skara Brae was uncovered in 1850.

McGovern (1990) sees a solidification of centralised political systems across the Norse North Atlantic happening at the same time as the onset of the LIA, which led to changes in adaptive strategies. Early on in the Norse colonisation process, he theorizes, settlers were quicker to adapt to new environments because they had less centralised authority making rules about agricultural practices; as these political systems solidified, rules about pasturage and other land use also solidified, and society became less able to adapt to rapid changes in climate.

2.3 Previous archaeological research throughout the North Atlantic

In the past twenty years, archaeological studies focusing on environmental change have been fairly common in the North Atlantic, but many, particularly outside of the major studies in Iceland, have lacked chronological resolution. The major finding from this research is that cultural knowledge about practices in the landscapes of the North Atlantic had a substantial environmental impact at a local level in all their colonies: deforestation, widespread erosion from grazing mammals, and the creation of new synanthropic habitats, which replaced more diverse 'natural' habitats (Dugmore et al. 2005). Meanwhile, changes to the environment unrelated to human activity and operating at a larger scale impacted the lives of the people living there, causing them to adapt at both local and regional scales.

The success of landscape management at Marwick Bay seems to have been something of an exception. Landscape degradation through farming practices is a theme in many other studies of the Norse North Atlantic. This is particularly true of Iceland, where deforestation both for fuel and to open up grazing areas seem to have rapidly led to the breakdown of topsoils and widespread erosion in habitable areas. This has also been reported in Shetland, the Faroe Islands, and Greenland (Simpson et al. 2001: 177). To many researchers, this is explained by the 'tragedy of the commons': communal management allowed more animals onto the landscape than it could support. This

management stemmed from cultural knowledge developed over time (Crumley 1999, in Simpson et al. 2001: 187). Cultural knowledge in this instance provided a rationale for community actions and defined how actions were to be undertaken, as well as where and when that would happen (Sackmann 1991). Simpson et al.(2001) find that, although Icelandic settlers arrived with cultural knowledge about landscape management from different environments, they had modified their attitudes towards landscape within the first fifty years of settlement to suit the Icelandic environment. In the LIA, however, when climatic fluctuations became severe, cultural knowledge stagnated, perhaps because there was not a concerted effort to make policy for 'bad years' because they were not perceived as normative (*ibid.* 189). Other reasons for cultural knowledge stagnation might be the rise of tenant farmers and the lack of connection to a single farmstead that Hastrup (1990) and Edwardsson (2004) describe. In all these cases, landscape management, and its attendant socio-cultural and socio-economic policies, may have played a large role in slowing community response to climate/environmental change: the presence of decades or even centuries of received wisdom about how to manage the annual agricultural cycle may have prevented the acceptance or adoption of any initiatives to change. Likewise, in the face of yearly variation, cultural knowledge that was sometimes successful may have seemed a better solution than experimentation.

Beyond Orkney and Iceland, other North Atlantic islands have also been studied at the interaction between archaeology and environmental science. Edwards et al. (2005) approach the relationship between humans and their landscape using a series of hypotheses about the environmental effects of agriculture entering into a 'pristine' environment in *landnám*-era Suðuroy, in the Faroe Islands. They employ radiocarbon dating, geoarchaeology, and palynology. Church et al. (2013) update the narrative of settlement in the Faroe Islands with new dating and palynological evidence.

In Norse and medieval Greenland, likewise, the demands of agricultural production played a large role in how members of the European settlements negotiated the landscape. Norse Greenland is most famous for its ultimate collapse, and determining the causes of that collapse has been an active area of North Atlantic scholarship for over three decades. For example, the fragile soils in Greenland led to a need for irrigation. Adderley and Simpson (2006: 1675) found that this was related to climatic fluctuation: in warmer years, grass for fodder would grow more, requiring more water; in colder years, there would be moisture deficits, which also required water. It is unclear if irrigation systems were used in Iceland in this period, but the immediate

need for them in Norse Greenland suggests that, in order for the colony to be initially successful, its founders needed to devise an irrigation strategy very early on. The irrigation systems devised were extensive (Arneborg 2005) and must have required labour and the cooperation of landowners to create, as well as leadership to initiate their construction.

The study of palaeoecological and historical evidence for manuring and irrigation at Garðar, the Norse Eastern Settlement of Greenland, by Buckland et al. (2009: 114), is a study at the local level of those irrigation systems. The settlement was a large farm, whose owners seem to have had contact with Norway. It is unclear if the irrigation systems at Garðar were part of local innovation, or inspired by cultural knowledge of agriculture in sub-Arctic regions at home in Norway. Irrigation systems had to be introduced shortly after *landnám*, when the stripping of turf for building resulted in a radical change to the lithology, seems to indicate radical anthropogenic change. Erosion from livestock grazing was widespread after *landnám*, but farmers responded by changing manuring and irrigation practices (*ibid.* 114).

From all of these studies, a pattern emerges of evidence for humans in the landscape negotiating both with their changing environment and with each other. There are no set rules that apply across the islands of the North Atlantic for how humans responded – or, for that matter, that apply across an individual island. Although they were part of the national and international socio-economic sphere, as with the intensification of fishing in Orkney, responses are locally-driven, with local consequences. Each of the studies above focused on small areas or single settlements, demonstrating the need to narrow our research focus in order to achieve meaningful and accurate results. Therefore, it is necessary to work at the level of individual excavations to untangle these relationships on the most precise time scale possible; only then can we attempt analysis at the regional level with any confidence.

2.4 Theoretical frameworks for conceptualizing human/environment interaction in the North Atlantic ca. AD 800-1800

From all of the above studies, some general themes emerge framing the current archaeological understanding of how humans in the coastal North Atlantic reacted to environmental change:

How landscape marginality affects responses Landscapes in the North Atlantic had to be carefully managed or lose productivity. Even in relatively lush Orkney, this led to the creation of local councils that met to regulate grazing rights (Simpson et al. 2001). In Greenland's Eastern Settlement, the landscape's fertility had to be carefully regulated through manuring and the construction of irrigation systems in order to provide enough fodder for the cattle-based economy (Buckland et al. 2009). In Iceland, meanwhile, a lack of community organization, especially early in the settlement period, seems to have led to erosion with serious consequences for agricultural viability (Dugmore et al. 2009). However, in some parts of Iceland, farmers were able to compensate for reduced grazing area due to both erosion and the LIA by developing technologies to enhance soil fertility and also by exploiting marine resources (e.g., McKinzey et al. 2005: 330).

'Crossing the threshold' Simpson et al. (2001) use this phrase to describe the moment when a group or settlement reaches a turning point that lies between success and failure. A number of questions arise from this notion. For example, when does a particular group move from success in a landscape to failure, and how is that recognisable archaeologically and in modern-day societies? Is the point of failure total abandonment, or depopulation, or forced migration within a small area leading to natural forces reclaiming once useful land? Or is it something more subtle, something crucial but largely unnoticed that happens months or years before the humans living in the landscape are noticeably affected? What are the social, cultural, or economic factors that might prevent acknowledgement or response to a threshold crossing? Finally, is 'crossing the threshold' an irreversible step? In lived-in landscapes, there will always be a negotiation between humans and environmental forces. However, in landscapes like the islands of the North Atlantic, particularly those that are more agriculturally marginal (Iceland and Greenland), even small changes in climate or environmental conditions can have very serious consequences for human settlement.

Success vs failure in a landscape That the notion of 'crossing the threshold' has become an important part of climate impact research emphasises the widespread tendency, in both academic and popular writing on the subject, to interpret Norse colonies in terms of their ultimate failure or success. Some researchers describe it as failure when the Greenland colonies died out, leaving behind gruesome evidence of the last days of a struggling community (Wallace 1990; Buckland et al. 1996;

Wallace 2003). Meanwhile, Iceland, the Faroe Islands, and the Northern Isles of Scotland are considered successful, and national identities in the region have been constructed on the legacy of ultimate triumph over centuries of environmental adversity (Karlsson 2000). However, thinking of the former Norse colonies as failures or successes superimposes the end results over years- or centuries-long occupation periods. For example, the Greenland colonies were successful in terms of survival for a relatively long time, engaging in trade with the rest of the medieval world for several centuries, while the Icelandic settlements struggled for centuries in the medieval and pre-modern period with famine and disease (Karlsson 2000). More precise dates may correlate economic, social, and environmental shifts that characterise settlements in a dynamic time scale, allowing theories about settlement change to move beyond the success/failure dichotomy.

Not overstating the case for climate or environment forcing societal change Part of understanding human settlement as a constantly negotiated relationship with the landscape is considering the role of non-anthropogenic factors like weather, climate, and catastrophic events (e.g., volcanic eruptions). However, the extent to which environmental and climatic conditions played a role in the Norse colonies during the Viking and medieval periods remains unclear. Lacking accurate and precise chronologies, it is impossible to correlate an environmental event with an archaeological one. In many coastal settlements throughout the Norse North Atlantic, for example, settlements in coastal areas follow the same pattern of movement across the landscape over time – Viking settlements clustered along the shoreline, but by the medieval period they had often moved away from the coast to sit atop hills. This may have been the result of shifting shorelines, but it may also have been the result of shifting economic foci or a defensive manoeuvre (B. Douglas, pers. comm., 1 August, 2009; K. Milek, pers. comm., 25 June, 2011). If it was possible to chronologically link the movement of the coastline to the movement of the settlement, then the theoretical connection between local environmental change and human movement could be strengthened.

Cultural memory about landscape use planning Anthropologists, archaeologists, and geographers often speak of memory as a social activity embedded in the landscape (for a review, see Hoelscher and Alderman 2004). Memory adds an additional chronological dimension to the archaeological study of land use; it asks archaeologists to consider both how landscapes have changed over time and how the

inhabitants of those landscapes experienced that change over time. Two recent studies highlight some of the major issues that are current research questions in the integrated study of human and landscape change. In the first, McKinzey et al. (2005) integrate oral tradition and scientific evidence about the LIA in southeast Iceland, finding that, even in the early twenty-first century, there is still a strong cultural memory in the region of the LIA and its impact on the agriculture and social life of the landscape. In the second, Dugmore et al. (2007) use tephrochronology to untangle the chronology of Þjórsárdalur, a valley with twelve to fifteen abandoned farms, including several abandoned after the Hekla 1104 eruption. They find that, while environmental factors had a major effect on land use in the valley, the socio-economic choices made by a series of local bishops had an equally strong effect. The bishops controlled who could gather wood in the forest and how much wood could be taken from it, and in this way the birch forest in this location was preserved long beyond when it had been depleted in many other inhabited areas of Iceland.

The research of McKinzey et al. (2005) and Dugmore et al. (2007) research serves as an introduction to the importance of cultural memory and historical perceptions of landscapes, changes in landscapes, and human responses to landscape change. Human practice in the landscape relates to a complex societal structure of shared knowledge about what works and what doesn't in a local context (Ingold and Kurrtila 2000). Thus, cultural memories about landscape, climate, and weather are crucial to an understanding of how societies cope with environmental conditions. Change within human-occupied landscapes cannot be related to environmental changes alone; there must be a certain amount of interplay between human settlement and landscape (Dugmore et al. 2007a). As a result, the importance of cultural memory and knowledge about the environment to interpreting human response to climate change cannot be overstated. Simpson et al. (2001: 187) define cultural knowledge as 'what is known by a social group about the dynamics of a landscape, as well as what is known about landscape responses to the activities of that social group.' This knowledge becomes cultural memory when a temporal component is added – as time progresses, the knowledge is remembered and used to make decisions about current conditions. Cultural memory and knowledge are therefore defined not just by purely pragmatic considerations, but by a wide range of factors.

This is related to Ingold and Kurtila's (2000) notion of a type of tradition that comes from inhabiting the landscape, wherein having knowledge about a place is part of what makes one local. Although much of the cultural knowledge from the Norse and

later periods in the North Atlantic is based on practicalities – for example, Zilmer (2008) discusses cultural memory in the context of references to seafaring and islands in the Icelandic sagas, and finds that many references to landscape in the sagas are strictly informative rather than embellished with supernatural elements – Amorosi et al. (1997: 505-506) note, 'Strategic issues are those directly affected by individual and group planning: how many children to raise, what mix of animals to keep, how to lay out a settlement – all inter-connected and interdependent with simultaneous decisions made by other human players. The parametric contexts, rainfall, growing season, depth of topsoil, are less subject to strategic contingency, yet interact with the predominantly social strategic choices.' Simpson et al. (2001) stress that early settlers in Iceland, despite coming to the unsettled landscape armed with knowledge about agricultural practices from very different environments, recognised the problems of soil erosion and land degradation early on and took steps to modify it; these steps are codified in documentary sources. They note that the lack of further modification is striking in the medieval and later periods, and suggest that this may be the result of stagnation of cultural knowledge during a period of wide but short-term climatic fluctuations. That cultural knowledge may have stagnated in the face of changing environmental conditions, or it may have stagnated because it was advantageous to powerful people in the landscape.

The idea that cultural knowledge can stagnate because of human factors raises the question of power: whom does cultural memory benefit, and whom does it penalise? For whom are the remembrances optimal? These people are the key social actors in the landscape, and will shape landscape organisation (Amorosi et al. 1997: 507). Hoelscher and Alderman (2004: 349) speak of the 'shared dimension of remembering, and the equally social nature of how space is produced', while emphasising the importance of power relationships, and therefore access to resources. These, they write, affect social memory about landscape. In both Orkney and Iceland, wealthy landowners would have been the primary shapers of the landscape, and presumably economic practices would have been remembered in a way that reinforced their past successes. Therefore practices at high-status settlements may have been passed down for generations, encoding in the landscape the successes of a previous generation. Even innovations to old practices probably related to the manipulation of cultural knowledge by the most powerful people in the landscape. In coastal medieval Orkney, for example, the dynamic interplay between new and old – traditional agrarian versus export-based fishing economies – may have been the result of a powerful few indi-

viduals seeing an opportunity to cement their position in society by forming trading alliances with outside partners.

2.5 Using chronology to understand archaeological landscapes within regional frameworks of cultural and environmental change

The events of the North Atlantic during the MWP and LIA have now been described in general terms, and individual case studies discussed. The weakness of many of these case studies is a lack of chronological precision or accuracy (or both) that forces the researchers involved to link changes at individual excavations only to general environmental change. With such a broad chronological scale, it is impossible to reliably correlate change in one record with change in another. The power of archaeology is its ability to relate the events at a single excavation to those in nearby localities as well as in the wider region; therefore, the heightening of accuracy and precision for archaeological and environmental chronologies at individual excavations will allow them to be linked to other archaeological investigations as well as well-dated environmental records.

3 | Archaeological and Environmental Chronologies in the North Atlantic

Archaeological and environmental chronologies rest on a framework of prior research. In this chapter, I review that framework. First, I discuss tephrochronology, including evaluating the sources of eruption geochemistry that are, as of the time of writing this thesis, available to correlate tephra layers in the North Atlantic. Second, I describe radiocarbon dating and OSL dating. I conclude with a discussion of Bayesian modelling.

3.1 Tephrochronology

Tephra is the ash and larger fragments that have been ejected from a volcano; the main focus of tephrochronology is the vitreous glass component of volcanic ash (Þorarinsson 1944; 1974; cf., Lowe 2011). Tephra may be either proximal to the volcano or distal from it, and visible or micro- (sometimes called crypto-) (Lowe 2008). Tephrochronology is a geochronological method using the pyroclastic fall component of tephra as marker horizons in stratigraphic sequences, and is used for dating and correlating archaeological, geological, palaeoenvironmental, and palaeoclimatic sequences. Tephrochronology relies upon the notion that the span of a tephra-producing volcanic event is short enough and discrete enough that it appears to be instantaneous in the stratigraphic record. The fall zone for tephra can span hundreds or even thousands of miles,[1] creating isochrones within otherwise chronologically floating sequences from

[1] e.g., In the admittedly extreme case of the Toba Super Eruption, tephra from Indonesia was deposited in a thick layer in India (Jones 2007), while microtephra from the small Eyjafjallajökull eruption in 2010 reached southern Europe (Lettino 2011; Rossini 2011).

separate study areas (e.g., Newnham and Lowe 1999). These isochrones can be extracted from the depositional record with field and laboratory techniques.

The discovery in the late 1980s that it was possible to isolate and identify individual shards of vitreous microtephra revolutionised the use and scope of tephrochronology. Microtephra linked to known eruptions became an extremely useful tool for correlating environmental and archaeological records across wide regions (e.g. Dugmore 1989; Pilcher and Hall 1992; Turney et al. 1997; 2004; Wastegard et al. 2000a; 2000b; van den Bogaard and Schmincke 2002; Davies et al. 2002; 2003; Lowe et al. 2004). The identification of these layers within stratigraphic features relies upon shard counts per gram of dry sediment and geochemical analysis, which is discussed further in Section 5.2 (Davies et al. 2007: 320). Some particularly well-preserved tephras have been used to independently test climatic synchroneity between Greenland and Europe as far south as the Alps, and current research is creating a European-wide framework for tephra studies linking Icelandic and Italian volcanoes (Blockley et al. 2007; Lowe 2008: 320; Lane et al. 2011). Tephrochronology can also provide an alternative to radiocarbon dating, which is often troubled by contextual and statistical limitations, including marine reservoir effects (Pyne-O'Donnell 2010).

Tephrochronology relies upon the supposition that each volcanic eruption produces a unique geochemical signature and so distal tephra layers can be matched to proximal layers by their glass chemistry. In practice, identifying individual eruptions by proximal glass chemistry has been one of the greater obstacles to be overcome as the methods of tephrochronology develop, as is discussed further in Section 3.3.[2] However, under the right conditions, tephrochronology presents researchers with an opportunity for extremely precise and accurate dates. Where there is historical information about volcanic eruptions, clear stratigraphy, and geochemical data from proximal deposits, it is possible to determine exact dates from tephra and microtephra. Dugmore et al. (1996) provide a good example of this with the Loch Portain tephra Group A, from western Scotland. Geochemically, this tephra could have been from either the Hekla 1510 or 1947 eruptions; stratigraphically and palaeoecologically, however, Hekla 1947 was impossible (Dugmore et al. 1995). Proximal tephra from the 1510 eruption has been dated with a reference from the *Biskupa Annálar* (Bishops' Annals), which describes an eruption in that year on the eve of St James's Day (25 July) that caused

[2]Another obstacle is that the age of tephras when there is no historical record of eruption relies upon other dating methods – for example, Hekla-4 has been wiggle-match dated to 2310 ± 20 (Hall et al. 1994). However, almost all of the tephras referenced in this thesis are from the Icelandic historical record. The provenance of their dates are discussed in Chapter 7 and Chapter 8.

earthquakes and 'other geological phenomena' (Thórarinsson 1967: 58; Dugmore et al. 1996: 513). The fraction of the microtephra that Dugmore et al. describe contained shards from the initial silicic phase of the eruption, suggesting that the tephra fall originated from the eruption on 25 July. Finally, using data about tephra transport from southeastern Iceland to the northern British Isles from the 1947 eruption of Hekla, which was of a similar scale and had a similar distribution area, Dugmore et al. suggest that it took 24-36 hours for the tephra from Hekla 1510 to pass over the Scottish peat bog in which they found the microtephra. Therefore, the microtephras found at Loch Portain have a high probability of dating to 26 or 27 July, 1510. This is just one example of how precise tephrochronology can be, especially when combined with other research methods.

As it stands now, tephrochronology needs to improve in two key areas. First, methods for detecting and extracting microtephras must improve so that smaller shards can be found and analyzed. Second, the dataset of published proximal eruption chemistry must continue to expand. However, in its current state, it can be a very powerful tool when combined with the correct research plan.

3.2 Tephra and distal microtephra deposition in the landscape

This thesis is primarily concerned with distal microtephra, as most of the study areas are located relatively far from active volcanic production zones in the Holocene period. Orkney is nearly one thousand kilometres from the active volcanoes of Iceland, while the Vestfirðir region of Iceland is the oldest geological part of the island and has not seen active volcanism since ca. 6-7 Ma (Roberts et al. 2007: 244). Geographically, it is located relatively far (over 100 km) from the most active volcanic centres of Iceland, as is shown in Figure 3.1. Therefore, it is crucial to understand both the transport pathways of tephra and microtephra in the atmosphere, and the factors affecting tephra and microtephra deposition in a variety of environments.

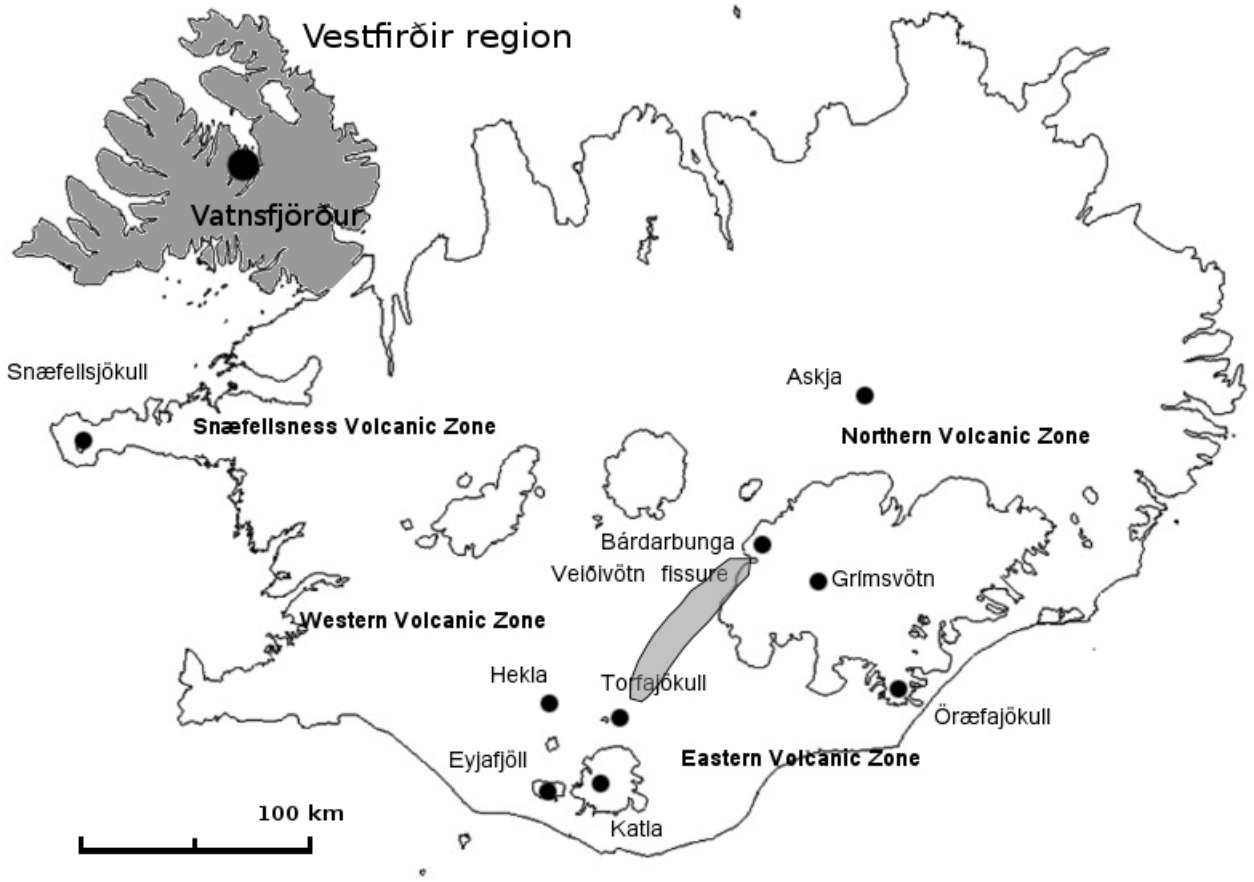


Figure 3.1: Location of volcanoes active in the last 2000 years BP in relation to the location of Vestfirðir. The nearest volcano – Snæfellsjökull – last erupted ca. AD 200. The Vestfirðir region is shown as dark shading, while the Veiðivötn fissure system is shown as light shading.

3.2.1 Transport pathways of tephra

Ash layers decrease exponentially in thickness and grain size the further they are from their volcanic source. This is a result of the sorting of particle size and density as tephra fall through the atmosphere (Pyle 1989). The mechanics of ash dispersal are not entirely understood at this point in time, and future research in tephrochronology has great potential for reconstructing the historical transport pathways of ash plumes (e.g. Lacasse et al. 2001). However, in the past two decades, the advent of the study of microtephra has resulted in the enlargement of known pathways from many eruptions (Lacasse 2001; Wastegard and Davies 2009). The least dense portions of ash clouds – those that can travel such great distances – form the basis for microtephra studies. Recent eruptions have demonstrated that the geographic spread of an ash cloud does not necessarily relate to size of eruption (Davies et al. 2010). Dispersion models based on twenty-first century Icelandic eruptions show that ash clouds from even relatively small eruptions can travel thousands of miles (e.g. the Grimsvötn eruption of 2004 and the Eyjafjallajökull volcano eruption of 2010), although only in the latter eruption was there confirmed tephra fall outside of Iceland (Davies et al. 2010).

Surviving tephra output from any eruption can be variable across the landscape, with variability increasing as distance from the volcanic source increases. This seems to be influenced by weather patterns at the time that the ash cloud is floating over the landscape. For example, tephra from the Hekla 1947 eruption fell in a large part of Finland, Ireland, and Scotland, but has not yet been detected in England, despite the cloud itself blowing over both of these areas; this differential tephra distribution over the landscape has been correlated to sleet and rain in Finland at the time (Dugmore et al. 1995: 263; Thórarinsson 1967; Rea et al. 2012). Following on the Hekla 1947 research, the spread of distal tephra from Hekla 1104 has also been correlated to areas with high precipitation (Langdon and Barber 2004; Wastegard and Davies 2009). Related to weather, Lacasse (2001) has used computer modelling to demonstrate how seasonality, in conjunction with wind and precipitation patterns, strongly influences the way that tephra spreads across the atmosphere and subsequently the landscape. The Eyjafjallajökull volcano eruption in 2010 provided non-model evidence to confirm that wind patterns have a major role to play in the spread of tephra as well (Davies et al. 2010). As a result, it is important to develop maps of ash fall – although they will not guarantee that a certain tephra will be found, they can provide guides to

likely tephras to be found in an area. Dugmore et al. (2011) call for the creation of this type of map.

Once on the ground, site-specific processes also may result in the uneven distribution of tephra, and so ash layers may be missed in some sequences. Davies et al. (2010) caution that, although shard concentrations within microtephra horizons can be used as a guide to map the highest ash densities, site-specific sedimentation processes may also have strongly influenced the placement of tephra within stratigraphy. As a result, it is necessary to understand the depositional processes that may have affected each tephrochronological sample. Many of these processes are specific to the depositional environment.

3.2.2 Terrestrial deposits

In the North Atlantic, peat is the most common terrestrial soil type to be cored for use in microtephra studies, and there are a number of methods for extracting tephrochronological information from these cores (for a review, see Gehrels et al. 2008). Peat develops in climates that are both wet and cool, and factors such as precipitation, ground and air temperature, amount of waterlogging within the soil, and topographic and drainage constraints all are important to its development (Tipping 2007: 2097). Furthermore, the development of peat is the result of specific regional factors: local topography, geomorphology, pedology, and climate all contribute at the local level (Tipping 2007: 2110). Peat deposits are generally treated as reliable sources for tephrochronologies because, as numerous studies have shown, tephra shards are generally not mobile within peat profiles (e.g., Langdon and Barber 2004: 21). They may be confined to less than 1 cm of peat stratigraphy, meaning that the vertical diffusion of individual shards may, in ideal conditions, be on the millimetre scale (Langdon and Barber 2004: 21; Dugmore and Newton 1992; Hall et al. 1994; Dugmore et al. 1996; Wastegard 2002; Bergman et al. 2004). In practice there is a wider distribution in the sediment column, as will be discussed further throughout the thesis.

Tephrostratigraphy for microtephra has in general been based upon 'shards per gram of dry sediment weight', done visually using a microscope (although in the future, XRF (x-ray fluorescence) may become an alternate method (Gehrels et al. 2008)). The concentrations of microtephra in a given vertical interval from a peat sample

are then used to determine areas to target for glass chemistry. The peaks and gullies described by shard counts theoretically form the record of tephra fall across a landscape; however, there are a number of factors that can affect this.

This is not to say that microtephra in peat cannot be affected by post-depositional processes that may influence the accuracy and precision of peat-based tephrochronology. Indeed, recent research indicates that tephra deposition across all landscapes is highly heterogeneous (Payne and Blackford 2008). Many of these factors are particularly pronounced at high latitudes, like the test cases studied in this dissertation, and so will be discussed here. Microtephra can move vertically in a stratigraphic column, affecting the stratigraphic age interpretation, and it can move horizontally, affecting concentration counts (Payne et al. 2005: 148). For example, Bjarnason (1991) noted the sinking of microtephra in a section of peat in northern Iceland through a moss carpet, affecting vertical placement and therefore accurate interpretation of tephra age. Meanwhile, Dugmore and Newton (1992) used x-radiography to show that there was horizontal shifting among microtephra in Scottish peat layers, documenting instances where microtephra concentrated in hollows in the peat, probably due to either wind or water movement. This affected their ability to determine the concentration of microtephra in a given layer because of the reliance upon shard counts within sub-samples of peat cores, and the likelihood that the sub-sample would not represent an accurate concentration of shards. Similarly, Bergman et al. (2004) describe secondary deposition of microtephras by wind in environments where the ground is frozen for part of the year, preventing the microtephra from settling into the peat surface. They note that long-lasting snow cover, permafrost, and exposure to strong winds all must be taken into account when considering post-depositional processes upon microtephras (*ibid.*: 245). Hunt (1994) and Boygle (1999) confirm this viewpoint, documenting wind and water movement in peat and its affect upon microtephra secondary deposition. Payne and Gehrels (2010), using rainfall simulation after planting Icelandic microtephra into a peat deposit in Scotland, determined that in their experiment microtephra had a tendency to clump together into hollows in the peat, which, again, could affect the observed concentration. Previously, rainfall had led Caseldine et al. (1998; 1999) to conclude that there is variability in microtephra taphonomy across replicated profiles, while Payne and Blackford (2008) document the differences in microtephra occurrence and concentration between closely adjacent sites and even within sites. The lack of replicable results is currently a notable research problem in tephrochronology, but the variability of deposition may explain it. Tephra layers may also act as active barriers to water flow in peat deposits, particularly when they

are fine grained (20 μm) and the layer is thick (>1 cm) (*ibid*: 3826). All of these factors are discussed in Chapter 7 and Chapter 8 in relation to the interpretation of data from this dissertation.

A final point for consideration in peat environments – or anywhere else that microtephra is deposited – is the presence of a background signal of microtephra. Pyne-O'Donnell et al. (2008: 77) provide several examples of what is meant by 'background signal' – a constant or near constant presence of microtephra shards throughout a wide vertical spread of the peat core. Charman et al. (1995) and Pilcher and Hall (1992) note their presence in Scottish peat records but offer only an explanation of inwash from surrounding slopes. More recently, Pyne-O'Donnell et al. (2008) demonstrate a complex tephrostratigraphy for peat cores containing Icelandic microtephras, noting that the Borrobol tephra (ca. 12,300 BP) always presents a stratigraphically diffuse distribution. They attribute this to harsh climatic conditions at the end of the last stadial period. Generally, however, microtephra background signals have not been well-documented in the literature. For example, Holmes et al. (1999) note the presence of a background signal in their study that expands tephrochronology to the Falkland Islands, but do not take it into account in their interpretation. Shard counts should always be included in tephra studies, as background signals provide important information about depositional conditions or post-depositional movement. These are therefore presented for the data gathered in this thesis in Section 6.2.

Payne et al. (2005) and Payne and Gehrels (2010) call for further studies into tephra taphonomy due to what they term extensive evidence of post-depositional movement. Where vertical movement downward can be explained largely by water processes, movement upward in a sedimentary column requires more explanation. Payne and Gehrels (2010: 20-21) offer three explanations: 1. Secondary deposition due to snow melt or other releases of microtephra into a peat system; 2. Movement of microtephra with a rising water table in a peat deposit; and 3. plant growth within peat pushing microtephra upwards. However, in two separate experiments, Payne and Gehrels (2010) determine that, in general, peat environments provide the best possible stratigraphic environment in which to study microtephra deposition. Furthermore, most post-depositional processes occur shortly after deposition, when the tephra-bearing surface is exposed to wind and rain. Their major point is that, despite the general rule that peat is the best depositional environment for microtephra, awareness of potential secondary deposition factors are crucial to understanding the tephrostratigraphy of a

peat core. Therefore, microtephra studies must both take these factors into account and document them for future understanding.

3.2.3 Lacustrine deposits

In lacustrine sequences, in contrast to most peat sequences, there is typically a wide vertical spread of volcanic sediments (Gehrels et al. 2006). Distribution is marked by a peak in shard concentration and then a gradual decline in the overlying sediment; sometimes sediments also have small distribution stratigraphically below the peak (Turney et al. 1997; Davies et al. 2005; Davies et al. 2007). As a result, microtephra deposits corresponding to a single volcanic event can be present across 5-10 cm of a lacustrine stratigraphic column. This has serious implications for precision in tephrochronology: 5-10 cm can represent a very long time span. Therefore, a discussion of depositional processes within lacustrine settings are crucial to understanding the timing of the primary ash fall (Davies et al. 2007).

In addition to the considerations above, placement of peak shard concentration within a sediment column may also be deceptive. The peak shard concentration has traditionally been labelled as the point of primary ash fall; however, there are arguments to be made for lower ash concentrations either below and above the peak corresponding more accurately to the primary volcanic event (Davies et al. 2007). For example, although ash concentrations stratigraphically below the peak may logically represent the beginning of a volcanic event, they may be the result of reworking or downward migration of shards within a column (Ruddiman and Glover 1972; Anderson et al. 1984; Enache and Cumming 2006). Meanwhile, microtephras from later eruptions may be masked within the tail of a peak from a large eruption (Gehrels et al. 2006). This is further complicated by depositional factors for lacustrine sediments, specifically those at high latitudes or altitudes where ice cover and snow-beds may present seasonal issues, or those in catchment areas where there is a low amount of vegetation cover to prevent erosion into the lake.

The impact that ice cover and snow-beds may have on sedimentation in high-latitude lakes is studied in a comparison between cores from two Swedish lakes by Davies et al. (2007). They find that shards from a single eruption can span 120 years of sediment column in a lake catchment, and suggest a number of explanations for this. For example, an initial low concentration of shards may represent the small amount of an ash cloud that is deposited primarily in a lake; a later peak may be the

result of deposition on the surrounding landscape and subsequent water catchment. Topography and vegetation in the lake's immediate region play a role in the speed with which water and sediments flow into it; Davies et al. (2007) find that a lake with patchy vegetation cover and steep slopes around it had evidence for a rapid inwash of shards, whereas the lake with a larger catchment area and forested slopes may have had a delayed tephra inwash. Snow-beds, or perennially lying snow, may also form tephra traps, holding sediments until seasonal or longer-period melting. One of the lakes in the Swedish study is located in an area where the fluctuations of the Little Ice Age, and subsequent periods of snow-bed melting, can be seen in the tephra shard counts from roughly the eruption of Askja in AD 1875 until a period of warmer weather and extensive melting in the 1930s.

Davies et al.'s conclusions are derived from an example where site-specific processes in areas with seasonal snow and ice cover can influence the accuracy and precision of chronologies derived from microtephras found in lacustrine sediments. Their study is also one of the first about the effects of snow-beds on microtephra sedimentation. Their results argue that this is an important factor that requires further study, especially as it relates to tephrochronology derived from lacustrine sediments in high latitudes.

Type of catchment and presence of vegetation can also play a large role in determining the stratigraphic distribution of tephra or microtephra within a lacustrine core. Pyne-O'Donnell et al. (2008) describe the distribution of microtephra in cores from Scottish lakes and palaeo-lakes. One layer found was the Borrobol tephra, the result of an Icelandic eruption shortly after the Dimlington Stadial (GS-2), ca. 22,000 and 13,000 years BP. Glaciers had recently retreated across the landscape, leaving in their wake little vegetation and large quantities of loose sediment. Pyne-O'Donnell et al. write, 'Shards of the Borrobol Tephra would thus have become mixed and entrained into this sediment and continually reworked into the lake until such time as the shards were depleted from the catchment or further sediment became unavailable for transport through slope stabilisation by vegetation development.' This may have resulted in a bimodal distribution of tephra throughout the core, which the authors conclude would mean that the second peak is invalid as an isochron, but may have value for timing climate change on the regional scale. Mangerud et al. (1984) note a similar distribution in depositional environments left denuded by the retreat of glaciers for Vedde Ash reworking from catchment into lakes. Therefore, lakes can be successfully studied for microtephra, but, much like peat cores, there is a range of depositional

and post-depositional considerations to take into account when interpreting their tephrostratigraphies. This is discussed further in Chapter 7.

3.2.4 Other records of tephra fall

Tephra and microtephra are also deposited in marine sediments and across ice caps, leaving a record of tephra fall that has been found in marine cores as well as ice cores. Several Icelandic tephras have been found in marine sediment cores throughout the North Atlantic (Ruddiman and Glover 1972; Kvamme et al. 1989; Sejrup et al. 1989; Sjoholm et al. 1991; Hunt et al. 1995; Lacasse et al. 1996; Lackschewitz and Wallrabe-Adams 1997; Bond et al. 2001; Wastegard and Rasmussen 2001; Jennings et al. 2002; Knudsen and Eiriksson 2002; Wallrabe-Adams and Lackschewitz 2003; Austin et al. 2004; Eiriksson et al. 2004; Kristjánsdóttir 2007). These records may be correlated to terrestrial and lacustrine records (e.g., Kristjánsdóttir 2007). Marine records from the North Iceland Shelf have been used in the last decade to reconstruct a high-resolution climate proxy record throughout the Holocene, although few studies have touched upon the most recent millennium (see Knudsen et al. 2009: 457 for a summary). Many of these records have been dated by tephrochronology. Similarly, tephra layers have been found within the Greenland ice core records (Hammer et al. 1980; Gronvold et al. 1995; Zielinksi et al. 1995; Mortensen et al. 2005). These layers are reflected as distinctive peaks of enhanced electrical conductivity and sulphate within the cores (Mortensen et al. 2005; Hammer et al. 1980; Zielinski et al. 1996). In the past, researchers have used these peaks to correlate timing with known tephra layers from Iceland, but there has been little glass chemistry on microtephra shards from Greenland, leading to ambiguities in data (Mortensen et al 2005). Identifying these tephras geochemically is crucial for the accuracy of future research of establishing a chronology for environmental changes. This is discussed further in Section 3.3.

3.3 Icelandic tephra-producing eruptions from the last 2000 years

Now that depositional factors have been discussed, the next question to address is the origin of these tephra layers. In the North Atlantic, the answer is overwhelmingly Iceland. There have been hundreds of volcanic eruptions in Iceland in the last 2000

years, many of which erupted after the island's settlement ca. AD 870. The known eruptions from this period are described in tables in Larsen and Eiriksson (2008) and Haflidason et al. (2000). The geochemistry of some Icelandic tephras is recorded in an online database, Tephrabase (Newton et al. 2007). This section will describe the known tephra-producing eruptions from the last 2000 years BP, and will then focus specifically on those that have published geochemistry. Although that time scale goes beyond the archaeological remit of the thesis, expanding it pertains to findings within several of the sample cores that make up the results of this thesis. In some cases, there are multiple publications documenting tephra layers, particularly in the case of Hekla 1104 and the *landnám* layer. In these cases, an effort has been made to choose the most representative proximal geochemistry for a more complete dataset covering the range of each composition. However, in other cases, there is very little published data available – a single grain measurement, or no glass chemistry at all. Therefore, a major limitation of the research in this thesis has been the availability of published (or obtainable) proximal glass chemistry from Icelandic eruptions.[3]

Holocene Icelandic volcanism is characterised by explosive eruptions, particularly explosive basaltic volcanism. The explosivity is due to ice caps covering volcanic zones, and the interaction between magma and ice. Icelandic eruptions from volcanic systems that take place underneath ice can produce phreatomagmatic eruptions, the most recent documented example of which is the Eyjafjallajökull eruption of 2010. Phreatomagmatic eruptions are hydrovolcanic events, when magma interacts with water to produce a steam-rich plume of fine ash particles in addition to volcanic gases. Approximately 60% of Icelandic eruptions in the past 1100 years were from volcanoes under icecaps or glaciers (Larsen 2002: 88).

75% of Icelandic known eruptions during the Holocene emitted tephra; of these, 80% are basaltic (Larsen and Eiríksson 2008). The tephrostratigraphy of the country is complex, with over 900 eruptions in the past 9000 years, and just less than 150 eruptions from the last millennium that have left tephra layers on the ice of Vatnajökull.

Despite the prevalence of basaltic tephras from Icelandic eruptions, silicic tephras represent the majority of distal tephras known from Iceland. Distal basaltic tephras from the same period thus far have only been found from three eruptions (Wastegard and Davies 2009). Reasons for this are discussed in Section 3.2.1.

[3] I did not obtain my own proximal data because of the difficulties in doing so for Icelandic tephras (e.g., Larsen and Eiríksson 2007); the most recent case of newly obtained proximal material formed the entirety of a PhD thesis (Meara 2012).

Distinguishing tephra layers from each volcanic system on the grounds of their geochemistry alone can, however, be difficult. Examples illustrating this problem in the case of Hekla tephra have been presented by Larsen et al. (1999). Another example is found in seven tephra layers with near-identical chemistry erupted by Hekla during the interval 950-550 BC,[4] two of which (layers H-M and H-N) were erupted within 50 years of each other and had similar southeastward dispersals (Larsen and Eiríksson 2007: 115). Larsen and Eiríksson note that tephra erupted during the initial phase of an eruption may also have a different chemical composition, in part due to the inclusion of lithics from the throat of the volcano. Therefore, the initial output from an eruption may have a different geochemistry than later phases.

In fact, geochemical composition of tephra from a single eruption can also change throughout the duration of the eruption. For example, Þórarinsson (1967) describes how some silicic Icelandic eruptions have decreasing silica content over time, which is particularly evident with Hekla eruptions (Langdon and Barber 2004: 23). As silica content decreases, tephra passes from silicic into more mafic (i.e., higher oxide percentages of iron and magnesium) phases: dacitic, andesitic, and basaltic (Carmichael 1979). A visual tool for understanding geochemical composition is the total alkali-silica (TAS) plot, which classifies the type of volcanic rock, particularly those with glassy elements, as shown in Figure 3.2. The type of glass that the tephra is composed of has implications not only for geochemical identification of tephra layers, but also for mapping dispersal: when dacitic and andesitic shards are recovered from a distal tephra deposit, then that may be evidence for the later stages of the eruption having reached that distal area (Langdon and Barber 2004: 23-24). Further information on distinguishing tephra layers geochemically is found in Section 5.4.4.

Below is a list of volcanic systems and their eruptions. A volcanic system is defined as a fissure swarm erupting basaltic magma and a central volcano erupting other evolved magmas (Larsen 2002: 81). Each of Iceland's major volcanic systems has major element characteristics that allow their products to be correlated to their source (Larsen et al. 1999; Larsen 2002: 82). A map of all volcanic systems discussed here is in Figure 3.1.

The eruptions that have known geochemistry and that were considered in this thesis are shown in Table 3.1.

[4]All dates are quoted as published – either as BC, AD, or BP – unless otherwise specified.

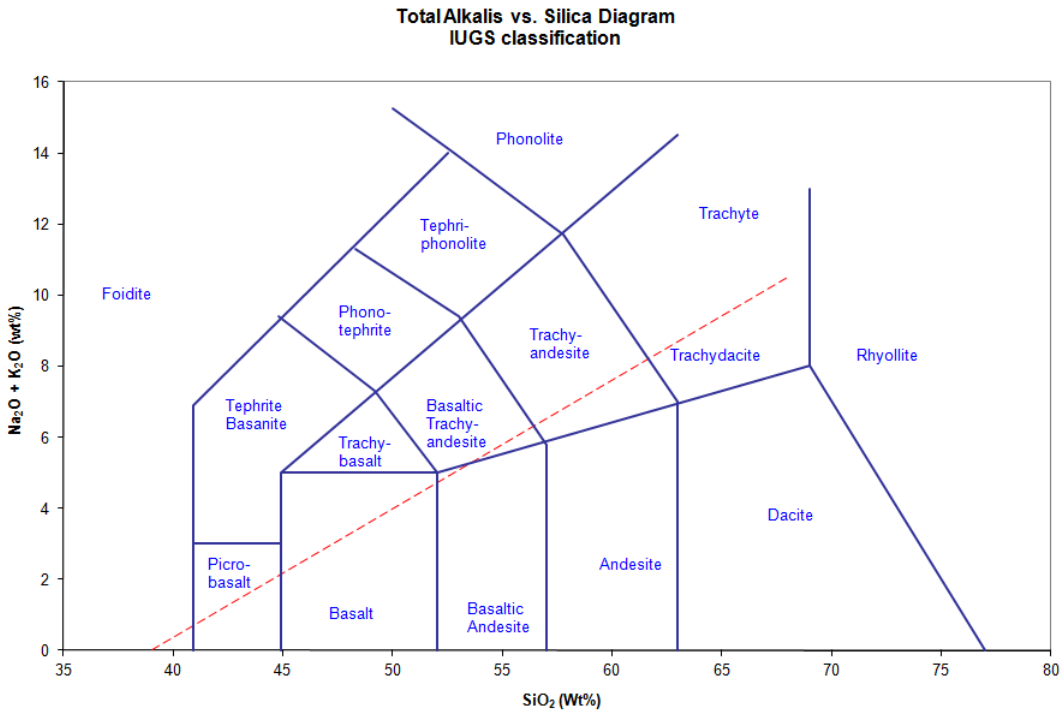


Figure 3.2: Plot of NaO_2+KO_2 against SiO_2, from le Bas et al. (1986: 747).

Table 3.1: All eruptions used for tephra correlation in this thesis.

Eruption	**Volcanic system**	**Approx. Age (AD)**	**How dated?**	**Citations**
H3	Hekla	approx 3000 cal yr BP	radiocarbon	Eiriksson et al. 2000
Snæfells	Snæfellsjökull	ca. 200	radiocarbon	Larsen et al. 1999
860 A	unknown	ca. 860	radiocarbon	Pilcher et al. 1995
860 b	unknown	ca. 860	radiocarbon	Pilcher et al. 1995
Landnám	Torfajökull	870	Greenland ice core	Grönvold et al. 1995
E935	Katla	935	radiocarbon	Dugmore et al 2007
Hekla 1104	Hekla	1104	historical source	Larsen et al. 1999; Boygle 1999
MOR-T4	unknown	between 1104 and 1362; older than GB4-50	tephrochronology	Chambers et al. 2004
GB4-50	unknown	between 1104 and 1362; younger than GB4-50	tephrochronology	Hall and Pilcher 2002

Table 3.1 — *Continued from previous page*

Eruption	**Volcanic system**	**Approx. Age (AD)**	**How dated?**	**Citations**
BGMT-1	unknown	ca. 1120	radiocarbon	Langdon and Barber 2001; Larsen et al. 1999; Pilcher et al. 1995
Hekla 1158	Hekla	1158	historical source	Larsen 1992
Hekla 1300	Hekla	1300	historical source	Dugmore et al 2007
Katla 1357	Katla	1357	historical source	Einarsson 1980
Oræfajökull 1362	Oraefajökull	1362	historical source	Larsen et al. 1999
MOR-T2	Beerenberg, Jan Mayen?	ca. 1400	radiocarbon	Chambers et al. 2004; Wastegard and Davies 2009
Veiðivötn 1477	Bárdarbunga	1477	historical source	Larsen et al. 2011
Hekla 1510	Hekla	1510	historical source	Larsen et al. 1999
Hekla 1693	Hekla	1693	historical source	Dugmore et al 2007
Katla 1721	Katla	1721	historical source	Haflidason et al. 1992; Larsen et al. 2011
Oræfajökull 1727	Oraefajökull	1727	historical source	Larsen et al. 1999
Hekla 1766	Hekla	1766	historical source	Larsen et al. 2011
Lakí 1783	Grímsvötn	1783	historical source	Metrich et al 1991
Eyjafjallajökull 1821	Eyjafjallajökull	1821	historical source	Larsen et al. 1999
Hekla 1845	Hekla	1845	historical source	Larsen et al. 1999
Askja 1875	Askja — Dyngjufjöll	1875	historical source	Sigurdsson and Sparks 1981

Table 3.1 — *Continued from previous page*

Eruption	**Volcanic system**	**Approx. Age (AD)**	**How dated?**	**Citations**
Hekla 1947	Hekla	1947	historical source	Larsen et al. 1999; Rea et al. 2012

3.3.1 Askja

Askja is a stratovolcano located in northeastern Iceland, a part of the Dyngjufjöll volcanic system in the Northern Volcanic Zone, which is tholeiitic (basaltic and subalkaline). Askja has erupted explosively once in historical times, on 29 March, 1875, when it produced tephra with a wide compositional range, for example with SiO_2 ranging from 67.4-75.9%. Although the eruption lasted only eight hours, tephra layers produced by it have distinct phases (Sigurdsson and Sparks 1981). This tephra can be discerned from other historical tephras with similar SiO_2 ranges based upon its relatively high MgO and TiO_2 content. On a ternary plot of CaO, FeO, and K_2O, it looks similar to Hekla 1104 (Larsen et al. 1999).

3.3.2 Eyjafjöll

This volcanic system is located on the south coast of Iceland, beneath the glacier Eyjafjallajökull, and is part of the Eastern Volcanic Zone. It is an east-west trending stratovolcano, with fissure-fed lava flows on the eastern and western flanks of the volcano. This system has erupted three times in the historical period: 1613, 1821-1823, and 2010. All three of these eruptions were at some stage phreatomagmatic, creating very fine-grained tephra deposits, mostly silicic and andesitic in composition. The 1821-1823 eruption (Larsen et al. 1999) and the 2010 eruption (Davies et al. 2010; Sigmarsson et al. 2011) are the only eruptions from the Eyjafjöll system to have published geochemistry. The 1821-1823 eruption, which dispersed ash to the north of the volcano, produced tephra with a high Na_2O and FeO content, which distinguishes it from other Icelandic silicic tephras recorded from historical times (Larsen et al. 1999). The 2010 eruption is still being studied, but its time-sequence sample suite is better than any other eruption documented before it and as a result Sigmarsson et al. (2011) have been able to observe that from Mg-rich basalt drove the eruption.

3.3.3 Grímsvötn

Grímsvötn is the most productive Icelandic volcano in historic times, with about 70 eruptions attributed to it (Thordarson and Larsen 2007: 142). Grímsvötn has two central volcanoes are located beneath a 200 m-thick ice cap that is part of Iceland's largest glacier, Vatnajökull, and is part of the Eastern Volcanic Zone (EVZ). Melting

of the ice covering the caldera lake leads to frequent jökulhlaup[5]. Fissure systems extend from the central volcano trending NE-SW, including the Lakí (Skaftar) fissure, which was responsible for the world's largest known historical lava flow in 1783 (Grimsvotn, Smithsonian Institution website 2011). That fissure eruption was the only one documented in historical times; all others came from the central volcanoes. The Saksunarvatn tephra (ca. 9000 BP), one of the largest and most widespread tephra layers in the North Atlantic, originated in the Grímsvötn system (Grönvold et al. 1995; Ingólfson et al. 1995). Tephra volumes from central volcano eruptions are difficult to determine due to the ice cap, and only a fraction of the tephra produced makes it beyond the ice to be dispersed in the atmosphere (Thordarson and Larsen 2007: 143). Grímsvötn is characterised by an eruption pattern of 50-80 year periods of high activity, followed by periods of low activity of roughly the same length (*ibid.*; Larsen et al. 1998). Glass chemistry from the Lakí eruption in 1783 is relatively Fe-Ti rich, with a TiO_2 range of 2.48-3.63 wt-% (Metrich et al. 1991). The glass chemistry of other eruptions from Grímsvötn are collected in Haflidason et al. (2000) and Óladóttir et al. (2011) have published mean tephra oxide weight percentage ranges for recent Grímsvötn eruptions. Many Grímsvötn eruptions have produced tephra, most recently the Gjálp 1996 event (which has a different name because it occurred between Grímsvötn and Bárdarbunga), Grímsvötn 1998, Grímsvötn 2004, and Grímsvötn 2011 (e.g., Gudmundsson et al. 2004).

3.3.4 Hekla

Hekla is a rift zone, snow-capped stratovolcano located in southwestern Iceland and has been the second most active volcano during Iceland's historical period (Thordarson and Larsen 2007: 141-142). It is part of the transitional-alkalic province of the Eastern Volcanic Zone (Larsen et al. 1999; 2008). The central volcano is part of a fissure called Heklugjá that trends ENE-WSW and that has given the volcano its distinct elongated shape (Hekla, Smithsonian Institution website 2011). Eruptions are centred on this central volcano/fissure area, and are generally mixed eruptions of tephra and lava. Mixed eruptions begin with a short-lived (0.5-2 hours long) Plinian or sub-Plinian phase, which is then followed by a longer lasting phase of lava fountaining and effusion that produces basaltic andesites (Thordarson and Larsen 2007:

[5]Glacial floods caused by volcanic activity; although the word is originally Icelandic, it has been adopted into English and is also used to describe ice-dammed lake drainage (e.g., Tweed and Russell 1999).

142). Tephras from Hekla have a wide range of SiO_2 values by oxide wt-%, with single layers ranging from 57-74% (Dugmore et al. 1992). TiO_2 and MgO values are consistently low, however (Larsen et al. 1999). A number of different researchers have concluded that the length of repose between eruptions affects the SiO_2 wt-% of Hekla's eruptions (e.g., Gudmundsson et al. 1992; Sigmarsson et al. 1992). More so than any other volcanic system in Iceland, proximal tephra from these eruptions have been documented and published.

Icelandic annals provide descriptions of Hekla eruptions. Þórarinsson (1967) brings these accounts together with early tephra studies. Hekla's record of explosive volcanism has had an impact on human habitation as well as the environment in Iceland. Notable eruptions from the historic period include: Hekla 1104, Hekla 1158, Hekla 1206, Hekla 1222, Hekla 1300, Hekla 1341, Hekla 1389, Hekla 1510, Hekla 1597, Hekla 1636, Hekla 1693, Hekla 1766, Hekla 1845, and Hekla 1947. The details of eruptions that correlate to tephra layers studied in this thesis are discussed in Chapter 7.

There are many documented cases of tephra from the Hekla volcano affecting human settlement, most notably at Þjórsárdalur, 'the Pompeii of Iceland', which is discussed more in Section 2.4 (Dugmore et al. 2007b). Hekla's location close to inhabited areas has made its tephra fall more of a hazard than similarly productive volcanoes located in more remote areas (e.g. Grímsvötn).

Tephra from Hekla eruptions has been found distally in the British Isles (e.g., Dugmore et al. 1995; Pilcher and Hall 1992), the Faroe Islands (e.g. Wastegard et al. 2001), Germany (van den Bogaard et al. 2002), and Scandinavia (e.g. Davies et al. 2007), as well as in marine and ice core records (e.g. Kristiansdottir et al. 2007; Davies et al. 2010). Hekla tephra currently dominates overseas distal records because its Plinian and sub-Plinian phases are composed of silicic, rather than basaltic, tephra. As discussed in Section 3.2.1, many researchers have theorised that, because silicic tephra is lighter, it therefore travels further during an eruption. Others have suggested that basaltic tephra dissolves over time (Blockley et al. 2003).

3.3.5 Katla

The Katla volcano is part of the Eastern Volcanic Zone and the majority of it lies beneath the Mýrdalsjökull ice cap, where it produces explosive sub-glacial eruptions. Katla is composed of a fissure swarm with a central volcano at its southwestern end. Most known eruptions have originated in the central volcano (i.e., under the ice cap),

but one large event that occurred along the exposed fissure was the Eldgjá fires, from AD 934-940 (Óladóttir et al. 2007: 478). In historical times, Katla has been the third most productive system in Iceland, producing 21 eruptions since human habitation of Iceland began (Larsen et al. 1999; Thordarson and Larsen 2007). During the Holocene, there have been between 150 and 300 sub-glacial eruptions at Katla (Larsen et al. 2001; Thordarson and Larsen 2007). All known historical eruptions have been accompanied by jökulhlaup. Eruptions are generally bimodal, consisting of high-Ti transitional basalts and rhyolites (Óladóttir et al. 2007; Lacasse et al. 2006). Both the whole-rock and the glass chemistry from Katla show narrow compositional ranges; the basalts are high in TiO_2 (4-5 wt%) (Lacasse et al. 2006). Silicic tephra from Katla also has a narrow compositional range with little variation across a 5000 year record of tephra output (Larsen et al. 2001: 128). Explosive eruptions of this volcano during historical times took place in AD 920, 935±2 (Eldgjá fissure/fires), 960, 1177±2, 1210, 1245, 1262, 1311, 1357, 1416, 1440, 1500, 1550, 1580, 1612, 1625, 1660, 1721, 1755, 1823, 1860, and 1918 (Historical Eruption Data, Smithsonian Institution 2011).

3.3.6 Öræfajökull

This volcanic system is east of the Eastern Volcanic Zone, and is the largest central volcano in Iceland, as well as encompassing the highest point in Iceland. It is a stratovolcano covered by the Vatnajökull icecap, with a small caldera at the top. The rock suite of this volcano is calc-alkaline (subalkaline rocks with relative enrichment in silica and alkalies and little enrichment in Fe) (Prestvik 1980; Larsen et al. 1999).

Öræfajökull has erupted explosively twice in historical times, once in 1362 and once in 1727. The 1362 eruption was the most voluminous explosive silicic eruption from the historical period in Iceland; the majority of the tephra was carried southeast (Þórarinsson 1958; Larsen et al. 1999). Distal tephras have been recorded in Scandinavia, Ireland, and Greenland (Palais et al. 1991; Pilcher and Hall 1992; Pilcher et al. 1996; Wastegard and Davies 2009). Both Sigurdsson and Sparks (1981) and Larsen et al. (1999) have published EPMA (electron probe micro-analyzer) data for the 1362 eruption. Larsen et al.'s data, which are used in this dissertation, are from the stratigraphic lowermost layers of ash from the eruption, which may have been a phreatomagmatic phase in the eruption. This tephra is characterised by high Na_2O and very low MgO. Tephra from this eruption has been found in Scandinavia, Ireland, and Greenland, but glass chemistry is uniform for all of those areas (Wastegard and

Davies 2009: 505). Larsen et al. (1999) also presented published EPMA data from the 1727 eruption, which are characterised by a Hekla-like range in SiO_2, but can be distinguished from eruptions of that volcano by higher FeO and lower MgO content. Selbekk and Tronnes (2007) found that tephra from Öræfajökull also had relatively high Na_2O content (2007).

3.3.7 Snæfellsjökull

The Snæfellsjökull volcano is an ice-capped stratovolcano in western Iceland that forms the prominent western tip of the Snæfells peninsula. It is an isolated volcano located in its own volcanic zone. Its explosive eruptions are silicic, and have taken place several times throughout the Holocene, most recently ca. AD 200 (Kjartanson 1967). A distal tephra layer identified in Ireland (QUB-141) has a geochemical affinity with Snæfellsnes, as does a layer from Sweden (Björck and Wastegard 1999; Haflidason et al. 2000). However, this volcano has not been well studied and the compositions of its eruptive produdcts are not well known.

3.3.8 Torfajökull

The Torfajökull stratovolcano is located north of Mýrdalsjökull, in southern Iceland. It consists of a large caldera with a small ice-cap to the southeast (Torfajokull, Smithsonian Institution 2011). Torfajökull volcano is responsible for the *Landnám* tephra layer, dated by the Greenland ice cores to 871 $\pm$ 2 and traditionally used as an approximate starting date for Icelandic settlement (although in recent years there have been some discoveries in the Reykjavik area stratigraphically beneath this tephra layer) (Gronvold et al. 1995; Larsen et al. 1999). Tephra from the *Landnám* eruption has recently been found as far afield as northwestern Scotland (Cage et al. 2011). A second explosive eruption from Torfajökull took place in approximately 1170. Tephra output from this system is characterised by high K_2O content relative to other Icelandic tephras (Larsen et al. 1999). Silicic lavas from the Torfajökull system sometimes contain tholeiitic basalt from the Veiðivötn system, suggesting that eruptions in both are linked (Larsen 1984: 34).

3.3.9 Veiðivötn/Bárdarbunga

This volcanic system consists of the Bárdarbunga stratovolcano and the Trollagigar and Veiðivötn fissures, located in the southeast of Iceland, and is part of the Eastern Volcanic Zone. Most of the historical eruptions in this system have taken place below the Vatnajökull ice cap and have emitted small to moderate amounts of basaltic tephra; many of these eruptions have produced jökulhlaup (Thordarson and Larsen 2007:143). Eruptions between these two and the Torfajökull volcano are linked and they are often active simultaneously, as in the tephra-producing eruption of 1477. However, each eruption has two unrelated magmas, one silicic and alkaline (Torfajökull) and the other basaltic and sub-alkaline (Larsen 1984; 1999). The bimodal tephra glass chemistry from the *Landnám* eruption is the result of linked volcanism between the Veiðivötn fissure and Torfajökull (Larsen et al. 1999: 468). Óladóttir et al. (2011) have published calculated mean tephra geochemistry for recent eruptions from this system.

3.3.10 Distal tephras from unknown systems/eruptions

A number of distal tephras have been found in the British Isles dating from the last two thousand years that have not been geochemically linked to known Icelandic proximal deposits (Pilcher et al. 1995; Langdon and Barber 2001; Hall and Pilcher 2002; Chambers et al. 2004). Although it is best practice to correlate with proximal glass chemistry, in some cases, particularly for far distal locations (i.e., the British Isles, Scandinavia, or continental Europe), it may be necessary to correlate with distal geochemistry. Below are unidentified layers that have been stratigraphically linked to the past 2000 years BP.

'AD 860 A': this tephra has been found in Scotland and Ireland (Pilcher et al. 1995; Langdon and Barber 2001).

MOR-T4, ca. AD 1000 and GB4-50, ca. AD 1250: These tephra layers have been found in single profiles in Ireland between Hekla 1104 and Öræfajökull 1362 (Hall and Pilcher 2002; Chambers et al. 2004). MOR-T4 has a range of SiO_2 wt-% of 67-70 (Chambers et al. 2004: 709) while GB4-50 has SiO_2 70 wt-% (Hall and Pilcher 2002: 226).

BGMT-1, ca. AD 1120: Langdon and Barber (2011) date this to 830 cal BP (they do not provide an error range) using an age-depth model from a peat sequence sampled

from the Isle of Skye, Scotland; this tephra consists of a mixed population of silicic tephra of Icelandic origin.

MOR-T2, ca. AD 1400; Beerenberg volcano?, Jan Mayen: This tephra layer, identified in an Irish lake by Chambers et al. (2004: 707), has geochemistry that lies outside of the range of Icelandic volcanism. Instead, particularly due to its concentrations of SiO_2, K_2O, and Na_2O, this tephra layer has been attributed to Beerenberg volcano, on Jan Mayen. Its age has been estimated at c. AD 1400 based upon placement within stratigraphy. This tephra layer may be correlated with others found elsewhere in northern Europe (Wastegard and Davies 2009: 505). Mt Beerenberg is known to have erupted at least three times in the last 1000 years, and seems to have an eruptive frequency of 150 +/- 75 years, but there is not yet any evidence for a c. AD 1400 eruption (Sylvester 1975).

3.4 Distal deposition in the North Atlantic

As mentioned above, Icelandic tephras have been found terrestrially in the UK and Ireland (Hall et al. 1994; Dugmore et al. 1995; Pilcher et al. 1995; Lowe and Turney 1997; Turney et al. 1997; Wastegard et al. 2000a; Davies et al. 2001; Langdon and Barber 2001; Plunkett et al. 2004; Ranner et al 2005), Germany (van den Bogaard and Schmincke 2002; van den Bogaard et al. 2002), Scandinavia (Mangerud et al. 1984; Birks et al. 1996; Gulliksen et al. 1998; Bjorck and Wastegard 1999; Zillen et all. 2002; Davies et al. 2003; Boygle 2004; Wastegard 2005; Pilcher et al. 2005), the Faroe Islands (Mangerud et al. 1986; Dugmore and Newton 1998; Wastegard et al. 2001; Wastegard 2002) and Russia (Wastegard et al. 2000b).

The majority of distal microtephra is from the silicic component of eruptions. The reasons for a lack of distal basaltic microtephras relate to volcanism, deposition factors, and study bias. For several years, preservation conditions for basaltic tephras were thought to be poor in peat cores, though this may also be due to sampling techniques (Dugmore et al. 1995). However, in recent years, there have been several finds of distal basaltic microtephras. For example, cores from the Mjáuvøtn lake system in the Faroe Islands yielded several basaltic microtephras (Wastegard et al. 2001: 106). Some of these were from the *Landnám* tephra, which is known from Icelandic sources and the Greenland ice cores to have a basaltic component (Thórarinsson 1944; Larsen 1984; Hafliðason et al. 1992; Gronvold et al. 1995; Zielinski et al. 1997; Wastegard

et al. 2000). Basaltic microtephra from the early Holocene has also been found in Scotland (Pyne-O'Donndell et al. 2008).

In recent years, new distal finds have been published with increasing frequency and recent eruptions like Eyjafjallajökull in 2010 have demonstrated the large tephra fall range of even relatively small volcanic events. Therefore it seems likely that distal tephra studies will continue to play an increasingly large role in chronology building for both archaeological and environmental research in the range of explosive volcanic systems. Below, distal tephra finds specific to the two case studies considered in this thesis are discussed.

3.4.1 Previous tephra finds in Vestfirðir

There has been a limited amount of research into the tephrochronology of Vestfirðir. Northwest Iceland has few visible tephra layers present in its soils; the majority of visible layers described relate to the early Holocene (e.g., Andrews et al. 2002). Late Holocene tephra layers originating in the Snæfellsjökull volcanic system have been found in soils in the southern part of Vestfirðir, but these date to before the historical settlement of Iceland (Sigurgeirsson 2006). Written sources describe three accounts of tephra falls in northwest Iceland; these are the Hekla eruptions of 1693 and 1766 and the Katla eruption of 1721 (Þórarinsson 1955; 1967). The 1766 eruption was one of the largest in recorded history (Thordarson and Larsen 2007: 141). Annals record that in 1766, the ash fall in the northern part of the country was so heavy that, of sixty horses in one region, only six survived the winter (from ash fall covering the vegetation) and therefore the landowners of the region were excused by the bishop Gisli Magnusson from attending the *Althing* (Hjartarson 1995). The Katla 1721 eruption, meanwhile, covered most of the country and was recorded in letters and annals from Vestfirðir to the southeast of Iceland (Þórarinsson 1955: 89). However, none of these layers has been identified geochemically in Vestfirðir until the research presented in this thesis.

There have been a limited number of late Holocene tephra studies from nearby areas, notably one from a lake just south of Vestfirðir and several covering marine cores from the North Iceland Shelf (Kristjánsdóttir et al. 2007; Geirsdóttir et al. 2009b; Quillman et al. 2010). Geirsdóttir et al. (2009b) explore climatic changes at a lake near Stykkishólmur, on the north side of the Snæfells peninsula, however their focus was on visible layers of tephra within their cores rather than microtephras. A study of Efstadalsvatn, a lake one peninsula to the west of Vatnsfjörður, only recorded tephra

to 3500 BP (Caseldine et al. 2003), while Jóhannsdóttir (2003) described terrestrial tephras from the early-mid Holocene in Vestfirðir but did not touch upon the later period. Kristjánsdóttir et al. (2007) found the Hekla 1104 layer within a marine core, while Quillman et al. (2010) focus on earlier time periods but do touch briefly upon the past 1000 years in their study of cores from Ísafjarðardjúp, the deep fjord that bisects Vestfirðir. Therefore, although the area is important for reconstructing climate in Iceland and elsewhere, as well as for establishing a chronology to link with the Greenland ice cores, there has been little research into the Late Holocene tephrochronology of Vestfirðir.

3.4.2 Previous microtephra finds in Orkney

In the past twenty years, a number of Icelandic tephras have been identified in the British Isles (e.g., Hall et al. 1994; Dugmore et al. 1995; Pilcher et al. 1995; Lowe and Turney 1997; Turney et al. 1997; Wastegard et al. 2000a; Langdon and Barber 2001; Davies et al. 2001; Plunkett et al. 2004; Ranner et al 2005). However, microtephra specifically found on Orkney is rare, having thus far been identified on the islands of Hoy (Hoy tephra, ca.5600 BP) and Mainland (Saksunarvatn tephra, ca. 10,800 BP and an unknown layer from the Loch of Knitchen), with no microtephras from the past two thousand years present (Dugmore et al. 1995; Bunting 1996; Bunting 1996b; Mangerud et al. 1986; Haflidason et al. 2000). Similarly, Shetland has only had microtephra finds from the early and mid-Holocene (see Meara 2011: 30-32 for a list). Northern mainland Scotland and the Western Isles, however, have had a number of late Holocene microtephras found there. BGMT-1, dating to 830 cal BP, has been found on the Isle of Skye, while the *landnám* tephra, ca. AD 870, and the 'AD 860 A' tephra have been found in Scotland and Ireland (Pilcher et al. 1995; Larsen et al. 1999; Langdon and Barber 2001). Notably absent from the British Isles – but found in Scandinavia – is Hekla 1104 (also known as Hekla 1) (Wastegard and Davies 2009: 505). Hekla 1158 may match to GB4-57, found in Ireland, showing a south-easterly path for tephra deposition from that eruption (Hall and Pilcher 2002). The Oræfajökull 1362 eruption dispersed widely, with finds in Greenland, Scandinavia, and Ireland, but not Britain, perhaps suggesting that it fell in Ireland because of rainfall there, and did not fall in Britain because it was dry (Wastegard and Davies 2009; Pilcher and Hall 1992). Hekla 1510, meanwhile, was one of the first tephra layers described in Britain, found in the Western Isles, Scotland and Ireland (Dugmore et al. 1995; Pilcher et al. 1996). Tephra from the initial phase of the Hekla 1845

eruption was blown to the southeast and documentary sources record tephra fall in the Faroe Islands, Shetland, and Orkney; the ash fell on the deck of a ship off the coast of Orkney at 5 a.m. the day after the eruption began at Hekla (Þórarinsson, 1981: 111-112; Wastegard and Davies 2009). Dugmore (1989) notes that this tephra was chemically analysed in the 19th century. Although Hekla 1947 had tephra fall recorded to the southeast, so far no shards from this event have been identified in the British Isles (Wastegard and Davies 2009).

The lack of tephra finds in Orkney therefore may be a product of research locations or taphonomic processes rather than a dearth of tephra fall on the islands. Orkney's rainfall patterns are similar to those of Scotland's Western Isles and Ireland, suggesting that tephra should be found there in similar quantities (Met Office Historical Data 2011). Further searching for microtephra in Orkney should continue to reveal distal tephra layers. Successful correlations in Ireland and elsewhere in Scotland suggest that these layers will be valuable chronological tools for archaeological and environmental research.

3.5 Other chronological methods

3.5.1 AMS radiocarbon and OSL

AMS radiocarbon dating and OSL dating play roles in interpreting the results of this thesis, but my research focuses on Bayesian modelling of existing dates rather than the laboratory methods for obtaining these dates. Therefore their description below is brief. Radiocarbon dating is based upon the carbon cycle: the radioactive isotope of carbon, ^{14}C, enters plants and animals throughout their lifespan via photosynthesis or the food chain. They exist in equilibrium with atmospheric ^{14}C until their death. After death, no atmospheric exchange occurs, and the ^{14}C of the sample is depleted by nuclear decay to form stable ^{14}N, emitting a β particle (an electron). The half-life of ^{14}C is 5568 years. Therefore, anything composed of carbon can be dated by the extent of its ^{14}C depletion with respect to initial conditions. ^{14}C also enters the earth's oceans as part of an exchange with the atmosphere, and also as dissolved carbonate. All ^{14}C together is known as the carbon exchange reservoir (Aitken 1990).

In the mid-1980s, the ORAU (Oxford Radiocarbon Accelerator Unit) began to use AMS (Accelerator Mass Spectrometry) for radiocarbon dating, which has increased the accuracy of radiocarbon dates as well as allowing for much smaller samples to

be dated. This sensitivity is required because the natural isotopic ratio of ^{14}C is 10-12, a minute concentration. Like all dating methods, AMS dating has its own set of problems and requires rigorous quality control as well as (if possible) independent verification of its results (e.g., Bayliss and Hey 2004: 259).

One such problem is the reservoir effect, which mainly affects bone and shell. The radiocarbon ages of sample materials whose organic matter formed in the ocean are, on average, 400 years older than those formed in terrestrial environments; this is known as the marine reservoir effect (MRE) (Stuiver and Braziunas 1993; Lanting and van der Plicht 1998). This happens because ^{14}C is only formed in the atmosphere, and it takes time to circulate through different reservoirs (in this case, the ocean). Therefore, a correction is necessary to correlate terrestrial and marine samples. Due to regional variation in oceanic currents, there is also a correction, designated ΔR, defined as a marine correction for a given area (Reimer et al. 2004).[6] The freshwater reservoir effect (FRE) is more variable by region than the MRE; it is caused by the exchange in gas state of carbon from the atmosphere and the dissolved inorganic carbon from groundwater. The latter often causes dates to appear older than they should. However, some sources, like volcanoes, may influence radiocarbon dates to appear too young, again due to an influx of carbon from a source besides the atmosphere. It is also important to know whether the freshwater is from a running or stagnant source (Lanting and van der Plicht 1998: 155).

One recent example of trying to calibrate the MRE and FRE comes from Mývatnssveit, Northern Iceland. There, human remains found beneath a known tephra layer were radiocarbon dated as older than expected. Archaeologists theorise that in life the humans had consumed a diet depleted in ^{14}C, but it was unclear what the source of that depleted carbon was(Ascough et al. 2007: 948). The Norse settlers in the area are known to have exploited terrestrial, marine, and freshwater resources, and to have traded all of these further inland (McGovern et al. 2006). Ascough et al. attempt to determine the percentage of dietary carbon affected by MRE vs. FRE by taking the average between animals known to eat only terrestrially-sourced food (cattle) and then sea- and freshwater-sourced animals.[7] Their results highlight that large quantities of information about individual diets, as well as large-scale dating

[6]The determination of ΔR is discussed further in Chapter 9.

[7]It is important to understand the potential dietary sources for every animal used in such a study; for example, in Orkney, there are sheep who eat seaweed and whose bones are therefore subject to the MRE (Balasse et al. 2009).

schemes, are necessary to gain a precise picture of how the MRE and FRE have affected human bone dates from any given place and time.

Once a radiocarbon date has been obtained, it must be matched to an absolute date via a calibration curve of atmospheric carbon levels. An inherent assumption of radiocarbon dating is that there is a constant amount of ^{14}C in the atmosphere at any given time; this is not the case. In order to achieve a high level of dating accuracy, the amount of atmospheric ^{14}C for the expected time period must be determined. Traditionally, wood samples dated by dendrochronology provided a check for the levels of ^{14}C in the atmosphere at a certain calendar date. A terrestrial calibration curve has been generated by plotting the radiocarbon age of wood samples versus the calibrated (dendrochronological) ages back to 12.4 cal ka BP, with earlier samples going back to 26 cal ka BP coming from marine records (corals and foramfinera) with their calendar ages converted to atmospheric equivalents via site-specific marine reservoir corrections and a Northern Hemisphere atmosphere/ocean offset. This curve has been revised and re-published many times, with the most recent version IntCal13 (Northern Hemisphere atmospheric radiocarbon calibration curve 2013) published in 2013 (Reimer et al. 2013). IntCal13 is used for the majority of the thesis, and it is noted where not.

OSL dating measures the length of time that a charge has been trapped within a crystal structure. It is used to determine when quartz, feldspar, and other minerals were last exposed to a light source; it is used primarily in geology but also has applications for dating archaeological materials and, as is the case for the majority of the OSL dates referenced in this thesis, sediments laid over archaeological deposits (e.g., Roberts 1997).

OSL samples are extracted from stratigraphic profiles using opaque tubes; it is crucial that the samples are not exposed to daylight or other bright light sources, because they will reset the radiation clock by emptying the previously trapped charge. Once in the laboratory, the samples are exposed to infrared light in controlled doses. Subsequently, charge is released in the form of visible and ultraviolet light; the trapped charge population is measured in sub-samples called aliquots (Yukihara and McKeever 2011). Because quartz is one of the major sample materials, this means that sediments composed of sand, such as the windblown material of Orkney and northern Scotland, are ideal for dating with this method (e.g., Morocco et al. 2007; Sommerville et al. 2007).

3.6 'Chronometric Hygiene'

'Chronometric hygiene', coined by Spriggs (1989) and Spriggs and Anderson (1993), and based on their work evaluating previously published radiocarbon dates from Island Southeast Asia and East Polynesia, is a set of critera for evaluating the validity and usefulness of published scientific dating material for use in further studies. Spriggs and Anderson (1993) established three criteria for rejecting radiocarbon dates and four criteria for accepting them (1993: 207-208), and found that of 109 dates from Hawaii, they rejected 60, suspected 28, and accepted only 21 (1993: 208). Although the science of radiocarbon dating has advanced greatly since those studies, current research suggests that it is still crucial to evaluate published chronological information using standardised criteria (e.g., Fitzpatrick 2006; Kuzmin 2006; Anderson 2008; Hunt and Lipo 2008; Pollard et al. 2012). For example, Ramsey (2009) suggests that outliers be dealt with on an individual basis if there are a small enough number of data points. These criteria eliminate non-AMS radiocarbon dates on bone, any date without a clear context, and dates on unclear sample material (for example, mixed pollen). They also eliminate dates that may have been affected by the MRE and have not been corrected for it.[8] For other types of chronological information, like OSL and tephrochronology, dates have been evaluated individually for irregularities. In addition to the original criteria, I have added one more, which is that the radiocarbon dates must be published with all the information necessary to re-interpret them in Bayesian models; poor methods of publication remain a major problem for studying radiocarbon dates (as discussed most recently in Wood 2015).

Once chronological information has been evaluated for accuracy on the basis of individual data points, it can be considered in the context of a body of chronological information - however, this is a type of data evaluation that has not often been considered. It is rare, for example, that radiocarbon or OSL dates are considered across regions or even beyond the unit of the archaeological site. There are several reasons for evaluating chronological information in this manner:

1. Excavators often assign phasing information to radiocarbon dates based on stratigraphic context or other diagnostic material. However, statistical analysis of radiocarbon dates from the Anglo-Saxon period in England suggests that,

[8]There are many dates on bone from the published sets used in this thesis, despite the acknowledged problems with the reservoir effect in the North Atlantic (e.g., Ascough et al. 2006). This is discussed more in Chapter 9.

at least for that area/time period, this phasing often does not match up with the calibrated radiocarbon phases. For example, the phase that is listed as being Late Anglo-Saxon by archaeologists is often described as being from ca. 850-1066 CE; however, the radiocarbon dates on material from the Late phase generally calibrate to earlier than that time period, as I discussed in my 2008 MPhil thesis. This can be applied to the Norse colonisation and later settlement in the North Atlantic wherever researchers have provided phasing information for dated materials. This is particularly true where archaeological phasing has relied on diagnostic, architectural, or even literary sources for creating phases – Iceland, for example. Looking at modelled radiocarbon dates can answer whether or not the perceived phases match up to the scientific dates, as well as seeing if phasing is uniform across an area or locally different.

2. Connecting large-scale population movements, like the colonisation of the North Atlantic islands during the Norse period, requires linking archaeological sites chronologically.

3. Determining if there are lag times in cultural responses to known environmental changes like the end of the MWP or the coldest years of the LIA.

4. Placing cultural changes such as the development of farm mounds or the expansion of the fishing industry within a regional chronological framework – asking, were these changes region-wide, or is there a range of variation amongst localities?

3.6.1 Bayesian modelling and OxCal: statistical methods for refining chronological information

Lowe (2008: 319) writes, 'Statistical correlation is an area poised for significant improvement but which ultimately will rely on the development of more comprehensive, stratigraphically constrained regional tephrostratigraphic and geochemical databases of uniformly high quality.' Statistical analysis is only as good as the raw data derived from tephrochronology, radiocarbon dating, and other methods. However, it is the most effective tool for combining different types of chronological information about environmental and archaeological data, both at single locations and across regions (Blockley et al. 2004).

Bayesian statistics are based upon Bayes Theorem, which is a way of thinking about probability. Steier and Rom (2000:183) describe it as allowing 'us to combine measured data from a sample with our knowledge on the corresponding sample before (prior to) the measurement. Both the measured data and the prior information must be formulated mathematically as probability distributions.' Chronological information expressed as probabilities (to 1σ or 2σ) – can be combined with stratigraphy, to place dated samples into a probable chronological series. In order to compute the highest probable accuracy of these stochastic systems, in which there will never be an exact result, many Bayesian models employ a type of algorithm known as the Monte Carlo Markov Chain. These algorithms rely upon the generation of random or pseudo-random numbers to reveal a probability distribution (Gill 2008). Bayesian modelling is most effective with large amount of information; the more dates available for analysis, the more accurate the results will be (Blackwell et al. 2006: 409). All dates in this thesis given as calibrated values are at 2σ.

There are a number of computer programs available to assist archaeologists in running these computations; the one used in this thesis is OxCal 4.2 (Bronk Ramsey 2007-2014). OxCal is a computer program both for calibrating radiocarbon dates in accordance with the latest internationally approved updates to the calibration curve and for providing statistical analysis of calibrated dates (Bronk Ramsey 2001: 355).

Bayesian modelling of chronological information has greatly expanded archaeologists' ability to understand their dated materials, and, in turn to phase their study locations and place them within wider regional contexts. Bayesian results can rule out entire calendar date ranges for some samples, reducing the effect of plateaux in the curve (Blackwell et al. 2006: 412).

3.7 Conclusions

This chapter reviewed the existing literature on tephrochronology, with specific attention paid to areas that are of critical importance to the research undertaken in this thesis.

The first was the importance of depositional factors to interpreting chronostratigraphies, especially in peat and lacustrine sediments. The main point of this discussion is that there are a range of factors affecting deposition of microtephra; these are largely determined by the type of sediment that the microtephra is deposited within,

but there are also site-specific factors (e.g., drainage patterns, standing snow fields) that will determine the ultimate record of microtephra deposition. These factors will affect tephrostratigraphies to varying degrees at each sampling location and must be addressed in tephra studies, particularly for microtephra layers, which are more likely to be mobile in sediment than thick visible layers.

The second topic reviewed in this chapter was the existing published literature that provides researchers with the geochemistry for known tephra layers. This highlighted the problems with the existing dataset and review literature, as well as recent developments.

The third was a review of the current record of distal microtephra found throughout the North Atlantic, with a specific focus on Orkney and northwestern Iceland. This highlighted gaps in the known record, specifically for Late Holocene eruptions in both locations.

4 | Study Locations

This chapter is an in-depth introduction to the archaeological and environmental records at Vatnsfjörður and the Bay of Skaill, the two individual landscape case studies in this dissertation. It also describes the off-site locations chosen for sampling from environmental records.

4.1 Selection of case studies

The positions of Vatnsfjörður, in the Vestfirðir (West Fjords) region of Iceland and the North Bay of Skaill on the Orkney Mainland, Scotland relative to one another are shown in Figure 4.1. Both are coastal settlements in the North Atlantic cultural zone, settled sometime after AD 800, and both have a range of local environmental records that may provide insight into the archaeologies of each settlement. The two case studies have divergent dating strategies, offering the opportunity to compare not only the possible impacts of environmental change on coastal settlements but also different chronological methods for linking archaeological and environmental records. Further, both are ongoing landscape-wide research projects, including excavations of material from the study period, and so this research directly contributes to current projects whilst taking advantage of the ability to participate in field work. In addition to the archaeological excavations, three external peat cores were also sampled: Hobbister and Spretta Meadow, both from Mainland, Orkney, and Kaldalonsjökull, from Vestfirðir, Iceland. These were chosen for their proximity to the archaeological excavations.

In many ways, the two landscapes are very similar. The placement of the buildings in both is along the coast but sheltered from the full force of the ocean – the Bay of Skaill, a deep, curving horseshoe bay protects the East Mound while the fjord Ísafjarðardjúp protects Vatnsfjörður. They are not unique in the context of their

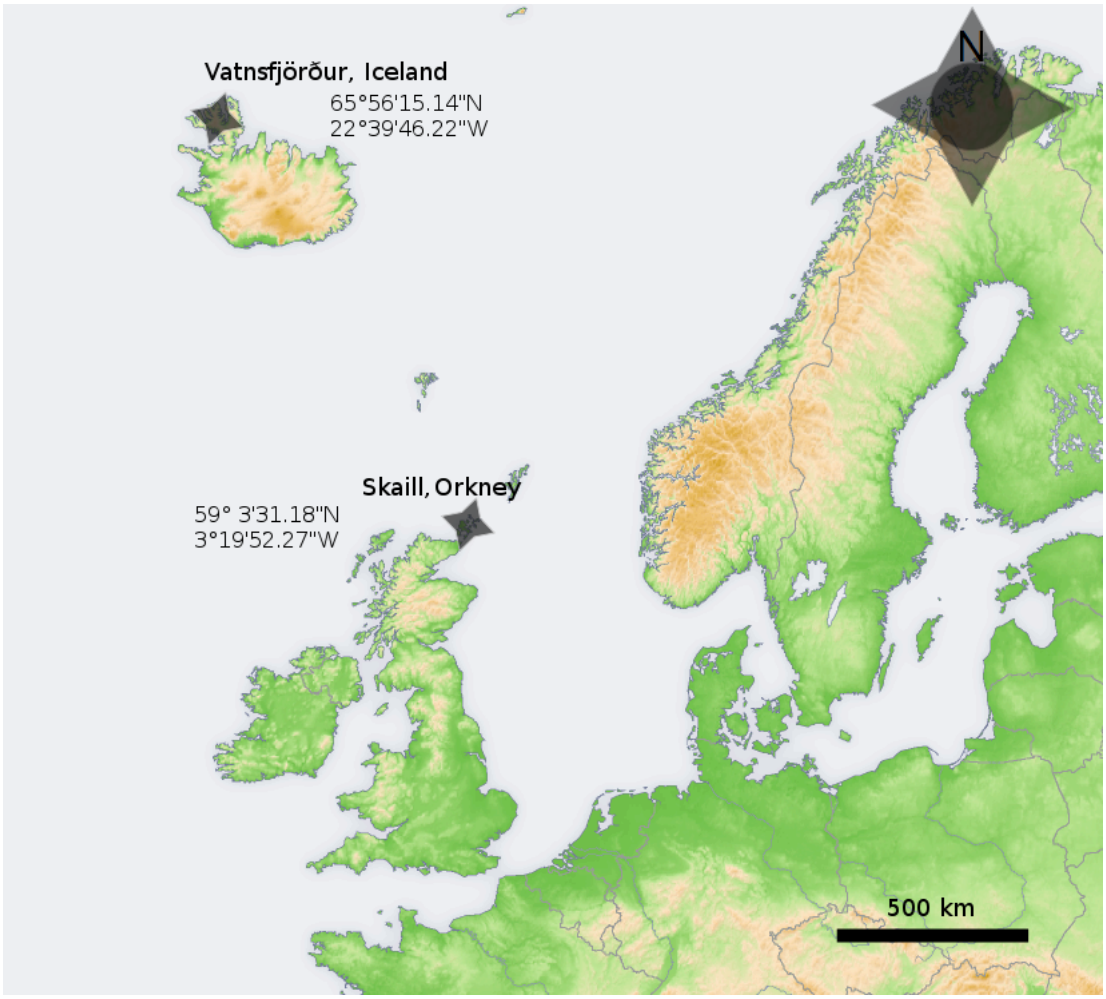


Figure 4.1: The location of the studied landscapes in relation to each other and northern Europe (map source EU Mapinfo base).

region, either: similar coastal settlements are known throughout the islands of the North Atlantic and seem characteristic of Norse settlement patterns (e.g., Bigelow et al. 2005). Architecturally, they share some similarities too: both contain longhouse-style buildings and both have as central features a settlement mound containing multiple layers of construction and occupation. Inhabitants at both places most likely supplemented their diets with marine resources and the presence of thousands of fish bones in both excavations as well as ethnographic analogies from later periods suggest that the people who lived there dealt directly with the acquisition of these resources.

The most striking difference between the two case studies is the longevity of settlement at each location. The farm at Vatnsfjörður was a central place in the landscape from

the settlement period until ca. 1700 and was inhabited until ca. 1900. On the basis of current excavated evidence, the Norse settlers at the East Mound were present only for a short period of time before the mound was abandoned.

Developing a chronology of these landscapes will illuminate how these differences grew more pronounced over time. Many of the similarities described above are related to a relatively brief period in the lives of these settlements: the creation of a shared island culture that developed with Norse immigrants during that period of expansion and colonization in the North Atlantic. What followed after, as these immigrants became inhabitants and then natives, was cultural adaptation to the different conditions – cultural, environmental, economic – in their individual islands. Geographically, although they are both located on the northwest coasts of North Atlantic islands, they are part of very different ecozones and settlers at each would have employed different agricultural and land management strategies. These would have become especially pronounced after the many warm years of the MWP faded away and the harsher climate of the LIA began. For example, at Skaill, environmental studies suggest that the inhabitants of the longhouse would have grown some cereal crops, perhaps flax and barley, throughout the life of the settlement (Alldritt in Griffiths and Harrison 2011); this seems unlikely for the inhabitants of Vatnsfjörður. At the level of individual farms, settlement patterns in Iceland were dispersed amongst individual farmsteads, particularly in the relatively uninhabited Vestfirðir region, whereas in Orkney settlement was denser (Vésteinsson 2000). By the end of the Norse period, Orkney had a capital and a cathedral, something Iceland would not have until the nineteenth century.

By comparing the two landscapes and their inhabitants' adaptation over time, through creating accurate and precise chronologies for them, the goal is to illuminate the importance of local conditions. Ordering events with scientific chronologies becomes the basic tool for imagining how humans in the past negotiated their environments. Vatnsfjörður has the potential to have many tephra and microtephra layers, while the East Mound at the Bay of Skaill has a large body of recent radiocarbon and OSL dates which can be refined using Bayesian modelling to produce a precise chronology there. The comparison of these two methods for their purpose, of facilitating the discussion of how environmental change may have affected these coastal settlements, will lead to a better understanding of how to study the links between archaeological and environmental records in future research.

4.2 Vestfirðir (the West Fjords), Iceland

Vestfirðir, shown in Figure 4.2, is a unique region in Iceland, different geologically, geomorphically, environmentally, and culturally from the rest of the country. The geology of Vestfirðir is layered Tertiary basalt lava flows 4-5 km thick, interspersed with thin interbedded sedimentary layers (Principato et al. 2006: 272). Vestfirðir has not been volcanically active since ca 6-7 Ma, when the last major shift in the North Atlantic Rift occurred; as a result, the oldest rocks in Iceland, approximately 16 Ma, are found in this area (Roberts et al. 2007: 244). Unlike other parts of Iceland, Vestfirðir does not have any active volcanism; the nearest active volcano, as shown in Figure 3.1, is Snæfellsjökull volcano, which is not a part of the Vestfirðir peninsula. Located approximately 150 km from Vatnsfjörður, this volcano was last active in approximately AD 200 (Kjartanson 1967). It is a landscape of glacial erosion, characterised by NW-SE deep fjords, of which there are over thirty. The geomorphology is highly dissected upland plateau, ranging from 500-970 m above sea level, with an icecap at the Drangajökull glacier and permanent snowfields to the west, as shown in Figure 4.2. The deepest fjord is Isafjarðardjúp, which bisects the peninsula. The climate is classified as subpolar maritime and average temperatures in the past century range from 10.1°C in July to -2.1°C in January (Stötter et al. 1999; Lloyd et al. 2009). The fjord itself is often locked with sea-ice. Spring avalanches, such as the one that killed a number of people and destroyed a town in 1995, are a continuing concern in the steep-sided fjords (Decaulne 2004).

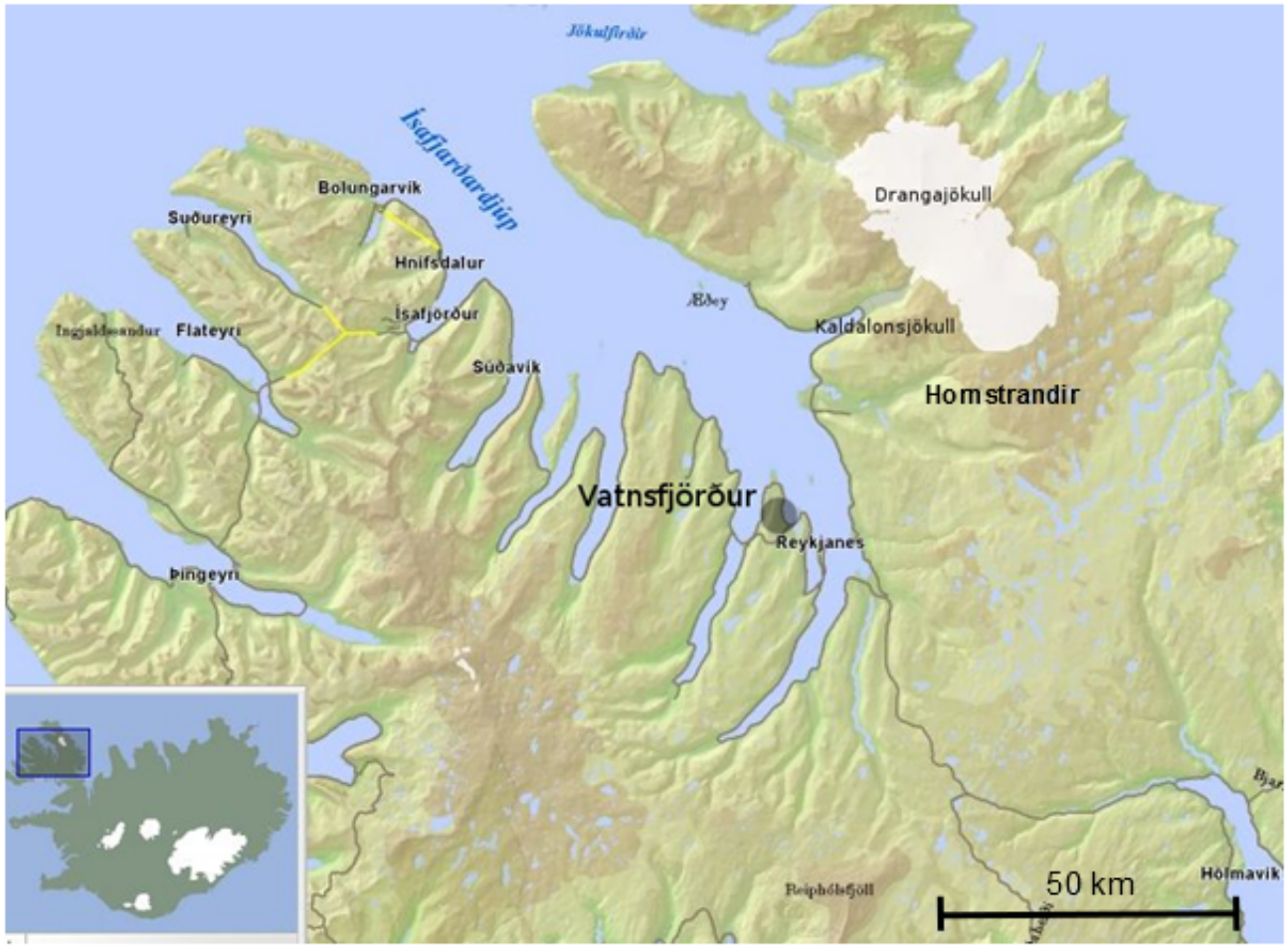


Figure 4.2: Map of modern day Vestfirðir with key locations labelled (Base map source is Korta 2011).

The Vestfirðir region's proximity to the Greenland ice sheet, coupled with its location within colder currents than the rest of Iceland, give it a more Arctic climate than the more inhabited southern and eastern parts of the country. Vestfirðir is affected by the same weather systems as northeast Greenland and the Greenland Sea, and so the effects of the LIA for this region were most likely similar to those recorded in the Greenland ice cores, rather than those in the rest of Iceland (Hjort et al. 1985: 26). The currents affecting northwest Iceland are the warm Irminger Current and the cold East Iceland Current, which spins off the polar East Greenland current; when the colder currents are stronger, heavy sea ice and icebergs develop in the region and glaciers advance (Malmberg 1985; Hopkins 1991; Principato 2008: 134). The Hornstrandir and Drangajökull ice caps in Vestfirðir are particular areas of interest to researchers reconstructing past climate because, unlike Iceland's larger and more southerly glaciers, they have not been affected by Holocene volcanic activity. Furthermore, Drangajökull is one of Iceland's smaller glaciers, and smaller glaciers are more sensitive to climate change than larger ones (Patterson 1994). During the LIA, glaciers covered an extensive part of the region; at the height of the LIA, the glaciated areas of the Hornstrandir peninsula, in the north of Vestfirðir, for example, covered 8-10 km^2, in contrast to the 1980s, when they covered an area of 1.5 km^2 (Hjort et al. 1985: 25). Lichenometric studies from the Hornstrandir glaciers indicate that the maximum extent of the glaciers occurred around 1860, with a rapid decline over the next sixty years (Hjort et al. 1985: 25). For Drangajökull, the figures are similar, further demonstrating the sensitivity of this environment (Principato 2008: 134). Glacier fluctuations in the area have also had an impact on its archaeology and history; Grove (2004) writes that, in eastern Vestfirðir, either over-riding ice or flooding associated with glacial advance led to farm abandonment during the LIA.

Another climatic factor in the region with archaeological significance is temperature variability, which has a major impact on vegetation growth and therefore agricultural yields. The effects of temperature variance are heightened in sub-polar environments. One study of twentieth century agriculture found that, comparing the 0.8 – 1.8°C lower average temperature from 1873-1922 against the 'normal' temperature in 1931-1960, there was up to 30% lower production from sheep rearing and 20% from cattle (Bergþórsson 1985). A similar study found that, for every 1°C increase in yearly average temperature, hay yields increase by 15-25% (Landnýting á Íslandi 1986; Sveinbjarnardóttir 1992: 15). Sveinbjarnardóttir (1992: 15) writes, 'It is inevitable that many small farms would have found it hard to survive downward changes in temperature of this magnitude.' McGovern et al. (1988) conclude that a -1.5°C

change in temperature would negatively affect both pasturage and barley growing in Iceland. Although there is little direct archaeological evidence from Vestfirðir, these figures demonstrate that the transition from the agriculturally favourable climate of the MWP to the colder and more variable LIA would have had a significant impact on the economic and social fortunes of Vestfirðir.

Perhaps the key to survival during the LIA was that the people of Vestfirðir were able to focus on marine resources. The peninsula is mountainous and has very little arable or pasturable land except along the coast, and as a result, early settlements were positioned from the perspective of the sea. For example, at Bolungarvík, on the northwest coast of Isafjárðardúp, the earliest settlements were longhouses built in good anchorage spots, rather than at places reachable by travel overland (Edvardsson and McGovern 2005). With the resource base of the region always looking towards the sea, the main resources in Vestfirðir were fish, things that drifted to shore (whales, wood), and oil (cod and shark liver). Edvardsson and McGovern (2005) argue that, for people in the region, farming was a method of subsistence, but wealth came from the sea. Tenant farmers paid their rent to landowners with dried fish or other marine items (*ibid.*).

Vestfirðir has received little archaeological attention compared to southern and eastern Iceland. It is sparsely populated part of the country and a trend of depopulation that began after World War II has continued into the twenty-first century. Most archaeological research there has been has focused on marine resources (e.g., Edvardsson 2004). The major exception to this has been the excavation and landscape surveys at Vatnsfjörður.

4.2.1 The Vatnsfjörður archaeological landscape

Vatnsfjörður was settled soon after *landnám* and became, for a period, a high status farm despite apparent agricultural infertility. From the thirteenth to the seventeenth century, it was one of the central places in Vestfirðir and Milek (2009) argues that the changes it underwent from the period of settlement until its decline, with the abandonment of the last farm house in 1906, may be seen as a microcosm of settlement shifts in Vestfirðir itself. A plan view of the farm and associated area is shown in Figure 4.4, and a satellite view of the area is shown in Figure 4.3. As a powerful farm, Vatnsfjörður collected rents from smaller farms it owned in the region and pooled locally-derived marine resources for export out of Vestfirðir (Edvardsson and

McGovern 2005; Tulinius 2005). First mentioned in written sources in the twelfth century, it was most likely the main farm in the region and the core of the original Norse settlement in Vestfirðir (Edvardsson and McGovern 2005), and may have functioned similarly to a manor in the medieval European sense described for Iceland by Juliusson (2010). It is mentioned as the home of Þorvaldur Snorrason (ca. 1160-1228), who was the chieftain of the Isafjörður area in *Hrafns saga Sveinbjarnarsonar*. In the centuries following, evidence for the farm comes from legal documents describing the fight over property rights between the owners and the church (Tulinius 2005: 13). Tulinius argues that there was an aristocracy in Vestfirðir until the seventeenth century, meaning that the area was a place with resources that could create wealth. From the fourteenth century onward, as fishing became more and more important to the Icelandic economy (both in terms of exports to Europe with newly formed fishing guilds and internal trade), the fertile fishing grounds of the Vestfirðir region enriched many people (*ibid.*).

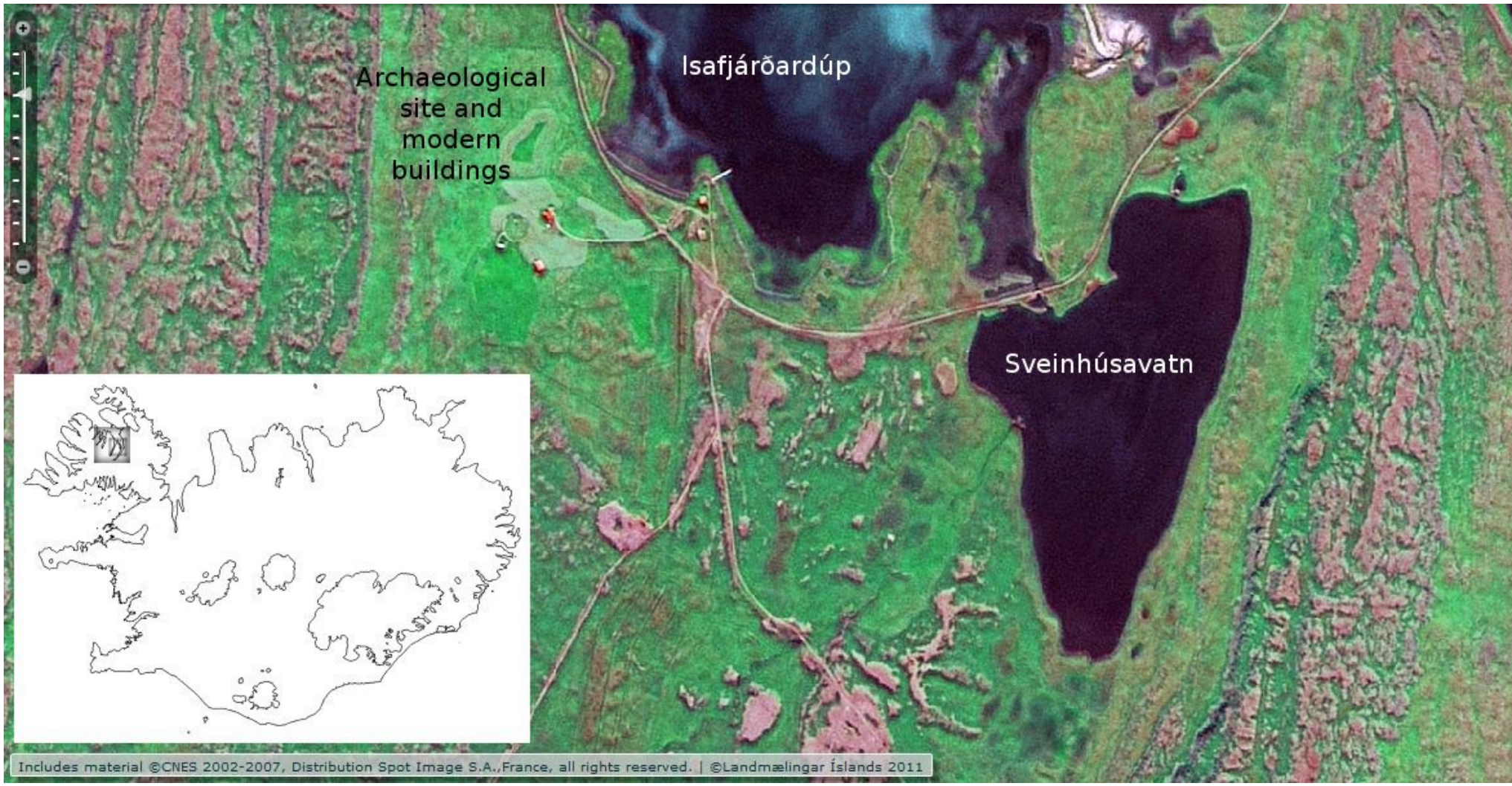


Figure 4.3: This satellite image shows the landscape around Vatnsfjörður (Landmælingar Íslands).

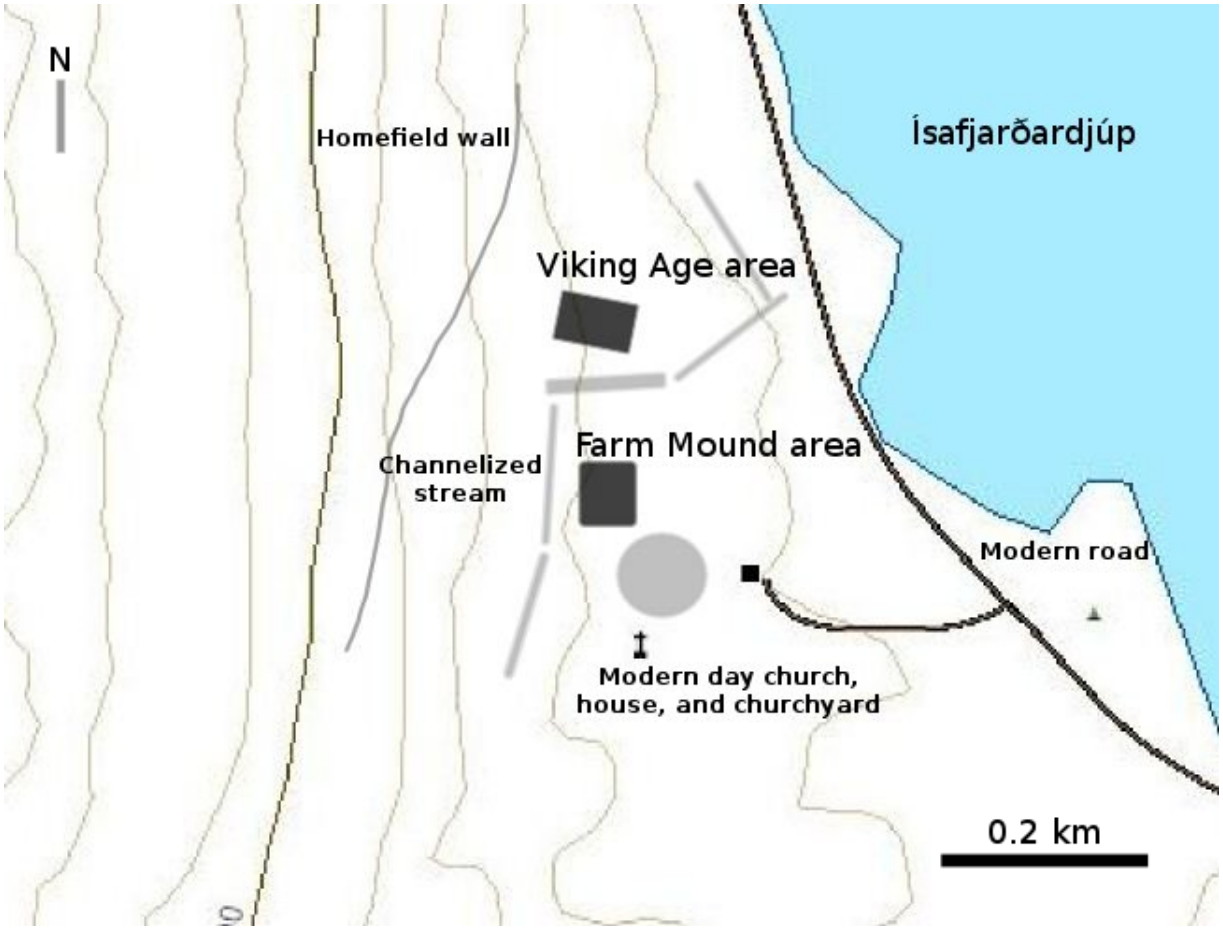


Figure 4.4: The layout of the Vatnsfjörður excavations in relation to the fjord (Landmælingar Íslands).

A likely sign of this new prosperity was the expansion of the farm. In addition to the main farm buildings, there was also a church built at Vatnsfjörður, probably in the twelfth century. This was a rich and important church until the Reformation in the mid-sixteenth century; it remained a parish church until the second half of the 20th century (Edvardsson and McGovern 2005). In the beginning of the 16th century, power in the region shifted away from Vatnsfjörður to Ögur, a few fjords away, but Vatnsfjörður remained an important and wealthy farm, and continued to hold land in other parts of Vestfirðir.

Annual archaeological excavations at Vatnsfjörður began in 2003 and have continued through 2014 as a joint project between the North Atlantic Biocultural Organisation (NABO) and *Fornleifastofnun Íslands* (FSÍ), an Icelandic archaeological unit. There are two main areas of excavation: a Viking Age area consisting of a number of grouped remains, and the farm mound, in use until the early twentieth century. Thus far, Vatnsfjörður is the only Viking age farmhouse to have been excavated in Vestfirðir (Vésteinsson 2004). The landscape at Vatnsfjörður is shown in Figure 4.5. The Viking Age portion of the excavation is close to the fjord, while the farm mound is on higher terrain and set further back from the edge of the water. The farm mound is in close proximity to a cemetery and church that are still in occasional use today (as shown in Figure 4.5), but neither the age of the cemetery nor the church are known and their relationships to the farm mound and the Viking Age farmstead are also unknown.

The Viking Age portion of Vatnsfjörður is shown in Figure 4.4. This area contains a bow-sided Viking home (*skáli*) and several potentially associated outbuildings. The Vatnsfjörður *skáli* is typical in size (approximately 15 m x 5 m) and layout of the majority of Viking homes found in Iceland, with a hearth in the centre of the building and two entrances in the long eastern wall (Edvardsson and McGovern 2005). During the excavation of the *skáli*, which was completed in 2005, several artefacts that date typologically to the tenth century were uncovered. These included five glass beads and a gold pendant that was originally mounted in an Irish brooch (Friðriksson in Milek et al. 2007). Since 2005, other areas around the *skáli* have been excavated, including a cooking area, a smithy, and some other outbuildings with unknown functions, which cover an area roughly 40 m x 40 m. Due to proximity to the *skáli*, it has been assumed that these buildings are all contemporaneous, but the chronology of the area was unclear (Milek et al. 2010). Excavation at the Viking Age area finished in 2010. This is discussed further in Chapter 7.

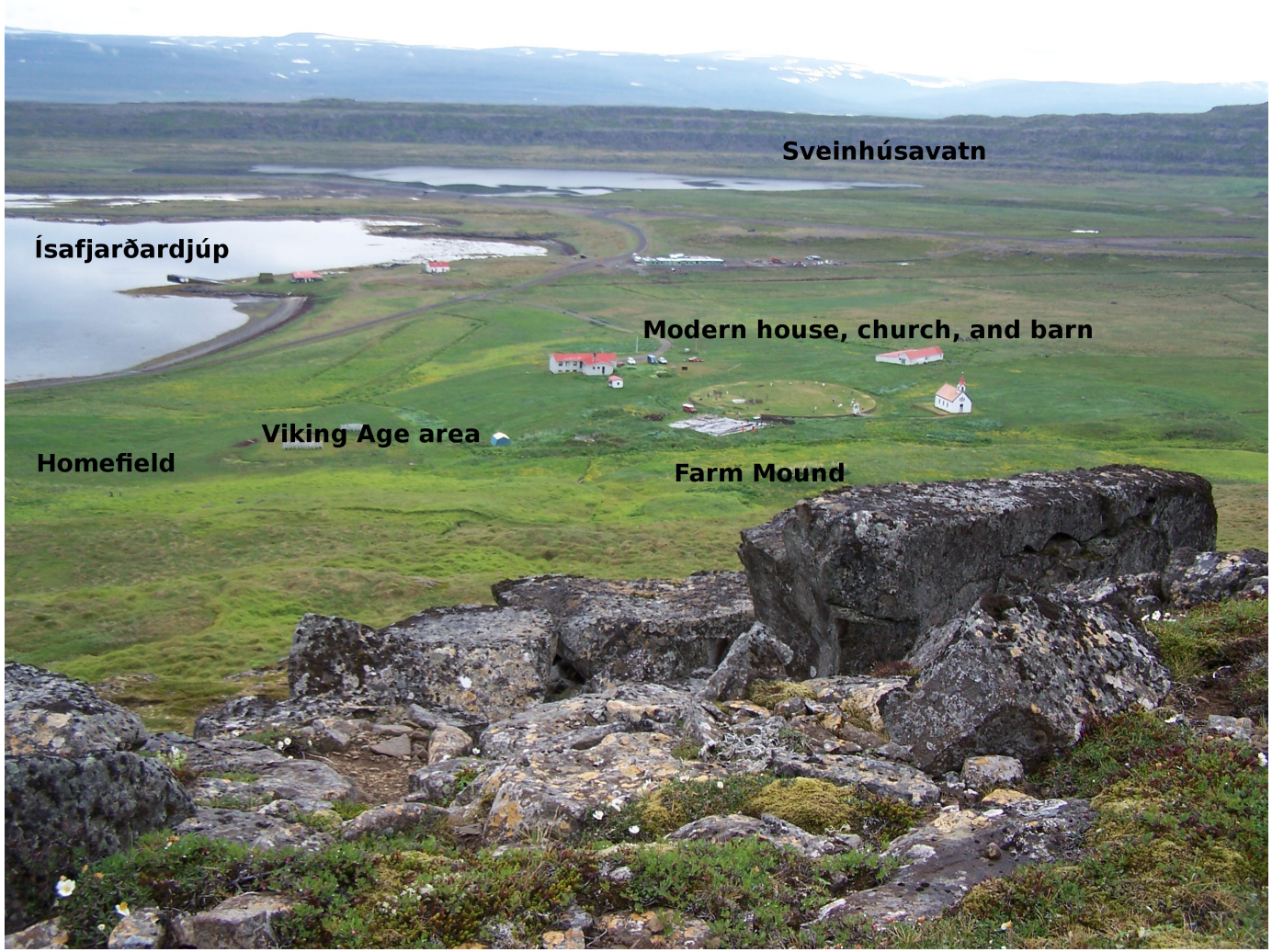


Figure 4.5: Photograph taken by the author looking to the east, showing key locations in the landscape around the Vatnsfjörður site.



Figure 4.6: The above pictures, taken by the author in 2009, show the Glaumbær turf house, in Skagafjörður, northern Iceland. The bottom image shows the interior of the turf walls. Glaumbær represents one type of turf house architecture that became popular in the 18th century, *burstabær*, which refers to the wooden facades at either end of the house. The Vatnsfjörður turf house on the farm mound was probably not of this style, but the general turf construction would have been very similar.

The farm mound is an artificial hill that developed over time as a result of turf building and associated refuse piles.[1] Currently, the excavated area measures approximately 40 m x 40 m (Isaksen in Milek et al. 2011). Turf houses, like the one shown in Figure 4.6, were the most common type of farm house built in Iceland from the late medieval period until c. 1910 (Forbes et al. 2010; Karlsson 2000a). The last turf dwelling at Vatnsfjörður dates from 1884-1906; Milek et al. (2009: 17) speculate that the development of the mound itself may have begun as early as the late ninth or tenth century, but this is not currently supported by any chronological data (Milek et al. 2009: 17). The quality of life in turf houses seems to have varied, but in general, they were dark and close spaces. They often included separate rooms for a variety of different functions, including pantries, storage areas, areas for processing different types of food (for example, the turf house at Glaumbær in northwest Iceland has a room devoted to the production of dairy products), and byres. The living areas of the turf houses were restricted to a small area because of the constraints of the climate: Karlsson (2000: 192) writes that, 'In the late Middle Ages people seem to have begun using the bathrooms for sleeping in, probably because they were the only rooms at the farms that could be heated.' He goes on to note that the word for 'bathroom', *baðstofa*, came to mean the word for living area in a turf house sometime in this period. As a result, people lived in close quarters, and, as Forbes et al. (2010) note in their study of archaeoentomology within the Vatnsfjörður farm mound, sanitation conditions were poor by today's standards. However, the farm was no worse off than any other farm known from Iceland in the early modern period, and, later, there are signs that the farm was better off than many others. For example, a number of high status artefacts have been found in nineteenth and twentieth century deposits, including wine bottles, porcelain, and tobacco-related paraphernalia (Lucas in Milek 2009). In 1906, the farm mound was succeeded by a large timber house, utilizing building methods that would not become common in Iceland until the 1920s (Forbes et al. 2010: 105). Excavation on the farm mound began in 2006 and has continued through 2014 (Milek et al. 2010).

Although saga and documentary sources give us more information on the political aspects of life at Vatnsfjörður than we know about the East Mound, Vatnsfjörður has very few archaeological dates. The *skáli* has been dated by a single AMS radiocarbon date on a cow bone that has been calibrated to the tenth century AD (Milek 2007). Further chronological data comes from the layout and size of the longhouse, which is

[1] 'Viking Age area' and 'farm mound' are the common terms used by the excavators for these two areas of excavation at Vatnsfjörður and will be referred to as such throughout.

very similar to one excavated in Aðalstræti, Reykjavik, that dates to the late ninth century. This suggests that the longhouse is from the settlement period in Iceland (Edvardsson and McGovern 2005).

However, more chronological data are obviously desirable, and as a result in 2009, 2010, and 2011, several previously unstudied visible stratigraphic layers that seemed likely to be tephra were sampled for geochemical analysis by myself. These were located in both the Viking Age area and the Farm Mound area. Prior to my research, a single visible tephra layer near to the Farm Mound had been correlated tentatively to Hekla, but not a specific eruption, by Sigurgeirsson (2006). Sampling procedures for tephra layers from the archaeological excavation are described in Section 6.1.1.3.

4.2.2 Sveinhúsavatn (Svein's House Lake)

To the east of Vatnsfjörður is a body of water called Sveinhúsavatn, named for its proximity to a now-abandoned homestead called Sveinhús. The lake's location is shown in Figure 4.3 and its position in the landscape is in Figure 4.5. Today it is a coastal freshwater lake with a stream exit to the sea over bedrock. The altitude of the lake is very close to the current height of high tide, but it has been determined that the lake rarely receives seawater input today (Lloyd et al. in Milek 2011). In the past, when sea-level was higher, the lake would have been flooded more often; if the sea level was only a few metres above present, the lake would be a marine embayment. This type of water body is known as an 'isolation basin', i.e. a coastal basin whose relationship with the sea – and saltwater – differs depending on sea level over time (Lloyd et al. 2009). Isolation basins are discussed further in Chapter 7.

The geomorphological and environmental history of the past two thousand years in Vestfirðir has not been well studied, and most studies end at the last major deglaciation of the region (e.g., Hjort et al. 1985; Jóhannsdóttir 2003; Roberts et al. 2007; Principato 2008; Lloyd et al. 2009). Therefore, the extent to which the MWP and LIA affected sea-level in the region – if at all – is largely unknown. The closest study comes from Gehrels et al.'s (2006) research into rapid sea-level rise in the North Atlantic around northwestern Iceland from the nineteenth century onwards. This study comes from the salt marshes at Viðarhólmi in Snæfellsnes, western Iceland, which is the peninsula directly south of Vestfirðir. They find that sea level in the Snæfells peninsula rose from AD 100-500, fell from then until the first half of the nineteenth

century, and then rapidly rose until the present. They attribute this to isostatic rebound and changes in sea temperature. However, Vestfirðir, with its sheltered fjord coastline, is very different from the jutting volcanic peninsula of Snæfellsnes. Sea-level rise throughout the country is highly localised because of its recent glaciations and in some areas potential landform deformation due to volcanism. Gehrels et al.'s (2006) conclusions therefore can only be taken as a possibility for the record of sea-level change in Vestfirðir.

Archaeologically, sea-level rise and its effect on Sveinhúsavatn is a major research question for the Vatnsfjörður site. If the sea-level has changed dramatically – similar to what Gehrels et al. (2006) document for the Snæfellsnes peninsula – then inundation of low-lying areas may have led to abandonment or movement around the landscape. This may explain why the focus of settlement, like many other settlement-era farms around Iceland, shifted upslope at some point in its history. The work presented in this thesis provides a detailed tephrostratigraphy for the lake which, combined with work on foraminifera in the lacustrine core done by Dr Jerry Lloyd and graduate students at Durham University, will reconstruct the depositional and environmental history of the lake in order to determine the extent of sea-level change and if or when the lake was part of the fjord.

From a tephrochronological point of view, lacustrine records also provide value in refining the technique as well as illuminating landscape history. Thompson and Bradshaw (1986) write, 'The stratigraphic variations within an ash layer preserved in a lake sediment record the effects of several sedimentation processes including catchment erosion, ash transport by water and wind, fluctuations in deposition patterns, bioturbation and mixings...' Tephrostratigraphies uncovered from Sveinhúsavatn's sediments may reveal the influence of melting snowbeds on deposition within the lake, as well as demonstrating periods when snowbeds did not melt for several years or even decades (e.g., Davies et al.'s 2007 study of microtephra deposition in two lakes in west central Sweden, described in Section 3.2.3). Further, samples from a lacustrine sequence near to an archaeological excavation may allow the precise dating of environmental and anthropogenic events affecting the lake itself, such as damming, draining, or other uses for irrigation that affected the lake in the past. Sampling procedures for this lacustrine core are described in Section 5.1.

4.2.3 Vatnsfjörður Homefield

The 'homefield' or 'infield' is the land that surrounded the domestic settlement, and is considered to have been one of the most important parts of Viking, medieval, and post-medieval settlement (Simpson 1997; Adderley et al. 2000; Simpson et al. 2002; Adderley and Simpson 2005). Homefields generally had an area for livestock grazing and then plots for fodder (usually hay) and cereal production, although the variety of crops changed based upon the constraints of latitude and climate. A homefield had to be carefully managed. For example, livestock spent significant portions of the year indoors in Iceland and Greenland, and to a lesser extent in the Faroe Islands, Shetland, and Orkney, so foddering needs for a fluctuating number of livestock as well as the domestic agricultural needs of the settlers had to be taken into account (Adderley and Simpson 2005). As topography and climate limited the arable land available, many of these homefields were used from the period of Norse settlement until farming in an area ceased (*ibid.*).

At Vatnsfjörður, the homefield is a low-lying meadow to the immediate north-east of the archaeological excavations, and is shown in Figure 4.4 and Figure 4.5. This particular homefield had been a mystery for researchers: despite study over several field seasons, there had been no evidence found for any management of or improvements to the area that would have been crucial to the success of the large farm at Vatnsfjörður (Barclay et al. in Milek 2011). Even during the MWP, northwestern Iceland was at the limits of viable agriculture, implying that careful management of the Vatnsfjörður homefield would have been necessary. An auger survey from 2008 revealed that the main body of homefield soils were relatively shallow, and underlain by beach sands and gravels; this led to leaching, podzolic development and concurrent nutrient deficiency in the soils of the homefield (Barclay et al. in Milek 2011; E. Tisdall pers. comm.). As a result, the homefield had poor agricultural potential, which made the success of Vatnsfjörður – a large, wealthy farm in a society where cattle husbandry was the key to high-status – even more confusing. After the 2009 season, understanding the homefield became a key research goal.

The homefield also contained a peat accumulation approximately 45 cm deep, which may have been the source of the turf walls of the houses and outbuildings as well as for fuel. This peat accumulation created a surface wet meadow which persists to this day. It is composed of peat overlying basal beach gravels, separated by a layer of charcoal that has been radiocarbon dated and calibrated to the tenth century AD.

The radiocarbon dates from the homefield are in Table 4.1. The formation of peat in this location seems unlikely given the underlying gravelly substrate, which should have created well drained conditions. Therefore it is unclear if the peat deposit is entirely anthropogenic, is a natural formation, or is the result of settlers cultivating what was originally a natural formation. One theory is that early Norse settlers created the meadow by burning an area covered in birch and leaving the charcoal to decay in order to reduce drainage and create a damp area. Naturally occurring peat within the area may have been kept wet by damming the nearby stream or irrigating the area in a different manner. Evidence for it being natural comes from the beach gravels immediately to the north of the homefield. These form a beach ridge very similar to other deposits along the coast that also have peat accumulation behind a beach ridge, and that have no evidence to indicate archaeological interference. A third hypothesis is that at Vatnsfjörður, settlers may have come upon the natural accumulation of peat from this beach ridge and enhanced it to make the wet area larger and maintain the meadow. The beach ridge at Vatnsfjörður is not as large as others down the coast, so the area may have needed to be altered by the settlers in order to form such a large area of peat (E Tisdall, pers. comm.).

Establishing a tephrostratigraphy of the homefield peat, which is one of the goals of the current research and is described in Section 6.2.1.1, will provide answers to archaeological questions as well as contributing to the science of tephrochronology. The homefield played a crucial role for the people who inhabited Vatnsfjörður by providing them with necessary resources. At present, only two reliable radiocarbon date comes from the homefield core, which are shown in Table 4.1. They were funded by NERC (Natural Environment Research Council) and done at the SUERC (Scottish Universities Environmental Research Centre) facility in East Kilbride. The research presented here, in conjunction with pollen data from Dr Eileen Tisdall and Rebecca Barclay at the University of Stirling, aims to establish a chronology of the homefield's use. This will be done with new tephrochronological research in conjunction with the radiocarbon dates presented in Table 4.1 to provide a clearer picture of how landscape use at the homefield changed over time. This research will also aim to answer how the peat was formed. There may have been a ditch dug down the hillside to the west of the homefield that brought water from the hill into the homefield; there is evidence for irrigation ditches at other Norse settlements, notably at Garðar, Greenland (Adderley and Simpson 2006), and a visual survey of the area to the west of the homefield showed possible evidence for a ditch. If the area was being irrigated, then it seems likely that microtephra could have moved within the soil, and that

a tephrochronology of the meadow would not contain discrete layers, but a strong background signal and mixing of tephras. If there are discrete layers of tephra, then it may indicate that the area was not irrigated. Further, if tephra begins mixing at a certain point in the tephrostratigraphy of the homefield, that might indicate when intentional irrigation began. Finding evidence that the people at Vatnsfjörður played a role in cultivating the peat of the wet meadow may shed light upon how the farm generated its agricultural wealth, while establishing a chronology for the wet meadow will illuminate the changing fortunes of the farm over time as it related to this crucial area for its agricultural resources.

Table 4.1: Radiocarbon dates associated with the Homefield (Milek 2007; Parkin et al. in Milek 2008; and Milek, pers. comm., April 2011). All dates are from SUERC.

Lab Code	Material	Site	^{14}C Age	Error ±	- δ ^{13}C	Calibrated
SUERC-8386	Charcoal – *Betula*	Wet Meadow (homefield)	1090	35	26.7	888-1018 cal AD
SUERC-8391	Charcoal – *Pinus sylvestris*	Wet Meadow (homefield)	1050	35	24.5	896-1031 cal AD

4.2.4 Kaldalonsjökull

Due to the uncertainty about whether or not the homefield peat had been anthropogenically altered to the point of not providing a useful tephrochronology, another nearby peat field was sought. The goal of examining this additional peat core was to create a tephrostratigraphy as close to baseline environmental conditions as possible. This peat field had to satisfy three conditions. First, it had to be located relatively close to Vatnsfjörður, so that the tephrostratigraphy would be roughly representative of the area as a whole. Second, it had to be separate from any known archaeological remains to prevent anthropogenic interference in the tephra taphonomy. Third, the core from the peat field needed to have minimal to no cutting by stream beds or other water sources to prevent movement of microtephra within the sediment column.

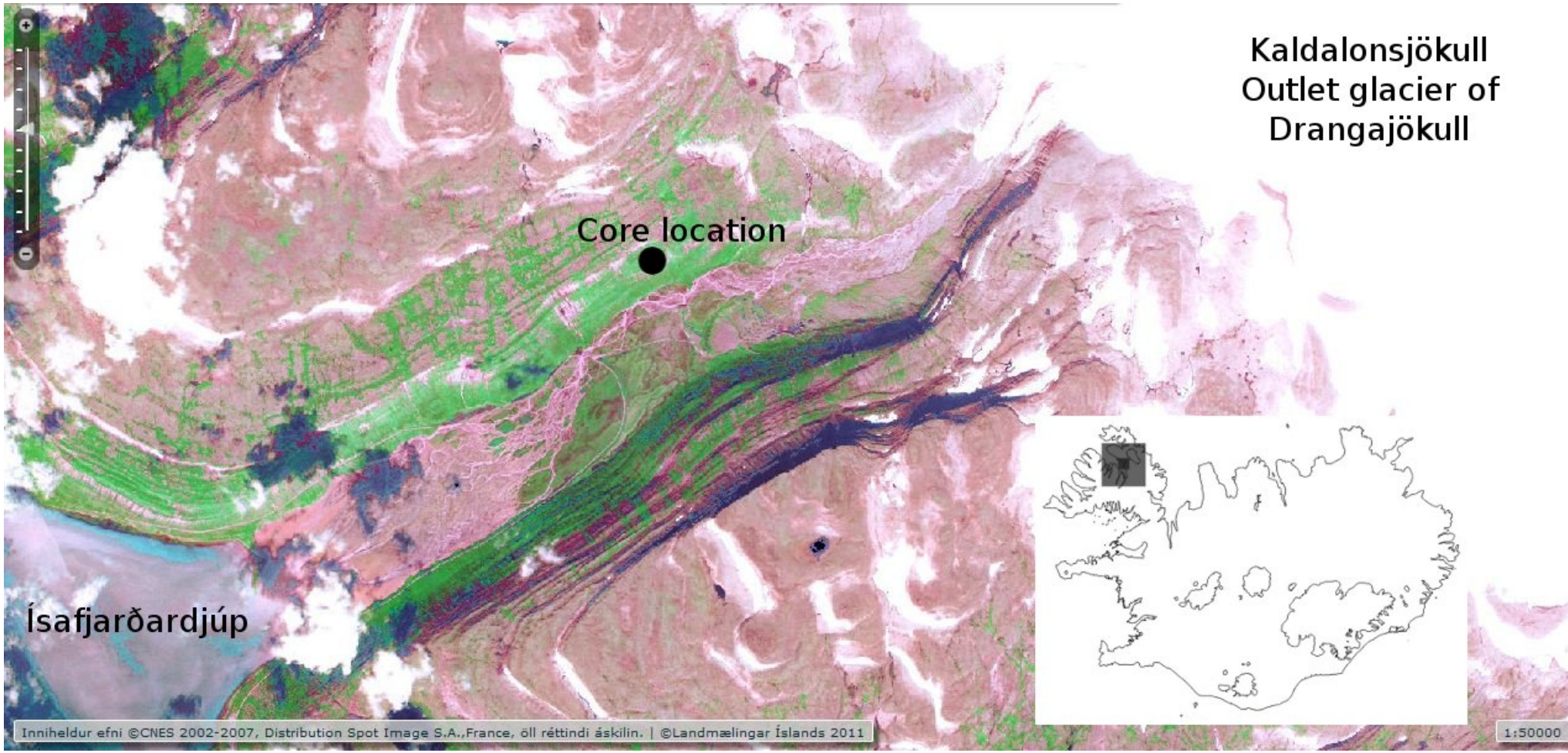


Figure 4.7: This satellite image shows the Kaldalonsjökull outlet glacier (part of the larger glacier, Drangajökull) and the core location on a hillside above the glacial outlet (*Landmælingar Íslands*) The distance of the core location is approximately 15 km from Vatnsfjörður (Sarah Principato, pers. comm., 12 October, 2010).

The resultant core is from near to Kaldalonsjökull, with GPS coordinates of 66.10494, -22.35192. Figure 4.7 shows this location. In Iceland it is common to name outlet glaciers separately from main glacial ice caps due to their fluctuating state; Kaldalonsjökull, therefore, is an outlet glacier from the southwest of the main Drangajökull ice cap, located to the east of Isafjarðardjúp. Kaldalonsjökull is across the fjord from Vatnsfjörður, less than 20km to the north-northeast. In the late Quaternary, the area was covered in ice; the most recent glacial incursion into the valley below where the sample came from was during the LIA, in the mid-1800s (Principato 2008; Principato pers. comm. April 2010). There are three radiocarbon dates from the peat section, indicating a basal depth of approximately 2500BP. These are shown in Table 4.2. They were funded by the US National Science Foundation and done at Beta Analytic, a commercial radiocarbon company in Miami, Florida, USA, because the principal investigator for this research, Dr Sarah Principato, is based at Gettysburg College, Pennsylvania.

Table 4.2: Radiocarbon dates from the Kaldalonsjökull core (Sarah Principato, pers. comm., 17 August, 2011). All dates are from Beta Analytic, Miami, Florida.

Lab Code	Depth	^{14}C Age	Error ±	-δ^{13}C	Material	Site	Calibrated
282599	310 cm	2470	40	26.1	moss	Kaldalonsjökull	768-430 cal BC
282600	310 cm	2503	59	25.9	sedge	Kaldalonsjökull	796-430 cal BC
282603	310 cm	2623	68	26.2	sedge	Kaldalonsjökull	930-541 cal BC

Environmental information from this core comes from Dr Principato and several of her undergraduate students.

4.3 Mainland, Orkney, Scotland

Mainland is the largest and most populated island in Orkney. Figure 4.8 shows its location. Orkney is an archipelago of low-lying islands (with the exception of the higher topography of Hoy) composed of Old Red Sandstone. Landscape features like shoreline cliffs and arches, sea-stacks, caves, and shore platforms all reflect the erosion patterns of the horizontally bedded sandstone (Hansom 2007). The geology of the two Orcadian areas studied here are shown in Figure 4.9. Orkney is a glaciated landscape and, although its geomorphology has not been extensively studied, it is thought that the islands were under an ice sheet for most of the Devensian period; as a result, isostatic rebound has played and continues to play a role in their geomorphology (Sutherland and Gordon 1993: 73). Following the last glacial period, Orkney's climate became temperate and maritime due to the warming influence of the North Atlantic current. This created relatively favourable conditions for human settlement. The larger islands of Orkney have been inhabited since the Mesolithic (Wickham-Jones 2006) and, during the period discussed here, were settled by the Norse, who integrated with the existing population (peacefully or not), and in the medieval period were part of the Norwegian and later Scottish kingdoms (e.g., Barrett et al. 2000). The case study in this thesis from Orkney focuses on the Viking, medieval, and post-medieval archaeological landscape of the East Mound in the north Bay of Skaill and two peat bogs in the south of Mainland.

4.3.1 The Birsay-Skaill Landscape Project

Like many archaeological landscapes in the Northern Isles, the Bay of Skaill is threatened by coastal erosion, and so was targeted by Historic Scotland as an urgent area for research (Griffiths et al. 2009).The Bay, shown in Figure 4.10, is a semi-circular and exposed directly to the western North Atlantic. Like the Bay of Birsay to its north, the land around the Bay of Skaill is a low-lying landscape with farmland and aeolian deposits of sand, the latter formed in part by the erosion of the underlying sandstone and from the redeposition of marine silts and sands in a high-energy coastal environment (Griffiths et al. 2009). It is a high-energy coastal environment,

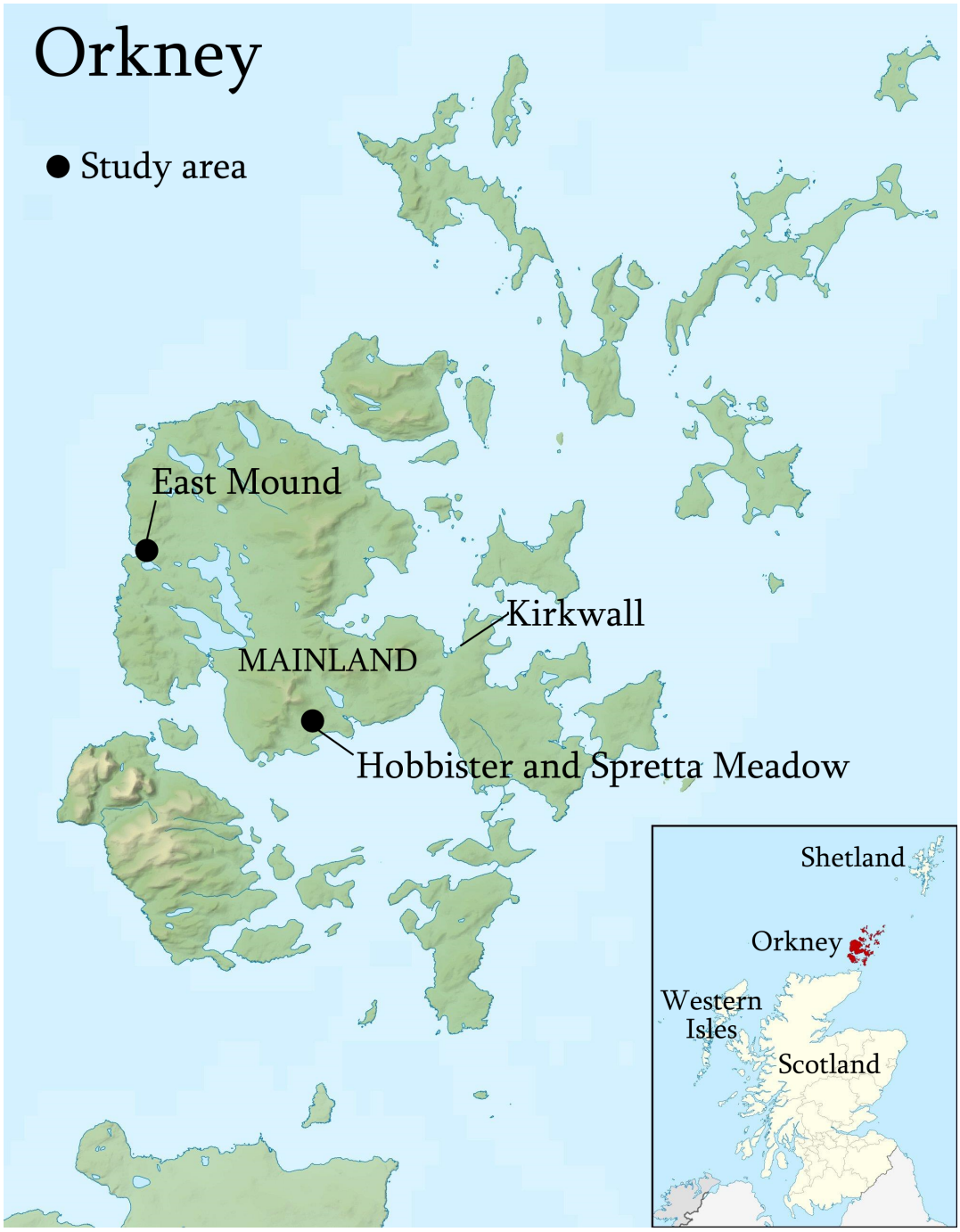


Figure 4.8: The location of the Bay of Skaill, Hobbister, and Spretta Meadow in Orkney (map base from Wikimedia 2015).

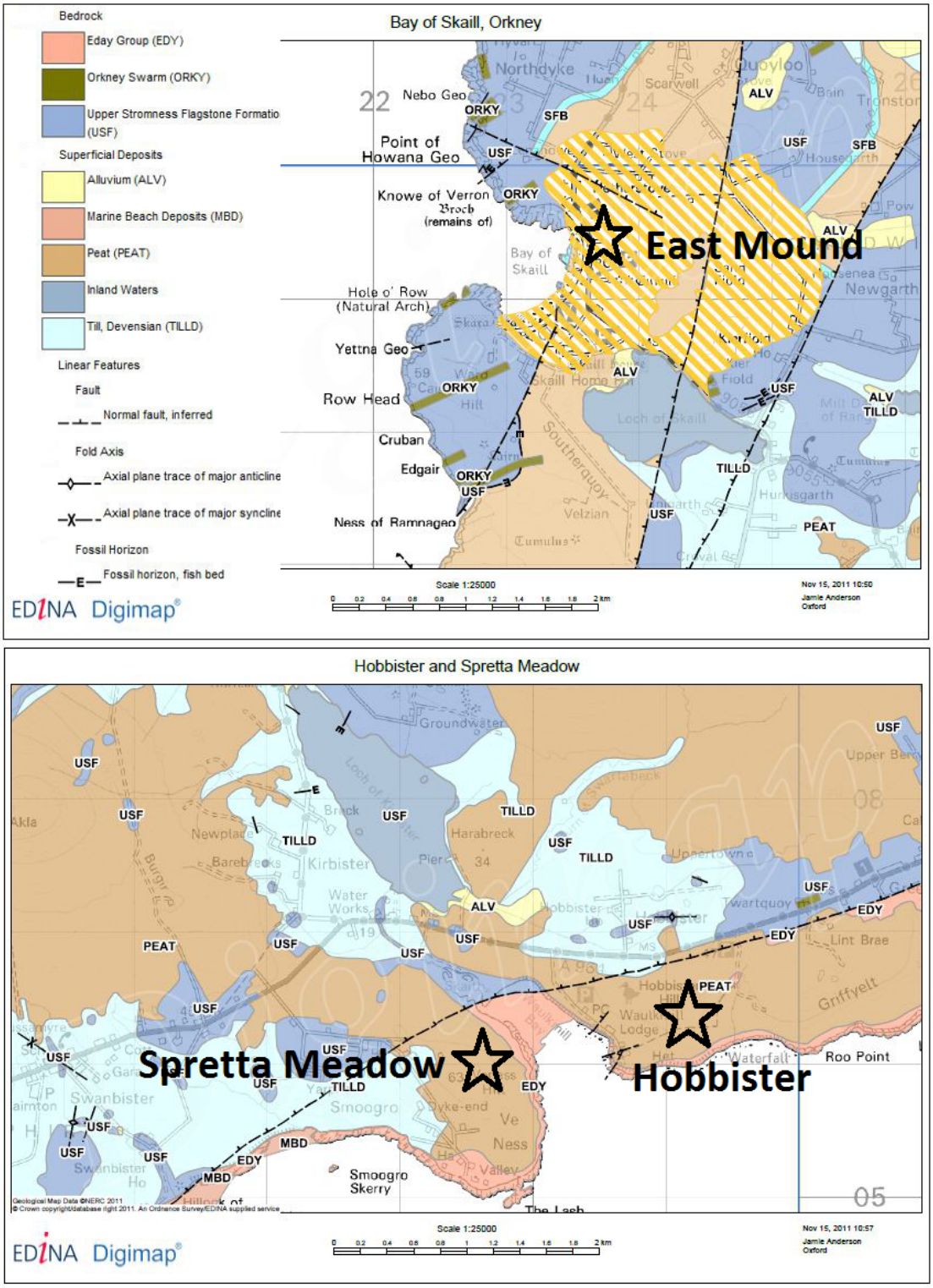


Figure 4.9: Geology surrounding the two studied areas (map from Digimap 2010).

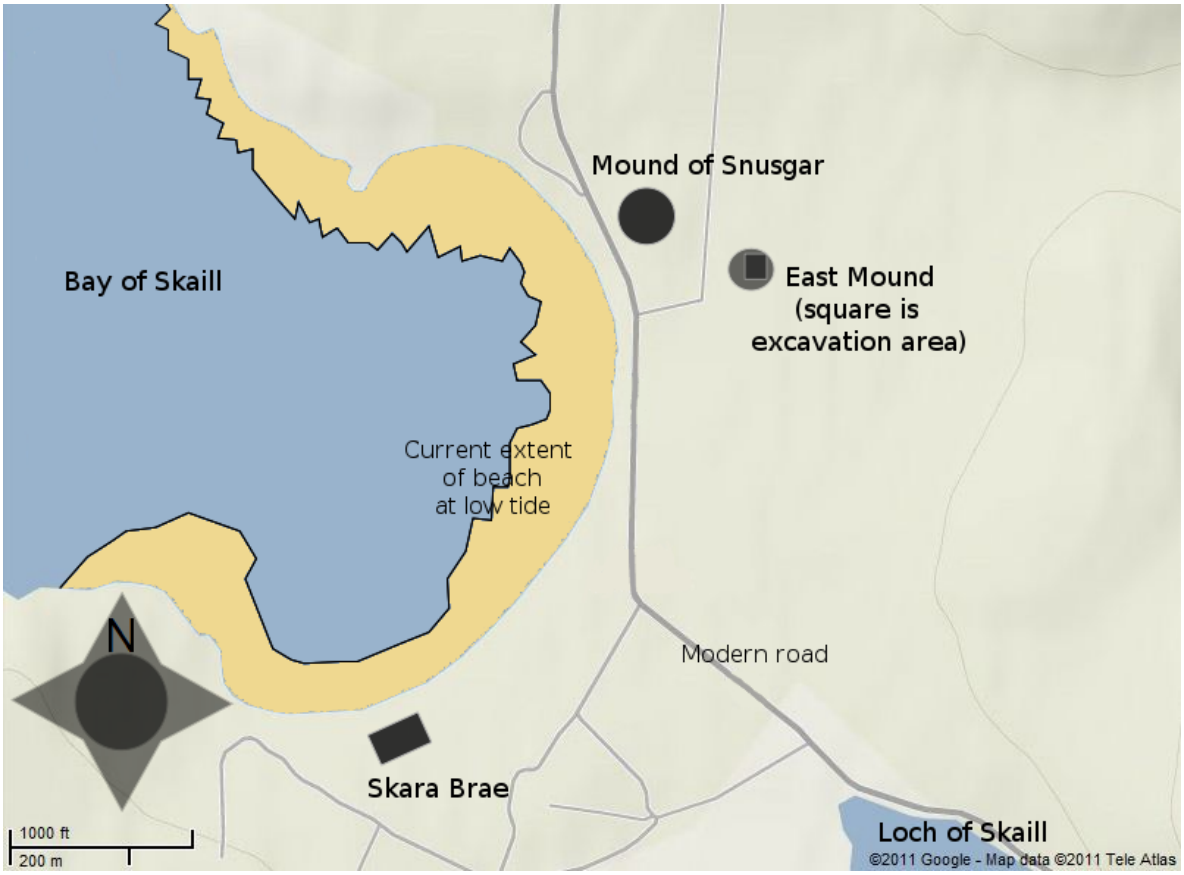


Figure 4.10: Plan of Bay of Skaill showing landscape features and location of archaeological excavation (background map data from maps.google.com).

and immediately inland from the bay is a machair, a low-altitude coastal landform consisting of windblown, mostly calcareous sand (Leinert et al. 2000). Keatinge and Dickson (1979), in what constitutes the seminal work on palaeoenvironment in this area, found that the bay was once a freshwater loch, but that sometime around 5 ka, probably due to rising sea level, increasing wind speed, and increasing storminess, the loch was breached and became part of the sea. Stratigraphy in the inland portion of the bay is characterised by wide bands of windblown sand and the area is well known through the twentieth century for its destructive, sand-shifting storms, such as the one that uncovered nearby Skara Brae (e.g., Hall et al. 2006).

The Birsay-Skaill Landscape Project began in 2003 and continued until 2011 with the intention of being a geophysical and topographical survey of the area with selective excavation. Post-excavation research and analysis continues to this day. Prior to this project, the archaeology of Viking and medieval period Orkney had taken place at a number of major excavations like the Brough of Birsay but had not had a landscape

focus. In 2003, magnetic studies, made possible because of the sandstone that characterises the geology of the region, revealed areas of interest under two large mounds on the northern part of the Bay; these were named the Mound of Snusgar and the East Mound (Griffiths et al. 2009). Along with areas in Birsay, Snusgar and the East Mound were selectively excavated in various field seasons from 2004-2010 (Griffiths et al. 2005; 2006; 2007a; 2007b; Griffiths forthcoming).

The dating strategy for Snusgar and the East Mound consists of a mixture of AMS radiocarbon dates and relative dating based upon artefact types and stratigraphic position (Griffiths et al. 2009: 7). In addition to that information, the excavators also had samples taken for OSL dating and tephrochronology, although these methods were seen to be more experimental. It was hoped that they could be used to build age models for the excavation in conjunction with the AMS and relative dates. As part of the current research, the East Mound excavation was sampled for microtephra, as is described in Section 6.1.2. The AMS radiocarbon dates and the OSL dates are presented in Appendix E, and are modelled using Bayesian statistics in Chapter 8.

When excavated, the East Mound revealed a longhouse with six phases of building (Griffiths forthcoming). Figure 4.11 shows the excavated area photographed from above at the end of the 2010 excavation season, showing the yard, an area for metalworking, and the majority of the longhouse. These structures may have been built upon a pre-Norse structure, using its foundations, but if so, excavators have not been able to uncover it. Windblown sand had filled the remains of the structure and this layer was cleared away by hand during the 2006-2008 field seasons. A range of artefacts including beads, whetstones, fragments of steatite vessels, and combs, as well as a strong faunal and environmental record, have all contributed to the ongoing analysis of life at the East Mound (Griffiths et al. 2009: 14).

Archaeologically, the East Mound is comparable to other coastal settlements in the Northern Isles, but it has the added component of being from a dynamic sand landscape that seems to have been a theme of Norse period settlement there. Three similar sites are Broo, Shetland (Bigelow et al. 2005), Bornais, Western Isles (Sharples ed. 2012), and Skaill Deerness (Buteux 1997), all coastal settlements exposed to the North Atlantic and prone to frequent and intensive storms. Broo and Bornais are similar to the East Mound stratigraphically too: Broo is characterised by sequences of 'cultural deposits interrupted with apparently pure sand strata that seem to be the products of aeolian transport and deposition' (Bigelow 2005: 90) while Bornais has a period of abandonment. This type of stratigraphy has a major role to play in developing



Figure 4.11: Plan view photograph of the East Mound excavation, showing the central longhouse being uncovered in the 2010 field season, facing east (Birsay Skaill Landscape Archaeology Project, University of Oxford).

the chronology of excavations as well as being a potential record of environmental change. Chapter 6, Chapter 8, and Chapter 9 describe my contribution to the dating and interpretation of the human settlement at the East Mound as it relates to environmental change in the area.

4.3.2 East Mound samples

The East Mound excavation area was chosen for tephrochronological research for a number of reasons. Orkney lies within the range of tephra fall from Icelandic volcanoes, and tephra has been found there before, albeit from long before the Viking period (Bunting 1994; Dugmore et al. 1995), as discussed in Section 3.4.2. The East Mound excavation in 2008 had exposed stratigraphic sections that could potentially provide a complete tephrostratigraphy for the site. The excavators were eager to try tephrochronology as a supplement to the radiocarbon record and to link the East Mound to local and regional environmental records. The location was also advantageous from a tephrochronological point of view because, given the distance between Orkney and late Holocene volcanic sources, it was helpful to have the radiocarbon and OSL dates to supplement any tephrochronological results.

The aim of the chronological research at the East Mound – and throughout the Birsay-Skaill Landscape Project's activities – has been to link archaeological data from excavation and survey with environmental data about landscape and climate change. The microtephra study conducted as part of this thesis was meant to supplement the AMS radiocarbon and OSL dates as the proposed way to do this.

Details of sampling from the East Mound and results are located in Chapter 6. Interpretation is located in Chapter 8.

4.3.3 Spretta Meadow and Hobbister A and B samples

After an archaeological landscape had been chosen for study in Orkney, I sought local environmental records to link to the archaeology using microtephra isochrons. Initially, the nearby Loch of Skaill seemed like a good candidate for coring. However, after an initial assessment it became clear that there were practical access problems there, as well as potential environmental constraints including European Protected

Species regulations.[2] As a result, I turned to cores that had already been taken. These came from Dr Jane Bunting at the University of Hull, and her then-PhD student (and now post-doctoral researcher) Michelle Farrell. The three cores came from similar environments, and were taken in 2006. They are labelled after their locations, Spretta Meadow, Hobbister A, and Hobbister B. Following coring, they were stored in a refrigerated area at the University of Hull. These were sub-sampled from for tephra studies in August 2009, as described in Section 6.1.2.2.

Prior to that, the cores were radiocarbon dated and sub-samples were taken for pollen studies. The radiocarbon dates are listed in Table 4.3 and the environmental studies are discussed later, in Chapter 8, as they relate to the interpretation of the chronology. The radiocarbon dates were acquired as part of Dr Farrell's PhD research. They were funded by NERC and done at the SUERC facility in East Kilbride. Radiocarbon dating of the Spretta Meadow core is planned for the future, partially pending the results of tephrochronological research in this dissertation.

Coring locations are shown in Figure 4.9. Spretta Meadow is a valley mire lying in a near-circular enclosed basin in the West Mainland hills, located at OS HY 23605 14642. The basin is clearly defined by the 50 m contour and is approximately 250 m in diameter. The surface supports a poor fen vegetation dominated by *Menyanthes, Molinia, Equisetum, Potentilla, Ranunculus* and various sedges. The core was taken from the centre of the basin (Michelle Farrell, pers. comm., 2009-2010).

Hobbister is an area of fairly extensive blanket peat covering approximately 4 km in Orphir, on the southern coast of Mainland. Vegetation in the area is dominated by *Calluna vulgaris, Molinia caerulea, Eriophorum angustifolium* and *Sphagnum moss.* Small patches of *Salix* scrub are also present in places. Hobbister A is located at OS HY 39612 06640 and Hobbister B is located at OS HY 39637 06562 (Michelle Farrell, pers. comm., 2009-2010).

The basal radiocarbon dates for these cores indicated that they were much earlier than the period of interest for this dissertation, which is focused on linking the environmental studies to the Viking Age and later archaeology; as a result, Spretta Meadow was scanned for microtephra down to 100 cm, Hobbister A down to 70 cm, and Hobbister B down to 100 cm.

[2]There was also concern about complications from the possible run-off effects of agricultural activity, which is heavy around the Loch. My supervisors advised me that it would not be in my interest as an individual researcher to persist with my plans to core the Loch. For a larger team able to call upon a more advanced infrastructure, and funded to pay ecological consultants to produce any necessary environmental assessments prior to fieldwork, it may well produce useful data.

Table 4.3: Radiocarbon dates associated with the Hobbister A and B cores (Michelle Farrell, pers. comm., 2011).

Lab Code	Depth	Site	^{14}C Age	Error ±	Calibrated
SUERC-22858	**61 cm**	**Hobbister A**	**1550**	**30**	**423-574 cal AD**
SUERC-19831	**173 cm**	**Hobbister A**	**3005**	**35**	**1387-1124 cal BC**
SUERC-22859	**253 cm**	**Hobbister A**	**3820**	**30**	**2448-2144 cal BC**
SUERC-19832	**370 cm**	**Hobbister A**	**6205**	**35**	**5293-5053 cal BC**
SUERC-22860	**81 cm**	**Hobbister B**	**1230**	**30**	**689-882 cal AD**
SUERC-19833	**124 cm**	**Hobbister B**	**2205**	**35**	**377-186 cal BC**
SUERC-22864	**167 cm**	**Hobbister B**	**3340**	**30**	**1729-1531 cal BC**
SUERC-19837	**195 cm**	**Hobbister B**	**3920**	**35**	**2547-2293 cal BC**

4.4 Summary

Two archaeological landscapes have been targeted for tephrochronological and other chronological research. They are:

1. Bay of Skaill Landscape Project, Orkney
2. Vatnsfjördur Landscape Project, Iceland

They were chosen because of their coastal locations, their potential for relevant local environmental records, and the different dating strategies employed by their excavators.

Related to the archaeological excavations are environmental and archaeological records also targeted:

1. Hobbister, Orkney
2. Spretta Meadow, Orkney
3. Sveinhúsavatn, Iceland
4. Homefield, Iceland
5. Kaldalonsjökull, Iceland

5 | Experimental procedures and methods

This chapter describes the field techniques, laboratory procedures, analytical methods, and the integration of laboratory results and archaeological theory that I have used in this dissertation.

5.1 Sampling for distal tephra from archaeological and environmental sites

Section 3.2 describes the range of depositional conditions in which tephra and microtephra are preserved, as well as the likelihood of tephra preservation, destruction, or chemical alteration in these different conditions. It is reasonable to choose certain locations as being likely places to find preserved and unaltered tephra, because of soil composition, placement in the landscape with relation to water movement, bioturbation, human disturbance, and /or other factors. Once likely sources of preserved tephra have been identified within an excavation or landscape, there are a range of methods available to extract the soil needed to establish an accurate tephrostratigraphy. Specific details of each individual sampling location are described in Chapter 4 and Chapter 6.

Archaeological excavations can present a range of challenges for identifying valid locations to construct tephrostratigraphies, particularly if there is evidence for infilling or soil disturbance due to past human activity. A strong understanding of the stratigraphy of the site, and in particular of the area where the tephra samples have come from, is necessary to develop accurate interpretations of the placement of tephra layers in context with human occupation layers or environmental fill.

Ideally, samples taken for establishing distal tephrochronologies should represent a continuous profile down the stratigraphy of an archaeological or environmental site. For marine, lacustrine, and many non-archaeological terrestrial sites with compacted sediment, this is achieved with the use of a core of sediment. Shorter cores in the field, including those studied in this thesis, are often taken with a Russian corer (for further discussion of technique, see Jowsey 1966 and Schofield et al. 2008). However, at sites with loosely compacted sediment, samples may be taken in individual containers from appropriately-sized intervals (generally, every 2 cm, but this will vary with what is possible with the condition of the sediment). Sediment within samples must be held tightly in place during transport and storage and any moisture in the sample must be maintained to prevent displacement of sediment. Stored samples are refrigerated.

5.2 Laboratory procedures for the extraction of tephra and microtephra

The data used in this thesis come largely from microtephras rather than visible tephras, and so this section will focus on microtephra extraction. The general procedure for the extraction of microtephra as used at the RLAHA (Research Laboratory for Archaeology and the History of Art) at the University of Oxford is shown in Figure 5.1, and for the most part follows Blockley et al. (2005). In some cases, Canada balsam, used to mount extracted tephra on slides, may cause phytoliths (opaline Si) to look like tephra under cross-polarised light, but this is a rare occurrence and the use of SPT is a less destructive method for tephra shards than previous methods that would have removed phytoliths (Blockley et al. 2005). Once mounted, individual shards are visually counted using a microscope to determine the amount of shards per dry gram of sediment in each sample. In addition to samples, during each extraction, two blank slides are prepared and visually scanned, one from the sieving stage and one from the heavy liquid flotation stage, in order to test against cross-contamination of samples or other forms of contamination.

For any samples where vitreous glass shards are found in high enough densities, the same sieving and extraction process takes place again. The amount present will vary by site, generally governed by proximity to volcanic sources. As discussed in Section 3.2, a volcanically distal location in Iceland almost certainly will yield a much higher shard count per gram of dry sediment than a site in Orkney. During this second extraction, the density of the SPT may be altered to suit the likely compositions of

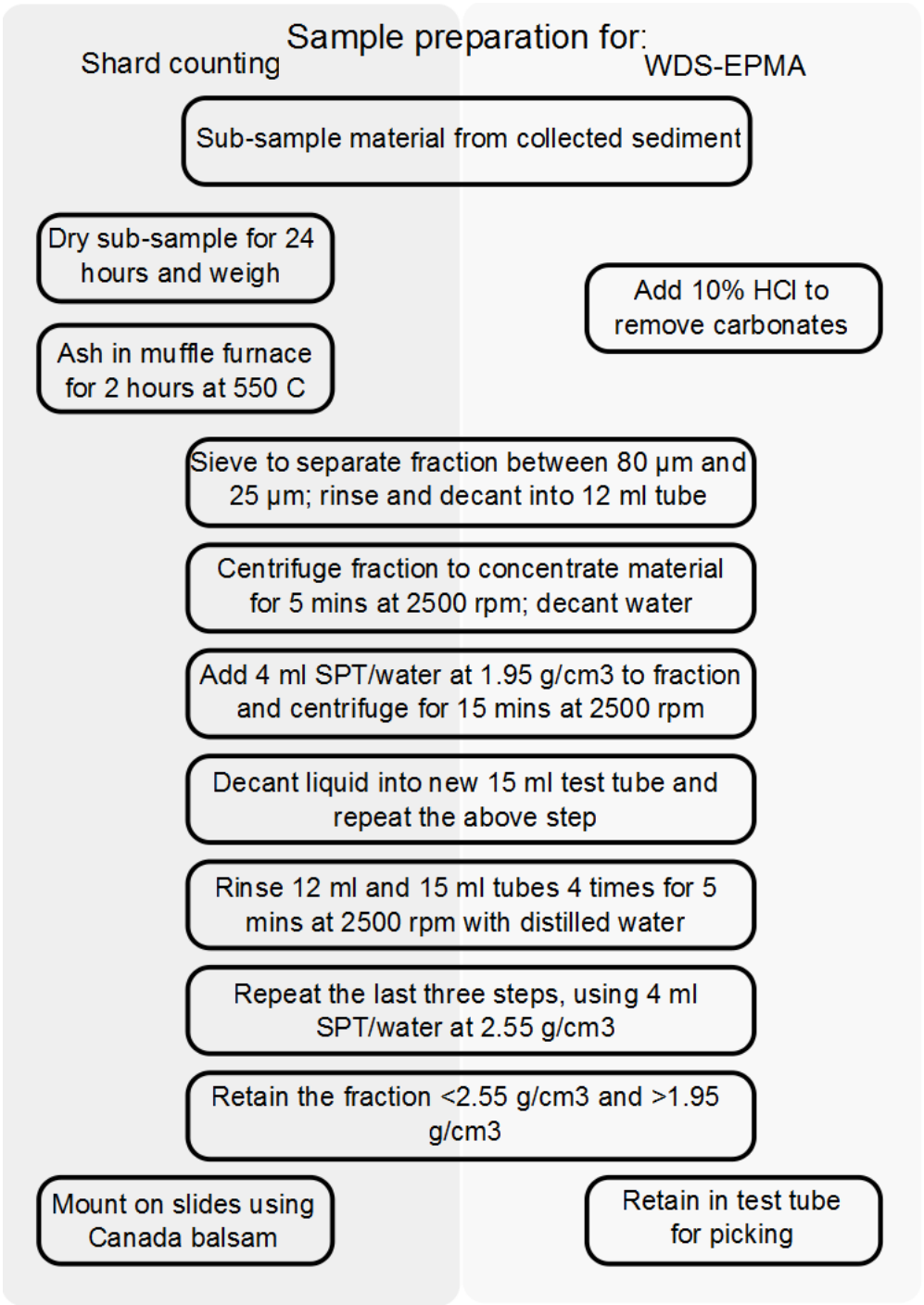


Figure 5.1: Method for extracting microtephra from collected sediment, modified from Blockley et al. (2005: 1957).

individual samples. Likewise, the sampling increment may be changed to suit the individual sample. For example, if a sample initially extracted in increments of 5 cm yields a large shard count, and if the core or samples taken will allow it, then it may be divided into 1-2 cm fractions for the next round of extraction in order to create a more precise tephrostratigraphy.

The next steps are shown in Figure 5.2. Where possible, approximately sixty shards are extracted per sample to ensure at approximately thirty shards large enough for geochemical analysis. In practice, this is only possible under ideal conditions and as few as two or three shards large enough for the beam of the WDS-EPMA may be extracted from entire samples. One reason for extracting a much larger number of shards in the syringe phase than will be analyzed is because the three-dimensional shards lie at various depths within the plane of the resin stub, and the end goal of hand grinding is to expose a proportionally large quantity of shards without grinding through or plucking out shards nearer to the surface.

The final step in the preparation of samples for geochemical analysis on the WDS-EPMA is carbon coating. Coating the stubs with carbon adds a conductive layer to prevent charging under electron bombardment in the probe (Reed 2005). The stubs are placed into a vacuum chamber with a carbon evaporation source and coated to a thickness of approximately 20 nm. At this point, they are ready for analysis on the microprobe. If, after initial WDS-EPMA, there are not enough analyses to characterise the tephra, it is possible to grind and polish the same stubs to expose the more deeply mounted shards. In practice, this is done commonly when shards are very small or there are very few available and so every one possible must be probed.

5.3 Wavelength Dispersive Spectrometry – Electron Probe MicroAnalysis (WDS-EPMA)

EPMA is a technique for analyzing the chemistry of a number of small selected areas across a sample. It was first developed by Froggatt (1983). It utilises X-rays by exciting them with a focused electron beam; because the X-ray spectrum contains lines characteristic of the elements present, the lines can be identified by their wavelengths and related to known standard samples. Standards consist of pure elements, and so it is also possible to determine the concentrations of the elements quantitatively in prepared samples (Reed 2005). EPMA beam width permits the

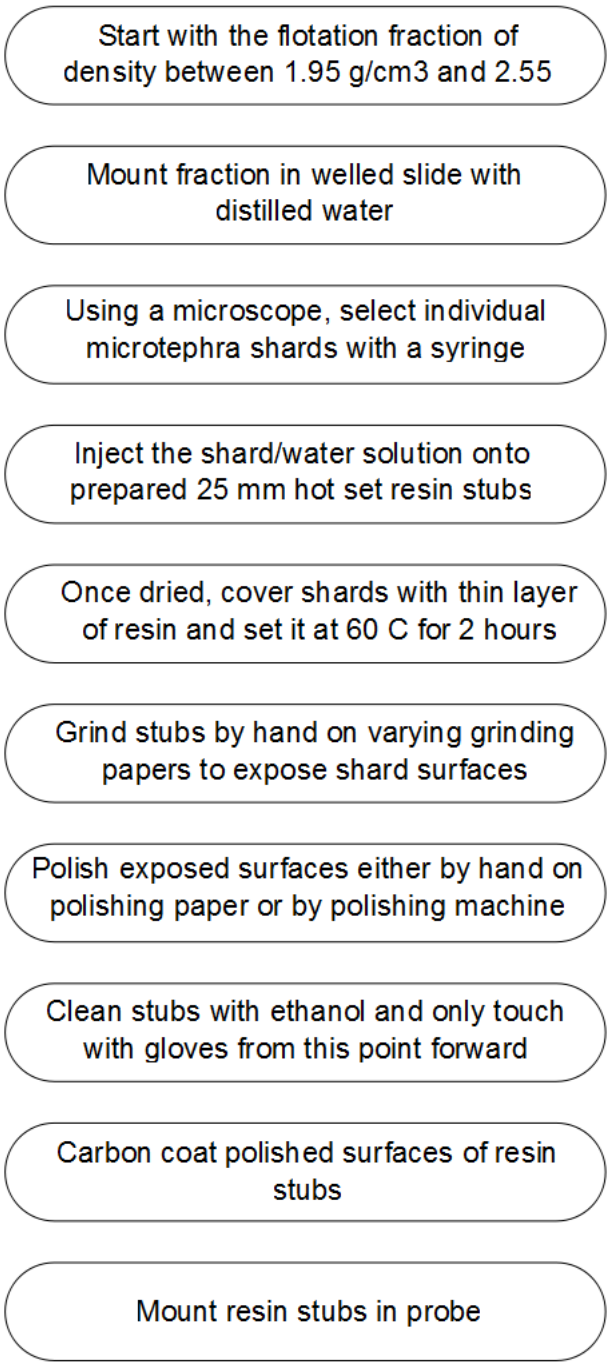


Figure 5.2: Steps for preparing samples for WDS-EPMA.

targeting of individual shards of microtephra. As a result, it is also ideal for the low concentrations of microtephra typically found within distal deposits (Hunt and Hill 1993).

Wavelength dispersive spectrometers disperse X-rays according to their wavelength by means of Bragg reflection, resulting in high spectral resolution but a lower intensity for a given beam current (complementary to EDS – for more detail, see Reed 2005: 88-91). The difference between WDS (wavelength dispersive spectroscopy) analysis and EDS analysis is that WDS acquires elemental data sequentially, whilst EDS acquires it simultaneously (Hunt and Hill 1993: 273). For both WDS and EDS, it is important to adjust count time and probe current (which relates directly to count rate) to their lowest possible limits while maintaining a predetermined precision. This is to minimize sodium mobilisation which becomes more of an issue the longer the sample is exposed to the beam. Therefore, adjustments to individual probes are made to maintain a balance between high counts per element (higher precision) and minimum sodium mobility (higher accuracy) (Hunt and Hill 1993: 274).

The 1992 International Quaternary Union (INQUA) Inter-Congress Committee on Tephrochronology recommended that the calibration of analytical instruments as well as the use of a common set of glass standards were necessary to advance accurate and precise research into tephrochronology. As a result, an inter-laboratory comparison of EPMA results for known standards was undertaken in the mid-1990s and again in the 2000s (Hunt and Hill 1993; Kuehn et al. 2011). The reproducibility of elemental analyses must be verified, and for this purpose a set of secondary standards of known composition is used. Ideally this standard will contain most of the major elements found within the tephra itself (Hunt and Hill 1993). All EPMA analysis in this dissertation was carried out on a JEOL8600, refurbished in November 2008, at the RLAHA, University of Oxford. The instrument was calibrated using a suite of mineral standards, and accuracy and precision during each analytical run was assessed using MPI-DING glass standards (see Jochum et al. 2000; Jochum et al. 2006). It is standard practice for analyses of these standards to be published alongside new EPMA data (Lowe 2011). For each group of analyses in this dissertation, these are given in Appendix 1.

Alongside the two secondary standard samples, seven of the resin stubs described above may be loaded into the microprobe at any one time. Samples are viewed through an in-built microscope, and may be viewed using a backscattered electron imaging mode, although the latter is not to be used too frequently or for long periods

as direct exposure to the beam will deteriorate the samples. Individual sample surfaces are scanned and the areas for analysis targeted by the operator. The distinctive morphology of vitreous tephra shards, in addition to the degree of surface polish in contrast to the surrounding resin or other minerals, makes them easily identifiable. In many cases, microtephras may be just on the boundary of the size necessary for the microprobe to take an accurate reading (i.e. without including nearby microtephras, minerals, or in most cases resin), and as a result it is necessary to target as many potential points as possible for each sample. Data from the accidental analysis of non-vitreous glass material can be filtered during the data analysis phase, as described in Section 5.4.1. The x and y coordinates for each point targeted on the plane surface of the resin stub are recorded by a computer; when all points have been targeted, the computer then analyses the points sequentially. There can be machine drift over time, which is one reason why it is important to compare values from the standards with published values.

5.3.1 Potential analytical problems

There are a variety of potential analytical problems associated with WDS-EPMA. In order to understand the data obtained from the use of these machines, it is necessary to know what sort of problems might arise during analysis. The sections below review these and assess their potential to present difficulties in interpreting the data obtained for this dissertation.

5.3.1.1 Sample preparation errors

If samples are not prepared correctly prior to probing, it can lead to serious analytical errors. For example, a scratched surface will result in fewer X-rays arriving at the detector because of absorption by the sample itself (Hunt and Hill 1993). Similarly, if, during the grinding and polishing process, the tephra shards are ground too thin, some of the X-rays will travel into the resin stub that they are mounted in, which will affect analytical results negatively (*ibid.*).

5.3.1.2 Alkali mobilization

Precise determination of alkali elements in tephra glass shards is made difficult by a loss in intensity over time by sodium and potassium signals (Nielsen and Sigurdsson

1981). Essentially, as the electron beam heats the sample, the alkali atoms interact with oxygen atoms and form two ions; the alkali ions diffuse throughout the sample. A space charge layer forms several microns beneath the surface of the sample and acts as a sink for the mobile alkali ions. As a result, there is decreased X-ray production from the alkalis (Lineweaver 1962; Nielsen and Sigurdsson 1981). Therefore, analytical results often have lower than anticipated sodium and potassium percentages, and higher than anticipated percentages for silicon and, to some extent, aluminium. In terms of tephra analysis, Hunt and Hill (2001) find that these effects are more of a problem for glasses with higher silicic composition by weight-% – rhyolite and dacite – and less of a problem for basalt and andesite.

Fortunately, this process of alkali mobilization does not occur immediately. Instead, there is an incubation period, with little to no depletion of alkalis; however, once the sample has been heated by the electron beam to a specific temperature, the alkali diffusion begins (Vassamillet and Caldwell 1969; Nielsen and Sigurdsson 1981). As a result, a method for decreasing the effects of alkali mobilization is to ensure that the sample temperature is kept relatively cool. Diffusing the heat across the sample by moving the beam across its surface only applies to large, homogenous samples, which is a rarity when analysing tephras. Nielsen and Sigurdsson (1981) suggest lowering the sample temperature to -90°C before beginning analysis, but this is obviously time consuming and only feasible under very specific circumstances. In order to minimise alkali mobilisation, the machine used for analysis here has a Faraday cage that minimises the samples' exposure to the beam.

5.3.1.3 Low totals

The sum of all elements within a reading ideally should be 100%. In reality, that number varies, so an acceptable range must be defined. Readings with low totals (less than 90%) should be rejected because of the similar chemistry between different tephras and the difficulties of correlation (Hunt and Hill 1993). There are several reasons for low totals of elements. One cause is errors in focusing the microprobe correctly for a reading; others are the result of the composition of the shards themselves.

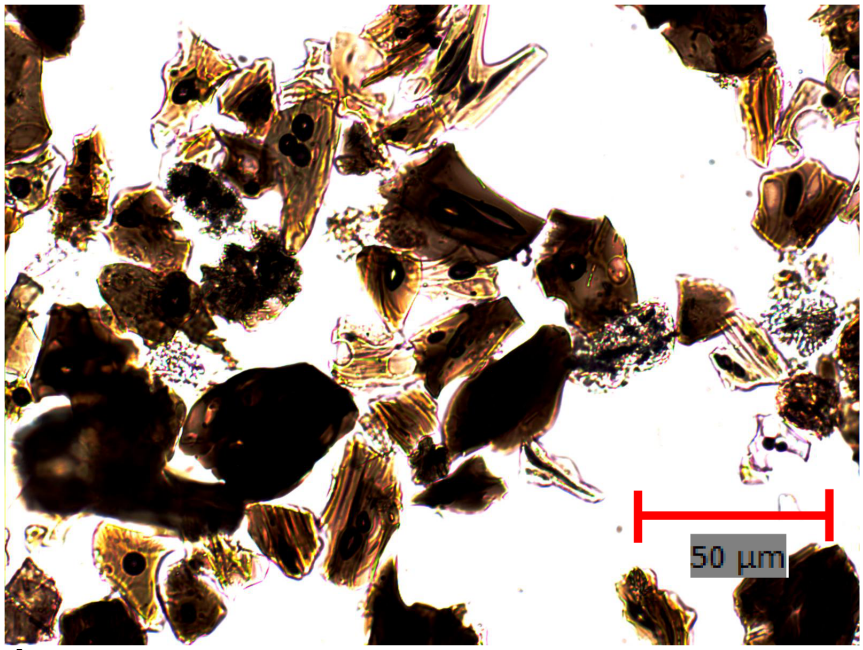
Water within tephra is the most common reason for low totals, and in fact explains why totals are never 100%. EPMA cannot determine the water content of tephras, as

hydrogen does not generate X-rays.[1] It is therefore important to determine a reasonable percentage of water content, and discard all samples with a lower total than that percentage. The water content of natural glasses can be altered by explosive eruption melts (resulting in vesiculation of the tephra), or by hydration and devitrification (Hunt and Hill 1993). Carmichael (1979) has suggested a range of 2-7% water for some types of igneous rocks, with most being in the 2% range. Conversely, Hunt and Hill (1993) see high water content (greater than 2%) as the result of leaching, which would alter the primary geochemical fingerprint of the glass and make its analysis useless for determining tephra identity. Hunt and Hill (*ibid.*) therefore disagree with the International Union for Quaternary Research (INQUA) recommendation that totals above 90% are acceptable (Froggatt 1992). They write, 'As few unaltered glasses contain more than 2% water, and fluorine and chlorine are not abundant, totals lower than 98% should, in theory, be excluded. In practice, this would exclude a high proportion of analyses and an arbitrary lower limit of 95% has proved practicable' (Hunt and Hill 1993: 274). Hunt and Hill go on to suggest that in cases of difficult geochemical correlations between tephras, 98% should be used (*ibid.*). To strike a balance between these opinions, in this thesis, analyses with totals below 95% have not been used.

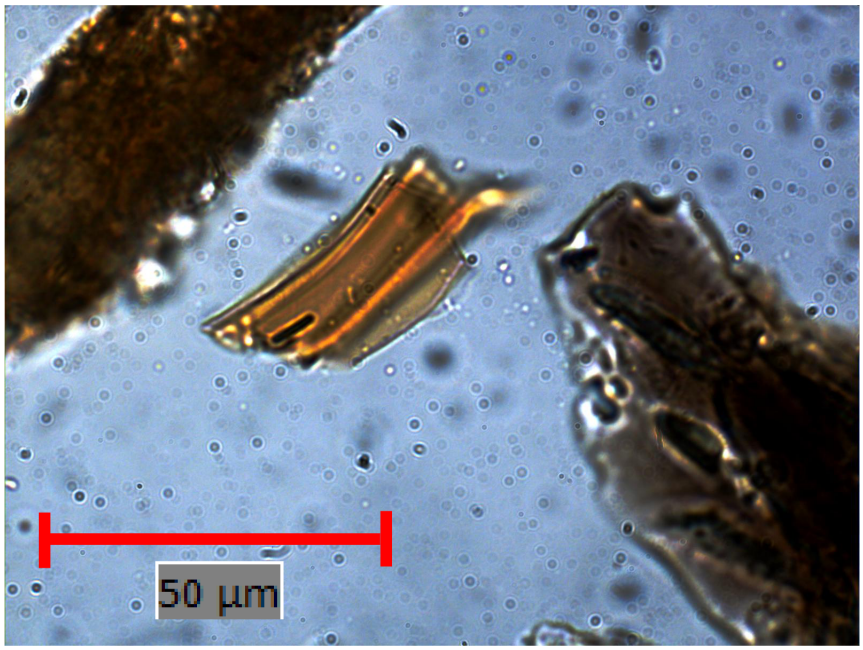
5.3.1.4 Sample shape/microlites

Berger (1992) suggests that the analyses of the smallest shards possible with beam size should be the most reliable, as microcrystallite content is inversely related to shard size; the characteristics of the shards themselves may present problems. Highly pumiceous shards of any size can create problems for probing, as the glass walls can be very thin, and much of the surface covered with vesicles. The beam size may be too large to probe these shards successfully, and therefore small shards with vesicles may result in low totals. Microlites (small inclusions within the glass) or feldspar contamination may also present problems (Hunt and Hill 2001). For this reason, Hunt and Hill recommend detecting crystalline heterogeneities by viewing tephras in transmitted light prior to EPMA analysis.

[1] X-ray spectroscopy works by exciting inner shell (a.k.a., K-Shell) electrons which are ejected, leaving a hole. If possible, a valence electron drops into the hole and emits the difference in energy as electromagnetic radiation. Larger atoms emit larger quantities of energy, which are x-rays; however, hydrogen is the least energetic element and has only enough energy to emit an ultraviolet photon. EPMA is unable to detect all but the lightest elements (H, He, and Li); meaning that the water in hydrous minerals cannot be analysed (Reed 2005).



A.



B.

Figure 5.3: Different types of microtephra shards. A. shows both vesicular and striated shards while the pale orange shard in B. has a microlite. A. is shown at 10x magnification and B. is shown at 25x.

Many of the shards analyzed in this dissertation have vesicles, striation, and microlite inclusions that have led to there being relatively few surfaces for microprobing. Examples of these shard variations are shown in Figure 5.3. As a result, most of the samples studied here were probed several times with further grinding and polishing between sessions. This was done to reveal as many clean, beam-sized tephra surfaces as possible. This meant that many more readings were possible than would have been if the resin stubs were only polished and beamed once.

5.4 Data processing and statistical methods

The analysis of probe data for use as a geochronological tool requires several steps: first, determining if probe data accurately reflect the composition of the probed shards; second, identifying the general composition of the shards; and third, if possible, correlating the probe data with known proximal and distal tephra layers. The third step is, for chronological purposes, the most important part of the analysis. This requires first narrowing down possible correlative volcanic events using purely chemical data, and then, if there are a number of possible correlatives, using stratigraphic or other chronological information to select the best match. If a match is not possible, trace or rare earth element analysis, using ICP-MS (Inductively coupled plasma mass spectrometry), may aid the identification (Pearce 2004; Pearce et al. 2007). However, this method may not be useful for tephra identification in instances where tephras cannot be separated using major elements as in most magmatic systems, trace element substitution for major elements follow systematic pathways (Pollard et al. 2006). Further, a number of studies have demonstrated that correlations are most statistically viable when made using only the major and minor elements (for a review, see Payne and Blackford 2008). For those reasons, and for reasons of funding and time, trace and rare earth element analyses have not been used in this thesis.

Key to the identification process is the use of both representative diagrams and statistical methods. Below, a number of methods are discussed for presenting and interpreting data, with an emphasis on those methods that have been used in this thesis.

5.4.1 Filtering data

It is standard practice in the WDS-EPMA analysis of tephra shards to filter data (Hunt and Hill 1993). Extraction procedures, as outlined in Section 5.2, do not solely isolate vitreous tephra, and both mineral matter and biological silica remain in samples for picking. Picking for tephra shard mounting also is not a clean process, and so each resin stub representing a single layer of tephra will often have a number of non-tephra units within it, which may later be mistaken for tephra and microprobed. These can easily be recognised in chemical analysis: particular totals are a sign of minerals (for example, biological silica will be 100% SiO_2; K feldspar ($KAlSi_3O_8$) will have approximately 17% K_2O and 18% Al_2O_3). Several samples used in this dissertation had a high number of minerals and biological silica during their initial picking, particularly those from Sveinhúsavatn, and upon visual inspection under the microscope, these were then picked again in an attempt to eliminate silica and minerals from analysis.

The other major reason to filter data is low total percentage, as discussed in Section 5.3.1. This can be the result of poor beam focus or aim, poor polishing of resin stubs, or microlites or vesicles in the shards themselves. Although the percentage varies dependent upon author, 95% is generally recognised as the cut-off point, and that number has been used in this thesis (Pollard et al. 2006).

5.4.2 Visual assessment of data

Visual assessment of bi-plots or tri-plots of the nine to twelve major and minor elements detected by WDS-EPMA are a standard method for identifying and correlating tephra layers with known tephra sequences (e.g. Larsen et al. 1999; Kristjánsdóttir et al. 2007), as well as being a standard method for interpreting geochemical data across the earth sciences. Bi-plots display selected pairs of oxides plotted against one another. For tephra studies, these oxides are chosen based on known information about likely magmatic composition, so for example SiO_2 is a common oxide to plot against others. Bi-plots are popular in the geological literature because they can demonstrate a linear gradient of composition across data points. Often, multiple bi-plots are used to demonstrate the full range of composition of a given data set. TAS (total alkali-silica) plots may also be used. Kuehn and Foit (2006) note that, while graphical comparison can be difficult for large datasets, it allows strongly heterogeneous tephra units to be compared effectively.

5.4.3 Sources for correlation and the creation of a database of proximal data

The above section presupposes that one has access to a database of quality proximal eruption data. As tephrochronology is a recent field of study, these databases do not always exist or may contain incomplete data. Furthermore, new publications periodically add to the proximal record for these volcanic systems (e.g. Larsen et al. 2011). This is true for Late Holocene Icelandic volcanism, despite being one of the most well-studied subjects in tephrochronology.

Prior to the research done here, there were two major sources publically available for Late Holocene Icelandic tephras. The first was a publication by Haflidason et al. (2000) that contained a list of the known Icelandic eruptions through the present day. The list is detailed and contains citations for the geochemistry of many of these eruptions, but the geochemistry is often from unpublished sources and Haflidason et al. have chosen to only publish single data points for each. Single data points are not useful for fingerprinting tephra from most eruptions, which can contain multiple phases and a spread of glass chemistry. The second major source is Tephrabase.org, which is described in Section 3.3. Perhaps because Tephrabase relies upon others to report their data to the maintainers of the database, it is not up to date for most eruptions and also contains some older data that may need to be revised (e.g. Boygle 1995 for Hekla 1104, which is discussed more in Chapter 7. Furthermore, in some cases (e.g. that from Chambers et al. 2004), Tephrabase does not make a distinction between proximal and distal glass chemistry data, when proximity to volcanic source may have some impact on the accuracy of the glass chemistry. This is because distal sources may contain only the less dense tephras.

As a result, an important step in correlating the data from the locations described in this thesis was to create an up-to-date database of glass chemistry from proximal and, where proximal data was not available, some distal sources. This database is drawn from published data entirely, but much of the data have not previously been collected together. It is in Appendix 3. The eruptions described are listed in Table 3.1.

5.4.4 Correlating sample layers with known geochemistry

The most complex analysis of geochemical data in this thesis occurs when correlating the geochemistry of sample layers with known eruptions from published sources.

Tephra layers within the context of the stratigraphy of an archaeological excavation or an environmental core can form an internal, relative chronology; it is only through geochemical correlation of those tephra layers with layers of known age from proximal volcanic sources that tephra layers become absolute chronostratigraphic markers. This section of the chapter deals with the methods used for correlation of tephra layers identified in the course of this research with published geochemical data from eruptions of known age, using a published example with Icelandic proximal data.

The first step is to attempt to narrow down the range of possible correlative eruptions based on geographical location and any available chronological information. The geographic range of ash fall from a given event is still unknown for most eruptions, but a general geographic region can often be determined. For example, in their study of Holocene cryptotephras from the North Iceland Shelf, Kristjánsdóttir et al. (2007) started from the assumption that all of their tephras would be Icelandic because of the geographic location of their study, and from there they used isopach maps, which show the extent of known ash fall across the landscape, to narrow the range of possible eruptions to those where ash had fallen in the north of Iceland. Likewise, given relative stratigraphic positions for tephra layers, it is unlikely that one will have to attempt to identify a tephra layer with no given age range. Once a range of possible correlative tephras have been identified, the second step is to visually compare the glass chemistry of these tephras to the distal data using bi-plots. For example, Kristjánsdóttir et al. (2007) use bi-plots of FeO vs. CaO and FeO vs. TiO_2 wt-% to compare the different glass chemistries of known eruptions and their core data. In that case, FeO and TiO_2 were chosen because of the known composition of Icelandic volcanoes.

In many cases, bi-plot comparisons will be conclusive enough to correlate distal and proximal layers. However, it is difficult to quantify the results of a bi-plot and there are some cases where the results may not be conclusive. One example of this is where there has been a series of eruptions with similar compositions, as many Hekla eruptions are. In this instance, tephrostratigraphy and other chronological information may be necessary to supplement the bi-plots and determine the identity of the tephra layer. Another example is where proximal datasets are small or incomplete. In this case, the sampled tephra layer may have a wider range of geochemistry than that of the known proximal geochemistry. As a result, there is some degree of personal judgment that must be used in making a correlation.

5.4.5 Statistical transformations of data

In addition to graphical representation, several statistical methods have been used in the past few decades to analyze data suites of tephra: for example, SC (similar coefficients), PCA (principal components analysis), and /or DFA (discriminant function analysis) (for a review, see Kuehn and Foit 2006). DFA in particular has been applied to Icelandic tephras in the North Atlantic, although at the time of that research the authors were hampered by a lack of proximal data with which to compare their results (Charman and Grattan 1999). Recently, some researchers have argued that visual assessment, particularly of bi-plots, can be misleading because it does not allow the consideration of all elemental variations together, and that statistical methods, and in particular multivariate analysis, present solutions for identifying geochemical data from tephra (Pollard et al. 2006; Lane 2008).

Before such statistical analysis is possible, there are several issues of data handling to be addressed relating to the normalisation of analytical totals from WDS-EPMA to 100% (Pawlowsky-Glahn and Egozcue 2006). Normalisation leads to the 'unit sum problem' (Aitchison 1986), which has been an issue in the analysis of tephra and similar geochemical data for a number of years (e.g. Pollard et al. 2006). The 'unit sum problem' relates to the numerical analysis of any compositional data, i.e., data that are constrained to add up to 100%. The oxide concentration expressed in geochemical datasets as a percentage relates not only to itself, but also to the percentages of all other oxide concentrations. Therefore, when data are normalised, if the composition of any oxide concentration changes then the percentage of all other components must change, and so the correlations between pairs of oxides must be influenced by the 'unit sum' constraint – i.e., that all percentages summed must equal 100%. This poses two problems: first, that for a variety of reasons outlined in Section 5.3.1, data do not equal exactly 100% and for certain analyses must be normalised to that; and, second, some correlations must be negative as a result of the 'unit sum', and therefore result in false correlation. Although one solution is simply to not normalise the data, this is not possible for all types of analysis. Aitchison has systematically challenged the use of geochemical data that do not address the 'unit sum problem' and for the past several years many tephrochronologists have used logratios to solve the problem (for a review, see Pollard et al. 2006).

Mahalanobis distances have been used in some cases in this thesis to aid in correlations. Mahalanobis distances are a measure of distance based on correlations between

variables (Mardia et al. 1989). In the case of tephra analysed by WDS-EPMA, these variables are oxide weight percentages. The method is often used in DFA. Stokes and Lowe (1988) seem to have been the first to use this technique for tephra correlation, while Lee and Bacon-Shone (2005) have used the technique to successfully identify unknown tephras from New Zealand. Analysis for this thesis was performed using the R statistics package/programming language and the code for computing Mahalanobis distances in this thesis is shown with an example in Appendix 4.

5.4.6 Chronostratigraphies and OxCal

Once all of the above data were assembled, and any tephra layers found in the course of this research correlated, they then had to be combined with any other chronological information (such as radiocarbon dates) in order to complete a chronology for each site. Finally, those chronologies had to be linked to other related studies. Both of these things were done in OxCal (Bronk Ramsay 2012) using Bayesian statistics, which produce statistical age models to refine raw dates. These are described more in depth in Section 3.5. In OxCal, the user inputs chronological information (radiocarbon dates as 'R_dates', other dates as 'C_dates') along with uncertainties. The user sorts these dates into sequences and phases based upon the prior knowledge required to make a Bayesian model, such as stratigraphic information linking dates. Figure 5.4 shows an example of OxCal input for a simple model, where all dates entered were in a stratigraphic sequence. They are listed from oldest to youngest. The bottom date, C_date, is an OSL date.

Figure 5.5 shows the results of running the simple OxCal model in table form. The program has taken into account the prior information (that the dates were in stratigraphic sequence) and then calibrated the radiocarbon dates with the most recent calibration curve (INTCAL13). The dates listed as 'unmodelled' are just calibrated while the 'modelled' dates are those with the model taken into account. The 'indices' show that the A_{model} and $A_{overall}$ are both above 95%, indicating a successful model. A value over 60% means that a model is statistically valid. Finally, Figure 5.6 shows the dates plotted; dark grey represents the modelled values, superimposed over the light grey unmodelled. In this model, the range of the dates is more precise.

Models that do not have good A values are often indicative of inaccurate dates or mistakes in understanding the stratigraphic relationships at a study site. OxCal therefore also provides a check on any kind of date that has been entered into it.

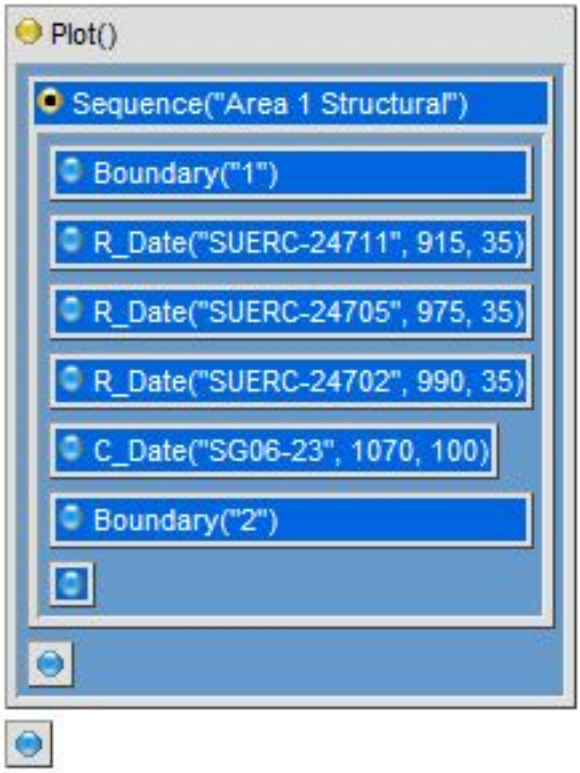


Figure 5.4: Example entry into OxCal version 4.2 (Bronk Ramsey 2015).

Name Show all Show structure		Unmodelled (BC/AD)			Modelled (BC/AD)			Indices A_{model}=96.1 $A_{overall}$=97.8				
		from	to	%	from	to	%	A_{comb}	A	L	P	C
▼ Sequence Area 1 Structural												
Boundary 1					940	1149	95.4					98.2
R_Date SUERC-24711		1029	1204	95.4	1023	1138	95.4		101.3			99.3
R_Date SUERC-24705		997	1155	95.4	1026	1149	95.4		101			99.3
R_Date SUERC-24702		986	1155	95.4	1027	1156	95.4		80.7			99.4
C_Date SG06-23		870	1270	95.4	1029	1195	95.4		115.8			99.1
Boundary 2					1027	1292	95.4					97.8

Figure 5.5: Example table output of model from Figure 5.4, from OxCal version 4.2(Bronk Ramsey 2015).

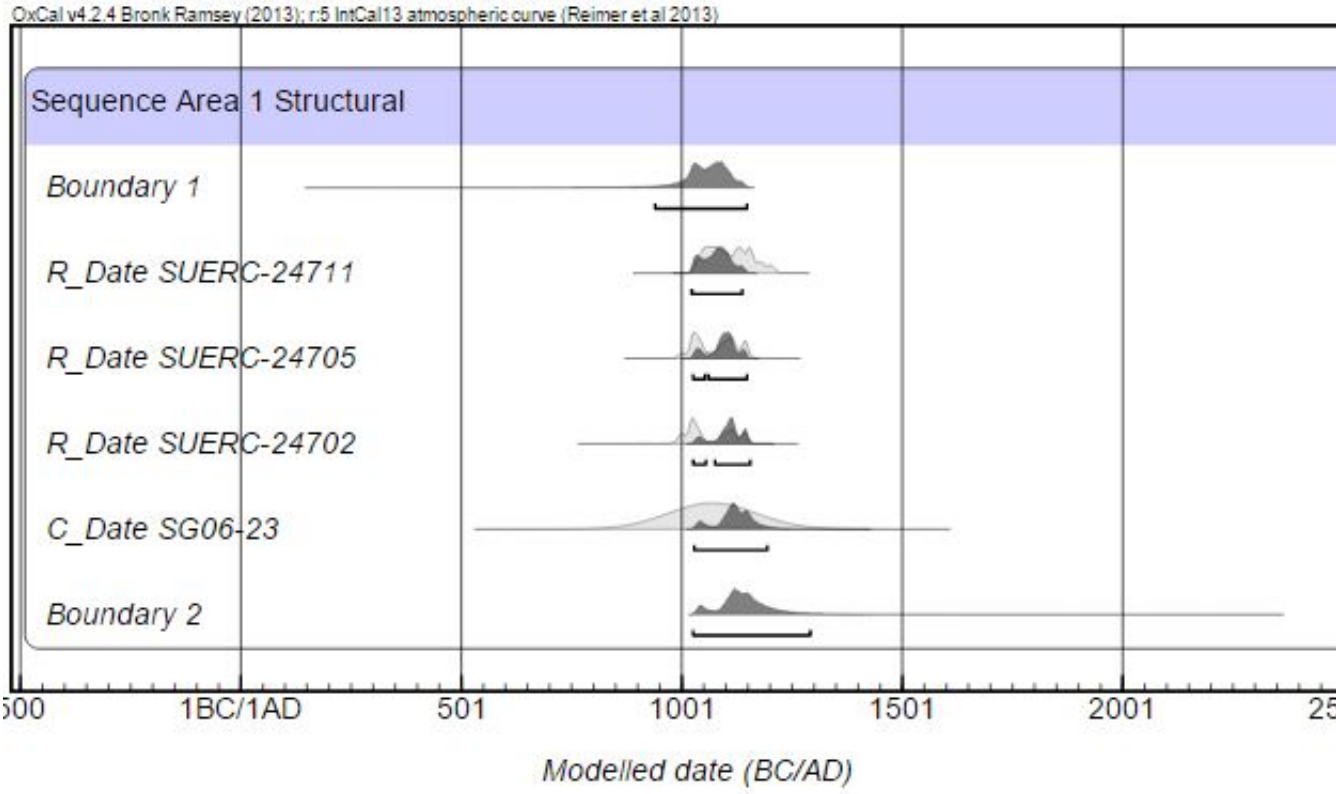


Figure 5.6: Example plot output of model from Figure 5.4, from OxCal version 4.2 (Bronk Ramsey 2015).

However, because these models rely upon their internal data, they are only as good as the data put into them. Therefore it is best to rigorously interrogate stratigraphic relationships and date quality before entering it into any model.

5.5 Integrating scientific results with archaeological interpretations

Tephrochronology and other chronological methods are tools for gaining an understanding of archaeological research questions. Chapter 7, Chapter 8, and Chapter 9 describe the integration of the results in Chapter 6 with archaeological data from the test cases studied as well as environmental data, both from the sites and from the wider region. Partly this has been done through Bayesian age modelling, which was discussed above. Beyond statistical models, the results have been integrated with chronological data from other archaeological excavations and environmental studies.

Integration consists of two main steps. First, tephra data have been combined with

other chronological data and the stratigraphy from the sampled locations and cores to create age models of events, both archaeological and environmental, for each landscape (Vatnsfjörður and the Bay of Skaill). Second, these chronologies have been expanded with published environmental and archaeological data from the surrounding regions. The aim of these two steps is to link the archaeological findings with records of environmental change both locally and regionally, therefore allowing an exploration of the links between the records with the most accurate and precise chronology currently possible.

The published data sources were chosen for a number of reasons. Primarily, the authors needed to use recent (approximately the past twenty years) and well-documented chronological methods. A few exceptions have been made for works of great importance or works that are often cited as sources for later research (e.g. sea-ice documented from historical sources in Ogilvie 1990), but in general dates from the Icelandic Sagas or other historical chronicles have not been used due to questions about their accuracy and this thesis's focus on scientifically-derived chronologies.

Sources had to be relevant not just to the islands of the Norse North Atlantic but also to the interpretation of the archaeological records at Vatnsfjörður and the Bay of Skaill; however, they could cover a range of topics: for example, landscape formation or the MW/LIA. Sources that focused on implementing models rather than describing past events were not used (e.g. Simpson et al. 2001 and Thomson and Simpson 2006). Lack of agreement between proxies is a well-recognised problem (Newnam and Lowe 1999; Blauuw 2010), and so although in some of the cases presented here, they do not agree, they have been presented side by side with the goal of suggesting possibilities.

In Chapter 9, I expanded the area of study to include the wider region of Norse colonisation, stretching from the northern British Isles to Greenland. Using Bayesian modelling, I performed several transformations on the chronological data from those locations to attempt to answer wider regional questions.

5.6 Summary

There were five main methods used in gathering the data to write this dissertation:

1. Archaeological field work: both excavation and field sampling for tephra and microtephra samples.

2. Preparation of those samples for the identification of major tephra layers using WDS-EPMA.
3. Statistical and visual data analysis to correlate the tephra layers with known eruptions and integrate them into local and regional chronologies, as well as the creation of a database of proximal geochemistry from Icelandic Late Holocene eruptions.
4. Use of Bayesian models to compare chronological data where stratigraphic relationships could be established.
5. Comparisons of the data with published environmental and archaeological studies using chronological information.

6 | Field and laboratory results

This chapter presents the results of the field and laboratory methods described in Chapter 5.

6.1 On-site sampling

Section 5.1 has a description of general sampling methods for microtephra.

6.1.1 Iceland

6.1.1.1 Sveinhúsavatn samples

In summer 2009, Dr Jerry Lloyd (University of Durham) and I cored the bottom of the lake nearest the Vatnsfjörður site, Sveinhúsavatn, whose location is shown in Figure 4.5. The purpose of taking cores from the lake bottom was to determine first, when the lake became freshwater (i.e. separate from the fjord); second, what implications this may have had for sea-level changes in the area; and third, the relationship that the lake had with the settlement over time.

Coring was performed using a Russian corer. Two cores were taken, one from the centre of the lake (at a depth approximately 1.35 m below the lake surface) and one from nearer to the shore (approximately 0.33 m below the surface). Ultimately, the core that was chosen for study was that from the centre of the lake, to maximise the length and structural integrity of the core as well as to avoid shore-area disturbances caused by thirsty local sheep. There were no visible tephra layers in the core. It was very uniform in composition, as shown in the photograph in Figure 6.1 and the sediment log in Figure 6.2. The lack of a visible tephra layer, given that many of the trenches in the archaeological excavations contained one, seemed surprising, but may



Figure 6.1: Sveinhúsavatn core from the centre of the lake showing the inside of the Russian corer. Picture taken by the author in August 2009.

be explained by how fine the ash in that layer is. As is described in Section 7.6, ash from that eruption formed a significant microtephra layer within the lake core.

6.1.1.2 Vatnsfjörður Homefield samples

Drs Eileen Tisdall and Ian Simpson (University of Stirling) cored the Vatnsfjörður homefield during the 2008 field season. This section of peat was chosen for study because of the relationship between the homefield and the Vatnsfjörður farmstead, which is described in depth in Section 4.2.3. Drs Tisdall and Simpson used a plastic tube 50cm in length and 5cm in diameter and forced it into the ground in order to collect the sample. Dr Tisdall and her student Rebecca Barclay then sampled the length of the core for pollen before sending it to the RLAHA for tephrochronological research. There, it was sampled in continuous 2 cm sections. A sediment log of the core is shown in Figure 6.3.

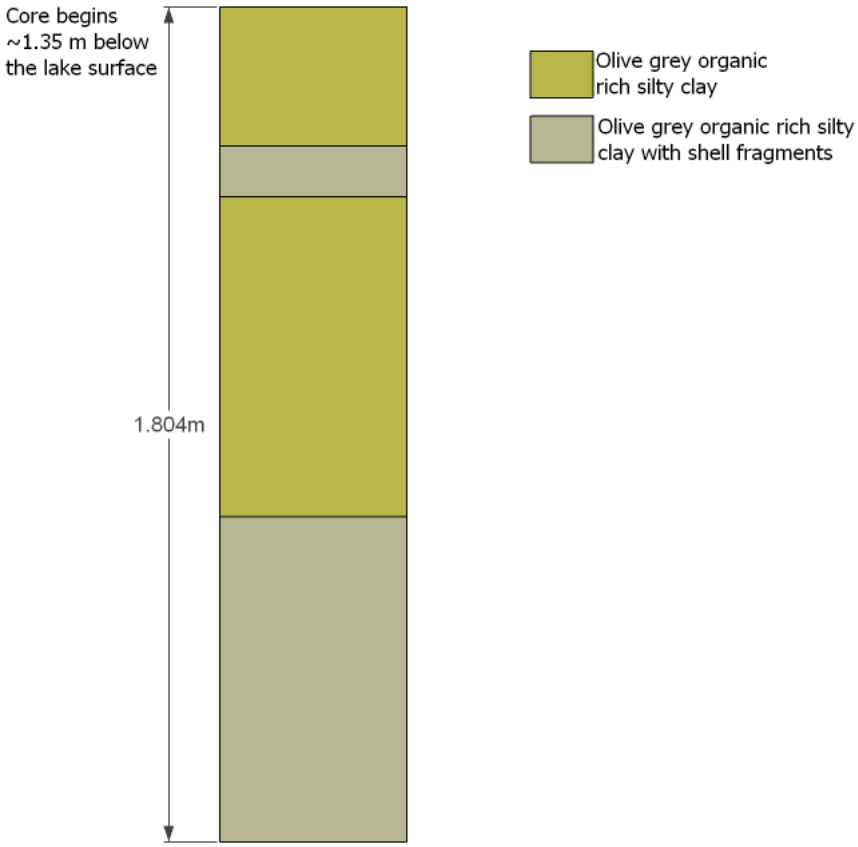


Figure 6.2: Sediment log of Sveinhúsavatn core.

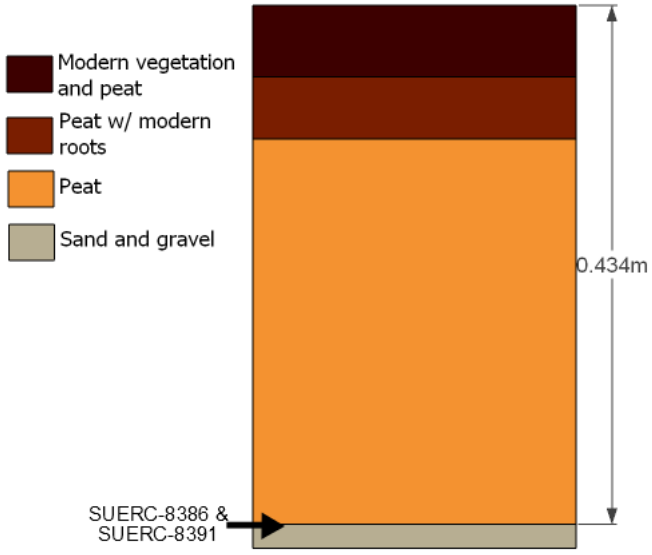


Figure 6.3: Sediment log of Homefield core.

6.1.1.3 Vatnsfjörður visible tephra layer samples

The Vatnsfjörður landscape archaeological research project is described in Section 4.2.1. Ten samples of visible tephra layers from the excavations were taken in bags by various archaeologists in the 2009, 2010, and 2011 field seasons. These samples came from different locations around the site, which is split into a Viking-age area and a farm mound that dates from an unknown time before its abandonment in the first decade of the twentieth century. The locations of the samples within the different areas of the excavations are shown in Figure 6.4, Figure 6.5, and Figure 6.6. One of the tephra layers is shown in situ in Figure 6.7; similar records for each sample are found in Chapter 7.

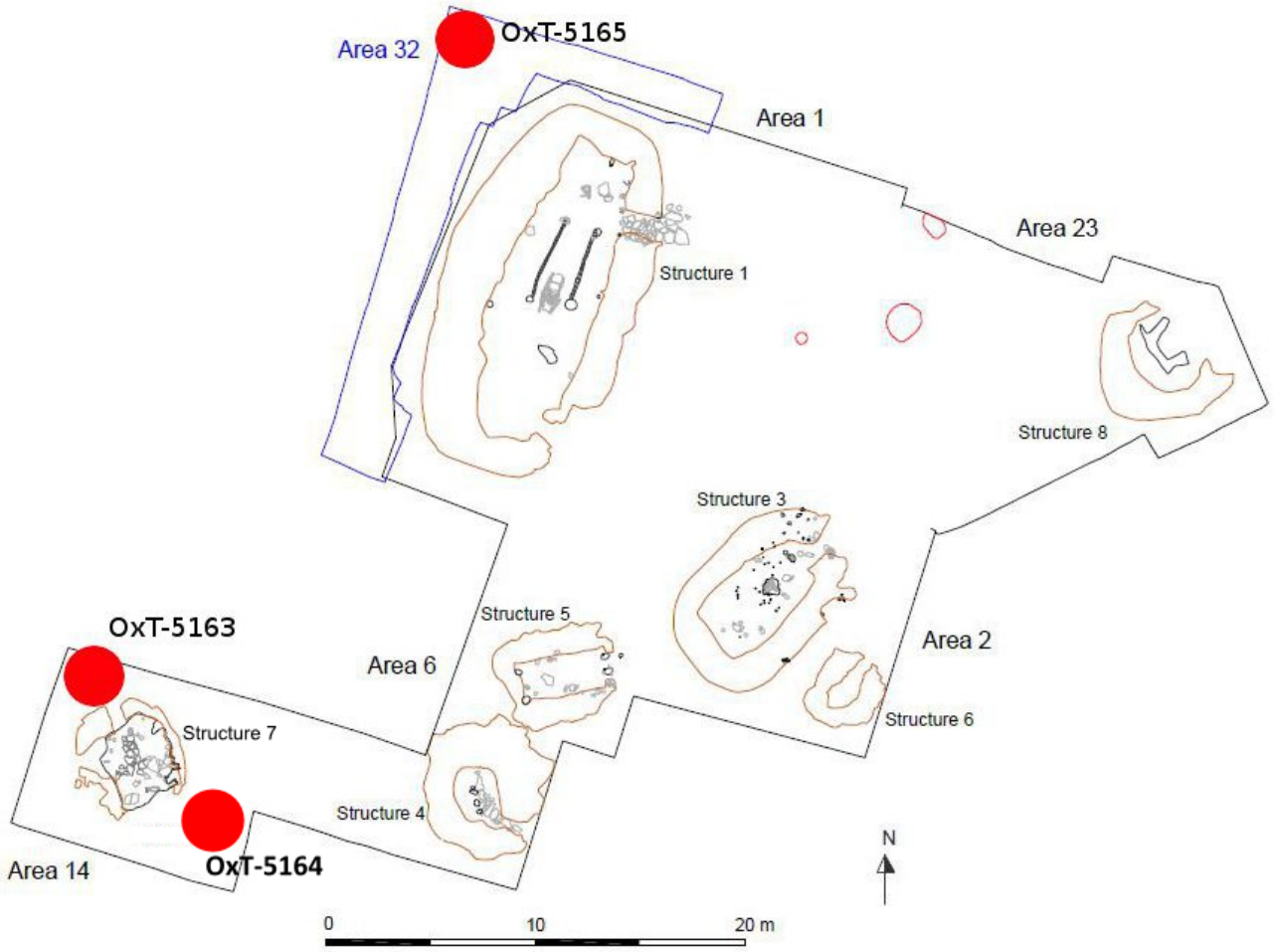


Figure 6.4: Plan of the Viking Age area locations of tephra samples marked in red. The plan shows the buildings (turf walls in brown), structural features such as stones (grey) and post holes (black), and pits (dark red) and is after Milek et al. (2011: 30).



Figure 6.5: Aerial view of the Farm Mound portion of the Vatnsfjörður site, with locations of tephra samples marked in red. The stone walls divide different areas and phases of the mound. Photo from Milek et al. (2011).

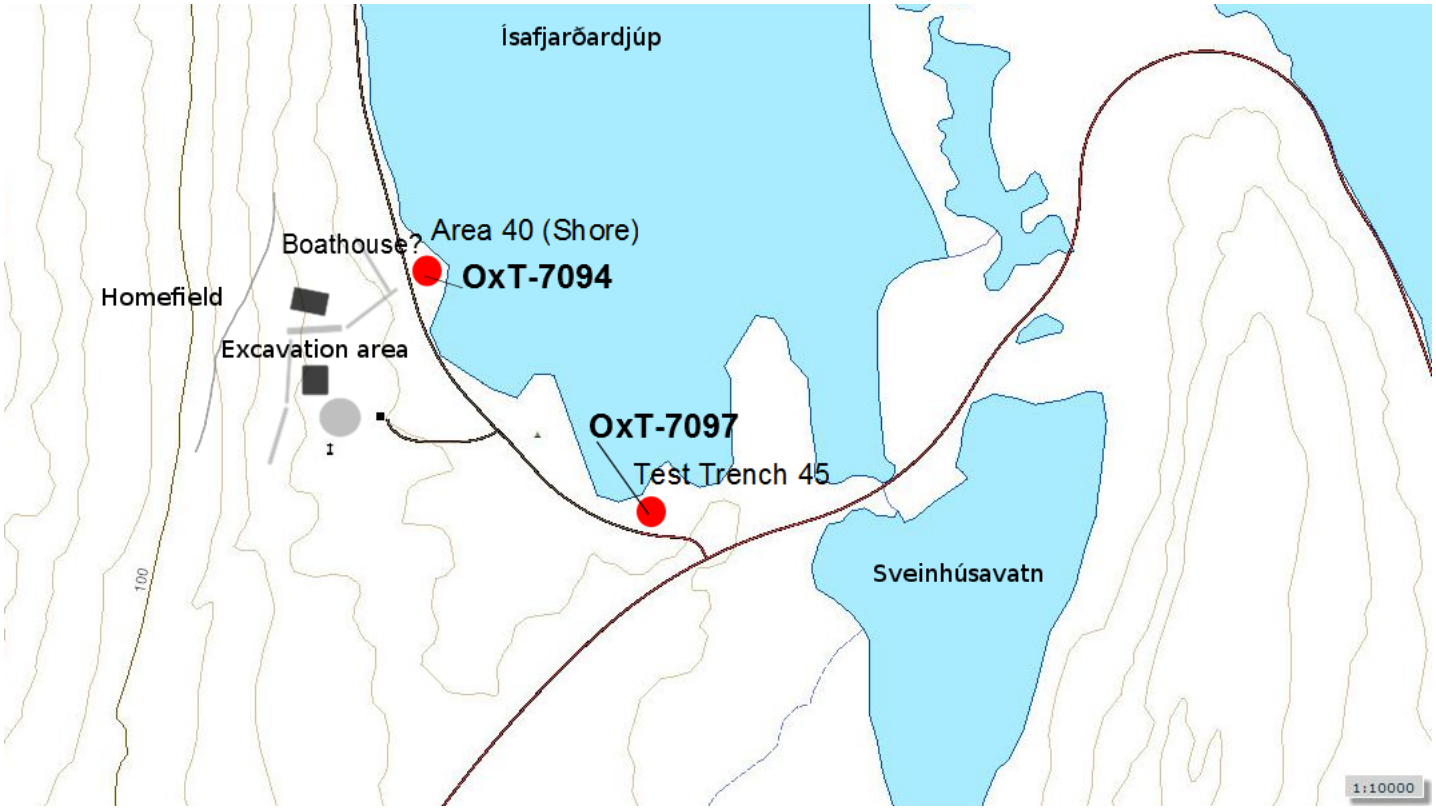


Figure 6.6: Location of Area 40 and Test Trench 45 in relation to the Viking Age and Farm Mound areas (base map source: *Landmælingar Íslands*).



Figure 6.7: In situ photograph of one example of a visible tephra layer from the Vatnsfjörður site, from Milek (2008). Similar visible tephra layers are found throughout the site. One of the goals of the research here was to determine if these tephra layers were the result of the same eruption or represent multiple eruptive events.

The sample labelled OxT-5163 was taken from the tephra layer visible in the section exposed on the edge of excavation area 14, and the sample labelled OxT-5165 was taken from the section exposed on the edge of excavation area 32, which is next to the Viking Age house (the *skáli*). I found that OxT-5164, although it was sampled and tested, was not in fact a tephra layer at all. It is from black sand that is part of the turf that formed the walls of structure 7 in the Viking Age portion of the site. The turf was reddish and may have been from a bog off-site, so preservation conditions may have caused the sand to look black (Karen Milek, pers. comm., 1 July, 2009). OxT-5166 came from context 10661 in Group 10515 in the Farm Mound. OxT-7099 was taken from within a turf cutting in a turf collapse layer on the Farm Mound, from context 10602 in Group 8562. OxT-7095 came from Group 10515. OxT-7098 came from Structure 10662 in Context 10605 (Oddgeir Isaksen, pers. comm., 16 October, 2011). OxT-7097 came from Test Trench 45, which is located along the shore southeast of main excavation areas; OxT-7094 came from Area 40, also located along the shore, northeast of the main excavations (Dawn Elise Mooney, pers. comm., 1 December, 2011).

Prior to this research, it was unclear what the relationship between these visible tephra layers was, and if they represented the same tephra-producing event or different

ones. In some cases, they had a similar physical appearance: a <1 cm thick greyish black composition that felt silky to the touch. In some other contexts, they were described as greenish or grey-green. In 2006, Magnús Sigurgeirsson, then a student at the University of Iceland, attempted to geochemically identify a similar-looking tephra layer from peat to the east of the archaeological site. However, this did not yield conclusive results (Sigurgeirsson 2006). Although Sigurgeirsson states that the visible tephra layer he sampled is 'from the Hekla system', it is unclear what this means as there is no diagnostic way to define a characterisation for the geochemistry of tephra from the entire volcanic system (e.g. the different geochemistry from Hekla 1104 versus Hekla 1300; see more in Chapter 7). Similarly, although many of the tephra layers found throughout the excavations have a similar appearance in situ, appearance is not a diagnostic characteristic for tephra. Therefore it is crucial to identify these tephra samples in order to understand the chronology of the site, as well as the relationships of these tephra layers to the site's stratigraphy. A large tephra fall may also have had an impact on life at the farm, which can be investigated by the identification of these tephra layers.

The turf construction that characterises the Farm Mound may be considered as a complication when interpreting the position of tephra layers relative to the actual chronology of the site, as is discussed further in Section 7.1. Stratigraphic diagrams showing the location of each tephra layer within the site's stratigraphy are also in Section 7.1.

6.1.1.4 Kaldalonsjökull

The environmental core from Kaldalonsjökull is described in Section 4.2.4. Approximately 50 samples in 2 cm intervals were collected in the summer of 2010 from an exposed peat slope near Kaldalonsjökull, which is across the fjord and slightly north from Vatnsfjörður. The samples were collected in bags to a depth of 192 cm. The samples could not be collected continuously because of rocky and sandy intrusions through the sediment column. The sediment log is shown in Figure 6.8. There were no visible tephra layers within this peat. The samples arrived at Oxford in July 2010.

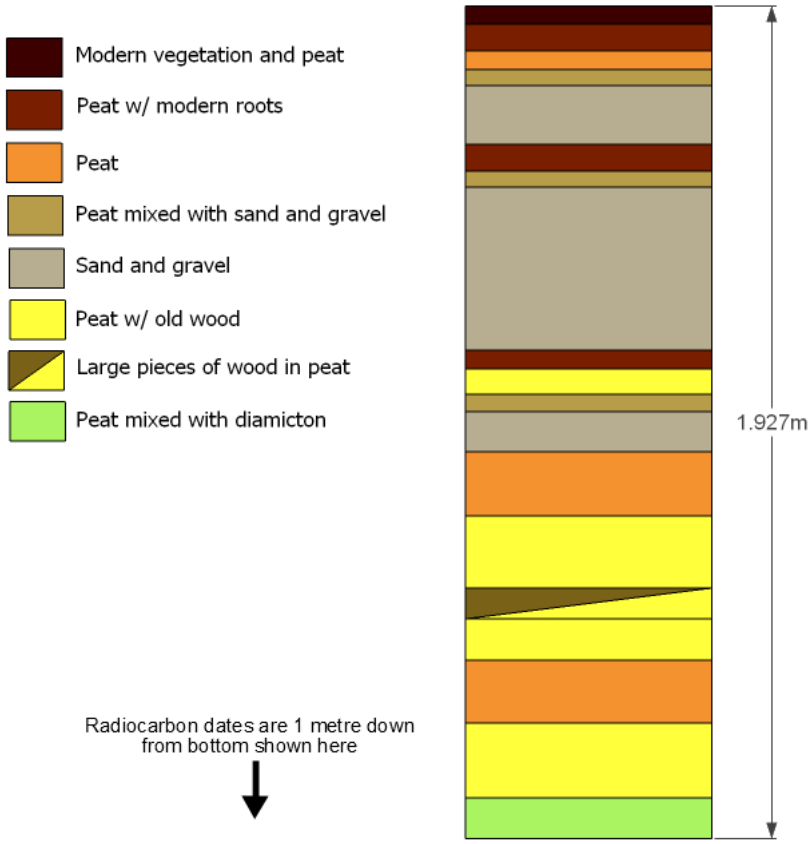


Figure 6.8: Sediment log of Kaldalonsjökull core.

6.1.2 Orkney

6.1.2.1 East Mound samples

The East Mound, part of the Birsay-Skaill Landscape Project, is an excavated mound containing a longhouse and its surroundings; it is described more thoroughly in Section 4.3.1. Samples for tephrochronology from the East Mound excavation came from seven stratigraphic sections located in different areas of the site. These samples were taken on the final day of excavation in the 2008 field season (28 August). Within the excavation, they correspond to the diagram of the area shown in Figure 6.9. Samples were taken from SG08 Section 8 (#1 and #2), Section 38 (north face), and #175 and #176 (west face). Labelled photographs of the stratigraphic sections sampled are shown in Figure 6.10, Figure 6.11, Figure 6.12, Figure 6.13, and Figure 6.14. The East Mound, part of the Birsay-Skaill Landscape Project, is an excavated mound containing a longhouse and its surroundings; it is described more thoroughly in Section 4.3.1. Samples for tephrochronology from the East Mound excavation came from

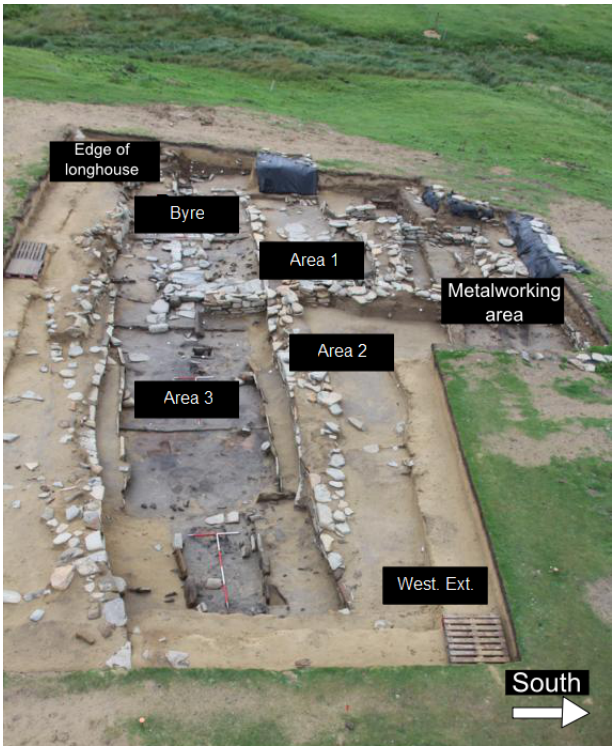


Figure 6.9: Locations of areas discussed in East Mound excavation.

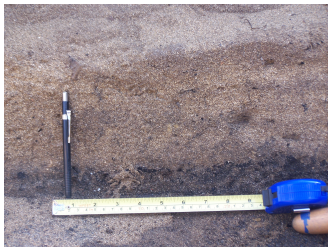


Figure 6.10: Stratigraphy of SG08 Section 8 (from Area 1), #1.

seven stratigraphic sections located in different areas of the site. These samples were taken on the final day of excavation in the 2008 field season (28 August). Within the excavation, they correspond to the diagram of the area shown in Figure 6.9. Samples were taken from SG08 Section 8 (#1 and #2), Section 38 (north face), and #175 and #176 (west face). Labelled photographs of the stratigraphic sections sampled are shown in Figure 6.10, Figure 6.11, Figure 6.12, Figure 6.13, and Figure 6.14.

6.1.2.2 Hobbister A and B and Spretta Meadow samples

The Hobbister A and B and Spretta Meadow peat cores are from southern Mainland, Orkney, and their exact locations are described in Section 4.3.3. These cores were



Figure 6.11: Stratigraphy of SG08 Section 8 (from Area 1), #2.



Figure 6.12: Stratigraphy of SG08 Section 38 (from Area 2).



Figure 6.13: Stratigraphy of SG08, Unit #175 (from the metalworking area).



Figure 6.14: Stratigraphy of SG08, Unit #176 (from the metalworking area).

sampled from for this thesis in August 2009. The sampling method was to take small (<5 g) sediment samples in plastic bags in continuous 2 cm intervals down the length of the Spretta Meadow core (whose sediment was less densely packed than that of the other cores), and to use 2 cm diameter plastic tubes to take a continuous sample down the length of the more solid cores Hobbister A and B. 2 cm intervals were judged to be the smallest unit possible for sampling based on the nature of the sediment in these cores. Further information on these cores is found in Farrell (2010: 239-244).

6.2 Tephrostratigraphies

Following field sampling, the cores and archaeological samples were prepared for visual analysis and shard counting. Tephrostratigraphies are the stratigraphic record of tephra layers, which can be displayed visually as counts of shards per dry weight of sediment per measurement unit within a stratigraphic profile, and are crucial records of tephra and particularly microtephra placement in a landscape. They can provide detailed and useful information not only about the location of particular proximally-correlated tephra layers but also about depositional processes at sampling sites that affect the placement of tephra in the stratigraphic column. For example, large ash fall events often cover wide depositional ranges (e.g. the Borrobol tephra: Pyne-O'Donnell et al. 2008 and others). This has obvious consequences for understanding a tephrostratigraphy and isolating an ash fall event; therefore it should be best practice to publish shard counts as tephrostratigraphies alongside other tephrochronological information. Below, the tephrostratigraphies of the sections sampled for this research are presented.

6.2.1 The results of initial microtephra extraction

As discussed in Section 5.2, each sediment core or archaeological group of samples was initially extracted using the methods outlined by Blockley et al. (2005). This initial tephra extraction was visually scanned with a microscope and two shard counts (described in Section 5.2) were produced and their results averaged in an attempt to make the shard counts less subjective. These shard counts combined with stratigraphic information produced the tephrostratigraphies presented below. Each core or group of sample materials was then re-sampled and re-extracted in areas with relatively high concentrations of microtephra for WDS-EPMA analysis. Amount of

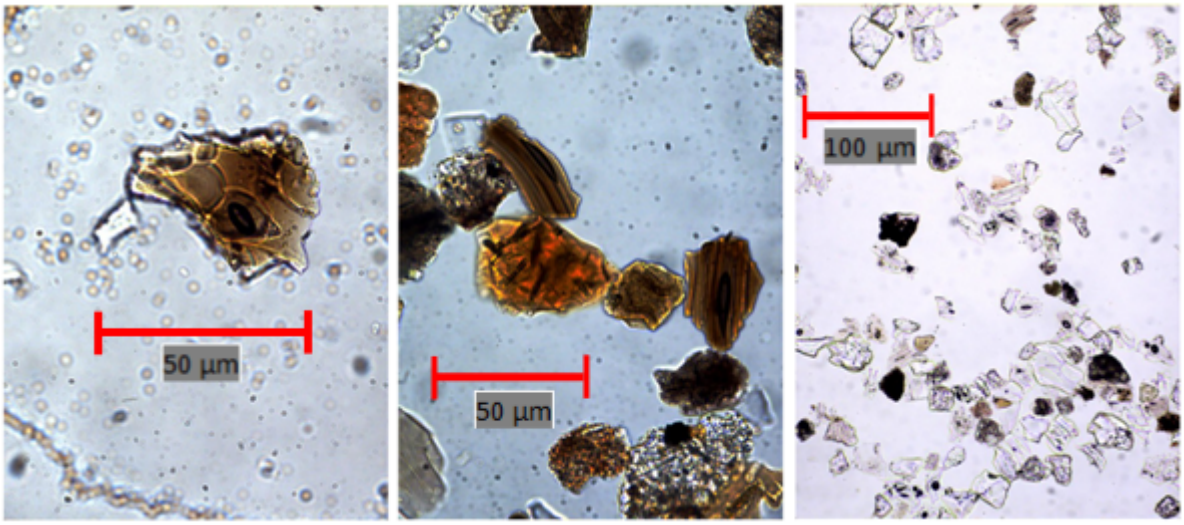


Figure 6.15: Different colours for individual microtephra shards. Left to right: brown, orange (centre, surrounded by brown), clear/white/purple. All photos by the author.

microtephra per sample is given as approximate shards/gram (s/g). Throughout this section, individual tephra shards are often described by colour. The most common are clear/white/purple, brown, and orange. Examples of each are shown in Figure 6.15. Giving colour descriptions are standard practice in tephra research (e.g. Larsen et al. 2001); colour descriptions are sometimes used to denote the SiO_2 percentage of the shards (with white /clear indicating a higher relative percentage than brown) but because that would be assigning an objective label to what is in reality my subjective judgment of individual shard colouration, that will not be done here.

6.2.1.1 Iceland

Sveinhúsavatn (OxT- 4308, 4309, 4310, 4682, 4685): This core was sampled in 5 cm increments, which corresponds to the foram study discussed in Section 7.6, and is common practice for tephra studies of lacustrine cores (e.g. Caseldine et al. 2003). At that resolution, there were four pronounced peaks of microtephra, three smaller peaks,[1] and a generally low but constant background signal of microtephra,[2] as shown in Figure 6.16. Visual inspection during scanning indicated that three of

[1]What constitutes a 'peak' of microtephra is related roughly to proximity to volcanic sources and therefore depth of ash fall. For example, a 'peak' in Orkney, as is discussed later, may be several orders of magnitude smaller than a 'peak' in Iceland.

[2]The issue of microtephra background signals is a matter of interpretation and is discussed at length in Chapter 7.

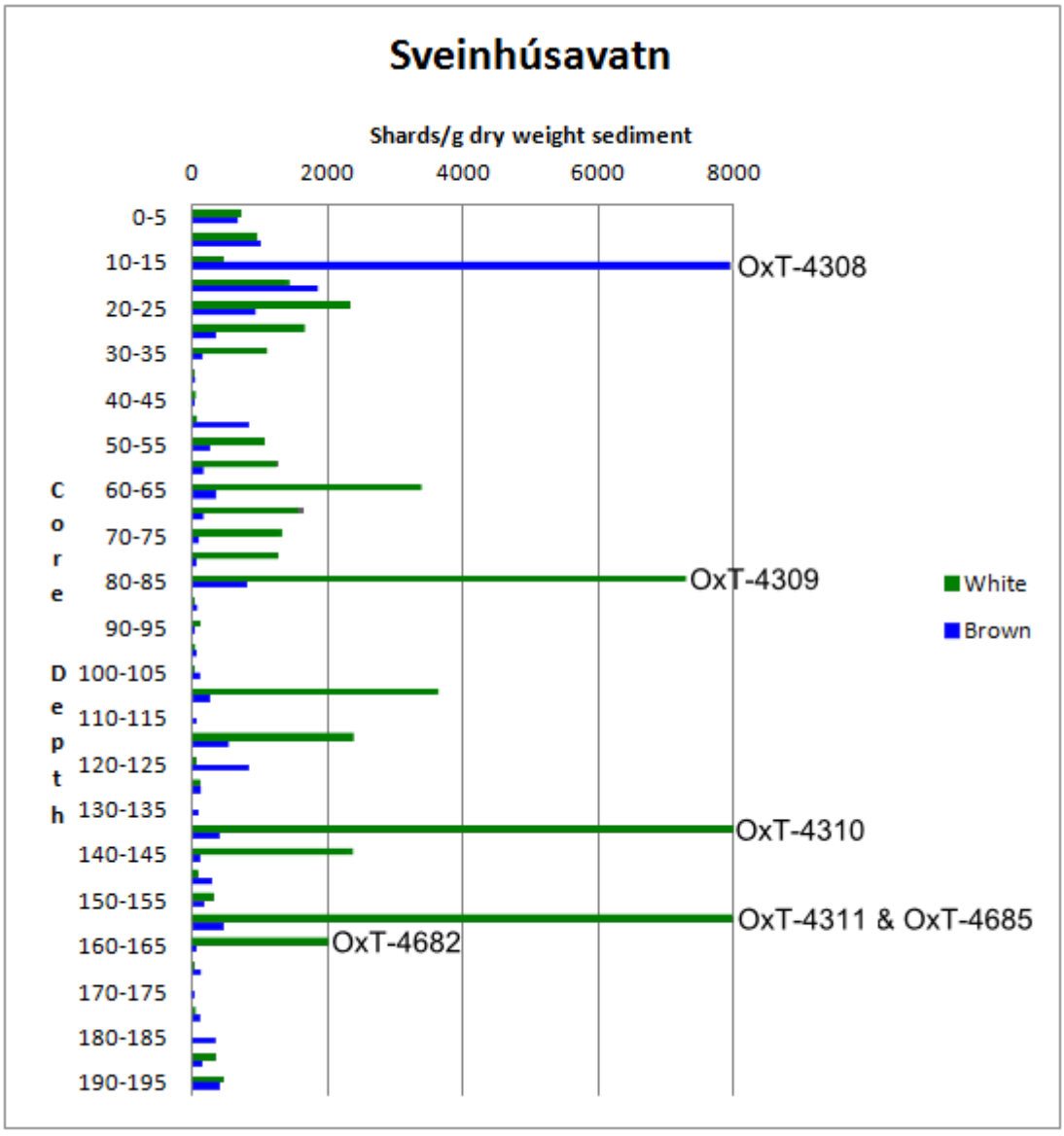


Figure 6.16: Tephrostratigraphy for Sveinhúsavatn; shard counts that appear to be exactly 8000 are actually >8000. The smaller peak at 160-165 cm (OxT-4682) was chosen for study after the four largest peaks because of an unclear correlation for OxT-4681, which is discussed in Chapter7.

these peaks were composed chiefly of white /clear vitreous shards, whilst the fourth was primarily brown in composition. The lowest (earliest) peak, designated OxT-4685 for WDS-EPMA and located between 155-160 cm within the core, is a white/clear layer with >8000 s/g.[3] It is immediately preceded in the core by a much smaller peak at 160-165 cm (OxT-4682); it is immediately followed by a sharp decrease to 80 s/g at 150-155 cm. The next peak (OxT-4310) follows a similar shape: a sudden rise in white/clear tephra at 140-145 cm, and then a steep increase at 135-140 cm, again of >8000s/g, followed by a complete absence of white/clear tephra from 130-135 cm. The next peak chosen for single grain WDS-EPMA analysis is also white/clear, at 80-85 cm (OxT-4309). This also has a concentration of >8000 s/g. While it has no microtephra in the layer immediately preceding it, the layers above it form a curve around a lower peak, from 45-80 cm. The final peak chosen for WDS-EPMA analysis is brown, from 10-15 cm (OxT-4308). This peak is the pronounced part of a rough bell curve of brown shards that ranges from 30-35 cm to the top of the core, at 0-5 cm. The peak itself is >8000 s/g.

The shape of the peaks between 140-145 cm and 155-160 cm suggest that they represent single ash deposit events with discrete start- and end-points. Although the sediment core appeared to be of uniform composition visually, it may be that lower in the core, conditions were such that microtephra could shift downwards over time. Another explanation for the stepped peaks may be that ash fall events started with a lower density of ash and then had an increase in ash production (Larsen et al. 2001). However, the chronological resolution necessary to show such a sudden change is almost certainly not possible in this record.

The third peak, from 80-85 cm, rises abruptly and then has a long and uneven tail of white /clear shards in higher (later) layers of the core. This may indicate a long-lasting eruption with a strong initial event (Dugmore et al. 1995). Alternately, it may indicate a depositional event that was initially catastrophic (such as the melting of a decades-old permanent ice cover, something proposed by Davies et al. (2007) for lakes in Sweden), followed by a period of annual deposition from water sources. This idea is revisited in Section 7.6.

While brown shards are found throughout the core in consistently small numbers (with the exception of the peak at 10-15 cm), the distribution of white/clear shards shows much greater variability throughout the core. This may relate to relative mass

[3]Although 8000 seems like an arbitrary number, it is because the slides are manually divided into eights in the visual counting process.

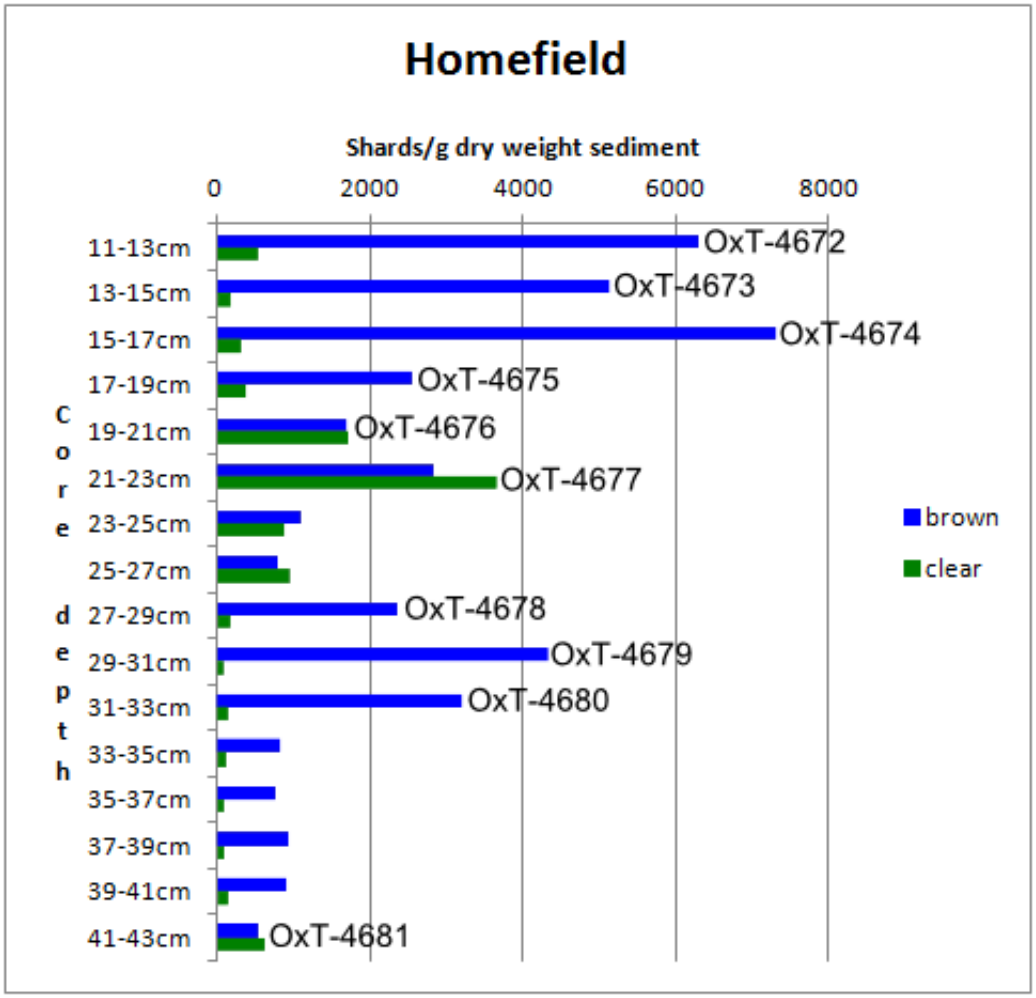


Figure 6.17: Tephrostratigraphy for the Homefield core.

differences between the compositions and settling within the sediment column (e.g. Tomlinson et al. 2010); alternately, Pollard et al. (2006) suggest that basaltic tephra are less chemically stable and may break down in certain depositional environments.

Vatnsfjörður homefield (OxT-4672, 4673, 4674, 4675, 4676, 4677, 4678, 4679, 4680, 4681): The Vatnsfjörður homefield is described in Section 4.2.3, and the sediment log is in Figure 6.3. The tephrostratigraphy for this core is shown in Figure 6.17. This was a peat core, and so it was sampled at 2 cm resolution, which is standard practice for peat cores sampled for tephrochronology. The homefield core ranges from 6-43 cm and contains vitreous microtephra shards ranging in colour from white/clear to dark brown. The section from 6-11cm was not sampled due to severe bioturbation from grass roots throughout the top of the core. The homefield core

contained microtephra throughout its length but it also had clearly defined peaks, much like the Sveinhúsavatn core.

The stratigraphic and chronologic bottom of the core, 41-43 cm (OxT-4681) was re-extracted for WDS-EMPA, but the section of the core from 33-41 cm was not because of its low levels of tephra relative to the rest of the core. Based on the tephrostratigraphy above it, it most likely represents the bottom edge of a curve of tephra that continues upwards through the core to approximately 25 cm, with a microtephra concentration of approximately 4200 s/g at its peak, 29-31 cm (OxT-4678, OxT-4679, and OxT-4680). The section from 23-27 cm contained a relatively small amount of microtephra and so was not sampled for microprobing. At 21-23 cm, there is another peak of microtephra, with approximately 3700 s/g (OxT-4677); this appears to be part of an uneven curve ranging from 17-21 cm (OxT-4675 and OxT-4676). As a result, the section from 11-17 cm (OxT-4672, OxT-4673, and OxT-4674) may represent the middle of an ash fall event following a curved distribution, with the uppermost layer not having been extracted and scanned because of the likelihood of disturbance by extensive root movement. It may also represent two distinct tephra layers chronologically close enough to have some overlap. Again, however, this is speculation based on the tephrostratigraphy.

Initially, it was not clear why the homefield has such a consistently small background signal of microtephra. Although it did not necessarily impact the ability to correlate the peaks with known eruptions, I speculated that it may have been a sign of post-depositional effects, like water movement within the sediment column that shifted microtephra between layers. If this were the case, it may have had implications for tephra and pollen studies. The resolution to this issue is discussed in Section 7.3.

In order to better understand the tephrostratigraphy of the homefield, I compared it to a peat core that was unlikely to have experienced anthropogenic effects. This is the core from Kaldalonsjökull whose tephrostratigraphy is discussed in Section 6.2.1.1. The addition of a second peat core from Vestfirðir to the study also contributed the goal of creating chronologies that link archaeological and environmental records.

Archaeological site: In addition to microtephra layers, there were also ten visible tephra layers within the archaeological stratigraphy at Vatnsfjörður targeted for geochemistry. These are described in Section 6.1.1.3, and are shown in stratigraphic profile in Section 7.1.1.

Kaldalonsjökull: This peat core is described in detail in Section 4.2.4, and a sediment log is shown in Figure 6.8. An initial scan in 6 cm intervals revealed that there was microtephra in peat layers throughout the core, so the core was scanned again at the higher resolution of 2 cm. The tephrostratigraphy of the core, derived from the 2 cm scan, is shown in Figure 6.18. This only shows the sections of sediment that could have contained microtephra, with breaks for rock /gravel layers excluded. These rock /gravel layers likely represent glacial incursion over the study area as the size and placement of the Kaldalonsjökull glacier shifted over time (Sarah Principato, pers. comm.).

The core from Kaldalonsjökull did not have any visible tephra layers, but it did have nine peaks that had a relatively high shard count compared to the rest of the core. It also had a section between 79 cm and 90 cm that had a continuous high concentration of microtephra. The core was only sampled for microtephra to 108 cm because radiocarbon dates on nearby peat sections suggested that the base of the 192 cm core would date to roughly 2500 cal BP (Sarah Principato, pers. comm. 10 August, 2010). Similar to the cores from the homefield and Sveinhúsavatn, there is also a background signal of microtephra present in this core, but as Figure 6.18 shows, several discrete peaks are discernible. The earliest (lowest) from the sampled section is from 103-106 cm. This layer is immediately below a thick layer of gravel, so the peak seems isolated. The next peak is from the cluster of high microtephra density between 79 cm and 90 cm. Visual scanning indicated that the topmost portion of this – the segment between 79 cm and 82 cm – was composed of clear shards that were very fragmentary. Otherwise, these layers look similar under the microscope. Above that, there is another break in sediment between 42 cm and 78.5 cm. There is a small peak composed of brown shards from 36-38 cm. There is another peak that may have distributed shards in the 4 cm below it at 12-14 cm. The highest peak is between 8-10 cm from the top of the core and contains both clear and brown shards, although the majority are clear.

There does not seem to be a persistent background signal and visual inspection of the layers suggests that the microtephra within them are of different compositions (e.g, some layers have microtephra consistently more vesicular than others). I chose several of the peaks described for WDS-EPMA to further understand the tephrostratigraphy of this core and area.

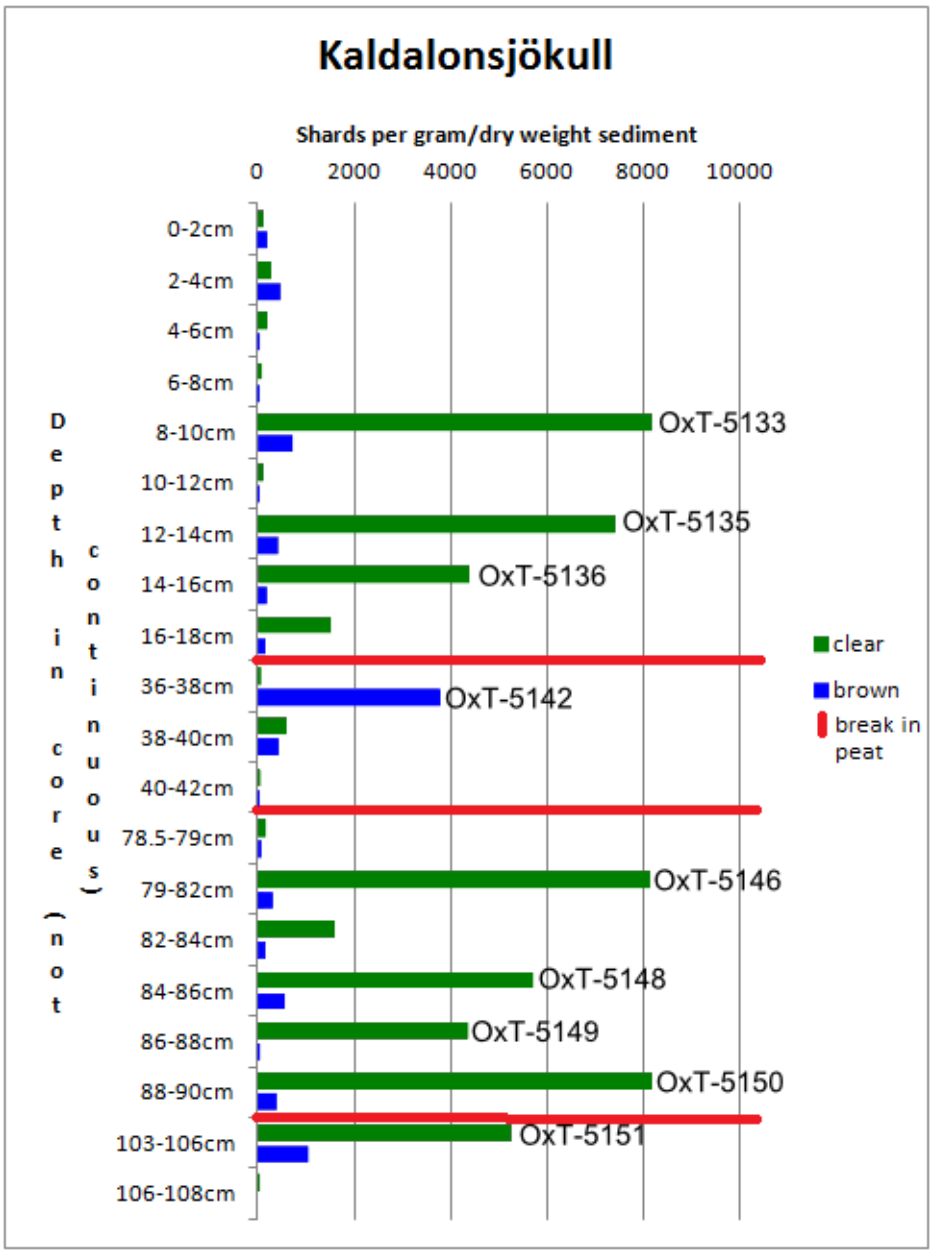


Figure 6.18: Tephrostratigraphy for Kaldalonsjökull; red lines indicate a break in sediment collection due to sand/gravel layers.

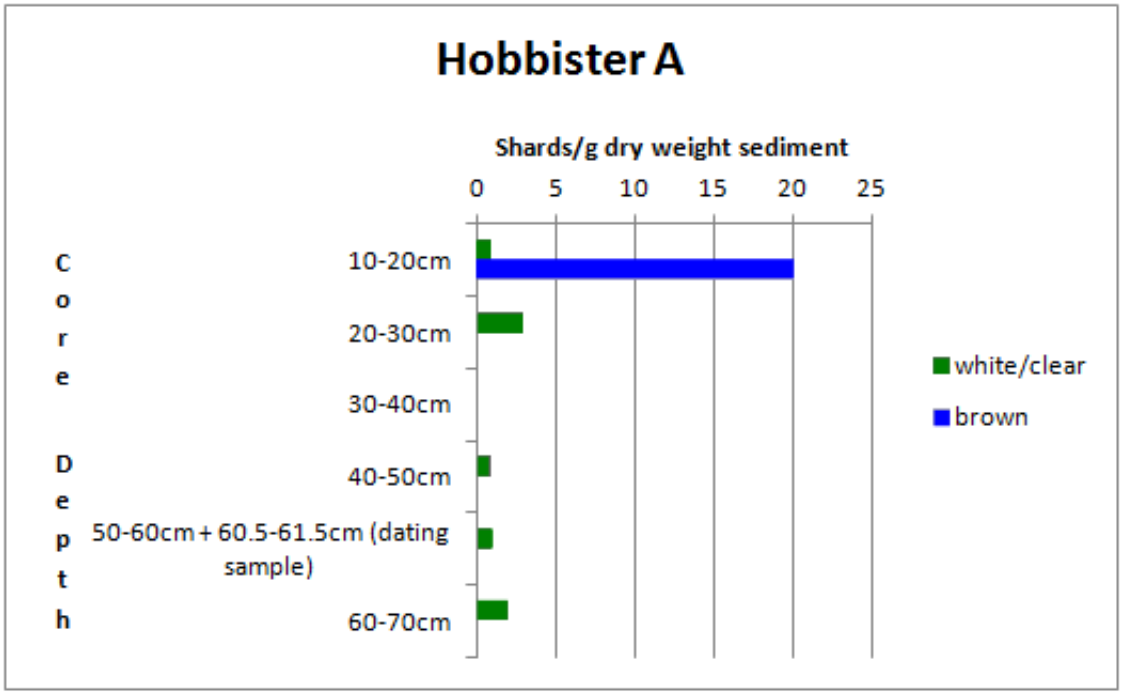


Figure 6.19: Tephrostratigraphy for Hobbister A.

6.2.1.2 Orkney

East Mound The East Mound samples were extracted twice, but both times no microtephra were found during visual scanning with the microscope. Although it seems likely that microtephra fell in the area sometime in the past because of nearby tephra finds (e.g. Dugmore et al. 1995; Bunting 1996; and the microtephra found by me in the Hobbister and Spretta Meadow samples), the relatively fragile shards were probably destroyed post-deposition. Sediments throughout the archaeological excavation contained a large amount of sand, as is discussed in Section 4.3.2, and this abrasive composition likely led to the breakdown of any microtephra.

Hobbister A and Hobbister B (OxT- 4765, 4766, 4767, 4770): Cores Hobbister A and Hobbister B are described in Section 4.3.3. These samples contained very low concentrations of microtephra and very little background signal, as is consistent with other microtephra studies from the British Isles (e.g. Hall et al. 1994; Housley et al. 2010). As a result, they were sampled at 10cm intervals to try to maximise the amount of tephra available per section for WDS-EPMA. The results of visual scanning and shard counting are in Figure 6.19 for Hobbister A and Figure 6.20 for Hobbister B.

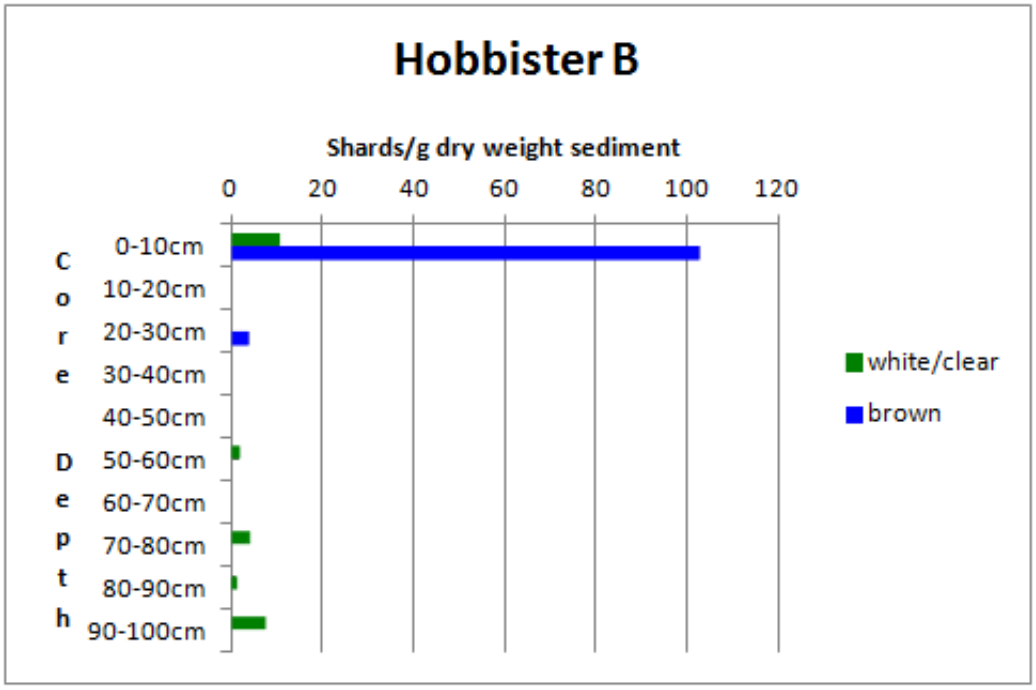


Figure 6.20: Tephrostratigraphy for Hobbister B.

Hobbister A contained a small number of white/clear shards scattered throughout the core (around 2-6 s/g), and a single peak near the stratigraphical and chronological top of the core, from 10-20 cm, with around 40 s/g. Hobbister B, likewise, contained a small number of white /clear shards, with three peaks around 6 s/g. In the core, the lowest of these is from 90-100cm, with approximately 14 s/g of white/clear shards. From 20-30 cm, there is a concentration of approximately 8 s/g, again composed of white/clear shards. The most notable peak from any of the Orkney samples comes from 0-10 cm within the core, with a concentration of approximately 20 s/g of white /clear colour and approximately 200 s/g of brown colour. This, along with the peak from 10-20 cm in Hobbister A, is notable due to the rarity of known mafic distal microtephra. This is discussed further in Section 8.2.

It seems likely that the peak in Hobbister A, from 10-20 cm, is the tail end of the event that is recorded in Hobbister B from 0-10 cm. However, unfortunately the top of Hobbister A had suffered in storage, and could not be reliably sampled. The soil from the top 10 cm of Hobbister A may have been compressed into the 10-20 cm range, leading to the small peak of microtephra.

A sample from the peak in Hobbister A could not be obtained during re-extraction for microprobe mounting, most likely due to the small concentration of microtephra

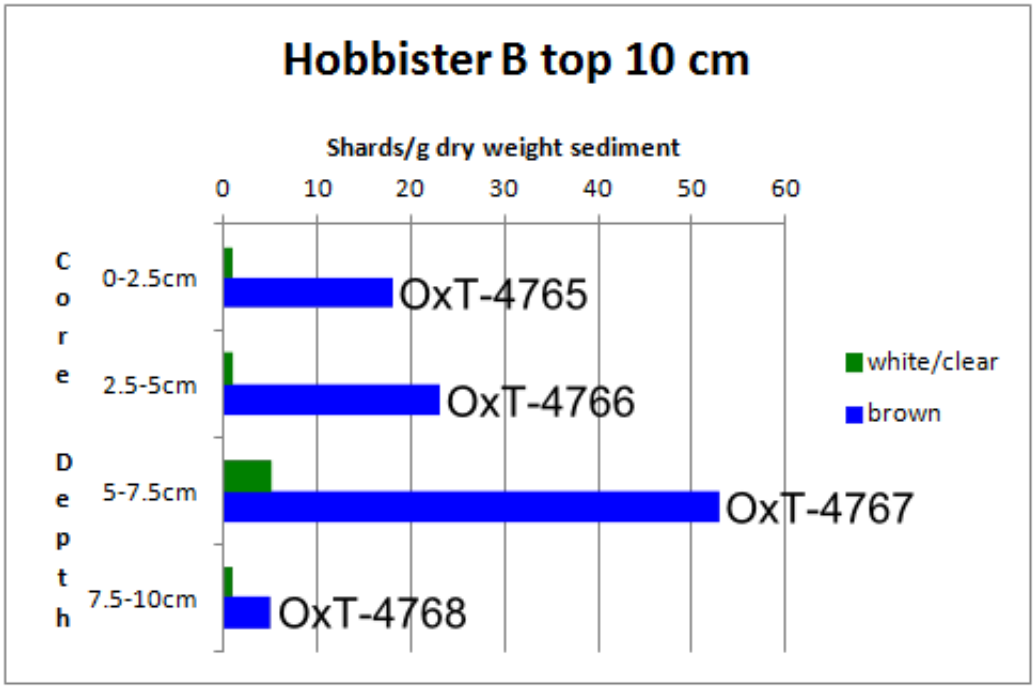


Figure 6.21: Tephrostratigraphy for the top 10 cm of Hobbister B.

in the original sample. In order to increase resolution, and therefore usefulness as a chronological tool, the peaks in Hobbister B (0-10 cm) were divided into 2.5 cm, re-extracted, and targeted for WDS-EPMA. Figure 6.21 shows the shard count for the 0-10 cm portion of the core. OxT-4765 corresponds to 0-2.5 cm; OxT-4766 to 2.5-5 cm; OxT-4767 to 5-7.5 cm; and OxT-4768 to 7.5-10 cm. A fifth sample from Hobbister B, OxT-4770, was successfully extracted and mounted for microprobing; this corresponds to 42.5-45 cm within the core.

The Hobbister A and Hobbister B samples relate to cores that have had a number of radiocarbon dates, which are listed in Table 4.3. One of these radiocarbon dates bounded the potential tephrochronological sources for these samples with a date of 1230±30 BP at a depth of 80 cm. This provided a lower boundary for possible microtephra-derived dates in the cores.

Spretta Meadow (OxT- 4774): Similar to the samples from Hobbister A and B, Spretta Meadow yielded extremely low shard counts. It had three peaks larger than approximateluy 6 s/g. These are shown in Figure 6.22. The most notable of these was from 30-40 cm, with approximately 35 s/g of white/clear colour. The other two were from 60-70 cm (approximately 14 s/g, white/clear) and 80-90 cm (approximately

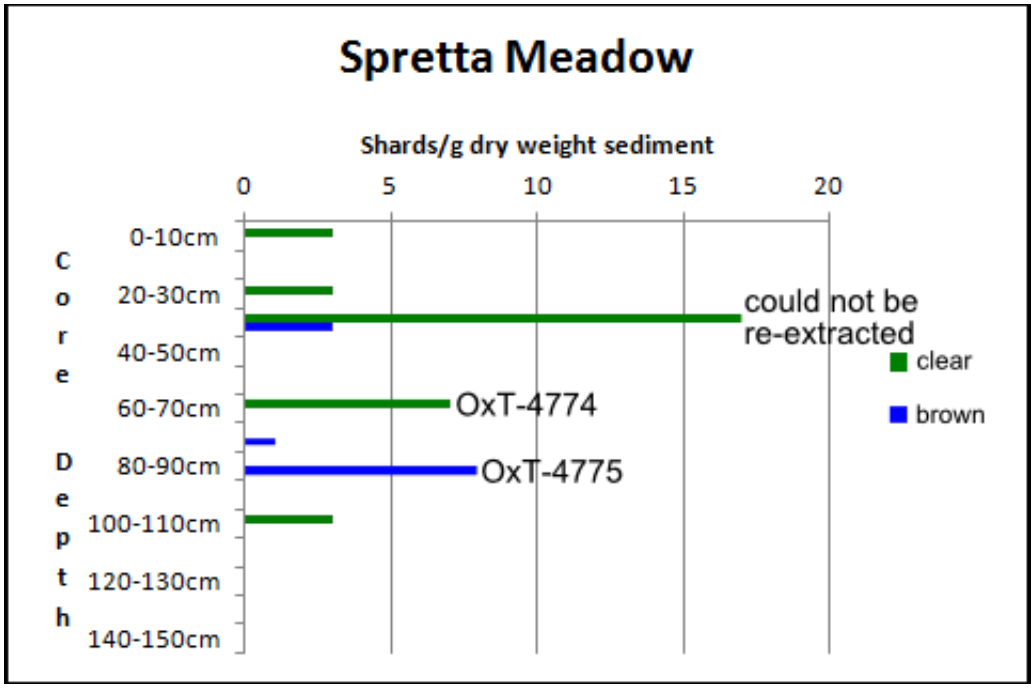


Figure 6.22: Tephrostratigraphy for Spretta Meadow.

16 s/g, brown). Only one sample could be successfully re-extracted for WDS-EPMA from the Spretta Meadow core, and that came from 60-70 cm (OxT-4774). This highlights one of the limitations of distal tephrochronology: the method relies upon the vagaries of the sampled material, and, with such low densities of microtephra, it is understandable that it may not always be possible to re-extract enough for a successful analysis. Unless a different extraction method becomes available, this does not seem likely to change, and is an acknowledged (or sometimes unacknowledged but obvious) problem in many distal tephra studies (e.g. Hall and Pilcher 2002; Balascio et al. 2010; and discussed by Payne et al. 2005).

Conclusions The small quantity of microtephra in samples from Hobbister A, B, and Spretta Meadow was not unexpected, and has precedent in a number of microtephra studies from the British Isles (e.g. Pilcher and Hall 1992; Dugmore et al. 1995; Rea et al. 2012). The stepped shape of the shard counts when graphed versus position in the cores may relate to the lower resolution of sampling – there may be curves with defined peaks present, rather than single peaks, but they are indistinguishable at 10 cm. The low numbers of shards within each peak suggest that increasing the resolution of the study to 5 cm or more would not have provided new information given the constraints of WDS-EPMA for shard size and quantity.

6.2.1.3 Summary

The tephrostratigraphies presented here demonstrate some of the challenges facing researchers studying distal tephrochronology. One of the most notable differences between the different sample sets here lies in the level of resolution that it is possible to obtain when sampling from cores; the precision of the chronology is greatly enhanced by heightened resolution, but this is sometimes not possible due to the physical condition of sample materials. This is particularly influenced by sediment type – i.e., sediment that is crumbling or sandy will be more difficult to divide into smaller sections than sediment with a high percentage of clay. Perhaps even more crucial to establishing a precise chronology is the ability to determine peaks and curves in the shape of shard distributions throughout a core. Several authors have written about some of the possibilities that these shapes represent: mapping the different stages, both in terms of composition and ash concentration, of an eruption that may have lasted for a year or several years; determining shifting of ash within the sediment column; or marking melting events that trap ash for seasons or years and then release it (i.e., Blackford 2000; Davies et al. 2007; Davies et al. 2010).[4] Although a reliable, high-resolution sample set is desired, it is not always possible to obtain this.

As shown by the samples from the Vatnsfjörður homefield, an excess of microtephra in a sediment column can result in confusing data. The method of shard counting itself relies upon visual assessment under a microscope and therefore is subjective, particularly when there are high concentrations of microtephra; it may be impossible to distinguish peaks due to the sheer number of individual shards. Overlaying of potential ash fall curves as well as a strong background signal may also contribute to several competing explanations for the deposition of microtephra in samples. The determination of what might have caused a strong background signal is crucial to the interpretation of tephrochronology for a core. This is discussed further in Section 7.3.

6.2.1.4 Layers targeted for WDS-EPMA

Using the tephrostratigraphies above, several layers were chosen for WDS-EPMA analysis. These are shown in Table 6.1.

[4]This is discussed more in Chapter 9.

Table 6.1: Stratigraphic and archaeological layers targeted for WDS-EPMA. Sample numbers labelled 'Successful?' had enough WDS-EPMA analyses that survived data filtration (discussed in Section 5.4.1) to be used for identifying the distal microtephra.

OxT-	Location	Depth	Successful?
4308	Sveinhúsavatn	10-15 cm	yes
4309	Sveinhúsavatn	80-85 cm	yes
4310	Sveinhúsavatn	135-140 cm	yes
4672	Homefield	11-13 cm	yes
4673	Homefield	13-15 cm	no
4674	Homefield	15-17 cm	yes
4675	Homefield	17-19 cm	yes
4676	Homefield	19-21 cm	yes
4677	Homefield	21-23 cm	yes
4678	Homefield	27-29 cm	no
4679	Homefield	29-31 cm	yes
4680	Homefield	31-33 cm	yes
4681	Homefield	41-43 cm	yes
4682	Sveinhúsavatn	160-165 cm	yes
4685	Sveinhúsavatn	155-160 cm	yes
4765	Hobbister B	0-2.5 cm	yes
4766	Hobbister B	2.5-5 cm	yes
4767	Hobbister B	5-7.5 cm	yes
4768	Hobbister B	7.5-10 cm	no
4769	Hobbister B	40-42.5 cm	no
4770	Hobbister B	42.5-45 cm	no
4771	Hobbister B	45-47.5 cm	no
4772	Hobbister B	47.5-50 cm	no
4773	Hobbister B	90-100 cm	no
4774	Spretta Meadow	60-70 cm	no
4775	Spretta Meadow	80-90 cm	no
5133	Kaldalonsjökull	8-10 cm	yes
5135	Kaldalonsjökull	12-14 cm	yes
5136	Kaldalonsjökull	14-16 cm	yes
5142	Kaldalonsjökull	36-38 cm	yes
5146	Kaldalonsjökull	79-82 cm	no
5148	Kaldalonsjökull	84-86 cm	yes
5149	Kaldalonsjökull	86-88 cm	yes
5150	Kaldalonsjökull	88-90 cm	yes
5151	Kaldalonsjökull	103-106 cm	no
5163	Vatnsfjörður	Area 14	yes

Continued on next page

Table 6.1 — continued from previous page

OxT-	Location	Depth	Successful?
5164	Vatnsfjörður	Farm Mound	no
5165	Vatnsfjörður	Area 32	yes
5166	Vatnsfjörður	context 10661 group 10515	yes
7094	Vatnsfjörður	context 10602 in Group 8562	yes
7095	Vatnsfjörður	Group 10515	yes
7097	Vatnsfjörður	Test Trench 45	yes
7098	Vatnsfjörður	Context 10605 (structure 10662)	yes
7099	Vatnsfjörður	Area 40	yes

6.3 WDS-EPMA data: Major and minor element composition of samples

All unfiltered geochemical data are available in Appendix 1, and there are summary tables in each section below. The data presented in the summary tables has been filtered according to the criteria described in Section 5.4.1. Due to the possibility that each of these samples represents a geochemically variable tephra layer, each will be described individually in this section.

As noted in the text above, some of the samples have multiple colours of glass, with white/clear/purple and orange/brown shards found in almost all samples. For WDS-EPMA analysis, there may be a sampling bias towards darker shards as they are easier to recognise visually during the single-grain targeting of the microprobe. Initially, it seemed as if the colouration of the shards would have some bearing on the geochemical results, but, perhaps due to the subjectivity of the viewer, they did not consistently correspond to geochemistry. However, attempts have been made to represent both, particularly for stratigraphic layers where there was a pronounced peak of one colour.

6.3.1 Iceland

6.3.1.1 Sveinhúsavatn

This section describes the glass chemistry of the microtephra peaks extracted from the lacustrine core from Sveinhúsavatn. Figure 6.2 shows the composition of the core, and

Figure 6.16 shows the placement of microtephra layers within the core. A summary table of the glass chemistry data from Sveinhúsavatn is in Table 6.2. Grain size for these samples was 20-80 μm; the composition and characteristics of each sample will be described below.

OxT-4308: This corresponds to 10-15 cm in this core, which had the highest concentration of microtephra in the core. These microtephra were brownish in colour and, like much of the microtephra throughout this lacustrine core, highly vesicular. None of the microtephra here showed any signs of weathering or degradation. The single grains probed here are andesitic or trachy-andesitic. Their SiO_2 values cluster tightly between 57.88 and 59.74 wt-%. They have relatively low TiO_2 values (1.2-1.5 wt-%) and FeO values between 8.67 and 10.02 wt-%.

OxT-4309: This corresponds to 80-85 cm in this core. Microtephra in this sample were highly vesicular and striated, with the result being that although >60 shards were picked for single grain analysis, very few shards had a surface large enough to beam for WDS-EPMA. An example of a vesicular tephra from this layer is shown at 40x magnification in Figure 6.23. None of the microtephra here showed any signs of weathering or degradation. Although during shard counting this particular peak was mostly composed of clear/white glass, a number of brown shards were also included in the WDS-EPMA analysis because, as noted above, these were much easier to visually identify. The shards in this analysis was generally basaltic, with a single rhyolitic and a single trachyandesitic grain. They ranged from 46.81-49.54 wt-% SiO_2, with high FeO of 13.33-14.76 wt-%. Significantly, they have an average TiO_2 wt-% of 3.73, which is generally indicative of a Katla eruption (Lacasse et al. 2006).

OxT-4310: This corresponds to 135-140 cm in this core. This sample contained both brown and white/clear shards; however, these were less vesicular than those of OxT-4309 and therefore a higher number of successful single grain analyses were possible as there were large enough surfaces for beaming with the WDS-EPMA. None of the microtephra here showed any signs of weathering or degradation. Seven of the single grain analyses were basaltic, five were rhyolitic, and one was trachyandesitic. For each compositional group, aside from the single trachyandesitic grain, the samples were fairly homogenous and therefore clearly divided into two groups. Group 1 had SiO_2 wt-% of 49.25-49.75, and a relatively high TiO_2 wt-% of average 2.29. Shards

Table 6.2: Summary WDS-EPMA data (after filtering) for the samples extracted from Sveinhúsavatn. This table shows the average compositional percentage, as well as the numerical range and standard deviation to 1σ. Where applicable, the data have been divided into compositional groups. The data in this table have not been normalised. The full results are available in Appendix 2.

Label		SiO2	TiO2	Al2O3	FeO	MnO	MgO	CaO	Na2O	K2O
OxT-4308	mean	58.81	1.31	15.14	9.34	0.27	1.84	5.27	4.14	1.55
n=16	max	59.74	1.50	16.27	10.02	0.37	2.12	6.00	4.68	1.78
	min	57.88	1.20	14.56	8.67	0.17	1.62	4.71	2.82	1.34
	standev	0.65	0.07	0.43	0.45	0.06	0.14	0.40	0.50	0.13
OxT-4309	mean	48.18	3.73	12.72	14.19	0.21	5.17	9.73	2.99	0.62
n=4	max	49.54	4.66	13.09	14.76	0.38	5.66	10.14	3.34	0.83
	min	46.81	2.87	12.35	13.33	0.05	4.79	9.23	2.67	0.43
	standev	1.27	0.97	0.32	0.66	0.14	0.43	0.43	0.29	0.20
OxT-4310	mean	49.43	2.29	13.31	12.68	0.20	6.43	10.99	2.34	0.29
Group 1	max	49.72	3.08	13.93	14.30	0.28	7.26	11.97	2.66	0.44
n=7	min	49.25	1.68	12.80	11.17	0.13	5.41	9.54	2.10	0.15
	standev	0.15	0.70	0.49	1.39	0.06	0.94	1.19	0.24	0.14
OxT-4310	mean	69.36	0.21	14.94	2.86	0.14	0.08	1.02	5.24	4.68
Group 2	max	69.97	0.25	15.29	2.93	0.17	0.09	1.03	5.41	4.82
n=5	min	68.91	0.17	14.70	2.74	0.11	0.07	0.99	5.09	4.62
	standev	0.53	0.03	0.26	0.07	0.02	0.01	0.02	0.13	0.09
OxT-4682	mean	67.27	0.35	15.17	3.66	0.13	0.20	1.42	5.05	4.37
n=11	max	69.45	0.58	16.40	5.18	0.20	0.47	2.26	5.84	4.72
	min	64.95	0.19	14.42	2.79	0.02	0.07	0.96	3.87	3.76
	standev	1.88	0.15	0.64	0.95	0.05	0.16	0.54	0.67	0.40
OxT-4685	mean	69.34	0.24	14.57	2.92	0.13	0.09	0.98	5.17	4.77
n=5	max	70.00	0.26	15.19	3.19	0.18	0.10	1.10	5.73	5.10
	min	68.26	0.21	13.95	2.78	0.08	0.07	0.84	4.06	4.55
	standev	0.69	0.02	0.55	0.16	0.04	0.01	0.12	0.64	0.23



Figure 6.23: Photograph by the author of microtephra shards from OxT-4308 under 40x magnification.

in Group 2 had SiO_2 wt-% of 64.44-69.97, with an average of 68.54 reflecting the uniformity of all but one sample; TiO_2 values for these shards were very low, with an average 0.27 wt-%.

OxT-4682: This corresponds to 165-170 cm in this core. The peak in shard count for this sample was almost entirely composed of white/clear shards. These shards were vesicular and striated, again making it difficult to find large enough surfaces to beam for single grain analysis. The majority of shards here were white/clear. In terms of glass chemistry, they largely plot to be rhyolitic, but four are trachydacitic. SiO_2 ranges from 64.95-69.45 wt-%. TiO_2, FeO, and MgO are all relatively low, with averages of .35, 3.66, and 0.20 wt-% respectively.

OxT-4685: This corresponds to 155-160 cm in this core. This layer, like all the others from this lacustrine core, had highly vesicular and striated microtephra. In general, this sample was composed of white/clear glass, although brown glass was present; the white/clear glass was specifically targeted for microprobe analysis during the picking stage because of the peak in this type of glass discovered during shard counting. Although there is a low total number of successful single grain analyses (n=6), all but one is rhyolitic. They have a relatively homogenous composition, with

an average SiO_2 wt-% of 68.32; a low average TiO_2 wt-% of 0.29; and low average FeO and MgO wt-%, 3.29 and .16 respectively.

6.3.1.2 Homefield

This section describes the glass chemistry of the microtephra peaks extracted from the peat core from the Vatnsfjörður homefield. For more information on this core, see Section 4.2.3. Figure 6.3 shows the sediment log for this core. A summary table of the glass chemistry data from the homefield is in Table 6.3.1.2. Grain size for these samples was 20-80 μm; the composition and characteristics of each sample will be described below.

Table 6.3: Summary WDS-EPMA data (after filtering) for the samples extracted from the Homefield core. This table shows the average compositional percentage, as well as the numerical range and standard deviation to 1σ. Where applicable, the data have been divided into compositional groups. The data in this table have not been normalised. The full results are available in Appendix 2.

Label		SiO2	TiO2	Al2O3	FeO	MnO	MgO	CaO	Na2O	K2O
OxT-4672	mean	59.91	1.30	15.35	9.22	0.25	1.77	5.32	3.51	1.45
n=15	max	61.18	1.41	16.12	9.70	0.31	1.89	5.48	4.25	1.59
	min	58.55	1.13	14.42	8.07	0.19	1.43	5.04	2.76	1.34
	standev	0.68	0.07	0.40	0.39	0.05	0.15	0.15	0.40	0.08
OxT-4674	mean	58.65	1.36	15.13	9.95	0.27	1.87	5.21	3.58	1.38
n=4	max	59.73	1.43	15.49	10.12	0.40	1.90	5.36	3.64	1.43
	min	57.17	1.26	14.69	9.81	0.20	1.85	5.12	3.53	1.34
	standev	1.32	0.09	0.41	0.16	0.11	0.03	0.13	0.06	0.05
OxT-4675	mean	58.53	1.28	15.17	9.60	0.29	1.84	5.20	3.74	1.74
Group 1	max	59.58	1.43	15.64	10.03	0.37	2.06	5.48	4.18	3.93
n=11	min	56.42	1.17	14.65	8.32	0.22	1.54	4.65	3.10	1.41
	standev	0.97	0.08	0.36	0.53	0.06	0.14	0.25	0.31	0.82
OxT-4675	mean	71.07	0.19	14.55	2.47	0.12	0.09	1.05	4.43	5.07
Group 2	max	72.89	0.25	15.41	3.00	0.20	0.22	1.32	5.59	7.36
n=5	min	69.64	0.09	12.62	1.95	0.03	0.04	0.74	1.94	4.25
	standev	1.48	0.07	1.30	0.50	0.09	0.09	0.24	1.69	1.53
OxT-4676	mean	60.68	1.13	14.81	8.54	0.25	1.28	4.58	4.36	1.86
n=8	max	63.89	1.41	15.79	10.27	0.30	1.97	5.85	5.83	3.13
	min	58.10	0.57	13.58	5.05	0.17	0.51	2.41	3.10	1.33
	standev	2.09	0.35	0.89	1.98	0.05	0.52	1.20	0.96	0.65

Label		SiO2	TiO2	Al2O3	FeO	MnO	MgO	CaO	Na2O	K2O
OxT-4677	mean	49.23	3.65	13.05	14.41	0.20	5.22	9.79	1.20	0.60
Group 1	max	50.91	4.63	13.60	15.12	0.31	6.47	11.08	1.74	0.80
n=8	min	47.98	1.77	12.76	12.39	0.13	4.85	9.25	1.00	0.25
	standev	1.31	1.07	0.26	0.89	0.07	0.52	0.63	0.23	0.21
OxT-4677	mean	59.37	1.29	15.35	9.47	0.26	1.84	5.34	3.55	1.42
Group 2	max	59.95	1.35	15.63	9.70	0.32	1.94	5.49	3.90	1.50
n=8	min	58.51	1.24	15.13	9.18	0.20	1.75	5.23	2.56	1.35
	standev	0.44	0.04	0.18	0.22	0.04	0.06	0.09	0.43	0.06
OxT-4679	mean	59.83	1.29	15.57	9.46	0.24	1.76	5.33	3.65	1.42
n=22	max	61.09	1.42	16.51	10.11	0.36	2.09	5.78	4.45	1.63
	min	58.99	1.06	14.24	8.38	0.17	1.45	4.61	2.83	1.02
	standev	0.42	0.09	0.52	0.45	0.04	0.13	0.23	0.50	0.15
OxT-4680	mean	59.58	1.29	15.39	9.51	0.27	1.80	5.33	3.39	1.42
n=17	max	60.68	1.49	15.64	9.88	0.39	1.99	5.72	4.19	1.59
	min	57.79	1.13	15.01	9.13	0.16	1.62	5.04	2.34	1.27
	standev	0.71	0.08	0.19	0.21	0.07	0.08	0.20	0.69	0.08
OxT-4681	mean	62.56	0.95	14.96	6.35	0.19	1.55	3.97	4.38	2.60
n=16	max	69.56	1.90	18.21	12.45	0.27	6.63	11.06	5.86	4.70
	min	49.53	0.20	13.74	2.64	0.09	0.06	1.00	1.77	0.24
	standev	6.22	0.56	1.15	3.17	0.06	2.07	3.18	1.33	1.51

OxT-4672: This corresponds to 11-13 cm in this core. Similar to the samples from Sveinhúsavatn, these microtephra were highly vesicular, and therefore there were few tephra shards of a great enough size to be beamed. The majority of shards were brown in colour, which corresponds to the shard count. This particular sample contained andesitic and basaltic andesitic/basaltic trachyandesitic single grain analyses. Of these, the majority were andesitic. They ranged in SiO_2 from 58.55-61.18 wt-%.

OxT-4674: This corresponds to 15-17 cm in this core. The majority of shards extracted here were brown in colour and either highly vesicular or striated. For the most part, they were andesitic, with a single grain analysis being trachydacitic. These had an average range of SiO_2 of 57.17-59.73 wt-%. TiO_2 and CaO values were relatively low: an average of 1.36 and 5.21 wt-% respectively.

OxT-4675: This corresponds to 17-19 cm in this core. Under the microscope, this microtephra was generally brown, with some white/clear shards. These shards had a very wide range and for averaging purposes in Table 6.3.1.2, they were split into two groups: values ranging from 56.42-59.58 and values ranging from 69.64-72.89 wt-% SiO_2. The first group ranged from purely basaltic to andesitic and trachy-andesitic, while the other group was solidly rhyolitic. Group 1 had a very uniform composition, as shown in Table 6.3.1.2. The second group also had a uniform composition, marked by relatively low TiO_2 values, on average 0.19 wt-%, and low FeO and CaO values, 1.95-3.00 and 1.05-1.32 wt-% respectively.

OxT-4676: This corresponds to 19-21 cm in this core. This portion of the core had nearly equal concentrations of brown and white/clear shards; correspondingly, the compositions of single grain analyses here are widely distributed. The majority are andesitic, with one dacitic, one trachydacitic, and two rhyolitic readings. These shards were not degraded or weathered in any visible way, but like many of the others analysed here, they were vesicular and striated. The range of SiO_2 here was relatively broad: 58.10-63.89 wt-%. FeO and K_2O were similarly varied: 5.05-10.27 and 1.86-3.13 wt-% respectively.

OxT-4677: This corresponds to 21-23 cm in this core. This section of the core contained both brown and white/clear shards in relatively high concentrations. Unlike higher levels within the core, although these shards were vesicular, they were of a size

large enough to obtain a high number of single grain analyses. Single grain analyses here were basaltic, andesitic, trachydacitic, and rhyolitic. Much like OxT-4675, the compositions here can be divided into two clear groups. Group 1 ranged from 47.98-50.91 wt-% SiO_2, while Group 2 was very uniform, ranging from 58.51-59.95. TiO_2 wt-% for Group 1 has an average of 3.65 wt-%. TiO_2 values around 4 wt-% are indicative of tephra from the Katla volcano (Lacasse et al. 2006).

OxT-4679: This corresponds to 29-31 cm in this core. This portion of the core had a high concentration of brown shards, and a low concentration of white/clear shards. These were vesicular, but large enough to have a high number of single beam analyses, much like OxT-4677. The majority of single grain analyses here were andesitic, with a few scattered basaltic, trachydacitic, dacitic, and rhyolitic analyses. The range of SiO_2 wt-% is 58.99-61.09.

OxT-4680: This corresponds to 31-33 cm in this core. Brown microtephra made up the majority of shards visible under the microscope; these were for the most part neither vesicular nor striated. They did not show any signs of weathering or degradation. Single grain analysis of samples from this section of the core are uniformly andesitic and cluster together tightly in elemental composition. They range from 57.79-60.69 wt-% SiO_2 with an average of 59.58. TiO_2 values are relatively low, ranging from 1.13-1.49 wt-%. FeO values range from 9.12-9.89 wt-%. Only Na_2O values show variation, ranging from 2.33-4.19 wt-%.

OxT-4681: This corresponds to 41-43cm in this core. This section of the core had similar concentrations of brown and white/clear shards, both of which were low relative to other sections of the core. These shards were not vesicular or weathered. They showed a wide range of compositions, although most were relatively high in SiO_2 content. There was one basaltic analysis, with the rest scattered among andesitic, dacitic, trachydacitic, and rhyolitic silica-alkali content. The range of SiO_2 was from 49.53-69.56 wt-%, with an average of 62.56 wt-%. These samples had the highest Al_2O_3 of any, 18.21 wt-%. That, like the other compositional percentages, as shown in Table 6.3.1.2, had wide ranges, indicating a mixed population.

6.3.1.3 Kaldalonsjökull

This section describes the glass chemistry of the microtephra peaks extracted from the environmental core from Kaldalonsjökull. For more information on the core, see Section 4.2.4. Figure 6.8 shows the sediment log for this core. A summary table of the glass chemistry data from Kaldalonsjökull is in Table 6.3.1.3. Grain size for these samples was 20-80 μm; the composition and characteristics of each sample will be described below. Microtephra throughout this core consisted of a mix of highly vesicular orange-brown and white/clear shards. There were no signs of weathering or degradation.

Table 6.4: Summary WDS-EPMA data (after filtering) for the samples extracted from the Kaldalonsjökull core. This table shows the average compositional percentage, as well as the numerical range and standard deviation to 1σ. Where applicable, the data have been divided into compositional groups. The data in this table have not been normalised. The full results are available in Appendix 2.

Label		SiO2	TiO2	Al2O3	FeO	MnO	MgO	CaO	Na2O	K2O
OxT-5133	mean	58.07	1.30	14.90	9.32	0.24	1.87	5.28	3.90	1.46
Group 1	max	58.96	1.35	15.09	9.72	0.27	1.92	5.47	4.06	1.54
n=5	min	57.50	1.22	14.67	8.96	0.20	1.81	5.06	3.68	1.37
	standev	0.55	0.06	0.15	0.27	0.03	0.05	0.15	0.14	0.07
OxT-5133	mean	76.12	0.17	11.93	1.50	0.04	0.03	1.64	4.79	0.93
Group 2	max	78.27	0.21	12.53	2.78	0.06	0.06	1.82	4.84	1.38
n=3	min	74.76	0.12	11.16	0.79	0.02	0.00	1.53	4.74	0.45
	standev	1.88	0.05	0.70	1.11	0.02	0.03	0.16	0.05	0.46
OxT-5135	mean	59.31	1.25	15.11	9.23	0.28	1.75	5.11	3.94	1.48
Group 1	max	59.90	1.28	15.41	9.54	0.39	1.86	5.37	4.41	1.55
n=6	min	58.33	1.21	14.76	8.87	0.16	1.69	4.88	3.18	1.33
	standev	0.58	0.03	0.24	0.26	0.08	0.06	0.17	0.52	0.08
OxT-5135	mean	75.63	0.19	12.29	1.56	0.03	0.04	1.36	4.91	1.99
Group 2	max	80.03	0.24	14.60	2.96	0.08	0.08	1.54	5.88	3.96
n=6	min	67.60	0.13	11.18	0.42	0.00	0.00	1.08	3.35	0.42
	standev	4.56	0.05	1.23	0.87	0.04	0.03	0.16	0.85	1.45
OxT-5136	mean	69.06	0.34	13.65	3.19	0.12	0.21	1.62	4.70	3.00
n=6	max	74.36	0.65	15.93	4.99	0.22	0.50	2.36	5.89	4.44

Label		SiO2	TiO2	Al2O3	FeO	MnO	MgO	CaO	Na2O	K2O
	min	62.47	0.11	11.56	1.88	0.00	0.01	0.99	2.95	0.47
	standev	5.29	0.21	1.94	1.39	0.08	0.20	0.61	1.06	1.35
OxT-5142	mean	59.05	1.29	15.07	9.31	0.24	1.80	5.08	3.76	1.45
n=14	max	60.41	1.42	15.54	10.17	0.32	2.17	5.35	4.21	1.54
	min	58.23	1.06	14.57	8.77	0.14	1.41	4.51	2.98	1.27
	standev	0.52	0.09	0.21	0.38	0.06	0.16	0.24	0.36	0.08
OxT-5148	mean	69.67	0.23	14.79	2.76	0.12	0.14	0.98	5.10	4.55
n=9	max	71.14	0.28	14.99	3.10	0.18	0.24	1.08	5.62	4.76
	min	68.30	0.21	14.63	2.09	0.03	0.07	0.81	3.81	4.25
	standev	1.06	0.02	0.14	0.37	0.04	0.07	0.10	0.71	0.17
OxT-5149	mean	59.30	1.32	15.13	9.39	0.23	1.80	5.27	3.71	1.39
n=2	max	59.68	1.35	15.26	9.47	0.27	1.81	5.33	3.71	1.42
	min	58.93	1.28	15.01	9.31	0.19	1.78	5.20	3.71	1.36
	standev	0.53	0.05	0.18	0.11	0.06	0.02	0.09	0.00	0.04
OxT-5150	mean	79.13	0.24	11.74	1.22	0.03	0.03	1.65	4.74	0.56
n=9	max	80.25	0.33	12.38	2.23	0.09	0.07	2.13	4.95	1.01
	min	78.18	0.18	10.85	0.25	0.00	0.01	1.08	4.47	0.21
	standev	0.71	0.05	0.49	0.62	0.04	0.02	0.36	0.16	0.29

OxT-5133: This corresponds to 8-10 cm of the Kaldalonsjökull core. Under the microscope, this section of the core was dominated by clear /white shards, but also contained brown shards. Relative to the rest of the core, this section had one of the highest concentrations of tephra shards. The geochemical composition of microtephra in the section can be divided into two clear groups, as is shown in Table 6.3.1.3. The first group, which contains the majority of shards probed, is andesitic, with little deviation from the mean for all oxides. The second group is at the upper end of SiO_2 values to be classified as rhyolitic; however, this group is not as uniform, particularly in its SiO_2 and FeO values.

OxT-5135: This corresponds to 12-14 cm in the core, and its concentrations of white/clear to brown shards were similar in ratio to OxT-5133. Also much like OxT-5133, the geochemical composition of the microtephra from this section can be divided into two groups: one andesitic and one rhyolitic. The rhyolitic group has a large standard deviation, whereas the andesitic group does not.

OxT-5136: This corresponds to 14-16 cm in the core. Microtephra in this section was almost entirely white/clear, with very few brown shards. The geochemical composition of microtephra from this section is highly varied, as shown by the standard deviation for SiO_2 in Table 6.3.1.3. Shards were both trachydacitic and rhyolitic.

OxT-5142: This corresponds to 36-38 cm in the core. Unlike every other section in the core, microtephra in OxT-5142 was entirely brown. Under the microscope, the shards within this section also looked distinct from other brown shards found throughout the core. These shards were large and very few were vesicular or striated. OxT-5142 is bounded by a layer of small gravel above it that was not studied for microtephra, and unprobed peat layer OxT-5143 which also had a strong brown microtephra presence. All probed shards were andesitic and geochemically very similar. SiO_2 values were 58.23 - 60.41 wt-%.

OxT-5146: This corresponds to 79-82 cm in the core. Under the microscope, this layer was very different from most others in the core. Microtephra here was composed almost entirely of white /clear shards but they were all very small and fragmentary. As a result, it was not possible to find large enough shard surfaces for WDS-EPMA analysis.

OxT-5148: This corresponds to 84-86 cm in the core. The majority of these microtephra shards were white /clear and vesicular. All were rhyolitic. SiO_2 ranged from 68.30 - 71.14 wt-%. Na_2O and K_2O values were relatively high, with means of 5.10 and 4.55 wt-% respectively.

OxT-5149: This corresponds to 86-88 cm in the core. These shards all appeared to be white /clear. Much like OxT-5148 and OxT-5150, they were highly vesicular. Both microtephra shards probed were andesitic. SiO_2 for these shards was 59.30 wt-% on average, while CaO was relatively high at 5.27 wt-% on average.

OxT-5150: This corresponds to 88-90 cm in the core, with the majority white /clear, although there were also a number of brown shards. This microtephra was highly vesicular. All were rhyolitic, with very high SiO_2 values, ranging from 78.18-80.25 wt-%. Na_2O values were also high, ranging from 4.47-4.95 wt-%.

OxT-5151: This corresponds to 103-106 cm in the core. Much like OxT-5146, microtephra in this section was small and fragmentary, composed of both white /clear and brown shards, and WDS-EPMA analysis was not possible.

6.3.1.4 Vatnsfjörður archaeological site

This section describes the glass chemistry of the tephra from the Vatnsfjörður archaeological site. A summary table of the glass chemistry data from Vatnsfjörður is in Table 6.3.1.4. The grain size for these samples varied greatly, with the portion >20 μ m used for analysis. The composition and characteristics of each sample will be described below.

Table 6.5: Summary WDS-EPMA data (after filtering) for the samples extracted from the Vatnsfjörður archaeological site. This table shows the average compositional percentage, as well as the numerical range and standard deviation to 1σ. Where applicable, the data have been divided into compositional groups. The data in this table have not been normalised. The full results are available in Appendix 2.

Label		SiO2	TiO2	Al2O3	FeO	MnO	MgO	CaO	Na2O	K2O
Label		SiO2	TiO2	Al2O3	FeO	MnO	MgO	CaO	Na2O	K2O
OxT-5163	mean	59.24	1.32	15.18	9.41	0.26	1.82	5.36	4.32	1.52
n=41	max	61.78	1.44	15.93	10.70	0.37	2.93	5.91	4.70	1.69
	min	58.28	1.10	14.41	7.42	0.15	1.39	4.72	3.17	1.38
	standev	0.62	0.08	0.27	0.54	0.05	0.22	0.18	0.26	0.07
OxT-5165 group 1	mean	49.90	2.85	13.52	13.31	0.22	5.51	10.33	2.75	0.45
n=7	max	50.53	4.37	13.93	13.05	0.29	6.12	11.14	3.25	0.77
	min	48.81	1.93	13.16	12.66	0.19	4.75	9.93	2.82	0.19
	standev	0.60	1.15	0.38	0.95	0.05	0.88	0.97	0.34	0.29
OxT-5165 group 2	mean	59.59	1.33	15.44	9.46	0.26	1.80	5.39	4.07	1.51
n=40	max	60.62	1.54	16.17	9.97	0.35	1.89	5.71	4.59	1.62
	min	58.78	1.25	13.92	8.95	0.19	1.59	5.17	2.56	1.38
	standev	1.30	0.06	0.38	0.33	0.03	0.06	0.04	0.24	0.07
OxT-5165 group 3	mean	67.36	0.47	15.28	4.42	0.19	0.42	2.10	5.07	3.81
n=11	max	70.96	1.03	16.00	8.07	0.29	1.25	4.55	5.70	4.77
	min	62.25	0.21	14.64	2.10	0.12	0.07	0.84	4.12	1.77
	standev	3.39	0.32	0.37	2.39	0.07	0.48	1.58	0.45	1.30
OxT-5166	mean	58.68	1.31	15.08	8.97	0.26	1.61	5.09	4.24	1.62

Label		SiO2	TiO2	Al2O3	FeO	MnO	MgO	CaO	Na2O	K2O
n=15	max	62.20	1.49	15.36	10.52	0.32	1.90	5.50	5.41	1.86
	min	56.62	0.90	14.60	7.48	0.19	1.08	4.35	2.83	1.39
	standev	1.61	0.16	0.24	0.87	0.04	0.24	0.35	0.65	0.14
OxT-7094	mean	58.68	1.24	14.89	8.74	0.25	1.80	4.99	3.83	1.59
n=1	max	58.68	1.24	14.89	8.74	0.25	1.80	4.99	3.83	1.59
	min	58.68	1.24	14.89	8.74	0.25	1.80	4.99	3.83	1.59
	standev	0.00	0.00	0.00	0.00	0.00	0.00	0.00	0.00	0.00
OxT-7095	mean	58.29	1.28	14.94	9.30	0.27	1.79	5.18	4.33	1.53
n=19	max	59.48	1.43	15.21	9.92	0.35	1.94	5.49	4.65	1.65
	min	57.10	1.04	14.68	8.56	0.21	1.23	4.61	3.95	1.44
	standev	0.60	0.08	0.14	0.36	0.04	0.16	0.22	0.19	0.06
OxT-7097	mean	58.26	1.22	15.21	9.01	0.22	1.81	5.32	4.31	1.47
n=13	max	60.79	1.37	17.64	9.69	0.30	2.69	6.08	5.10	1.66
	min	56.13	0.74	14.55	6.19	0.13	1.23	4.95	3.98	1.21
	standev	1.06	0.17	0.79	0.89	0.05	0.34	0.33	0.28	0.14
OxT-7098	mean	59.02	1.26	15.17	9.15	0.20	1.76	5.14	4.09	1.58
n=10	max	60.16	1.32	15.67	9.72	0.25	1.92	5.34	4.64	1.67
	min	58.29	1.19	14.88	8.59	0.11	1.67	4.78	2.82	1.48
	standev	0.64	0.05	0.24	0.36	0.04	0.08	0.17	0.48	0.06
OxT-7099	mean	58.49	1.27	15.01	9.10	0.23	1.73	5.22	4.41	1.51
n=11	max	60.47	1.40	15.68	9.60	0.37	1.97	5.65	4.96	1.67
	min	56.95	1.07	14.46	7.94	0.17	1.43	4.87	4.08	1.30
	standev	1.18	0.08	0.34	0.52	0.06	0.15	0.21	0.23	0.13

OxT-5163: This sample is VSF09 Viking Age in the report (Anderson in Milek et al. 2011). This sample was part of a visible tephra layer in the archaeological excavation that was composed of dark, almost black sediment. Following sieving to remove the <20 μm fraction, the remainder was dark brown in colour and very fine grained. Under the microscope, this layer had a number of vesicular and striated shards. The glass chemistry of this sample is more uniform than any of the other samples from the archaeological site, with all but one analysis falling into the andesitic category (and the single analysis on the line between andesitic and dacitic). The range of SiO_2 is between 58.28-61.78 wt-% for all n=43 analyses. TiO_2 is 1.10-1.44 wt-%, and the widest range of any oxide is FeO, 7.42-10.70 wt-%.

OxT-5164: This sample is VSF09 7157 in the report (Anderson in Milek et al. 2011). This sample did not contain any tephra.

OxT-5165: This sample is VSF09 Area 32 in the report (Anderson in Milek et al. 2011). Following sieving to remove the <20 μm fraction, the remainder was dark brown/black in colour and very fine grained. Under the microscope, this layer had a number of vesicular and striated shards. Due to the density of tephra within the sample, which, when viewed at magnification, seemed to be the entirety of the sample, it was probed once without picking. This was the only sample in the course of this research that was not treated using the procedures for extracting microtephra based on Blockley et al. (2005) and detailed in Section 5.2. The glass chemistry results from the first probing were based on what were most likely the largest tephra shards within the sample as they were hand-picked. However, because the sample had in general appeared to be quite fine-grained when viewed at magnification, it was hypothesised that the range of glass chemistry results derived from these larger grains might not be representative of the sample as a whole. The sample was re-extracted following the microtephra procedure (Blockley et al. 2005) and these results showed a slightly wider spread. In order to clarify whether or not that spread of results was the sign of a distinct tephra layer, the sample was extracted again at a heavier density than the others (2.80 g/cm^3). Therefore OxT-5165 has a large number of single grain analyses and also shows much greater variation than other samples. This is discussed in Section 7.1.1.

Taken in total, the results show a varied range of glass chemistry, but divided they form two distinct groups. Although the vast majority of analyses are andesitic, there

are significant numbers of rhyolitic and basaltic analyses, in addition to a single trachydacitic analysis.

OxT-5166: This sample is VSF-09 Farm Mound from the report (Anderson in Milek et al. 2011). Much like OxT-5163, this sample was part of a visible tephra layer in the archaeological excavation that was composed of dark, almost black sediment in situ. Following sieving to remove the $<$20 μm fraction, the remainder was dark brown in colour and very fine grained. Under the microscope, this layer had a number of vesicular and striated shards. Unlike OxT-5163, this sample was not tightly clustered on the TAS plot, although most analyses were andesitic, with two near the border with dacitic and a few near the border into trachy-andestic. SiO_2 was between 56.62-62.20 wt-%. TiO_2 was relatively low, with an average of 1.30 wt-%; FeO and Na_2O showed relatively wide ranges, with 7.49-10.52 wt-% and 2.82-5.41 wt-% respectively.

OxT-7094: This sample is from context 10602 in Group 8562, located along the shore to the northeast of the main archaeological excavations. Although only one shard of microtephra was successfully probed from this sample, the sample itself had a large quantity of microtephra shards. Shards were both vesicular and striated. The sample is andesitic, with SiO_2 of 58.68 wt-%.

OxT-7095: This sample is from Group 10515 in the Farm Mound. Shards were striated, vesicular, and brown in colour under the microscope. Geochemically, the microtephra from this sample is very uniform, with low standard deviations. It is andesitic bordering on trachy-andesitic.

OxT-7097: This sample is from Test Trench 45, located near the shore to the east of the main archaeological excavations. Much like other samples from the archaeological excavations, shards were striated, vesicular, and brown in colour under the microscope; on a TAS plot, they are andesitic bordering on trachy-andesitic. Compositionally, there is more variation than OxT-7095: SiO_2 ranges from 56.13-60.79 wt-%, while both Al_2O_3 and NaO also have relatively wide ranges.

OxT-7098: This sample is Structure 10662 in Context 10605 in the Farm Mound. Much like other samples from the archaeological excavations, shards were striated, vesicular, and brown in colour under the microscope; on a TAS plot, they are andesitic bordering on trachy-andesitic. This sample is compositionally uniform, with very low standard deviations in every oxide except Na_2O, which has a range of 2.82-4.64 wt-%.

OxT-7099: This sample is from Area 40, in the Farm Mound. Much like other samples from the archaeological excavations, shards were striated, vesicular, and brown in colour under the microscope; on a TAS plot, they are andesitic bordering on trachy-andesitic. OxT-7099 shows some compositional variation, particularly in SiO_2 and FeO, which range from 56.95-60.47 and 7.94-9.60 wt-% respectively.

6.3.2 Orkney

This section describes the glass chemistry of the microtephra peaks extracted from the peat cores in Hobbister. For more information on the cores, see Section 6.1.2.2 and Section 6.2.1.2. A summary table of the glass chemistry data from the core Hobbister B is in Table 6.6. Due to the low numbers of tephra shards, only layers from Hobbister B were successfully probed. The composition and characteristics of each sample will be described below. Both low concentration of shards within layers and small shard size contributed to a low number of single grain analyses possible for these samples; however, as stated above, small sample sizes are common in distal microtephra studies.

6.3.2.1 Hobbister

OxT-4765: This corresponds to 0-2.5 cm in this core. This section of the core contained a low concentration of shards in comparison to the Icelandic cores, but the concentration was relatively high in comparison with the scarce number of shards found in the Orkney cores in general. Microtephra here was both brown and white /clear as well as vesicular. Striations were not common. Although the shards did not show signs of weathering, they were more fragmentary than the average shards observed in cores in Iceland, most likely due to distance from source. Single grain analyses indicate that the glass chemistry from these samples does not have a wide range of variation, indicating that, despite a small sample size, they are representative.

Table 6.6: Summary WDS-EPMA data (after filtering) for the samples extracted from Hobbister. This table shows the average compositional percentage, as well as the numerical range and standard deviation to 1σ. The data in this table have not been normalised. The full results are available in Appendix 2.

Label		SiO2	TiO2	Al2O3	FeO	MnO	MgO	CaO	Na2O	K2O
OxT-4765	mean	59.93	1.15	15.17	8.96	0.20	1.59	4.86	3.24	3.41
n=4	max	60.16	1.18	15.55	9.51	0.27	1.68	5.11	3.59	4.14
	min	59.61	1.11	15.01	8.38	0.14	1.45	4.55	2.94	2.71
	standev	0.25	0.03	0.26	0.50	0.05	0.10	0.23	0.30	0.66
OxT-4766	mean	60.57	1.07	15.25	8.34	0.22	1.47	4.73	3.83	2.53
n=6	max	62.02	1.13	15.50	9.04	0.30	1.62	4.93	4.33	3.15
	min	59.31	0.99	14.93	7.63	0.14	1.31	4.43	3.40	1.81
	standev	1.03	0.06	0.19	0.52	0.06	0.12	0.21	0.34	0.56
OxT-4767	mean	60.14	1.04	15.06	8.57	0.20	1.35	4.58	4.03	2.02
n=1	max	60.14	1.04	15.06	8.57	0.20	1.35	4.58	4.03	2.02
	min	60.14	1.04	15.06	8.57	0.20	1.35	4.58	4.03	2.02
	standev	0.00	0.00	0.00	0.00	0.00	0.00	0.00	0.00	0.00

They are borderline trachyandesitic/andesitic. The range of SiO_2 is 59.61-60.17 wt-%. Other major oxides have tight ranges, with the largest being K_2O, 2.71-4.14 wt-%.

OxT-4766: This corresponds to 2.5-5 cm in this core. Microtephra here was both brown and white/clear, relatively quite small and vesicular. Striations were not common. Much like OxT-4765, the shards were generally smaller than the average size of shards observed in cores in Iceland. They did not show signs of weathering. The single grain analyses here were more scattered than OxT-4765, but aside from one trachydacitic analysis, they were clustered between andesitic, dacitic, and trachyandesitic on a TAS plot. SiO_2, FeO, and K_2O values showed the most range: 59.31-62.02 wt-%, 7.63-9.04 wt-%, and 1.81-3.15 wt-%.

OxT-4767: This corresponds to 5-7.5cm in this core. Microtephra here was both brown and white /clear, relatively quite small and vesicular. Striations were not common. Much like OxT-4765 and OxT-4766, the shards did not show signs of weathering, and they were generally smaller than the average size of shards observed in cores in Iceland. The concentration of shards here was extremely low and only one good analysis could be achieved for this section of the core (others were filtered due to low wt-% of oxides). This single analysis was andesitic, with a SiO_2 value of 60.14 wt-% and an FeO value of 8.57 wt-%.

6.4 Summary

Sediment samples to be analyzed for the presence of tephra or microtephra were taken from several different areas related to two archaeological excavations. These are:

Orkney:

1. Archaeological excavation (seven samples)
2. Hobbister A and B core
3. Spretta Meadow core

Iceland:

1. Archaeological excavations (ten samples)
2. Sveinhúsavatn

3. Homefield

4. Kaldalonsjökull

Tephrostratigraphies, in the form of shard counts, were created for each of these except for the two archaeological excavations, and are presented in Figure 6.19, Figure 6.20, Figure 6.22, Figure 6.16, Figure 6.17, and Figure 6.18. From these tephrostratigraphies, a number of areas were targeted for further study because of their relatively high concentrations of microtephra shards, which are listed in Table 6.1. These were then re-extracted and prepared for geochemistry. Section 6.3 describes the geochemistry of microtephra that was successfully analysed with WDS-EPMA. Summaries of the geochemistry for each are in Table 6.6, Table 6.2, Table 6.3.1.2, Table 6.3.1.3, and Table 6.3.1.4. Chapter 7 and Chapter 8 interpret these results, and then relate them to a wider understanding of the archaeological themes introduced in Chapter 2.

7 | Interpretation: The chronology of Vatnsfjörður

In Chapter 1, I asked, 'How can scientific chronologies, in their current state, be used to understand the relationship between records of environmental and archaeological change?' and, 'How did environmental change in the landscape, both anthropogenic and natural, affect human life at coastal settlements in the North Atlantic?' Although Turney and Caseldine (2009) call for establishing accurate and precise chronologies is crucial to link these records, and is the area currently most in need of further research before these links can be made with confidence. Once accurate and precise chronologies have been established, the argument goes, then the process of interpreting archaeological and environmental relationships can begin. Lacking chronologies that link the two records, it is impossible to correlate records.

That argument, however, relies upon the existence of ideal study locations, landscapes, and records. Currently, linking chronologies across sites and record types is not possible in most cases. Tephrochronology, and particularly distal micro- tephrochronology, is a promising method but has drawbacks that are discussed in Section 3.2. Likewise, combining tephra studies with other methods does not always work: all methods do not apply at all sites, and there is no universal chronological strategy.

Acknowledging all of the caveats and limitations of chronology building, archaeological interpretation of environmental impacts is still possible. Although scientific methods have greatly enhanced the ability to identify and understand some components of the archaeological record, interpretation will always rely upon the methods of social science: the interpretative power of anthropological archaeology and its ability to illuminate the human past.

In this chapter, I interpret the results of the tephrochronological research described in Chapter 6 for the Vatnsfjörður archaeological landscape and surrounding area.

7.1 Vatnsfjörður archaeological site

7.1.1 Correlating distal layers with proximal glass chemistry

Section 5.4.4 describes the process of correlation, or 'fingerprinting' (Lowe and Hunt 2001) distal tephra layers with known eruptions. New data sets of identified glass chemistry are being made available with some frequency, and it is expected that Iceland's tephrostratigraphy will be continuously updated for several years; however, in some cases, older or less reliable data sets have had to be used because they are the only ones available. This is always noted in the text.

All sample data have been compared against the full dataset of possible correlation data, using both bi-plots and Mahalanobis distances; the figures presented here are used for illustrative purposes with most likely correlations shown rather than the full suite of correlative data. Each figure uses a different scale that fits its particular correlation.

During extraction, the sample OxT-5164 did not yield any tephra; however, the other samples, OxT-5163, -5165, -5166, and -7094, -7095, and 7097-7099, contained large quantities of tephra. These samples were probed for their geochemistry and the results filtered. The glass chemistry results are presented in Chapter 6. A complete and unfiltered record of the data is in Appendix 1.

Unlike other areas analysed in this dissertation, the Vatnsfjörður archaeological excavations had layers of tephra visible in their stratigraphy. Also unlike many of the other areas, these layers had a well-bounded temporal range, as their placement within the archaeological stratigraphy meant that they had to have been deposited sometime after the settlement of Iceland, ca. AD 870. Therefore, it seemed likely that these visible tephra layers would correspond to ash fall events that had been recorded historically by those living in the Vestfirðir region. Þórarinsson (1955; 1967) has collected historical records of Icelandic eruptions from the sagas through the twentieth century, and he lists the eruptions of Hekla 1693 and Hekla 1766 as having recorded ash fall in Vestfirðir. Larsen (1999; 2002) presents isopach maps that agree with Þórarinsson which are based on both those historical records and his own tephra analysis. The eruption of Katla in 1721, meanwhile, had ash fall recorded in areas that suggest its ash cloud should have drifted over Vestfirðir, but there are no historical records and thus far no geochemical evidence to indicate that the ash settled there (Þórarinsson 1955; Larsen 1999; Larsen 2002). Larsen (2002:84) suggests that ash fall from Katla

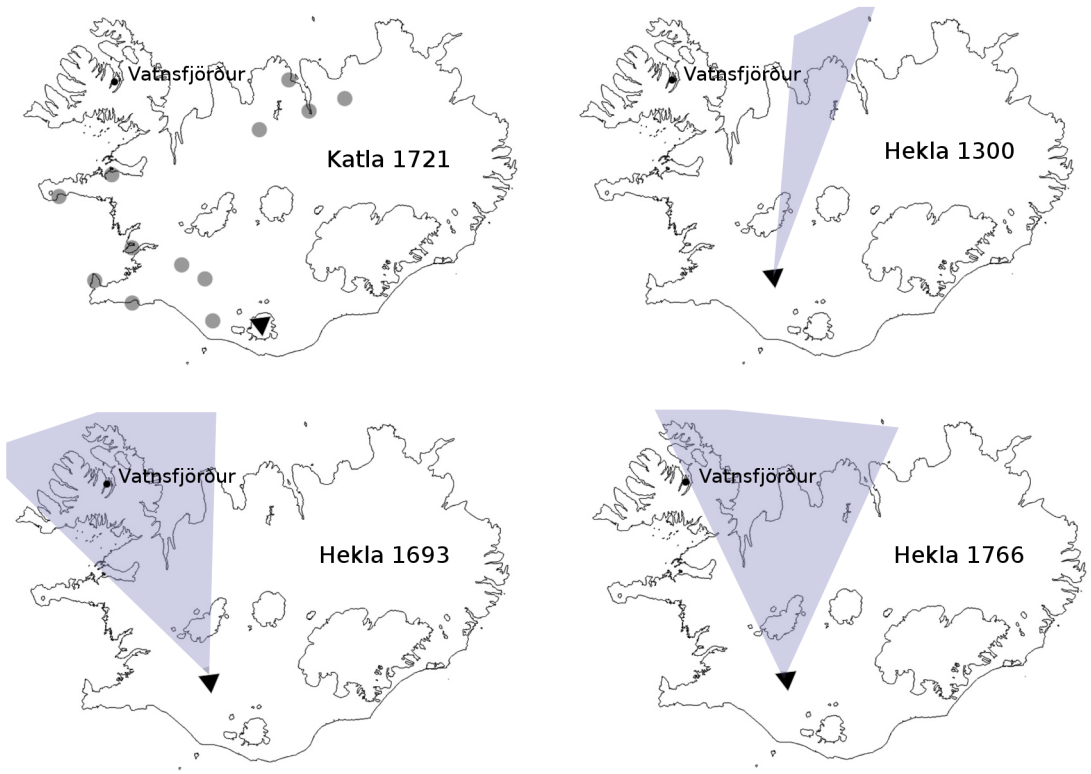


Figure 7.1: Isopach and tephra fall maps showing recorded tephra fall patterns prior to the research in this dissertation. The Hekla distribution maps are drawn with assumed fallout areas, while the Katla 1721 map has been drawn with circles representing recorded data. Hekla information comes from Larsen (1999: 465) and Þórarinsson (1967); Katla 1721 comes from Larsen (2002: 84) and Þórarinsson (1955: 90).

1721 may have been negligible in Vestfirðir, although she offers no explanation for why. Hekla 1300 also had ash fall in the north, but has not yet been found in Vestfirðir (Larsen 1999; Kristjansdóttir et al. 2007). Figure 7.1 shows the ash fall records for all of these eruptions.

These four eruptions and Hekla 1104 were all compared to the glass analyses from the archaeological samples. Hekla 1104 was included because it occurred after the settlement of Iceland, had a large, widely dispersed ash fall to the north, and has very little recorded historical information, so there is a chance that it may have fallen over Vestfirðir (Þórarinsson 1967; Larsen et al. 1999; Haflidason et al. 2000). Sigurgeirsson (2006) found that a visible tephra layer from a peat field close to the archaeology had glass chemistry that he described as having originated in the Hekla system. However, it is difficult to derive any useful information from that statement because Hekla

tephras show a wide variability across eruptions (e.g., Hekla 1104 versus Hekla 1693).

The published glass chemistry data used to correlate these samples comes largely from three sources. The data sets used for Hekla 1300 and Hekla 1693 come from Dugmore et al. (2007), who derived them from soil profiles in the valley of Þjórsárdalur. This valley is located immediately north of Hekla.

The geochemical data for Katla 1721 comes from Haflidason et al. (1992) and Larsen et al. (2011). Haflidason et al. record fourteen data points; seven analyses from the University of Iceland and seven from the University of Bergen. These tephras were identified from gravity cores from the deepest part of Þingvallavatn, which is located approximately 125 km west-northwest of Katla. Based on the published information, it is unclear how Haflidason et al. came to the conclusion that this particular layer is Katla 1721. They write, 'The top layer in the section, band 1 (0.2 cm thick) is taken to be the Katla 1918 tephra layer and band 3b is taken to represent the K 1721 tephra... Band 3b is, however, rich in lenses of windblown material which is reflected in several glass types of this horizon in addition to the Katla glass type' (1992: 85-86). Their glass chemistry has a wide spread, as shown in Figure 7.2. Larsen et al. (2011) also found tephra they have identified as Katla 1721 in a lake core, this one from Hvítárvatn, which is approximately 70 km north of Hekla. They base their analysis of Katla 1721 on data from an unpublished PhD (Jagan 2010). Their data, also shown in Figure 7.2, is more uniform than that recorded by Haflidason et al. (1992).

The data set for Hekla 1766 is also from Larsen et al. (2011), but is based on only seven analyses. Previously, the only set of data available for this eruption came from an unpublished MSc thesis summarised by Haflidason et al. (2000).

The data set for Hekla 1104 comes from Larsen et al. (1999) and Boygle (1999) and is also shown in Figure 7.2. Larsen et al. collected their samples from open sections of stratigraphic profiles proximal to Hekla where the historical tephrostratigraphy is well known. Boygle's samples come from Svínavatn, a lake in the northern Icelandic region of Húnavatnsýssla located approximately 200 km north of Hekla.

7.1.1.1 OxT-5163

As noted in Section 6.3.1.4, OxT-5163 has tightly constrained glass chemistry. It was therefore clear that the sample did not match either Hekla 1104 or Katla 1721. Using

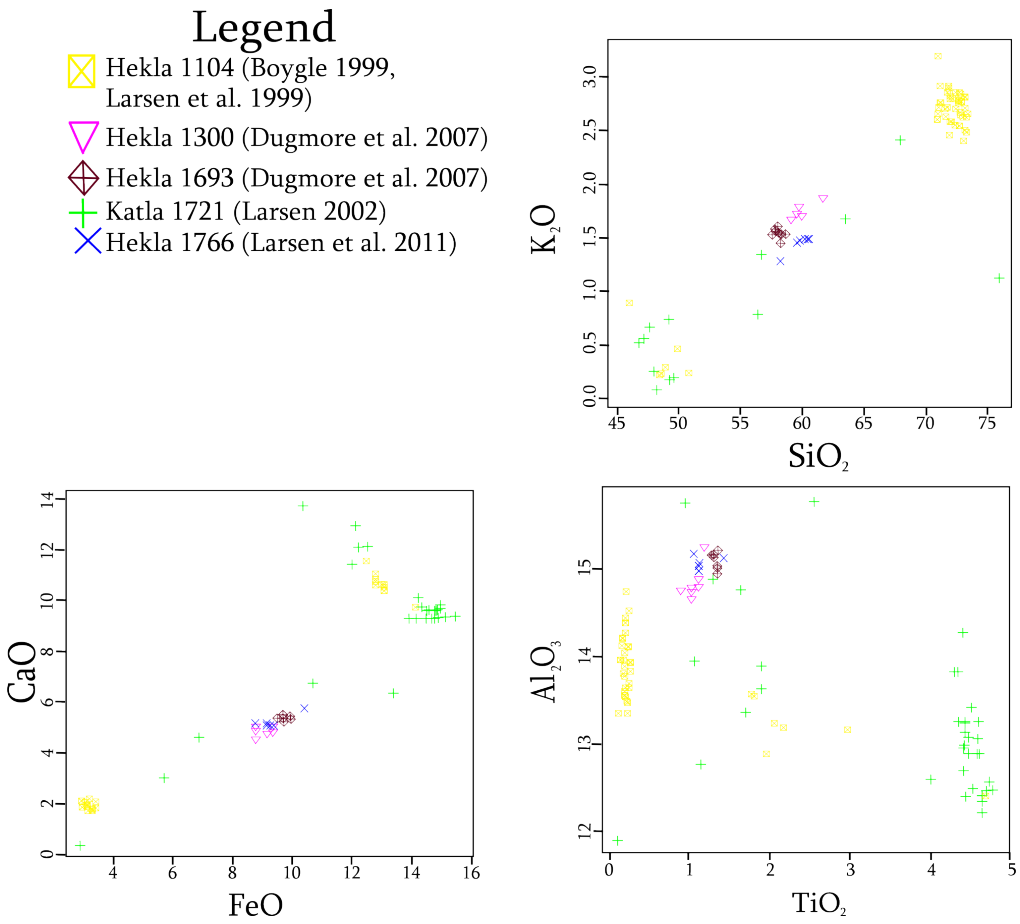


Figure 7.2: Glass chemistry of Katla 1721 from Haflidason et al. (1992) and Larsen et al. (2011); Glass chemistry of Hekla 1300 and Hekla 1693 from Dugmore et al (2007); Glass chemistry of Hekla 1766 from Larsen et al. (2011); Glass chemistry of Hekla 1104 from Boygle (1999) and Larsen et al. (1999). All units are wt-%.

bi-plots, the sample was compared to Hekla 1300, Hekla 1693, and Hekla 1766. This comparison is shown for selected major element wt-% in Figure 7.3.

OxT-5163 most closely resembles the analyses of Hekla 1693, although the spread of data from OxT-5163 is not as tightly constrained as Dugmore et al.'s (2007) for Hekla 1693. Notably, OxT-5163 has a wider range of SiO_2 wt-% values, which spread it across the range of values for both Hekla 1300 and Hekla 1766. However, none of the other major element bi-plots show close correlation between OxT-5163 and these two eruptions. Therefore, it seems likely that this sample correlates to the eruption of Hekla 1693.

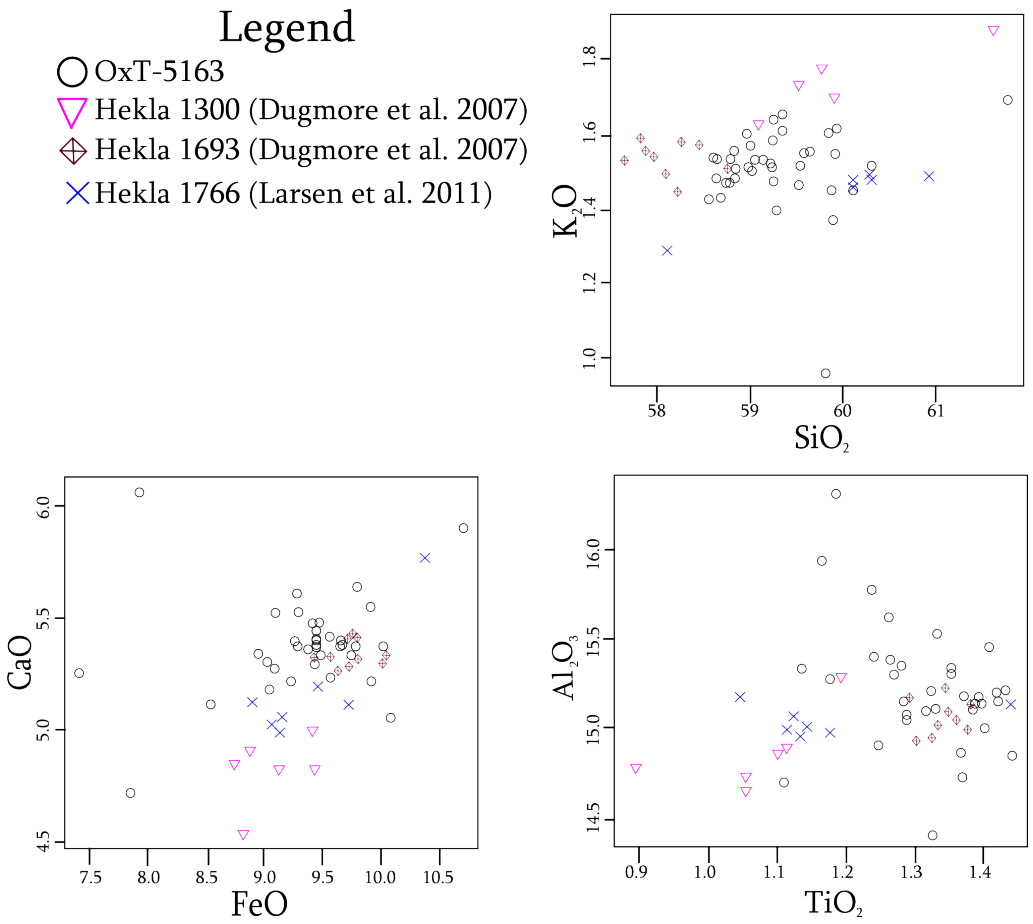


Figure 7.3: Comparison of OxT-5163 with published proximal data for Hekla 1300, Hekla 1693 (Dugmore et al. 2007b) and Hekla 1766 (Larsen et al. 2011). All units are in wt-%.

7.1.1.2 OxT-5165

As noted in Section 6.3.1.4, OxT-5165 has the widest spread of glass chemistry analysis of the samples from the Vatnsfjörður excavations. It seems most likely that the glass chemistry of this sample should primarily be identified as Hekla 1693. There is also a possibility that a limited number of shards within the sample come from Katla 1721. This tephra layer, as noted in Section 6.3.1.4, is very dark in colour. Larsen (1984), who records visible tephra layers from both eruptions at Veiðivötn, describes them as equally dark in appearance, but (at least at that location) the tephra from the layer he identified as Katla 1721 had larger grain size that that from Hekla 1693. Therefore, there is little visual evidence to distinguish tephra from these eruptions from one another.

As described in Section 6.3.1.4, this sample underwent multiple extractions, and pro-

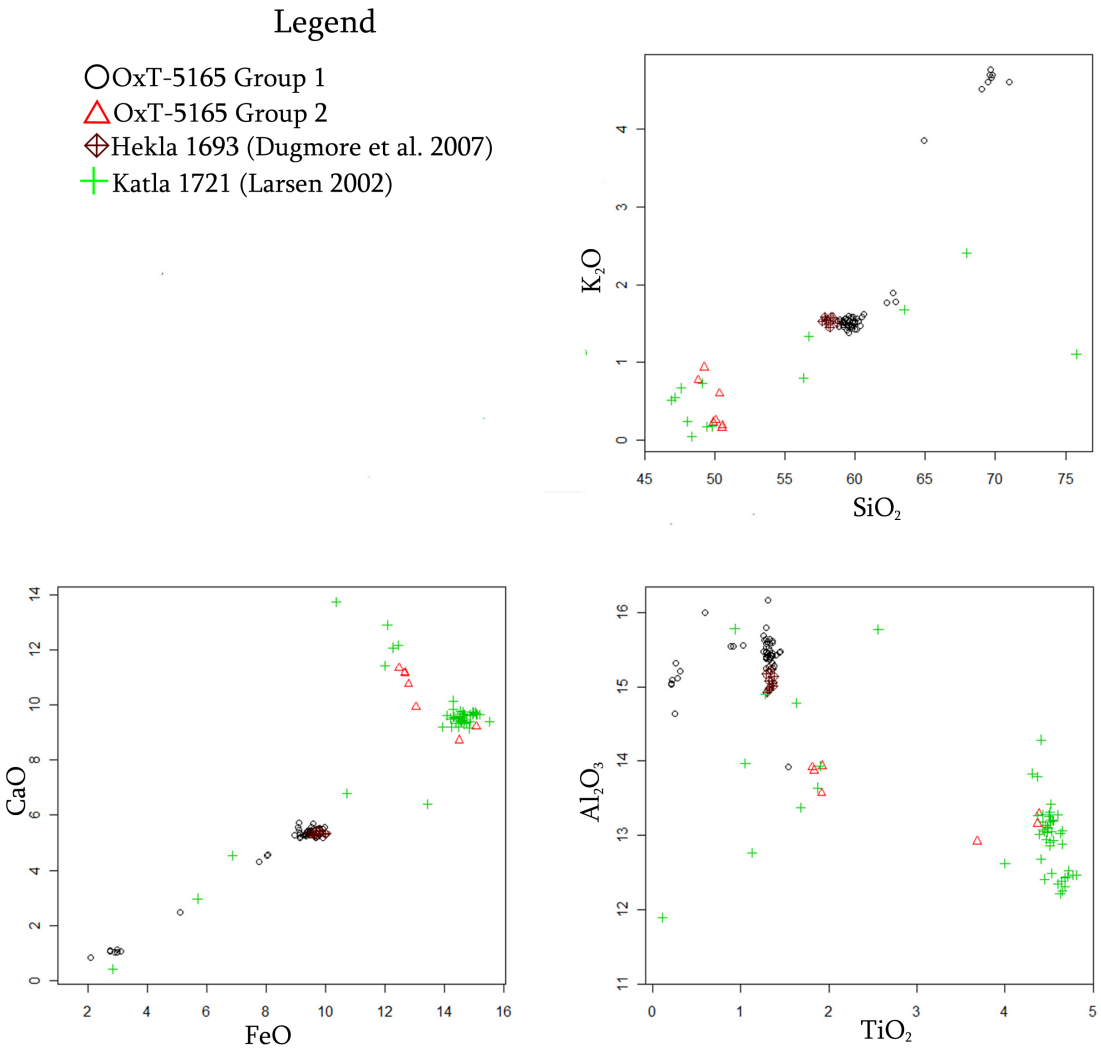


Figure 7.4: Comparison of OxT-5165 analyses broken into Group 1 and Group 2 alongside proximal data for Hekla 1693 (Dugmore et al. 2007b) and Katla 1721 (Haflidason et al. 1992) . All units are wt-%.

duced two distinct sets of results. Figure 7.4 shows all analyses from OxT-5165, divided into Group 1 and Group 2, alongside Hekla 1693 and Katla 1721.

It may be that some of those analyses from Group 2 are in fact products of Katla 1721, as shown in Figure 7.4. These might have blown into an exposed tephra layer and stuck there, for example if this layer was exposed for several years, perhaps as part of a roof section or exposed wall that has since collapsed, so that the products of another eruption fell onto it. These shards were more dense than those from Group

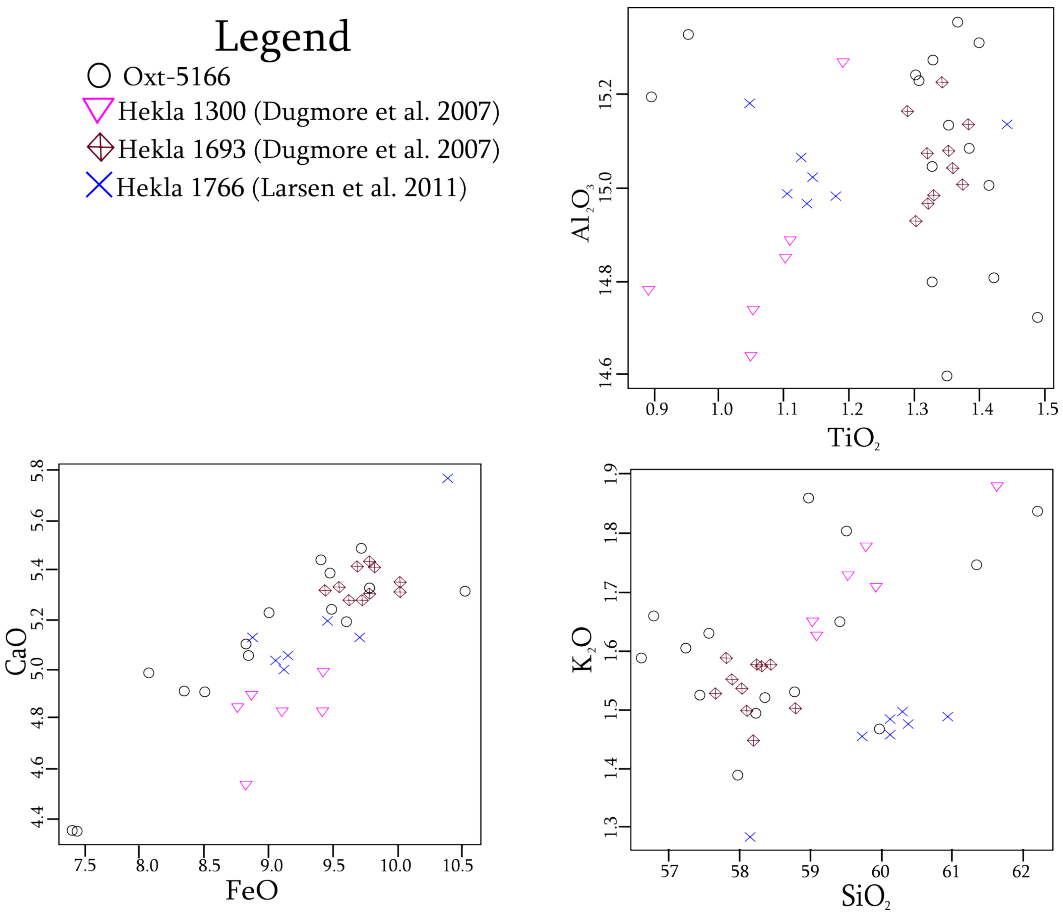


Figure 7.5: Comparison of OxT-5166 with published proximal data for Hekla 1300, Hekla 1693. and Hekla 1766. All units are in wt-%.

1, which, based on Larsen's (1984) description of the difference between Hekla 1693 and Katla 1721 visually, may be another reason to identify them as being incursions from Katla 1721. However, due to the small number of single shard analyses that are similar to Katla 1721, as well as the little published proximal data available, it is impossible to make any definitive statements.

7.1.1.3 OxT-5166

Much like OxT-5163, this sample was constrained enough that it was obvious it did not correlate to Katla 1721 or Hekla 1104, and as a result was only compared to Hekla 1300, Hekla 1693, and Hekla 1766. These comparisons are shown in Figure 7.5

Although OxT-5166 has several outliers, the main cluster of single shard analyses matches with Dugmore et al.'s (2007) Hekla 1693 analyses in major element bi-plots.

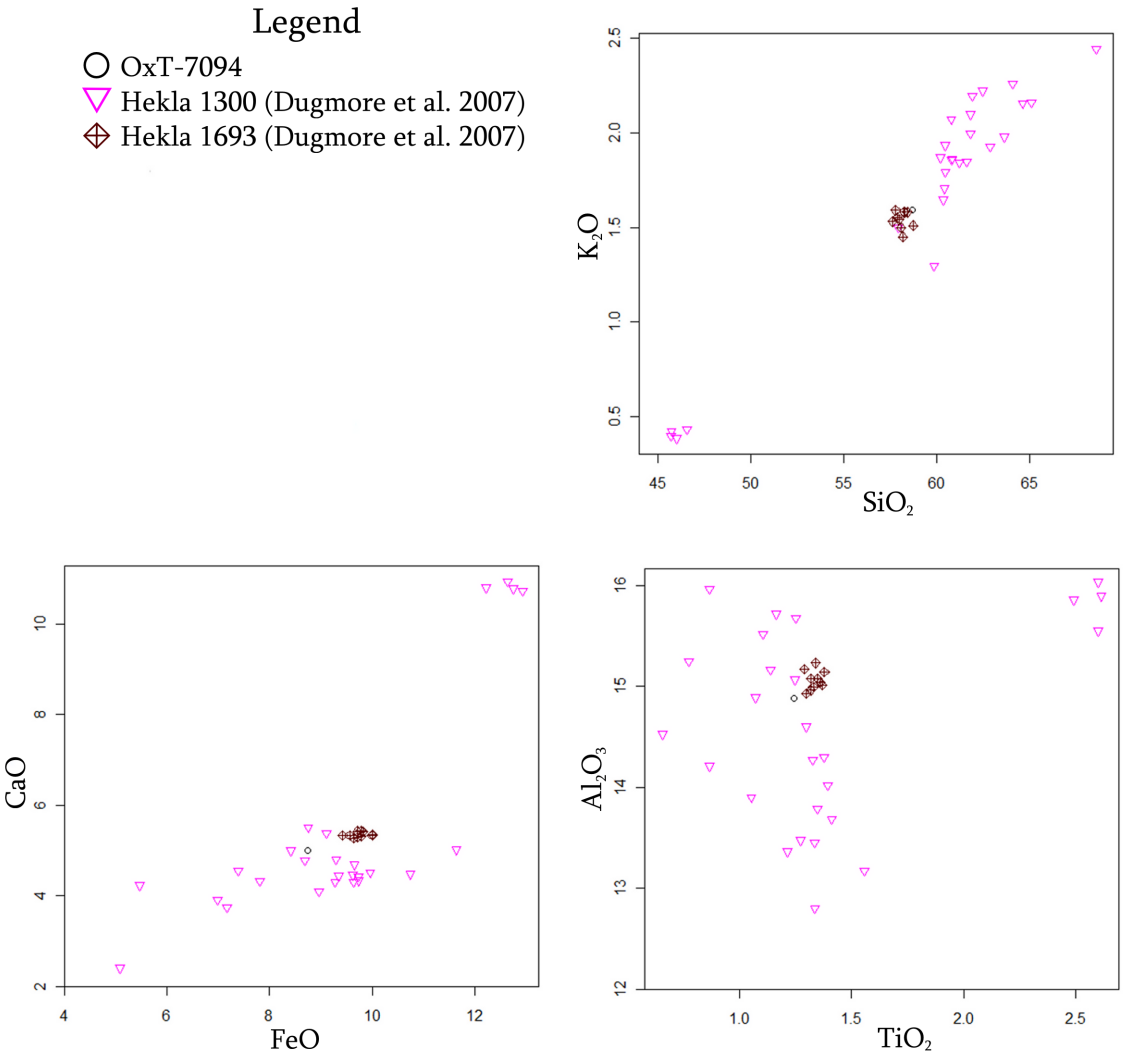


Figure 7.6: Comparison of OxT-7094 with published proximal data for Hekla 1300 and Hekla 1693 (Dugmore et al. 2007b). All units are in wt-%.

7.1.1.4 OxT-7094

Subsequent analyses from the Vatnsfjörður archaeological excavations were compared against Hekla 1300 and Hekla 1693 (Dugmore et al. 2007b). OxT-7094, despite having only a single data point from WDS-EPMA, can be assumed to correlate to Hekla 1693 because of the correlations of the other tephras from the area. This is shown in Figure 7.6.

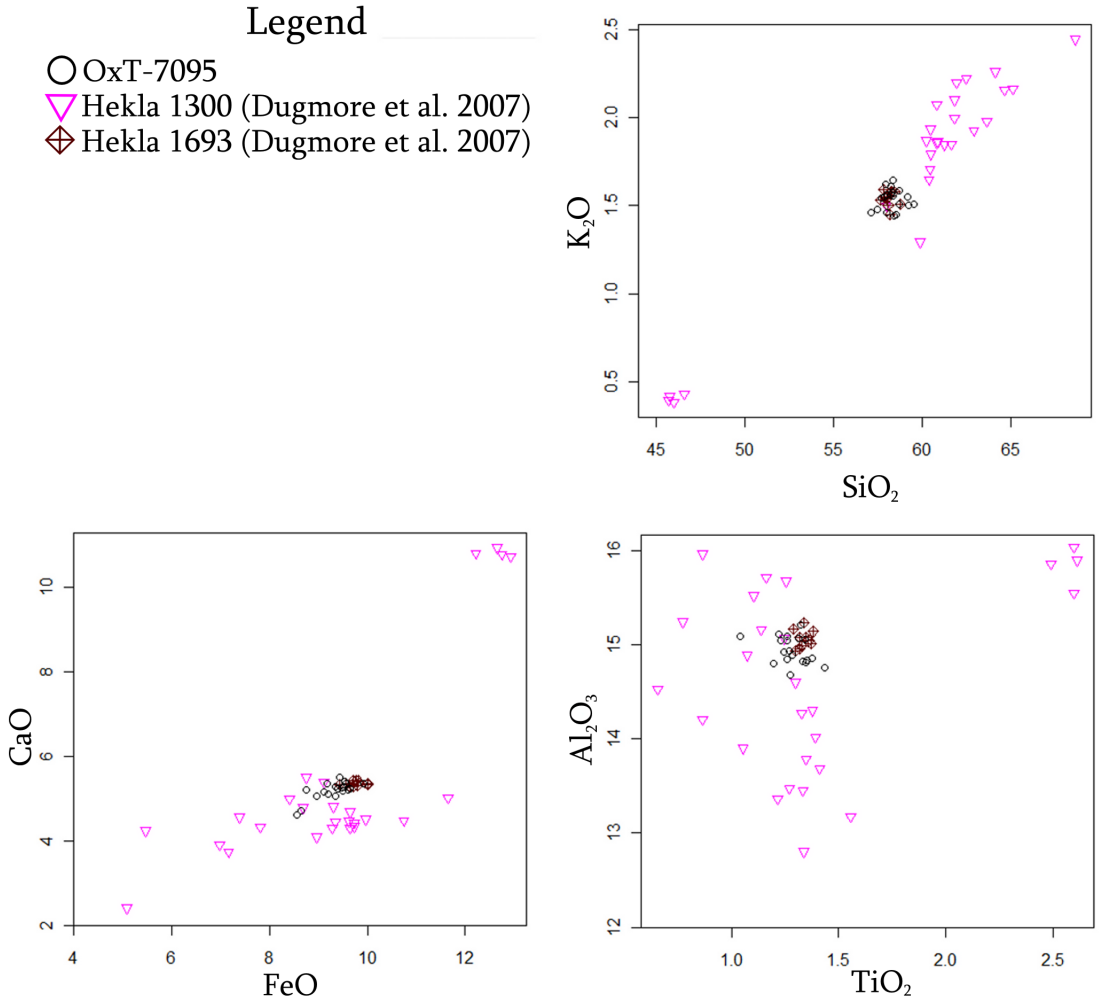


Figure 7.7: Comparison of OxT-7095 with published proximal data for Hekla 1300 and Hekla 1693 (Dugmore et al. 2007b). All units are in wt-%.

7.1.1.5 OxT-7095

OxT-7095 correlates to Hekla 1693 (Dugmore et al. 2007b).

7.1.1.6 OxT-7097

OxT-7097 correlates to Hekla 1693 (Dugmore et al. 2007b).

7.1.1.7 OxT-7098

OxT-7098 correlates to Hekla 1693 (Dugmore et al. 2007b).

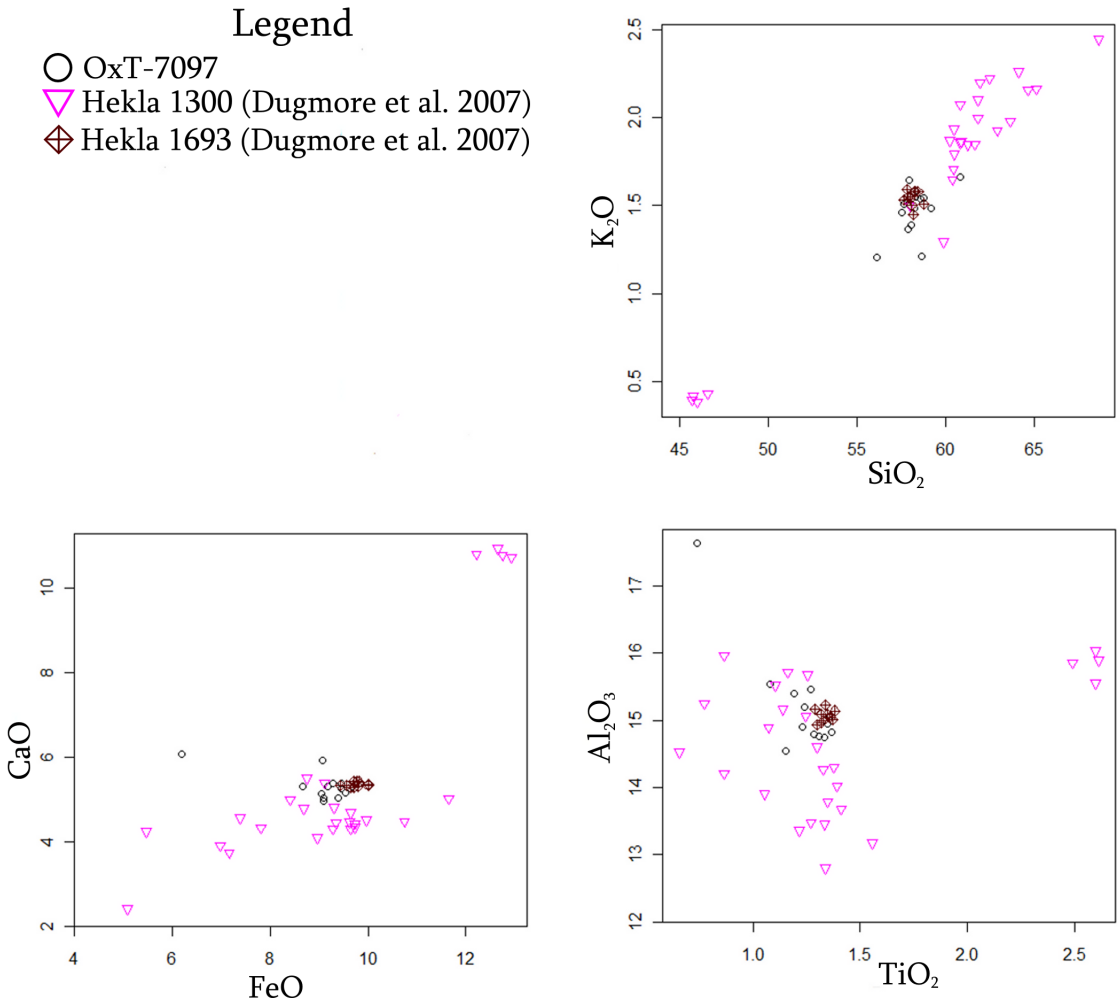


Figure 7.8: Comparison of OxT-7097 with published proximal data for Hekla 1300 and Hekla 1693 (Dugmore et al. 2007b). All units are in wt-%.

7.1.1.8 OxT-7099

OxT-7099 correlates to Hekla 1693 (Dugmore et al. 2007b).

7.1.1.9 Conclusions

The availability and quality of proximal tephra single shard analyses for known eruptions has been crucial in being able to correlate these tephra layers. Prior to the publication of Larsen et al. (2011) in July of that year, the only published analysis of Hekla 1766 was listed in a table in Haflidason et al. (2000) that came from an unpublished Icelandic thesis written in 1985. As it is, both Hekla 1766 and Hekla

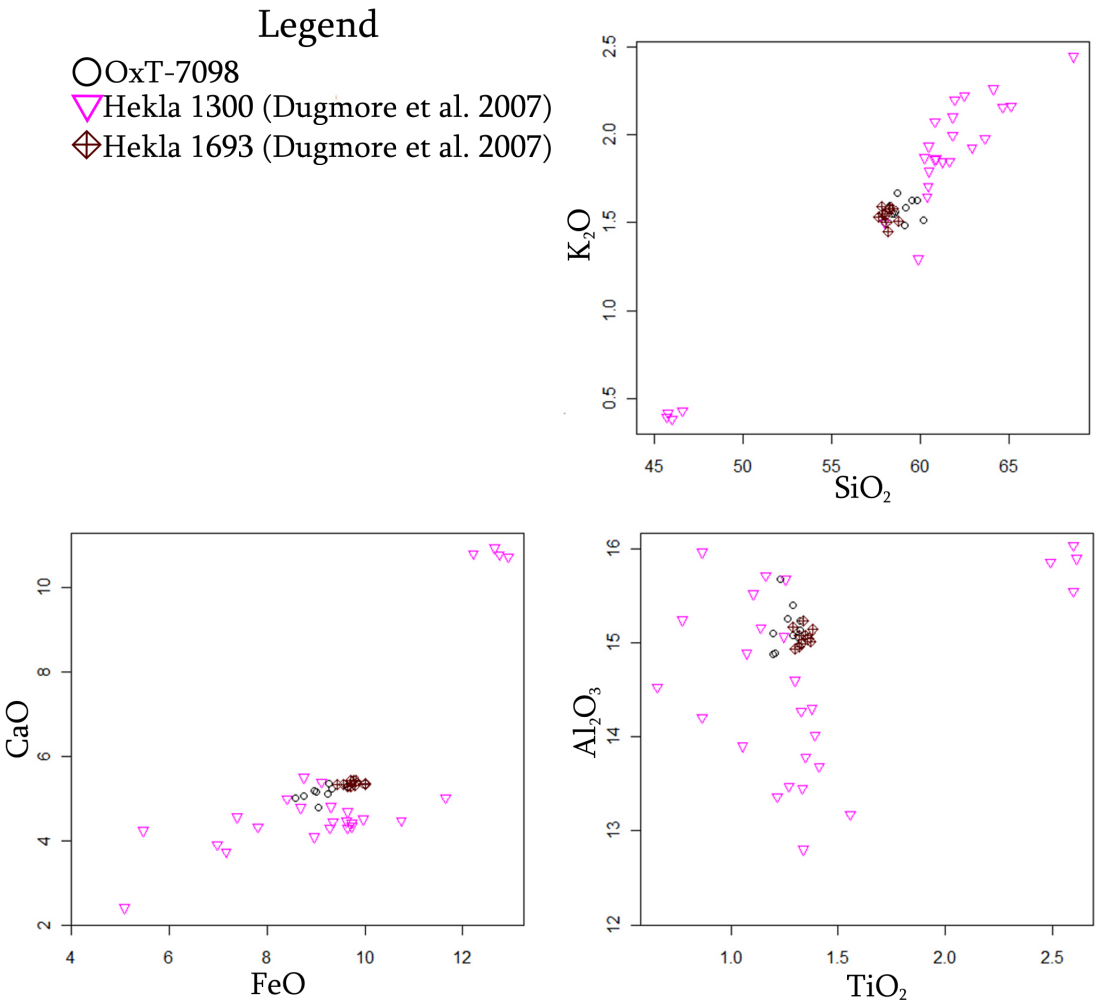


Figure 7.9: Comparison of OxT-7098 with published proximal data for Hekla 1300 and Hekla 1693 (Dugmore et al. 2007b). All units are in wt-%.

Table 7.1: Correlation results for samples from the Vatnsfjörður site.

Sample Number	Probable Correlation	Other Possible Correlations
OxT-5163	Hekla 1693	
OxT-5164	not tephra	
OxT-5165	Hekla 1693	possible inclusion of Katla 1721
OxT-5166	Hekla 1693	
OxT-7094	Hekla 1693	
OxT-7095	Hekla 1693	
OxT-7097	Hekla 1693	
OxT-7098	Hekla 1693	
OxT-7099	Hekla 1693	

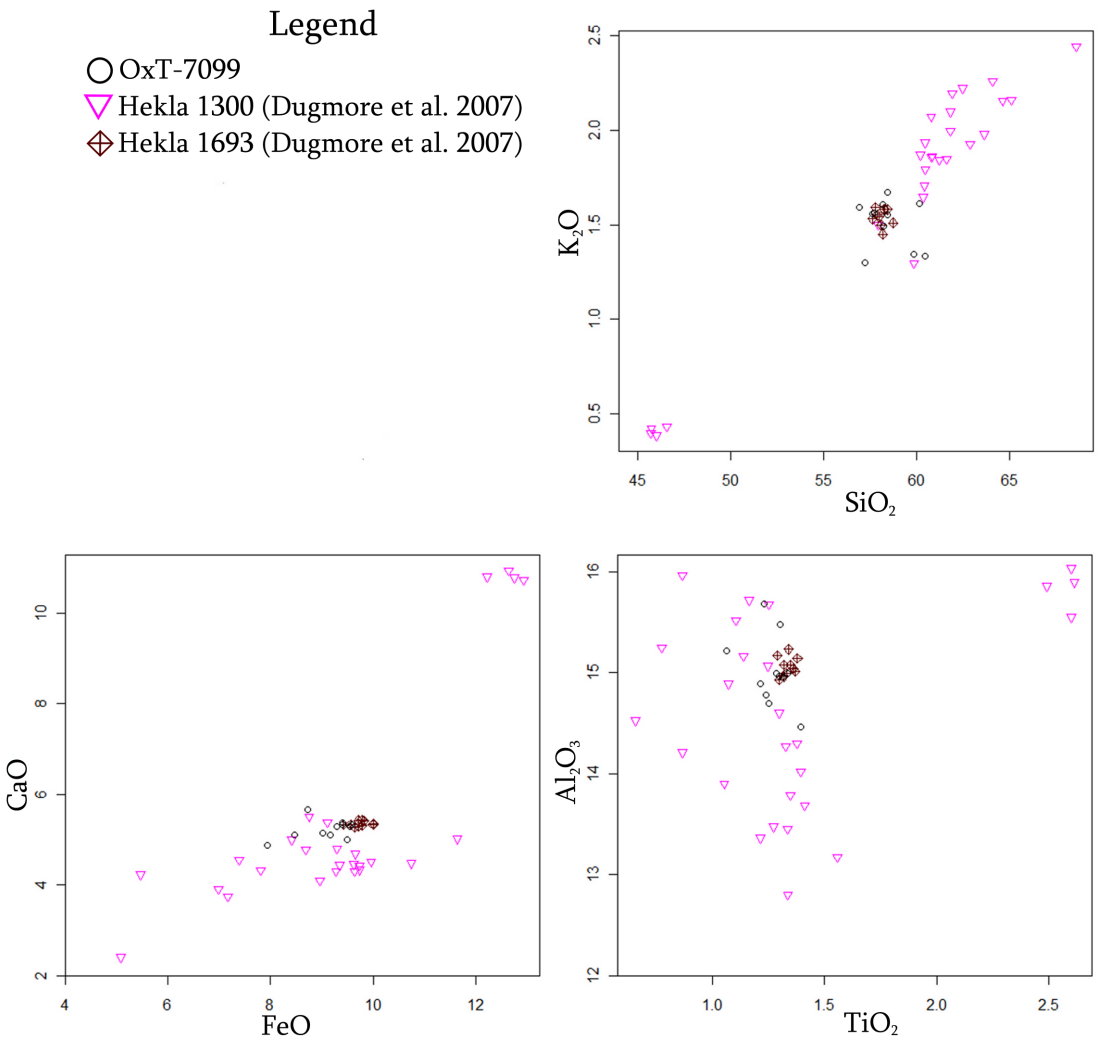


Figure 7.10: Comparison of OxT-7099 with published proximal data for Hekla 1300 and Hekla 1693 (Dugmore et al. 2007b). All units are in wt-%.

1693 have fewer than ten single shard analyses each published today. As discussed in Section 3.3, Hekla's eruptions are often geochemically complex, with eruptions that can last for months (Þórarinsson 1967). For example, Hekla 1104 has a wide range of glass chemistry, as shown in Figure 7.2. Although the explosive phase of Hekla eruptions is often only a few hours or days, the nature of the tephra ejected changes over that time period as the magma pool is depleted (Thordarson and Larsen 2007). Therefore it can be expected that the limited single shard analyses published from these eruptions will not encompass the full range of ejected tephra. This may explain why some of the analyses from the Vatnsfjörður samples are not as tightly constrained geochemically as Dugmore et al.'s (2007) analysis. It may also explain why, for example, for OxT-7097, -7098, and -7099, FeO values are consistently lower than those

recorded by Dugmore et al. (2007) for Hekla 1693.

However, the results presented here — that the visible tephra layers found throughout the archaeology at Vatnsfjörður most likely correlate to the Hekla 1693 eruption — provide new chronological information about the Vatnsfjörður site. With archaeological interpretation, this will aid in reconstructing the sequence of events as well as linking the chronological position of the Vatnsfjörður archaeological landscape to that of the wider region.

7.2 Hekla 1693 in the Vatnsfjörður archaeological site

The overall aims of the Vatnsfjörður project, which are discussed in more depth in Section 4.2.1, are to identify the relationship between the farm's evolution and the evolution of the surrounding landscape, and to identify why this farm in an apparently infertile region became a chieftain's seat and was a centre of power in the Vestfirðir region from the thirteenth century until its decline at the end of the seventeenth century (NABO 2011).

The results of the tephra correlation presented above for Vatnsfjörður contribute greatly to the understanding of the site. Briefly, through sampling in multiple areas, it has been determined that the visually identical tephra layers found throughout the stratigraphy represent the same eruptive event. This has been correlated to the eruption of Hekla in 1693. Following the identification of these tephra layers, they will now be put it into their context at each sampled location at the site. This then leads to using Hekla 1693 as an isochron to interpret change at the local level, within the Vatnsfjörður landscape, and from there to discussion of some questions in Icelandic and North Atlantic archaeology generally. Following that, this isochron will be used to connect Vatnsfjörður to local environmental records.

For interpreting a crucial moment in the history of Vatnsfjörður, the Hekla 1693 tephra layer is in an advantageous position, as the farm is known from historical documents to have declined in the late seventeenth century. The tephra layer takes on additional importance in light of the problems with radiocarbon dating archaeological material at Vatnsfjörður. This is due to a lack of preserved non-bone material and the

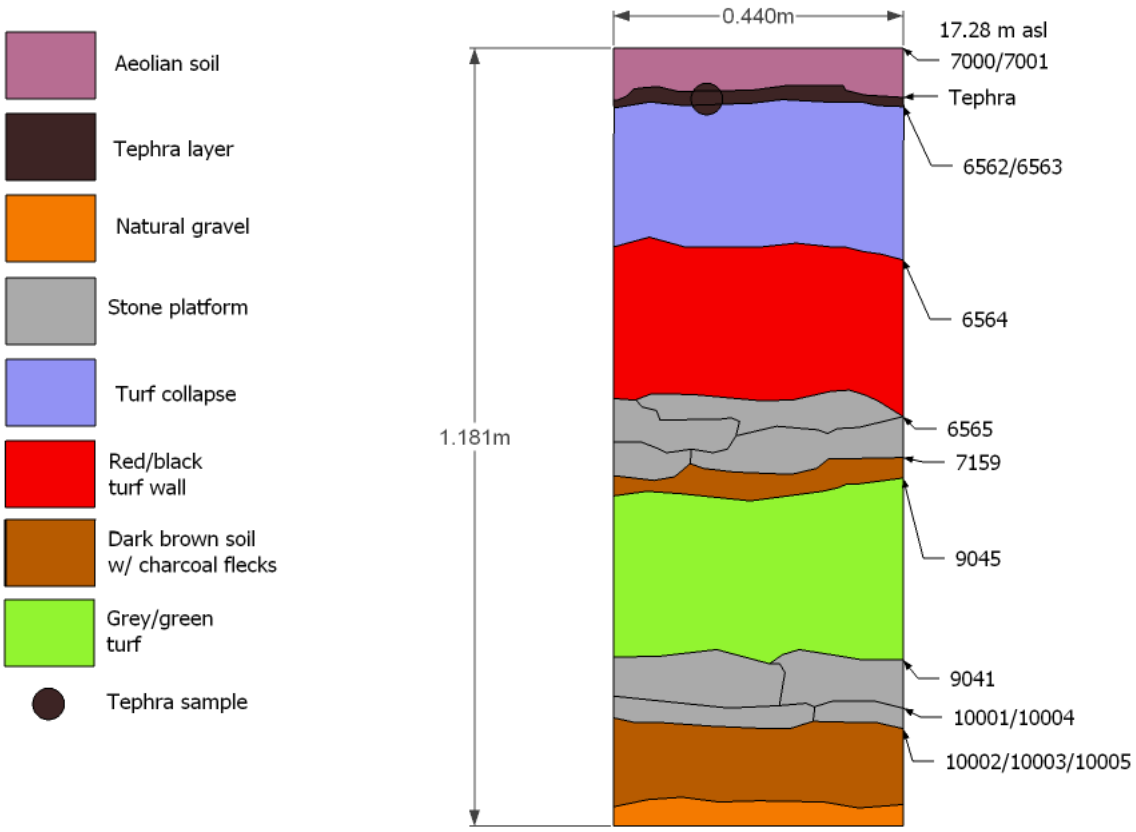


Figure 7.11: Stratigraphic profile of Area 14, which contains tephra sample OxT-5163 (labelled as 'tephra' near the top of the profile). The four and five digit numbers correspond to context numbers from the site, whose descriptions are found in Milek (2008; 2009; 2010; 2011).

Icelandic reservoir offset problem for non-herbivores, as well as generally low numbers of datable bones (e.g., Ascough et al. 2006; 2007; 2011).[1]

7.2.1 Area 14

First, the individual tephra samples will be considered in their respective contexts. OxT-5163 comes from Area 14, and its placement in the stratigraphy of Area 14 is shown in Figure 7.11, while its location on a plan of the area is shown in Figure 6.4. This sample was chosen to be representative of the visible tephra layer in an archaeologically complex part of the Viking Age area of the site. Area 14 was opened as a test trench in 2006, then excavated in 2007-2010 (Milek 2008: 65-68; Milek 2009: 55-56;

[1]New research techniques are being developed to deal with the reservoir offset, including using different elemental isotopes (e.g., Sayle et al. 2014).

Milek 2010: 53-59; Milek 2011: 31-36). Area 14 contained the remains of three structures, the relative positions of which are shown in the stratigraphy, separated by stone floors. Structure 7, which overlayed Structures 9 and 10, had a thick turf wall made of reddish black turf that has been associated throughout the excavations with the medieval period because of its stratigraphic position. The walls of Structure 7 contained some small bones identified as belonging to juvenile cattle and adult ovicaprine, but not enough to be a midden dump, so it has been suggested that their placement was deliberate and meaningful (Milek 2010: 55). Stratigraphically below this are layers associated with Structure 9, which belonged to an early construction phase based on the presence of grey podsols that have been associated with the *skáli* and other structures that have contained artefacts from the tenth century. Unit 9038, the dark brown, organic floor deposit in Structure 9, contained a rich faunal assemblage that included arctic fox, cattle, pig, ovicaprine, fish, and small phocids (Dupont-Hébert in Milek 2010). Beneath this was Structure 10, a very small building containing a collapsed hearth and possibly an oven, and constructed of the same grey podsol turf as Structure 9. Structure 9 seems to have been built over Structure 10 very quickly (Milek 2011: 31-32). Structures 9 and 7 are thought to have been associated with animals, while Milek (pers. comm. 4 January, 2012) has identified Structure 10 as a pit house, a common feature in Icelandic Viking Age farmsteads.

OxT-5163, the Hekla 1693 ash layer in this stratigraphic profile, overlies all three of the structures. It is separated from Structure 7 by mixed layers of turf debris, indicating that the ash fell some time after its collapse. Contexts 7000 and 7001, which overlay the Hekla 1693 tephra layer, contained no archaeological finds and were composed entirely of aeolian topsoil. Therefore, Hekla 1693 arguably provides a date to cap the archaeological phases in Area 14. The importance of this to the interpretation of the site, as well as to answering a longstanding question in Icelandic archaeology, is discussed further below.

7.2.2 Area 32

OxT-5165 came from Area 32, which is also located in the Viking Age area of the excavation. Its location is shown in plan in Figure 6.5. This sample was chosen because although Area 32, as shown in the stratigraphy in Figure 7.12, contained very little archaeology, it was stratigraphically connected to the *skáli*, which had been closed after the 2004 excavation (Edvardsson and McGovern 2005) and so could not

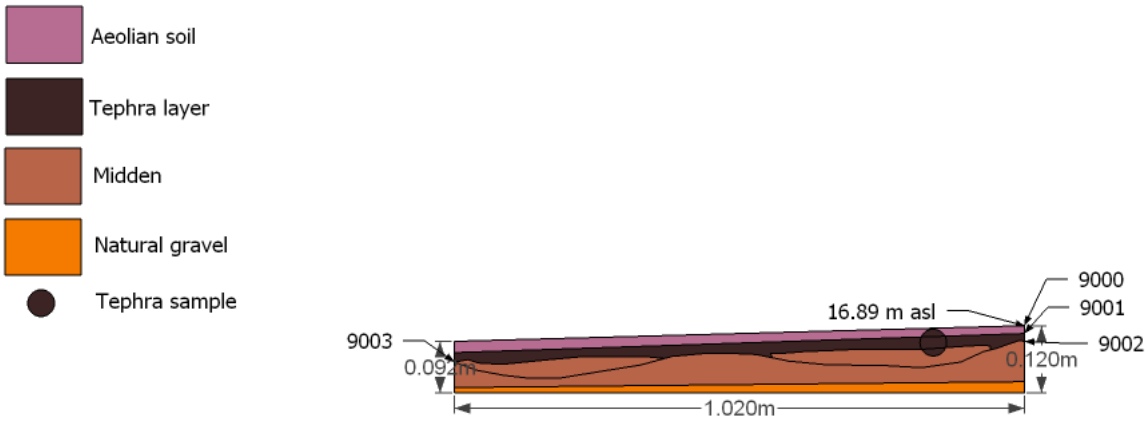


Figure 7.12: Stratigraphic profile of northwestern side of Area 32. The four and five digit numbers correspond to context numbers from the site, whose descriptions are found in Milek (2010).

be sampled. Therefore this sample provides an important link to the main building of the Viking Age part of the site. Area 32 is located along the west and north sides of the *skáli*. Area 32 was excavated entirely in 2009 (Milek 2010: 60-62), and consists of contexts 9000 and 9001, surface turf and aeolian topsoil, which overlie the tephra layer sampled for OxT-5165, which in turn overlies two thin, lensed turf/sheet midden layers with very few artefacts and some poorly preserved bone debris. There is no evidence of turf collapse from the *skáli*, which came as a surprise to the excavators given its proximity. Nearer to the door of the *skáli*, and hence not shown in the stratigraphic profile above (as the doorway is on the eastern side of Area 32), was a layer that seemed to be trampled debris from people entering and exiting the building. Beneath these thin midden layers was the natural gravel which underlies all of the Viking Age area excavations at Vatnsfjörður. Once again, Hekla 1693 caps the archaeology in this area, and the contexts above it are devoid of archaeological material, putting a final date on archaeological activity next to the *skáli*. The confirmation that the visually similar tephra layer found above the archaeology throughout the Viking Age area is Hekla 1693 in two places at opposite sides of the area means that archaeological activity throughout that portion of the excavation has an end date. Also, although the majority of the Viking Age excavation was officially 'closed' due to reaching the bottom of the archaeological area in 2009 (aside from Area 14, which was closed in 2010), not all of the component areas of the excavation have been linked to one another stratigraphically. The Hekla 1693 tephra layer provides a useful marker to link them together chronologically and stratigraphically.

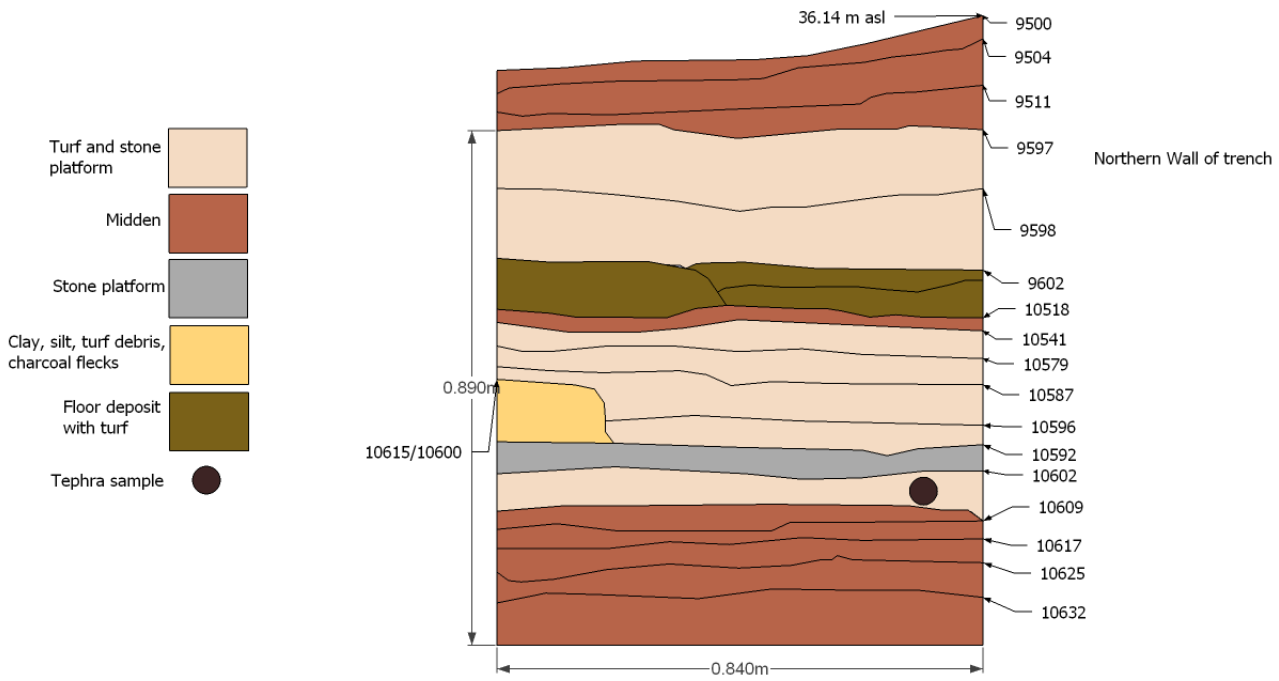


Figure 7.13: Stratigraphy of Group 8562 in the Farm Mound. The four and five digit numbers correspond to context numbers from the site, whose descriptions are found in Milek (2010; 2011).

7.2.3 Group 8562

Unlike the tephra samples from the Viking Age area, the samples from the Farm Mound were embedded between archaeological layers. Farm mound construction, which is described in more depth in chapter four, was a style common in Iceland, Orkney (as at the East Mound), Shetland, the Faroe Islands, and Norway for centuries, from before the settlement of Iceland until the early twentieth century in some cases. People built homes immediately atop of the remains of previous ones, so that the farm area gained elevation over time. People almost never rebuilt an entire house, instead building new rooms or reusing walls from older rooms in a piecemeal style of construction (Vésteinsson et al. 2002:14-15). The tephra samples therefore must be considered as embedded within the archaeology of the farm mound, and the tephra layer to have played a role within the life of the farm, much as other layers of sediment would have done.

Sample S-557 (OxT-7094) comes from context 10602 in Room 8562 of the Farm Mound portion of the site, which was excavated in 2009-2010 (Isaksen in Milek 2011: 52-54) and whose stratigraphy is shown in Figure 7.13. The placement of this sample



Figure 7.14: Aerial photograph of Room 8562 showing location within the Farm Mound (from Isaksen in Milek 2011).

in plan and that of the others from the Farm Mound are shown in Figure 6.5. This sample was chosen for analysis because of its importance in the sequence of developments at the farm mound, and also because the tephra layer in it was relatively intact compared to other occurrences of the visible tephra layer throughout the farm mound. The upper portion of this group (contexts 9500, 9504, 9511, 9597, 9598, and 9602) was excavated in 2009 and consisted of various midden deposits rich in animal bones on top of a sequence of turf collapse layers. In 2010, the area of excavation was extended to the west, and the full extent of the room was revealed. Context 10518 was another midden deposit, located above an alternating sequence of six turf and stone layers, the bottom of which (context 10602) was ultimately found to be part of the same platform as 9597 and 9598. The tephra layer analysed here (OxT-7094) was found amongst the stones in context 10602, as if the tephra had been swept away (either deliberately or by the movement of feet) and pushed into crevices in the floor. This seems to imply that the surface was in active use in 1693. Below 10602 were five soft deposits containing turf, silt, and animal bones that may be midden deposits. The last of these deposits, context 10632, was the final one excavated due to the discovery that the walls of the room were running under deposits in an adjacent

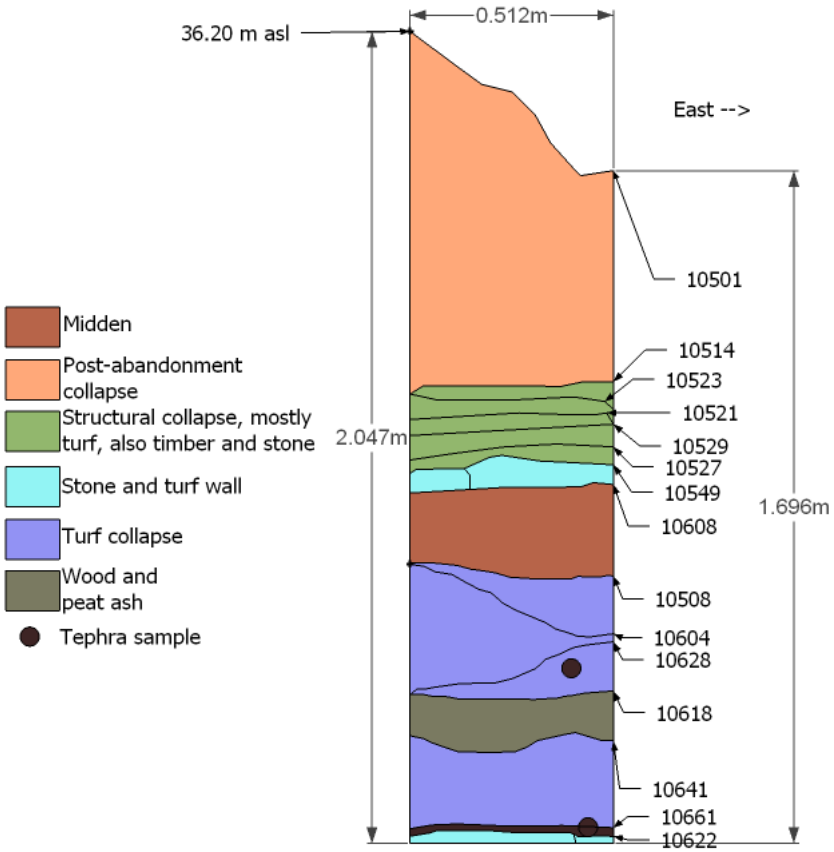


Figure 7.15: Stratigraphy of group 10515. The five digit numbers correspond to context numbers from the site, whose descriptions are found in Milek (2011).

group.

7.2.4 Group 10515

Sample S-556 (OxT-7095) comes from Group 10515 in the Farm Mound, which was first excavated in 2010 as part of the extension of the western edge of the Farm Mound excavation to investigate the north-south running wall remains uncovered in 2009 (Isaksen in Milek 2011: 46-50). This group contains all the deposits excavated from this western expansion, which was approximately 40 cm by 330 cm. Below the turf and topsoil was a thick mixed material context (10501) that most likely formed when the farm mound was finally abandoned and began to collapse in 1906; it was composed of a mixture of sandy silt, turf debris, and gravel (Isaksen in Milek et al. 2011). Below this thick (30 cm – 100 cm) collapse layer was a series of structural collapse layers composed mostly of turf but containing bits of timber and rocks. Seventeenth to

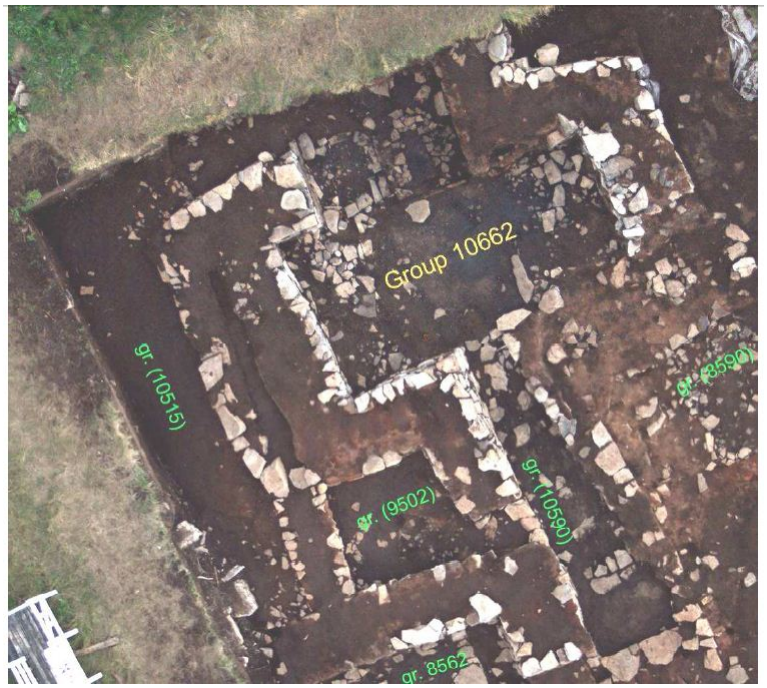


Figure 7.16: Group 10515 photographed from above before the removal of layers stratigraphically above Hekla 1693 (Oddgeir Isaksen, pers. comm., 16 October, 2011).

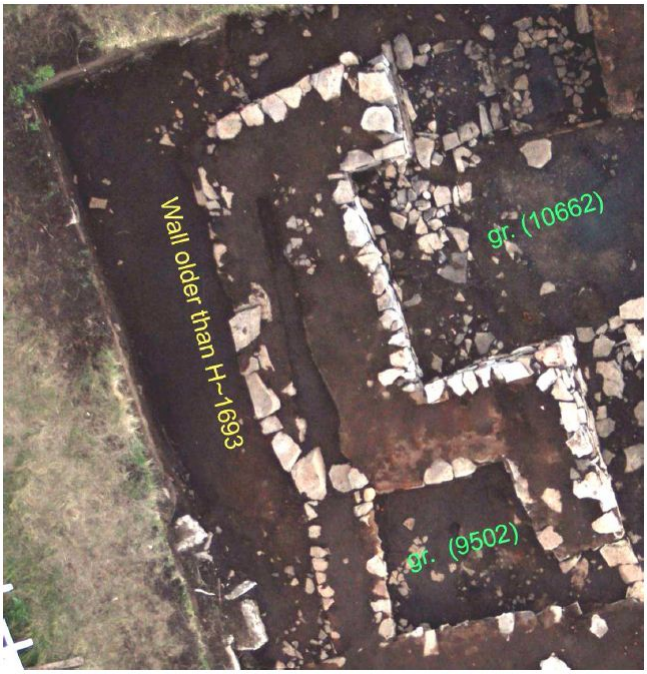


Figure 7.17: Group 10515 photographed from above after the removal of layers stratigraphically above Hekla 1693 and Hekla 1693 (Oddgeir Isaksen, pers. comm., 16 October, 2011).



Figure 7.18: Photograph of Group 10515, facing north, showing hearth (10540) and wall (10549) (from Isaksen in Milek 2011).

eighteenth century pottery sherds were found throughout these layers. The northeast corner of the room contained deposits relating to a hearth that extended beyond the western /northern boundary of excavation, with a sequence of floor deposits spilling out across the floor in front of the hearth. The hearth area had postholes near to it, suggesting that there was some sort of framework built over it, and a 15 cm high turf wall around it, most likely used to contain burning material. The hearth was almost certainly external, lying beyond the turf wall that this western expansion was originally opened to examine. That turf wall was 300 cm thick and ran through the middle of Group 10515; the thickness of the wall suggests that it was an external wall. None of these contexts are shown in Figure 7.15 because the tephra sample was taken from the opposite side of the excavation area for this group; however they relate to the interpretation of the group.

The stratigraphy of the north side of the wall is shown in Figure 7.15. Below context 10501, there are several layers of structural collapse deposits. Below that is a wall unit, 10549, which consists of a turf core with stone facing on either side. Below that is a thick sheet midden deposit containing fish bones, glass, iron, and wood, followed by several layers of turf collapse. Tephra from the Hekla 1693 eruption (OxT-5166) is flecked throughout these turf collapse layers in small quantities. As discussed in chapter four, it was initially thought that finding the visible tephra layer on the remains of turf walls or other turf building materials would cause problems in the interpretation of the chronology. This was because the tephra layer could have been

deposited either when the turf was growing, or later, when it was part of the house. At least in this case, it was easy to tell in the field that the tephra here had been deposited on the peat some time before it was used in this location as a building material because the tephra was jumbled throughout the peat rather than lying atop it (Oddgeir Isaksen, pers. comm., 3 December, 2011). This suggests that the tephra fell on the turf before it was cut and used for construction, and that the turf collapse in these layers therefore post-dates 1693. Below the turf collapse is a soft deposit composed of wood and peat ash, context 10618, followed by another thick layer of turf collapse that did not contain any visible tephra. Immediately below that, with sharply delineated boundaries both above and below the layer, is the visible tephra layer (context 10661), sample OxT-5166, which has been correlated with Hekla 1693. Unlike the tephra found in Group 8562, which was found amongst stones, the layer clearly lay atop a thick turf and stone wall that is the western end of structures 10662 and 9502. This was beneath turf collapse. Therefore it seems that the tephra was able to lie upon the wall without being disturbed so that when the turf collapsed onto it, it remained in a solid layer.

7.2.5 Area 40

The location of Area 40 in relation to the Farm Mound and Viking Age areas of excavation is shown in Figure 6.6. It is located to the northeast of the main excavation areas, and excavation there began in summer 2011. Thus far, a number of thin/lenses of cultural material have been revealed, lying above two walls, one at the south end of the excavation area (which is 7.5 x 5 m) and one at the north end. The tephra studied here came from context 11057. This context is the uppermost phase of the south wall. It is composed of turves which were mostly dark brown and reddish orange in colour, with some bright orange and pale beige striations. The turves contained a grey-green tephra within them as a recurring band (Dawn Elise Mooney, pers. comm. 1 December, 2011). Therefore the tephra (OxT-7099), which has been correlated with Hekla 1693, pre-dates the construction of this phase of the wall. It must have fallen some time prior to the cutting of the turves for use in construction. Therefore this portion of the wall is contemporaneous with other layers within the Farm Mound that also contain the tephra.

Area 40 contains other small amounts of tephra of a similar visual description as that found throughout the archaeology and identified geochemically as part of this research

as Hekla 1693. However, not all of it was sampled for geochemistry because of the incomplete excavation. Most interesting are two contexts. Context 11085, contained tephra in situ in the south wall, visible only at the far western end of the wall. The tephra appeared to overlie/lip up against the earliest phase of wall construction. Context 11086, meanwhile, also contained tephra in situ at the east end of the north wall, where tephra was lying underneath the eastern extension of the north wall. The north wall itself is similar to Context 11057, composed of turves banded with tephra. Whatever Area 40 was, it seems to have been constructed contemporaneously with or shortly after the Hekla 1693 ash fall.

7.2.6 Area 45

Area 45 is a test trench that is 1 x 2 m located to the east of the main excavation areas of the Vatnsfjörður. Its location is shown in Figure 6.6. The tephra came from context 11004, which formed the north wall of Structure 5. This is a large, horse-shoe shaped structure which may have been a workshop or a smithy, but as of summer 2011 it has only been excavated in this small test trench, so its purpose remains unclear (Dawn Elise Mooney, pers. comm., 1 December, 2011). The tephra (OxT-7097) came from immediately above the stone wall, as shown in Figure 7.19. No cultural layers were found above the tephra layer, but again, as this is a test trench, results remain preliminary. However, it seems likely that Hekla 1693 provides a *terminus ante quem* for this structure.

7.2.7 Tephra from Hekla 1693 and the interpretation of the Vatnsfjörður excavations

The names 'Viking Age' and 'Farm Mound' that are used to delineate the different parts of the excavation have persisted from the period when the former consisted solely of the *skáli*, and the name should not be taken as an indication of the true age of the archaeology found in that area of excavation. In fact, the time of the transition between the two areas is a matter of debate that is mirrored at excavations throughout Iceland. Vésteinsson (2001: 11-12) identifies a general pattern of settlement for early-founded high status farms in Iceland. Those farms that were founded shortly after the *landnám* tephra layer fell are often situated very close to the beach, and often at the mouth of a stream. These early settlers would build a dwelling, like a *skáli*, near the beach. At some point this dwelling would be abandoned and settlement

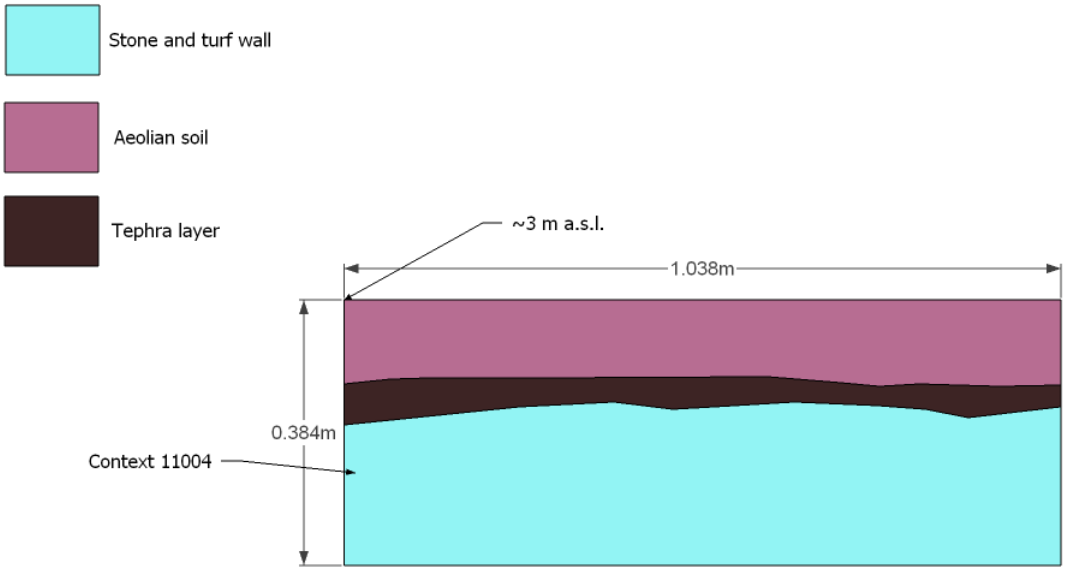


Figure 7.19: Stratigraphy of test trench Area 45. The five digit number corresponds to context numbers from the site, whose descriptions are found in Milek (forthcoming).

would move upslope, away from the beach. A church building would follow and exploitation and cultivation of a nearby wet meadow would provide the farm with the majority of its agricultural needs. Vésteinsson theorises that the shift from the initial settlement location to the upslope area took place in the time of only one or two generations, suggesting that this was due to clearance of birches and other trees from the upslope area that, in turn, led to erosion and flooding of the stream that the original farm had been founded upon. He uses the example of Grelutóttir in Arnarfjörður, where excavations of the original farm found it covered in rubble (2001:12). However, Vésteinsson's theory that the shift upslope occurred in one or two generations has been challenged by evidence from recent excavations of other early coastal settlements, such as Sauðarkrókur in Skagafjörður (Bolender et al. 2008), and the dating of that transition is now considered a major research question for Icelandic archaeology (Milek pers. comm., 7 December, 2011). Similarly, this pattern does not seem to apply to Vatnsfjörður, where there are at least three distinct building phases in the Viking Age area, as noted in the description of Area 14. Based on the presence of the Hekla 1693 tephra layer, all that can be said with certainty about the abandonment of the Viking Age area is that it took place at an undetermined time before that eruption. Although the tephra layer lies directly atop collapsed structures, as in Area 14 and Area 45, the generally low sedimentation rate throughout

the archaeology (e.g., Area 32) means that it is difficult to estimate how much time had passed between the abandonment and subsequent collapse of a structure and the deposition of the tephra layer.

The presence of archaeological layers below the Hekla 1693 layers in the Farm Mound area means that the farm mound was already in use in 1693. The tephra layer overlies at least one period of construction and excavation in the coming years may reveal more. Therefore it is possible that there was activity for an unknown amount of time both downslope in the Viking Age area by the beach, and upslope, on the Farm Mound. If such simultaneous use of these areas did occur, that would alter the traditional view of the complete abandonment of the original settlement area by the beach in exchange for an upslope farm development.

However, the lack of archaeological evidence above Hekla 1693 in the Viking Age area suggests that, ultimately, the shift upslope to the farm mound was a complete movement, with the people at the farm leaving behind the remains of workshops as well as living spaces and re-establishing these activities at new areas upslope. There is no evidence for coastal inundation in the stratigraphy, and indeed the sea-level study described in Section 7.6 indicates that sea-level was falling throughout the period. There is also no evidence that the small irrigation channel to the northwest of the settlement buildings ever flooded any portion of the archaeology. Further research is needed to understand why the farm and its outbuildings shifted upslope entirely at some point before 1693.

Another consideration at the archaeological excavation is the effect that the ash fall in 1693 might have had on life at the farm. The tephra layer is 1-2 cm thick and has been found in every trench opened at the site, suggesting that, although it appears small in the stratigraphic record, it would have been a major event at the farm. Indeed, the ash fall from the eruption of Hekla in February 1693 is the only known ash fall event to be recorded historically at Vatnsfjörður. A churchman there wrote that so much ash had fallen on the homefield that, 'in the time needed to write a short letter ... it took the impression of footprints when walked on', while someone living in a neighbouring region noted that the black ash had travelled as far as Vestfirðir, and, 'The earth was blackened by sand [ash], so that in some places it was quite necessary to give hay to the beasts at pasture even though the ground was quite free of snow' (quoted in Þórarinsson 1967:92). The late seventeenth century was a bad time for Icelanders in a variety of ways, as discussed in Section 2.2.2, and so a disruptive volcanic eruption could have had serious consequences for the farm. After several

centuries of in general colder and less predictable weather than that from the halcyon days remembered in the sagas, the country was still reeling from population loss from famines and recurrent outbreaks of plague and other diseases. Increasing control by Denmark led, in 1602, to enforced changes to trading conditions that were extremely unfavourable to Icelandic interests; meanwhile, pirates raided the country's shores. All of these elements have led to this period being known as Iceland's 'Dark Ages' (Kristinsson 1973; Karlsson 2000).

Based on the archaeological excavations, however, there is little evidence from Vatnsfjörður to suggest that the eruption and subsequent ash fall had any permanent effect on the farm. Þórarinsson (1967: 95) provides a map of homesteads abandoned or affected by this eruption based on historical records. It shows that only six homesteads were abandoned, and all of these were within 15 km of Hekla. One of these has been excavated, Sandártunga, and it was covered in a heavy blanket of ash (Vésteinsson 2001). In general, Þórarinsson notes that farms affected by more than 25 cm of freshly fallen tephra were never resettled; farms affected by 10–15 cm were abandoned but only for a short period of time (1-4 years), whereas fallout less than 10 cm deep caused extensive damage but did not lead directly to abandonment. Farmsteads and crofts described by him as 'badly damaged' by the eruption extend to 40-50 km northwest from the volcano, but are all south of Langjökull. For the people at Vatnsfjörður, it may have been a once in a life time event to have such noticeable ash fall since they lived so far from active volcanic centres. The Lakí Fires of 1783 where probably the only other volcanic activity to have had any direct impact on Vatnsfjörður, and these are difficult to detect in the archaeological record because, instead of laying down tephra, they caused a dry fog that led to a multi-year famine (Vasey 1991; Stothers 1996). However, the effects of any disaster can be difficult to determine archaeologically. For example, Streeter et al. (2012) were unable to find archaeological evidence clearly connected to the demographic crises caused by Iceland's catastrophic plague outbreaks in the 1400s. Written sources say that Vatnsfjörður went into decline in the late seventeenth century (Tulinius 2005), and so perhaps the eruption of Hekla in 1693 did have profound effects.

7.3 Homefield

7.4 Correlating distal layers with proximal glass chemistry

As discussed in Section 6.2.1.1, the homefield core's tephrostratigraphy, which is shown in Figure 6.17, contained microtephra in every sampled interval, including several distinct, identifiable tephra layers. It was suggested that the abundance of microtephra in the core could have been caused by a relatively constant low-level influx of sediment from the surrounding bedrock. However, Hardarson et al. (1997) have published glass chemistry data from basaltic lavas in Súgandafjörður (Vestfirðir) that they believe is representative of the region as a whole. It is significantly different from any of the tephras analyzed from the homefield or, for that matter, elsewhere at the site, with SiO_2 values around 48 wt-% and TiO_2 values around 1.75 wt-%. Therefore it seems likely that the reasons for this density of microtephra deposition are the result of multiple eruptions from Hekla volcano with similar glass chemistry and the sensitivity of peat as a depositional environment for microtephra.

7.4.1 OxT-4672

The first notable peak of microtephra within the soil core, OxT-4672 (11-13 cm), correlates to the Hekla 1766 eruption (proximal glass chemistry from Larsen et al. 2011). The eruptions of Hekla 1300 and Hekla 1693 (Dugmore et al. 2007b) were also included in this analysis, but geochemically OxT-4672 most closely matches Hekla 1766. This is shown in Figure 7.20. Furthermore, this correlation fits with the stratigraphic position of the soil layer.

The ash fall path of Hekla 1766 is shown in Figure 7.1. Þórarinsson (1967) notes that the best contemporary account of this eruption comes from Einar Jónsson (1712-1788), who was at Ás in Hreppar, which is 32 km west-northwest of Hekla, indicating that the ash fall was moving in that direction. The eruption took place on the morning of 5 April. Other contemporary sources record that there was a great deal of tephra fall from the eruption, and that scoria 'as big as a man's fist' fell in Skagafjörður, in the northwest(*ibid*: 111). Tephra fell throughout the north of Iceland, and, although contemporary accounts place that fall to the east of Vatnsfjörður, it seems likely that,

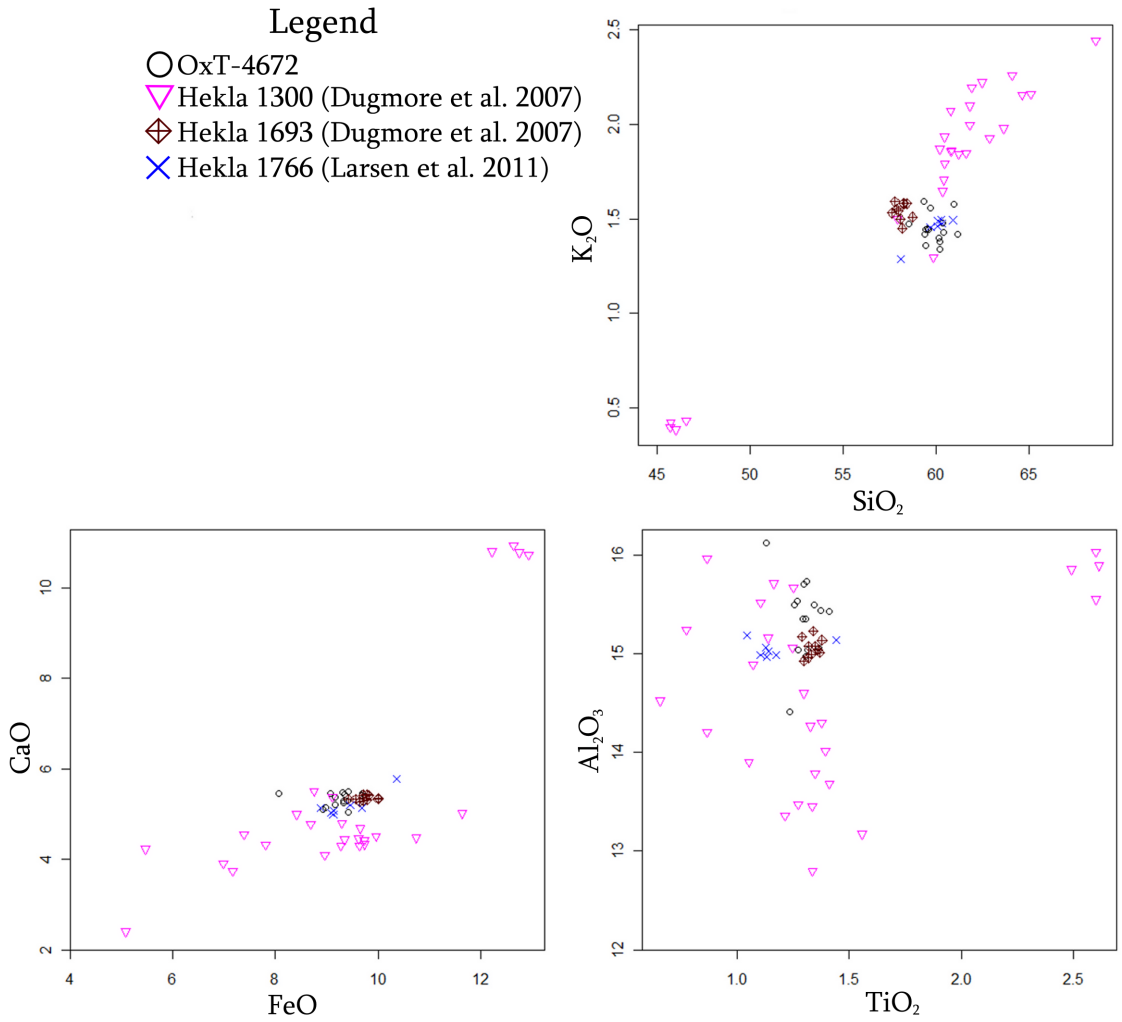


Figure 7.20: Comparison of OxT-4672 with published proximal data for Hekla 1300, Hekla 1693 (Dugmore et al. 2007b), and Hekla 1766 (Larsen et al. 2011). All units are in wt-%.

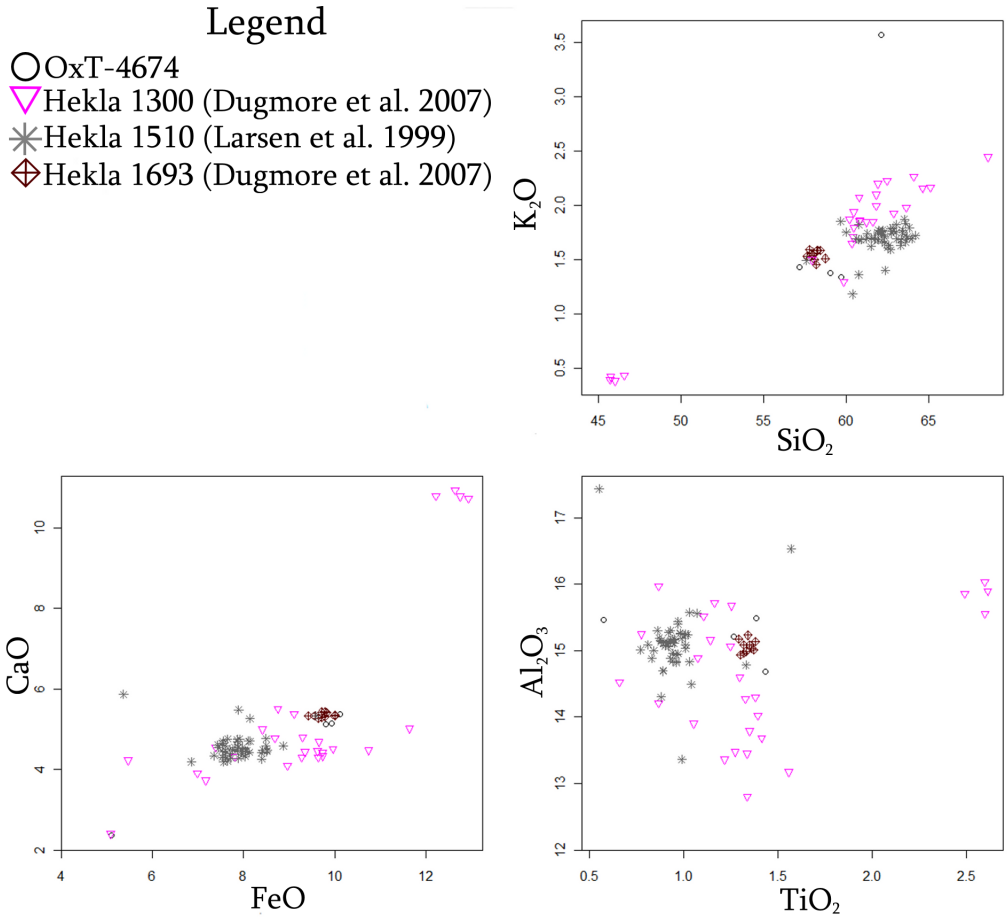


Figure 7.21: Comparison of OxT-4674 with published proximal data for Hekla 1693, Hekla 1300 (Dugmore et al. 2007b), and Hekla 1510 (Larsen et al. 1999). All units are in wt-%.

given the presence of visible tephra in nearby Skagafjörður, a fine layer of tephra could have fallen in Vestfirðir.

7.4.2 OxT-4674

The glass chemistry of OxT-4674, from 15-17 cm in the core, closely resembles that of OxT-4675, which is correlated in the section below to Hekla 1693 (Dugmore et al. 2007b). Given the quantity of tephra that fell at Vatnsfjörður as a result of that eruption, it seems likely that this tephra layer could span multiple segments of the homefield core. Figure 7.21 shows the correlation of tephra grains from this layer with Hekla 1693.

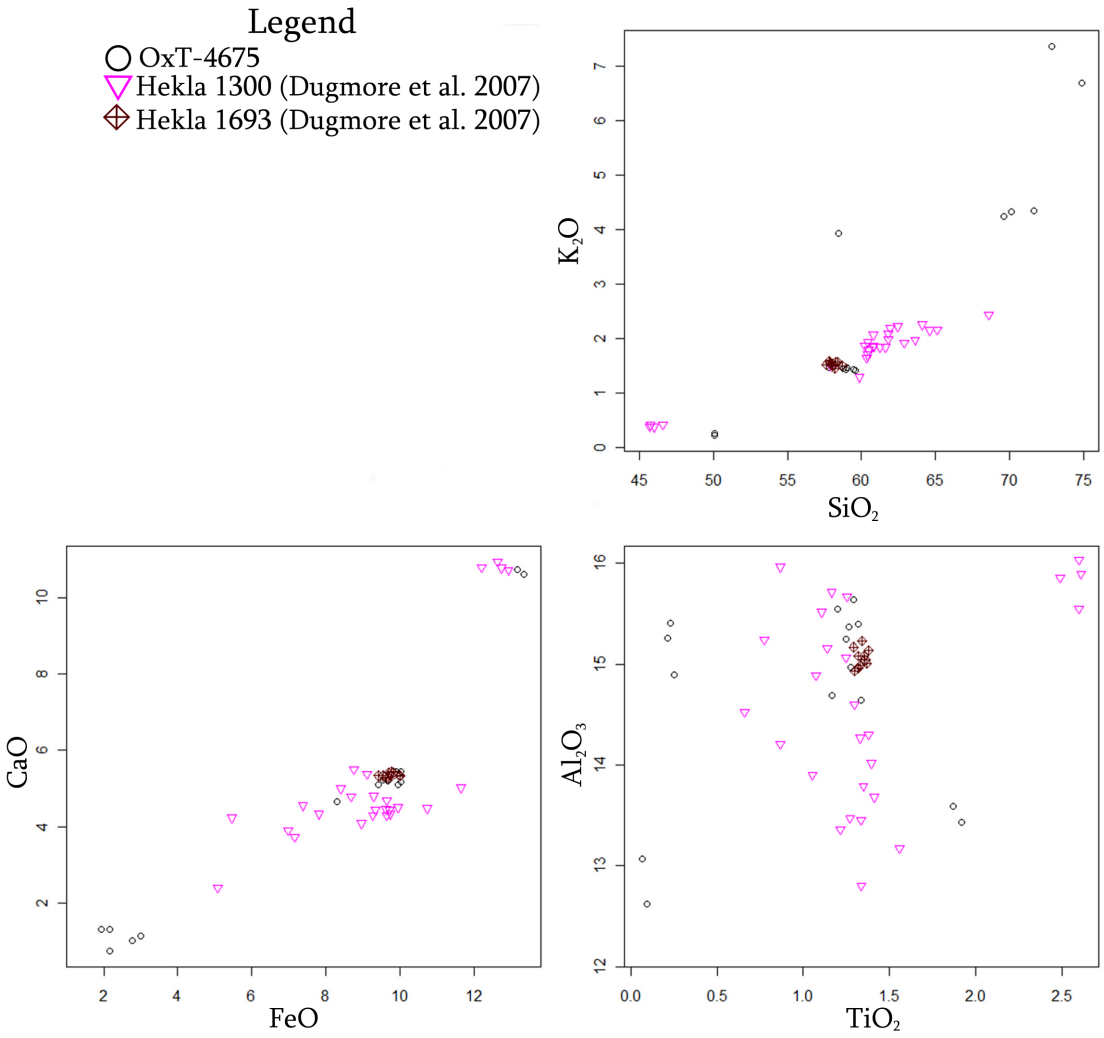


Figure 7.22: Comparison of OxT-4675 with published proximal data for Hekla 1693 and Hekla 1300 (Dugmore et al. 2007b). All units are in wt-%.

7.4.3 OxT-4675

OxT-4675 (17-19 cm) correlates to Hekla 1693 (Dugmore et al. 2007b). Based on the glass chemistry of OxT-4674, it seems that this large tephra fall has spread across multiple sampled sections of the Homefield core. The shard count shown in Figure 6.17 confirms this: the portion from 17-19 cm had the highest shard count in the core, and the portion from 15-17 cm can be interpreted as a smaller portion of the tephra fall. It could also be interpreted as tephra moving through the sediment post-deposition, as is discussed in Section 3.2. The glass chemistry is shown in Figure 7.22 compared to proximal glass chemistry from Hekla 1693 and Hekla 1300 (Dugmore et al. 2007b).

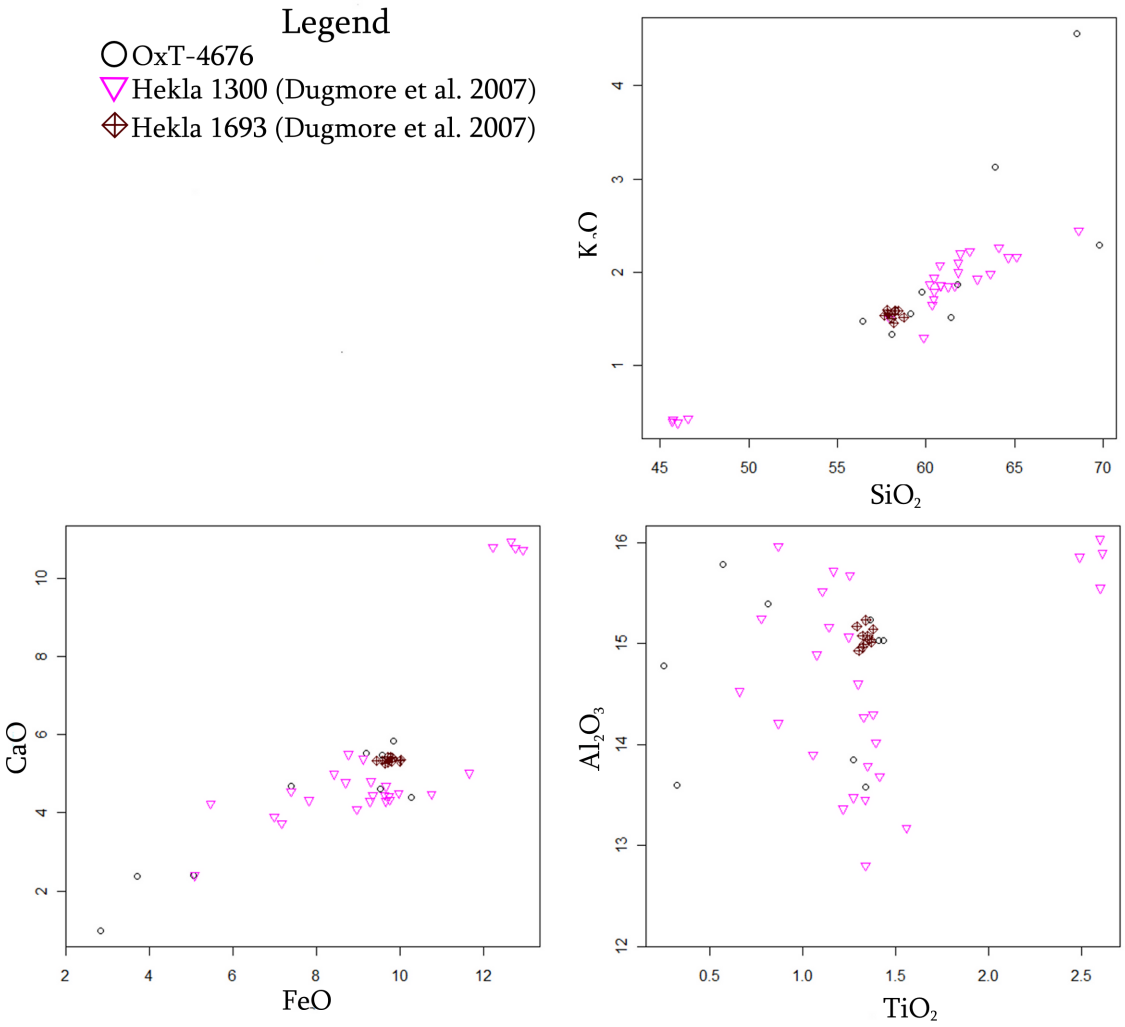


Figure 7.23: Comparison of OxT-4676 with published proximal data for Hekla 1693 and Hekla 1300 (Dugmore et al. 2007b). All units are in wt-%.

7.4.4 OxT-4676

OxT-4676 (19-21 cm) correlates to Hekla 1693, perhaps representing the lower limit of the eruption (although OxT-4677, 21-23 cm, may be the lower limit). This correlation is shown in Figure 7.23. This layer spans several centimetres of the Homefield core, which is consistent with how heavy the ash fall from this eruption was at other parts of Vatnsfjörður.

7.4.5 OxT-4677

The glass chemistry of OxT-4677 (21-23 cm) is split between two groups, as described in Section 6.3.1.2. Those two groups, as shown in Figure 7.24, are generally discrete. The first, with lower SiO_2 wt-%, cannot be correlated with any known proximal eruptions, but its geochemistry indicates that it is not from the Hekla volcanic system. Using Mahalanobis distances (which are discussed in Section 5.4.4), its nearest match from the available data set of published proximal data is Katla 1721, followed by Lakí 1783. The second group, with higher SiO_2 wt-%, may correlate to Hekla 1693, the same eruption as OxT-4676. Therefore this layer is constrained by Hekla 1693 above (at 21 cm) and Hekla 1300 below (at 29 cm).

Based on the date of an unknown Hekla eruption between 1300 and 1693 for the second compositional group, and the closer association of the glass chemistry of the first group with the Katla volcanic system, then perhaps the first group correlates to the eruption of Katla in 1357 or another Katla eruption, perhaps one closer to 1693. Unfortunately, only Einarsson et al. (1980) have published glass chemistry from any Katla eruption during that time period. From the 1357 eruption, they have published a single analysis without a recorded standard deviation. Figure 7.25 shows OxT-4677 plotted beside this single data point. There are some differences: notably, this group of OxT-4677 has higher CaO and lower NaO values than what Einarsson et al. recorded for Katla 1357, but their single data point does not take into account any compositional variation during the eruption. The SiO_2 and TiO_2 wt-% values are very similar. Therefore, based on stratigraphic position and other contextual evidence, as well as some oxide weight percentages, it seems likely that OxT-4677 contains tephra from a Katla eruption – possibly that of 1357 – in addition to the mystery Hekla eruption. During the 1357 eruption, the bulk of tephra from the eruption was found to the south of the volcano, but an annalist in the northwest (near Snæfellsnes) may have reported seeing it in the distance, indicating that an ash cloud may have been seen in the area (Einarsson et al. 1980). It is also possible that microscopic ash particles blew to the northwest with a change in wind. There were a number of other Katla eruptions during this time period, including in 1660, 1625, 1612, 1580, 1500, and 1416 (Haflidason et al. 2000). However, lacking a better proximal data set, it is impossible to be anything more than highly speculative about the identity of the possible Katla microtephra.

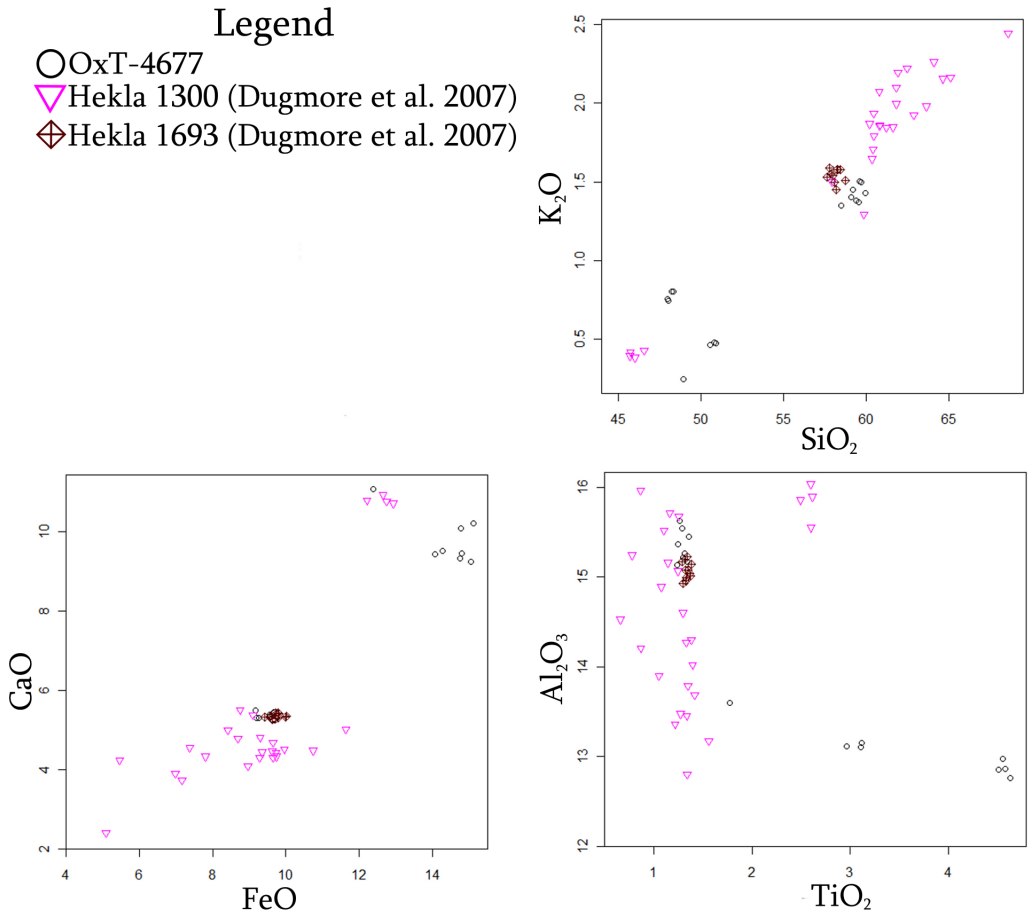


Figure 7.24: Comparison of OxT-4677 with published proximal data for Hekla 1300 and Hekla 1693 (Dugmore et al. 2007b). All units are in wt-%.

7.4.5.1 OxT-4679 and OxT-4680

OxT-4679 (29-31 cm) and OxT-4680 (31-33 cm) contain microtephra from the eruption of Hekla 1300, as shown in Figure 7.26. Based on the shard count shown in Figure 6.17, it seems likely that OxT-4679 represents the main depositional event, while OxT-4680 represents the lower limit or some downward movement of microtephra after its initial deposition.

The eruption of Hekla in 1300 is described by Þórarinsson (1967) as the second largest Hekla eruption in in the historical period. The ash fell largely to the north, as shown in Figure 7.1. This ash fall occurred during haymaking season and Þórarinsson speculates that it led to a recorded 'great mortality' during the following winter in Skagafjörður. Therefore it seems likely that some quantity of ash would have fallen at Vatnsfjörður, which is located not far to the west of Skagafjörður.

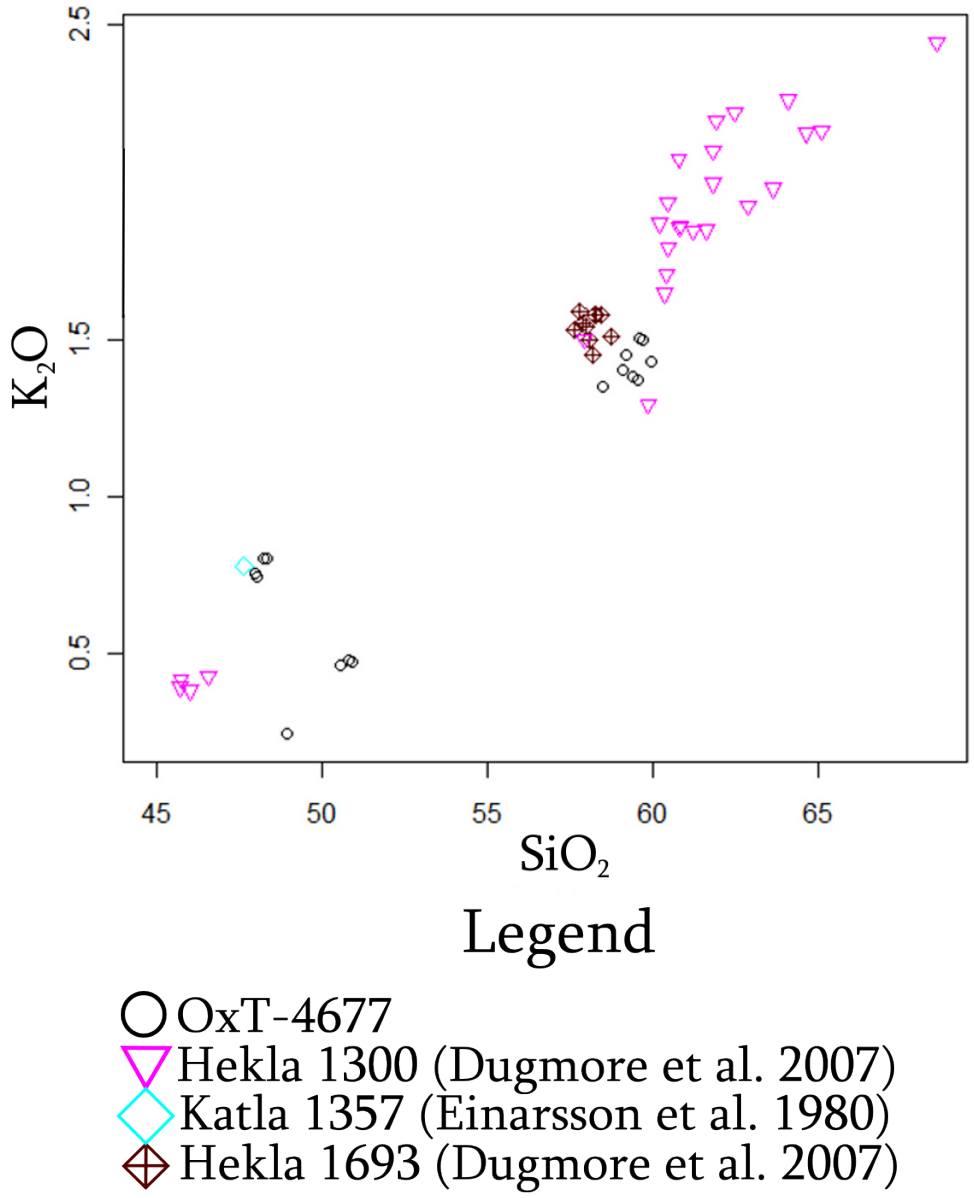


Figure 7.25: Comparison of OxT-4677 with published proximal data for Katla 1357 (Einarsson et al. 1980), Hekla 1693, and Hekla 1300 (Dugmore et al. 2007b). All units are in wt-%.

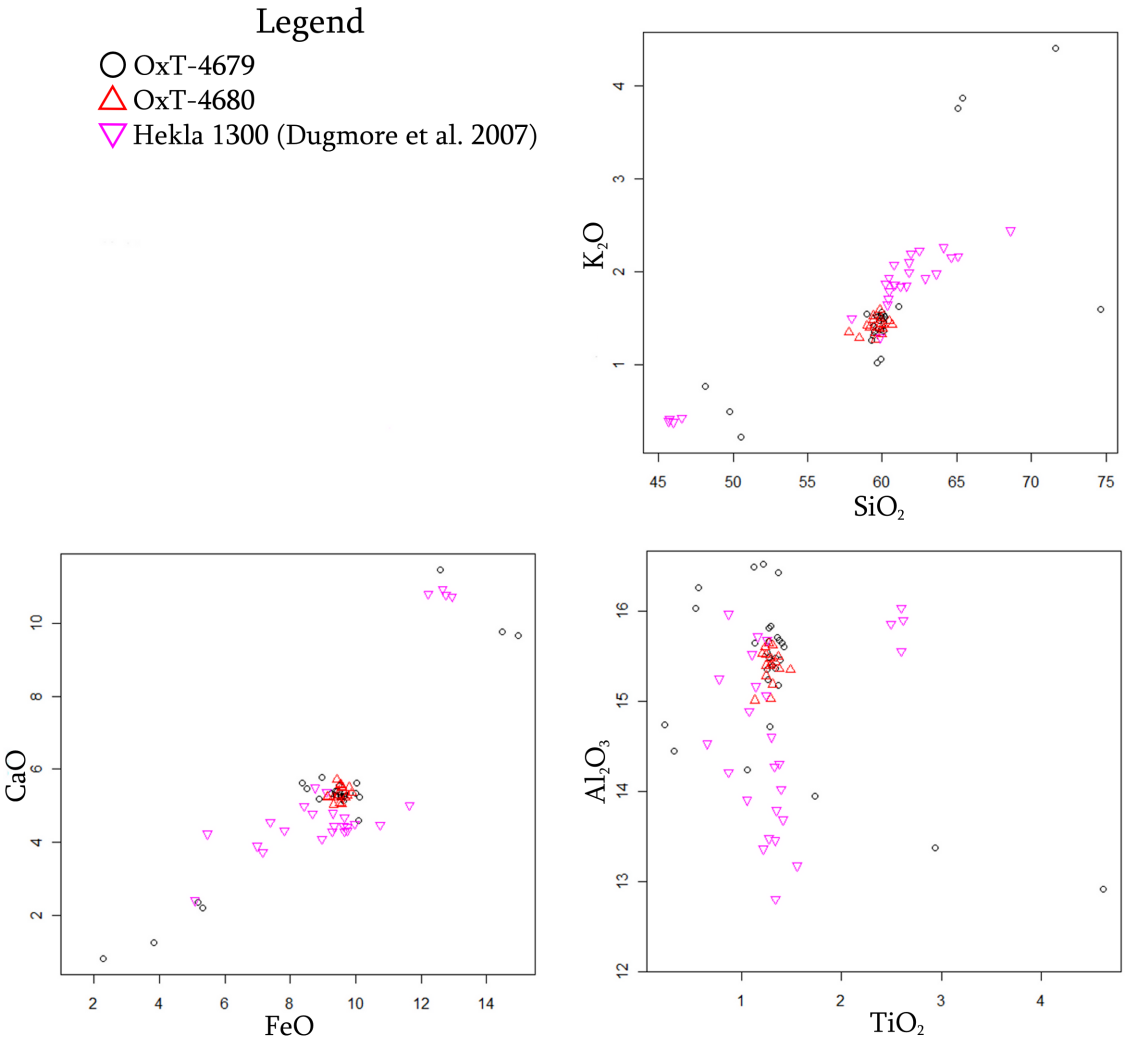


Figure 7.26: Comparison of OxT-4679 and OxT-4680 with published proximal data for Hekla 1300 (Dugmore et al. 2007b). All units are in wt-%.

7.4.5.2 OxT-4681

OxT-4681 does not correlate to any currently known eruption. It has a very mixed geochemical population, as discussed in Section 6.3.1.2. There is a small chance that it contains some shards from the rhyolitic phase of the *landnám* tephra layer (Larsen et al. 1999), as is shown in Figure 7.27. However, the basal radiocarbon dates for the core, which are shown in Table 4.1, indicate that the oldest the base of the core could be is 888 cal AD, and that is the absolute earliest date at two sigma so statistically unlikely. There is a chance that the tephra from that eruption was still present in the landscape when this peat began to form, and these may account for those few shards,

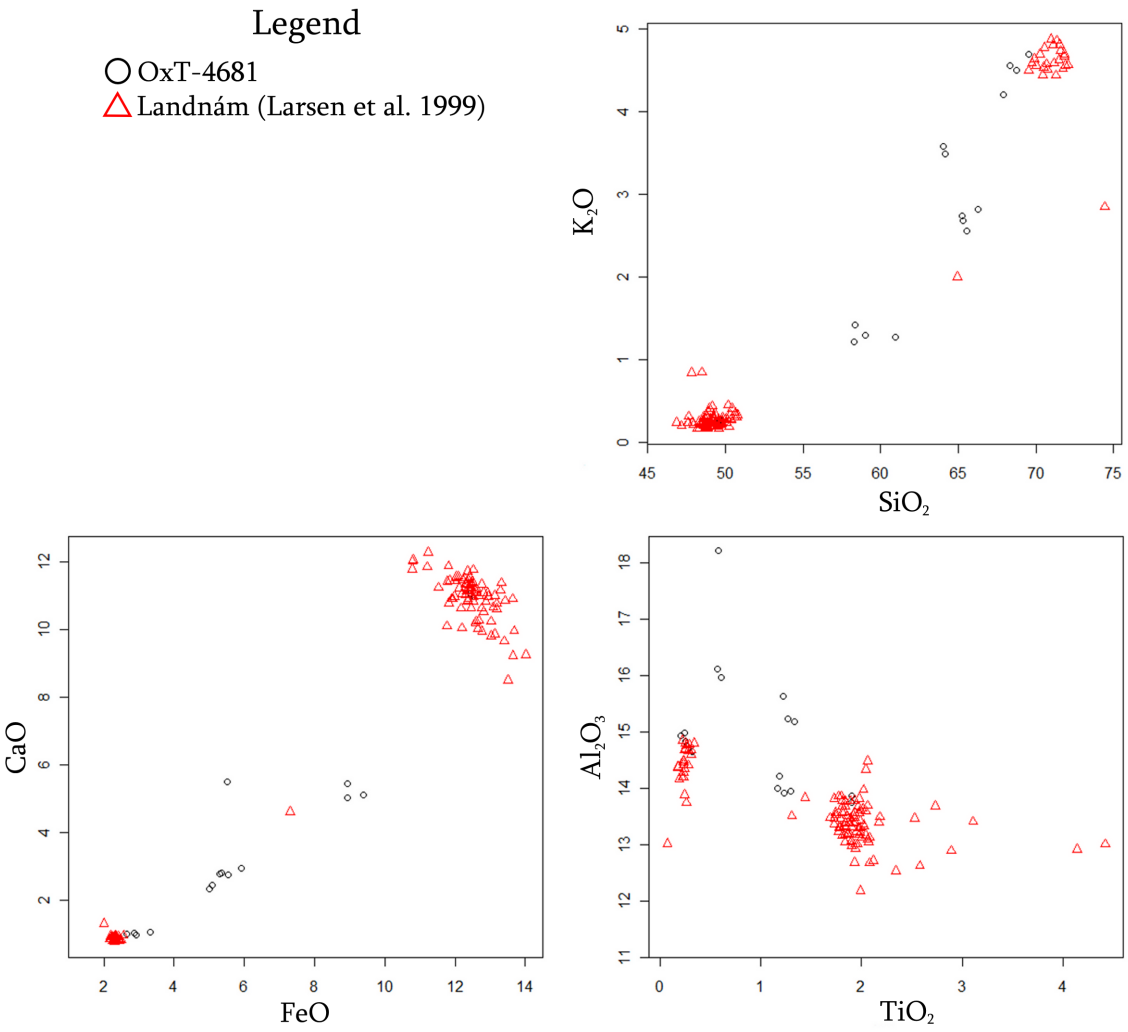


Figure 7.27: OxT-4681 is shown with the *Landnám* tephra, which dates to ca. AD 870 (Grönvold et al. 1985).

but this layer should not be considered positively correlated.

7.4.6 Conclusions

Ultimately, the peat record at the homefield revealed a number of clear microtephra layers. Table 7.2 lists the correlations of these layers. Further conclusions about this core are located in Section 7.5.2.

Table 7.2: Table showing the correlation results for samples from the Homefield core.

Sample Number	Probable Correlation	Other Possible Inclusions
OxT-4672	Hekla 1766	
OxT-4674	Hekla 1693 upper limit?	
OxT-4675	Hekla 1693	
OxT-4676	Hekla?	
OxT-4677	Hekla 1300 upper limit?	Katla 1357?
OxT-4679	Hekla 1300	
OxT-4680	Hekla 1300 lower limit	
OxT-4681	mixed population	rhyolitic component of *Landnám*?

7.5 Kaldalonsjökull

The WDS-EPMA results from the peat core from an outcrop near Kaldalonsjökull are in Section 6.3.1.3. The core had several pronounced peaks of microtephra as well as a small background signal. Below, the peaks are correlated with known eruptions where possible.

7.5.1 Correlating distal layers with proximal glass chemistry

7.5.1.1 OxT-5133

As shown in Figure 7.28, the basaltic component of OxT-5133 (8-10 cm) correlates to proximal glass chemistry for Hekla 1766 (Larsen et al. 2011). Compared to the homefield, this is higher in the sediment core. It may be that the accumulation of peat in the area slowed towards the end of the LIA for environmental reasons relating to the changing of the Drangajökull glacier, which reached its maximum a few decades after the 1766 eruption (Principato 2008). There are also three silicic shards, which were not found in the Homefield sample that seems likely to correlate to Hekla 1766. These may represent a different phase of the eruption that has not yet been documented in proximal geochemistry.

7.5.1.2 OxT-5135

OxT-5135 (12-14 cm) correlates to the eruption of Hekla 1693 (Dugmore et al. 2007b), as is shown in Figure 7.29. As is noted elsewhere, this eruption deposited relatively

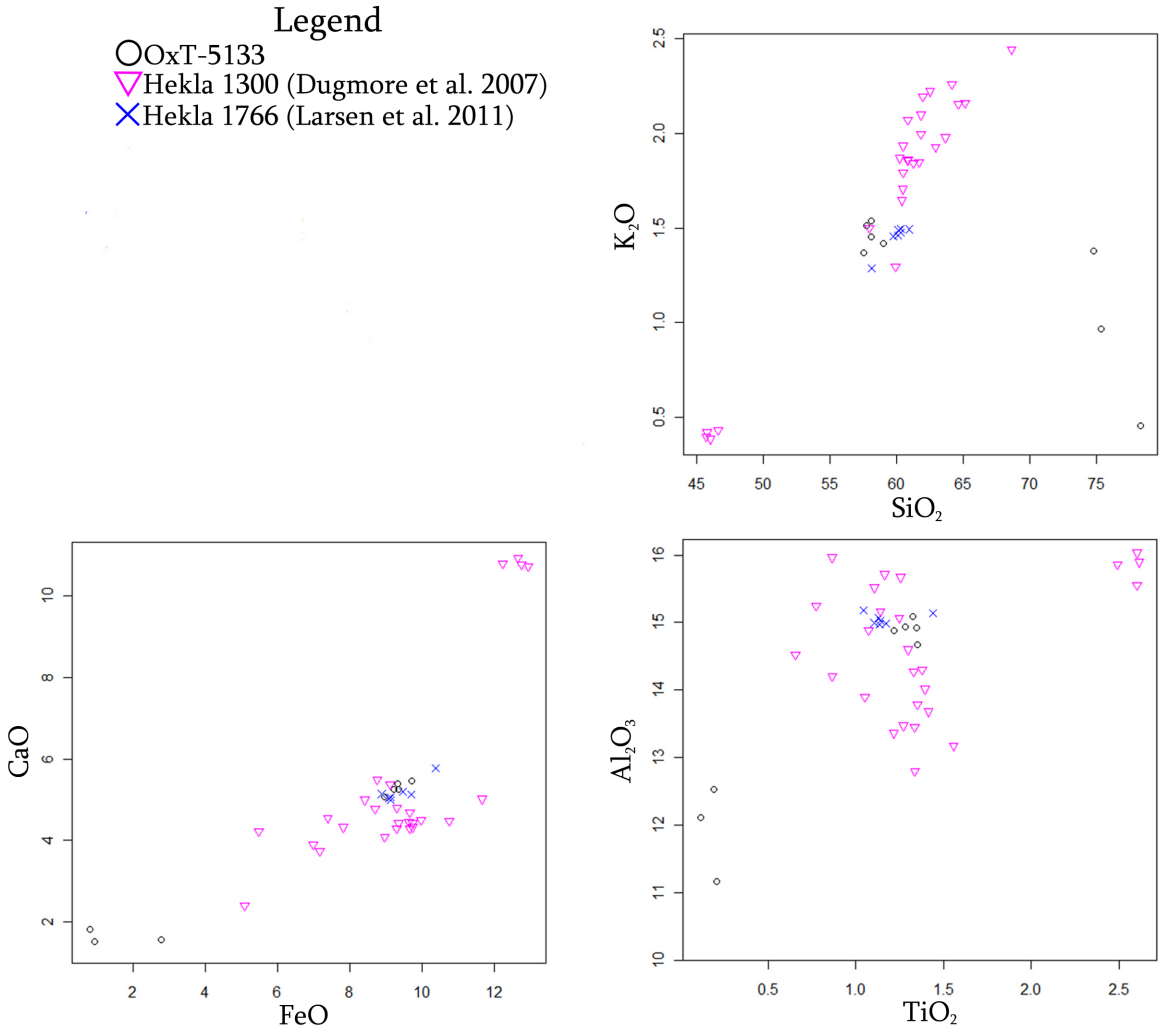


Figure 7.28: Comparison of OxT-5133 with published proximal data for Hekla 1300 (Dugmore et al. 2007b) and Hekla 1766 (Larsen et al. 2011). All units are in wt-%.

large amounts of tephra in Vestfirðir, and the tephrostratigraphy for this core (shown in Figure 6.18) reflects this, as this was the largest microtephra layer in this core.

7.5.1.3 OxT-5136

OxT-5136 (14-16 cm) has a very mixed population, although it may contain some tephra from Hekla 1693 that has moved downward through the peat. This would be consistent with the size of the ash fall in this area.

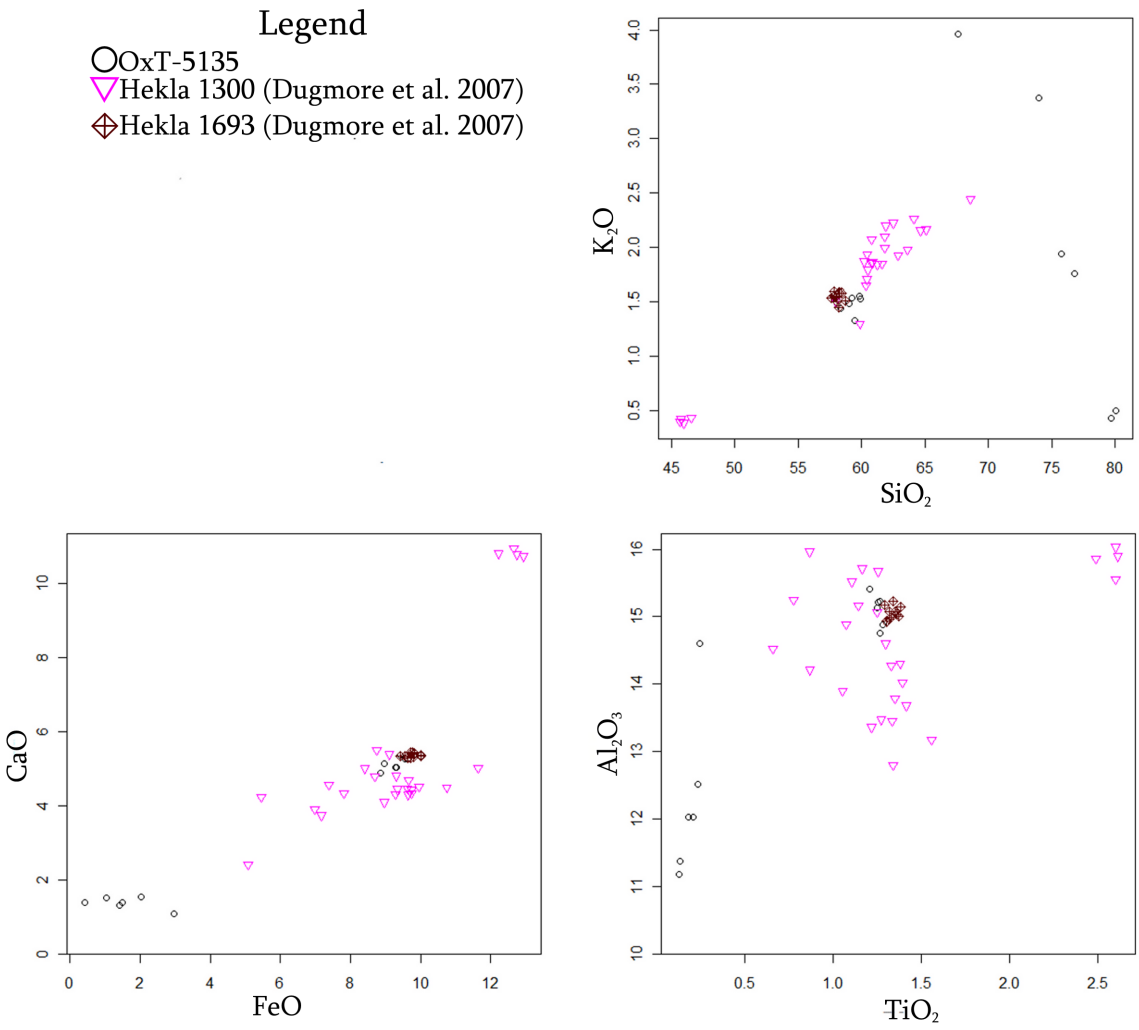


Figure 7.29: Comparison of OxT-5135 with published proximal data for Hekla 1300 and Hekla 1693 (Dugmore et al. 2007b). All units are in wt-%.

7.5.1.4 OxT-5142

Figure 7.30 shows the correlation of OxT-5142 (36-38 cm) with the eruption of Hekla 1300 (Dugmore et al. 2007b). This tephra layer was also found in the homefield core, at a depth of 29-31 cm. Figure 7.1 shows that the eruption had the potential to be widespread across Vestfirðir.

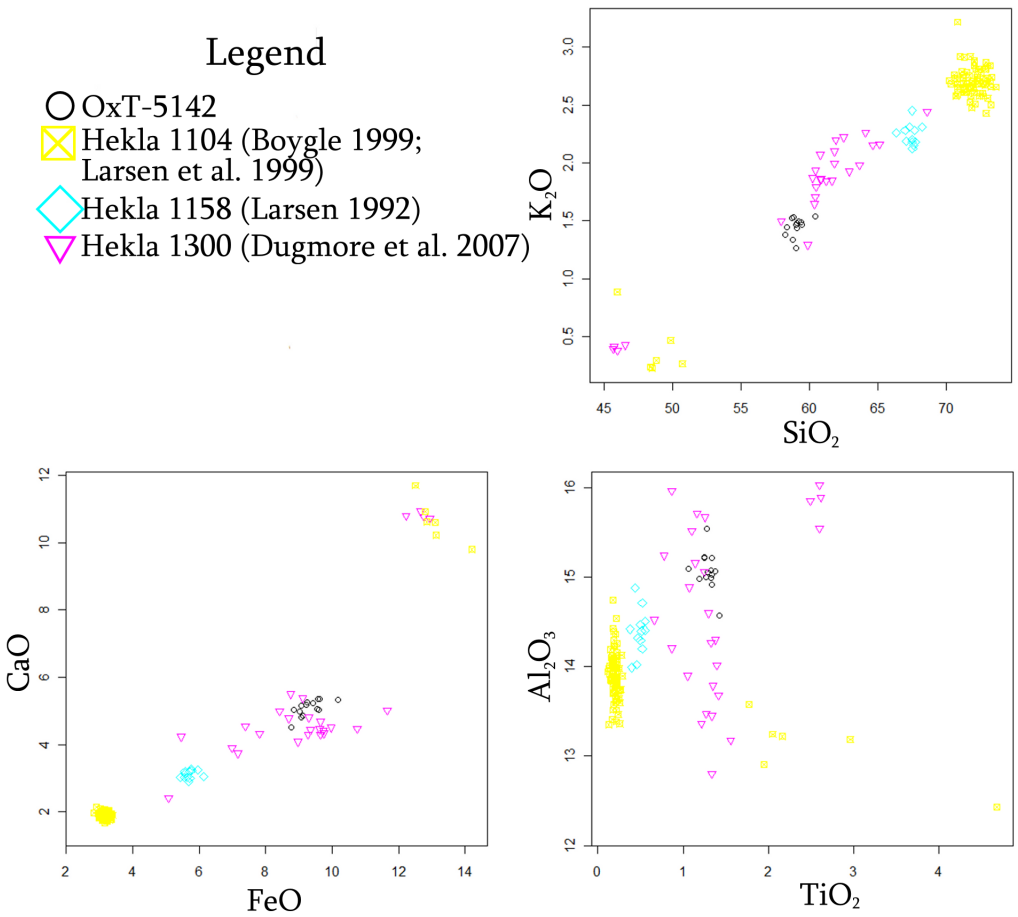


Figure 7.30: Comparison of OxT-5142 with published proximal data for Hekla 1300 (Dugmore et al. 2007b), Hekla 1104 (Larsen et al. 1999; Boygle 1994), and Hekla 1158 (Larsen 1992). All units are in wt-%.

7.5.1.5 OxT-5148

OxT-5148 (84-86) correlates to the *landnám* tephra layer, which has been dated to 871 ± 2 (Gronvold et al. 1995). This tephra event is described in more detail in Section 7.6.1.3.

7.5.1.6 OxT-5149 and OxT-5150

Neither OxT-5149 (86-88 cm) or OxT-5150 (88-90 cm) could be correlated to published proximal glass data. OxT-5149 is of a somewhat mixed composition and may represent a mixture of ash fall events, but OxT-5150 is well-constrained with few outliers. However, neither correlate with OxT-4682/-4685, from Sveinhúsavatn, which

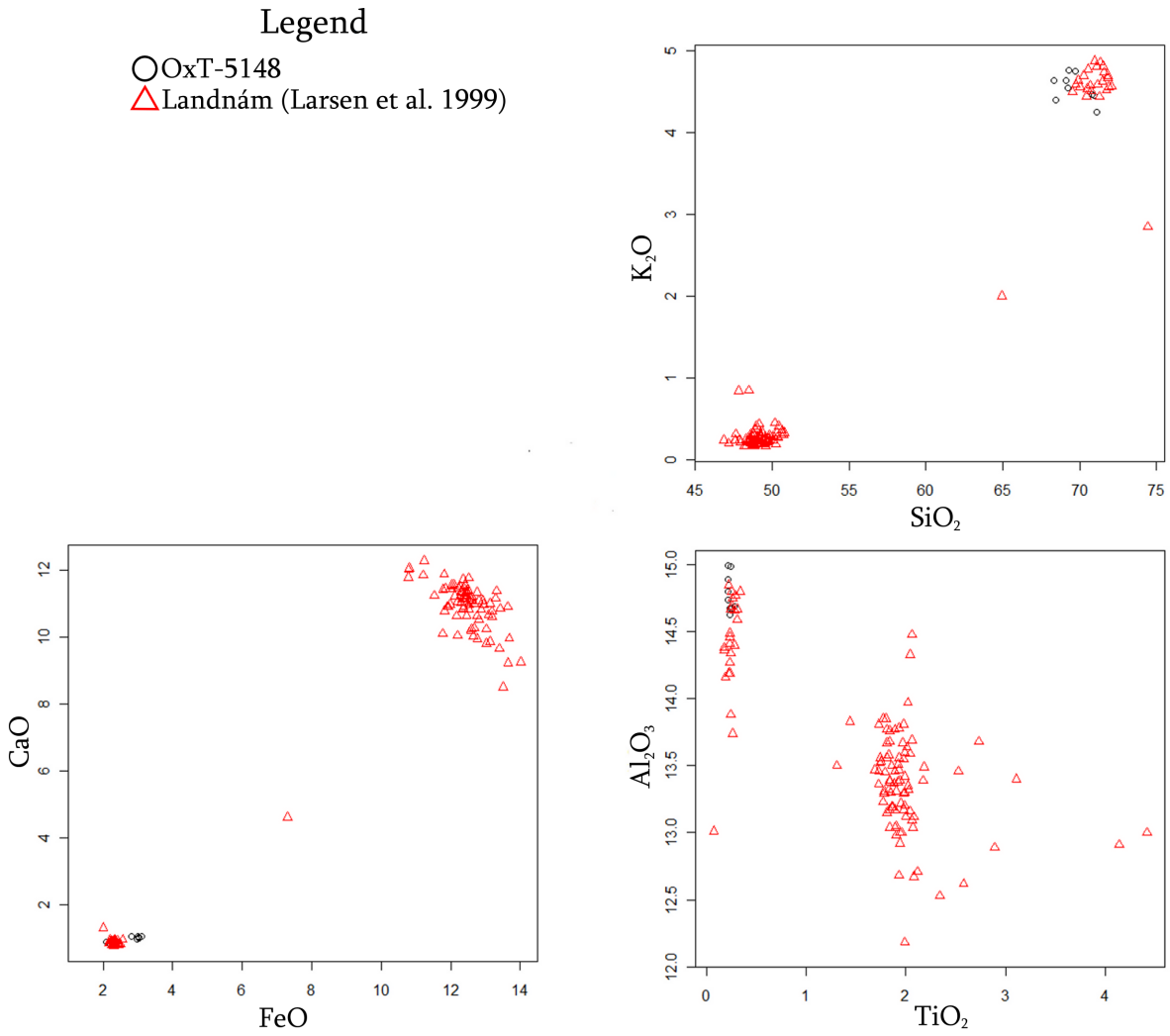


Figure 7.31: Comparison of OxT-5148 with published proximal data for the *landnám* tephra (Larsen et al. 1999). All units are in wt-%.

are other pre-*landnám* well-constrained ash fall events.

7.5.1.7 Conclusions

Table 7.3 shows the positive correlations from the Kaldalonsjökull core.

7.5.2 Homefield and Kaldalonsjökull chronologies

The Kaldalonsjökull core was brought into this study to provide a secondary peat record from Vestfirðir to compare to the homefield core in case the homefield core

Table 7.3: Table showing the correlation results for samples from the Kaldalonsjökull core.

Sample Number	Probable Correlation	Other Possible Inclusions
OxT-5133	Hekla 1766	
OxT-5135	Hekla 1693	
OxT-5136	Hekla 1693 lower limit?	mixed composition
OxT-5142	Hekla 1300	
OxT-5148	*landnám*	
OxT-5149	unknown	mixed composition
OxT-5150	unknown	

showed signs of anthropogenic alteration caused by water movement from irrigation, rainfall, or snow melt. After correlating the tephra layers in the cores to known eruptions, the tephrostratigraphy of Kaldalonsjökull is similar to that of the Homefield for the time periods in which they overlap. Due to the breaks in peat at Kaldalonsjökull caused by gravelly inclusions, this record appears much longer than that of the Homefield, when in fact the upper portion of it covers a similar amount of time. Figure 7.32 shows the tephrostratigraphies of the two peat cores. Microtephra from the eruptions of Hekla in 1766, 1693, and 1300 were found in both cores. Although there is some difference in placement of tephra layers, Payne and Blackford (2008) have found that to be true for peat profiles between nearby study locations (like these) or even between profiles from the same study site.

A secondary purpose for studying the Kaldalonsjökull core was to create a chronology for changes in the Drangajökull glacier, which has been used as a proxy for climate change (Principato 2008). Most research into the glacier has not taken into account the late Holocene, with the exception of a small amount done by Principato (2006). Although this research is ongoing, the chronology presented here will allow the record to be extended through the Little Ice Age.

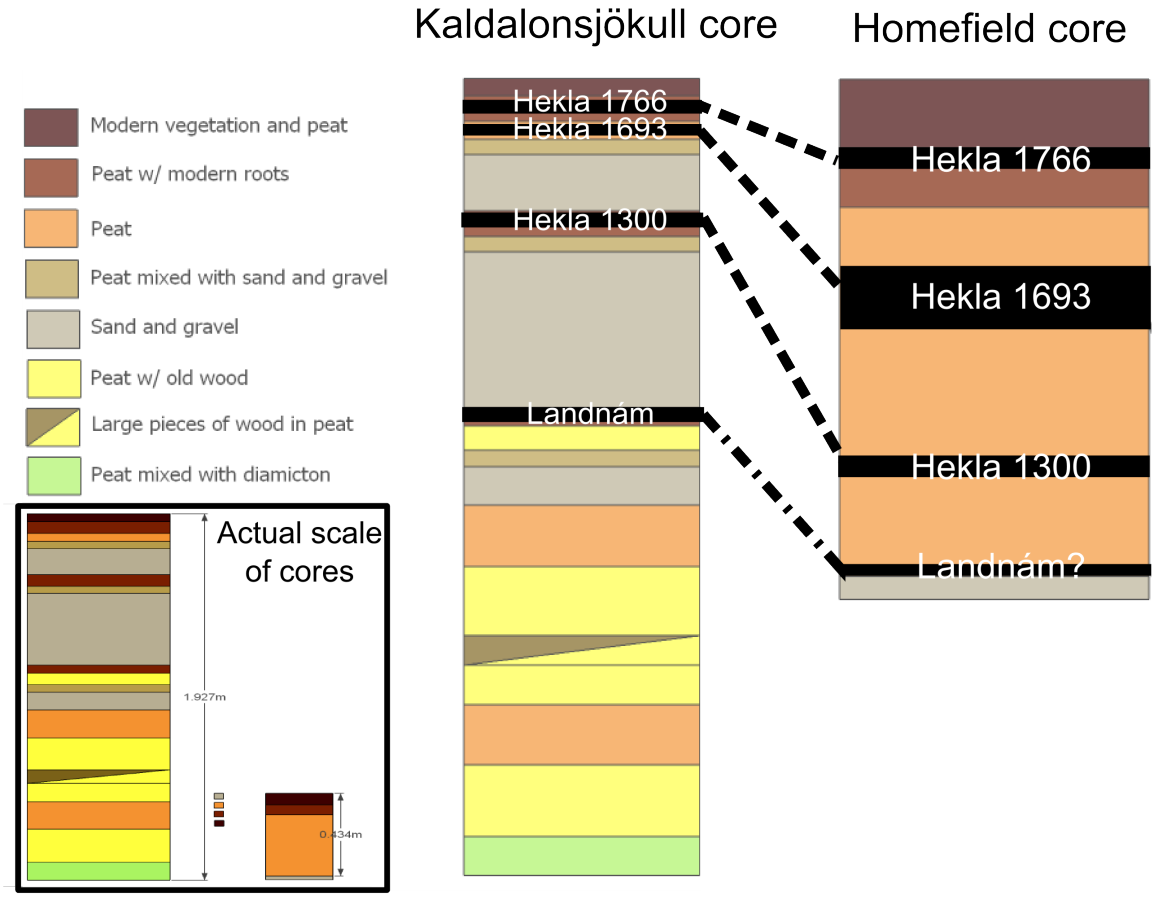


Figure 7.32: Tephra layers found in both the Homefield core and the Kaldalonsjökull core, overlaid on the sediment logs. Figure is not to scale, but scale is shown in the lower left.

The comparison of the peat cores provided valuable data to understand the densely-populated tephrostratigraphies of both cores. Although both had background signals – i.e., low levels of microtephra in every visually-inspected section – they also had discernible peaks. By comparing the records at both, it was possible to see similar patterns in the peaks. Similarly, after WDS-EPMA, comparing the glass chemistry of the layers in the two cores aided in correlation. This was especially true for the Hekla 1766, Hekla 1693, and Hekla 1300 layers, which all have very similar published proximal chemistry. When it was difficult to distinguish these layers, the corresponding layer in each core could have its glass chemistry compared for further confirmation. This is shown in Figure 7.33, which compares homefield and Kaldalonsjökull glass chemistry for Hekla 1766 with published data from Larsen et al. (2011).

Another example comes from a comparison of Hekla 1693 glass chemistry from across several records. Figure 7.34 shows OxT-4308 from Sveinhúsavatn, OxT-4675 from the homefield, OxT-5135 from Kaldalonsjökull, and OxT-5163 from the archaeological excavation, alongside published proximal data from Dugmore et al. (2007b). Using this research, there is a wider spread of glass chemistry associated with this eruption than accounted for by Dugmore et al., which may be related to the fact that they only published ten analyses.

The movement of microtephra within peat is demonstrated in the tephrostratigraphies of both cores. The best example of this is the Hekla 1693 tephra layer in the homefield core, which seems to have spread across a very wide range of the peat profile. Although shard counts allowed the eruptive event to be isolated to a 2 cm section of the profile, there was clear movement of tephra both up and down from that section. A variety of possibilities for why this might be the case are discussed in Section 3.2, which reviews a number of different studies on post-depositional processes for microtephra in peat. For example, Bergman et al. (2004) theorise that frozen ground, long-lasting snow cover, and exposure to strong winds could alter microtephra deposition, all of which seem likely to have occurred in Vestfirðir, particularly during the harsher winters of the LIA. In fact, frost heaving, which causes jagged upthrusts of thawing ground, is a common feature throughout peaty areas in this landscape, including in the homefield itself. While this might cause a delay in the deposition of microtephra or cause the tephra to move around horizontally (for example, being deposited in large quantities in an area of low ground where snow melt pooled), or experience upward vertical motion (because of a delay in the deposition of the microtephra, as described by

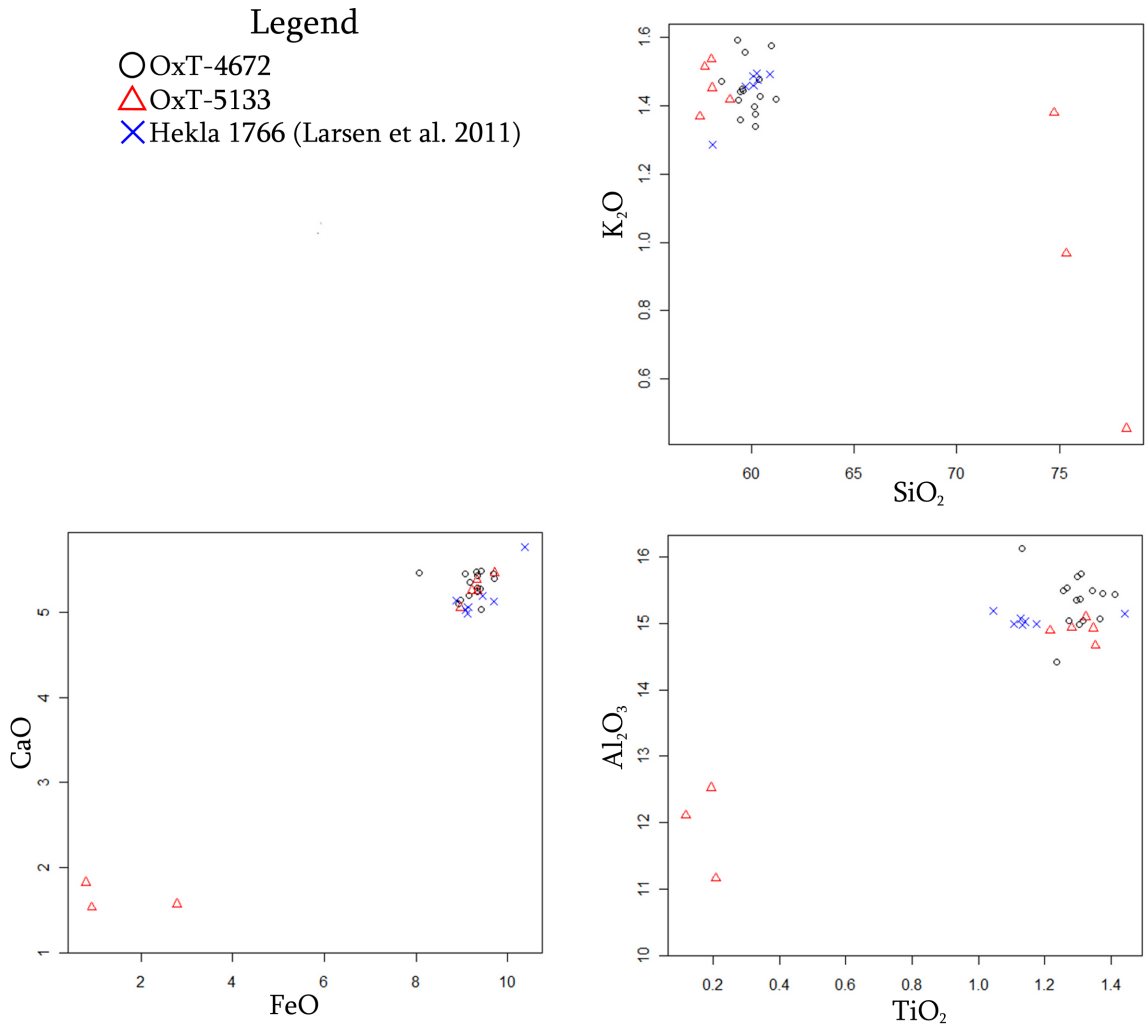


Figure 7.33: Comparison of proximal and distal data from Hekla 1766. OxT-4672 is from the homefield, OxT-5133 is from Kaldalonsjökull, and they are compared to data from Larsen et al. (2011).

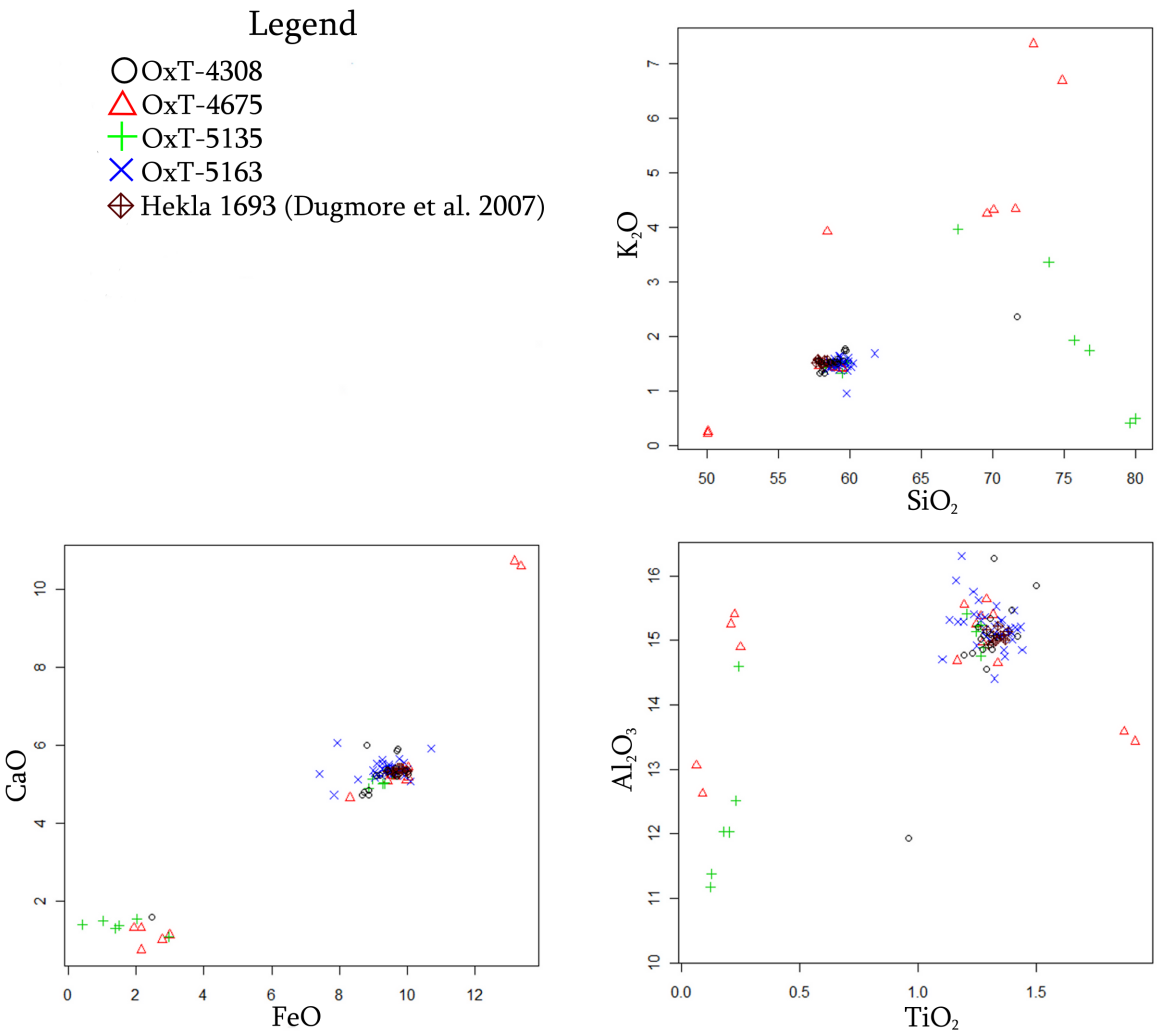


Figure 7.34: Comparison of proximal and distal data from Hekla 1693. OxT-4308 is from Sveinhúsavatn, OxT-4675 is from the homefield, OxT-5135 is from Kaldalonsjökull, and OxT-5163 is from the archaeological excavation, and all have been correlated to Hekla 1693. These are compared to published proximal data for this eruption from Dugmore et al. (2007).

Payne and Gehrels (2010), it does not fully explain the downward vertical shifts in the sediment column.

Vertical downward movement of microtephra seems to be more pronounced in the homefield core, and this may be explained by water movement in the homefield. However, this should not be a cause for concern about the integrity of the tephrostratigraphy. In a series of experiments by Payne and Gehrels (2010), they find that, although water movement in peat could shift microtephra downwards, it generally has only a very localised effect. Similarly, Swindles et al. (2013), in a study of microtephra from Shetland, found that there was reworking of microtephra that correlated to the Hekla 4 and Hekla-Selsund eruptions within the landscape. In their case, they found that, even with geochemically mixed populations between layers that they attributed to some reworking, there were also discrete and identifiable layers that went in chronological sequence. Finally, the comparison to the tephrostratigraphy for the Kaldalonsjökull core provides another indication that the the geochemical correlations from the homefield are correct.

7.5.3 Integrating the chronology of the Homefield with its pollen record

Archaeologically, the homefield has an important role to play in the interpretation of the farm at Vatnsfjörður. As discussed in Section 4.2.3, homefields were an important part of Viking and later North Atlantic farmsteads. The Vatnsfjörður homefield initially confused researchers because of its apparent infertility. The Vatnsfjörður farmstead is in an agriculturally difficult environment, even during the warmer years of the MWP, and so the productivity of the homefield, located in one of the few arable spaces around the farmstead, would have been crucial to its success. A further question for researchers was the extent to which the creation and maintenance of the homefield was anthropogenic. It was unclear if the peat formed there was entirely natural, naturally-occurring but maintained by irrigation, or deliberately cultivated from the earliest period of settlement at the farm.

Dr Eileen Tisdall and her student, Rebecca Barclay (University of Stirling) sampled the homefield core for pollen. Combined with the tephrochronological record shown above, the goal was to illuminate the record of the peat in the homefield from its formation until the present day. The pollen record that they developed, along with their preliminary report, is in Barclay et al. (in Milek 2011) and Barclay and Anderson

(forthcoming). Below is described how the tephrochronological research reported above provides a framework for understanding the pollen record. This is represented graphically in Figure 7.35. This then connects the pollen record to developments at the archaeological site.

The portion of the homefield sampled from and studied above was the wet meadow. The wet meadow is enclosed by the eastern boundary wall of the Viking Age area (Barclay 2008). It is underlain by a thin layer of charcoal, and beneath that the gravel that underlies the rest of the Viking Age area of the Vatnsfjörður excavations (and is discussed briefly in Section 7.2.2). The charcoal has had two radiocarbon dates, which are shown in Table 4.1. These calibrate (using INTCAL13) to 895-1020 cal AD and 895-1030 cal AD, suggesting a post-*landnám* date for the development of the peat in the wet meadow. Barclay (2008) has theorised that peat developed here either because of changes to the hydrology of the landscape caused by woodland removal during the early stages of settlement, or as a result of damming using the raised beach surface. The purpose of damming would have been to create a homefield that could support fodder production or grazing. The latter suggestion is supported by finds of microhorizons of cultural materials (bones, charcoal, and other midden materials) within the meadow, which could be the results of manuring and other management.

Barclay et al. (in Milek 2011) write, 'The pollen assemblage data suggest that the wet meadow site is predominately a herb and sedge rich grassland and remains so for the time recorded in this diagram. Throughout the peat core Poaceae (grasses) dominate each assemblage, dwarf shrubs and herb species dominate over tree and shrub species, and species diversity would appear to be low... The majority of species show limited fluctuations between zones.' Therefore the homefield did not show dramatic changes over time. Using the tephrochronology developed above, Barclay et al. divide the pollen record into five LPAZs (local pollen assemblage zones) based on local similarities between the communities. This is shown in Figure 7.35.

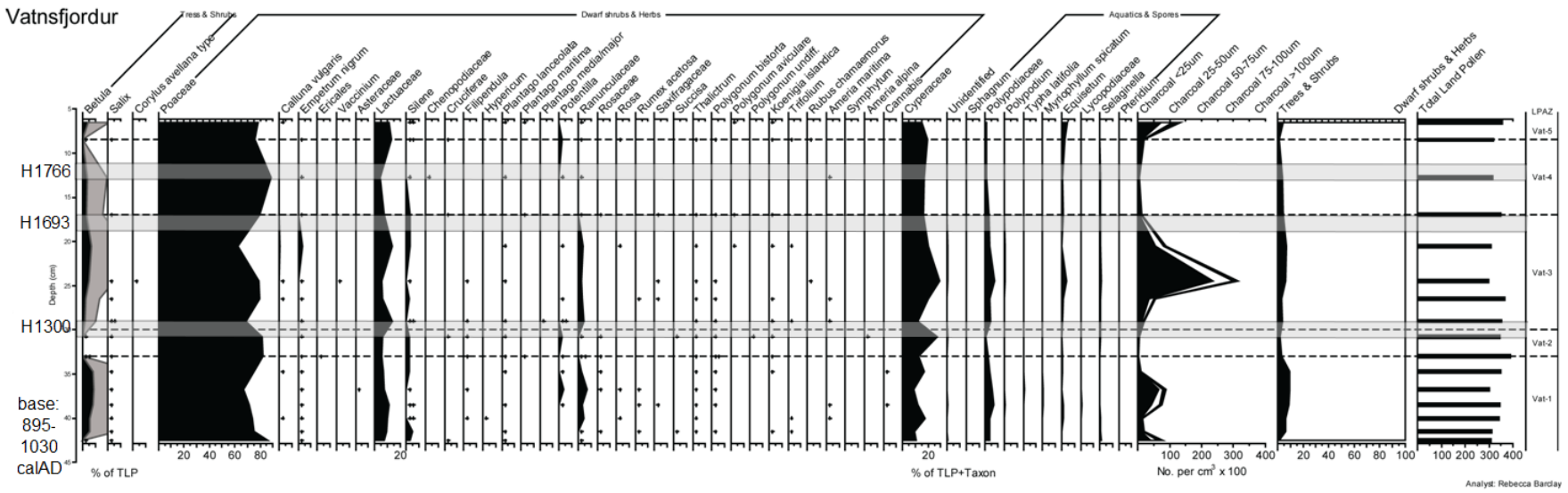


Figure 7.35: Pollen and spore percentage data for Vatnsfjörður wet meadow site, alongside charcoal concentration onsite. Data aside from chronology from Barclay et al. (in Milek 2011).

All pollen and charcoal information below is summarised from Barclay and Anderson (forthcoming).

The first zone, which dates from the creation of the peat meadow (ca. AD 900-1000) until ca. AD 1175, is dominated by grasses (Poaceae), with smaller percentages of Betula (birch) (10%) and Salix (willow), (<2%) throughout. Towards the top of this zone (so ca. AD 1175), there is a sharp decline in *Betula* to less than 1%.

The second zone, which is a shorter zone that terminates around 1300, is characterised by the absence of *Betula*, and very low concentrations of charcoal.

The third zone is neatly bracketed in time by the eruptions of Hekla 1300 and Hekla 1693. There is a decline in species diversity, and a sharp, well-defined peak in charcoal concentration which occurs ca. AD 1500, followed by a long decline.

The fourth zone progresses from 1693 until approximately the middle of the 19th century. According to many proxies, this was one of the coldest periods of the LIA in northwestern Iceland (Principato 2008; Geirsdottir et al. 2009b). Like the third zone, there is a decrease in species diversity, with very little charcoal.

The fifth zone represents the decline of the homefield in conjunction with the decline and abandonment of the farmstead, which is known to have been abandoned in 1906. At this point, the peat began to dry, which may be because of a loss of irrigation from the settlers at the farmstead. Charcoal increases towards the top of this zone, perhaps as an indication of later settlement at the new farmhouse that is still occupied at Vatnsfjörður.

By constructing the chronology for this peat record, several questions about the homefield have been answered. First, it seems likely based on the date of creation combined with the gravelly layer that the peat field is anthropogenic (Barclay et al. 2011; Barclay and Anderson forthcoming). The decline in birch around ca. AD 1175 was almost certainly related to fuel production, and is consistent with the decline in birch described by Church et al. (2007), Dugmore et al. (2007a), and Dugmore et al. (2009) in the Eyjafjallahreppur and Þjórsárdalur areas of southern Iceland. If this is correct, then it is the first instance of tree clearance to be documented from Vestfirðir. Barclay et al. also note that increased species diversity in the second zone may indicate purposeful cultivation of a variety of herbs.[2] It is interesting to note that the decline in charcoal at the end of the third zone occurs from around AD

[2]Cereal crops have only been found further south in Iceland thus far (Adderley and Simpson 2005; Adderley et al. 2008; Barclay and Anderson forthcoming).

1500-1693; the Jarðabók entry from 1710 describes this as a period of scarcity for Vatnsfjörður.

7.6 Sveinhúsavatn

Sveinhúsavatn is the lake to the southeast of the archaeological excavations at Vatnsfjörður, and is described in Section 4.2.2. The reason for studying the lake core is to understand how sea-level has changed in the area over time as well as to understand possible uses for the lake by settlers at Vatnsfjörður.

7.6.1 Correlating distal layers with proximal glass chemistry

From the Sveinhúsavatn core, shard counting revealed four microtephra peaks that were over 1000 shards per gram dry sediment weight, and these four peaks were subsequently re-extracted and underwent WDS-EPMA. The shard count is in Section 6.2.1.1 and the results of WDS-EPMA are in Section 6.3.1.1 . Below, three of the four are correlated to known eruptions, and possible matches for the fourth are discussed.

7.6.1.1 OxT-4308

OxT-4308 is andesitic, and correlates to the eruption of Hekla 1693, as shown using major element biplots in Figure 7.36. However, much like the data from the Vatnsfjörður archaeology, Hekla 1693 appears to have a wider spread of possible glass chemistry than that reported by Dugmore et al. (2007b).

7.6.1.2 OxT-4309

OxT-4309 is basaltic. As was discussed in Section 6.3.1.1, this particular tephra layer was highly vesicular and therefore, although this section of the lake core contained well over 1000 individual shards, they were not ideal for single grain analysis and ultimately only a small number were successfully microprobed. As shown in the biplots in Figure 7.37, the successful analyses correlate to the Eldgjá fissure eruption of ca. 935, using glass chemistry for that eruption from Dugmore et al. (2007b). Data from Boygle (1994) from a basaltic phase of the eruption that she identifies as

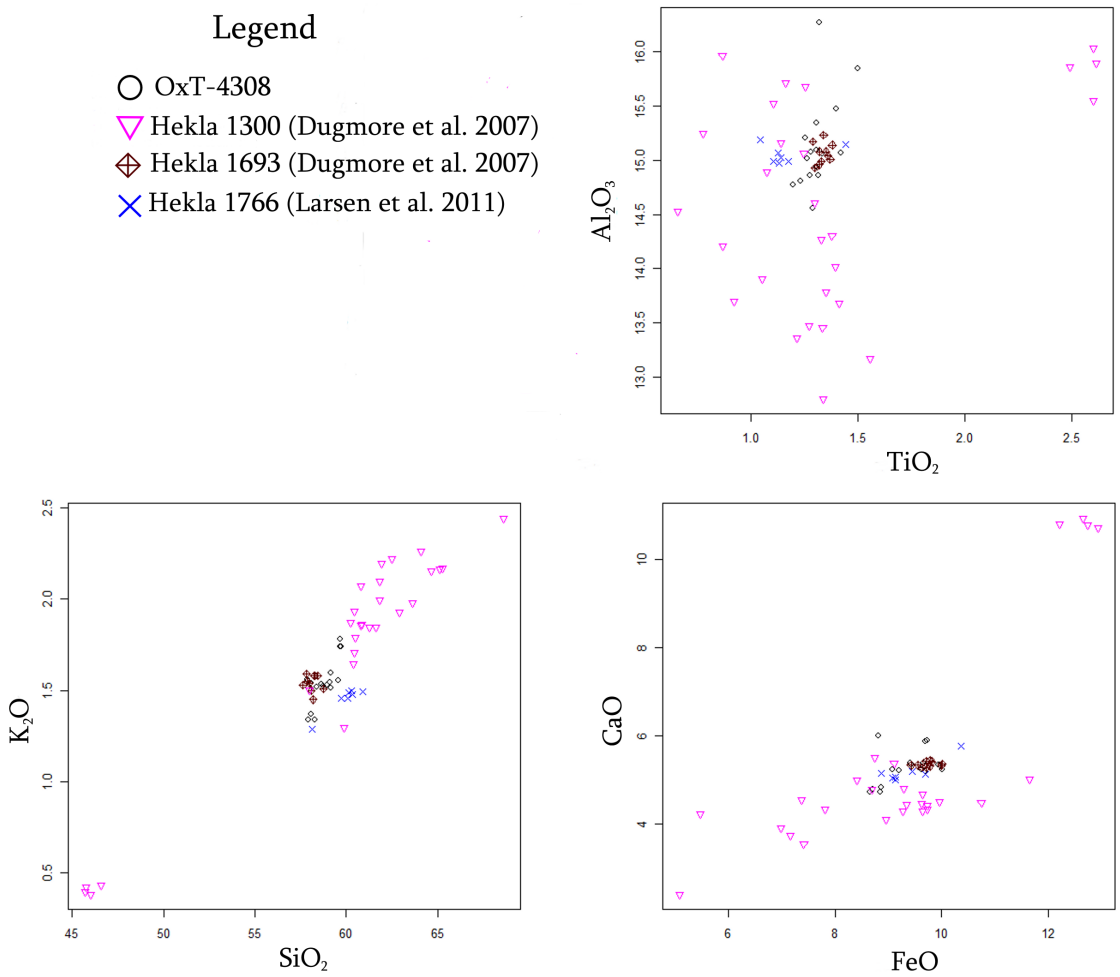


Figure 7.36: Comparison of OxT-4308 with published proximal data for Hekla 1300, Hekla 1693 (Dugmore et al. 2007b), and Hekla 1766 (Larsen et al. 2011). All units are in wt-%.

Hekla 1104 showed some similarities to OxT-4309. However, Boygle's (1994) data is the only current published example of the basaltic phase for this eruption, with all other published sources presenting SiO_2 wt-% values of 70 or greater (e.g., Larsen et al. 1999; Haflidason et al. 2000). In addition to Eldgjá 935 being a closer match in terms of glass chemistry for OxT-4309, it seems possible to consider Boygle's (1994) basaltic data anomalous.

Eldgjá is a fissure system that is part of the Katla volcanic system. Its tenth century eruption, which lasted for several years, produced one of the world's largest known Holocene lava flows (Katla, Smithsonian Institution 2011). During this time, the fissure eruption also produced ash fall in Iceland and elsewhere (Stothers 1998). Glass

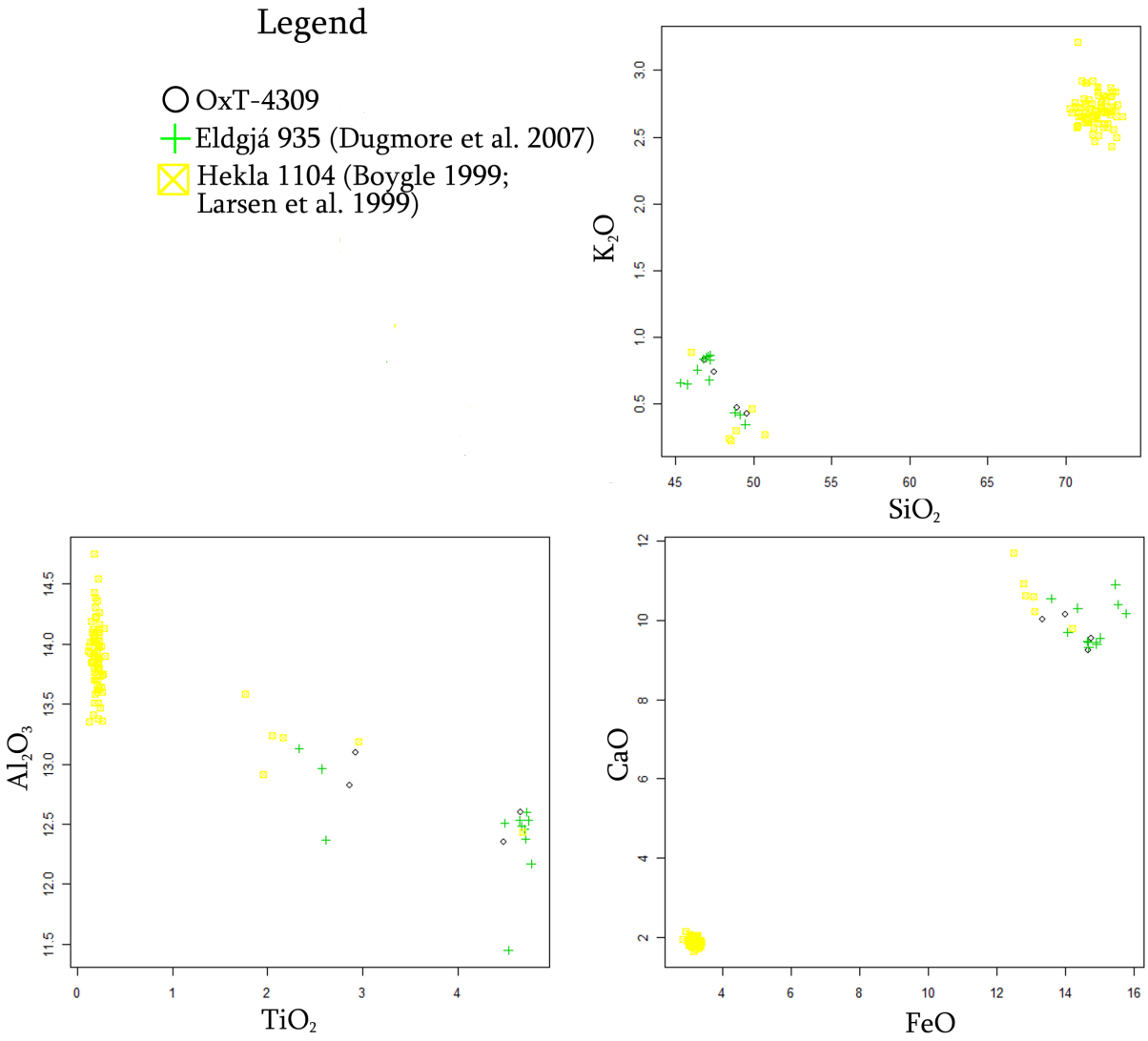


Figure 7.37: Comparison of OxT-4309 with published proximal data for Hekla 1104 (Larsen et al. 1999) and Eldgjá 935 (Dugmore et al. 2007b). All units are in wt-%.

shards matched to this eruption have been found in the GISP2 Greenland ice core, for example, proving that at least part of the ash fall event blew to the northwest of Katla, which would put Sveinhúsavatn and Vatnsfjörður directly in its path. This ash fall event has been dated by correlation of proximal data with glass shards found in the GISP2 Greenland ice core chronology to 938 ± 4 (Zielinski et al. 1995). Historical evidence suggests that the ultimate date of the eruption was over a period of several months, with disagreement about the exact year, but the most recent source uses AD 935 and this has become shorthand for this eruptive event (Þórarinsson 1958; 1967; Dugmore et al. 2007b).

7.6.1.3 OxT-4310

OxT-4310 has bimodal chemistry, split between basaltic and rhyolitic composition. It correlates to the Landnám tephra, as shown in Figure 7.38. Proximal glass chemistry for that eruption comes from a number of sources; those used here are from Larsen et al. (1999). The *landnám* tephra has been dated using a Greenland ice core to 871 ±2 (Grönvold et al. 1995). The eruption came from the Torfajökull complex in Iceland's Eastern Volcanic Zone and has been traditionally used to date the settlement of Iceland (Larsen et al. 1999:468).

7.6.1.4 OxT-4685

At present, it is not possible to correlate OxT-4685 with any known eruptions. However, comparatively few Icelandic eruptions are known prior to *landnám* simply because there are no written observations, so it seems likely that this eruption correlates to an unknown eruption or an eruption that does not have published data, similar to OxT-5150. The data is shown in Figure 7.39 with the last known Snæfells eruption, which has been dated to ca. AD 200 (Snaefellsjokull, Smithsonian Institution 2011). This eruption took place immediately south of Vestfirðir in the time before the *landnám*, but is not geochemically linked to OxT-4685. In the future, when there is better understanding of the pre-*landnám* eruptive history of Iceland, this layer may be identifiable. If a proposal for radiocarbon dates on the Sveinhúsavatn core is successful, then those dates may potentially constrain the tephra layer represented by OxT-4685 and lead to an identification.

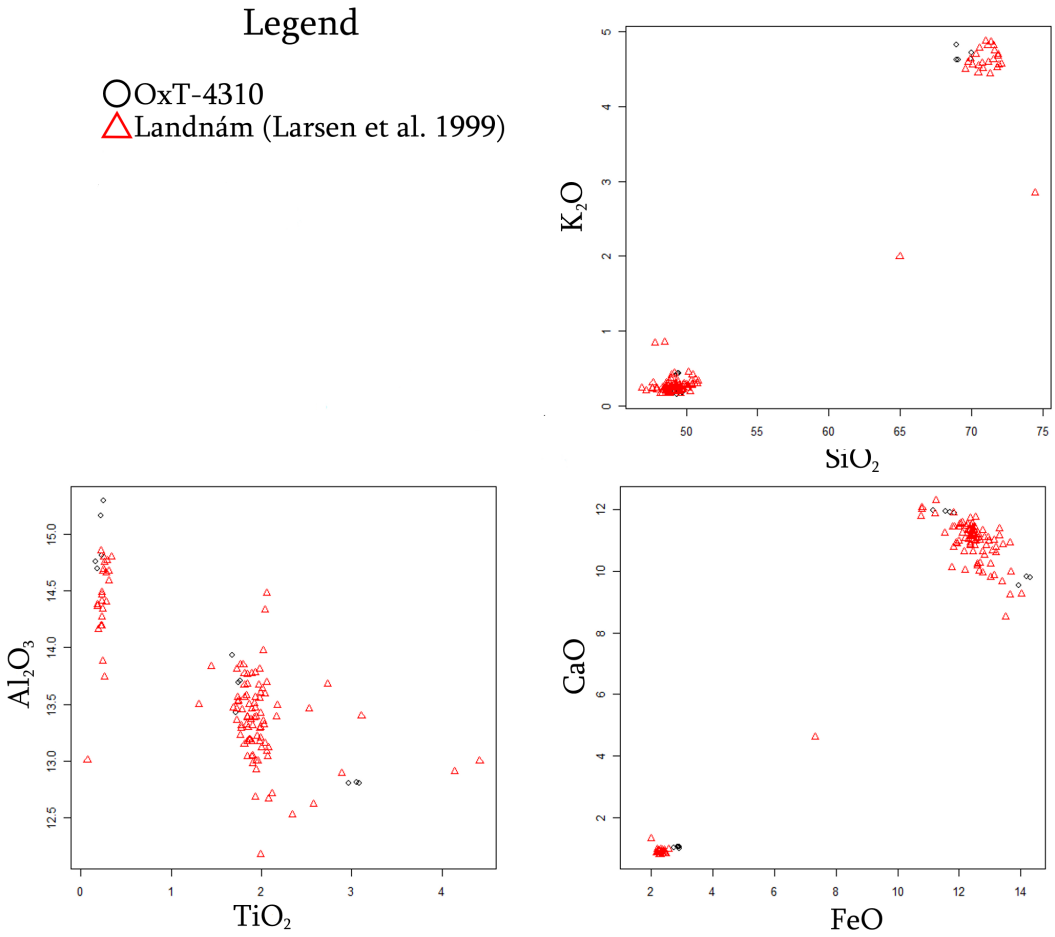


Figure 7.38: Comparison of OxT-4310 with published proximal data for the *landnám* tephra (Larsen et al. 1999). All units are in wt-%.

7.6.1.5 Conclusions

In summary, as shown in Table 7.4, OxT-4308 (10-15 cm) correlates to Hekla 1693; OxT-4309 (80-85 cm) correlates to Eldgjá 935; OxT-4310 (165-170 cm) correlates to the *landnám* tephra (871 ±2); and OxT-4685 (195-200) cannot be correlated to a specific eruption.

Although there is a slight background signal throughout the core, this is expected of tephra deposition in lake sediments (e.g., Thompson and Bradshaw 1986) and it does not seem to have affected analysis.

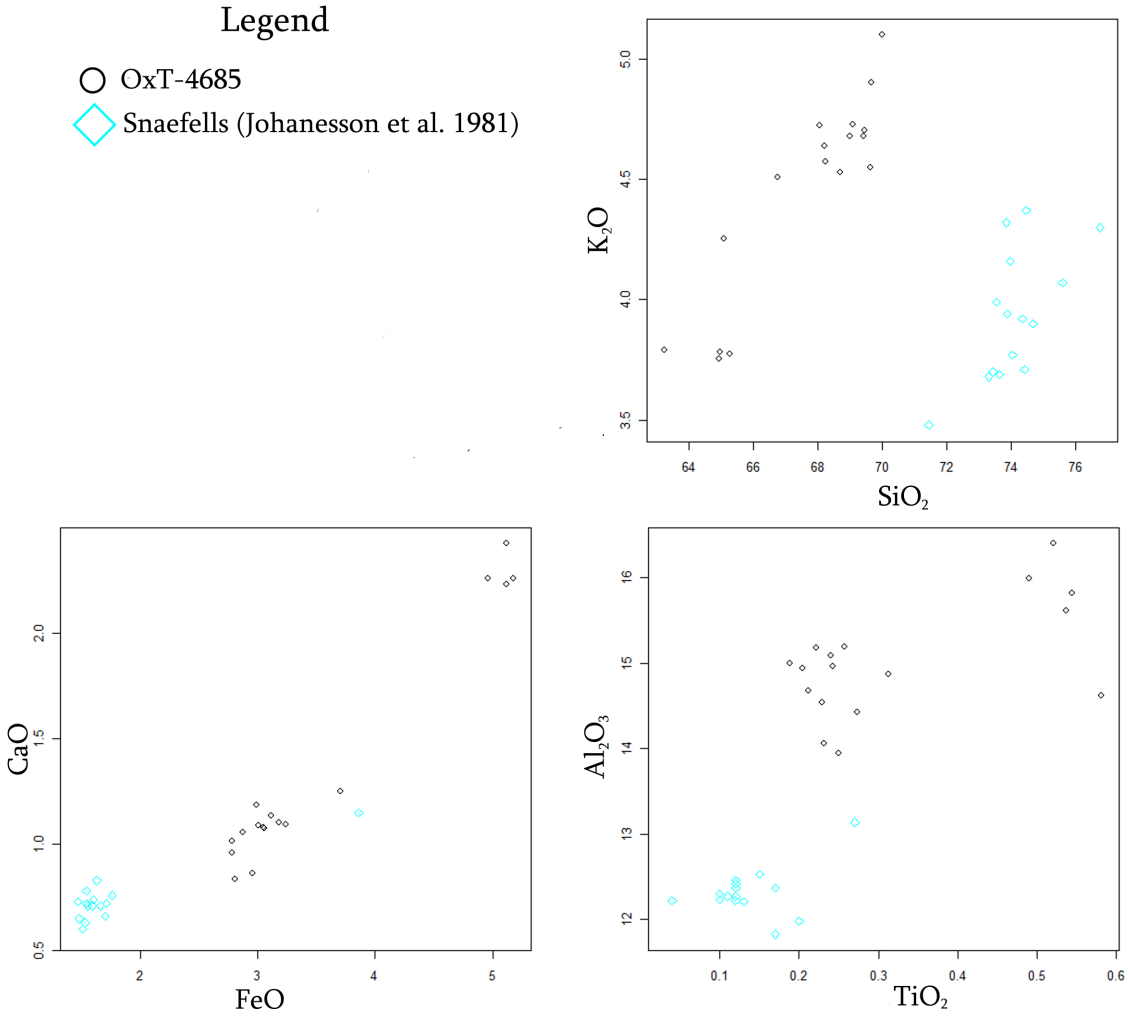


Figure 7.39: Comparison of OxT-4685 with published proximal data for the eruption of Snæfells ca. AD 200 (Larsen et al. 1999). All units are in wt-%.

Table 7.4: Table showing the correlation results for samples from the Sveinhúsavatn core.

Sample Number	Probable Correlation	Other Possible Correlations
OxT-4308	Hekla 1693	
OxT-4309	Eldgjá ca. 935	
OxT-4310	Landnám ca. 871	
OxT-4685	unknown	

7.6.2 Sveinhúsavatn chronology

As shown in the tephrostratigraphic diagram in Figure 6.16, the lake core from Sveinhúsavatn had four peak microtephra layers. Three of these were correlated to known eruptions. These are the eruptions of Hekla 1693, Hekla 1104, and the *landnám* tephra, which dates to 871 ±2 (Grönvold et al. 1995). The fourth microtephra peak could not be linked by glass chemistry to any known eruption. The core was sampled in 5 cm intervals to correspond with diatom research conducted by Dr Jerry Lloyd and his student William Dickens at Durham University. Their research focus is on sea-level changes over time in northwest Iceland, as measured by diatom changes. The chronology for the core was constructed from the microtephra record as part of this thesis, and the joint report on the diatom research can be found in Dickens et al. (Milek 2011) and Dickens (2011). Below, their diatom research combined with the chronological framework has been used to refine the interpretation of the wider archaeological landscape. This illuminates the role that Sveinhúsavatn may have had to play in the development of the farm at Vatnsfjörður.

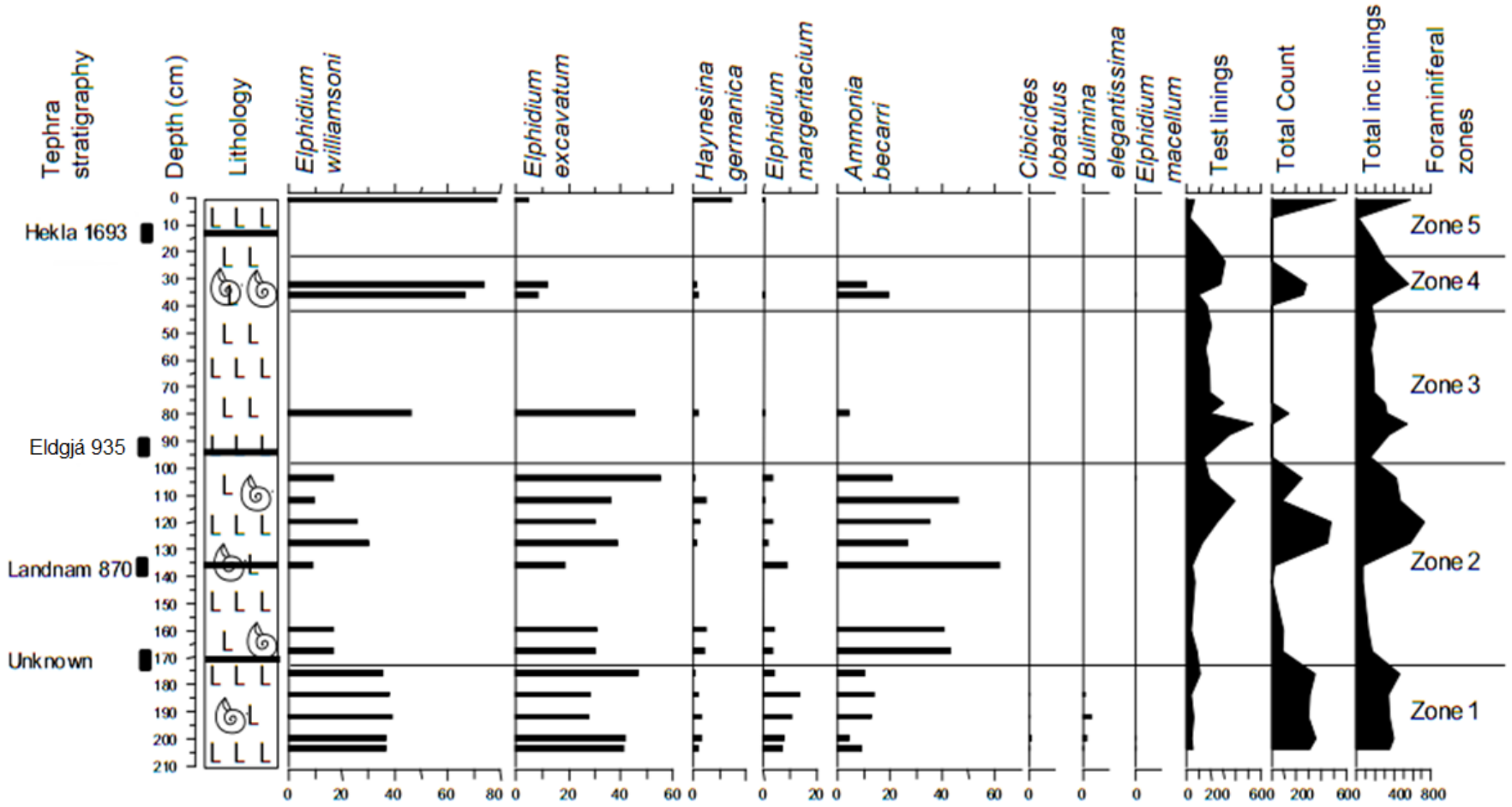


Figure 7.40: Foram counts with tephrostratigraphy of Sveinhúsavatn core. Further details, including a description of each foram species, are available in Dickson and Lloyd(in Milek 2010).

The reason for using tephra studies on the lake, as is discussed further in Section 4.2.2, was to closely date the different transitions that the lake underwent over time. Based on its position in the landscape, it seemed almost certain that the lake had once been a seawater-filled bay and part of Isafjarðardjúp. It was unknown when this was and, because sea-level is very much local in Iceland, it could not be determined without directly studying the lake. The diatom data shown in Figure 7.40 and Figure 7.41 show that the transition from seawater to freshwater occurred between 20-45 cm in the lake core, which corresponds roughly to between AD 1350 and 1600. Figure 7.42 shows the deposition rate for the core. This shift passed through several stages across centuries, and all available evidence suggests that it was a gradual change. As Figure 7.42 demonstrates, sedimentary deposition was much greater prior to the sea-level dropping low enough that Sveinhúsavatn became a lake.

Tephrochronology was necessary at the lake in order to produce this preliminary study; Pb^{210} dating was inconclusive, and as mentioned above, the freshwater reservoir effect leads to problematic lacustrine radiocarbon dates in Iceland (Ascough et al. 2011).

7.6.3 The importance of the bay/lake transition to the farm at Vatnsfjörður

The dating of the bay/lake transition at Sveinhúsavatn opens the way for further research into a long-standing research question at the site. As was discussed in Chapter 4, no boathouse has definitively been found at Vatnsfjörður, although geophysical and ground survey along the current coastline of the fjord has shown some possible locations (Gardela and Mikocewiz in Milek 2010; Dawn Elise Mooney, pers. comm., 1 December, 2011[3]). Boathouses were an important feature of coastal high status farms throughout the Norse cultural area for many centuries. Although their earliest and largest forms have thus far been found only in Norway, the smaller *hróf*, or light shelter, is mentioned repeatedly in the sagas of the Icelanders and similar styles of boathouse have been found in boat roosts at Jarlshóf in Shetland (Stylegar and Grimm 2005). In the *Landnámabók*, which describes the settlement of Iceland, Haukr Erlendsson notes a number of boathouses in the country (trans. Pálsson and

[3]Mooney suggested that the test trench at Area 45 may have uncovered the remains of a small boathouse, but based upon the tephra layer found there that wall, if it was a boathouse or related to a boathouse, it would have been in use after the bay/lake transition at Sveinhúsavatn (Dawn Elise Mooney, pers. comm., 3 March, 2012).

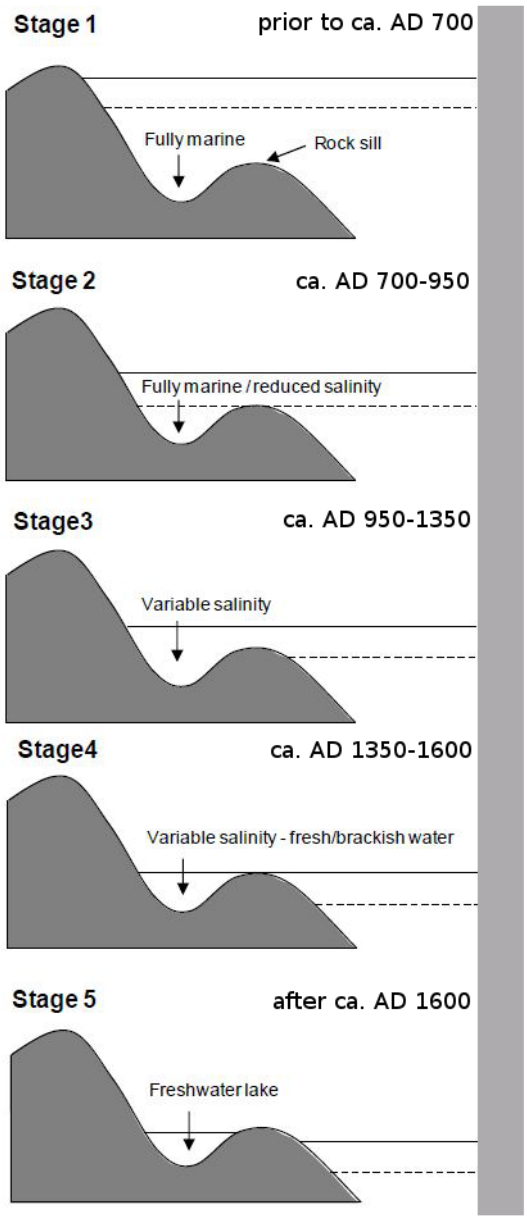


Figure 7.41: Example of the different transitional phases that Sveinhúsavatn may have undergone over time as sea level changed in the area (Dickens and Lloyd with data from Anderson in Milek et al. 2010).

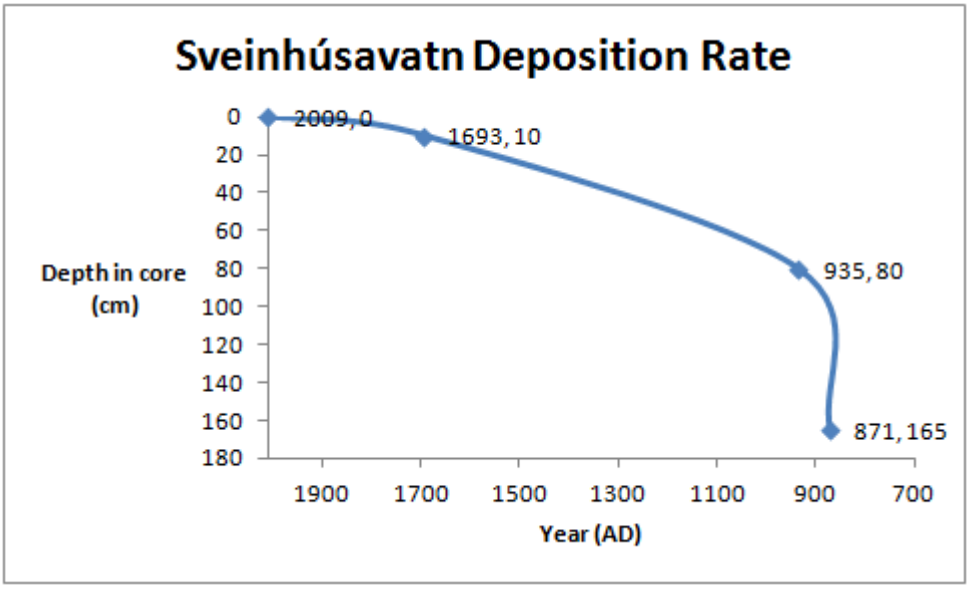


Figure 7.42: The deposition rate for sediment in the lake, based on tephrochronology through the lake core. Each point represents an identified tephra layer and its depth in the core.

Edwards). Boathouses could be large wooden structures, such as those found in Norway, variably-sized stone buildings, or small sheds with peat walls. Although little archaeological research has been done into Icelandic boathouses, unexcavated ruins suggest that the majority were built of stone (Stylegar and Grimm 2005: 265-266). One antiquarian survey describes finding both *hróf* and *naust* in Iceland, most notably one at a different Vatnsfjörður on the north of the Snaefellsnes peninsula (Erlingsson 1899: 87-88). He describes the five boathouses as being of the same form: 'an oblong square, with no wall in one end, that towards the sea.' Therefore it seems likely that some remains of the boathouse at Vatnsfjörður must exist, or must have left an impression on the landscape. The sea-level study indicates a lower sea-level for the present day than at the time of settlement, so it also seems likely that coastal erosion, which has been a problem at many Norse boathouses throughout the North Atlantic (Stylegar and Grimm 2005), will not have destroyed the evidence for this important building. As no boathouse has been found yet around the current coastline or near to it, and the lake has now been shown to have been an ideal harbour for the farm, the next area to be surveyed for the boathouse should be around the lake. Finding the boathouse would further reinforce the argument presented above, that what is today a lake played a crucial role as a harbour in the initial settlement of and centuries-long prosperity at the farm.

In addition to providing information about a likely harbour for the farm in its first five hundred years, the data from Sveinhúsavatn can be used to discuss the effects that sea-level change may have had upon the people who lived at the farm. This relates to the patterns of settlement in Iceland in general. It is not known when Vatnsfjörður was founded, aside from that it was some time after *Landnám* (although the home-field basal dates may provide a beginning point, given the evidence of anthropogenic creation of the peat there). However, it is generally accepted in Iceland that the oldest farms are named for natural features (like Vatnsfjörður, meaning 'lake fjord' or 'water fjord'), whereas a farm with a suffix denoting the word farm (*-gerði, -staðir*) means a later (and generally lower status) one (Vésteinsson 2001; Lárusdóttir 2006). Therefore Vatnsfjörður may have been one of if not the earliest settlement in Vest-firðir. This could mean that as Norse settlers entered the uninhabited countryside, the location that became the settlement at Vatnsfjörður was chosen before any other area in the surrounding landscape. The landscape feature that is now Sveinhúsavatn may have played a crucial role in this - and indeed, the name Vatnsfjörður may itself be derived from the presence of the bay.

Life in Vestfirðir, as a region, was very different from that in other parts of Viking and medieval Iceland. Callow (2006), in his study of Icelandic farm life based on the saga *Guðmundar saga dýra*, uses the 'valley' as the unit of community in medieval Iceland because most chieftaincies and their surrounding farmsteads were located in the long valleys that lead to most of the country's coastline. In Vestfirðir, however, the topography does not include many long valleys and most settlement is perched along narrow strips on the coast with towering hillsides behind. Instead, Vestfirðir had what Vésteinsson (2006: 97) has called a 'community of dispersed settlements', which after the settlement period only existed in that region, the far north, and the far east, Iceland's least inhabited regions. The majority of farms were isolated inside of the steep-sided fjords, with little space for maintaining agriculture. Vésteinsson (2000: 14) notes that Vatnsfjörður was the only farm anywhere in Iceland located in a fjord environment that was able to sustain a chieftaincy. He theorises that this was almost certainly due to the placement of the farm in the base of the fjord, meaning that other farms within Vestfirðir's dispersed settlement community could travel to it in their ships. Travel between farms via ship was not unheard of in northern Norway, particularly in places like the Lofoten Islands where travel would have been easier by ship than overland (Nielssen 1993), and so the first settlers in western Vestfirðir may have scouted the fjord environment of Isafjarðardjúp for the best location to establish a large farm that would then be able to control other, later settlements in

the landscape. As Sveinhúsavatn was a bay at this time, it seems likely that the presence of a bay large enough to shelter ships, which was not a common feature in the area[4], could have been a powerful draw for these first settlers. They may have chosen to settle in that particular location because of this advantageous natural feature.

The bay that is now Sveinhúsavatn may also have played a major role in the chieftaincy's development and prosperity. Vatnsfjörður was not an impoverished farm, although its agricultural potential by virtue of its location was much less than that of other chieftaincies in Iceland (Tulinius 2005). As discussed in Section 4.2.1, historical records indicate that by the thirteenth century, Vatnsfjörður was the most powerful farm in Vestfirðir and would remain so until the end of the seventeenth century. These same records also indicate that the farm was known to be powerful outside of the fjord environment of Vestfirðir, and that chieftains at Vatnsfjörður regularly engaged in the power struggles that the sagas tell us characterised aristocratic life in Iceland throughout the Viking and medieval periods. Vésteinsson (2000: 13) notes that fjord environments afforded access to a variety of resources because they stretched from the sea to the highlands: fish, homefield, pasture, forest, and driftwood. However, to become a chieftaincy and maintain that position for centuries, the farm at Vatnsfjörður also had to have power over other farms in the region (Tulinius 2005; Edvardsson and McGovern 2005). The bay may have been used as a harbour for nearby farmers and fisherman to bring their goods, which could then be moved on to markets further south in Iceland or further afield in Europe. The fall in sea level throughout the medieval period until roughly AD 1600 may have initially been a nuisance, forcing the people of Vatnsfjörður to move or rebuild boathouses and other buildings associated with the processing of trade goods and tithes, but when the sea level dropped low enough that the rock sill at the mouth of the bay was high enough relative to the water surface to keep out boats, the bay would have stopped being useful. By roughly AD 1600, the bay to lake transition had happened; the enclosed shape of the bay was gone as a useful resource for fjord-going vessels. Vatnsfjörður declined in status and wealth from the seventeenth century onwards. The timing of the loss of the bay may be purely coincidental, and without further investigation such as excavations on the former shore, it is impossible to say, but it is reasonable to theorise that the transition of the bay into the lake now known as Sveinhúsavatn would have dealt a serious blow to the ability of the people at Vatnsfjörður to control

[4]This statement is based on the lack of lakes, aside from the glacial lagoon by Kaldalonsjökull, in Ísafjarðardjúp.

commerce, and therefore rule the community, in Vestfirðir. By the end of the seventeenth century, power in Vestfirðir had shifted away from the farm at Vatnsfjörður to the fishing port at Isafjorður. The drop in sea level therefore may have had very serious consequences for the farm. Even if it did not, documenting sea level change provides local data for understanding the shoreline/environmental history of the area.

7.7 Linking records across Vatnsfjörður

Multiple records have now been documented from Vatnsfjörður and the surrounding landscape: three archaeological areas, Sveinhúsavatn, the Homefield, and Kaldalonsjökull. As shown in Figure 7.43, all of these are connected by the Hekla 1693 tephra/microtephra.

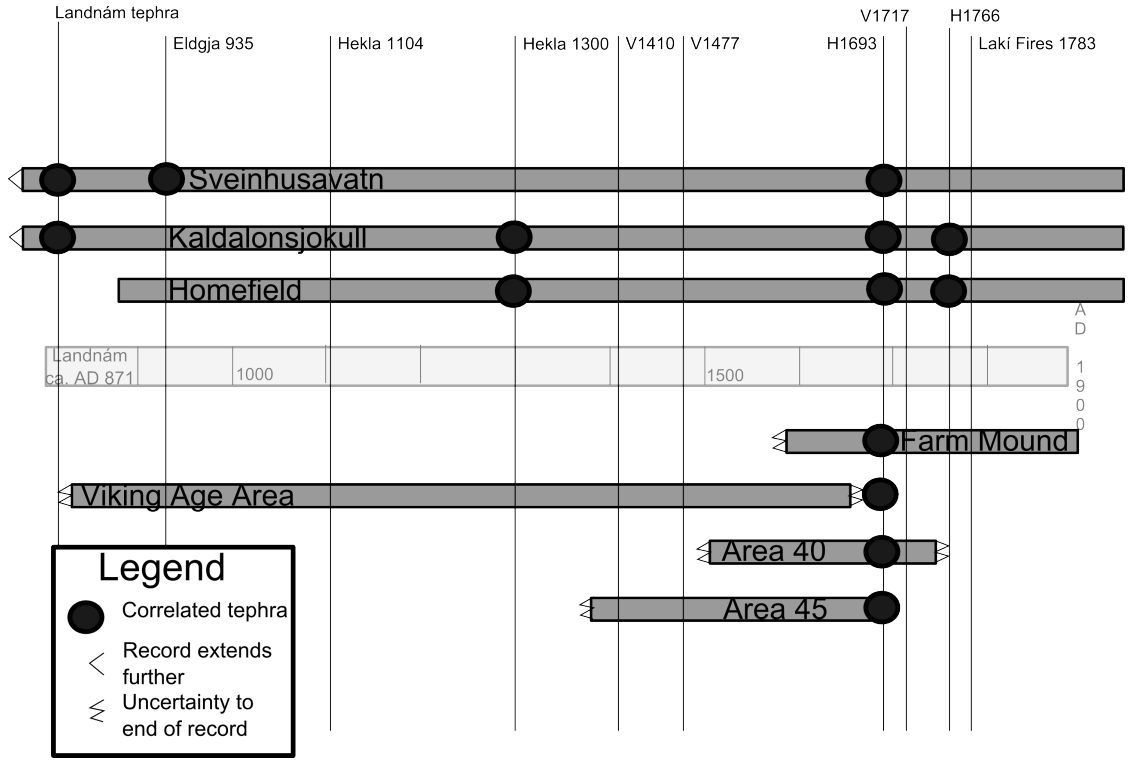


Figure 7.43: Diagram showing the different records sampled that relate to Vatnsfjörður and Vestfirðir, and how tephra and microtephra layers connect them.

Hekla 1693 is not a visible layer throughout the landscape. Although it is a visible layer across much of the archaeological site, it is not visible in the other records studied here, notably the Homefield, Sveinhúsavatn, and Kaldalonsjökull. However, the layer is present in the microtephra records. Further, it is not found in every sequence throughout excavated portions of the archaeology — for example, a cross-section of the Homefield boundary wall excavated in 2010 spans stratigraphy from the Viking Age until modern day, but does not have a visible tephra layer (Milek in Milek 2011: 67). One reason for this might be the very fine nature of the tephra grains from the Hekla 1693 eruption. As discussed above, even tephra shards from the visible tephra layer were generally too fine to be extracted without using microtephra techniques.

Another explanation may be differential deposition across the site. This would not be unprecedented. For example, Mairs et al. (2006: 369) have studied tephra from the eruption of Katla in 920 in the valley of Thórsmörk and found evidence for differential deposition even though Thórsmörk is close to Katla. Mairs et al. suggest that there is a connection between surface vegetation, erosion, and depth to determine the survival of tephra deposits. Differential deposition patterns may also explain why Sveinhúsavatn is the only record to have evidence for the Eldgjá 935 eruption. Similarly, lying snow fields or ice over on the lake (e.g., Davies et al. 2007) during the LIA may explain why Sveinhúsavatn does not contain tephra from Hekla 1766 or 1300.

The connection of the microtephra layers across these records has connected the archaeological excavations to environmental records of sea-level change, vegetation, and glacial change. The direct connection of Hekla 1693 allows for a very high resolution of events, but the tephrochronologies derived from the other records also tighten the chronological resolution of events happening in the landscape around Vatnsfjörður.

7.8 Connecting Vatnsfjörður to Icelandic archaeology

Chronology also connects the development of the farm at Vatnsfjörður to the development of settlement throughout Iceland and the North Atlantic. In Iceland, archaeology has traditionally lagged behind historical records as a source of information about the past, to some extent because the historical records provide well-dated, specific information and so many researchers have not seen a need to elaborate on

those records with archaeological information (Harrison et al. 2008). This lack of archaeological investigation extended to a neglect of post-medieval archaeology. Over the past decade, in particular, archaeology has begun to come into its own in Iceland, moving away from its roots in the literature of the sagas, but as a result at present there has been relatively little non-historically-based archaeological research, and much of that has been focused on specific areas (e.g., Eyjafjallahreppur and Mývatn) rather than considering the entire country. Moreover, as at Vatnsfjörður, there are many places in Iceland that do not have comprehensive historical records. Therefore archaeology is often the only source of information about this time period in Iceland. In order to move the story at Vatnsfjörður beyond the farm and connect it to the rest of Iceland, the chronology is now used as a framework to link it to environmental and archaeological studies in the wider region. The power of using chronology as the frame for integrating this data is its ability to link records beyond the immediate range of the site.

Individual archaeological excavations must be considered as part of a wider historical context. Figure 7.44 visually presents studies in Icelandic archaeology, environment, or both that have secure chronologies or have been otherwise selected because of criteria outlined in Section 5.5. The sources for Figure 7.44 are presented in the Excel table on CD. Figure 7.45 shows the location of the studies referenced.

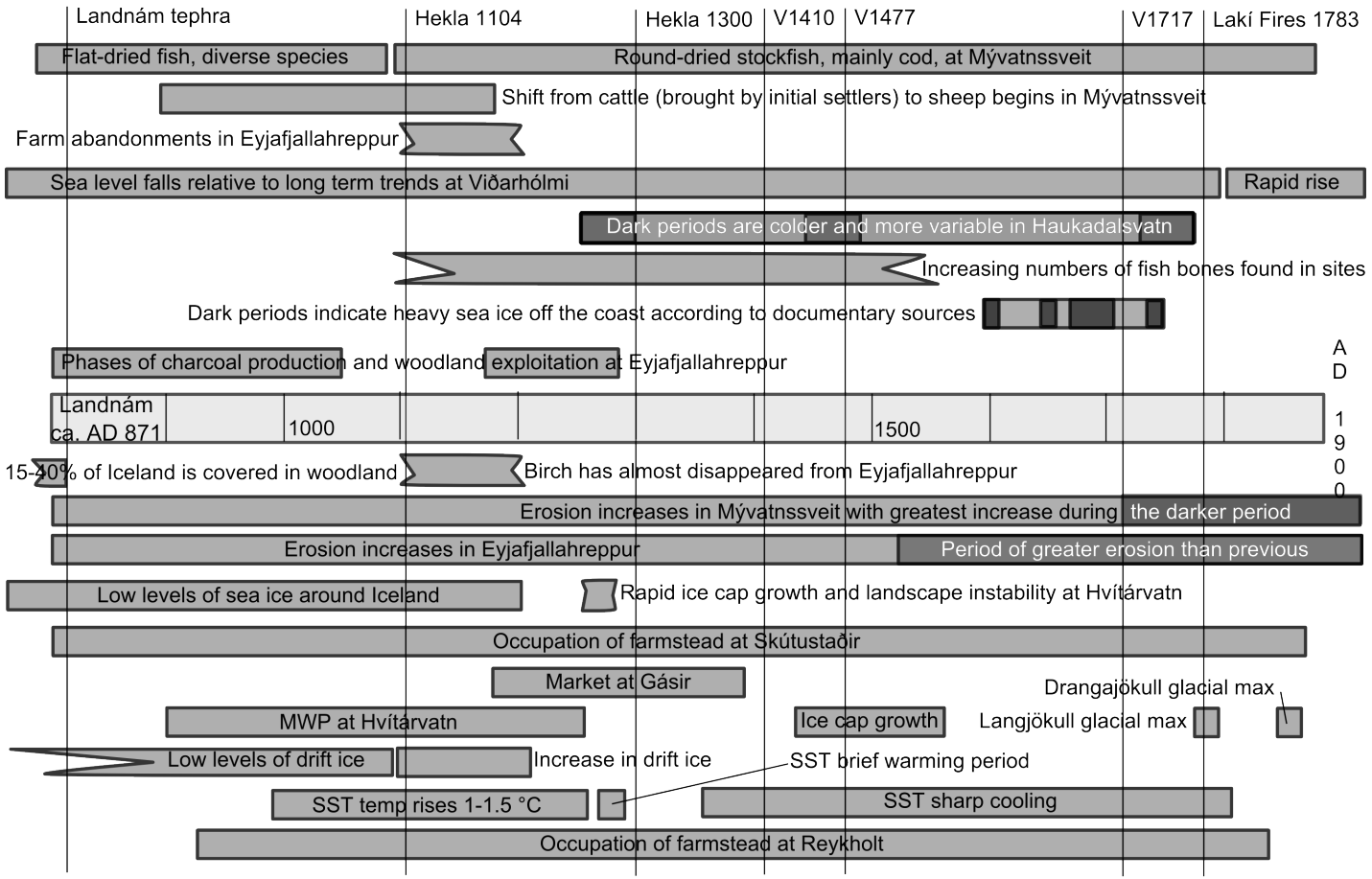


Figure 7.44: Timeline of selected environmental and archaeological records from Iceland, with sources listed under 'Iceland' in the Excel database CD. In some cases, data has been excluded from graphical representation that is similar to other data or that has been superceded by new studies (e.g., Knudsen et al. (2004), Grove (2000), and Crowley et al. (2000) all discuss similar material to the more recent Sicre et al. (2008) and Geirsdóttir et al. (2009b)). A broken line indicates that the endpoint is unknown.



Figure 7.45: Map of Iceland showing all locations mentioned in Figure 7.44, Figure 7.44. Glaciers are shown in white.

The first thing to note from Figure 7.44 is some trends in Icelandic environmental and archaeological studies. These were discussed in detail in Section 2.3. To summarise, there are three major trends. First, zooarchaeology has been a dominant research trend, mainly due to the work of McGovern, Perdikaris, and their respective students (e.g., Edvardsson 2004; Perdikaris and McGovern 2007; Hambrecht 2011). Many of these studies are focused on the dietary consumption of fish, and the intensification of cod fishing in medieval Iceland.

Second, studies about the environmental impacts of the Norse *landnám* in Iceland ask several questions: when were major periods of erosion? How did erosion relate to the settlement of the landscape? How did Icelandic settlers manage their woodland resources, and how did that relate to the production of fuel? When did the native birch that covered 15-40% of Iceland around *landnám* disappear (Church et al. 2007)? When were farms abandoned and what noticeable impact did that have on the landscape?

A third group of research is about non-anthropogenic environmental factors. This research seeks to answer questions such as, how did sea-level along the coasts change? What are the sea ice records for Iceland, and when were the periods of greatest sea ice encroachment? When did the MWP and the LIA occur? How did these periods manifest themselves: with consistently lower temperatures, cooler summers, or stormier periods? When were the late Holocene glacial maximums for Iceland's glaciers, and how does that relate to the LIA? Using chronology, each of these environmental factors can be linked back to reconstruct what may have affected the lives of Icelanders over time. This is not to say that environmental impacts always drove social change, or even had a role to play in it. Dugmore et al. (2007: 8) highlight the example of Þjórsárdalur, in southeastern Iceland, where, despite erosion and the impact of volcanic ash, there were still extensive birch forests in the sixteenth century, despite the valley being a marginal landscape for birch.[5]

In archaeology, it is almost impossible to prove a causal link between two events; however, scientific chronologies provide a way to highlight potential relationships and connections. Once chronologies have shown the potential for connection, then it is possible to apply archaeological interpretations to those connections.

[5]One major issue in Icelandic archaeology that has been the subject of much debate but that is not supported by scientific dates is the conversion to Christianity. Vésteinsson (2000) has written extensively about the topic. It is traditionally dated to AD 1000 by written sources.

Each of the three research trends noted above link to Vatnsfjörður. In North Atlantic archaeology, there is a general pattern of decline in domestic mammal bone from the early medieval to the early modern periods in proportion to increasing fish bones; this suggests a rise in the importance of marine resources over time (Edvardsson 2010). Stable isotope studies, although problematic for Iceland, show a similar subsistence pattern with a large enough sample size (Ascough et al. 2014). Edvardsson (2010) and Amorosi et al. (1997) attribute these changing sustenance strategies to responses to soil erosion, cooling climate, and changing social forces. Similarly, the shift from cattle to sheep as the dominant domesticated mammal at Mývatnssveit has implications for subsistence strategies that relate to environmental and social change. Much has been made of the settlers of Norse Greenland and their refusal to change from a farming-based (and likely rooted in Norway) subsistence strategy. In Iceland, at least in Mývatnssveit, there is a documented shift from the higher maintenance cattle to the hardier sheep (McGovern et al. 2007). The timing of this shift seems to have occurred relatively early: settlers arrived in the *landnám* period with cattle, sheep, goats, pigs, and horses. By the tenth century goats and pigs were increasingly rare. At Steinbogi, Mývatnssveit, early-13th-century archaeofauna indicate that there was a shift away from cattle production toward the sheep-dominated pattern of the classic 18th-century farm as described in the Jarðabók farm surveys (*ibid.*: 40).

At Vatnsfjörður, the moment of transition here is difficult to see. Unfortunately, bone preservation at the Viking Age area is poor, with most bones too fragmentary to identify (Dupont-Hébert in Milek 2010; Dupont-Hébert in Milek 2011). By 1693, fish represented the majority of archaeofauna found at least in one area of the Farm Mound. This was in room 8562, whose floor was dated in Section 7.2.3 using tephrochronology. The other species found in abundance in this room (which served as a midden), were ovicaprine, suggesting that fish and sheep were the main animals being exploited at Vatnsfjörður by this year (Dupont-Hébert in Milek 2011).

For Vatnsfjörður, the shift towards marine resources would have benefited the owners of the farm. Although their land was marginal for wealth based on livestock, it seems likely that their placement in the Vestfirðir landscape and proximity to the rich marine resources of Ísafjarðardjúp gave them an ideal location to exploit the fishing trade as it grew through the LIA. Likewise, the potential shift from cattle to the less-landscape-intensive sheep would also have benefited the farmers at Vatnsfjörður.

The second area of research, anthropogenic environmental change, particularly as it relates to fuel usage and woodland management, has not been studied in Vestfirðir

before now. The research from the homefield core described in Section 7.3 provides a chronological framework for the initial fuel usage and precipitous drop in birch resources at Vatnsfjörður. This chronology is similar to that recorded by others for similar resource use in Iceland.

The third research area, non-anthropogenic environmental change, also had a role to play in this study of Vatnsfjörður, specifically in the core from Sveinhúsavatn. The sea-level study revealed the potential impact of sea-level change on human settlement at the farmstead. There have been very few sea-level studies that relate to human settlement in Iceland, and this study is in many ways advantageous because of the placement of the lake beside the farmstead, but it provides a framework for interpreting sea-level change archaeologically at future locations in Iceland and beyond.

Finally, the tephrochronology for the Kaldalonsjökull core will contribute to future research reconstructing glacial fluctuations at Drangajökull. Very little research has been done on the Vestfirðir region itself, and because climate is local this means that some of our data must be extrapolated. However, in Vestfirðir, Principato (2008: 140) finds that the LIA glacial maximum for Drangajökull, the glacier in Vestfirðir, is in the mid-19th century. This corresponds with other parts of Iceland, including outlet glaciers in Vatnajökull and Myrdalsjökull (Þórarinsson 1944; Dugmore and Sugden 1991; Björnsson et al. 1996). The new tephrochronology described above will allow for a tightening of the chronological resolution of these records as the research that the author began with Dr Principato on this area continues (see more on this in Section 10.4).

Beyond issues directly studied in the records above, two further issues may have had an impact on Vatnsfjörður: coastal sea ice and tenant farming. Sea ice affected the northwest, north, and east of Iceland most strongly, and could have had serious consequences for fishing, trading, and communications at Vatnsfjörður. Ogilvie and Jónsdottir (2000: 390) describe the effects of heavy sea ice as lowering land temperatures, keeping vessels away, and cutting off fishing grounds. Some winters were particularly hard; for example, in 1374, annals records that there was sea ice through the end of August that prevented any ships from Norway reaching Iceland at all that year (translated in Ogilvie 1990: 244). Ogilvie (1984) has gathered records of sea ice off the coast of Iceland based on documentary sources. Unfortunately several centuries (the 1400s and 1500s) suffer from a lack of reliable sources, but she is able to record annual data from 1601-1780. She finds that the decades from 1680-1710 were particularly cold and had many years with sea ice that reached Iceland's coast, with

the 1690s in particular being one of the coldest decades on record (1984: 146). This period coincides with Vatnsfjörður's decline.

Tenant farming, meanwhile, had its roots in post-medieval Icelandic society. The practice and its social consequences are discussed by Hastrup (1990; 1992), Bolender (2006), and, particularly relating to Vestfirðir, Edvardsson (2004). A summary of this is provided in Section 2.2.2. Archaeologically, Simpson et al. (2003) have studied the differences between Sveigakot, a farm in the Mývatn region that was owned by successive tenants, and Hofstaðir, which was owned by an upper-middle ranking family. Simpson et al. note that Sveigakot is heavily eroded and went through several cycles of abandonment and reoccupation by progressively poorer and poorer householders. Meanwhile, Hofstaðir seems to have been highly successful at managing its soil, despite being in the same marginal conditions for growing crops and fodder as Sveigakot. Simpson et al. (2003: 46) note that impoverished farmers who may not be present at the farm for the next harvest cycle manage their resources differently from secure landowners who are concerned with passing on their farm as an inheritance to their kin. How this may relate to our interpretation of Vatnsfjörður may be found in the research described above for the homefield. One possible explanation may be that the sudden decline in charcoal, culminating in a complete drop-off right around 1693, is a sign of a time when resources were poorly managed by householders at the farm. The early 1700s were a time when the majority of farms in Iceland were owned by tenant farmers (Bolender 2006). Therefore Vatnsfjörður may have come under poor management, perhaps by tenant farmers, around the time when it is known from the Jarðabók to have declined. This is just one hypothesis – the decline in charcoal could also represent a period of conservation, as settlers slowed their destruction of the remaining woodlands, but based on the coinciding decline of the farm and the possibility that there were only tenant farmers present this seems less likely.

Some of the issues that affected other settlements in Iceland during this period would have had little bearing on Vatnsfjörður. For example, the devastation recorded by Þórarinsson (1967) for farms around the Hekla region following Hekla's eruption in 1693 was due to a layer of tephra over 25 cm thick, whereas the thickest tephra layer to have affected life at Vatnsfjörður was around 1 cm. Similarly, Vestfirðir was isolated enough from the rest of Icelandic society that during the plague outbreak of 1494-1495, that region alone was unaffected (Streeter et al. 2012).

Ultimately, building a chronology for Vatnsfjörður and local records has allowed its archaeology to be interpreted with respect to local environmental and anthropogenic

change, as well as providing a way to connect it to archaeological and environmental research also built on strong chronologies from outside of its small region.

7.9 Summary

Interpreting the chronology of the Vatnsfjörður archaeological landscape and surrounding region and relating it to the archaeological record took several steps. First, these were correlated with the WDS-EPMA data from Section 6.3.1.1, Section 6.3.1.2, Section 6.3.1.3, and Section 6.3.1.4 to known eruptions. Table 7.5 provides a summary of these correlations.

This number of possible correlations is relatively high for distal tephra studies.[6] These correlated tephra layers were then placed in the contexts of their respective locations through the landscape. The chronological markers that they provided were used to interpret the archaeology of the Vatnsfjörður farm, pollen studies and environmental change at the homefield (connected to the record from Kaldalonsjökull), and sea-level change from foram studies at Sveinhúsavatn.

Following the development of local chronologies, the chapter then turned to an interpretation that linked Vatnsfjörður's archaeological history to regional studies incorporating high-precision chronologies, archaeology, and/or environmental change. The next chapter is the interpretation of the second case study, the East Mound at the Bay of Skaill.

[6]For example, Wastegård et al. (2009) found six microtephra layers in their study of peat and lacustrine cores from the Faroe Islands; Gudmundsdóttir et al. (2011) found nine in their study from the North Iceland shelf.

Table 7.5: All correlations of WDS-EPMA data with known eruptions.

Sample Number	Location	Most likely correlation	Other possibilities?
4308	Sveinhúsavatn	Hekla 1693	
4309	Sveinhúsavatn	Eldgjá ca. 935	
4310	Sveinhúsavatn	Landnám ca. 870	
4672	Homefield	Hekla 1766	
4674	Homefield	Hekla 1693 upper limit?	
4675	Homefield	Hekla 1693	
4676	Homefield	Hekla?	
4677	Homefield	Hekla 1300 upper limit	Katla 1357?
4679	Homefield	Hekla 1300	
4680	Homefield	Hekla 1300 lower limit	
4681	Homefield	mixed population	Landnám?
4682	Sveinhúsavatn	unknown	
4685	Sveinhúsavatn	unknown	
5133	Kaldalonsjökull	Hekla 1766	
5135	Kaldalonsjökull	Hekla 1693	
5136	Kaldalonsjökull	Hekla 1693 lower limit?	mixed composition
5142	Kaldalonsjökull	Hekla 1300	
5148	Kaldalonsjökull	Landnám ca. 870	
5149	Kaldalonsjökull	unknown	mixed composition
5150	Kaldalonsjökull	unknown	
5163	Vatnsfjörður	Hekla 1693	
5164	Vatnsfjörður	not tephra	
5165	Vatnsfjörður	Hekla 1693	fraction Katla 1721?
5166	Vatnsfjörður	Hekla 1693	
7094	Vatnsfjörður	Hekla 1693	
7095	Vatnsfjörður	Hekla 1693	
7096	Vatnsfjörður	Hekla 1693	
7097	Vatnsfjörður	Hekla 1693	
7098	Vatnsfjörður	Hekla 1693	
7099	Vatnsfjörður	Hekla 1693	

8 | Interpretation: The chronology of the East Mound, Bay of Skaill

The East Mound archaeological excavation and surrounding landscape in the Bay of Skaill and Vatnsfjörður have many ways to be compared and contrasted: they are both coastal settlements where settlement began as a result of the Norse colonisation of the North Atlantic. Both settlements may have been affected by sea-level change, increased storminess, temperature change, and other environmental and climatic changes. However, whereas Vatnsfjörður was settled for roughly one thousand years, with settlement shifting upslope from the *skáli* to the farm mound, the occupation of the East Mound ended with the abandonment of the longhouse a few centuries after it has first been settled. Geophysical data and other field survey techniques in the area have found no evidence of a later settlement similar to the Vatnsfjörður Farm Mound (Griffiths et al. 2009). Therefore the timing of the settlement and abandonment of the East Mound, alongside the chronology of the local environmental record, are crucial to understanding why this coastal site was only inhabited for a short period of time. In this chapter, the chronological context for the Bay of Skaill archaeological landscape is interpreted and integrated with chronologically constrained local archaeological and environmental records.

The chronology of the East Mound, in contrast to Vatnsfjörður, does not rely upon tephrochronology. As is described in Section 4.3.1, the East Mound has had a large number of radiocarbon dates as well as OSL dates. Therefore studying the chronology of the East Mound provides an opportunity to construct chronologies in an entirely different manner from those at Vatnsfjörður. First, using Bayesian modelling to make the radiocarbon dates both more accurate and more precise, the chronological sequence of events as it is currently known from the East Mound is described. Following this, the archaeological chronology from the East Mound is linked to the environmental records from Hobbister (first correlating the tephra results described

in Section 6.2.1.2 with proximal eruption data where possible). Then the range of the palaeoenvironmental data is expanded to include a variety of other published studies, chosen using the criteria in Section 5.5. The concluding section of the chapter is a discussion of lessons learned in the course of interpreting the data relating to distal tephrochronology and archaeological analysis.

8.1 Bayesian Modelling and the East Mound

The East Mound is described in Section 4.3.1. The excavation ended in 2011 and the data gathered is currently in the final stages of publication (Griffiths forthcoming). The area excavated represents a longhouse-style building similar in shape and layout to the *skáli* at Vatnsfjörður and several associated outbuildings and ancillary areas. The East Mound underwent seven building phases, with reuse of masonry throughout the life of the buildings (Griffiths and Harrison 2011: 13; Griffiths forthcoming). Wind-blown sand filled the interior of the building complex and had to be cleared as part of excavation. The only building phase in the mound not associated with the longhouse is a later context that was a mix of beach cobbles and rough flagstones of ca. 0.4 m x 0.4 m that may have been a medieval or later animal pen (Griffiths and Harrison 2011: 30). Archaeological research at the East Mound has also included environmental and zooarchaeological sampling intended to supplement the history of the construction of the longhouse (Alldritt in Griffiths et al. 2009; Mainland in Griffiths et al. 2009; Alldritt in Griffiths and Harrison 2011; Mainland in Griffiths and Harrison 2011).

Although the microtephra study sampled from the stratigraphy at the East Mound and described in Section 6.1.2 and Section 6.2.1.2 did not provide any chronological information about the East Mound, the archaeology has a detailed chronology as a result of well-documented stratigraphy combined with 49 associated radiocarbon dates and four OSL dates. These dates are listed alongside their contexts in Appendix E.[1] The radiocarbon dates were processed by SUERC following the methods described by Dunbar et al. (2016). The OSL dates were processed at the Research Laboratory for Archaeology and the History of Art (RLAHA) at the University of Oxford using the methods outlined by Rhodes and Schwenninger (2007).

[1]There are three dates on bone from this sample: SUERC-47146, on a cow phalange, -47147, on a pig calcaneum, and -47158, an unidentified mouse bone. All of these have δ^{13}C values less than -21, so no marine reservoir correction is needed.

I have created a site-wide Bayesian model based on the stratigraphy of the East Mound site to make these radiocarbon and OSL dates more precise. This was done using OxCal v.4.3 (Bronk Ramsey 2009; Reimer et al. 2013). The method for using OxCal to create Bayesian models is described in Section 5.4. The model seeks to answer two questions: What are the dates of use for individual structures at the site, and what are the beginning and end dates for the use of the site?

The site stratigraphy at the East Mound contains some challenges, notably wind blown deposition layers from the storms that are prevalent in the Bay of Skaill and the disturbances associated with an occupation site that saw periods of rebuilding. Despite these challenges, the extensive radiocarbon sampling and well-documented excavation allowed me to create a Bayesian model encompassing nearly every date from the site. In the site nomenclature, Trench 5 and its extensions 5A and 5B comprise the area of the East Mound that was excavated and dated. Detailed site stratigraphy is available in Griffiths (forthcoming).

Using Bayesian modelling, the radiocarbon dates from the East Mound are significantly more precise. Nearly all of the radiocarbon and OSL dates can be fit into a site-wide model, and a slowly accumulated area of windblown sand that covered Trench 5, context 2001, has two OSL dates, X3100 and X3099, that provide a late terminus ante quem for activity at the site.

Four dates had to be eliminated from this overall model. On the first run with all dates included (N = 51), SUERC-24701 (carbonized barley grain) had A(individual) = 0; the A(model) = 9.6. That date is far too old for its context - indeed, its radiocarbon date is 1160 ±35 BP, making it approximately 95 years older than the next oldest date - and seems to be in error. After removing it, the model (N = 52) had A(model) = 50.4. Three other radiocarbon dates all had low A(individual) values and did not seem to fit within their contexts based on the dates around them: SUERC-17866 (A(individual) = 14), -24703 (A(individual) = 43), and -24711 (A(individual) = 35).

SUERC-17866 (carbonised barley grain) is from context 2111, a dump of domestic refuse, and dates to be later than contexts stratigraphically after it, suggesting it may be an intrusion into its context. After the probably erroneous SUERC-24701, SUERC-24703 (carbonised barley grain) is the oldest chronological radiocarbon date from the East Mound; however, its context, 2095, was thought by the excavators to be from a later occupation area; again, it may also be an intrusion. -24711 (charcoal: Salix) also modelled as too old to fit its context.

With those four dates eliminated, the model has A(model) = 158, with N = 47. Three dates have A(individual) values lower than 60, but none seem erroneous outside the model. SUERC-47150 (carbonised barley grain), which has the lowest individual A value (28), is the youngest date from the Norse period in the model, calibrating (unmodelled) to 1035 to 1222 cal AD at 95%. Although it is young, there is no reason to suspect a problem with the radiocarbon date itself, and it has been left in the model. SUERC-33719 (A(individual) = 51) and -33718 (A(individual) = 40) are a late and early date, respectively, and their lower individual A values do not seem to be the result of any error.

The most striking feature of the final model is how brief the period of occupation at the East Mound seems to have been.[2] Figure 8.1 shows the final model, and Table 8.1 shows the summary of the boundaries. Given this model, the absolute longest period for dated activity at the site is from 1000 to 1072 modelled cal AD, with much of the activity taking place in the early decades of the eleventh century AD.

Table 8.1: Boundaries from the East Mound model presented in Figure 8.1.

Boundary	Start 68%	Start 95%	End 68%	End 95%
Start Occupation at Site	1010	1000	1024	1029
Start Longhouse Occupation	1023	1018	1033	1037
End Longhouse Occupation	1030	1026	1043	1050
End Occupation	1040	1033	1060	1072

In the geography of the site, the longhouse seems to have been the main focus of activity, with the other areas surrounding it and supporting it. Modelled intervals for the various areas of the site are shown in Table 8.2 and indicate that, while the metalworking area and the southeast midden have the longest modelled durations of activity at the site, the ancillary buildings were only used for a brief period of time - perhaps under a decade. This model gives the occupation of the longhouse itself, at most, from 1018 to 1050 modelled cal AD at 95%. Pre-longhouse activity from Phase 2 of the site - represented by the dates SUERC-24714 and SUERC-24713, stratigraphically the oldest radiocarbon dates at the site - comes from artefact rich deposits that model, respectively, to 1008 to 1033 modelled cal AD at 95% and 1007 to 1043 modelled cal AD at 95%. These are accompanied by early walls and may represent the first construction at the site. The final use of the longhouse is in Phase

[2]All models in this thesis cite Bronk Ramsey 2009; Reimer et al. 2013; and OxCal v.4.3, referencing OxCal, the calibration curves used, and the version of OxCal used to create the model.

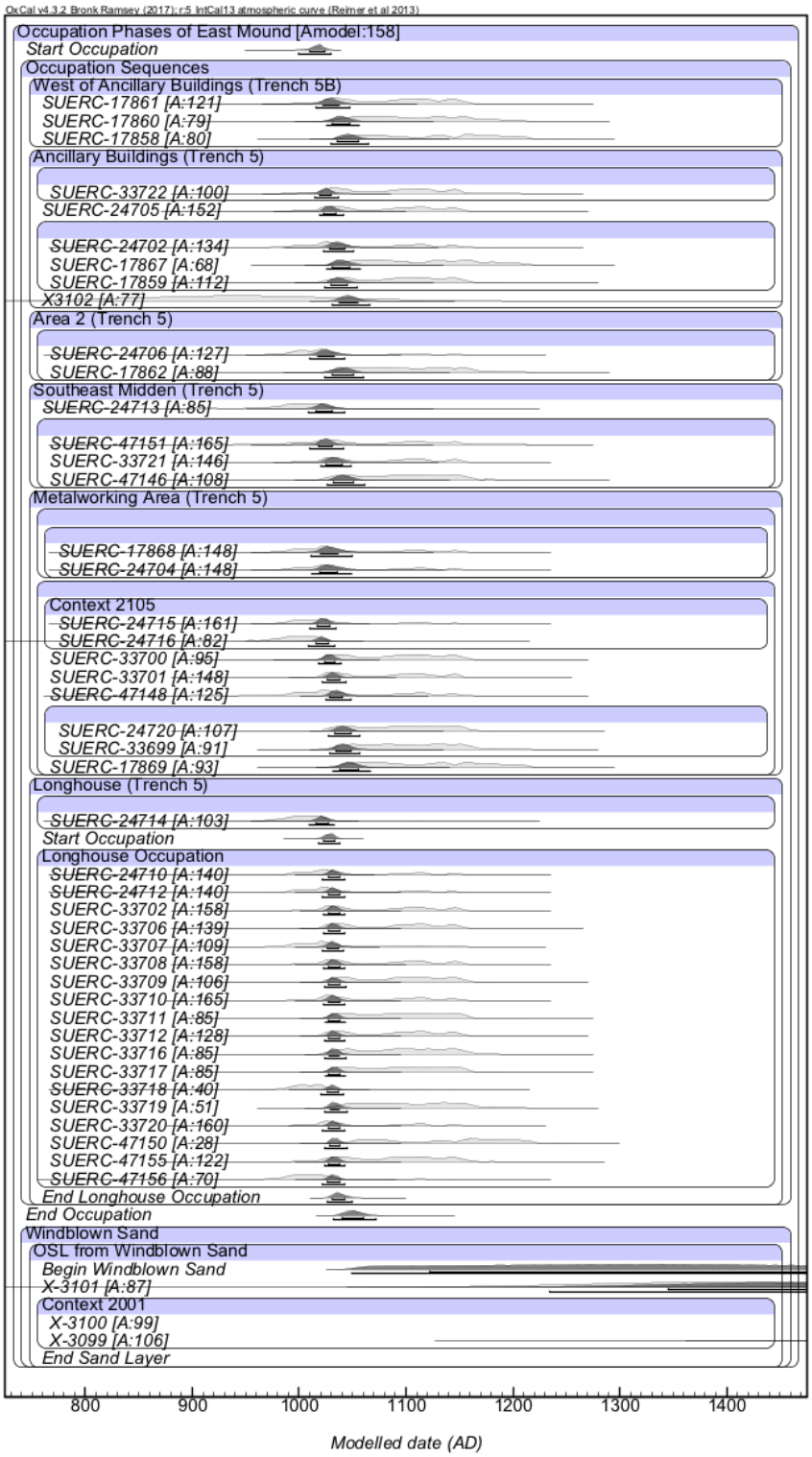


Figure 8.1: Results of the East Mound model (Bronk Ramsey 2009; Reimer et al. 2013; OxCal v.4.3), with N = 47 and A = 158. The final two dates, OSL dates on windblown sand that serve as a terminus ante quem for activity at the site, extend past the shown edge of the plot to much later in time.

6, with SUERC-47150, discussed above, representing the youngest date, which models to 1024 to 1045 modelled cal AD at 95%; unmodelled it calibrates to 1035 to 1222 cal AD, so the modelling may be pushing this date to appear older than its true age.

Table 8.2: Modelled intervals for different areas of activity at the East Mound. The interval query in OxCal calculates the interval between the start and end of a phase (i.e., its duration).

Area	Interval 68%	Interval 95%
West of Ancillary Buildings	0 to 8	0 to 17
Ancillary Buildings	0 to 8	0 to 16
Area 2	20 to 46	7 to 66
Southeast Midden	20 to 47	7 to 66
Metalworking Area	20 to 47	7 to 66
Longhouse	0 to 19	0 to 33

As will be discussed further in Chapter 9, other Norse sites containing longhouses in the Norse North Atlantic had lengthy periods of activity. Was the East Mound an unsuccessful farm? Ancillary buildings, like the metalworking area, a byre, and the southeast midden, all model to have dates close to the occupation period of the longhouse, and their presence means there were a great deal of activity around the house, which was itself large and constantly being added to or changed. This suggests a level of wealth for the people building it. The sand layer immediately above Phase 6 in the ancillary buildings, dated as X3102, models to 1030 to 1067 modelled cal AD at 95%. Perhaps this represents a storm event catastrophic enough to convince the inhabitants of the East Mound to leave behind their large home and to move elsewhere. Activity may have shifted away from the mound to areas further inland that have not yet been explored archaeologically.

8.2 Correlating distal layers with proximal glass chemistry

The results described in Section 6.3.2 will now be correlated geochemically with, where possible, published and unpublished eruption glass chemistry.

8.2.1 Hobbister B – OxT-4765, OxT-4766, OxT-4767

Section 3.4.2 discusses the current state of distal tephra studies in Orkney. Prior to the research presented here, there have been no published tephra finds in Orkney correlated to eruptions in the past 2000 years. The tephra presented here is almost certainly from that age.

The WDS-EPMA results for the successful samples from the Hobbister B core are described in Section 6.3.2. Following data filtering, there were a limited number of data points from these samples. However, small sample sizes are not unprecedented or even very rare in distal tephrochronology studies (e.g., Chambers et al. 2004; Balascio et al. 2010; Lane et al. 2011; Rea et al. 2012), so this study is not unprecedented. Thus far, there is no lower limit to statistical validity for tephra fingerprinting with small sample sizes, although a discussion about how realistic it is to make a correlation with very few data points is needed (see Section 10.4.

Radiocarbon dates from Hobbister B bounded the lower part of the core, as is shown in Table 4.3. Therefore the microtephra scanned from 0-7.5 cm had to be younger than that, and based on its position near the top of the core, it was possibly significantly younger. Based on the similarities between the WDS-EPMA data for OxT-4765, -4766, and -4767, as well as the peak shape of the tephras 0 - 10 cm deep within the Hobbister B core (as shown in Figure 6.21), it seemed likely that the WDS-EPMA data from these three samples could be combined and analysed as belonging to a single eruptive event. There is precedent for this: for example, Rea et al. (2012) combine microtephra geochemistry across several centimetres in their study of fourteen peat profiles from Ireland. As demonstrated in the bi-plots in Figure 8.2 and Figure 8.3, a visual comparison of the data shows that the microtephra from Hobbister B between 0-7.5 cm correlates to either Hekla 1947 or Hekla 1510.

8.2.1.1 Hekla 1510, Hekla 1947, and the British Isles

At first glance, the bi-plots presented in Figure 8.2 and Figure 8.3 clearly argue that both the Hobbister B samples and the data presented by Rea et al. (2012) should correlate to Hekla 1510 purely on the basis of the glass chemistry of the samples. Rea et al. argue that their samples correlate to Hekla 1947. As the data from Hobbister B is very similar to that which Rea et al. identifies as Hekla 1947, it is important to

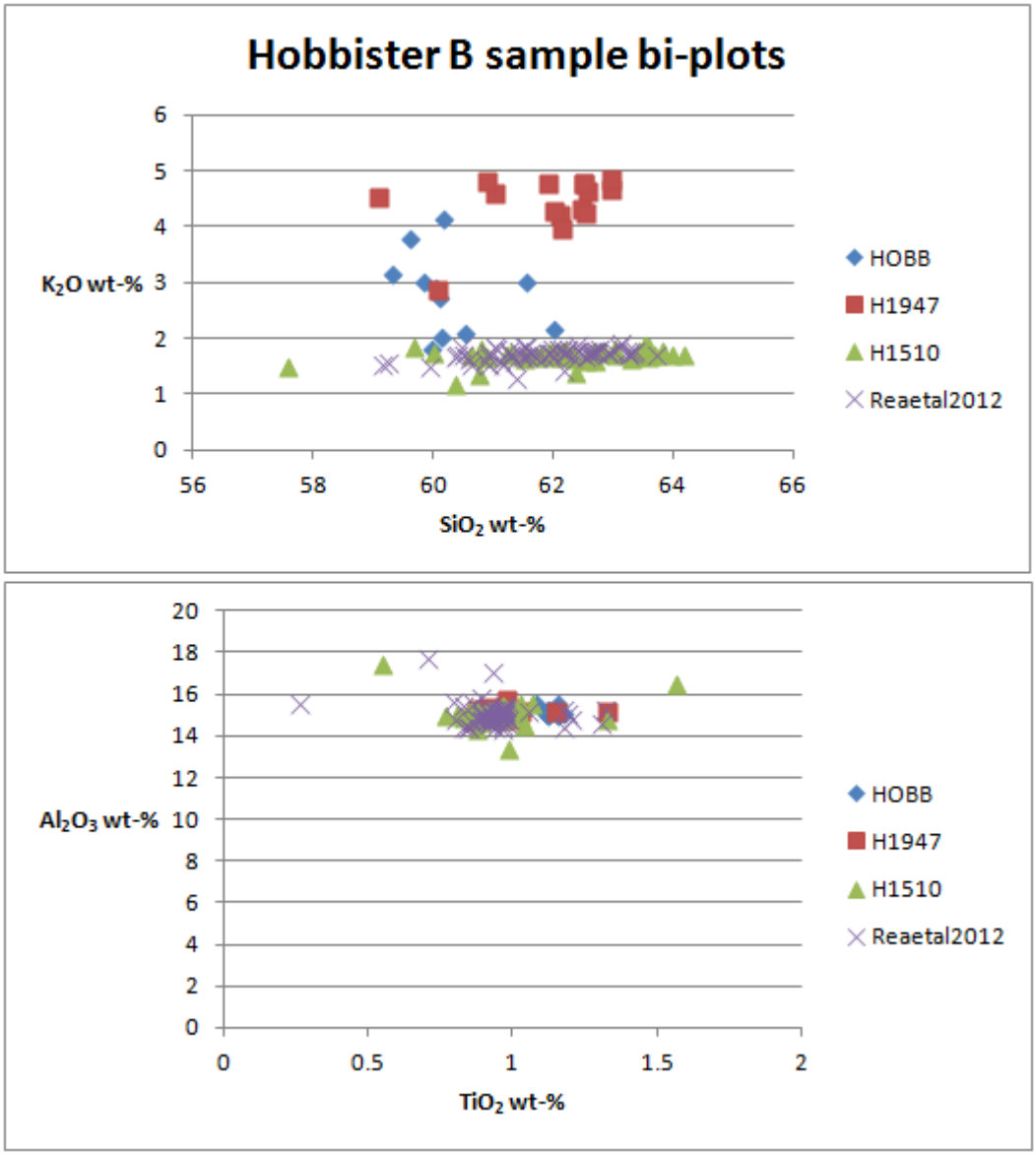


Figure 8.2: Correlation bi-plots for the Hobbister B core depth 0-7.5 cm (combined samples OxT-4765, -4766, and -4767 = HOBB). Hekla 1947 data is from Larsen et al. (1999). Hekla 1510 data is from Dugmore et al. (1995), Pilcher et al. (1996), and Larsen et al. (1999). 'Reaetal2012' comparative data is from the appendix of Rea et al. (2012).

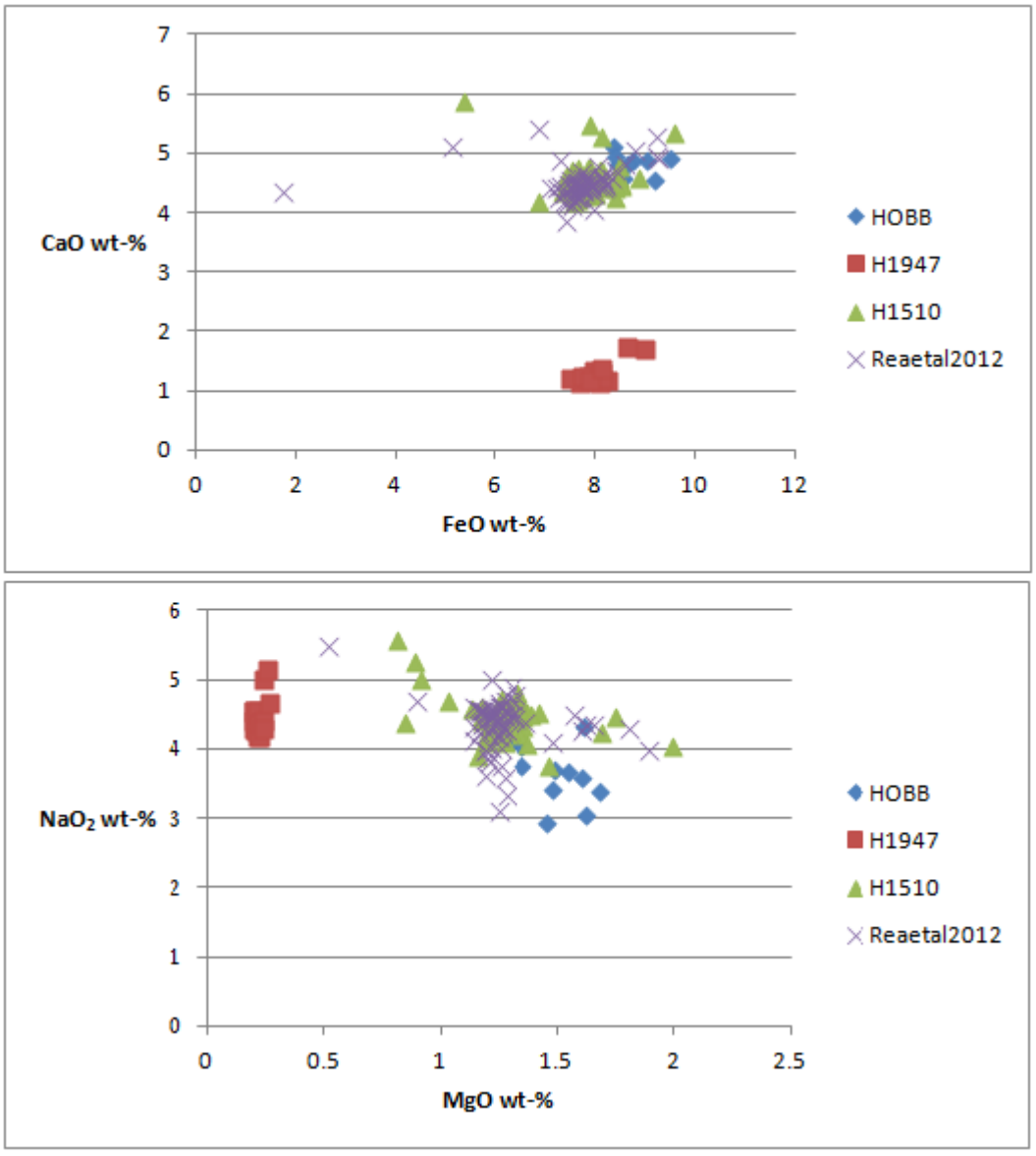


Figure 8.3: Correlation bi-plots for the Hobbister B core depth 0-7.5 cm (combined samples OxT-4765, -4766, and -4767 = HOBB). Hekla 1947 data is from Larsen et al. (1999). Hekla 1510 data is from Dugmore et al. (1995), Pilcher et al. (1996), and Larsen et al. (1999). 'Reaetal2012' comparative data is from the appendix of Rea et al. (2012).

discuss possible reasons why they have arrived at their conclusions and see if their reasons apply to the microtephra from Hobbister B.

Rea et al. give two reasons for unambiguously classifying their microtephra as Hekla 1947: first, the presence of SCPs (spheroidal carbonaceous particles) alongside the microtephra, and second, their depth within the peat profiles studied (between 0 and 18 cm). SCPs are described by Swindles (2010: 1) as, 'a component of fly-ash formed by the incomplete high-temperature combustion of fossil fuels, and are therefore unambiguous indicators of atmospheric deposition from industrial sources including power generation.' There was nothing resembling Swindles' (2010) description of these under the microscope with this sample.

Rea et al.'s argument for the depth of the ash layer within the profile is that it seems unlikely, based on rates of peat formation, that a sixteenth century layer would lie at a maximum 18 cm below the surface (and in many cases, very near the surface). They do not provide a citation for rates of peat formation within their study location, and there is obviously a great deal of difference between peat profiles even within their small study area in Northern Ireland: for example, at Ballynahone, the microtephra layer ranges from 0-6 cm, whereas at Tattenamona, it ranges from 10-18 cm. Similarly, in five peat profiles in Loch Portain, Scotland, Dugmore et al. (1996) found microtephra that they have identified as Hekla 1510 ranging in depth from 11-17 cm (512). Housley et al. (2010) record what they identify as Hekla 1947 at 19 cm and Hekla 1510 at 52 cm in Dunadd, western Scotland. Therefore peat depth varies greatly across the study area and may not be a reliable indicator of tephra identity.

The proximal glass chemistry that Larsen et al. (1999) published for Hekla 1947 is unequivocally different from both Rea et al.'s results and the results from Hobbister. For example, wt-% of the oxides MgO, CaO, and to some extent K_2O are very different. Confusingly, Rea et al. say that they have used Tephrabase (Newton et al. 2007) for their glass chemistry correlations, but provide very little visual evidence that supports their statement that Hekla 1947 and Hekla 1510 are 'geochemically similar'. The same Tephrabase sources have been used here as they were in the bi-plots in Figure 8.2 and Figure 8.3 and these figures clearly show differences in the glass chemistry data from these two eruptions. However, there is always the possibility that the data provided by Larsen et al. may not be diagnostic of the eruption, due to sampling a small fraction of the total compositional range. Housley et al.'s (2010) glass chemistry for layers they identify as Hekla 1947 and Hekla 1510 are virtually indistinguishable from each other.

The Hobbister B samples therefore seem geochemically to correlate to Hekla 1510, but based on depth of profile they seem to be too young, and therefore to correlate to Hekla 1947. Rea et al. state that Hekla 1510 has been detected in much greater concentrations than Hekla 1947 in the British Isles, and that therefore comparative shard counts should also give a good indication of which eruption a layer correlates to. However, their paper does not show evidence that they have identified the Hekla 1510 layer within their profiles, nor do they provide a citation for this statement. Based on this unreliable information, as well as the fact that tephra deposition has been shown to be highly variable across the British Isles (e.g., Dugmore et al. 1995; Chambers et al. 2004), it has not been considered in the interpretation of Hobbister.

Two further steps were taken to try to correlate the Hobbister data to either Hekla 1947 or Hekla 1510. The first was to note where previous examples of tephra from each eruption had been found, and the second was to check weather records for Orkney from 1947 to see if rain had fallen at the time of the 1947 eruption, as rain is known to increase the chance of microtephra deposition across a landscape (Lacasse 2001; Langdon and Barber 2004; Wastegard and Davies 2009). While Hekla 1510 isopach maps produced by Þórarinsson (1967) and Larsen et al. (1999) show the ash cloud moving to the southwest of Hekla, Dugmore et al. (1996) have recorded tephra from this eruption in northern mainland Scotland and Housley et al. (2010) record it in western Scotland. Therefore it is likely to have fallen across Orkney. Similarly, Hekla 1947 is known to have fallen in Finland and western Scotland (Þórarinsson 1967; Housley et al. 2010), so Orkney is a likely candidate for having microtephra from that eruption.

In 1947, Hekla produced tephra from the beginning of the eruption, on 29 March, until roughly June of that year, although only the initial explosion is known to have deposited tephra outside of Iceland (tephra fall was recorded in Finland at the time) (Þórarinsson 1967). Unfortunately, weather records for April-June of 1947 are not available for Orkney, and there are significant differences in data from the two nearest stations. For example, for April 1947, Wick Airport, on the north coast of mainland Scotland, reported 46 mm of precipitation for the month; meanwhile, Lerwick, Shetland, reported 107.8 mm for the same period[3]. Therefore the weather records recorded in 1947 are not a useful source for determining the identity of the Hobbister tephra.

[3](Met Office Wick Airport Data 2012; Met Office Lerwick Data 2012)

On the basis of the above – using the correlation with proximal glass chemistry, and the possibility that Hekla 1947 did not fall on Orkney (since it has not yet been found there) – the peak in Hobbister B is identified as Hekla 1510, with the caveat that it may be Hekla 1947. Whether the tephra is Hekla 1510 or Hekla 1947, it is the first recorded discovery of either tephra from Orkney. The next step is to determine how this tephrochronological date affects the environmental interpretation of the Hobbister core.

Interestingly, whichever Hekla tephra this corresponds to, it is andesitic, and has been found distally, which up until recently was considered to be rare. In Section 3.2, the reasons for silicic microtephra being the most commonly found distal tephra were described. Briefly, these were volcanism, deposition factors, and study bias. Blockley et al. (2003) have also suggested that basaltic tephra will dissolve in some peat bog environments. As recently as 2008, Larsen et al. wrote that only silicic tephras have the travelling power to create widespread distal layers. It remains true today that the most commonly found composition for microtephra by far is silicic, but recently basaltic microtephra from Icelandic eruptions has been found in the Mjáuvøtn lake system in the Faroe Islands and Scotland (Wastegard et al. 2001: 106; Pyne-O'Donndell et al. 2008).

Andesitic tephra commonly has heterogeneous glass composition, in some cases with a range between 2-10 wt% SiO_2 (Shane 2005). In historical times, andesitic volcanism in Iceland has been the result of mixed explosive and effusive eruptions, and these have been confined to Hekla, with the exception of the 1973 eruption of Eldfell (Thordarson and Larsen 2007: 134). These eruptions consist of three phases: a brief (generally less than one hour) Plinian event, a longer transitional phase with some tephra fall as well as fountain lava, and finally a Strombolian phase (Þórarinsson 1976; Larsen et al. 1992). All Hekla eruptions described in historical times follow this pattern. During the course of eruptions, the composition of the products changes from andesitic to basaltic-andesitic or other compositions, meaning that the Plinian phase, when tephra travels the furthest, is often andesitic (Sigmarsson et al. 1992: 21). However, the somewhat heterogeneous glass composition may explain the difficulty in distinguishing between Hekla 1947 and 1510.

8.3 Linking the East Mound to Hobbister B

Using the above tephra dates and the available radiocarbon dates from Table 8.3, I created two deposition models for the Hobbister B core, which are shown together in Figure 8.4. The pollen research from Hobbister B formed part of the PhD research of Dr Michelle Farrell (University of Hull). The tephra date for the section from the top of the core provides a constraint on the radiocarbon dates that Dr Farrell cites in her PhD thesis (Farrell 2009). Both agree well with the deposition rates shown by the radiocarbon dates, but for the rest of the discussion below will assume that this tephra layer is from Hekla 1510 for all the reasons listed above.

Farrell (2009) has studied the pollen for the Hobbister A and B cores, but was only able to reconstruct the Viking and medieval periods from Hobbister B. The chronological research presented here further constrains this data, placing an end date for the top of the Hobbister B core and allowing her phasing to be refined. Farrell finds that the general trend throughout time was continuity, from the Pictish period to the Norse settlement period, and from then until the present day. Heathland dominated the landscape, and there does not seem to have been deliberate burning to manage the woodland. There may have been rough grazing around the area, but there was no arable cultivation. Farrell notes that this was in contrast to Pool on Sanday and Quoygrew on Westray, where Bond (in Hunter et al. 2007a) and Barrett et al. (2005) have found evidence for cultivation. As in Iceland, fuel use in Orkney during this time period is something of a mystery. Hobbister B contains low levels of arboreal pollen (only 5% of the total pollen) (Farrell 2009: 302). Morris et al. (1986) found that, at the Brough of Deerness, only the local population of scrub willow (*Salix*) was exploited for fuel during the Viking period. Therefore the landscape seems to have been quite open, with only small patches of woodland. Donaldson et al. (1981) note that driftwood was an important source of fuel at the Brough of Birsay, but much like in Iceland, gathering resources for fuel must have been a constant concern for Viking settlers on Orkney.

Constraining the chronology of studies like Farrell's (2009) can inform our interpretation the Orcadian environment and how that may have affected life at the settlements there during the Viking and medieval periods. Although some areas, such as Quoygrew and Pool on Sanday seem to have been intensively cultivated, in general the evidence from Hobbister B argues that the landscape seems to have had little woodland or cultivation. There is also little evidence for animals grazing except in

Table 8.3: Radiocarbon dates associated with the Hobbister A and B cores (Michelle Farrell, pers. comm., 2011).

Lab Code	Depth	Site	^{14}C Age	Error ±	Calibrated
SUERC-22858	**61 cm**	**Hobbister A**	**1550**	**30**	**423-574 cal AD**
SUERC-19831	**173 cm**	**Hobbister A**	**3005**	**35**	**1387-1124 cal BC**
SUERC-22859	**253 cm**	**Hobbister A**	**3820**	**30**	**2448-2144 cal BC**
SUERC-19832	**370 cm**	**Hobbister A**	**6205**	**35**	**5293-5053 cal BC**
SUERC-22860	**81 cm**	**Hobbister B**	**1230**	**30**	**689-882 cal AD**
SUERC-19833	**124 cm**	**Hobbister B**	**2205**	**35**	**377-186 cal BC**
SUERC-22864	**167 cm**	**Hobbister B**	**3340**	**30**	**1729-1531 cal BC**
SUERC-19837	**195 cm**	**Hobbister B**	**3920**	**35**	**2547-2293 cal BC**

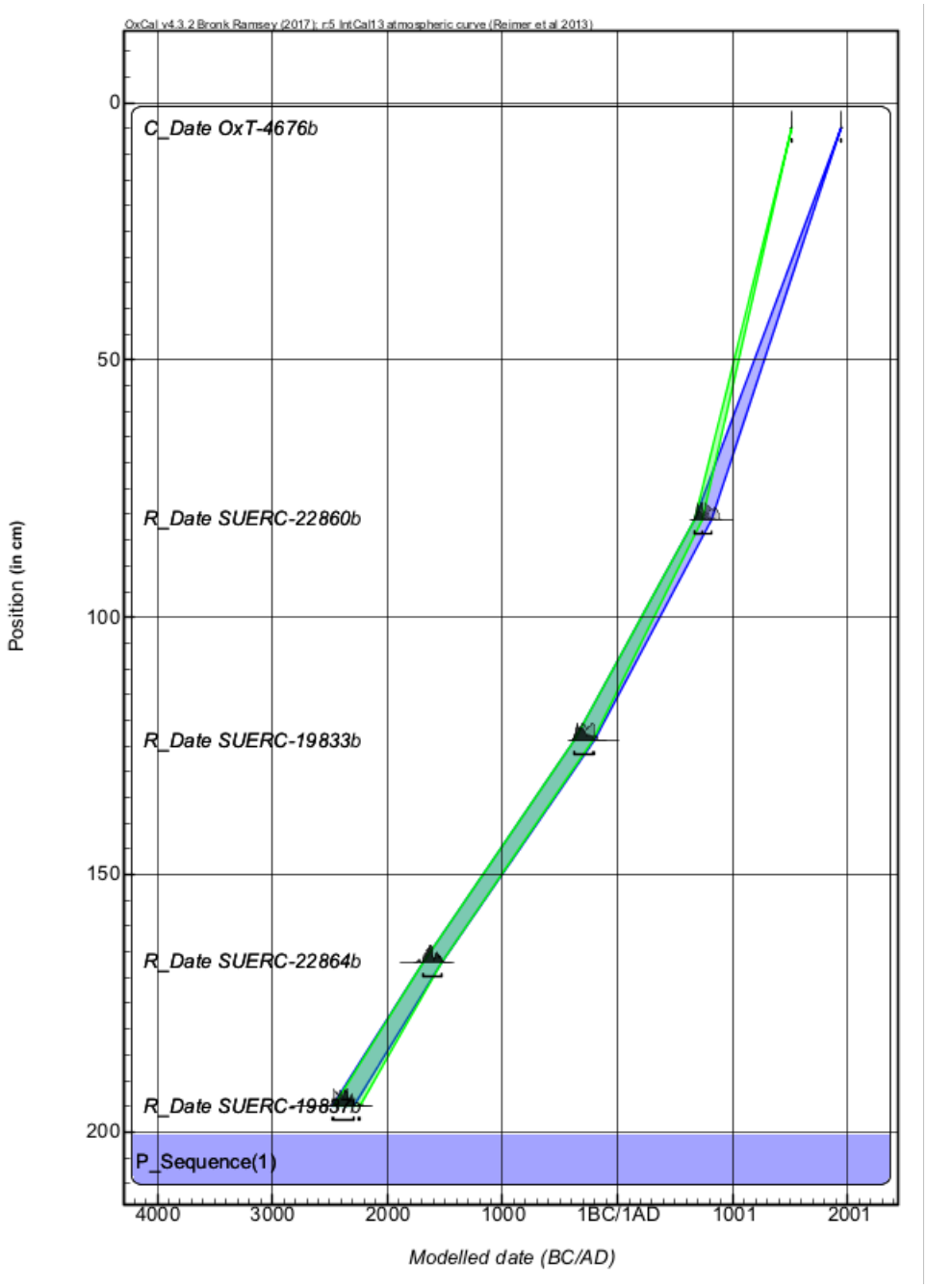


Figure 8.4: Hobbister B deposition model using the P_Sequence from OxCal using Hekla 1510 (green) and Hekla 1947 (blue). The P_Sequence creates a Poisson - process deposition model which allows for fluctuation in deposition rates (Oxcal v.4.3; Bronk Ramsey 2008; Bronk Ramsey 2009)

certain archaeological localities (Simpson 2003). Further pollen studies are needed from Orkney for this period before anything more firmly conclusive can be said.

8.4 Developing a combined archaeological and environmental chronology for the Bay of Skaill

One of the major research questions asked in this thesis is how chronology can be used to understand the relationship between records of environmental and archaeological change. The East Mound radiocarbon record has been made more precise by Bayesian modelling, and, although it could not be directly linked by microtephra layers as was originally hoped, its past environmental conditions have been theorised through the use of the Hobbister study. Now the East Mound and Hobbister will be discussed in the context of Viking and medieval Orkney. In order to bring the world of the Norse settlers at the East Mound into the discussion of the themes outlined in Section 2.4, the archaeology must be connected to preceding, contemporaneous, and later events in the local area.

The Norse archaeology from the Bay of Skaill is only a short phase in a dynamic cultural-environmental landscape. Unlike the settlers at Vatnsfjörður, who entered into a 'pristine' landscape in Vestfirðir, the people who built the longhouse and associated buildings at the East Mound were part of a long tradition of human habitation in Orkney, and more specifically in the Bay of Skaill itself. The nature of the transition between Norse settlers and the people who lived in Orkney before them is not known.[4] Therefore it is currently impossible to speculate about whether cultural knowledge about the landscape was passed between them, or if the Norse settlers had to begin from their base of cultural knowledge about inhabiting mainland Norway or the North Atlantic islands. Radiocarbon dating suggests that the East Mound was inhabited during the late tenth and eleventh centuries, after the initial Viking colonisation of Orkney, implying that the settlers there most likely would have already had some cultural knowledge of the Orcadian environment or at least ones similar.

In order to conceptualise the East Mound within the history of the landscape, it has been compared to other archaeological and environmental studies. The criteria for choosing those studies are discussed in Section 5.5; the key point of importance

[4]Whilst no evidence has yet been uncovered showing the East Mound longhouse superimposed over an earlier archaeological site, it is impossible to rule this out without significantly more excavation.

is that these studies need to have some form of recent chronological research unless they are particularly seminal or interesting. Table F.1 in Appendix F lists the studies chosen for comparison alongside a short description of the dates, methods, and events described. The locations for each of those studies are shown in Figure 8.5, emphasising their proximity to the East Mound and the Bay of Skaill. The results of these studies are conceptualised in time alongside the chronological information from Hobbister, Spretta Meadow, and the East Mound archaeology in Figure 8.6.

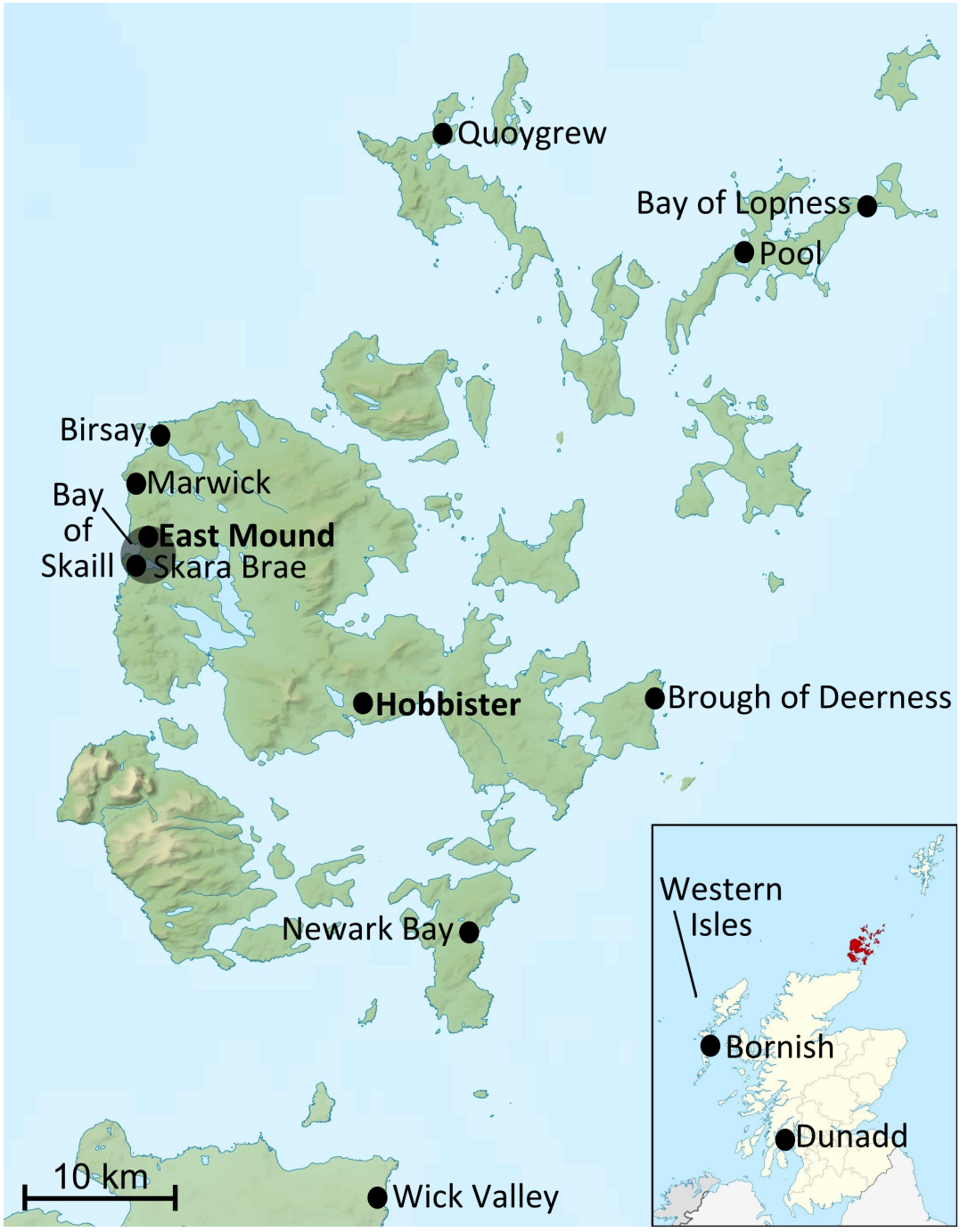


Figure 8.5: Location of all places named in Table F.1, with the shaded area representing the entirety of the Bay of Skaill (which contains Skara Brae and the East Mound).

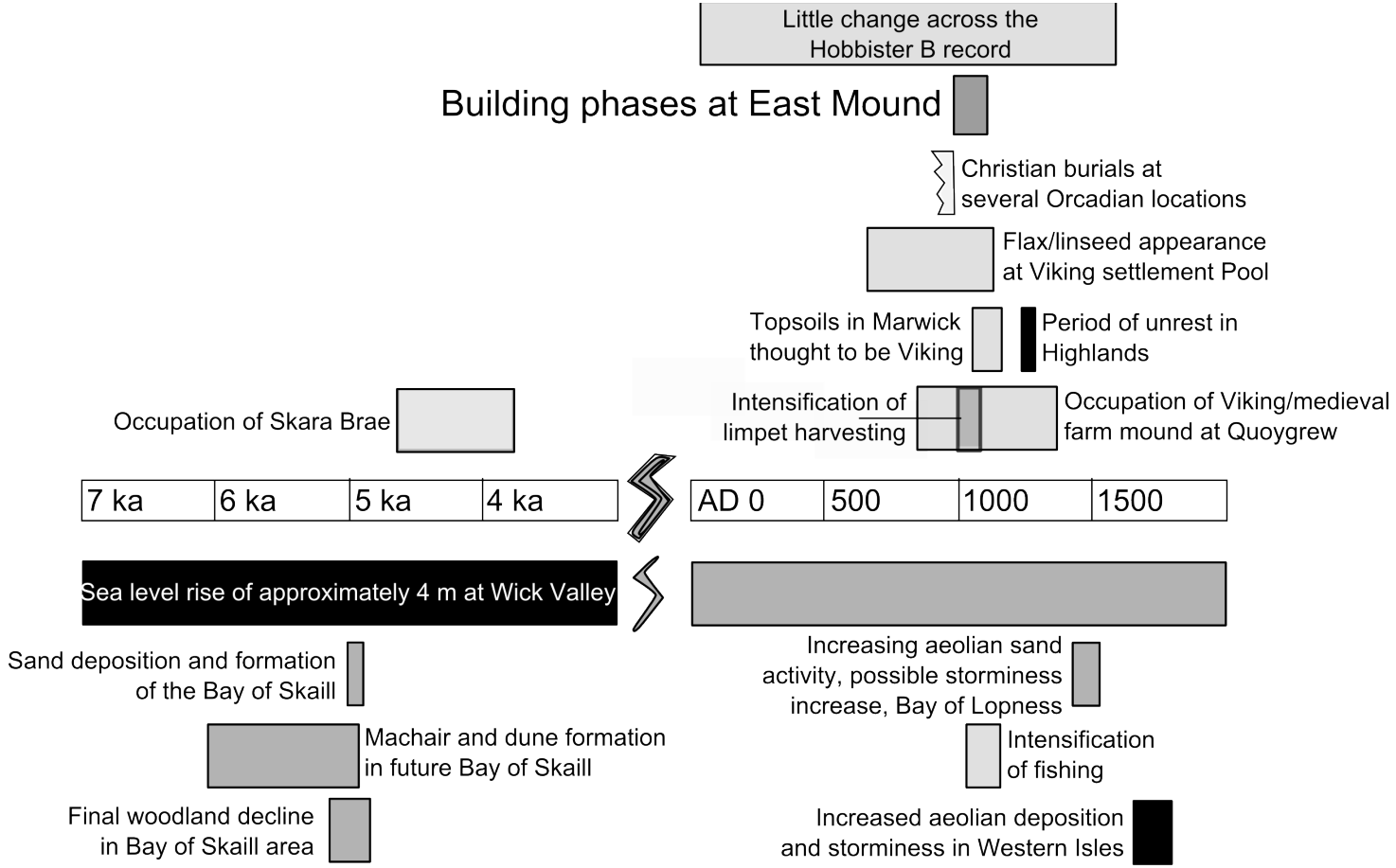


Figure 8.6: Timeline of Orcadian and nearby archaeological and environmental events. Events further afield than Orkney are shaded black. The sources for this information are listed in Appendix 5 and a map showing the locations in relation to the Bay of Skaill is Figure 8.5.

Beyond the non-anthropogenically-altered record at Hobbister B, the most obvious environmental record to compare the research from the East Mound to is the evidence of past plant life and any anthropogenic effects. There has been little published research on this topic since Keatinge and Dickson (1979). Hobbister B provided a detailed record, but there is also some evidence from the East Mound itself. Alldritt (in Griffiths et al. 2009; in Griffiths and Harrison 2011; in Griffiths forthcoming) has studied carbonised plant macrofossils and charcoal from areas across the Bay of Skaill Landscape Project. In Marwick Bay, which is two kilometres north of the Bay of Skaill, two contexts (1018 and 1019) contain a large quantity of charred cereal grain and occasional wood charcoal and burnt peat (Alldritt in Griffiths and Harrison 2011). These contexts have been radiocarbon dated to 776-973 cal AD; they may relate to human activity, but if so, it was from early on in the time of the East Mound's settlement. Throughout the East Mound, Alldritt found cereal grain (including oat and barley), particularly in the western extension of the longhouse; this means that they date from at least the eleventh century. She also found flax, which can be linked to Bond and Hunter's (1987) research that saw the appearance of flax from approximately AD 700 until AD 1200 at the Viking settlement of Pool. Alldritt also finds evidence for a possible homefield near the East Mound based upon charcoal from plant material from wet meadows and standing water environments.

Although there is little specific research about it, the MWP's effects on Orkney are discussed in Section 2.2.1. Climatic models for the Northern Hemisphere models indicate that the East Mound would have been inhabited during the generally warm and mild period of the MWP (IPCC 2007). Based on the radiocarbon dates, it seems likely that the mound was abandoned before the colder and less predictable weather of the LIA. However, a different kind of severe weather could still have had an effect on life there and seems likely to have contributed to its abandonment.

Construction and occupation at the East Mound has been constrained by radiocarbon dating and Bayesian modelling to a relatively short period. Section 4.3.1 discussed how occupation at the East Mound was capped by repeated incidents of windblown sand deposition. Some of the OSL dates, notably SG06-22, indicate that these sand deposition incidents could have occurred during the LIA, however, other sand deposition events occurred much earlier. One example relates to the construction of the longhouse. Context 2095, which has been radiocarbon dated (SUERC-24703), is part of Area 2. It is an occupation layer that is younger than the main floor of Area 2 and is immediately above a large quantity of sand, indicating that a storm

covered a large part of Area 2 in sand sometime after the initial construction of the area but while the settlement was still occupied. Context 2095 did not fit within the main model, but calibrated alone it dates to 894-1024 cal AD. It seems likely that there were storms moving large enough quantities of sand to leave their mark upon the settlement during the supposedly calmer years of the MWP. Even though fishing seems to have been a major source of food at the East Mound, sand storms would still have impacted the oats, barley, and flax grown there as well as the livelihood of their animals. There is evidence that they used organic admixtures and stones to stabilise soil layers in the face of large sand deposits (Griffiths forthcoming).

After the period of settlement, storms continued to lay down sand layers across this landscape. As far as current environmental research indicates, around ca. 1500 there seems to have been an increase in aeolian deposition (and therefore an increase in storminess) that is associated with the LIA throughout northwest Europe (Gilbertson et al. 1999; Wilson et al. 2004; Somerville et al. 2007). On coasts throughout the Highlands and Islands, this period may have been marked by long-lasting snowfields that prevented vegetation from growing and exposed the sandy soils underneath. Wind erosion then led to further incidences of aeolian deposition of large quantities of sand (Lamb 1977; Mitchell 1999; Morocco et al. 2007). This may mean that the storms that have left their mark upon the landscape from the LIA (e.g., Somerville et al. 2007) were even fiercer than those that left the sand behind in contexts 2095 and 2047; however, it may also mean a need for further research into levels of storminess throughout the MWP and LIA periods.

Likewise, further OSL dates may illuminate when these sand deposition incidents – likely the results of large storms, like those described in the Bay of Lopness (Somerville et al. 2007) – occurred. If they were common before the LIA, they may have contributed to the abandonment of the East Mound. The placement of context 2047 immediately over a rough flagstone floor/hearth area may suggest that this area of the longhouse was abandoned as the result of sand from a storm making an incursion into living space.

The landscape history was shaped by other events that have not left as obvious a mark on the the archaeological site. Some of the significant events in the landscape history of the Bay of Skaill occurred thousands of years before the construction of the East Mound long house. Those are shown in the left side of the timeline in Figure 8.6. The formation of the Bay itself occurs around the same time as the final woodland decline in the Skaill area (Keatinge and Dickson 1979; de la Vega Leinert et al. 2000). The

occupation of Skara Brae, which according to current radiocarbon research spanned roughly 1000 years, ended 3.8 ka before present (Ashmore 1998; Leinert 2000).

Sea level change was ongoing throughout the period. Although there has been no local research on sea level rise in the Bay of Skaill for the relevant time period, de la Vega Leinert et al. (2000) suggest that the research done by Dawson and Smith (1997) on sea level rise over the last 7 ka. in the Wick Valley, in the Highlands is analogous. Dawson and Smith find that, due to isostatic rebound, sea level has risen approximately 4 m over that time period, with some marine transgressions.[5]

Archaeologically, the occupation of the East Mound took place during a period that has become one of the most debated and discussed in Viking archaeology: the intensification of cod fishing (Barrett et al. 1997; Barrett 2000; Barrett et al. 2000b; Barrett et al. 2001). The farm at the East Mound was partly contemporaneous with several similar settlements in Orkney that have shown evidence of the intensification of fishing, and in particular cod fishing. At Quoygrew, for example, Milner et al. (2007) found that there was a measurable impact in the local limpet population caused by an increasing pressure on producing bait for fishing; this dated to the 11th and 12th centuries. At the East Mound, Ingrid Mainland (in Griffiths and Harrison 2011) has found that the large quantities of marine molluscs found at the site were dominated by the common periwinkle and the limpet; there seems to be no change in limpet quantities throughout the lifetime of the settlement, suggesting that the intensification of fishing did not have as marked an impact on the East Mound's economy as compared to Quoygrew. There were two large deposits of periwinkle in contexts 2225 and 2275 (which are found at comparable sites such as Beachview, Birsay (Morris 1996)); these are part of the western extension, so this may reflect different patterns of mollusc usage later on in the life of the settlement.

8.5 Summary

The conclusions from this chapter are twofold: archaeological and tephrochronological.

[5]One marine transgression occurred ca. 1200 BP, which calibrated is close to the occupation of the East Mound, but based on comparisons with nearby locations this event does not seem indicative of wider landscape trends (Dawson and Smith 1997: 76), and so will not be considered in the interpretation of the Bay of Skaill landscape history.

Archaeologically and environmentally, the East Mound fits into the general patterns of settlement already established for coastal North Atlantic settlements of the period. Its relationship to the coast and in particular to the large storms that deposit sand makes it most comparable to other coastal sandy sites like Broo, in Shetland (Bigelow 2005). These storms may have led to the abandonment of the longhouse; they may also have deterred anyone else from settling permanently in the same area. Radiocarbon and OSL dates from the East Mound have made its occupation period more precise, and Bayesian modelling of these dates suggests a very short time period for occupation. The longhouse was large by Orcadian standards, suggesting a high-status settlement, but the lack of continuation may suggest that something about the location made it ultimately unfavourable to the farming lifestyle of the Viking/medieval settlers. Based on the current evidence, the occurence of violent storms that shifted large quantities of sand may have contributed to its quick abandonment.

Chronologically, the use of Bayesian modelling of radiocarbon and OSL dates allowed the phases of the excavation to be much better understood. The lack of a truly local environmental record as well as the lack of either stratigraphic links to radiocarbon dates in any environmental record or tephra isochrons to connect them means that the archaeological and environmental record at the East Mound cannot be directly connected to outside sources. Although analysis has been possible in comparing the archaeological remains to well-dated environmental records, the chronological resolution is lacking still.

Based on the findings presented here, this thesis argues that sediments in Orkney should be further studied for microtephra deposits, including those from the past 2000 years BP. Although in some cases it may be impossible to correlate a microtephra layer due to small sample size, varied geochemistry, or poor preservation of shards (e.g., Bunting 1994 or several of the layers found here), there is also a great opportunity for future researchers to identify high resolution isochrons.

Distal microtephra studies of the Hobbister A and B and Spretta Meadow cores revealed several tephra layers and successfully identified one, which is a similar level of success to many current distal microtephra studies, including those from the British Isles (e.g., Balascio et al. 2010; Housley et al. 2010). As our understanding of microtephra deposition increases, as in studies like this one and others by Payne et al. (2005), Payne and Gehrels (2010), and Swindles et al. (2013), then hopefully our ability to successfully locate and extract for successful WDS-EPMA will increase.

It was the large suite of radiocarbon dates from the East Mound that allowed regional environmental records to be linked to the archaeology there. The tephra study here did identify a recent tephra layer in Orkney, something which had not previously been done. Several important points arose from studying the microtephra of these cores:

- Issues with the literature used to classify microtephra, as discussed in Section 8.2.1.1.
- Large possible ranges of deposition depths within peat: Correlation of microtephra layers is made more difficult by the large range of deposition depths that microtephra from one eruptive event can have across several peat profiles. The findings presented here as well as those listed as examples (Dugmore et al. 1996 and Rea et al. 2012) show that single eruptive events can span very different ranges, both in terms of depth and in terms of size (i.e., ranging from 1 cm to 10 cm within a profile). More studies are needed from distal locations that compare multiple profiles.
- There are potential large differences between proximal and distal glass chemistry. This could be caused by separation of different fractions in the ash cloud, but has implications for distal microtephra studies based on proximal data.

9 | The Chronology of the North Atlantic ca. AD 900-1800

In Chapters 7 and 8, I chronologically examined relatively contained archaeological landscapes. In this chapter, I gather published excavations and environmental studies and create regional chronological studies using Bayesian modelling throughout the Norse North Atlantic. First, I review current chronological information – specifically radiocarbon, OSL, and tephra – from Norse colonisation through the LIA. Then I create a series of models using OxCal to examine social trends and settlement change, and to evaluate how well the results from current chronological data and methods create a coherent archaeological record, with a focus on comparing change throughout the region.

9.1 Modelling dates from the North Atlantic islands

Constructing Bayesian models allows researchers to combine chronological information and create more accurate and precise timelines for individual sites, groups of sites, or regions, providing the original dates can be linked, as discussed in Section 3.6.1. Individual dates from the studies discussed in this chapter are described in the Excel table, included with the thesis on a CD-ROM. The majority of AMS radiocarbon dates used come from Aarhus (lab code: AAR) and the Scottish Universities Environmental Research Centre (SUERC/previously GU and SSR). Others are from Oxford (OxA), Toronto (TO), Radiocarbon Dating England (RCD) (later Harwell), NSF-Arizona AMS Facility (AA), Denmark National Museum (K), Poznan Radiocarbon Laboratory, Poland (POZ), Beta-Analytics (Beta), and the Center for Accelerator Mass Spectrometry, California (CAMS).

Most of the columns in the included Excel table are self-explanatory. Aside from Toftanes in the Faroe Islands, all of the radiocarbon dates have δ^{13}C values. The

'Percent Marine Diet' is discussed below, and contains the values I generated for each date that needed this field (rather than values provided by the study authors). 'Position (context)' is taken directly from site reports and so data such as, for example, context 15 for SUERC-5119 (Reykholt, Iceland) can be referenced directly in the report in Sveinbjarnardóttir et al. (2006). This information has been given to establish stratigraphic position. The column 'Relevance' is my description of why this study or individual date has been included in this research; if the date is archaeological, then it is implied that the context is Norse unless otherwise stated. Finally, 'Expected Age' gives information on what phase, if any, the authors of each study have assigned to the individual date. For example, Golding et al. (2010) believe that SUERC-21992 from Sandhavn, Greenland, is a date on material from the later part of the Norse period. Although I recognise that there are many distinctions to be made about what constitutes Early, Middle, and Late Norse (amongst other time period designations), the authors of the original studies' own terminology has been used in the database to make it a more accurate and user-friendly reference.

9.1.1 Orkney

Combined with the Bay of Skaill radiocarbon dates discussed in Chapter 8, Orkney has a relatively diverse group of dates available for study. Large numbers of radiocarbon dates come from Quoygrew (Simpson et al. 2005; Barrett et al. 2012), St Thomas's Kirk (Toolis 2008), and Newark Bay (Barrett et al. 2000; Barrett and Richards 2004). These are supplemented by two radiocarbon dates from Netherskaill, Marwick (Simpson 1997), three radiocarbon dates from boat burials at Scar (Owen and Dalland 1999; Barrett and Richards 2004), and OSL dates on sand deposits from Tofts Ness, Sanday, and the Bay of Lopness (Sommerville et al. 2007). The locations of these sites are shown in Figure 9.1.

9.1.2 Shetland

Although many important excavations from the Norse period have taken place in Shetland, such as at Jarlshof, Underhoull, The Biggins, and Sandwick South, there has been little scientific chronology building there (Ashford in Owen and Lowe 1999; Hansen 2000). Hansen places the Scandinavian period in Shetland from the earliest Norse raids of approximately AD 800 to 1469, when the Danish king gave the islands to the Scottish king. Norse cultural influence lasted until sometime beyond



Figure 9.1: Location of dated sites from Orkney (map source: ESRI).

1469 (and some say that it continues to this day). However, Hansen notes that the majority of major excavations in Shetland took place before AMS dating had been invented. There have thus far been no tephra finds relating to the Norse period from archaeological sites in Shetland[1]. Instead, saga evidence, diagnostic artefacts, and architectural styles have determined the archaeological chronologies for many Norse sites in Shetland.

There are six exceptions. The first is a preliminary study with very limited chronological information from Bigelow et al. (2005), which investigates how environmental change has affected settlement from the Norse period onwards at the coastal site of Broo. The second is Sandwick, Unst, which is a multi-period site that includes the foundation of a presumed Norse longhouse (Unst, Sandwick, Royal Commission on the Ancient and Historical Monuments of Scotland 2013), which has six radiocarbon dates associated with Norse or later material.[2] The third is the relatively large group of radiocarbon dates from Old Scatness, another multi-period site known mainly for its Pictish/Iron Age broch and village that also has a Norse period of occupation (Outram and Batt 2010). Kebister, north of Lerwick, has been excavated and published (Owen and Lowe 1999) with a radiocarbon dating scheme, but, as Ashford (in Owen and Lowe 1999) states, it is unclear what kind of Norse settlement, if any, there was at the site. He places it at ca. AD 1100 to 1400 based on the exploitation of steatite resources; there is also a grave that he says may be associated with Norse settlement there which has two radiocarbon dates that have been included here. Most recently, a monograph on Unst (Turner et al. 2013) documents an archaeologically-influenced palynological sequence at Belmont and a small number of archaeological radiocarbon dates from Norwick; these dates also reveal an early Norse presence in Shetland, but unfortunately their number is limited because of mechanical disturbance to the site (in volume: 229). The locations of these sites are shown in Figure 9.2.

9.1.3 Western Isles

There has been little scientific dating of archaeological sites in the Western Isles (Sharples and Pearson 1999). The major exception to this is the site of South Uist, Bornais, a multi-period large farm with an extensive radiocarbon dating programme

[1]There are several from much earlier non-Norse periods, however, e.g. Dugmore and Newton (in Owen and Lowe 1999) and Swindles et al. (2013).

[2]Sandwick, Unst has other AMS radiocarbon dates, but all of these are from the pre-Norse period (Edwards et al. in volume: 75-90).



Figure 9.2: Location of dated sites from Shetland (map source: ESRI).

from the Norse period(South Uist, Bornais, Royal Commission on the Ancient and Historical Monuments of Scotland 2013). The locations of this site and of the burial site at Cnip (Barrett and Richards 2004) which has two Norse-period radiocarbon dates, are shown in Figure 9.3.

9.1.4 The Faroe Islands

The majority of scientifically dated studies from the Faroe Islands focus on the Norse *landnám* period. The two with the most comprehensive dating schemes are Undir Junkarinsfløtti (Church et al. 2005) and Toftanes (Vickers et al. 2005; Edwards and Schofield in Stummann Hansen 2013). Radiocarbon dates also come from Á Sondum by Church et al. (2013); from Við Kirkjugarð, a possible pre-Norse settlement (Arge 2014); from Argisbrekka (Mahler 2007); and Sandur (Arge 2001; Arge et al. 2005).

Olsen et al. (2010) have a scientifically-dated environmental study from three lakes in the Faroe Islands whose results they have attempted to link to the archaeological record for Norse or earlier *landnám*. The results of that study are included with the archaeological dates here. Limited numbers of radiocarbon dates from environmental studies are available from Storavatn, Mjauvotn, Argisbrekka, and Brunavatn (Mahler 2007; Olsen et al. 2010; Church et al. 2013). Olsen et al. (2010) also include a single tephra date in their study, for Hekla 1104, which has been included here. Figure 9.4 shows the location of of each archaeological and environmental site listed above.

9.1.5 Iceland

Radiocarbon dating has not traditionally made many inroads into archaeological research in Iceland. Initially, this was because researchers associated archaeological findings with stories from the Sagas and other written records, often to the exclusion of findings that were not described by literary sources (Friðriksson 1994). More recently, concerns over both marine and freshwater reservoir effects, documented extensively by Ascough et al. (2006; 2007; 2011; 2012; 2014), have kept radiocarbon dating in Iceland to a minimum. Increasingly, tephrochronology is being used in Iceland to date archaeological sites (e.g., Vésteinsson and McGovern 2012), and is sometimes seen as a viable alternative to radiocarbon dating, although its use to accurately and precisely date widescale settlement at this stage has also been questioned



Figure 9.3: Location of dated sites from the Western Isles (map source: ESRI).

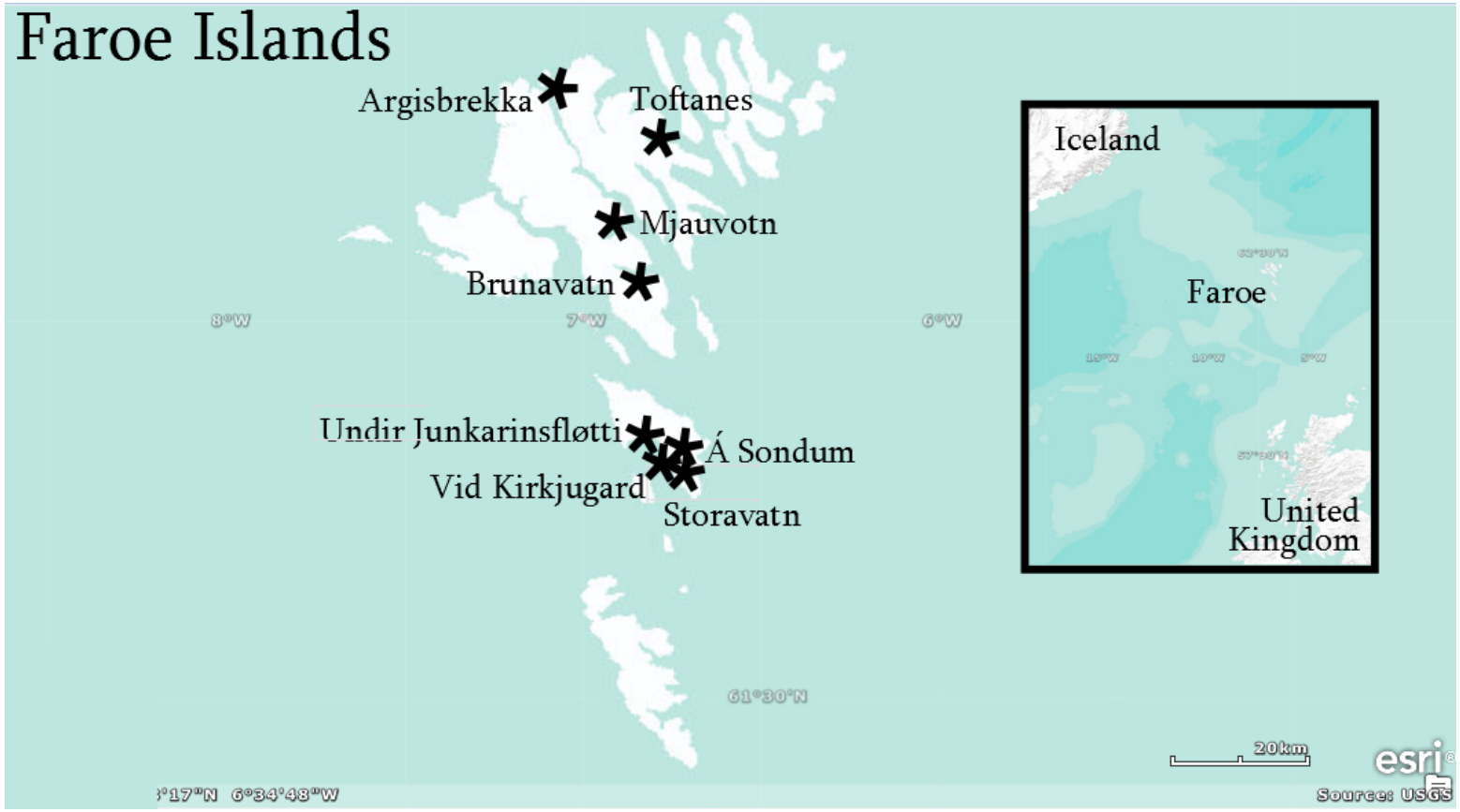


Figure 9.4: Location of dated sites from the Faroe Islands (map source: ESRI).

(e.g. Barrett 2012; Edwards 2012). The only current major study done with radiocarbon dates in Iceland is Sveinbjörnsdóttir et al. (2010), which dated 83 skeletons (79 humans, 2 horses, and 2 dogs). Almost all of the human remains had reservoir effects, which will be discussed further below. The location of the dates from Iceland used in this study are shown in Figure 9.5.

9.1.6 Greenland

Greenland has by far the largest and most diverse data set in this study, with 204 total dates, 152 from the larger Eastern Settlement, 38 from the smaller Western Settlement, and 14 from the less-studied and also small Middle Settlement. Figure 9.6, Figure 9.7, and Figure 9.8 show the locations of the sample sites.

These dates are from different strands of research interests. Archaeological study of the Norse colonisation of Greenland has focused in recent decades on the links between the settlements, their ultimate abandonment, and possible environmental change. Adderley and Simpson (2006), Edwards et al. (2008), and Schofield et al. (2008) have all published radiocarbon-based studies combining archaeological and environmental evidence. Pollen-based studies, using radiocarbon dates and other dating methods to create sequential chronologies for local pollen assemblage zones (LPAZ) like the one I created for Sveinhúsavatn at Vatnsfjörður in Chapter 7, are common from the Eastern Settlement (e.g., Edwards et al. 2013; Ledger et al. 2014a). Another large group of dates in the database comes from Arneborg et al.'s (1999; 2012; 2012b) multi-site studies of diet in Norse Greenland. The marine reservoir effect is a major consideration for radiocarbon dates on bone here, as is discussed below.

9.1.7 North America (Vinland)

For the sake of completeness, I will mention the radiocarbon dates from excavations at L'Anse aux Meadows in Newfoundland, Canada (Wallace 1982; 1988; 1990; 2003; Davis et al. 1988). The Norse remains at L'Anse aux Meadows are the first (and currently the only) clear evidence for a Norse presence in North America. In total, there are 148 radiocarbon dates from these excavations, of which Wallace identifies 50 as pertaining to the Norse period (2003: 11). Unfortunately, these radiocarbon dates, as Wallace (ibid.) acknowledges, have many problems including, most notably for this work, wide error ranges (ca. 400 years). There are few diagnostic artefacts

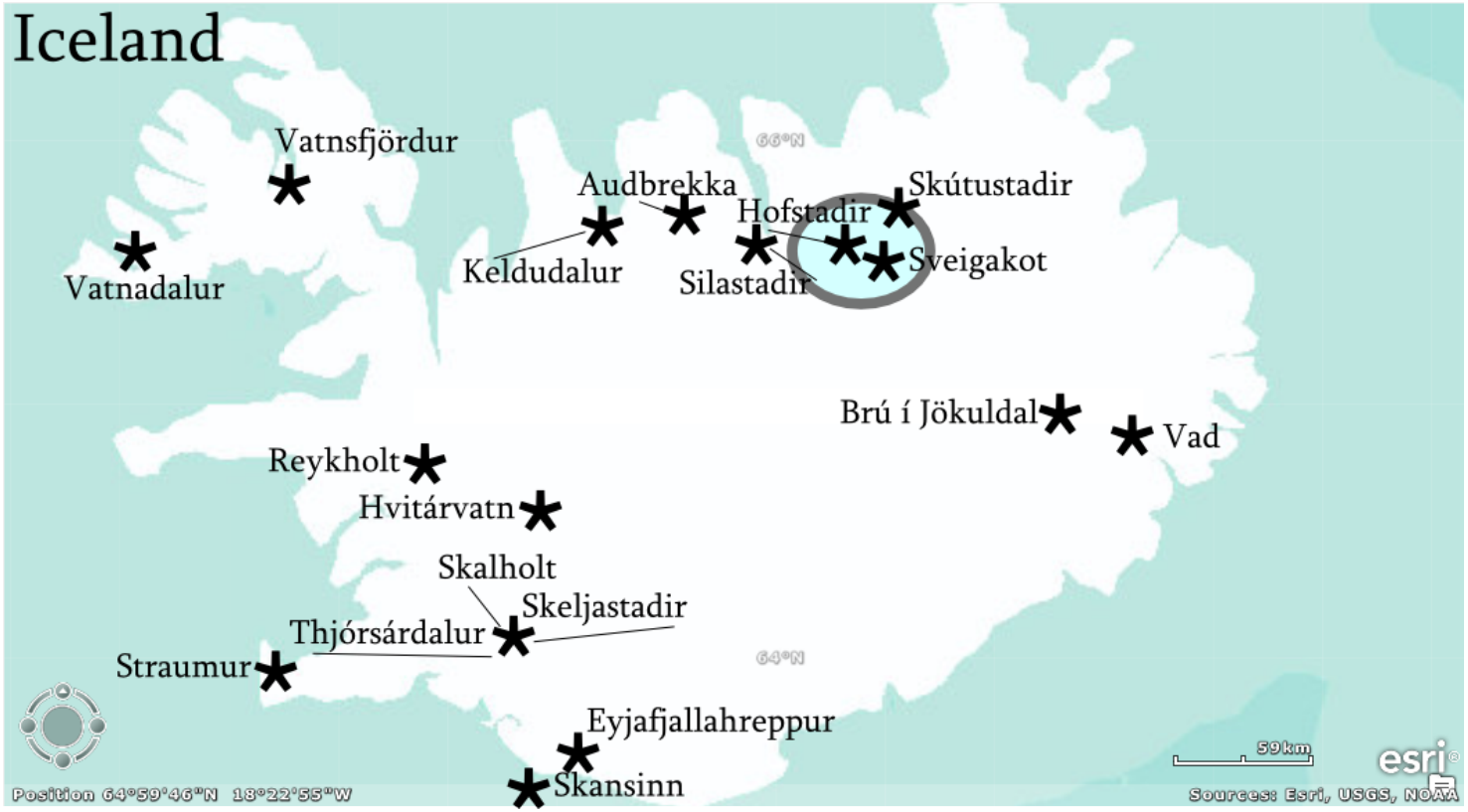


Figure 9.5: Locations of dated sites from Iceland. Shaded area contains all sites from Vésteinsson and McGovern (2012)(map source: ESRI).

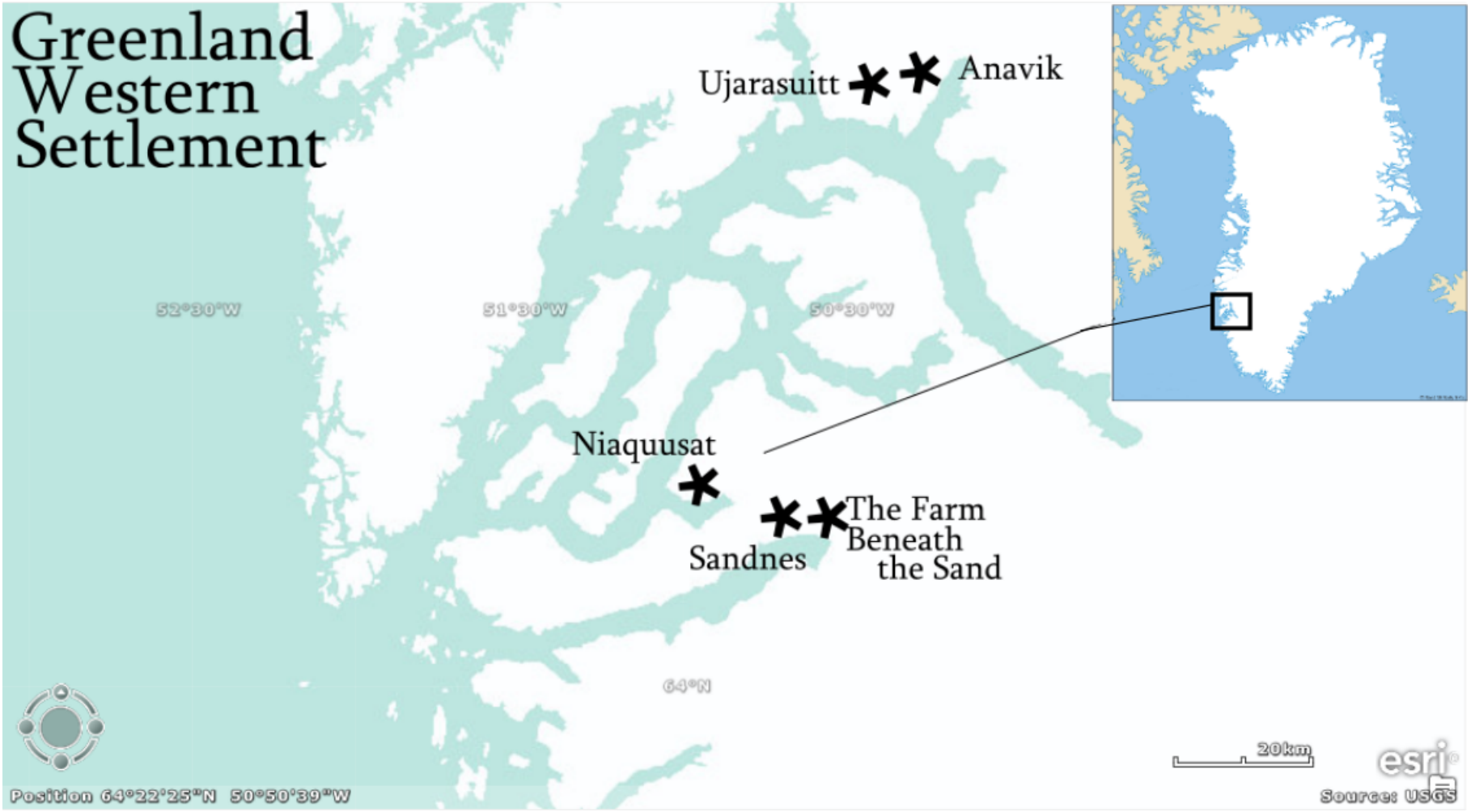


Figure 9.6: Location of radiocarbon dates from Greenland's Western Settlement (map source: ESRI).

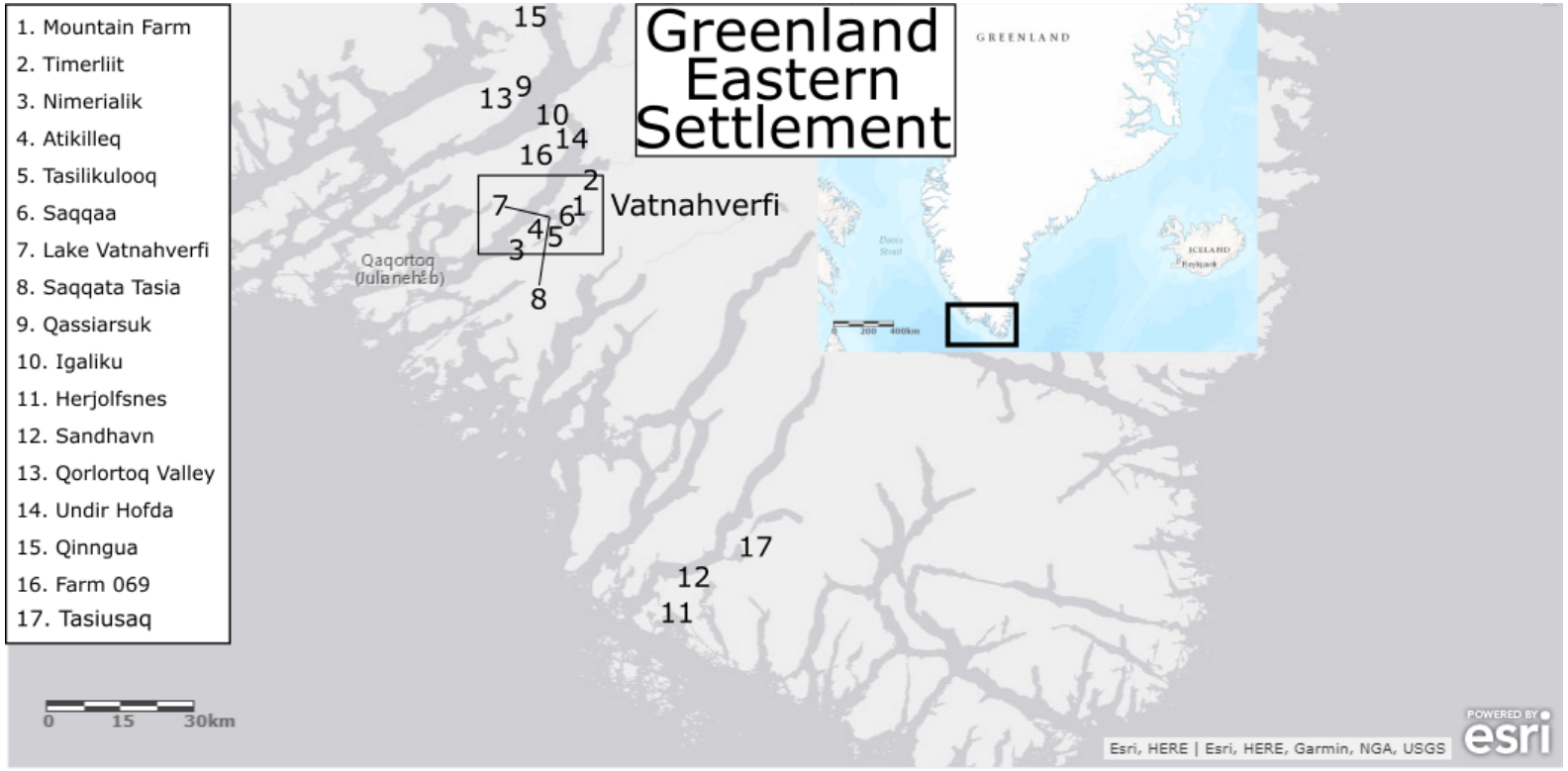


Figure 9.7: Location of radiocarbon dates from Greenland's Eastern Settlement (map source: ESRI).



Figure 9.8: Location of radiocarbon dates from Greenland's Middle Settlement (map source: ESRI).

from the Norse phase of the excavations, but the architecture is Icelandic, which Wallace dates by form to the tenth through thirteenth centuries (2003: 10). Until further radiocarbon dating can be done on this material, the Norse period at L'anse aux Meadows will remain without a refined chronological range. These radiocarbon dates are not considered here or included in the database.

9.2 Modelling Regional Change in Shetland, the Western Isles, and the Faroe Islands

Bayliss et al. (2007) quote Box (1979) in their passionate plea for statistical modelling of archaeological chronologies: 'All models are wrong; some models are useful.' They connect the creation of models to the seminal works of Shanks and Tilley (1987) and Ingold (e.g., 1993), positioning models as another useful method to think about archaeological time. Having identified the chronological data currently available, I will now use that information to model calendar dates for archeological phases from Shetland, the Western Isles, and the Faroe Islands, and to explore some major questions in Norse archaeology: the nature of religious conversion from paganism to Christianity in Orkney and Iceland, the settlement and abandonment of Norse Greenland, and the timing of *landnám* in different regions.

9.2.1 Correcting for the Marine Reservoir Effect

Many of the radiocarbon dates on bone analysed in this chapter exhibit the marine reservoir effect. The MRE has been brought up elsewhere in this thesis but has not played a major role in the results thus far; in this chapter, I deal specifically with radiocarbon dates on bone that have evidence for the marine reservoir effect.

When an invididual's diet is not 100% terrestrial, calibrated radiocarbon dates on their bones must combine the terrestrial and marine calibration curves based on the percentage of terrestrial sources in their diet. This is because organic material from the ocean is generally several hundred radiocarbon years older than their terrestrial counterparts (Stuiver and Polach 1977). Therefore, dates on matter with a marine diet (or that are marine life themselves) are calibrated using the Marine13 curve and a localized offset from the global average marine reservoir effect, ΔR. This is because ocean circulation patterns influence ΔR, meaning region-specific values are needed. Currently, known values by geographic region can be found in a database through the

Queen's University Belfast (Reimer and Reimer 2001; values in this thesis accessed in 2016-2017).[3] An average is taken of nearby values to yield the ΔR value and its error range for a given geographic area. This is standard practice, used in many of the papers I cite here (e.g. Barrett in Barrett ed. 2012). Cook et al. (2015) discuss best practice for the calibration of dates on organic matter that has been affected by the reservoir effect, including recommending a ±10% error range on the percentage marine diet component, as has been done here.

The percentage of marine sources in diet are based on δ^{13}C values from bone, which are long-term averages of dietary protein. Depending on the type of bone, these averages can range from five years to a lifetime of dietary history (Ambrose and Norr 1993). The percentage can vary with region, as is discussed more below in relation to Iceland and Greenland, but generally, δ^{13}C = -21 ± 1‰ is considered a 100% terrestrially-sourced diet, while -13 ± 1‰ is considered to be 100% marine (Barrett and Richards 2001). I wrote a Python script to generate the percent marine diet using linear interpolation between the two end points for each radiocarbon date that requires it in the database. The results are included in the table under 'Percent Marine Diet', and the Python script is in Appendix G. Cook et al. (2015) discuss best practice for the calibration of dates on organic matter that has been affected by the reservoir effect, including recommending a ±10% error range on the percentage marine diet component, as has been done here.

9.2.2 Calibration Curve

The radiocarbon calibration curve presents some difficulty for the period of Norse colonisation and settlement. As is discussed generally in Chapter 3, the radiocarbon calibration curve has a series of plateaux from ca. 800 to 1000 cal BP and ca. 1100 to 1200 cal BP, which impact the precision of calibrated dates from this period. Briefly, plateaux in the curve can be a result of rapid changes to radiocarbon concentration in atmospheric carbon (McCormac et al. 2004), which for this area is based on the Irish oak dendrochronology record (Turney et al. 2005; 2006). As a result, and as is obvious from some of the diagrams below, even dates with narrow (approximately ±35) error ranges may lack precision when translated to calendar dates because of their placement on the calibration curve. When this has been a significant issue with a model, it is discussed further.

[3]The Greenland and Iceland sections below discuss this further.

9.2.3 Modelled Calendar Ages for Relative Phases

One use of Bayesian modelling is to understand the chronology of current archaeological interpretations. Excavators using stratigraphy, typologies, or other dating methods often divide their sites into relative chronologies. In the Norse North Atlantic, archaeologists in some areas have divided their sites into phases within the broader Norse period. Below, I use models to suggest calendar dates for these relative chronologies for Shetland, the Western Isles, and the Faroe Islands, specifically focusing on the sites of Old Scatness and Bornais.

9.2.3.1 Shetland

Archaeologists have provided phasing information for several excavated and dates sites in Shetland. Sandwick can be broken down into two phases: the Norse period of occupation at the site, and the end of the occupation period for the house which the excavators have described as architecturally Norse (Unst, Sandwick, Royal Commission on the Ancient and Historical Monuments of Scotland 2013)[4]. Old Scatness has more phasing information, including radiocarbon dates that the excavators are able to attribute to the Early Norse phase and the Late Norse Phase (Outram and Batt 2010), which is reflected in the model; a significant number of the dates from this site can only be phased to a combined Iron Age and Norse period archaeologically, but they seem to run to earlier (the Iron Age) in terms of modelled and calibrated radiocarbon dates. Kebister and Norwick have relatively straightforward archaeological phasing information and both are in the Norse category, with the house excavated at Norwick going into the 'Early Norse' period.

A model combining all of this phasing information, and assuming that the periods described are contiguous (i.e., that there is a boundary between dates categorised as 'Early Norse' and 'Late Norse'), is presented in Figure 9.9. Table 9.1 summarises the results of this model.

Three dates were eliminated due to having unknown phasing. A further two, GU-11864 and -11098, dates on charred barley from Old Scatness, are much older than

[4]Although there were two dates on human bone, GU-1291 and -1291b, from Sandwick, neither had $\delta^{13}C$ indicating the need to take the MRE into account (possibly because they were pre-Norse, so did not have diets that utilized marine resources, as Barrett and Richards (2004) suggest for ore-Norse Orkney); ultimately, neither were included in the model because they had unknown archaeological phasing.

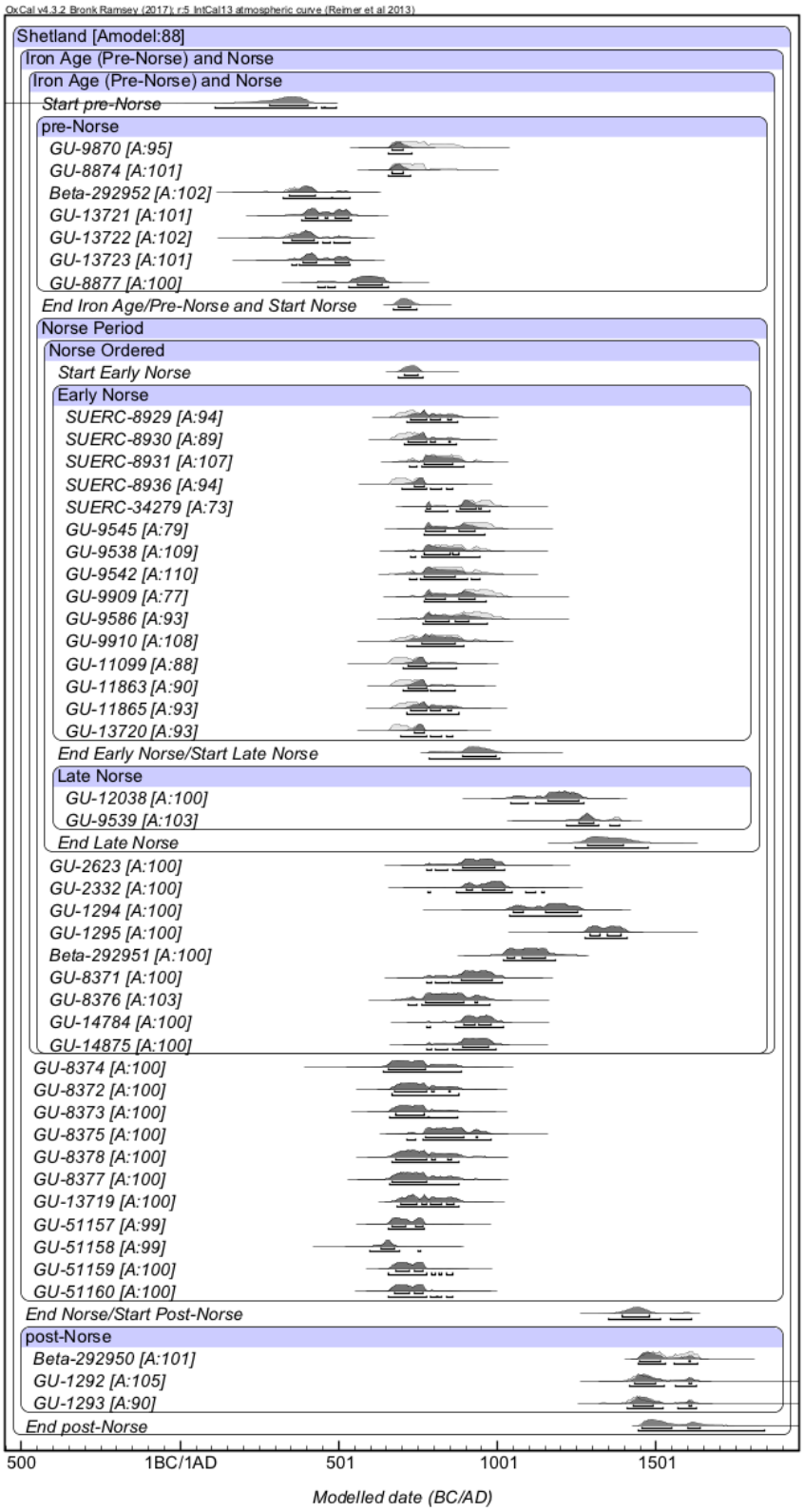


Figure 9.9: Model of dates from Shetland (Bronk Ramsey 2009; Reimer et al. 2013; OxCal v.4.3). N = 47, A = 88.

Table 9.1: Summary of boundaries from Shetland model presented in Figure 9.9.

Boundary	Start 68%	Start 95%	End 68%	End 95%
Start Pre-Norse/Iron Age	288	110	402	494
End pre-Norse/IA and Start Norse	688	674	728	748
Start Early Norse	707	686	750	764
End E. Norse/Start L. Norse	890	784	995	1010
End Late Norse	1285	1245	1397	1476
End Norse/Start Post-Norse	1395	1351	1480	1614
End Post-Norse	1456	1445	1641	1843

any other dates in their context and probably do not represent the Pictish/Viking interface that their excavators (Outram and Batt 2010) believed that they did; both are from Structure 11 and they may be intrusive. They also had to be eliminated in order for the model to run. After an initial run of the model, I also eliminated GU-8876 (another charred barley date from Old Scatness, *ibid.*) because it had an individual A value of 36.3 and appeared too young for its phasing; the authors had put a question mark on its position within the context, so it seems safe to assume this is an intrusive sample. Eliminated dates are shown in Table 9.2.

Table 9.2: Dates eliminated from the model presented in Figure 9.9.

Date	Location	Indiv. A value?	Reason for Elim.
GU-1291a	Sandwick, Unst		unknown phasing
GU-1291b	Sandwick, Unst		unknown phasing
GU-8370	Old Scatness		unknown phasing
GU-11864	Old Scatness		too old for phasing
GU-11098	Old Scatness		too old for phasing
GU-8876	Old Scatness	36.3	too young; position question

Hansen (2000) placed the start of the Shetland Norse period around ca. 800; here, it models to earlier, 678 to 756 modelled cal AD. Norse colonists may have arrived before the written records of Norse 'raids' began. The most striking result of the model is the extensive length of time that excavators have assigned to the Norse period. Dates that excavators consider to be from Norse contexts range, at 68%, from 688 to 1480 modelled cal AD. The longhouses at Sandwick and Old Scatness, classified as being Norse-style by the excavators, had occupation periods that, both modelled and just calibrated, spanned centuries. This is particularly true for Sandwick, where the end occupation phase, represented by GU-1292 and -1293, models to sometime between the 1420s and 1620s at 95%; comparatively, the Late Norse period middens at Old

Scatness, the last dated evidence for a Norse-associated phase at that site, range from 1285 to 1305 modelled cal AD. Culturally, Shetland was no longer considered 'Norse' by the time that the occupation period ended at Sandwick, and elsewhere in the North Atlantic the longhouse-style farms seem to have had shorter occupation periods than Old Scatness (e.g. Orkney's East Mound, where, in Chapter 8, I argue that the occupation period for the longhouse was quite brief, and at Quoygrew, where the evidence for the end of the Norse period and a shift into a 'medieval' culture is largely based on a shift in house style (Barrett in Barrett ed. 2012)).

Table 9.3: Summary of boundaries from the model of Old Scatness presented in Figure 9.10. All dates shown are modelled cal AD.

Boundary	Start 68%	Start 95%	End 68%	End 95%
Start Occupation of Site	313	151	490	517
Pictish Phase Begins	359	309	513	524
End Pictish/Start Norse	693	678	737	756
End Last Norse Phase	1060	1051	1310	1354
End Occupation	1072	1060	1392	1502

Old Scatness has, for 22 of its 33 dates (not including the four listed above in Table 9.2) clear stratigraphy, making it a good candidate for Bayesian modelling. Eleven dates, all the dates from Structure 6, are phased by the excavators only as belonging to the occupation phase at the site (Outram and Batt 2010). Figure 9.10 shows a model of only Old Scatness, with boundaries shown in Table 9.3. The model has A = 79.9, with two dates whose individual A values are between 45 and 60: GU-13722 and GU-9539. The former is the oldest date from the site and the latter is the youngest, so I have left them in the model rather than create artificial boundaries by excluding them. Once again, the period of occupation is lengthy - modelled cal AD 313 to 1392 at 68%. The Norse period ranges from modelled cal AD 693 to 1310 at 68%, which is also strikingly long. The latest possible date for the beginning of Norse activity at Old Scatness, according to this model based only on the site stratigraphy, is modelled cal AD 756 (at 98%). These modelled date ranges push back the boundaries of Norse occupation in Shetland, if they represent real events. The oldest dates in the model that Outram and Batt believe are from this early Norse period come from Structure 11, which they have interpreted as an area of interface between Pictish and Norse activity. GU-13720, in particular, is very early; unmodelled, it ranges from 659 to 772 cal AD at 95%. This date is not an outlier; GU-11099, GU-11863, and GU-11865,

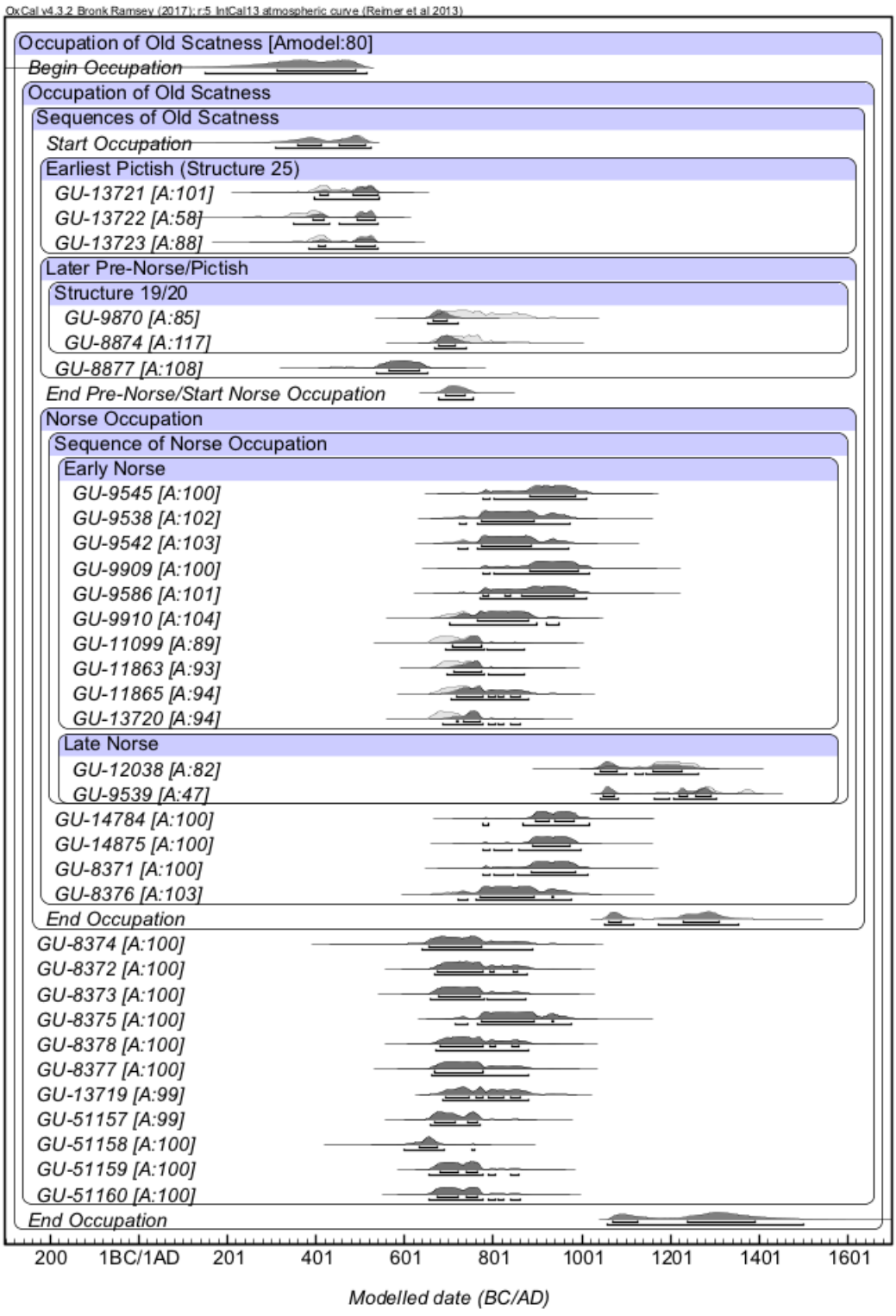


Figure 9.10: Model of dates from Old Scatness site (Bronk Ramsey 2009; Reimer et al. 2013; OxCal v.4.3). N = 33, A = 80.

all also from Structure 11, calibrate without modelling and also model to similar early ranges, as shown in Table 9.4.

Table 9.4: Calibrated (unmodelled) dates from the Early Norse period at Old Scatness.

Date	68% cal AD	95% cal AD	68% mod. cal AD	95% mod. cal AD
GU-13720	670-766	659-772	740-770	696-861
GU-11099	670-767	652-865	719-777	705-870
GU-11863	684-769	662-864	721-776	705-869
GU-11865	681-855	672-879	726-855	714-879

These radiocarbon dates, modelled according to the excavators' phasing, indicate that Old Scatness was occupied for a long time period (compared to, for example, the East Mound), and that its early Norse phases represent some of the earliest known Norse activity in Shetland. The long history of Pictish occupation of the area prior to the shift to the Norse - whether that was a peaceful transition or not - suggests that this site offered stability and prosperity. What ended this lengthy occupation period? Could the loss of value and subsequent abandonment of the farm at Broo, which Bigelow et al. (2005) believe was caused by increased storminess along the sandy coast of Shetland during the LIA, have also affected Old Scatness, which is located very near Broo? Sandwick, also located on the coast, was a rescue excavation, found eroding out of sand dunes, so there may be parallels between the reasons for abandoning all of these farms. Further refined dating information on the end of the occupation periods for these farmsteads alongside chronologically-based studies of coastal dune movement may help explain the abandonment of places that were previously occupied for so long.

9.2.3.2 Western Isles

The Western Isles currently have two Norse-period archaeological sites with scientific dating evidence: Cnip, with two Norse burials (Barrett and Richards 2004) and Bornais (which is also called Bornish), located on a machair with access to nearby beach on the island of South Uist (Sharples (ed.) 2012; South Uist, Bornish, accessed 2017).[5] Bornais began as an Iron Age settlement and became one of the largest Norse settlements along the Western seaboard of the British Isles. The Norse-period house was eventually abandoned and settlement shifted to a large farmhouse built

[5]Radiocarbon dates from Cille Pheadair are expected to be published soon.

nearby - but not in the same open field - sometime around the eighteenth century. The site's phasing and stratigraphy allow many of the dates from it to be modelled. Given that there were only two dates from Cnip, they were also added to the model, placed into the general Norse Period. Some dates on bone from Bornais and both dates from Cnip had some marine sources in their diets, and had a percent marine diet determined based on the recommendations of Barrett and Richards (2004) and Cook et al. (2015), using linear interpolation between δ^{13}C = -21 ± 1‰ (a 100% terrestrially-sourced diet) and -13 ± 1‰ (100% marine). ΔR for these dates is taken from Barrett and Richards (2004), 91±30. The initial run of the model, minus only the dates listed as 'unknown' in Table 9.5, had A(model) = 1.5 due to three dates.

These dates, all from Bornais, were OxA-9639 (A(individual) = 0), a cattle rib bone found in a context from the Norse period, SUERC-7625 (A(individual) = 0), an articulated red deer bone, also found in a Norse period context, and OxA-10274 (A(individual) = 2.5), a cattle bone found in the sand layer below the Viking Age house, because it was too young for its context. Bornais has complicated stratigraphy with occupations and re-occupations of the house in both the Iron Age and the Viking age (Sharples ed. 2012). There is precedent in Norse household architecture for embedding animal bones in walls or floors: walrus bones and tusks at Aðalstræti 14-18 (McGovern 2001) and cattle and sheep at Hofstaðir (McGovern 2002). Perhaps these were bones that were passed down (in the case of the ones that dated too old) or ones that were placed beneath the floor of the Viking Age house (in the case of the too young OxA-10274). The dates eliminated are in Table 9.5.

Table 9.5: Dates not used in the final model for the Western Isles shown in Figure 9.11. Complete descriptions for each date in this table, and all others in this chapter, are found under the 'Shetland' section of the table on the included Excel CD.

Date	Location	Indiv. A value?	Reason for Elim.
SUERC-7652	South Uist, Bornais		Unknown expected age
SUERC-7653	South Uist, Bornais		Unknown expected age
SUERC-7626	South Uist, Bornais		Unknown expected age
SUERC-7627	South Uist, Bornais		Unknown expected age
SUERC-7628	South Uist, Bornais		Unknown expected age
SUERC-7632	South Uist, Bornais		Unknown expected age
SUERC-7633	South Uist, Bornais		Unknown expected age
OxA-9639	South Uist, Bornais	0	too old
SUERC-7625	South Uist, Bornais	0	too old
OxA-10274	South Uist, Bornais	2.5	too young

The new version of the model, which has n = 47 dates, has A(model) = 114. Figure 9.11 shows the results of the model, and Table 9.6 summarises the results. Bornais, where the majority of the dates shown come from (aside from GU-3485 and -3489, the burials from Cnip), had a long period of occupation. Whether or not the people who lived there considered themselves culturally 'Norse' throughout that long period the excavators categorise as Norse or identified as something else is unclear.

Table 9.6: Summary of boundaries from the model of the Western Isles and Bornais presented in Figure 9.11. All dates shown are modelled cal AD.

Boundary	Start 68%	Start 95%	End 68%	End 95%
Start Iron Age	285	202	376	400
End Iron Age/Start Norse	855	818	920	947
Start Bornais Occ.	944	887	1012	1021
End Sand/Start Sec. Occ. Bornais	982	946	1029	1100
End Sec. Occ. Bornais	996	985	1109	1262
End Norse Period	1405	1360	1454	1494

Similar to Old Scatness, Bornais was originally settled in the Iron Age, and then transitioned into a Norse farm. The Norse period had multiple separate periods of activity, interrupted by periods of abandonment with windblown sand between occupation layers, one of which has been constrained by the radiocarbon dates used in this model. This model places those windblown sand events, as at the East Mound, Orkney, and Broo, Shetland, during the MWP - before the potentially increased storminess of the LIA (e.g., Somerville et al. 2007). Here, the interruption in Norse settlement takes place some time before 982 to 1029 modelled cal AD at 68%, and the site seems to have been resettled afterward. Unlike at the East Mound, something drew people back to this place in the landscape. Perhaps, as I suggested for Old Scatness, this was because of its proven legacy of success from the Iron Age.

9.2.3.3 The Faroe Islands

The Faroe Islands have a more diverse data set of dating information than Shetland or the Western Isles, with five archaeological sites from six different studies and three different core sampled lake locations from a single environmental study. Much of the research in the Faroe Islands has focused on the events surrounding Norse *landnám* and the possibility of pre-Norse settlement, maybe priests from Ireland (e.g., Church et al. 2013). To model these dates, I created an overlapping model with a 'pre-Norse'

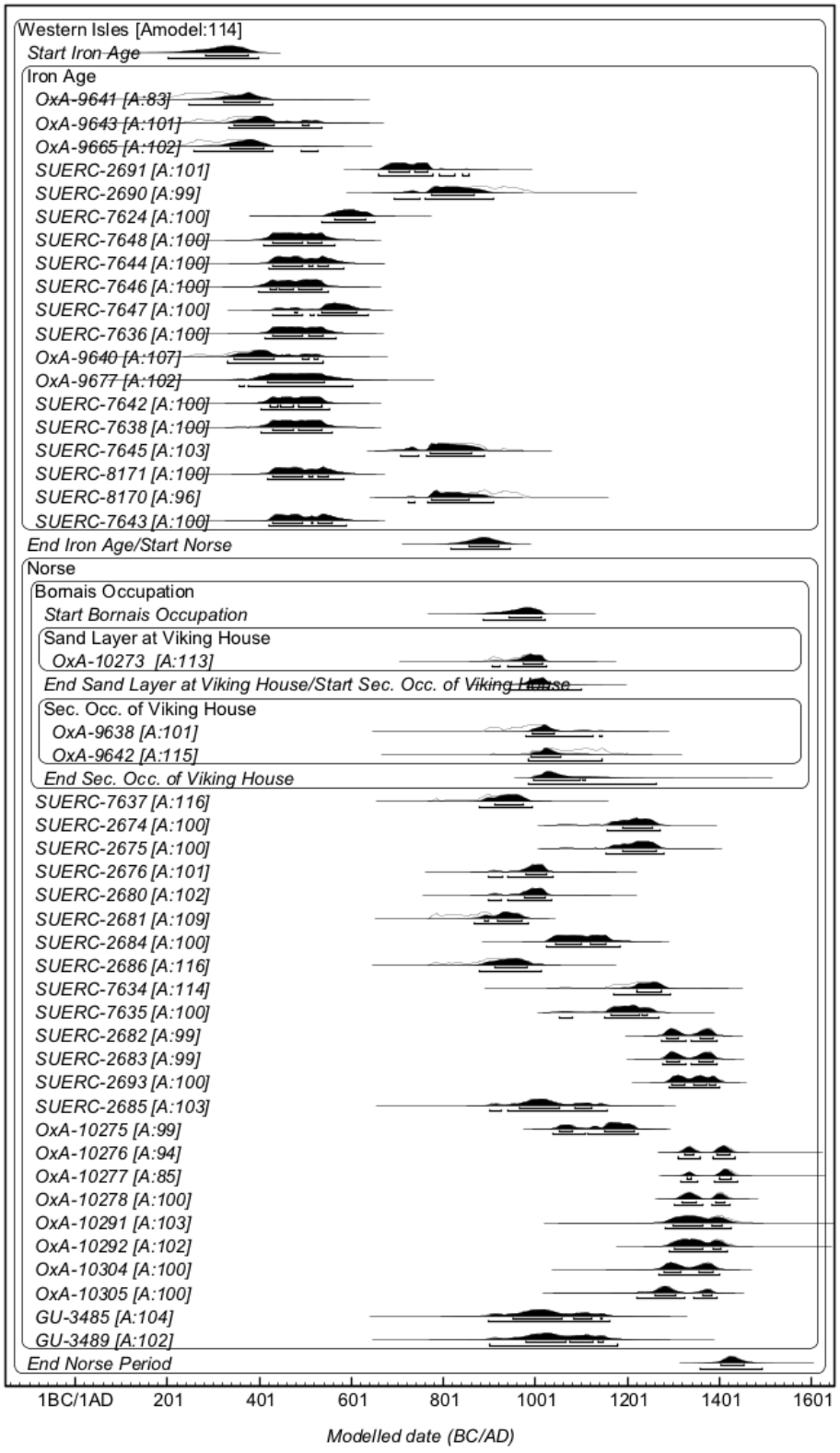


Figure 9.11: Model of dates from the Western Isles (Bronk Ramsey 2009; Reimer et al. 2013; OxCal v.4.3). N = 47, A = 114.

phase, a '*landnám*' phase, and a 'post-*landnám* Norse' period. Within the larger phases, there are sequences from Argisbrekka, Undir Junkarinsfløtti, Brunavatn, and Mjauvotn. The overlapping model assumes independence between sequences, rather than making them contiguous. If there was some period of time when the pre-Norse population coexisted with the Norse, then using an overlapping model will not obscure that. Although Church et al. (2013) find that the pre-Norse settlement at Á Sondum lies beneath Norse cultural layers, Arge (2014) does not record a similar terminus ante quem for the pre-Norse settlement at Við Kirkjugarð. Similarly, the use of the overlapping model allows the environmental sequences from Olsen et al. (2010) to be modelled in sequence. Four of the radiocarbon dates on animal bone from Undir Junkarinsfløtti (Church et al. 2005) are from individuals who had a marine percentage in their diet and they have been modelled to reflect that, using ΔR values of 23 $\pm$99 (Reimer and Reimer 2001; Olsson 1980) taken from Sorvag, Vago, the Faroe Islands.

Figure 9.12 and Figure 9.13 shows the results of the model for the Faroe Islands, and Table 9.7 summarises the results using the boundaries. K-5064 (birch dated from a layer prior to a rebuilding phase at Argisbrekka (Mahler 2007: 80)) is the only date eliminated from the final model because it was significantly earlier than it should have been, giving the model N = 70 dates, 69 of which were radiocarbon, and one tephra date from Hekla 1104, found in the Brunavatn core. AAR-6928 (a sheep bone from Undir Junkarinsfløtti that had 8% marine diet) is the only date in the model with an individual A value lower than 60 (A(individual) = 32.5), but, although it is an early date, it does not seem erroneous in its context, and the model itself has A = 110.5 with that date included.

Table 9.7: Boundaries of the model shown in Figure 9.12 and Figure 9.13. All dates are modelled cal AD.

Boundary	Start 68%	Start 95%	End 68%	End 95%
Start of Pre-Norse	229	3 BC	405	507
End of Pre-Norse	742	702	931	1175
Start of Landnám	779	763	889	891
End of Landnám	886	883	973	991
Start of Norse Period	825	710	957	990
End of Norse Period	1051	1038	1117	1200

The remarkably long period modelled for the boundary 'End of Pre-Norse' is 702 to 1175 modelled cal AD at 95%. In part this is because of a plateau in the calibration curve, as shown in Figure 9.14, but the few dates available from this period (n =

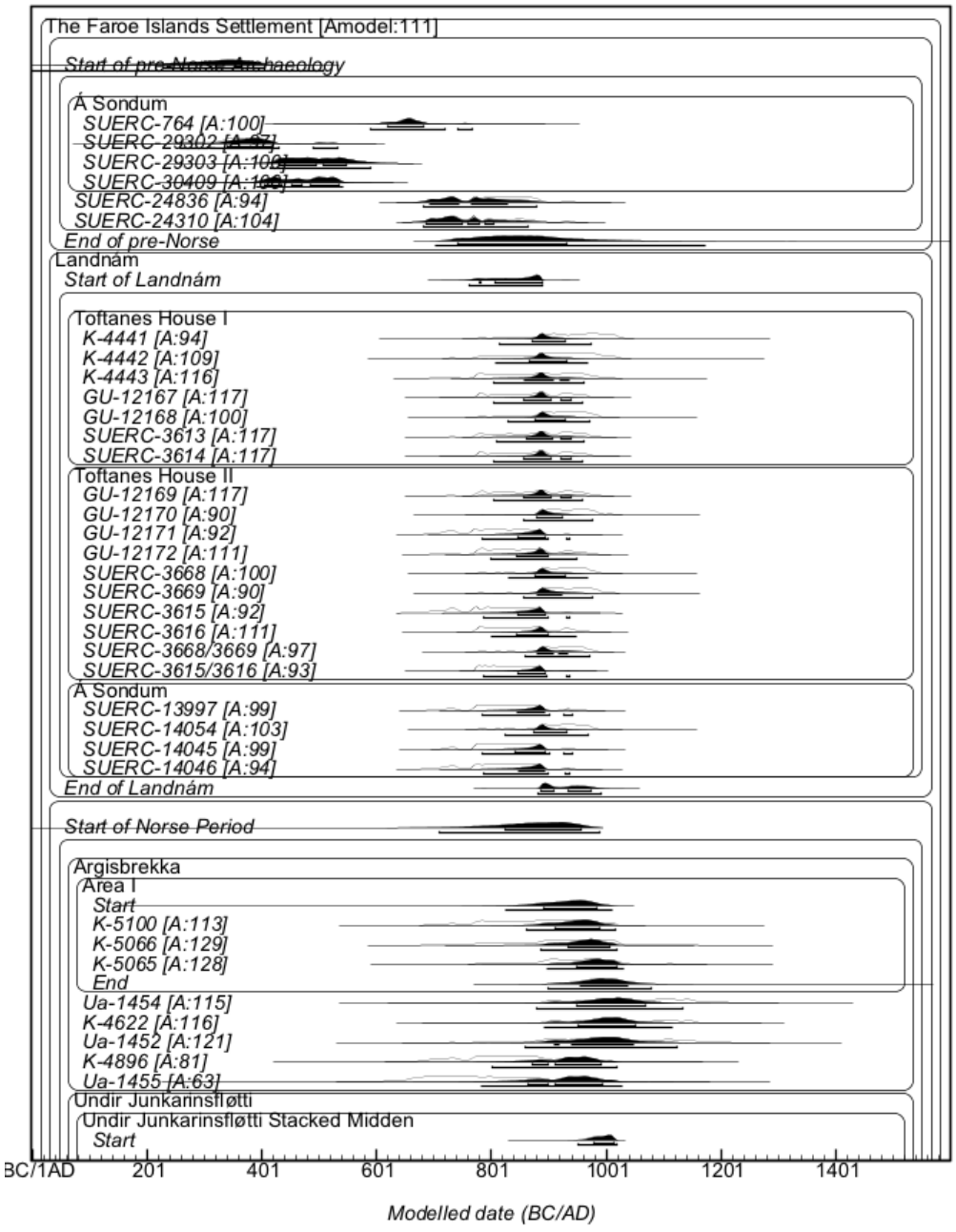


Figure 9.12: Faroe Islands model part A, from the start of the model to the Undir Junkarinsfløtti sequence. (Bronk Ramsey 2009; Reimer et al. 2013; OxCal v.4.3). For total model, N = 70, A = 110.5.

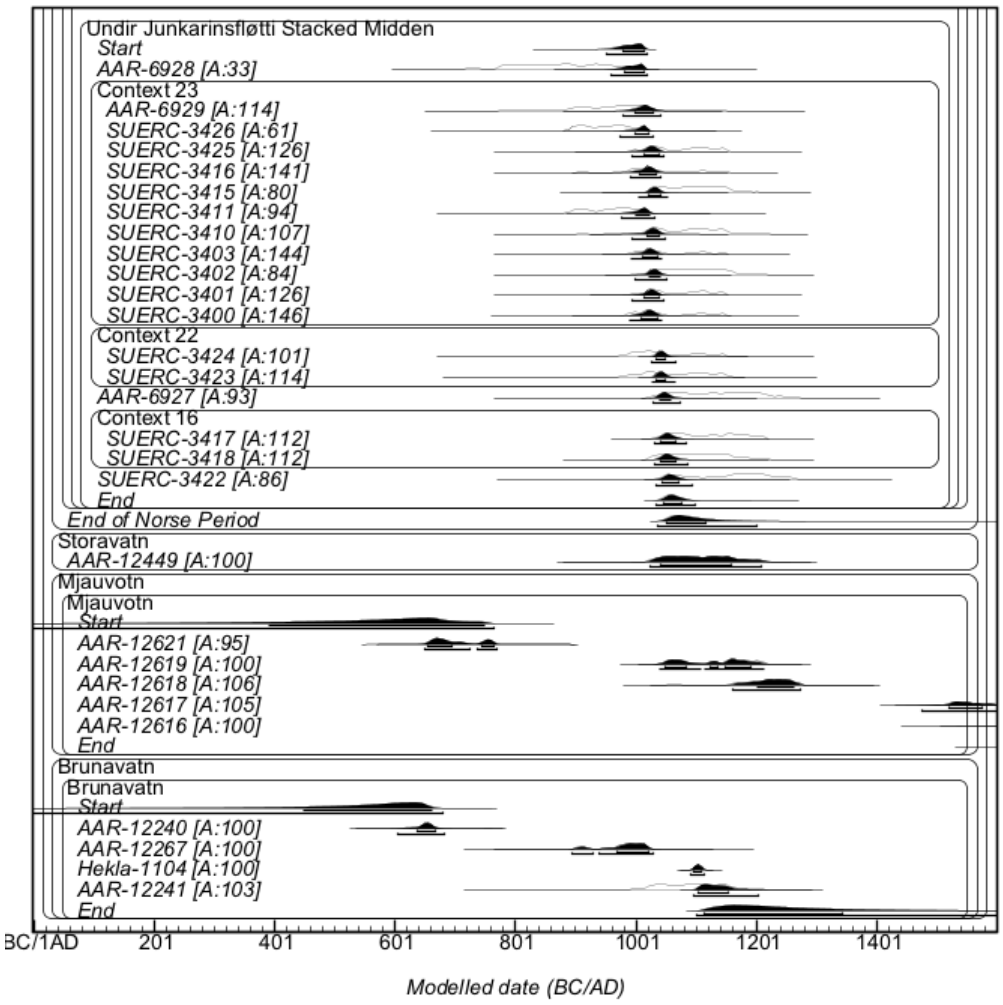


Figure 9.13: Faroe Islands model part B, from the start of the Undir Junkarinsfløtti sequence to the end of the model. (Bronk Ramsey 2009; Reimer et al. 2013; OxCal v.4.3). For total model, N = 70, A = 110.5.

7) and their variability are also pushing the model to have a wide range. The early start of the period is influenced by SUERC-29302, a carbonised barley grain from Á Sondum. Barley is not native to the Faroe Islands and must have been brought by humans (Church et al. 2013: 231), and the excavators see no reason for this date to be in error. The pre-Norse settlement seems to have taken place sometime between the 4th and probably 8th centuries AD; the Norse period begins very shortly thereafter, with, at least in this model, a potential period of overlap in the late 8th or early 9th century AD. Although there is scant evidence for pre-Norse settlement - much of it obscured by later, larger Norse settlements, which lie over the pre-Norse remains at Á Sondum as Church et al. lament - the Norse may have entered into a landscape in

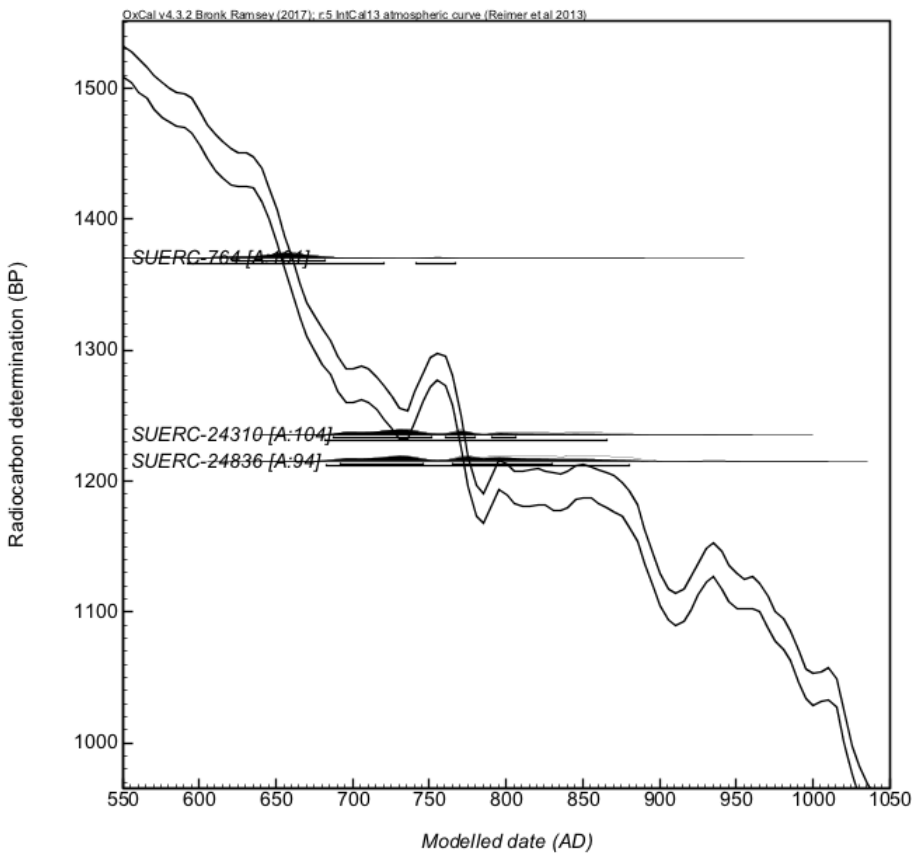


Figure 9.14: Excerpt of dates from the pre-Norse period of the model of the Faroe Islands on the calibration curve, showing the plateaux in the curve (Bronk Ramsey 2009; Reimer et al. 2013; OxCal v.4.3).

the Faroe Islands where the best places to farm were made obvious either by a small extant settlement or the recent ruins of one.

Dates from the Norse period end sooner (modelled to be by ca. AD 1200) than they do for the other places studied here, but that is a product of what kind of archaeological remains have been scientifically dated from the Faroe Islands, where most chronological research has focused on the *landnám* period.

9.3 The Chronology of Conversion

9.3.1 Orkney: Religious Conversion Modelled Part I

The timing - and nature - of the conversion from the Norse pagan religion to Christianity is a recurring research question in North Atlantic archaeology, and is often used to mark the end of the truly 'Norse' period and the beginning of the medieval. The dataset of radiocarbon dates from Orkney provides one way to examine this important transition.

Orkney has 195 dates in the database, of which all but eleven are radiocarbon (the others are OSL). Many of these are from a broad Norse/medieval chronological category, which it has been difficult to divide more finely. There does not seem to be a distinct, archaeologically-detectable cultural transition from a Norse/Viking period to the medieval in Orkney. For example, Barrett (2012) emphasises that Phase 3 at Quoygrew represents a shift in the main focus of the farm, but he does not describe a hard boundary between the Norse period and settlement afterward. The traditional date for the conversion of Orkney to Christianity is AD 995 (Barrett 2002), and a formal bishopric was established in Kirkwall, the largest city in Orkney, ca. AD 1048, but, as is discussed more below, the meaning of these dates as they relate to the lived culture is unclear. Nor is this the only way to look at the timing of cultural change in Orkney: for example, Barrett and Richards (2004) see a start to what they call the Viking Age from ca. AD 850 to 950 based on an increase in marine diet (especially for high status individuals and males). Historically, AD 1231, the end of the line of jarls established by Harold I of Norway (who initially claimed Orkney and Shetland for his Viking kingdom), has been used as a hard ending to the Norse period, but, much like when Roman legions withdrew from southern Britain several centuries earlier, it is likely that Viking/Norse cultural influences remained and that the transition to a post-Viking society in Orkney was a gradual one.

For all this ambiguity, there is an archaeological record of change that appears in the radiocarbon dates - burial practices. In general, the presence of grave goods like Thor's Hammers, and the practice of boat burials and cremation have been used to indicate a pagan grave, while crosses, placement of graves within churchyards, inhumation burials, and orientation of graves east to west have been used to indicate a Christian grave. Using recent anthropological theories of 'personhood', Lund (2013) critiques this understanding as simplistic, a 'check-list' to determine the religion of an

individual from limited evidence, and cautions against seeing the transition as hard, with a retroactive bias towards understanding Christianity in the formerly Norse pagan world as exactly comparable with Christianity elsewhere. Barrett (in Carver ed. 2006: 221) similarly emphasises the need to see the conversion period as one without a hard boundary, and he argues that it should be understood as including competing, probably coexistent ideologies, and suggests that there was a period of time when a Christian elite lived near the Brough of Deerness, in the eastern part of Orkney, while a pagan elite lived in the area around the Brough of Birsay, in the west.

While the conversion period seems to have represented a major change in the power structures that governed Orkney (and this is discussed further below in relation to Iceland), the extent to which the conversion was an ideological shift is perhaps unknowable. Barrett, for example, moves beyond this debate quickly in his opening paragraphs to move on to the evidence. We do not have contemporary accounts of what the subjects of the elite Orcadians choosing conversion felt about the process. Our closest contemporary source, the Orkneyinga Saga was written in 1230, over two centuries after some of the events it records, and it deals mainly with elite activities.

This leaves us with the burial evidence. New Archaeology, which later became processualism (e.g., Binford 1971), placed mortuary rituals within the social context of the society that created them, while post-processualism, and notably Hodder (1980 and 1982) and Parker Pearson (1982) argue against considering mortuary practices as having a one to one relationship with practices in life. Instead, they argue that burial practices and funeral ceremonies are almost always expressions of an ideal, mediated by the living. Parker Pearson goes on to emphasize that ideology played a major role in mortuary rituals, with the living manipulating the dead - and the expressions of grief and change surrounding their death - to advance their own positions in society. Both of these positions are based largely on ethnography, with all of the constraints and critiques that come with comparing long ago societies to still-living ones often far removed geographically, and more recent attempts have been made to reconcile the two. For example, Brown (1995) argued that archaeologists consider the context of funerary rituals - each one was not a carefully planned affair with the explicit goal of advancing an ideology, but rather a reflection of the political and ideological positions, and economic constraints, of the moment when these rituals took place.

Bayesian modelling of existing radiocarbon dates on human burials from this period offers another way to examine pagan to Christian transition period in Orkney, insofar

as it relates to burial practices. The results of the models below are considered within the anthropological framework built by processual and post-processual archaeology, considering the role that the living would have had in physically creating these burials and in choosing what level of wealth and piety went into them.

The question best explored through Bayesian modelling of the current data set is the duration of the conversion event, as told through grave evidence, and the nature of the transition from Pictish burials to Norse pagan to Christian. I have created three chronological groups for Orkney's radiocarbon dates from human burials: burial with Pictish grave goods ('Pictish') (e.g. T-7470 from Westness (Barrett and Richards 2004)), burial with Norse grave goods/boat burial, which I named 'Pagan Norse' (e.g. SUERC-1176 from Scar (Owen and Dalland 1999; Barrett and Richards 2004)), and 'Christian' burials from churchyards (e.g. SUERC-10687 from St Thomas's Kirk (Toolis 2008)). Many of these dates had δ^{13}C values consistent with the marine reservoir effect, and I calibrated these using ΔR values of 48 $\pm$47 (Reimer and Reimer 2001). For the percent marine diet, I used -21 and -13 as my end points for linear interpolation. Two dates, AA-50703 and AA-53127, have been left out of the model because, as Barrett and Richards (2004: 260-262) discuss, they are too recent to be plausible within their archaeological context.

OxCal offers multiple options to model archaeological phases. One models phases as independent of one another, assuming they may have some overlap, to estimate the start and end dates of each phase. Another models the phases as in order archaeologically, and estimates the timing of the transitions between each phase.

First, I created a model where each of the three phases overlapped and looked at the interval (the duration) of each phase. The overall model had A(model) = 135, with only one date with an individual A value below 60, TO-7195 (A = 56). This particular date is on human bone from a burial with grave goods identified as Pictich from Westness, on the southwest coast of Rousay (Barrett and Richards 2004), and dates older than any others in the dataset. There is nothing to suggest that the radiocarbon date itself is incorrect, and this may just represent an early find. In one iteration of the model, I removed TO-7195, but it had very little effect on the final results. As it seems likely that this date is correct and just represents an early burial, I have left it in the model.

In this model, the results of which are summarized in Table 9.8 and shown in Figure 9.15, the phases do have considerable overlap. Neither the start date for pre-Norse

Table 9.8: Summary of boundaries from the overlapping model of Orkney conversion period dates shown in Figure 9.15. All dates are modelled cal AD.

Boundary	Start 68%	Start 95%	End 68%	End 95%
Earliest Recorded Pictish	500	416	602	643
Pictish End	693	667	802	901
Pagan Norse Start	800	579	977	1023
Pagan Norse End	1049	1027	1212	1419
Christian Start	912	870	975	999
Latest Recorded Christian	1455	1439	1503	1540

burials nor the end date for Christian burials are representative (obviously Christian burials continue into the modern period), but are products of the samples examined in this study, which are presented in relation to change in the Norse world. The very early date at 95% for the start of the Pagan Norse period is the result of a limited number of dates (n = 11) with a wide chronological range; plateaux in the calibration curve may also be influencing the precision of the model.

Burials identified as Pictish by the excavators have, at 95% confidence, a potentially long period of overlap with Norse burials - and potentially even a very limited time overlapping with Christian burial practices. However, at 68% confidence, they have almost no overlap with the Pagan Norse period and none with the Christian. Looking at the model, shown in Figure 9.15, it is clear that the duration of the Pagan Norse period is being pulled later in time by a single date, AA-54929, which is a date from the boat burial at Scar.

The burial at Scar contained the remains of three people, identified as a man, a woman, and a child, who were buried at the same time based on the stratigraphy of the site. Each skeleton was dated, and all had a 9% marine diet. As Figure 9.16 demonstrates, these dates taken together and assumed to be from the same archaeological phase have a very wide chronological range. The excavators discuss the results of the radiocarbon dates (although they do not correct for the marine reservoir effect), and conclude that they will date the site between AD 875 and 950, which according to their research corresponds with an area of overlap between all three radiocarbon dates and artifact typologies from other finds at the site (Owen and Dalland 1999: 164-165). Correcting for the marine reservoir effect and modelling the dates in a single phase (as in Figure 9.16) or using the overlapping model (as in Figure 9.15), the dates from Scar move forward in time, with the junction between the three values becoming the early 11th century AD. This is a relatively late date for a boat burial

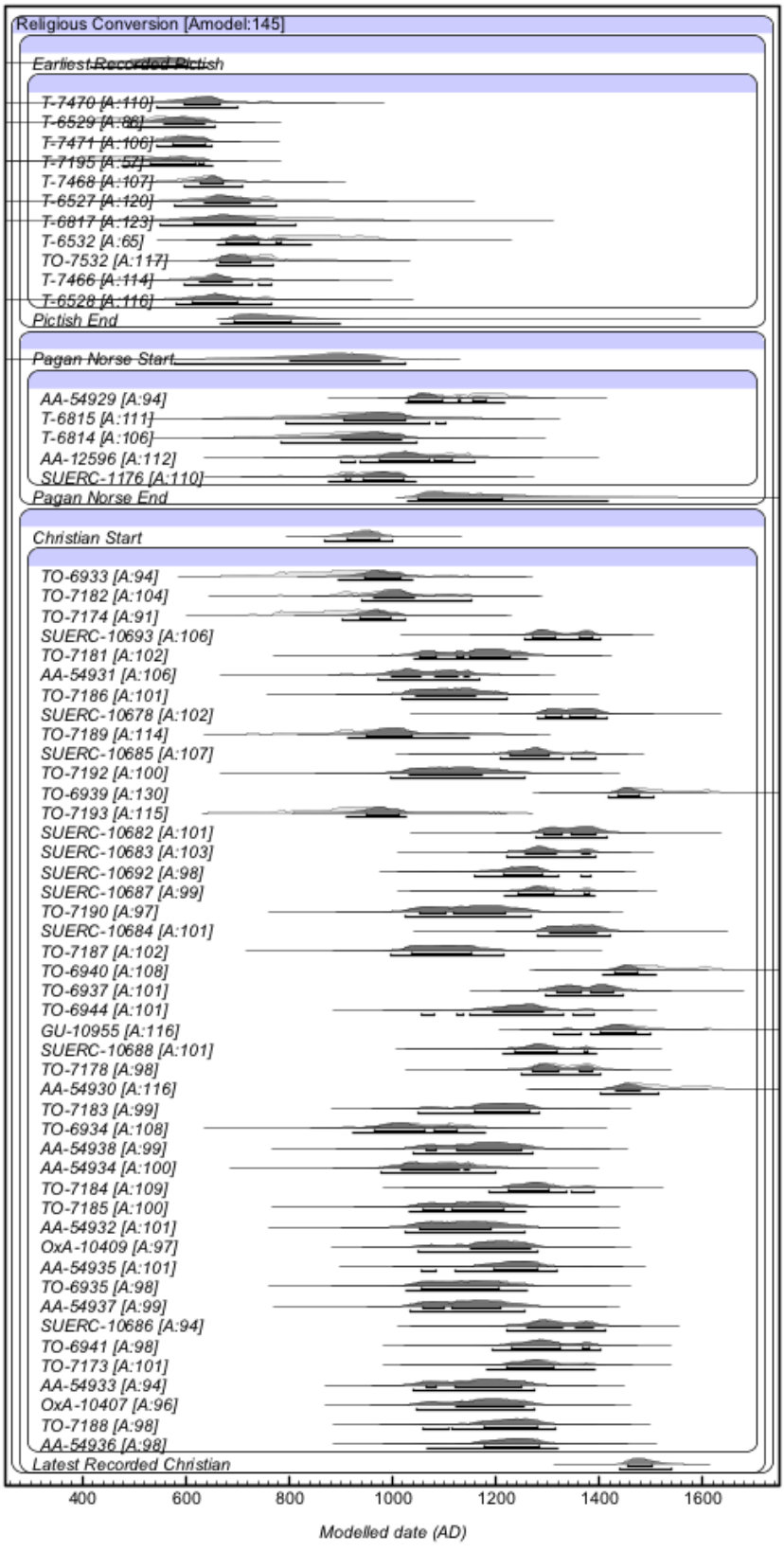


Figure 9.15: Results of overlapping phases model for dates relating to the conversion of Orkney (Bronk Ramsey 2009; Reimer et al. 2013; OxCal v.4.3). N = 61, A = 145.

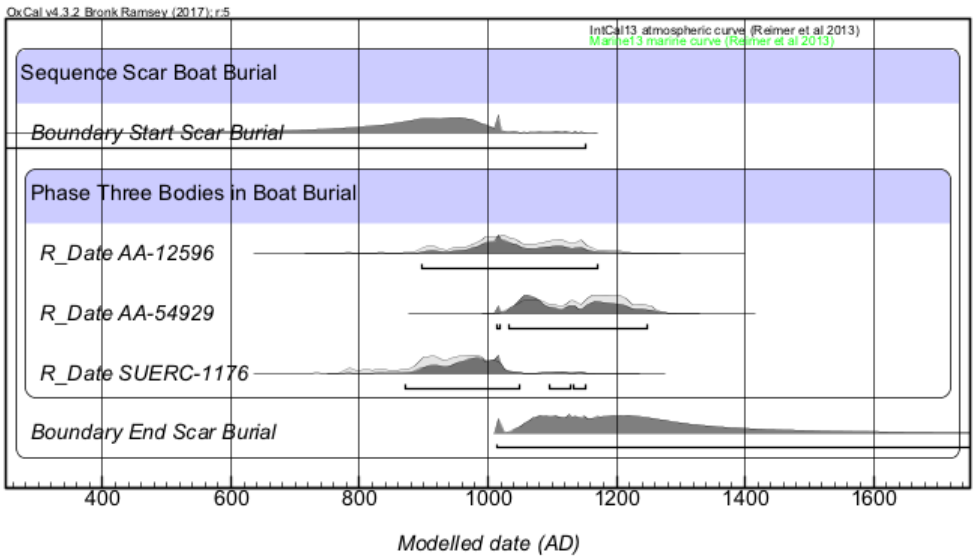


Figure 9.16: Model of the dates from Scar as a single phase (Bronk Ramsey 2009; Reimer et al. 2013; OxCal v.4.3). N = 3, A = 112.

in Scotland and the surrounding area, although many of those burials are dated by typology rather than scientific chronology (e.g., Graham-Campbell 2003; Batey 2011; Harris et al. 2017).

The other two burials included in the model from the pagan Norse period are from Westness, from graves where individuals were buried with Norse grave goods (there were also two small boat burials from the Norse period found in this cemetery) (Graham-Campbell 2003; Barrett and Richards 2004). There is no reason to suspect that any of these radiocarbon dates are incorrect, but, with such a limited sample size, the dating of the phase is affected by the relatively late date of AA-54929. It is notable that the three dates from the boat burial all have the same percentage of marine diet, 9%, while the two burials from Westness are almost identical - 35% and 36%. This suggests that of the five dated remains associated with Norse pagan burial practices, they are split into two groups in terms of diet. According to this model, the Westness burials are from an earlier date, but the individuals they represent had diets much richer in marine resources than the people buried at Scar. This provides a tantalizing clue as to the different circumstances of their lives.

Further radiocarbon or otherwise scientifically dated material from Orcadian Norse pagan graves would fill out this picture and create a larger sample size to model this time period. As Graham-Campbell (2003: e.g., 134) describes, most of the graves

from this time period have been dated by artifact typology. Future research will hopefully include more scientific dating.

Using the overlapping model, the transition between Pagan Norse burials and Christian burials has a long period of overlap, even at 68% confidence. The Christian period also starts early in this model: at 95% confidence, Christian burials may start as early as AD 890 or as late as AD 1007, a span of just over a hundred years; at 68% they start at AD 912 to 975, again earlier than the traditional date of AD 995 for conversion. As is discussed further below, this may relate to a particular group of burials from Newark Bay pushing the start date early. The overlapping model does suggest a considerable period where the relatively small Orcadian landscape had practising members of the two faiths.

In the second model, where I query OxCal to treat each phase ('Pictish', 'Pagan Norse', and 'Christian') as contiguous, there are some notable outliers - but, in general, the model is in agreement. Using all the same dates from the overlapping model, the contiguous model returned A(model) = 54.7. Three dates, all from the Christian phase, had individual A = under 10%: TO-7174 (A = 2.1), TO-6933 (A = 3.5), and TO-7193 (A = 7.3). Additionally, TO-7182 had A = 17.7. All four dates are churchyard inhumation burials from Newark Bay, and all date earlier than any other burials sampled at the site. Three of these dates have the lowest marine percentage in their diet of any of the dates from the Christian period - 9% to 12% - while the fourth, TO-7193, has a marine diet percentage of 25%, still well below the median percentage (34%) for all of the burials recorded here from the Christian period.

Removing the three dates with A(individual) = under 10%, the model has A = 121, shown in Figure 9.17. TO-7193 has A(individual) = 28 in this model, but removing it runs the risk of obscuring a real historical event. That grave, along with the three removed from the model, with their lower marine diet percentages, may represent some of the earliest Christian activity during the Norse period in Orkney (it is unclear if there was a Christian presence amongst the Pictish). Perhaps these were people who moved to Orkney from an already Christian area, acting as the vanguard of the religion. Aside from those early Christian dates, modelling these dates as contiguous phases provides clear boundaries around the pagan Norse period in a model with strong agreement (again the start of the Pictish phase and the end of the Christian phase are not representative). Table 9.9 shows these boundaries.

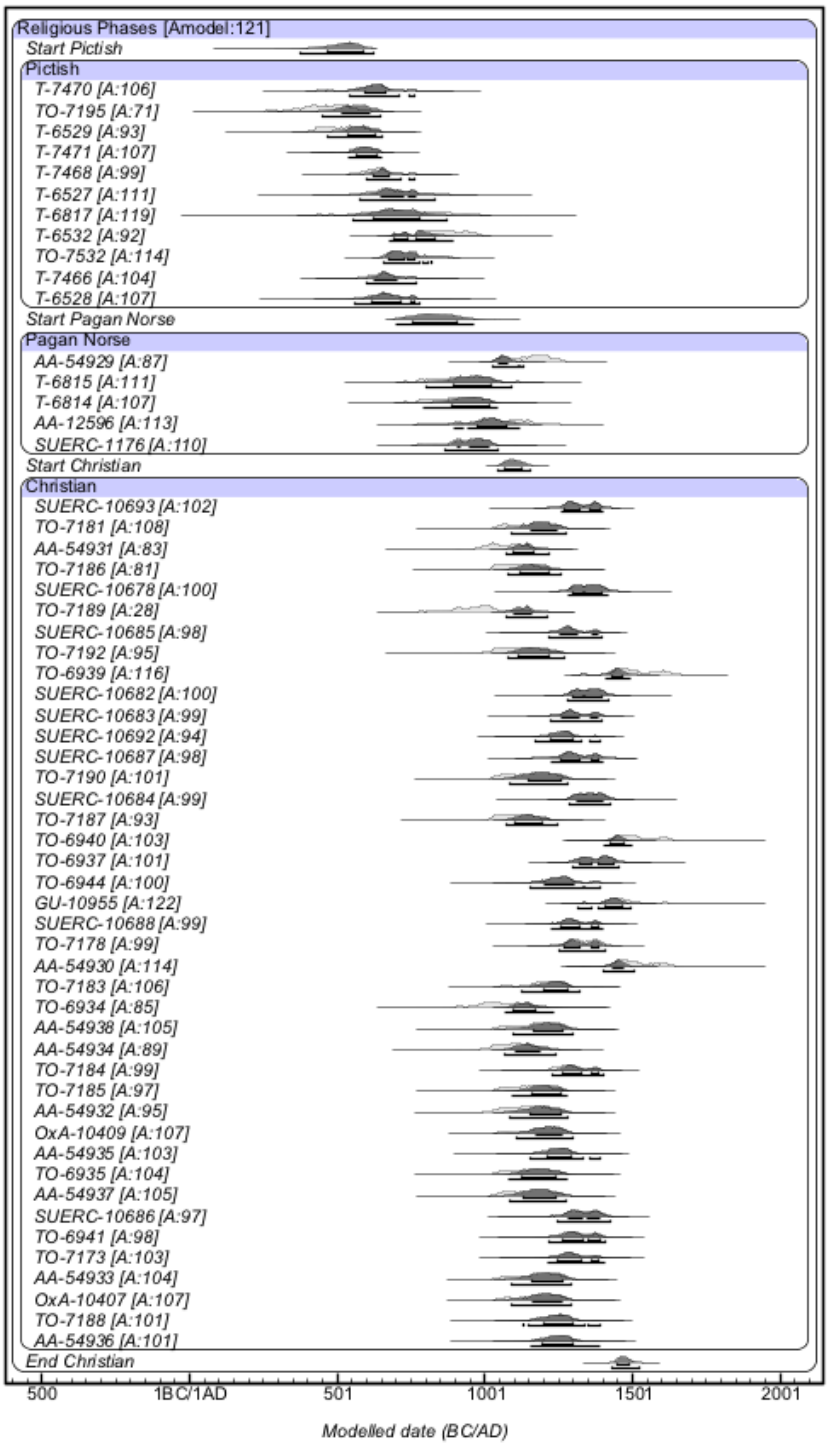


Figure 9.17: Contiguous model of dates from Orkney conversion period (Bronk Ramsey 2009; Reimer et al. 2013; OxCal v.4.3). N = 58, A = 120.5.

Table 9.9: Boundaries from contiguous model shown in Figure 9.17. All dates are modelled cal AD.

Boundary	Start 68%	Start 95%	End 68%	End 95%
Start of Pictish	471	377	587	626
End Pictish/Start Pagan Norse	758	699	905	963
End Pagan Norse/Start Christian	1065	1045	1125	1156
End Christian	1448	1430	1489	1522

The two models provide different ways of conceiving of the changes in burial practice in Orkney from radiocarbon dated samples. The overlapping model, especially for the Norse pagan to Christian transition, seems to be more representative, creating a space for earlier Christian burials located in the east side of the archipelago, consistent with Barrett's (in Carver ed. 2006) view that the west retained paganism longer than the east. Scientific dating from graves around the Brough of Birsay region would be useful to more clearly date the transition.

9.3.2 Iceland: Religious Conversion Modelled Part II

The conversion of Iceland is an enduring mystery in Icelandic archaeology (and history), described by Vésteinsson as 'one of the really strange events in the history of Christian missions' (2000: 17). One historical source for it is Chapter Seven of the Íslendingabók, which recounts these seemingly extraordinary events in detail. The story goes that, after a series of missions from Norway and increasing religious tensions in Iceland - with some Icelandic chieftains converting to Christianity and pleading their case before the Norwegian king - the summer meeting of the Alþingi in AD 999 or 1000 yielded a compromise from the pagan speaker, Þorgeirr Ljósvetningagoði: the island would convert to Christianity with three conditions. First, the exposure of newborns was still allowed, second, horsemeat could still be eaten, and third, pagan rituals could be practised privately (Þorgilsson, translated 2006).

The account of such an abrupt transition has generated many opinions from scholars. Most recent opinions see the transition as one related to increasingly complex structures of governance, with chieftains seeking to consolidate their power in the landscape (e.g., Vésteinsson 2000), and with consequences for the lived experiences of the Icelanders (e.g., Lund 2013). Others feel that an abrupt conversion is not shocking, and can be explained within the boundaries of pagan beliefs and the need for the elites in Iceland to prevent a religious-based civil war (e.g., Gunnell 2009).

As in Orkney, the archaeological evidence for conversion lies in a change in burial practices from often elaborate pagan rituals to churchyard burials of the Christian era. We can imagine that there were daunting logistical issues surrounding conversion - as Vésteinsson humorously suggests, if the conversion really did fully take place in the year 999 or 1000, the few Christian priests in the country that summer must have been tremendously busy baptising and educating (2000: 35).

Sveinbjörnsdóttir et al. (2010) present 44 radiocarbon dates on human bone, two on horse, and one on dog, all from a wide geographical range of graves from the pagan and early Christian periods. Using these dates, I have created a series of Bayesian models related to the conversion period. For Iceland, there are questions of absolute dating - for example, were some Icelanders already using Christian practice before AD 1000? - and of relative dating - for example, is there an overlap between pagan and Christian burial practices? - that models can explore. I created models, presented below, that offer some possibilities for the chronology of the conversion of Iceland as seen through this group of burials.

Before modelling, the dates from Sveinbjörnsdóttir et al. needed to be corrected for the marine reservoir effect, as their δ^{13}C values indicate that the individuals dated had a range of marine diet percentages. The range is notably wider for pagan burials than for Christian ones, as shown in Figure 9.18. Sveinbjörndóttir et al. do not provide corrected dates. Although they do provide their own marine diet percentages, I have recalculated those to the more recent recommendations of Cook et al. (2015) for Iceland (between -20.7‰, representing a fully terrestrial diet, and -13.3‰, representing a fully marine diet).

The ΔR values from the Queen's University Belfast Marine Reservoir Correction database for Iceland present some issues. There are presently a limited number of readings for local surface carbon reservoir from around the coast of Iceland, with most of the readings concentrated around the Reykjanes peninsula and just north of it. Icelandic currents are complex, and all of the readings available here were influenced by the Irminger Current, which sweeps up the western coast of Iceland and around the north (http://www.fisheries.is/ecosystem/oceanography/ocean-currents/); this yields ΔR value = 57, with standard deviation = 79. Sveinbjörnsdóttir et al. (2010) use ΔR value = 50 with standard deviation = 71. However, Ascough et al. (2007) recommend a ΔR value, for northern Iceland only, of 111 $\pm$ 10. Ascough et al. also caution against the presence of the freshwater reservoir effect, which they find to be seriously affecting their results from Mývatnssveit, which is located near the large

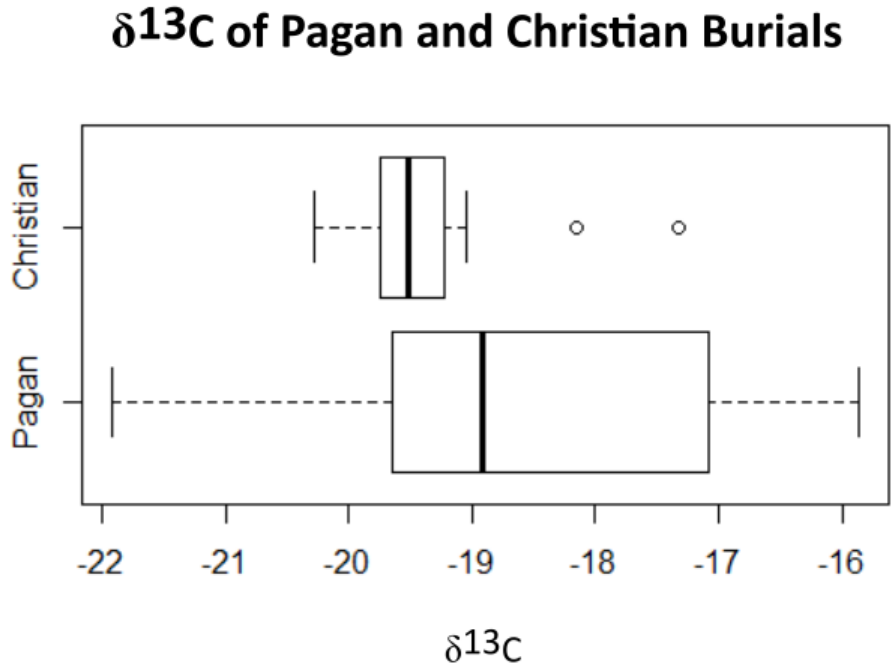


Figure 9.18: Boxplot comparing the δ^{13}C results from pagan burials and Christian burials.

freshwater lake Mývatn and which they argue has a seriously depleted carbon reservoir impacting the Arctic char who live in the lake and are consumed by, in the case of their study, a local pig. Compounding these potential problems with both variable ΔR and a potential freshwater reservoir effect, Eiríksson et al. (2004; 2011) find an increase in marine reservoir ages along the coast of Iceland after an influx of cold water in ca. AD 1300, coinciding with the onset of the Little Ice Age - although this does not affect the radiocarbon dates relating to the conversion.

First, I created a model that assumes a clear divide between pagan and Christian burial styles - similar in form to the contiguous model I created for Orkney. Before the model could run, I had to change some of the input to more accurately represent the marine reservoir effect. Initially, I modelled the dates using the same ΔR value and standard deviation from the Marine Reservoir Correction database for all of the dates, similar to the correction that Sveinbjörnsdóttir et al. (2010) applied, but I found disagreement with certain Christian-era graves - those from Keldudalur (northern Iceland, roughly 8 kilometres from the coast). The initial model had only A(model) = 1.3. Sveinbjörnsdóttir et al. (2010: 690-691) say that they found all of their dates to calibrate in such a way that accepted ranges showed Christian-era

burials later than AD 1000 and pagan burials earlier; however, I have not been able to replicate that using the provided values.[6] Sveinbjörnsdóttir et al. did not create any models, instead simply calibrating each date, but if their hypothesis that the timing and manner of the Christian conversion of Iceland as recorded in Íslendingabók is correct, then it should not be a problem to model pagan burials as earlier than Christian burials. As a result, I used Ascough et al.'s (2007) recommended values for north central Iceland, 111 ± 10, for dates from Keldudalur.

The result of this adjustment is a model with A = 108 and four dates with individual A values less than 60. One of those is from Keldudalur, AAR-9244 (A = 55), which dated older than all other Christian burials. The cemetery at Keldudalur had burials from both pagans and Christians, indicating a relatively long span of use; perhaps this individual was someone who had converted to Christianity before the others, maybe someone who had travelled abroad or been born elsewhere. The individual also had a marine diet percentage of 46%, the highest of any of the Christian period burials (which have a median percentage of 17%), but a number that fits comfortably within the wide range of values from the pagan period (from 11% to 65%, with a median of 34%), lending credence to the idea that this individual's remains are likely older than the other Christian burials.

The second date with a low A(individual) = value is AAR-5877 (A = 19.4), from Vad, Skriddalur, which appeared too young to be from the pagan period (and, interestingly, has a relatively low marine diet percentage of 18% - although pagan-era graves have a wide range of percentages, 18% is close to the median value from the Christian era). It is the only burial dated from that archaeological site. Perhaps this individual was buried in the pagan style after Christianity had become the dominant religion and burial style.

AAR-5916 (A(individual) = 42.5) and AAR-5917 (A(individual) = 33.6), both Christian burials from Audbrekka, Hörgárdalur, are the youngest dates from the study and presumably represent later burials than the others chosen for Sveinbjörnsdóttir et al.'s study. They are the only dates from this location.

A fifth date is worthy of attention to interrogate the accuracy of this model. AAR-5908 (A(individual) = 77.5) is from the remains of the Bishop of Skálholt, Páll Jónsson, said in written sources to have died in AD 1211 (Sveinbjörnsdóttir et al. 2010:

[6] I am using more recent calibration curves than they did - their paper used IntCal04 and Marine04 - so there may be some small differences in calibration.

691). He had a marine diet percentage of 16%, and calibrated (not modelled) his remains date from 1044 to 1270 cal AD. In this model, the date leans old, its modelled range just barely encompassing AD 1211 (1035 to 1212 modelled cal AD at 95%). Although his remains have an acceptable A value and are technically consistent with written sources, they are worth considering as a test of the model.

None of these dates seems to be in error, so they have been left in the model because its overall A value was greater than 60. Instead, they demonstrate that a contiguous model does not fully represent the complexities of the conversion period, because there are limited examples that fall outside of this version of the chronology. Still, it is noteworthy that of forty-seven radiocarbon dated individuals, only four do not adhere to a model with a clear division between the pagan and Christian burial periods - and two of those appear in error not because they disprove that division, but because they are plausibly newer than the dates around them.

Table 9.10: Boundaries of contiguous model of Icelandic conversions presented in Figure 9.19. All dates are modelled cal AD.

Boundary	Start 68%	Start 95%	End 68%	End 95%
Start Pagan Burials	886	859	960	977
End Pagan/Start Christian	941	910	990	999
End Christian Burials	1072	1065	1226	1245

The contiguous model supports the idea, discussed at length by Vésteinsson (2000: 25) and argued for by Gíslason (1990) and Gunnell (2009) amongst others that one reason that the official conversion happened so quickly and without bloodshed was because many Icelanders were already Christian. Table 9.10 shows the boundaries generated by this contiguous model, and Figure 9.19 shows the results of the model. In this version of the chronology, the transition between pagan and Christian burial practices takes place sometime in the 10th century AD, and the mid- to late- 10th century at 68%. Aside from AAR-5877, which calibrates to approximately the 11th century AD when not constrained by the model, all of the pagan burials have an end point that, at 95% confidence, is at AD 999. At 95% confidence, Christian burials may start as early as AD 910, only roughly fifty years after the Norse colonisation of Iceland.

Given the dates that do not fit into a contiguous model, the next step was to create an overlapping model, similar to the one created for Orkney, with two phases: 'Pagan Burials' and 'Christian Burials.' Table 9.11 and Figure 9.20 show the results of this

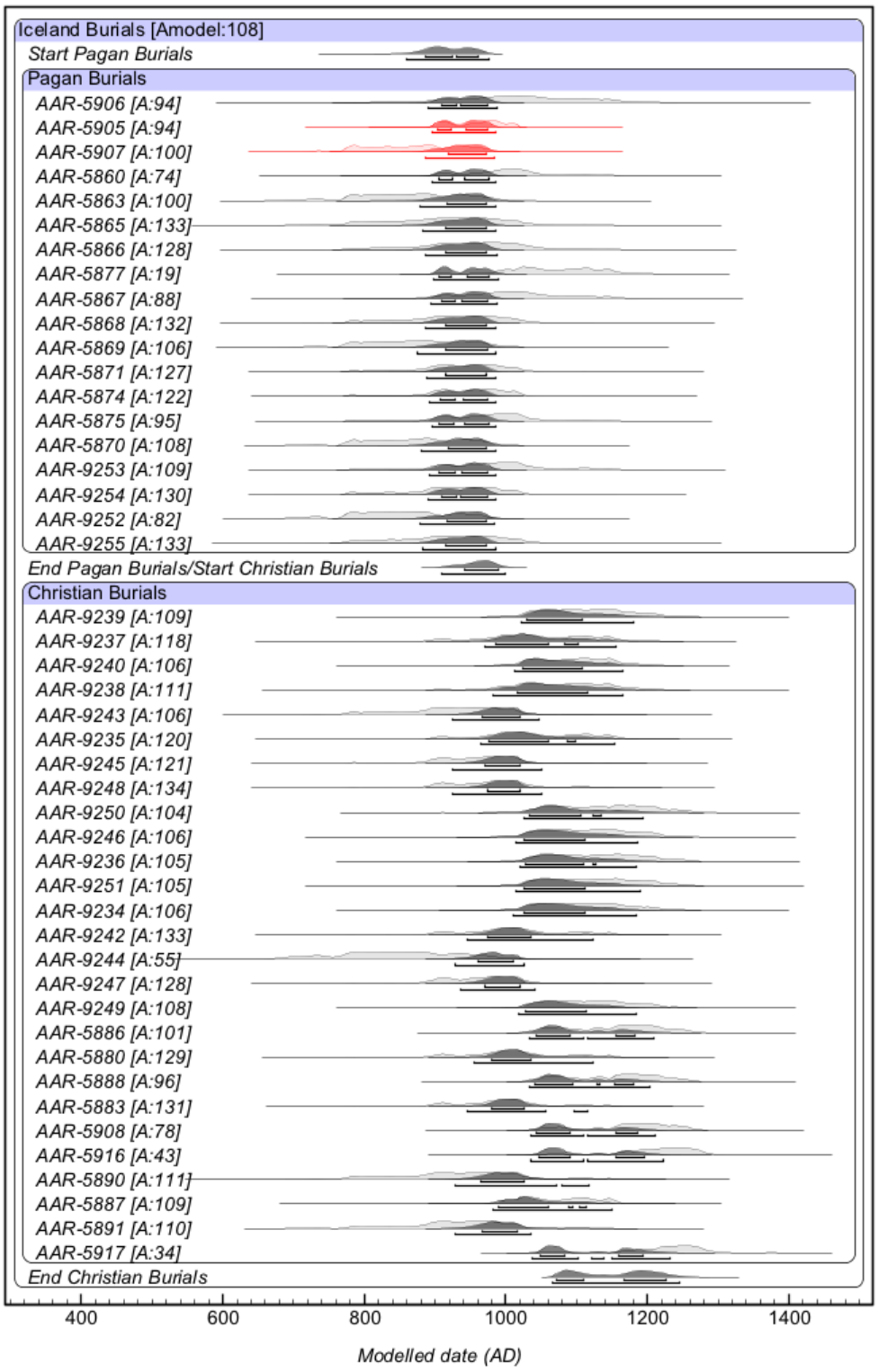


Figure 9.19: Results of the contiguous Icelandic burials model (Bronk Ramsey 2009; Reimer et al. 2013; OxCal v.4.3). The two dates appearing in red are on horse bone and are the only dates in the model that do not have a marine reservoir offset. N = 47, A = 108.1.

model. This model has A = 138.8. The earliest recorded pagan burials, especially at 68% confidence, accord well with the current understanding of the earliest settlement of Iceland, while the pagan period in both models benefits from being tightly constrained by that settlement event. Notably, even using this overlapping model, pagan burial practices have ended - at latest, even at 95% confidence - by AD 1031. Christian burials start in the early tenth century - and possibly even the late ninth century - again suggesting that Christianity was well known and practiced in Iceland before the official conversion.

Table 9.11: Boundaries from the overlapping Icelandic conversion model presented in Figure 9.20. All dates are modelled cal AD.

Boundary	Start 68%	Start 95%	End 68%	End 95%
Earliest Recorded Pagan	879	834	948	976
End of Pagan Burials	923	906	1015	1031
Christian Start	908	876	980	1011
Latest Recorded Christian	1066	1062	1243	1259

There are three dates in this model with individual A = lower than 60. As before, AAR-5877 (here A = 34.3) appears to be much younger than any other date from the pagan period. As an outlier, it is pushing the boundary 'End of Pagan Burials' forward in time. Also as before, AAR-5916 (A = 54.6) and AAR-5917 (A = 45.2) are younger than the other dates in the 'Christian Burials' phase. AAR-9244 (A = 66.1) now fits within the phase with an acceptable individual A value. AAR-5908 (Páll Jónsson) here has an A(individual) = 86.2, from 1036 to 1220 modelled cal AD, closer than the contiguous model to the written date for his death of AD 1211, but still relatively early.

Both of these models place the conversion - in terms of practice, rather than official declaration - of Iceland earlier than written sources suggest. It also places them earlier than the existing archaeological evidence for churches and churchyards suggest. It is reasonable to wonder if the marine reservoir effect is making these dates older. As has been discussed elsewhere in this document, Icelandic radiocarbon dates, especially those on bone, have presented difficulties for accurate calibration because of the MRE, and, in some cases, the freshwater reservoir effect (e.g., Ascough et al. 2010; Ascough et al. 2012). Combining dates with a varied range of marine diet percentages (0% to 65% across both pagan and Christian burials) resulting in plausible models with A values greater than 60 argues against there being a consistent MRE pushing these

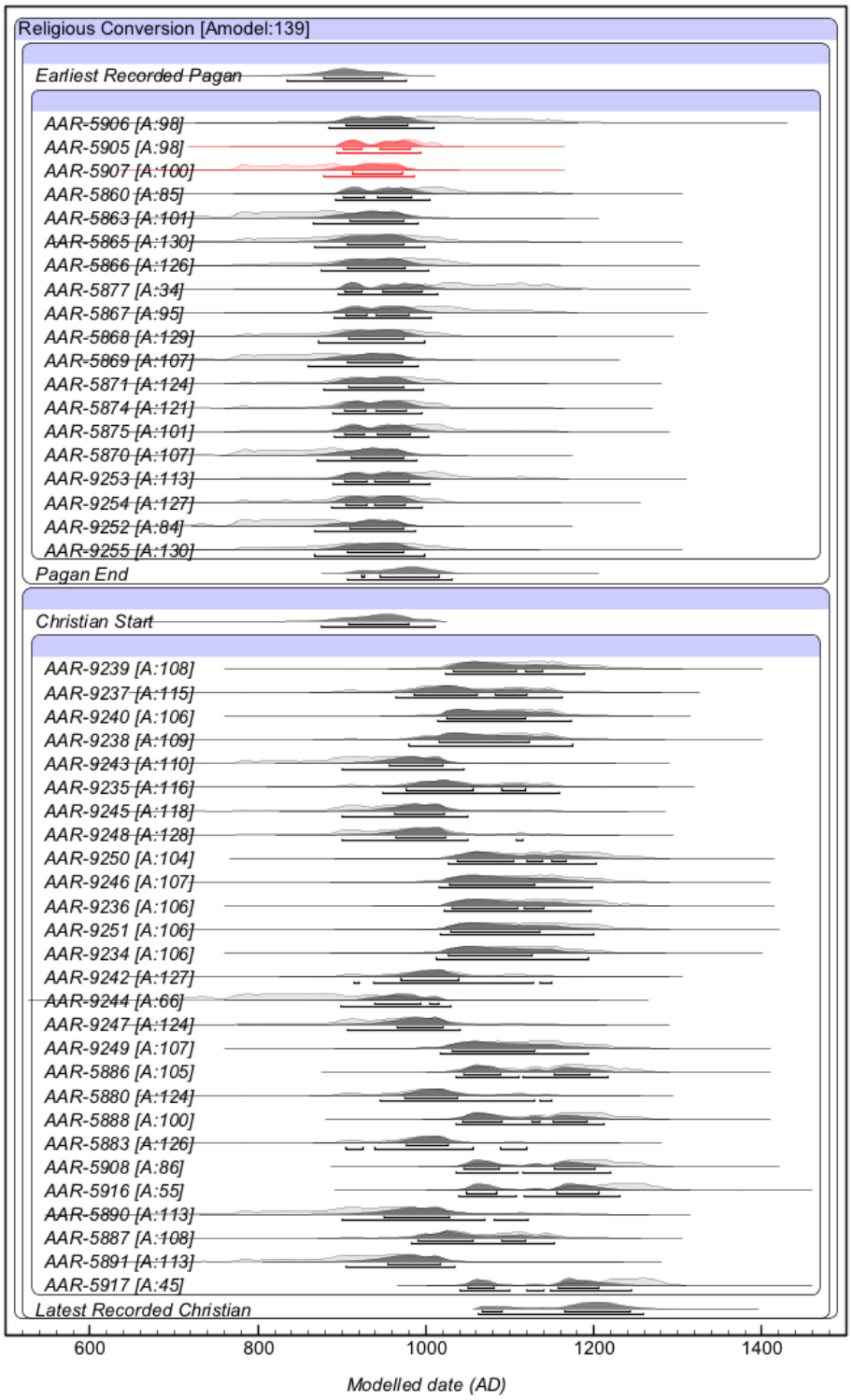


Figure 9.20: Results of the overlapping Icelandic burials model (Bronk Ramsey 2009; Reimer et al. 2013; OxCal v.4.3). The two dates appearing in red are on horse bone and are the only dates in the model that do not have a marine reservoir offset. A = 47, N = 138.8.

dates backward. For example, from the pagan period, AAR-5906 from Brimnes vis Dalvík has a marine diet percentage of 65%; AAR-5905, also from Brimnes vis Dalvík, has a marine diet percentage of 0%. These two dates model to be almost identical in age with the reservoir correction applied. There is no indication that dates with higher percentages of marine diet are skewing the model older.

Is there a geographical component to the chronology of conversion in Iceland? The results of these models suggest that there were no particular regions that either held on to pagan-style burials for longer than others or converted to Christian-style burials sooner than others. The five most recent pagan burials are from four different locations almost as geographically disparate as it is possible to be in Iceland - one each from Vad, in the east, Straumur, Tunguhreppur, in the southwest, Vatnsdalur, Patreksfjordur, in Vestfirðir, and two from Brimnes vis Dalvík, in the north. The earliest Christian burial dates are from Keldudalur (northern) and Skeljastaðir, Thjórsárdalur (southern lowlands). This information suggests a decentralised form of both religions, perhaps one driven by influential individuals. It also suggests that at least some Icelanders were well-travelled within their own country, allowing ideas to disseminate far and wide, supported by the mixture of ideas at the summer meeting at the Alþingi.

The results of the chronological models presented here make a strong case that the infrastructure (churches and churchyards) and personnel (priests able to baptise) to convert Icelanders to Christianity were present in tenth century Iceland - and not just concentrated in certain areas, but scattered and/or travelling throughout the country. Archaeologically, evidence for this implied infrastructure has not thus far been discovered. Vésteinsson (2000: 38-39) lists early churches described in the sagas, but very few of these can be verified archaeologically. Similarly, the cemeteries listed by Sveinbjörnsdóttir et al. (2010) are more limited in scope and cannot possibly account for all the burials from this period. The results presented here argue for a focus on searching for more of these early churches and churchyards.

9.3.3 Conversion Chronology - Orkney and Iceland

Comparing the timing of conversion in Orkney and Iceland using these models, there are some notable differences. As discussed in the section above this one, Orkney's conversion period had significant overlap between pagan burials and Christian burials, and an overlapping model, able to assume a significant period when Orcadians - probably located in different parts of the archipelago - simultaneously practiced both

pagan and Christian burial rituals seems to represent the period more accurately. Iceland, in contrast, is well represented by a contiguous model, and there are only a few outliers from this data set, seemingly representing individuals who were buried in a different manner than their contemporaries. The geography of conversion, based on these models, indicates that Iceland had a more homogenous culture, at least in religious practice, than Orkney.

Vésteinsson discusses the relatively unique nature of Icelandic settlement - small communities, controlled by local elites and often separated by steep fjords or other geographical barriers - and theorises that, especially in the early Christian period, elites may have built churches as a way to consolidate their power in the landscape (2000). They had entered an empty landscape without obvious centres of power aside from locations favourable to agriculture or maritime activities. It seems likely that early settlers were eager to make fortunes and establish themselves as chieftains, and supplying a centralised place of worship, conveniently located on the farm, would have been an excellent way to do so. The models presented here, which argue for an earlier conversion, within just a few decades of the settlement of Iceland rather than over a century afterward, agree with this reasoning - in the essentially unsettled land of opportunity, it makes sense that anything someone could do to attract more people to their new farm would be jumped at eagerly.

The Norse settlement of Orkney proceeded differently. Revisiting Section 2.2.1, the exact nature of the interactions between the arriving Norse and the long-time Pictish occupants is not known, but seems to have been varied, with a few elite centres in the landscape (e.g., the Brough of Birsay and the Brough of Deerness (Morris 1989; Morris 1996; Buteux 1997)) and some more independent, seemingly successful farms (e.g., the East Mound (Griffiths forthcoming), Pool (Hunter 2007), Westness (Kaland 1993), and Buckquoy (Ritchie 1977)). Presumably the Norse settlers in Orkney were able to take over - either peaceably, by marriage or purchase, or violently - farms and areas in the landscape that already had been proven to be successful. Although competition for elite status would have still be fierce, given what was already known about the landscape, the drive to build Christian churches as a way to further enhance the wealth of a farm and, crucially, draw in new arrivals, may have been less intense in Orkney.

9.4 Greenland - Timing of Settlement, Landscape Use, and Abandonment

The current body of dates from Norse Greenland can be divided geographically into the three settlements, Western, Middle (sometimes considered part of the Eastern), and Eastern. Below, I create a Bayesian model to understand the timing of settlement at each and to consider the relationships between the three.

Many of the dates from Greenland have been assigned more detailed phasing information by previous authors, but not all of it is useful to modelling the settlement history. Arneborg et al. (2012; 2012b) present a chronological division of Norse Greenland based on the dates in their study like this: Early Norse (AD 980-1160), Mid Norse (AD 1160-1300), Late Norse (AD 1300-1450). Their reason for creating these categories is changes in diet, with a steady increase in marine resource percentage throughout the period but a discernible levelling off around AD 1300 (with the highest percentages from the later period of the Eastern Settlement) (ibid: 123-124). All of the dates on human bone from burials are culturally Christian or from churchyards, as are all of the human burials from the study by Arneborg (et al. 1999), so aside from dietary percentage and any stratigraphic information, there is not another way to distinguish between discernible cultural periods (and no way to discuss if Norse Greenland was always Christian). Inputting these dates with these period distinctions into a larger model with the dates from the other studies would, because of the great number of them, mathematically force the model to conform to the idea of diet as the sole determinant in Norse cultural change throughout a period of nearly 500 years - something that does not align with the evidence from the other studies included in this database. For example, Schofield et al. (2008), in their pollen-based study of the archaeology of the Qorlortoq valley in the Eastern Settlement, see a gradual record of change, with subtle but noticeable effects on vegetation after *landnám*, including the possible cutting of peat for construction, but no clear boundary for a transition from an early Norse cultural period of settlement to a later one. Schofield and Edwards (2011), writing about Qinngua, also in the Eastern Settlement, describe what may be sustainable use of birch woodlands, in contrast to the prevailing picture of birch decline at other locations in the Norse North Atlantic. Further, although there is evidence for Norse diet changing throughout time from many other studies, especially zooarchaeological ones (c.f. McGovern 1985), there is not evidence for the Norse themselves considering a change in diet a major cultural change. As a result,

all of these studies together cannot be divided into culturally meaningful periods such as Early Norse, Mid Norse, and Late Norse. The clearest things that we can model with the entire dataset as it is currently are the periods of *landnám*, land use, and abandonment for the Eastern, Middle, and Western Settlements.

As elsewhere in the North Atlantic, radiocarbon dates on bone from Greenland need to be corrected for the marine reservoir effect. A substantial portion of dates in the database are on human bone from a study of Norse diet using stable isotopes across both the Eastern and Western Settlements of Greenland (Arneborg et al. 2012; 2012b). A second group investigating similar issues are from Arneborg et al. (1999). In both of these studies (Arneborg et al. 2012 and 2012b are one study), the authors used $\Delta R = 50$ to correct for the marine reservoir effect on their dates; this figure was derived from three textile samples compared to an archaeologically associated bone sample (AAR-1269) with a high (78%) marine diet percentage (Arneborg et al. 1999: 162). This is significantly different from the value given by the Queen's University Belfast Marine Reservoir Database (last accessed 22 February, 2016), $\Delta R = 135 \pm 65$, which is based on four readings from McNeely et al. (2006) and five from Olsson (1980), all taken from the western coast of Greenland. These are all within the West Greenland Current, which sweeps around the southern part of Greenland and up its western coast (Yang et al. 2016) past where the Eastern, Middle, and Western Settlements of Greenland were located. Further, this second value is consistent with those used by Edwards et al. (2013: 26) to correct their dates from the Middle Settlement, a more recent publication. I have chosen to use this most recent value, $\Delta R = 135 \pm 65$, to calibrate dates from human bone with a marine percentage in their diet.

As is standard practice (Cook et al. 2015), I used linear interpolation to determine the marine percentage of diet, using -21‰ as a 100% terrestrial diet and -12.5‰ as 0%. I have recalculated all percentages, rather than using the original authors' percentages where given. Python code for linear interpolation is located in Appendix G. Table 9.12 compares four dates across the spectrum of marine percentage possible in this dataset, ranging from $\delta^{13}C$ = -14.1 ‰ (AAR-1146) to $\delta^{13}C$ = -19 ‰ (AAR-1568). The results show some differences, especially for AAR-1267, where its range has widened considerably.

Aside from the dates on human bone, there are three animal bones that have also been given marine diet percentages: one from a dog, one from a pig, and one from a wild boar. Erle et al. (2012) have found that, aside from dogs and pigs, there is little

Table 9.12: All dates given are in calibrated age AD at the 1 sigma range. Comparison between published results and my calibration using $\Delta R = 135 \pm 65$. My calibration done using Intcal13, Marine13, and Oxcal (Bronk Ramsey 2009; Reimer et al. 2013; OxCal v.4.3).

Date	Arneborg et al. Correction	New Correction
AAR-1146	1323-1412	1311-1405
AAR-1570	1063-1227	1060-1210
AAR-1267	995-1043	960-1122
AAR-1568	1046-1218	1049-1205

evidence for needing to adjust for marine signal in Greenlandic domesticated animals, especially herbivores. However, Arneborg et al. (1999) and Edwards et al. (2013) note that reindeer (*Rangifer*), who were presumably eating seaweed and have slightly elevated δ^{13}C values, may demonstrate the marine reservoir effect. All animals with a δ^{13}C value higher than -21‰ have been calculated for marine diet percentages.

The history of the Western Settlement is bookended by AD 985, the traditional date for the foundation of the Greenland colony (which I have given an error range of ±10 for in the model to cover any uncertainty), and by a letter written by Ivar Bardarson to the Bishop of Bergen, in which he wrote about events that happened around AD 1341 to 1360: 'now the Skraeling [Inuit] have [destroyed] the whole of the Western Settlement. There are only horses, goats, cattle, and sheep all wild, but no inhabitants, neither Christian nor Heathen' (National Museum of Natural History, https://www.mnh.si.edu/vikings/voyage/subset/greenland/history.html, last accessed January 2016). Bardarson left Greenland behind, and by 1360 he was in Bergen, serving as the Canon of the Bergen Cathedral. As dramatic as his letter is, the modelled dates below place the end of the Western Settlement later - potentially much later.

The dates in the database from the Western settlement are on bone, both human from burials and animal from middens and farm deposits (Arneborg et al. 1999; Arneborg et al. 2012b). The locations of all of these are shown in Figure 9.7. CAMS-62001 and K-4119 were immediately eliminated from the model for being from unknown phases, and CAMS-62002 because its date is so recent as to seem intrusive or incorrect. Excavators placed some of the dates in the Inuit period prior to the Norse period, so the model consists of these two periods. I did not place the letter as an end-date because Arneborg et al. (2012b) reported several locations that appeared to have

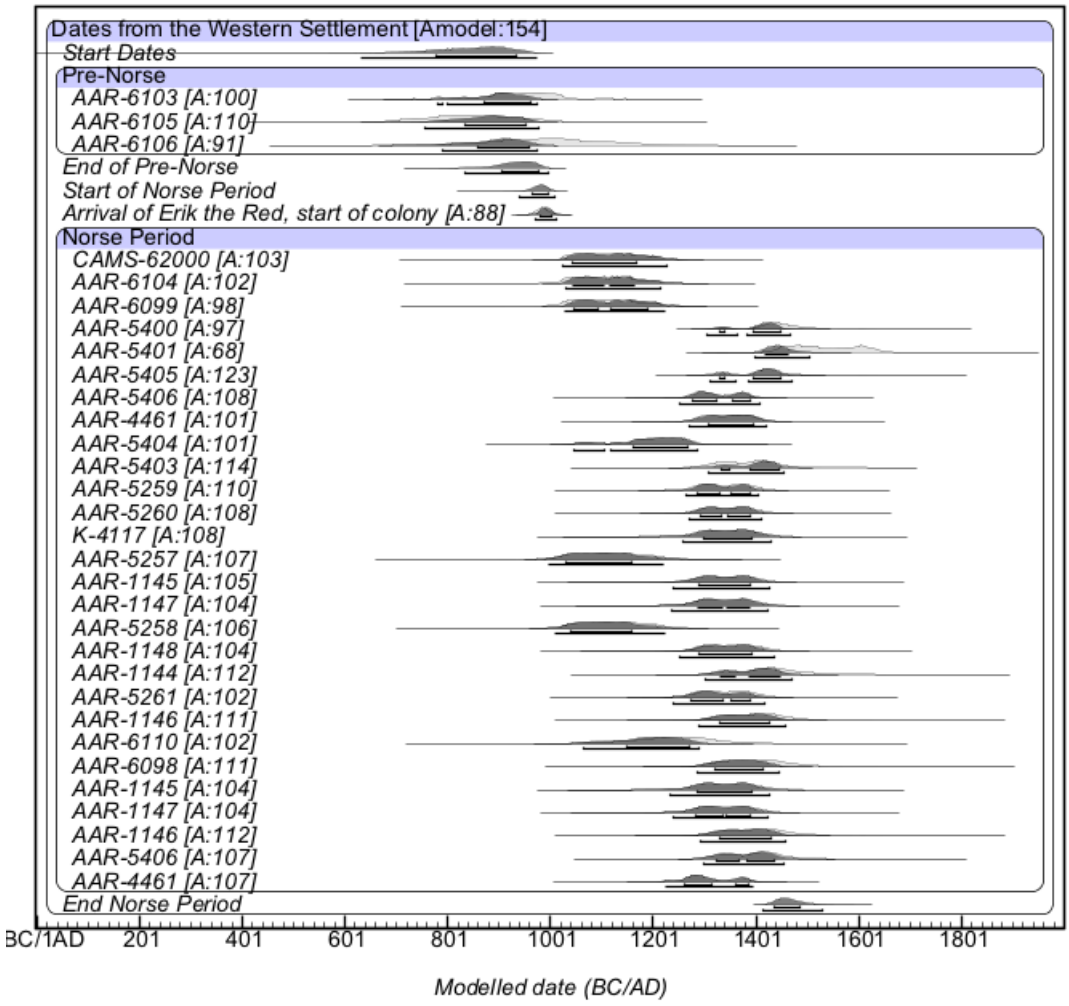


Figure 9.21: Model of the Western Settlement of Greenland (Bronk Ramsey 2009; Reimer et al. 2013; OxCal v.4.3). N = 31, A = 154.

been occupied after that: Anavik, the Farm Beneath the Sands, and one date, AAR-1144, on human bone from a churchyard burial at Sandnes. The results of the model are shown in Figure 9.21, with A(model) = 154 and no dates originally in the model needing to be eliminated from its admittedly simple structure. Table 9.13 shows the boundaries of the model.

Unsurprisingly, given that their paper is the source of every radiocarbon date in it, the model agrees with Arneborg et al. (2012b) that there is evidence for the Western settlement having a Norse presence at least fifty years - and possibly many more - beyond Ivar Bardarson's doom-laden letter. The boundaries of the Norse period here are from 941 to 1010 to 1416 to 1530 modelled cal AD at 95%. The latest

Table 9.13: Boundaries from the model of the Western Settlement shown in Figure 9.21. All dates are modelled cal AD.

Boundary	Start 68%	Start 95%	End 68%	End 95%
Start of Pre-Norse	730	632	936	976
End Pre-Norse	905	835	978	995
Start Norse	966	941	997	1010
End Norse	1435	1416	1485	1530

dates are AAR-5400, a date on animal bone from room 3 of the Farm Beneath the Sand (1307 to 1468 modelled cal AD) and AAR-5401 and -5405, both also on animal bone, from room 1, possibly the roof, of the Farm Beneath the Sand (1398 to 1505 and 1311 to 1470 modelled cal AD) (both at 95%). Overall, the model finds the duration of the Norse period at the Western Settlement is between 420 and 541 years at 95%. The marine reservoir effect should not be a factor in the accuracy of these most recent modelled dates, because their percentage of marine diets are only 13% and 0% respectively. These results posit a considerably longer period of time than the traditionally accepted written sources state for the Western Settlement, and than archaeologists have traditionally considered (e.g., Barlow et al. 1997).

Also in line with Arneborg et al.'s results are the majority of the human burials coming from individuals who died around or just before AD 1300; these individuals, aside from AAR-5404, all have marine percentage diets above 50%. Interestingly, two individuals buried in the churchyard at the high status farm of Sandnes (AAR-5257 and -5258) are earlier than many of the other dates from the Norse period (respectively 996 to 1222 and 1010 to 1225 modelled cal AD at 95%), but still have high percentage marine diets - does this represent individual choice? Immigrants from another area, as Fricke et al. (1995) suggest? Both are tantalizing possibilities.

The Middle Settlement has been much less studied than either of its larger neighbors. It is considerably smaller, with settlement focused on the fjord edge, and, thus far, no known large farms or church. Edwards et al. (2013: 3) describe it as a location with a less favourable climate for agriculture than the other Norse settlements in Greenland. The only scientific dating information from this site currently extant is from Edwards et al. and consists of fourteen dates, of which they assign nine to the Norse period. Three of the others are likely post-Norse Inuit, while the other two are probably modern and will not be included in this model. The model is divided into two phases, 'Norse' and 'Post-Norse,' with the Norse period additionally divided into

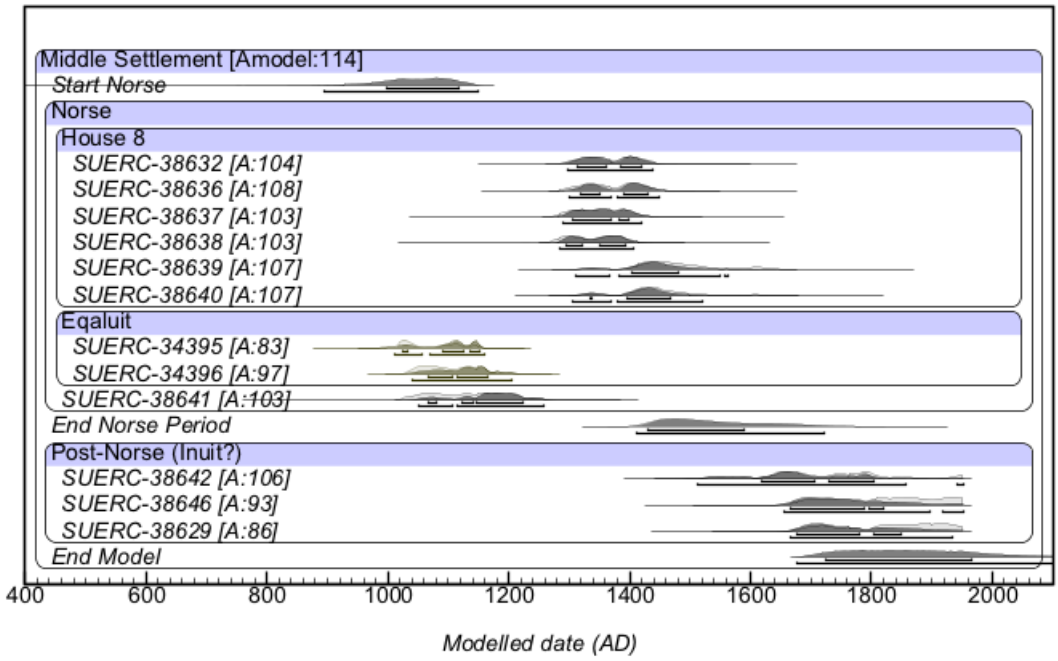


Figure 9.22: Model of the Middle Settlement of Greenland (Bronk Ramsey 2009; Reimer et al. 2013; OxCal v.4.3). N = 12, A = 114.

two phases, one for House 8 from the ruin group at Grønnedal and the other from Eqaluit. The Norse phase also includes a single date from the ruin group at Tissaluk. The two dates from Eqaluit, SUERC-34395 and -34396, were sampled sequentially from a midden. Although the dates are inverted, Edwards et al. show with a chi-squared test that they are statistically indistinguishable (10), so they are used in this model, grouped in a single phase but not sequentially. All dates but those from the midden have a marine diet percentage and have been modelled accordingly.

Table 9.14: Boundaries of the Middle Settlement model shown in Figure 9.22. All dates are modelled cal AD.

Boundary	Start 68%	Start 95%	End 68%	End 95%
Norse Start	997	893	1118	1149
Norse End	1429	1410	1590	1722
Model End	1725	1966	1677	n/a

Figure 9.22 shows the results of the model for the Middle Settlement, while Table 9.14 shows the boundaries of the model. This model should be understood as a starting point for exploring the chronology of the Middle Settlement, as it relies upon a small sample size of dates taken from three locations. As is also noted by Edwards et

al., the dates they have sampled cluster in two groups, with the dates from Eqaluit modelling earlier than those from House 8. The plateaux in the calibration curve mean that both groups have wide ranges, particularly at 95%. Keeping these things in mind, this model suggests that the Middle Settlement may have been occupied for as long as the Eastern and Western Settlements were. The results from House 8 are particularly interesting in light of the poorer agricultural potential of the landscape at the Middle Settlement, as the model indicates that it was a functional, if not large, farm during the colder and less predictable climate of the LIA.

Compared to the other two settlements, the Eastern Settlement has many more dates, and a much more diverse set of sample materials and study types. There are dates on bone, including many from human burials (Arneborg et al. 1999; Arneborg et al. 2012b) but there are also several environmental studies with internal chronology from position in core samples. As a result, the model for the Eastern Settlement is broken up into a series of sequences within the Norse activity period: Tasiusaq (Edwards et al. 2008), Qinngua (Schofield and Edwards 2011), one sequence from Igaliku (Gauthier et al. 2010), and another from Igaliku (Buckland et al. 2009), Qorlortoq Valley (Schofield et al. 2008), Sandhavn (Golding et al. 2011), Lake Vatnahverfi (Ledger et al. 2014a), Atikilleq (Ledger et al. 2015), Nimerialik (Ledger et al. 2015), and the Mountain Farm, Vatnahverfi (Ledger et al. 2013).[7] Some of these dates (as will be evident from the model results) have been separated from their sequences because they date from a pre- or post-Norse period in the landscape. The rest of the dates have been modelled as Norse period, with the inclusion of C Dates for the settlement of Greenland (AD 985 ±10) and AD 1408 ±5, the date of the letter from Icelandic papal envoys to the Vatican describing a wedding in Hvalsey Church, known as the final written record from Norse Greenland.

Figure 9.23, Figure 9.24, and Figure 9.25 shows the model for the Eastern Settlement, which has A(model) = 117.9, with N = 136 total dates. Only one date has A(individual) = lower than 60, which is SUERC-8901 (A = 44.8). This date is in sequence with SUERC-8905 in the post-Norse period and dates slightly younger than the date it is stratigraphically below. The two overlap within their error ranges, so this date does not seem to be incorrect and has been left in the model.

With the large number of dates available from the Eastern Settlement, this model has the most precision of any of the Greenland settlements. The modelled boundary for

[7]Saqqaata Tasia (Ledger et al. 2014) and Tasilikulooq (Ledger et al. 2017) have not been included because of issues with the dates and their sequences that the authors highlight.

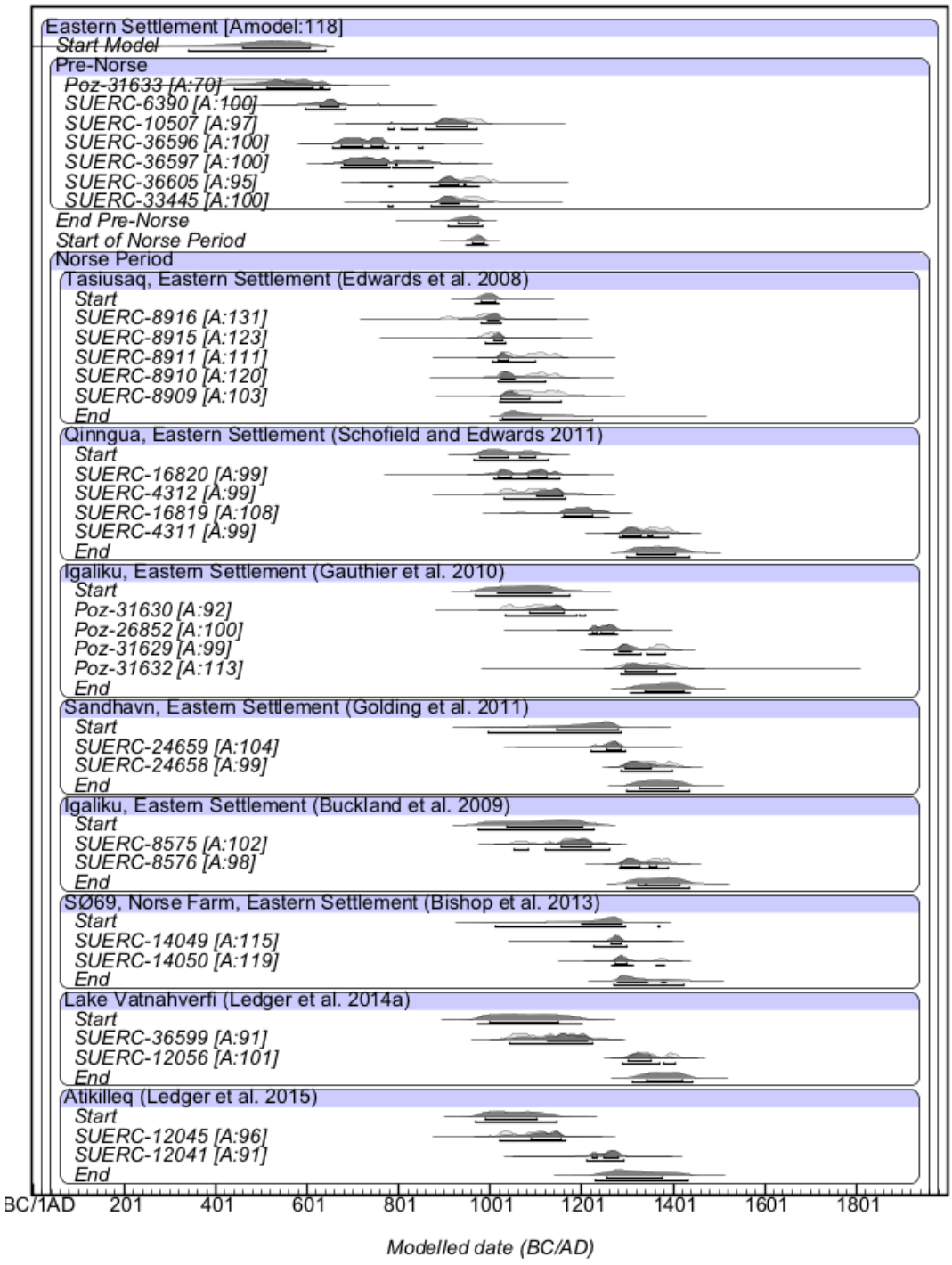


Figure 9.23: Eastern Settlement model part A, from the start of the model to the end of the Atikilleq sequence. (Bronk Ramsey 2009; Reimer et al. 2013; OxCal v.4.3). For total model, N = 136, A = 117.9.

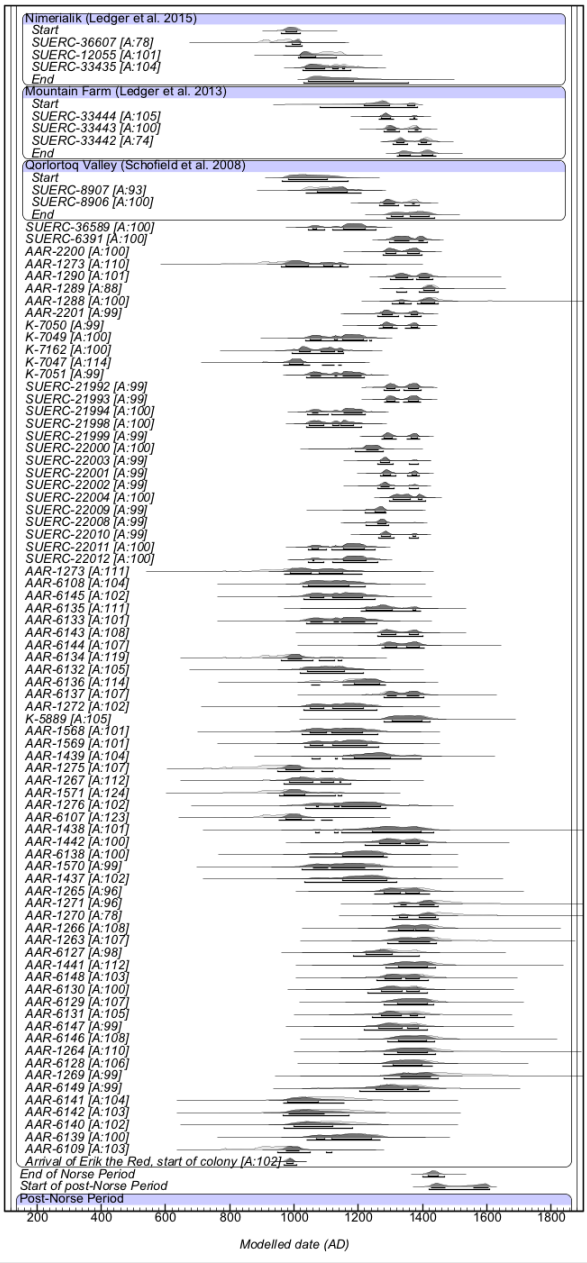


Figure 9.24: Eastern Settlement model part B, from the last date of the Atikilleq sequence to the end of the Norse period. (Bronk Ramsey 2009; Reimer et al. 2013; OxCal v.4.3). For total model, N = 136, A = 117.9.

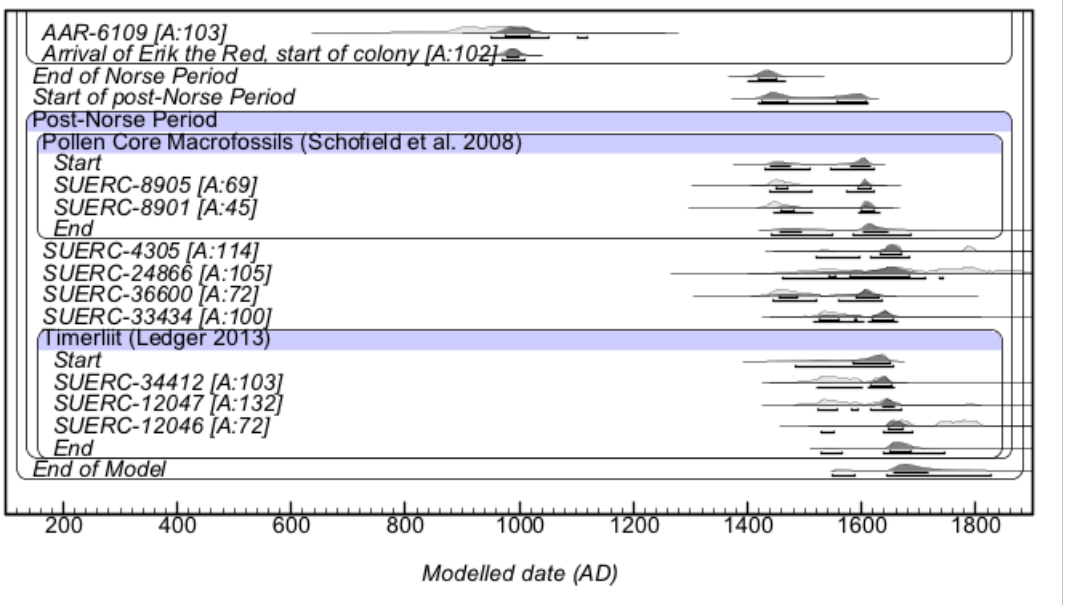


Figure 9.25: Eastern Settlement model part B, from the end of the Norse period to the end of the model. (Bronk Ramsey 2009; Reimer et al. 2013; OxCal v.4.3). For total model, N = 136, A = 117.9.

Table 9.15: Boundaries from the model for the Eastern Settlement shown in Figure 9.23, Figure 9.24 and Figure 9.25. All dates shown are modelled cal AD.

Boundary	Start 68%	Start 95%	End 68%	End 95%
Start Model	461	343	606	640
End Pre-Norse	931	910	974	985
Start Norse	961	946	986	996
End Norse	1418	1400	1449	1468
Start Post-Norse	1426	1420	1606	1610
End Model	1655	1548	1716	1827

the beginning of the Norse period, 946 to 996 modelled cal AD at 95%, agrees with the traditional date of AD 985 for the establishment of a Norse colony in Greenland. The modelled end of the Eastern Settlement, 1400 to 1468 modelled cal AD, fits with the traditional one: the Hvalsey wedding of AD 1408, supposedly the final major social event at the Eastern Settlement and in Norse Greenland, fits into the early part of that range.

The model uses two distinct strands of evidence: the sequences from cores and the direct dating of archaeological material like human burials and settlements. The former tends to place the end of Norse occupation at the Eastern Settlement in the

mid-15th century AD (e.g., Ledger et al. 2015). Is there agreement between the two on this later end date? Table 9.16 shows the modelled ends of the Norse period for each of the core sequences included in the Eastern Settlement model. Aside from Tasiusaq, which comes from a sequence focused on the early Norse period (Edwards et al. 2008), all have a range of modelled end dates that could plausibly see the end of the Eastern Settlement in the early to mid-15th century AD. The reasons given for dating this as the end of the Norse period at each location relate to a decline of farming activity (Igaliku (Gauthier et al. 2010), the Mountain Farm (Ledger et al. 2013), and Sandhavn (Golding et al. 2011)), a rise in Cyperaceae (sedges) indicating a return to a steppe and mire environment (Lake Vatnahverfi (Ledger et al. 2014a)), falling levels of charcoal (Atikilleq and Nimerialik (Ledger et al. 2015)), and a re-expansion of Salix (willows) at Qorlortoq (Schofield et al. 2008).

Table 9.16: Modelled ends of the Norse period for each of the core sequences included in the Eastern Settlement model

Core Location	Modelled End Date cal AD at 95%
Tasiusaq	1022-1225
Qinngua	1300-1435
Igaliku (Gauthier et al. 2010)	1304-1440
Igaliku (Buckland et al. 2009)	1298-1438
Sandhavn	1301-1438
Farm Ø69	1272-1424
Lake Vatnahverfi	1312-1441
Atikilleq	1229-1434
Nimerialik	1031-1357
Mountain Farm	1319-1443
Qorlortoq Valley	1288-1438

The archaeological evidence as modelled here agrees with the evidence from environmental studies. The two latest dates model, at 95% to modelled cal AD 1281 to 1440 (AAR-1264) and 1279 to 1450 (AAR-1269). Both are churchyard burials, implying that, even if they are from the latest point of their range, there was at least someone left in the Eastern Settlement to bury them - but, combined with the decline in agricultural activity as discerned through the use of local pollen assemblage zones, assigning an early to mid-15th century date to the abandonment of the Eastern Settlement seems correct.

According to the models presented above, the three settlements have strikingly similar periods of occupation, as shown in Table 9.17, belying the argument that the Eastern

Settlement was longer lasting than the Western, and bringing the Middle further into our understanding of the chronology of Norse settlement. The modelled longer end of the Western Settlement compared to the Eastern Settlement may be a result of a smaller sample size resulting in less precision in the model.

Table 9.17: Comparison of the modelled Norse periods from the three different settlements in Greenland. All dates are modelled cal AD.

Settlement	Begin 68%	End 68%	Begin 95%	End 95%
Western	966-997	1435-1485	941-1010	1416-1530
Middle	997-1118	1429-1590	893-1149	1410-1722
Eastern	961-986	1418-1449	946-996	1400-1468

9.5 Modelling *landnám*

Modelling is concerned with defining moments of change. There is not a clear distinction to mark the end of the Norse cultural period in any of the North Atlantic polities discussed above (aside from the Greenland colony - but it seems likely that the culture there had become similar to what we call 'medieval' elsewhere in the North Atlantic by the time of its abandonment). What about clear evidence for the beginning of the Norse period? The question of when the Norse settled in a particular landscape is one that has fascinated researchers and drawn research projects throughout the North Atlantic, and, given focused chronological data, often with an environmental focus on vegetational change, it can be modelled. On Orkney, Shetland, and the Western Isles, the Norse entered a landscape with settled human inhabitants, but the transition appears to have created new cultural types - Norse farms built over earlier Iron Age farms, like at Old Scatness, Shetland, or different burial styles, like the boat burials at Scar, Orkney. In the Faroe Islands, although there is evidence for limited amounts of human settlement before the Norse came, the evidence for Norse arrival is not just in the construction of farms but also in a changed pollen regime as their agricultural practices transformed the landscape. This landscape transformation is also evident from Greenland and Iceland. Finding a start date without specific environmental studies (as we have for the Eastern Settlement of Greenland and the Faroe Islands) presents difficulties because of the vagaries of archaeological sites - although we may have evidence for many settlements, as we do from Orkney, we do not know if these are the *first* settlements or just the ones we have been lucky enough to find.

Using the available evidence and the models presented above, it is possible to model *landnám* as understood by current scientific dating for each of the areas of Norse colonisation discussed in this chapter (aside from Vinland). Figure 9.26 compares the modelled chronological ranges of settlement across the landscape, using dates from each of the locations discussed above. The map highlights the waves of settlement across the landscape, with Shetland the earliest, followed by similar time frames for the Faroe Islands and Orkney. Next, Iceland and the Western Isles share a similar modelled date range. Finally, the Eastern and Western Settlements of Greenland have very similar modelled ranges for *landnám*, while the Middle Settlement models to very soon after.



Figure 9.26: Map comparing modelled dates for *landnám*, based on models created above.

9.6 Conclusions

There is a relatively large body of published chronogical information available from the Norse period in the North Atlantic which I have gathered together here, with some areas (e.g., Greenland's Eastern Settlement) more represented than others (e.g., the Western Isles). Drawing together chronological information, particularly from published sources, unsurprisingly demonstrates both the potential and the limitations of the current data set for constructing narratives linking archaeological and environmental change. We are fortunate as researchers of the North Atlantic to have the amount of scientific chronological information that we do, especially compared to many other study areas, and to have much of it from the last twenty-five years of AMS dating. There are still notable gaps in the record, highlighted by the influence of certain well-dated archaeological sites on models designed to simulate change in larger landscapes. The marine reservoir effect and plateaux in the calibration curve present challenges to calibration and modelling of radiocarbon dates from this region, but they are not barriers to using these crucial tools to understand the chronology of the past.

The cultural and settlement changes modelled above - length of use, religious conversions, and arrival and departure in the landscape - can all be studied using Bayesian modelling. A change in burials, as from Orkney and Iceland, signalling a large-scale conversion, is one of the most successful ways to see this from the evidence here - but individuals who chose not to convert or who were ahead of the trend need to be kept in mind when creating models, so that important evidence is not treated as an outlier. Changes in diet are murkier to interpret as periods of cultural change. Barrett (2000) has argued that the rise in consumption of fish in Norse/medieval Orkney can be linked to the rise of Christianity and its imperative to abstain from (terrestrial) meat at certain religiously proscribed times, but the rise in marine resource consumption in Greenland has been interpreted as being the result of proximity to marine food resources, limited terrestrial food resources (i.e., only people of high status having access to the most desirable meat products), and adaptation to the Greenlandic environment (Arneborg et al. 2012; 2012b). Use of resources in the landscape - peat (e.g. Schofield et al. 2008) or birch (e.g. Church et al. 2007) - or landscape modification like irrigation channels (e.g. Arneborg 2005) - throughout time are avenues to explore further for evidence of cultural change. Finally, as demonstrated by the long periods of occupation identified as Norse by excavators, particularly in Shetland,

cultural transition periods can be elusive even at the level of a single archaeological site.

Subjects for modelling across sites, and even up to the regional level, must be chosen carefully. Given a focused research question and sensitivity to circumstances that impact date choices and the outcome of statistical models, as demonstrated above, Bayesian modelling can shed new light on local and regional archaeological questions.

10 | Conclusions and Future Research

In the introduction to this thesis, I argued that improving archaeological site chronologies and creating linked regional chronologies would illuminate environmental and social change in the North Atlantic. Throughout this work, I have focused on ways to improve chronologies: both at the local level in the two archaeological landscape case studies, and by working with published chronological data from across the Norse colonisation zone to pose questions and suggest answers about the archaeology of the region.

10.1 Summary of qualitative results

The qualitative results of the thesis can be divided into three categories: tephra identifications, database construction, and refinement of existing chronological information.

First, I have identified over forty tephra and microtephra layers found in the two archaeological excavations, Vatnsfjörður and the East Mound; four peat cores, Hobbister B, Spretta Meadow, the Vatnsfjörður homefield, and Kaldalonsjökull; and one lacustrine core, Sveinhúsavatn. The majority of these tephra layers came from Iceland but some were also identified in Orkney, although none were found in the East Mound excavations. As the majority were microtephras, they were extracted using microtephra extraction techniques based upon Blockley et al. (2005) and those that were successfully extracted in large enough quantities were probed for geochemical classification. WDS-EPMA data from the tephra and microtephra layers studied are summarised in Table 6.1 and in Section 6.3.

Second, I have gathered together a database of published (and in some cases, unpublished) chronological data relating to the North Atlantic ca. AD 900-1800, which is included with this volume on a CD.

Third, both for the East Mound and with published data from across the North Atlantic islands, I have created Bayesian models in OxCal to explore archaeological questions through chronology building. In many cases, these have led to more precise and accurate chronologies: narrowed date ranges for successful models and identification of possibly problematic dates within the dataset.

10.2 Summary of main interpretation

In this thesis I correlated or 'fingerprinted' the tephra layers found in the sample materials with known eruptive events. These identifications are summarized in Table 7.5 for Iceland and in Section 8.2 for Orkney. They were then used to build chronologies for the various records studied. At the East Mound, the stratigraphy of the site was combined with the radiocarbon and OSL dates to create a Bayesian model in OxCal (Bronk Ramsey 2012). This model identified problems with some of the radiocarbon dates and made many of the others more precise. It allowed the linking of all but one of the excavation areas, much like the Hekla 1693 tephra tied together all the excavation areas at Vatnsfjörður. At Vatnsfjörður, the pollen and charcoal from the homefield and forams from Sveinhúsavatn provided supplementary environmental information to enhance the archaeological interpretation. By linking these records using chronology, they were used to interpret how environmental change may have affected the inhabitants at each location. This research was interdisciplinary, and like many studies of human/environment interaction, could not have been possible without some collaboration with environmental scientists, who have always been credited in the text.

These interpretations are in Section 7.9 and Section 8.5. Some of the major findings are:

At Vatnsfjörður:

- The visible tephra layer found throughout the site correlates strongly to published data for Hekla 1693 (Dugmore et al. 2007b). This tephra layer is advantageously placed from an archaeological point of view because the farm at Vatnsfjörður is known from historical sources to have gone into decline in the late seventeenth century. There is currently no evidence from the archaeology of any major shift around this date aside from the deposition of the tephra layer

which, although visible in the stratigraphy, was at most a few centimetres thick and so should not have had a long-lasting effect upon the farm.

- The current published glass chemistry data for Hekla 1693 (in Dugmore et al. 2007b) may not take into account some of the variations in the tephra. A large body of single shard analyses has been recorded in this thesis and may be used to better understand the composition of tephra from this eruption.

- The Hekla 1693 layer forms a *terminus ante quem* for the Viking Age area of excavation at Vatnsfjörður. There does not seem to have been a clear and abrupt transition from activities at the Viking Age area to the farm mound. In Area 14 (within the Viking Age area), the tephra layer lies immediately atop wall collapse from a building of some kind, while at Area 32 (also in the Viking Age area) it is separated from cultural layers by a layer that seems to have no cultural remains whatsoever. Usage in some specialised areas of the portion of the excavations labelled 'Viking Age' may have continued long after it had stopped in other areas.

- Sveinhúsavatn transitioned from a bay to a lake sometime between AD 1350 and 1600. This transition was most likely gradual. The bay may have served as a landing location for ships at Vatnsfjörður in its early days.

- The homefield was formed after *landnám*, and using tephrochronology and two basal radiocarbon dates can be divided into clear phases. There is a sharp drop-off in charcoal that coincides with the end of the seventeenth century and may relate to the decline of the Vatnsfjörður farm's power in the area.

- The tephra record in the peat from the homefield is similar to that of the peat core from Kaldalonsjökull, which is located across the fjord and slightly northwest of Vatnsfjörður. The chronology of the Kaldalonsjökull core confirms that the homefield core, despite being from an anthropogenically-altered peat field, has a valid tephrochronology, albeit with some movement of microtephra around the immediate deposition layer. In future, the tephrochronology of the Kaldalonsjökull core may be used for reconstructing temperature fluctuations in the area during the last 1000 years.

At the East Mound:

- The occupation period for the longhouse and associated areas within the mound models to the eleventh century AD.

- The different phases of construction on the longhouse and associated areas can be discerned with some precision; notably, the metalworking area and midden seem to have been in use throughout the period of occupation.
- Windblown sand layers played a major role in developing the stratigraphy of the mound. One sand layer (context 2095) was found between two occupation layers, suggesting that settlement at the mound continued after a serious storm, with settlers simply building over sand deposition. However, the youngest date at the site came from another layer of windblown sand, context 2047, which did not have any occupation layers over it. The sand, based on an OSL date, was deposited ca. AD 1093-1304. This suggests that the sand most likely covered an already abandoned longhouse.
- Cereals (barley and oat) and small quantities of flax that were found at the site have modelled dates for the early eleventh century. This suggests that the East Mound had a similar agricultural regime to contemporaneous farms in Orkney and either may have had a prosperous degree of local consumption or may have been growing additional crops for export.

For regional chronologies:

- The database of published dates from the North Atlantic is the product of an exhaustive literature search that sought to document any archaeological site found with radiocarbon dates, tephrochronological studies, or OSL dates that relate to the period studied have been included. Environmental studies and historical/documentary sources have also been included if they seemed relevant to understanding the archaeology.
- Bayesian models based on published phasing for each island in the North Atlantic refined existing dates with varying degrees of success, generally determined by quantity and quality of dates available. Models including the Norse settlements at Old Scatness and Bornais argue that their occupation periods were long-lived.
- Bayesian modelling can be used for posing different hypotheses about the timing of religious conversion, suggesting answers to longstanding questions about the pagan to Christian transitions in Orkney and Iceland. In Orkney, burials of both pagan and Christian nature seem to have overlapped in time. Conversion there may have been divided geographically, with Christianity adopted earlier in the eastern part of the archipelago than in the west. In Iceland, modelling

suggests that there was almost no overlap between the pagan and Christian periods aside from a few individuals. The conversion to Christianity models to the tenth century, which has implications for understanding the traditional conversion narrative presented in Íslendingabók of a sudden conversion in the summer of AD 999 or AD 1000. Modelling also suggests that Christianity in Iceland was widely geographically distributed from its earliest beginnings, and that archaeologists should look for further evidence of churches and churchyard burials throughout the country.

- Bayesian modelling suggests that the Western Settlement of Greenland lasted far beyond the traditional date for its abandonment, Ivar Bardarson's letter, dated to ca. AD 1348 to 1360. Instead, modelling suggests that it may have been occupied throughout the 15th century AD.
- Bayesian modelling also suggests that Greenland's Eastern Settlement was abandoned sometime around the early to mid-15th century AD, agreeing with multiple environmental studies.
- Greenland's Middle Settlement was modelled for the first time, also suggesting a lengthy period of occupation despite a less favourable agricultural environment.
- The modelled dates for *landnám* can be compared across the region, representing the most recent dates for this important period.

This thesis also contributed to tephrochronological research goals. The two test cases were in locations that, prior to this research, had almost no known tephra or microtephra finds from the Late Holocene. As discussed in Section 3.4.1 and Section 3.4.2, Vestfirðir has been little studied for any kind of tephrochronology, with no findings reported from the last thousand years; all tephras known from Orkney are from earlier than the last two thousand years. Therefore the tephra findings presented in this thesis represent expansion to the map of known tephra fall events, as was called for in a community statement from the Workshop on the Eyjafjallajökull eruptions of 2010 (Dugmore et al 2011).

For Vestfirðir, this study presents the first evidence of Hekla 1766, Hekla 1693, Hekla 1300, the *landnám* tephra, and Eldgja 935. This has extended the known range for these tephras and future researchers in the area will have a record to draw upon to confirm their own findings. A particular area of interest may be in the Late Holocene for marine cores off the North Iceland Shelf; thus far there have been several publications about these marine cores, but none going from the Late Holocene. The

data from this thesis will be published in the RESET (Response of Humans to Abrupt Environmental Transitions) database and if desired will also be sent to become part of Tephrabase; in this way, the raw WDS-EPMA data will be available to future researchers.

For Orkney, this thesis presents the first finding of either Hekla 1510 (more likely) or Hekla 1947; either would be the first instance of tephra from either eruption having been found in Orkney. This tephra was andesitic, making it a rare distal find of that type of volcanic glass.

10.3 Chronology as a tool for understanding the interaction between the human past and palaeoclimate

The first major research question asked in the thesis was, *How can scientific chronologies, in their current state, be used to understand the relationship between records of environmental and archaeological change?* The question was partially inspired by Caseldine and Turney (2010) stating that chronology is the area most in need of research for the field investigating the relationships between the human past and palaeoclimate to advance. It follows that without accurate and precise chronologies, the links between different records cannot be understood. If the sequence of events uncovered at an archaeological excavation is to be compared to an environmental proxy, those two records must share a common chronological scale. It is unclear if improving on current chronology-building methods will yield significantly better results. By selecting two case studies with very different chronological strategies, one of the goals in this thesis was to explore the possibilities offered by current methods for scientific chronology building to make connections between archaeological and environmental records.

The chronology building presented in this thesis demonstrates that current methods can achieve high levels of accuracy and precision, despite the need for improvement in some areas. Specifically, the tephrochronological record could benefit from the characterisation of more tephra layers from known eruptions and from better definition of the geochemical ranges of some tephra layers. The findings in this thesis also demonstrate the intractable fact that building these chronologies relies upon the availability and suitability of material to date, whether it be a tephra layer or a radiocarbon

sample. Tephra layers have to be erupted serendipitously to coincide with important archaeological moments (as the *landnám* tephra layer has). For radiocarbon, the calibration curve remains a problem in many periods, including the one studied here, but this is based upon atmospheric conditions and will be difficult to mitigate by improved methods beyond the Bayesian modelling that is already in use.[1]

With these difficulties in mind, two other questions arise: first, if achieving chronologies with the accuracy and precision necessary to show correlations between events that could have happened at the scale of human lifetimes or even the scale of short-lived settlements is the desired goal, then what are some ways forward? Second, is chronology as important to the future of human/palaeoclimate studies as Caseldine and Turney (2010) have argued that it is?

The answer to the first is to always use the chronological methods that are available. The database of others' published chronological data provided insight into the types of studies that have been conducive to building chronologies, which is discussed in more depth in Section 7.8 and Section 8.4. Many of these studies have been done by archaeologists with an interest in environmental science, which has relied upon scientific chronologies more than traditional archaeology. As a result, the types of studies that do include scientific dating evidence make it easy to assume environmental causes for archaeological change. This makes it difficult to see examples of human actions being driven by something other than the environment. The bias of what material is studied is very real; there may be plenty of other factors driving change but the typical studies that use scientific chronology building are prone to emphasising a non-human driver for change. The most thought-provoking studies are those that consider alternatives (e.g., Amorosi et al. 1997; Dugmore et al. 2012).

Part of archaeological interpretation is the informed imagining of the possibilities within the past, but that can sit somewhat uneasily alongside scientific data. For example, with Sveinhúsavatn, although the foram evidence demonstrates a phase change for a landscape feature, and the tephra layers provide a timing for that – a timing that occurs simultaneously to when Vatnsfjörður is known to have been prosperous, and that ends roughly one hundred years before the site entered decline – it is left to archaeologists to devise possible outcomes. Although it seems likely that the bay/lake must have been important to the settlement, even the best chronology combined with the best environmental record can never establish an exact causal link.

[1]Wiggle-matching has its limitations (Blaauw et al. 2004) and calibration curves will never be perfectly accurate.

Another example is the sand layer in context 2047 at the East Mound. The layer directly overlies the longhouse, no occupation layers are stratigraphically above it, and the OSL date indicates that it likely was laid down later than any construction or occupation at the mound. It certainly came from a later date in the period of occupation at the longhouse. The archaeological question then is, is there a case here for cause and effect? Were the storms in the bay so destructive that they forced people to abandon the longhouse? Then again, the people who lived there may have left for some entirely different reason, and a storm deposited sand over the surface sometime later. This can be extended to imagining all coastal settlements in exposed areas of sandstone environments, with their similar potential stormy weather. For many it must have been difficult to live with the threat of storms that could bury their homefield and lay thick sand layers over their yards; this may have driven some, if not these particular East Mound settlers, to leave a similar environment and settle elsewhere. Like the layer of ash from Hekla 1693 found in context 8562 at the Vatnsfjörður Farm Mound, which has been either tramped down or swept into the cracks in a stone surface, there are elements of physicality and human agency that are required to move beyond the sequence of events that accurate and precise chronologies can give to the study of the intersection between the human past and palaeoclimate.

10.4 Future research

Thinking about future research provides me a chance to reflect not just upon future ventures but also upon what might have been given unlimited time, money, and access. Furthermore, every research project is a learning process, and it is easy in hindsight to wish that one had known at the beginning what one knows now. Some future research avenues stemming from this thesis are:

- At Vatnsfjörður, we are still limited by a lack of chronological information that is not the Hekla 1693 tephra layer. As the farm mound is still being excavated, future research here should attempt to establish other chronological information. Radiocarbon dating has proved difficult there, but microtephra studies may present a way forward. In particular, if a small portion of the Viking Age area could be sampled for microtephra, then perhaps the foundation date for the *skáli* could be determined based on the presence of the *landnám* tephra having been found in Sveinhúsavatn and the peat at Kaldalonsjökull.

At the East Mound, the archaeological record is well documented and published to data structure report level thus far, with the main report forthcoming (Griffiths forthcoming). With the addition of Bayesian modelling as part of this study, it has a chronology that is both convincing and precise. The lack of nearby environmental records and the lack of chronological resolution for those records meant that the archaeology could not be closely linked to local environmental changes. The use of the Hobbister B core as an environmental proxy revealed how a non-anthropogenically-altered environment looked during the study period in Orkney, but it did not illuminate what changes may have been made near to the farm. Instead, it highlighted how local environmental records truly can be. Hopefully future studies will take into account a closer environmental record - Alldritt in Griffiths (forthcoming) has begun this work.

- Both case studies (and many of the published studies) seem to involve relatively high status sites. The longhouse at the East Mound is one of the largest found in the British Isles and Vatnsfjörður was a centre of power in Vestfirðir from the thirteenth to seventeenth centuries. An interesting, but potentially ambitious research project would be to investigate how high status coastal settlements fared during periods of environmental change in comparison to lower status settlements. As is discussed in Section 7.8, there is a difference between how the neighbouring inland high-status farm Hofstaðir and lower-status farm Sveigakot fared during the period, with the expected result that Sveigakot did more poorly over time (Simpson et al. 2003). Vésteinsson (2007) argues that holding territory was the key to success in medieval Icelandic society; it would be interesting to note whether or not there were coastal lower-status farms/settlements, or if in fact coastal resources were so valuable that elites dominated the ownership/occupation of those areas.

- Records of tephra geochemistry from known eruptions should improve over time and new ones are being studied with regularity (e.g. Meara 2012). So long as these are published and widely available, identifying distal tephra and/or microtephra layers will only become easier. The tephra geochemistry from this thesis will be uploaded to the RESET database so that future researchers can use that information. If they are desired, they will also be submitted to Tephrabase. Similarly, newer methods for identifying microtephra layers in cores like XRF (Kylander et al. 2011) and for identifying trace elements in glass shards like

ICP-MS (Pearce 2004) will continue to advance tephrochronology's ability to date archaeological and environmental materials.

- Thus far, there is no agreed-upon lower limit to statistical validity for tephra fingerprinting with small sample sizes (e.g., n=<5), but a discussion about how realistic it is to make a correlation with very few data points is definitely needed.

There is always room for more research questions, and as scientific chronology building becomes more common in archaeology – with AMS radiocarbon dating entering its third decade, and newer techniques such as microtephrochronology and OSL becoming better every year, there will be more dates available from across the Norse period. Large-scale chronological surveys which move beyond the notion of the archaeological site to the wider landscape – as at Vatnsfjörður and the Bay of Skaill in this thesis, among others, and then further out from that, to encompass an entire cultural area or region, provide a method to link a variety of records into a more complete story about archaeological change.

More chronological information would help answer questions about environmental change. As discussed in Chapter 2, there is strong evidence that the years from AD 900-1800 were characterised by environmental change that, in some parts of the North Atlantic, dramatically altered the natural and human landscape. The more temperate climate of the MWP, followed by the variable and colder climate of the LIA, have been linked by several researchers to changes in sea level, glacial and icepack extents, sea ice coverage, sea and land temperatures, and storminess. Sea level change, glacial extent and icepack change, temperature change, and increased storminess all played roles in shaping the settlement patterns at Vatnsfjörður and the Bay of Skaill, as discussed in Chapter 7 and Chapter 8. In several other archaeological studies, researchers have found evidence to suggest that these environmental changes altered human settlement as well. With further dates phased to later in the period, we could ask if these changes happened at the same time, and if archaeological evidence (movement of settlements, decline of some settlements, changes in economic strategies) for the MWP/LIA transition fits chronologically with environmental changes such as sea level changes, sea ice levels, and increased storminess, or if there is a lag time for culture to react to non-anthropogenic landscape change.

Further, if there is a lag time, we could explore if it is local – for example, if all of Iceland experienced the change later than all of the British Isles. We could

also explore if the explanation is a social one, as for example Dugmore et al. (2012) suggest in their paper on the Norse colony in Greenland. They attribute social factors as drivers for change more so than climate change. Adderley and Simpson (2006), also note that there may be a lag time for change caused by environmental factors as conservative forces within society attempt to keep traditional or trusted methods for agriculture, building, etc. despite environmental changes making them more difficult. It should also be considered that human-driven landscape management, crucial in the marginal agricultural economies of the Norse North Atlantic, must have played a role in shaping when effects show up in the archaeological and environmental records, as at Þórsmörk and Þjórsádalur, where woodland resources seem to have been managed once it became clear that they were being depleted faster than they could regenerate (Dugmore et al. 2006; Dugmore et al. 2007b).

Another question of interest that could be answered with more data is when the transition from longhouse to farm mound took place. In some cases, such as at the Bay of Skaill, longhouses seem to have been occupied for a brief period, perhaps only a few generations; is this a trend or an exception? As discussed in Chapter 4, construction on the Farm Mound at Vatnsfjörður began at an unknown date; in fact, the timing of the development of farm mounds throughout the Norse North Atlantic, and with it the often-accompanying upslope shift of settlement, remains unclear. Comparing the chronological data from where the base of farm mounds have been excavated and considering those within their regional context would provide a possible foundation period for the construction of these common landscape features.

Economic questions, such as those that Simpson et al. (2005) and Barrett et al. (2000) ask about Orkney, could also be answered with more clarity with further dates: when did arable land improvement to homefields and topsoils take place, such as that observed by Simpson et al. (2005) at Quoygrew? Was this a trend that spread across the landscape, or did it happen independently? When did certain industries (e.g., fishing) become important in certain places?

10.5 Final thoughts

This thesis began by agreeing with Mitchell (2008) when he said that archaeologists are uniquely placed to interpret the relationship between past human life and the

palaeoenvironment. Climate impact research will continue to be an important contribution, not just to academic research but, if archaeologists choose to reach out, to the public debate. Socially-driven actions can have an environmental impact on the local, regional, or even global scale. Coastal settlements in the Norse cultural zone experienced this: for example, cutting down forests for fuel led to permanent deforestation and widespread erosion in Iceland. Continuing to consider archaeological change that is grounded in a solid chronology and can be correlated to environmental change – as this thesis, and other research like it, does - is vital to understanding, in the twenty-first century, how we can coexist with our constantly-changing environment.

Bibliography

Adderley, W.P., Simpson, I. A, 2006. Soils and palaeo-climate based evidence for irrigation requirements in Norse Greenland. *Journal of Archaeological Science* 33, 1666-1679.

Adderley, W.P., Simpson, I. A., 2005. Early-Norse Home-Field Productivity in the Faroe Islands. *Human Ecoloy* 33, 711-736.

Adderley, W.P., Simpson, I. A., Vésteinsson, O., 2008. Local-scale adaptations: A modeled assessment of soil, landscape, microclimatic, and management factors in Norse home-field productivities. *Geoarchaeology* 23, 500-527.

Ahronson, K., 2000. Further Evidence for A Columban Iceland: Preliminary Results of Recent Work. *Norwegian Archaeological Review* 33, 117-124.

Ahronson, K., 2007. *Viking-Age Communities: Pap Names and Papar in the Hebridean Islands*, British Archaeological Reports British Series 450, Oxford.

Aitchison, J., 1986. *The statistical analysis of compositional data.* Chapman and Hall, London.

Aitken, M.J. 1990. *Science-based Dating in Archaeology*, Longman.

Ambrose, S.H., Butler, B.M., Hanson, D.B., Hunter-Anderson, R.L., Krueger, H.W. 1997. Stable isotopic analysis of human diet in the Marianas archipelago, Western Pacific. *American Journal of Physical Anthropology* 104: 343–362.

Amorosi, T., Buckland, P., Dugmore, A., Ingimundarson, J. H., McGovern, T. H., 1997. Raiding the landscape: human impact in the Scandinavian North Atlantic. *Human Ecology* 25, 491-518.

Anderson, R. Y., Nuhfer, E. B., Dean, W. E., 1984. Sinking of volcanic ash in uncompacted sediment in Williams Lake, Washington. *Science* 225, 505-8.

Andrews, J. T., Geirsdóttir, A., Hardardóttir, J., Principato, S., Grönvold, K., Kristjansdóttir, G.B., Helgadóttir, G., Drexler, J., Sveinbjórnsdóttir, A., 2002. Distribution, sediment magnetism and geochemistry of the Saksunarvatn (10,180 - 60 cal. yr BP) tephra in marine, lake, and terrestrial sediments, northwest Iceland. *Journal of Quaternary Science* 17, 731-745.

Andrews, J.T., Belt, S.T., Olafsdottir, S., Masse, G., Vare, L.L., 2009. Sea ice and marine climate variability for NW Iceland/Denmark Strait over the last 2000 cal. yr BP. *The Holocene* 19, 775-784.

Arge, S. V., Sveinbjarnardóttir, G. Edwards, K. J., Buckland, P. C., 2005. Viking and Medieval Settlement in the Faroes: People, Place and Environment. *Human Ecology* 33, 597-620.

Arge, S.V., 1991. The *Landnám* in the Faroes. *Arctic Anthropology*, 28 (2), 101–120.

Arge, S. V., 2014. Viking Faroes: Settlement, Paleoeconomy, and Chronology. *Journal of the North Atlantic*, 7, 1-17.

Arneborg, J., 2005. Greenland irrigation systems on a West Nordic background: an overview of the evidence of irrigation systems in Norse Greenland c. 980-1450 AD. In: Klapste, J. (Ed.), *Water management in medieval rural economy*: *les usages de l'eau en milieu au Moyen Age*.

Arneborg, J., Heinemeier, J., Lynnerup, N., Nielsen, H. L., Rud, N., Sveinbjörnsdóttir, A. E., 1999. Change of Diet of the Greenland Vikings Determined from Stable Carbon Isotope Analysis and 14C Dating of Their Bones. *Radiocarbon*, 41(2), 157-168.

Arneborg, J., Lynnerup, N., Heinemeier, J., Møhl, J., Rud, N., Sveinbjörnsdóttir, Á. E., 2012a. Norse Greenland dietary economy ca. AD 980-ca. AD 1450: Introduction. *Journal of the North Atlantic*, 3, 1-39.

Arneborg, J., Lynnerup, N., Heinemeier, J., 2012b. Human diet and subsistence patterns in Norse Greenland AD c. 980-AD c. 1450: Archaeological interpretations. *Journal of the North Atlantic*, 3, 119-133.

Ascough, P. L., Church, M. J., Cook, G. T., Dunbar, E., Gestsdóttir, H., McGovern, T. H., Dugmore, A. J., Friðriksson, A., Edwards, K. J. 2012. 'Radiocarbon reservoir effects in human bone collagen from northern Iceland.', *Journal of Archaeological Science*, 39 (7), 2261-2271.

Ascough, P. L., Church, M. J., Cook, G. T., Einarsson, Á., McGovern, T. H., Dugmore, A. J., Edwards, K. J. 2014. Stable isotopic (13C and 15N) characterization of key faunal resources from Norse period settlements in North Iceland. *Journal of the North Atlantic*, Special Volume 7, 25-42.

Ascough, P. L., Cook, G. T., Church, M. J., Dugmore, A. J., Arge, S. V., McGovern, T. H., 2006. Variability in North Atlantic marine radiocarbon reservoir effects at c. AD 1000. *The Holocene* 16, 131-136.

Ascough, P. L, Cook, G. T., Church, M. J., Dugmore, A. J., McGovern, T. H., Dunbar, E., Einarsson, Á., Friðriksson, A., 2007. Reservoirs and radiocarbon: ^{1}4C dating problems in Mývatnssveit, Northern Iceland. *Radiocarbon* 49, 947-961.

Ascough, P. L., Cook, G. T., Hastie, H., Dunbar, E., Church, M. J., Einarsson, A., McGovern, T. H., Dugmore, A. J., 2011. An Icelandic freshwater radiocarbon reservoir effect: Implications for lacustrine ^{14}C chronologies. *The Holocene* 21, 1073-1080.

Ashmore, P. J., 1998. A list of Historic Scotland archaeological radiocarbon dates, in: Turner, R. (Ed.), *Discovery and Excavation in Scotland.* Council for Scottish Archaeology Publishers, 125-128.

Austin, W. E., Wilson, L. J., Hunt, J. B., 2004. The age and chronostratigraphical significance of north Atlantic ash zone II. *Journal of Quaternary Science* 19, 137-146.

Axford, Y., Geirsdóttir, Á., Miller, G. H., Langdon, P. G., 2008. Climate of the Little Ice Age and the past 2000 years in northeast Iceland inferred from chironomids and other lake sediment proxies. *Journal of Paleolimnology* 41, 7-24.

Balascio, N. L., Wickler, S., Erik, L., Bradley, R. S., 2010. Distal cryptotephra found in a Viking boathouse: the potential for tephrochronology in reconstructing the Iron Age in Norway. *Journal of Archaeological Science* 38 (4), 1-8.

Balasse, M., Mainland, I., Richards, M.P., 2009. Stable isotope evidence for seasonal consumption of marine seaweed by modern and archaeological sheep in the Orkney archipelago (Scotland). *Environmental Archaeology* vol. 14, issue 1, 1-14.

Ballantyne, C. K., 1991. Late Holocene erosion in upland Britain: climatic deterioration or human influence? *The Holocene* 1, 81-85.

Barber, K., Langdon, P., Blundell, A., 2008. Dating the Glen Garry tephra: a widespread late-Holocene marker horizon in the peatlands of northern Britain. *The Holocene* 18, 31-43.

Barclay, R., 2008. *Homefield Formation and Management at Vatnsfjörður, NW Iceland – A Geoarchaeological Interpretation.* Unpublished MSc dissertation, University of Stirling.

Barclay, R. and Anderson, J. K., forthcoming. Homefield Formation and Management at Vatnsfjörður, NW Iceland – A Geoarchaeological Interpretation.

Barclay, R., Tisdall, E., McCulloch, R., Simpson, I. A., 2011. Pollen Analysis wet meadow site, in (eds.) Milek et al., Vatnsfjörður 2010 Interim Report.

Barlow, L. K., Sadler, J. P., Ogilvie, A. E. J., Buckland, P. C., Amorosi, T., Ingimundarson, J. H., Skidmore, P., Dugmore, A. J., McGovern, T. H., 1997. Interdisciplinary investigations of the end of the Norse Western Settlement in Greenland. *The Holocene* 7, 489-499.

Barrett, J. H., 2008. What caused the Viking Age? *Antiquity* 82, 671-685.

Barrett, J. H., 2012. Comments on Orri Vésteinsson and Thomas H. McGovern: 'The Peopling of Iceland'. Counting Invisible Icelanders. *Norwegian Archaeological Review*, vol. 45, No. 2, 218-220.

Bartett, J.H., ed., 2012. *Being an Islander: production and identity at Quoygrew, Orkney, AD 900-1600.* Cambridge: McDonald Institute Monograph.

Barrett, J. H., Beukens, R. P., 2000. Radiocarbon dating and marine reservoir correction of Viking Age Christian burials from Orkney. *Antiquity* 74, 537-543.

Barrett, J., Beukens, R., Simpson, I. A., Ashmore, P., Poaps, S., Huntley, J., 2000. What Was the Viking Age and When did it Happen? A View from Orkney. *Norwegian Archaeological Review* 33, 1-10.

Barrett, J. H., Locker, A. M., Roberts, C. M., 2004. The origins of intensive marine fishing in medieval Europe: the English evidence. *Proceedings. Biological sciences / The Royal Society* 271, 2417-21.

Barrett, J. H., Richards, M. P., 2004. Identity, gender, religion and economy: new isotope and radiocarbon evidence for marine resource intensification in early historic Orkney, Scotland, UK. *European Journal of Archaeology* 7, 249-271.

Barrett, J. H., Slater, A., 2009. New Excavations at the Brough of Deerness: Power and Religion in *Viking Age Scotland New Excavations at the Brough of Deerness*: *Power and Religion in Viking Age Scotland Structure Report*, 81-94.

Barret, J. H. in Carver, M. (ed.), 2006. Christian and Pagan Practice during the Conversion of Viking Age Orkney and Shetland. *The Cross Goes North: Processes of Conversion in Northern Europe, AD 300-1300*, Boyles: 207-226.

Bas, M. J. L. E., Maitre, R. W. L. E., Streckeisen, A., 1986. A Chemical Classification of Volcanic Rocks Based on the Total Alkali-Silica Diagram *Journal of Petrology* 27 (3), 745-750.

Batey, C. E., 2011. Viking Burials in Scotland: Two 'New' Boat Burial Finds, in *Shetland and the Viking World*, ed. Val E. Turner, Olwyn A. Owen, and Doreen J. Waugh, Shetland Heritage Publications, 39-45.

Bayliss, A., Bronk Ramsey, C., van der Plicht, J., Whittle, A. 2007. Bradshaw and Bayes: Towards a Timetable for the Neolithic. *Cambridge Archaeological Journal*, 17:1, 1-28.

Bayliss, A. and Hey, G. 2004 Scientific dating, in *Yarnton*: *Saxon and medieval settlement and landscape*, Oxford Archaeology Thames Valley Landscape Monograph No 20, 255-266.

Beattie, K. G., Bond, W. G., Manning, E. W., 1981. *The Agricultural Use of Marginal Lands*: *a Review and Bibliography.* Lands Directorate, Environment Canada.

Bending, J., Buckland, P.C., Christensen, K., Edwards, K.J., Hunter, F., Jouttijarvi, A., Schofield, J.E., Hansen, S.S., and Vickers, K. 2013 Toftanes. A Viking Age Farmstead in the Faroe Islands. *Acta Archaeologica* 84, no. 1, 8-239.

Bennett, K., Boreham, S., Sharp, M., 1992. Holocene history of environment, vegetation and human settlement on Catta Ness, Lunnasting, Shetland. *Journal of Ecology* 80, 241-273.

Benson, L., Petersen, K., Stein, J., 2006. Anasazi (Pre-Columbian Native-American) Migrations During The Middle-12th and Late-13th Centuries – Were they Drought Induced? *Climatic Change* 83, 187-213.

Berger, G. W., 1992. Dating volcanic ash by use of thermoluminescence. *Geology* 20, 11-14.

Bergman, J., Wastegård, S., Hammarlund, D., Wohlfarth, B., Roberts, S. J., 2004. Holocene tephra horizons at Klocka Bog, west-central Sweden: aspects of reproducibility in subarctic peat deposits. *Journal of Quaternary Science* 19, 241-249.

Bergthorsson, P., 1985. Sensitivity of Icelandic agriculture to climatic variations. *Climatic Change* 7, 111-127.

Bigelow, G., Ferrante, S. M., Hall, S. T., Kimball, L. M., Proctor, R. E., Remington, S. L., 2005. Researching catastrophic environmental changes on northern coastlines: a geoarchaeological case study from the Shetland Islands. *Arctic Anthropology* 42, 88-102.

Binford, L. R. 1971. Mortuary Practices: Their Study and Potential. *Approaches to the Social Dimensions of Mortuary Practices*, ed. J. A. Brown. Washington, DC: Memoirs of the Society for American Archaeology 25, 6–29.

Birks, H. H., Gulliksen, S., Haflidason, H., Mangerud, J., Possnert, G., 1996. New Radiocarbon Dates for the Vedde Ash and the Saksunarvatn Ash from Western Norway. *Quaternary Research* 45, 119-127.

Bjarnason, A.H., 1991. Vegetation on lava fields in the Hekla area, Iceland. *Acta Phytogeographica Suecica* 77, 7-114.

Björck, J., Wastegård, S., 1999. Climate oscillations and tephrochronology in eastern middle Sweden during the last glacial-interglacial transition. *Journal of Quaternary Science* 14, 399-410.

Björnsson, H., Gjessing, Y., Hamran, S.-E., Hagen, O., Liestol, O., Palsson, F., Erlingsson, B., 1996. The thermal regime of sub-polar glaciers mapped by multi-frequency radio-echo sounding. *Journal of Glaciology* 42, 23-37.

Blaauw, M., Van Geel, B., Mauquoy, D., Van Der Plicht, J., 2004. Carbon-14 wiggle-match dating of peat deposits: advantages and limitations. *Journal of Quaternary Science* 19, 177–181.

Blaauw, M., 2012. Out of tune: the dangers of aligning proxy archives. *Quaternary Science Reviews* 36, 38-49.

Blackford, J., 2000. Palaeoclimatic records from peat bogs. *Trends in Ecology & Evolution* 15, 193-198.

Blackwell, P.G., Buck, C.E., Reimer, P.J., 2006 Important Features of the new radiocarbon calibration curves, *Quaternary Science Reviews* 25, 408-413.

Blake, S., 1984. Magma mixing and hybridization processes at the alkalic, silicic Torfajökull central volcano triggered by tholeiitic Veiðivötn fissuring, South Iceland. *Journal of Volcanology and Geothermal Research* 22, 1-31.

Blinman, E., 2008. 2000 Years of Cultural Adaptation to Climate Change in the Southwestern United States. *AMBIO*: *A Journal of the Human Environment* 37, 489-497.

Blockley, S. P. E., Donahue, R. E., Pollard, A. M., Ward, K. R., 2003. Establishing Late-glacial and Holocene marine reservoir radiocarbon offsets in the northern North Atlantic: the potential for improving the chronology of Arctic archaeology. *Physics in Canada* 59, 263-268.

Blockley, S.P.E., Edwards, K.J., Schofield, J.E., Pyne-O'Donnell, S.D.F., Jensen, B.J.L., Matthews, I.P., Cook, G.T., Wallace, K.L., Froese, D., 2015. First evidence of cryptotephra in palaeoenvironmental records associated with Norse occupation sites in Greenland. *Quaternary Geochronology* 27, 145–157.

Blockley, S. P. E., Lane, C. S., Lotter, A. F., Pollard, A. M., 2007. Evidence for the presence of the Vedde Ash in Central Europe. *Quaternary Science Reviews* 26, 3030-3036.

Blockley, S. P. E., Pyne-O'Donnell, S. D. F., Lowe J. J., Matthews I. P., Stone A., Pollard A. M., Turney C. S. M., Molyneaux, E. G., 2005. A new and less destructive laboratory procedure for the physical separation of of distal glass tephra shards from sediments. *Quaternary Science Reviews* 24, 1952-1960.

Bogaard, C. van den, Dörfler, W., Glos, R., Nadeau, M.-J., Grootes, P. M., Erlenkeuser, H., 2002. Two Tephra Layers Bracketing Late Holocene Paleoecological Changes in Northern Germany. *Quaternary Research* 57, 314-324.

Bogaard, C. van den, Schmincke, H.-U., 2002. Linking the North Atlantic to central Europe: a high resolution Holocene tephrochronological record from northern Germany. *Journal of Quaternary Science* 17, 3-20.

Bolender, D., 2006. *The Creation of a Propertied Landscape*: *Land Tenure and Agricultural Investment in Medieval Iceland.* Unpublished PhD thesis, Northwestern University.

Bond, G, Mandeville, C., Hoffman, S., 2001. Were rhyolitic glasses in the Vedde Ash and in the North Atlantic Ash Zone 1 produced by the same volcanic eruption? *Quaternary Science Reviews* 20, 1189-1199.

Bond, J. M., Hunter, J. R., 1987. Flax-growing in Orkney from the Norse period to the 18th century. *Proc. Soc. Antiq. Scot.* 117, 175-181.

Bonsall, C., Macklin, M. G., Payton, R. W., Boroneant, A., 2002. *Climate, floods and river gods*: *environmental change and the Meso-Neolithic transition in southeast Europe Before Farming.*

Box, G. E. P., 1979. Robustness in scientific model building. *Robustness in Statistics*, ed. by L. Launer and G.N. Wilkinson. Academic Press, 201–36.

Boygle, J., 1999. Variability of tephra in lake and catchment sediments, Svínavatn, Iceland. *Global and Planetary Change* 21, 129-149.

Boygle, J., 2004. Towards a Holocene tephrochronology for Sweden: geochemistry and correlation with the North Atlantic tephrostratigraphy. *Journal of Quaternary Science* 19, 103-109.

Bronk Ramsey, C., 2008. Deposition models for chronological records. *Quaternary Science Reviews*, 27(1-2), 42-60.

Bronk Ramsey, C., 2009. Bayesian analysis of radiocarbon dates. *Radiocarbon*, 51(1), 337-360.

Brown, J. 1995. On mortuary analysis - with special reference to the Saxe-Binford Research Program, in Lane Anderson Beck, ed. *Regional Approaches to Mortuary Analysis*, Plenum Press, New York.

Buckland, P. C., Amorosi, T., Barlow, L. K., Dugmore, A. J., Mayewski, P. A., McGovern, T. H., Ogilvie, A. E. J., Sadler, J. P., Skidmore, P., 1996. Bioarchaeological and climatological evidence for the fate of Norse farmers in medieval Greenland. *Antiquity* 70, 88-96.

Buckland, P. C., Dugmore, A. J., Edwards, K. J., 1997. Bronze Age myths? Volcanic activity and human response in the Mediterranean and North Atlantic regions. *Antiquity* 71, 581–593.

Buckland, P. C., Edwards, K. J., Panagiotakopulu, E., Schofield, J. E., 2009. Palaeoecological and historical evidence for manuring and irrigation at Garðar (Igaliku), Norse Eastern Settlement, Greenland. *The Holocene* 19, 105-116.

Buckland, P. C., Panagiotakopulu, E., 2005. Archaeology and the Palaeoecology of the Norse Atlantic Islands: A Review in *North Atlantic Islands. Smithsonian Institution Press*, Washington DC, 167-181.

Bunting, M. J., 1994. Vegetation history of Orkney, Scotland: Pollen records from two small basins in West Mainland. *New Phytologist* 128, 771-792.

Bunting, M. J., 1996. The development of heathland in Orkney, Scotland: pollen records from Loch of Knitchen (Rousay) and Loch of Torness (Hoy). *The Holocene* 6, 193-212.

Bury, J. D., 1923. *History of the Later Roman Empire from the Death of Theodosius I to the Death of Justinian, AD 395 - AD 565.* Macmillan.

Buteux, S., 1997. *Settlements at Skaill, Deerness, Orkney.* BAR British Series 260, Oxford.

Butzer, K. W., 1971. *Environment and archeology. An ecological approach to prehistory.* Aldine Publishing Co.

Cage, A. G., Davies, S. M., Wastegård, S., Austin, W. E. N., 2011. Identification of the Icelandic *Landnám* tephra (AD 871 ± 2) in Scottish fjordic sediment. *Quaternary International* 246, 168-176.

Callow, C., 2006. Geography, Communities, and Socio-Political Organization in Medieval Northern Iceland, *People and Space in the Middle Ages*, 65-86.

Canmore, `http://canmore.rcahms.gov.uk/en/mycanmore/`, Royal Commission on the Ancient and Historical Monuments of Scotland, last accessed 20 April, 2015.

Cant, R. G., 1984. Society, and Church Organisation in the Northern Isles. In: Fenton, A., Pálsson, H. (Eds.), *The Northern and Western Isles in the Viking World.* John Donald Publishers Ltd, Edinburgh, 169-179.

Carmichael, I. S. E., 1979. Glass and the glassy rocks *The evolution of the igneous rocks.* McGraw Hill.

Caseldine, C. J., Baker, A., Barnes, W. L., 1999. A rapid , non-destructive scanning method for detecting distal tephra layers in peats. *The Holocene* 9, 635-638.

Caseldine, C. J., Geirsdottir, A., Langdon, P., 2003. Efstadalsvatn–a multi-proxy study of a Holocene lacustrine sequence from NW Iceland. *Journal of Paleolimnology* 30, 55–73.

Caseldine, C. J., Hatton, J., Huber, U., Chiverrell, R., Woolley, N., 1998. Assessing the impact of volcanic activity on mid-Holocene climate in Ireland: the need for replicate data. *The Holocene* 8, 105-111.

Caseldine, C. J., Turney, C., 2010. The bigger picture: towards integrating palaeoclimate and environmental data with a history of societal change. *Journal of Quaternary Science* 25, 88–93.

Chambers, F. M., Daniell, J. R. G., Hunt, J. B., Molloy, K., O'Connell, M., 2004. Tephrostratigraphy of An Loch Mór, Inis Oírr, western Ireland: implications for Holocene tephrochronology in the northeastern Atlantic region. *The Holocene* 14, 703-720.

Charman, D. J., Grattan, J., 1999. An assessment of discriminant function analysis in the identification and correlation of distal Icelandic tephras in the British Isles. *Geological Society, London, Special Publications* 161, 147-160.

Charman, D. J., West, S., Kelly, A., Grattan, J., 1995. Environmental change and tephra deposition: The strath of Kildonan, Northern Scotland. *Journal of Archaeological Science* 22, 799-809.

Church, M. J., Arge, S. V., Brewington, S., McGovern, T. H., Woollett, J. M., Perdikaris, S., Lawson, I. T., Cook, G. T., Amundsen, C., Harrison, R., Krivogorskaya, Y. Dunbar, E., 2005. Puffins, pigs, cod and barley: palaeoeconomy at Undir Junkarinsfløtti, Sandoy, Faroe Islands. *Environmental Archaeology*, 10(2), 179-197.

Church, M. J., Arge, S. V., Edwards, K. J., Ascough, P. L., Bond, J. M., Cook, G. T., Dockrill, S. J., Dugmore, A. J., McGovern, T. H., Nesbitt, C., Simpson, I. A. 2013. The Vikings were not the first colonizers of the Faroe Islands. *Quaternary Science Review* 77, 228–232.

Church, M. J., Dugmore, A. J., Mairs, K., Millard, A., Cook, G. T., Sveinbjarnardóttir, G., Ascough, P. A., Newton, A. J., Roucoux, K., 2007. Charcoal production during the Norse and early medieval periods in Eyjafjallahreppur, Southern Iceland. *Radiocarbon* 49, 659–672.

Cook, G.T., Ascough, P.L., Bonsall, C., Hamilton, W.D., Russell, N., Sayle, K.L., Bownes, J.M., Scott, E.M., 2015. Best Practice Methodology for 14C Calibration of Marine and Mixed Terrestrial/Marine Samples. *Quaternary Geochronology.*

Crowley, T., 2000. Causes of climate change over the past 1000 years. *Science* 289, 270-7.

Davies, S. M., Branch, N. P., Lowe, J. J., Turney, C. S. M., 2002. Towards a European tephrochronological framework for Termination 1 and the Early Holocene. *Phil. Trans. of the R. Society of London Series A* 360, 767-802.

Davies, S. M., Elmquist, M., Bergman, J., Wohlfarth, B., Hammarlund, D., 2007. Cryptotephra sedimentation processes within two lacustrine sequences from west central Sweden. *The Holocene* 17, 319-330.

Davies, S. M., Hoek, W. Z., Bohncke, S. J. P., Lowe, J. J., O'Donnell, S. P., Turney, C. S. M., 2008. Detection of Lateglacial distal tephra layers in the Netherlands. *Boreas* 34, 123-135.

Davies, S. M., Larsen, G., Wastegård, S., Turney, C. S. M., Hall, V. A., Coyle, L., Thordarson, T., 2010b. Widespread dispersal of Icelandic tephra: how does the Eyjafjöll eruption of 2010 compare to past Icelandic events? *Journal of Quaternary Science* 25, 605-611.

Davies, S. M., Turney, C. S. M., Lowe, J. J., 2001. Identification and significance of a visible, basalt-rich Vedde ash layer in a Late-glacial sequence on the Isle of Skye, Inner Hebrides, Scotland. *Journal of Quaternary Science* 16, 99-104.

Davies, S. M., Wastegård, S., Abbott, P. M., Barbante, C., Bigler, M., Johnsen, S. J., Rasmussen, T. L., Steffensen, J. P., Svensson, A., 2010a. Tracing volcanic events in the NGRIP ice-core and synchronising North Atlantic marine records during the last glacial period. *Earth and Planetary Science Letters.* 294, 69-79.

Davies, S. M., Wastegard, S., Wohlfarth, B., 2003. Extending the limits of the Borrobol Tephra to Scandinavia and detection of new early Holocene tephras. *Quaternary Research* 59, 345-352.

Dawson, A. G., Elliott, L., Mayewski, P., Lockett, P., Noone, S., Hickey, K., Holt, T., Wadhams, P., Foster, I., 2003. Late-Holocene North Atlantic climate 'seesaws', storminess changes and Greenland ice sheet (GISP2) palaeoclimates. *The Holocene* 13, 381-392.

Dawson, S., Smith, D. E., 1997. Holocene relative sea-level changes on the margin of a glacio-isostatically uplifted area: an example from northern Caithness, Scotland. *The Holocene* 7, 59-77.

Decaulne, A., 2004. Combining geomorphological, historical and lichenometrical data for assessment of risk due to present-day slope processes, a case study from the Icelandic Westfjords. *Risk Analysis*, 177–186.

Department of Continuing Education, University of Oxford, Humanities and Social Science Research - Archaeology, Orkney Excavation 25 July - 27 August, 2010 http://www.conted.ox.ac.uk/research/projects/birsay-skaill/excavations_2010.php, accessed 12 December, 2011.

Diamond, J., 2005. *Collapse*: *How societies choose to fail or succeed.* Penguin.

Dickens, W., 2011. *Reconstruction of the coastal morphology in Vestfirðir, north west Iceland, during the late Holocene.* Unpublished MSc thesis, Department of Geography. Durham University.

Donaldson, A. M., Morris, C. D., Rackham, D. J., 1981. The Birsay Bay Project: Preliminary investigations into the past exploitation of a coastal environment at Birsay, Main- land, Orkney, in: Brothwell, D., Dimbleby, G. (Eds.), *The Environmental Aspects of Coasts and Islands.* BAR.

Dugmore, A. J., 1989. Icelandic volcanic ash in Scotland. *Scottish Geographical Magazine* 105, 168-172.

Dugmore, A. J., Borthwick, D. M., Church, M. J., Dawson, A., Edwards, K. J, Keller, C., Mayewski, P., McGovern, T. H., Mairs, K.-A., Sveinbjarnardóttir, G., 2007a. The role of climate in settlement and landscape change in the North Atlantic Islands: an assessment of cumulative deviations in high-resolution proxy climate records. *Human Ecology* 35, 169-178.

Dugmore, A. J., Church, M. J., Mairs, K.-A., McGovern, T. H., Newton, A. J., Sveinbjarnadóttir, G., 2006. An over-optimistic pioneer fringe? Environmental perspectives on medieval settlement abandonment in Þórsmörk, South Iceland, in *Dynamis of northern societies*: *proceedings of the SILA NABO conference on Arctic and North Atlantic archaeology.* Aarhus University Press, Copenhagen, 335-345.

Dugmore, A. J., Church, M. J., Buckland, P. C., Edwards, K. J., Lawson, I., McGovern, T. H., Panagiotakopulu, E., Simpson, I. A., Skidmore, P., Sveinbjarndóttir, G., 2005. The Norse *Landnám* on the North Atlantic Islands: an environmental impact assessment. *Polar Record* 41, 21-37.

Dugmore, A. J., Church, M. J., Mairs, K., McGovern, T. H., Perdikaris, S., Vésteinsson, O., 2007b. Abandoned Farms, Volcanic Impacts, and Woodland Management: Revisiting Þjorsardalur, the 'Pompeii of Iceland'. *Arctic Anthropology* 44, 1-11.

Dugmore, A. J., Gisladottir, G., Simpson, I. A., Newton, A., 2009. Conceptual models of 1200 years of Icelandic soil erosion reconstructed using tephrochronology. *Journal of the North Atlantic* 2, 1-18.

Dugmore, A. J., Larsen, G., Newton, A. J., 1995. Seven tephra isochrones in Scotland. *The Holocene* 5, 257-266.

Dugmore, A. J., McGovern, T. H., Vésteinsson, O., Arneborg, J., Streeter, R., Keller, C., 2012. Cultural adaptation, compounding vulnerabilities and conjunctures in Norse Greenland. *Proceedings of the National Academy of Sciences*, 1-6.

Dunbar, E., Cook, G. T., Naysmith, P., Tripney, B. G., 2016. AMS 14C Dating at the Scottish Universities Environmental Research Centre (SUERC) Radiocarbon Dating Laboratory. *Radiocarbon*, Volume 58, Issue 1: 9-23.

Dugmore, A. J., Newton, A. J., 1992. Geochemical stability of fine-grained silicic Holocene tephra in Iceland and Scotland. *Journal of Quaternary Science* 7, 173-183.

Dugmore, A. J., Newton, A. J., 1992. Thin tephra layers in peat revealed by X-radiography. *Journal of Archaeological Science* 19, 163-170.

Dugmore, A. J., Newton, A. J., 1998. Holocene tephra layer in the Faroe Islands. *Fróðskaparrit* 46, 191-204.

Dugmore, A. J., Newton, A. J., Cook, G. T., Larsen, G., 2000. Tephrochronology , Environmental Change and the Norse Settlement of Iceland. *Environmental Archaeology* 5, 21-34.

Dugmore, A. J., Newton, A. J., Edwards, K. J., Larsen, G., Blackford, J. J., Cook, G. T., 1996. Long-distance marker horizons from small-scale eruptions: British tephra deposits from the AD 1510 eruption of Hekla, Iceland. *Journal of Quaternary Science* 11, 511-516.

Dugmore, A. J., Newton, A. J., Smith, K. T., 2011. Report and Community Statement: Workshop on the Eyjafjallajökull eruptions of 2010 and implications for tephrochronology, *Volcanology and Quaternary Studies*, 1-15.

Dugmore, A. J., Sugden, D. E., 1991. Do the anomalous fluctuations of Sólheimajökull reflect ice-divide migration? *Boreas* 20, 105-113.

Edvardsson, R., 2004. Fornleifarannsókn í Vatnsfirði við Ísafjarðardjúp 2004.

Edvardsson, R., 2010. *The role of marine resources in the medieval economy of Vestfirdir, Iceland.* Unpublished PhD thesis: City University of New York.

Edvardsson, R., McGovern, T. H., 2005. Archaeological Excavations at Vatnsfjörður 2003-04. Archaeologica Islandica, 16-30.

Edvardsson, R., Perdikaris, S., McGovern, T. H., Zagor, N., and Waxman, M. 2004. Coping with hard times in NW Iceland: Zooarchaeology, history, and landscape archaeology at Finnbogastaðir in the 18th century. *Archaeologica Islandica* 3, 20-46.

Edwards, K. J., 2012. Was The Peopling of Iceland a Trickle, a Steady Stream or a Deluge? *Norwegian Archaeological Review*, vol. 45, No. 2, 220-223.

Edwards, K. J, Borthwick, D., Cook, G. T., Dugmore, A. J., Mairs, K.-A., Church, M. J., Simpson, I. A., Adderley, W. P., 2005. A Hypothesis-Based approach to landscape change in Suðuroy, Faroe Islands. *Human Ecology* 33, 621-650.

Edwards, K. J., Buckland, P. C., Dugmore, A. J., McGovern, T. H., Simpson, I. A., Sveinbjarnardóttir, G., 2004. Landscapes circum-landnám: Viking settlement in the North Atlantic and its human and ecological consequences: a major new research programme. In *North Atlantic connections and adaptations*: *economies, environments and subsistence in lands bordering the North Atlantic.* Oxbow Books.

Edwards, K.J., Cook, G.T., Nyegaard, G., Schofield, J.E., 2013. Towards a first chronology for the middle settlement of norse greenland: ^{14}C and related studies of animal bone and environmental material. *Radiocarbon* 55, no. 1, 13-29.

Edwards, K. J., Schofield, J. E., 2013. 7.6. Radiocarbon dating at Toftanes and the wider Faroese context. *Acta Archaeologica*, 84(1), 177-185.

Edwards K. J., Schofield, J. E., Macquoy, D., 2008. High resolution paleoenvironmental and chronological investigations of Norse landnám at Tasiusaq, Eastern Settlement, Greenland. *Quaternary Research* 69, 1-15.

Einarsson, E. H., Larsen, G., Þórarinsson, S., 1980. The Sólheimar tephra layer and the Katla eruption of 1357. *Acta Naturalis Islandica.*

Eiríksson, J., Knudsen, K. L., Haflidason, H., Heinemeier, J., 2000. Chronology of late Holocene climatic events in the northern North Atlantic based on AMS ^{14}C dates and tephra markers from the volcano Hekla, Iceland. *Journal of Quaternary Science* 15, 573-580.

Eiríksson, J., Knudsen, K.L., Larsen, G., Olsen, J., Heinemeier, J., Bartels-Jónsdóttir, H.B., Jiang, H., Ran, L., Símonarson, L.A., 2011. Coupling of palaeoceanographic shifts and changes in marine reservoir ages off North Iceland through the last millennium. *Palaeogeography, Palaeoclimatology, Palaeoecology*, Volume 302, Issues 1–2, 95-108.

Eiríksson, J., Larsen, G., Knudsen, K., Heinemeier, J., Simonarson, L., 2004. Marine reservoir age variability and water mass distribution in the Iceland Sea. *Quaternary Science Reviews* 23, 2247-2268.

Enache, M. D., Cumming, B. F., 2006. The Morphological and Optical Properties of Volcanic Glass: A Tool to Assess Density-induced Vertical Migration of Tephra in Sediment Cores. *Journal of Paleolimnology* 35, 661-667.

Erlingsson, T., 1899. *Ruins of the Saga Time*: *Being an Account of Travels and Explorations in Iceland in the Summer of 1899.* David Nutt, 270, Strand, W.C., London.

Evans, S., 1990. The Productivity of Maguey Terrace Agriculture in Central Mexico during the Aztec Period. *Latin American Antiquity* 1, 117-132.

Farrell, M., 2010. *The environmental context of later prehistoric human activity in Orkney, Scotland.* Unpublished PhD thesis, University of Hull.

Fenton, A., 1997. *The Northern Isles*: *Orkney and Shetland.* Dundurn Press Ltd.

Fitzpatrick, S. M. 2006. A Critical Approach to Dating in the Caribbean: Using Chronometric Hygiene to Evaluate Chronological Control and Prehistoric Settlement. *Latin American Antiquity* Vol. 17, No. 4 (Dec., 2006), 389-418.

Forbes, V., Bain, A., Alda, G., Milek, K. B., 2010. Reconstructing aspects of the daily life in late 19th and early 20th century Iceland: archaeoentomological analysis of the Vatnsfjörður farm, NW Iceland, *Archaeologica Islandica* 8, 77-110.

Fornleifastofnun Íslands, 2009. *Ágrip af sögu u Vatnsfjarðar (A short history of Vatnsfjörður).* Reykjavík.

Fricke, H. C., O'Neil, J. R., Lynnerup, N. 1995. Oxygen isotope composition of human tooth enamel from medieval Greenland: Linking climate and society, *Geology.* Volume 23, Number 10: 869-872.

Friðriksson, A., 1994. *Sagas and Popular Antiquarianism in Icelandic Archaeology.* Avebury.

Friðriksson, A., Vésteinsson, O., McGovern, T. H., 2004. Recent investigations at Hofstadir, northern Iceland in *North Atlantic connections and adaptations*: *economies, environments and subsistence in lands bordering the North Atlantic.* Oxbow Books.

Froggatt, P. C., 1983. Toward a comprehensive upper Quaternary tephra and ignimbrite stratigraphy in New Zealand using electron microprobe analysis of glass shards. *Quaternary Research* 19, 188-200.

Froggatt, P. C., 1992. Standardization of the chemical analysis of tephra deposits. Report of the ICCT Working Group. *Quaternary International* 13-14, 93-96.

Gauthier, E., Bichet, V., Massa, C., Petit, C., Vannière, B., Richard, H. (2010). Pollen and non-pollen palynomorph evidence of medieval farming activities in southwestern Greenland. *Vegetation History and Archaeobotany*, 19(5-6), 427-438.

Gehrels, W. R., Marshall, W. A., Gehrels, M. J., Larsen, G., Kirby, J. R., Eiriksson, J., Heinemeier, J., Shimmield, T., 2006. Rapid sea-level rise in the North Atlantic Ocean since the first half of the nineteenth century. *The Holocene* 16, 949-965.

Gehrels, M. J., Newnham, R. M., Lowe, D. J., Wynne, S., Hazell, Z. J., Caseldine, C., 2008. Towards rapid assay of cryptotephra in peat cores: Review and evaluation of various methods. *Quaternary International* 178, 68-84.

Geirsdóttir, Á., Miller, G. H., Axford, Y., 2009a. Holocene and latest Pleistocene climate and glacier fluctuations in Iceland. *Quaternary Science Reviews* 28, 2107-2118.

Geirsdóttir, Á., Miller, G. H., Thordarson, T., Ólafsdóttir, K. B., 2009b. A 2000 year record of climate variations reconstructed from Haukadalsvatn, West Iceland. *Journal of Paleolimnology* 41, 95-115.

Gilbertson, D. D., Schwenninger, J.-L., Kemp, R. A., Rhodes, E. J., 1999. Sand-drift and Soil Formation Along an Exposed North Atlantic Coastline: 14,000 Years of Diverse Geomorphological, Climatic and Human Impacts. *Journal of Archaeological Science* 26, 439-469.

Gíslason, J. 2014. Acceptance of Christianity in Iceland in the year 1000 (999). *Scripta Instituti Donneriani Aboensis*, Volume 13: 223-255.

Golding, K. A., Simpson, I. A., Schofield, J. E., Edwards, K. J., 2011. Norse–Inuit interaction and landscape change in southern Greenland? A geochronological, pedological, and palynological investigation. *Geoarchaeology*, 26(3), 315-345.

Graham-Campbell, J. 2003. The Vikings in Orkney. *The Faces of Orkney: Stones, Skalds and Saints*, ed. Doreen J. Waugh, Scottish Society for Northern Studies, 128-137.

Grattan, J., Pyatt, F. B., 1994. Acid damage to vegetation following the Laki fissure eruption in 1783 - an historical review. *The Science of the Total Environment* 151, 241-247.

Griffiths, D. (ed) forthcoming 2017. Beside the Ocean: Viking and Medieval settlement at the Bay of Skaill, Marwick, and Birsay Bay, Orkney. Landscape Survey and Excavation 2003-11, Oxford: Oxbow Books and Historic Scotland.

Griffiths, D., Ashmore, P. (eds.) 2011. *Aeolian Archaeology*: *the Archaeology of Sand Landscapes in Scotland.* Scottish Archaeological Internet Report 48.

Griffiths, D., Harrison, J., 2011. *Birsay-Skaill Landscape Archaeology Project, Orkney Phase XI and Phase XII*: *Data Structure Report 2011.* Oxford.

Griffiths, D., Harrison, J., Hanshaw, S. 2009. *University of Oxford Birsay-Skaill Landscape Archaeology Project , Orkney, Phase X Data Structure Report 2008-9.* Oxford.

Grimsvotn, Smithsonian Institution, Global Volcanism Program, `http://www.volcano.si.edu/world/volcano.cfm?vnum=1703-01=`, accessed 4 April, 2011.

Grönvold, K., Óskarsson, N., Johnsen, S. J., Clausen, H. B., Hammer, C. U., Bond, Gerard, Bard, E., 1995. Ash layers from Iceland in the Greenland GRIP ice core

correlated with oceanic and land sediments. *Earth and Planetary Science Letters* 135, 149–155.

Grove, J., 2004. *Little Ice Ages*: *Ancient and Modern*, 2nd ed. Routledge.

Gudmundsson, A., Oskarsson, N., Gronvold, K, Saemundsson, K., Sigurdsson, O., Stefánsson, R., Gíslason, S. R., Einarsson, P., Brandsdottír, B., Larsen, G, Jóhannesson, J., Thordarson, T, 1992. The 1991 eruption of Hekla, Iceland. *Bulletin of Volcanology* 54, 238-246.

Gudmundsson, H. J., 1997. A Review of the Holocene Environmental History of Iceland. *Quaternary Science Reviews* 16, 81-92.

Gudmundsson, M. T., Sigmundsson, F., Björnsson, H., Hígnadóttir, T., 2004. The 1996 eruption at Gjálp, Vatnajökull ice cap, Iceland: efficiency of heat transfer, ice deformation and subglacial water pressure. *Bulletin of Volcanology* 66, 46-65.

Gulliksen, S., Birks, H. H., Possnert, G., Mangerud, J., 1998. A calendar age estimate of the Younger Dryas-Holocene boundary at Krakenes, western Norway. *The Holocene* 8, 249-259.

Gunnell, T. 2009. Ansgar's Conversion of Iceland. *Scripta Islandica* 60: 105-118.

Haflidason, H., Eiriksson, J., Kreveld, S. V., 2000. The tephrochronology of Iceland and the North Atlantic region during the Middle and Late Quaternary: a review. *Journal of Quaternary Science* 15, 3-22.

Haflidason, H., Larsen, G., Ólafsson, G., Larsen. 1992. The Recent Sedimentation History of Thingvallavatn, Iceland. *Oikos* 64, 80.

Hall, A. M., Hansom, J. D., Williams, D. M., Jarvis, J., 2006. Distribution, geomorphology and lithofacies of cliff-top storm deposits: Examples from the high-energy coasts of Scotland and Ireland. *Marine Geology* 232, 131-155.

Hall, V. A., Pilcher, J. R., 2002. Late-Quaternary Icelandic tephras in Ireland and Great Britain: detection, characterization and usefulness. *The Holocene* 12, 223-230.

Hall, V. A., Pilcher, J. R., McCormac, F. G., 1994. Icelandic volcanic ash and mid-Holocene Scots pine (Pinus sylvestris) decline in the north of Ireland: no correlation. *The Holocene* 4, 79-83.

Halsall, G., 2003. *Warfare and society in the Barbarian West 450-900.* Routledge, London. Hambrecht, G., 2009. Zooarchaeology and the Archaeology of Early Modern Iceland. *Journal of the North Atlantic* 2, 3-22.

Hambrecht, G., 2011. *Faunal analysis of the early modern bishop's farm at Skálholt, Arnessysla, Iceland.* Unpublished PhD thesis, City Univerity of New York.

Hamilton, J. R. C., 1956. *Excavations at Jarlshof, Shetland.* Her Majesty's Stationery Office, Edinburgh.

Hammer, C. U., Clausen, H. B., Dansgaard, W., 1980. Greenland ice sheet evidence of post-glacial volcanism and its climatic impact. *Nature* 288, 230-235.

Hansen, S., 2000. Viking settlement in Shetland. *Acta Archaeologica*, 71, 87-103.

Hansom, J. D., 2007. West coast of Orkney. *Geological Conservation Review* 28, 1-7.

Harris, O. J. T., Cobb, H., Batey, C. E., Montgomery, J. 2017. Assembling places and persons: a tenth-century Viking boat burial from Swordle Bay on the Ardnamurchan peninsula, western Scotland. *Antiquity*, Volume 91, Issue 355, 191-206.

Harrison, R., Roberts, H. M., Adderley, W. P., 2008. Gásir in Eyjafjörður: International Exchange and Local Economy in Medieval Iceland. *Journal of the North Atlantic* 1, 99.

Hastrup, K., 1990. *Nature and Policy in Iceland 1400-1800.* Clarendon Press, Oxford.

Hastrup, K., 1992. Uchronia and the two histories of Iceland, 1400-1800. In: Hastrup, K. (Ed.), *Other Histories.* Routledge, European Association of Social Anthropologists, pp. 102-121.

Hekla, Smithsonian Institution, Global Volcanism Program, `http://www.volcano.si.edu/world/volcano.cfm?vnum=1702-07=`, accessed 5 April, 2011.

Helama, S., Timonen, M., Holopainen, J., Ogurtsov, M. G., Mielikäinen, K., Eronen, M., Lindholm, M., Meriläinen, J., 2009. Summer temperature variations in Lapland during the Medieval Warm Period and the Little Ice Age relative to natural instability of thermohaline circulation on multi-decadal and multi-centennial scales. *Journal of Quaternary Science.* 24, 450–456.

Hill, D., Cowie, R., 2001. *Wics*: *the early medieval trading centres of Northern Europe*. Sheffield Academic Press., Sheffield.

Historical Eruption Data, Smithsonian Institution, Global Volcanism Project, `http://www.volcano.si.edu/world/volcano.cfm?vnum=1702-03=&volpage=erupt`, accessed 5 April, 2011.

Hjartarson, E., 1995. Heklugos fyrr á öldum. *Lesbók Morgunbladsins* 37, 1-2.

Hjort, C., Ingólfsson, Ó., Norddahl, H., 1985. Late Quaternary geology and glacial history of Hornstrandir, Northwest Iceland: a reconnaissance study. *Jökull* 35, 9-28.

Hodder, I. 1980. Social Structure and Cemeteries: A Critical Appraisal. *Anglo-Saxon Cemeteries*, ed. P. Rahtz, T. Dickinson, and L. Watts. Oxford: British Archaeological Reports 82, 161–9.

Hodder, I. 1982. *Symbols in Action: Ethnoarchaeological Studies of Material Culture*. Cambridge: Cambridge University Press.

Hodges, R., 2006. Goodbye to the Vikings?, in: Hodges, R. (Ed.), *Goodbye to the Vikings? Re-reading Early Medieval Archaeology*. Duckworth, London, pp. 157-62.

Hoelscher, S., Alderman, D., 2004. Memory and place: geographies of a critical relationship. *Social & Cultural Geography* 5, 347-355.

Holmes, J., Hall, V., Wilson, P., 1999. Volcanoes and peat bogs. *Geology Today* 15, 60-63.

Hopkins, T.S., 1991. The GIN Sea – a synthesis of its physical oceanography and literature review 1972-1985. *Earth Science Reviews* 30, 175-318.

Housley, R. A., Blockley, S. P. E., Matthews, I. P., MacLeod, A., Lowe, J. J., Ramsay, S., Miller, J. J., Campbell, E. N., 2010. Late Holocene vegetation and palaeoenvironmental history of the Dunadd area, Argyll, Scotland: chronology of events. *Journal of Archaeological Science* 37, 577-593.

Hunt, J. B., Fannin, N.G.T., Hill, P. G., Peacock, J. D., 1995. The tephrochronology and radiocarbon dating of North Atlantic Late-Quaternary sediments: An example

from the St. Kilda Basin. *The tectonics, sedimentation, and palaeoceanography of the North Atlantic Region* 90, 227-248.

Hunt, J. B., Hill, P. G., 1993. Tephra geochemistry: a discussion of some persistent analytical problems. *The Holocene* 3, 271-278.

Hunt, J. B., Hill, P. G., 1996. An inter-laboratory comparison of the electron probe microanalysis of glass geochemistry. *Quaternary International* 34-36, 229-241.

Hunt, J. B., Hill, P. G., 2001. Tephrological implications of beam size – sample-size effects in electron microprobe analysis of glass shards. *Journal of Quaternary Science* 16, 105-117.

Hunt, T. L. and Lipo C. P. 2008. Evidence for a Shorter Chronology on Rapa Nui (Easter Island). *The Journal of Island and Coastal Archaeology*, Vol. 3, Iss. 1, 140-148.

Hunter, J., 2003. The Early Norse Period. In: Edwards, Kevin J., Ralston, I.B.M. (Eds.), *Scotland After the Ice Age*, 2nd ed. Edinburgh University Press, Edinburgh, pp. 241-254.

Hunter, J., 2007a. The Interface and Scandinavian Settlement. In: Hunter, J., Bond, J., Smith, A.N. (Eds.), *Investigations at Sanday, Orkney Volume 1*: *Excavations at Pool, Sanday.* Historic Scotland, Kirkwall, 121-137.

Hunter, J., 2007b. Later Norse Settlement. In: John Hunter, Julie Bond, and A.N.S. (Ed.), *Investigations at Sanday, Orkney Volume 1*: *Excavations at Pool, Sanday.* Historic Scotland, Kirkwall, 147-168.

Hunter, J., Bond, J., Smith, A.N., 2007. Overview. In: Hunter, J., Bond, J., Smith, A.N. (Eds.), *Investigations at Sanday, Orkney Volume 1*: *Excavations at Pool, Sanday.* Historic Scotland, Kirkwall, 515-522.

Ingold, T. 1993. The Temporality of the Landscape. *World Archaeology.* Volume 25, No. 2: 152-174.

Ingold, T., Kurttila, T., 2000. Perceiving the Environment in Finnish Lapland. *Body & Society* 6, 183-196.

IPCC, 2007. *IPCC, 2007: Climate Change 2007: The Physical Science Basis. Contribution of Working Group I to the Fourth Assessment Report of the Intergovernmental Panel on Climate Change.* Cambridge University Press.

Jagan, A. 2010 Tephra stratigraphy and geochemistry from three Icelandic lake cores: a new method for determining source volcano of tepra layers, unpublished PhD thesis, University of Edinburgh.

Jennings, A. E., Gronvold, K., Hilberman, R., Smith, M., Hald, M., 2002. High-resolution study of Icelandic tephras in the Kangerlussuaq Trough, southeast Greenland, during the last deglaciation. *Journal of Quaternary Science* 17, 747-757.

Jochum, K. P., Dingwell, D. B., Rocholl, A., Stoll, B., Hofmann, A. W., Becker, S., Besmehn, A., Bessette, D., Dietze, H.-J., Dulski, P., Erzinger, J., Hellebrand, E., Hoppe, P., Horn, I., Janssens, K., Jenner, G. A., Klein, M., McDonough, W. F., Maetz, M., Mezger, K., Müker, C., Nikogosian, I. K., Pickhardt, C., Raczek, I., Rhede, D., Seufert, H. M., Simakin, S. G., Sobolev, A. V., Spettel, B., Straub, S., Vincze, L., Wallianos, A., Weckwerth, G., Weyer, S., Wolf, D., Zimmer, M., 2000. The Preparation and Preliminary Characterisation of Eight Geological MPI-DING Reference Glasses for In-Situ Microanalysis. *Geostandards and Geoanalytical Research* 24, 87-133.

Jochum, K. P., Stoll, B., Herwig, K., Willbold, M., Hofmann, A. W., et al., 2006. MPI-DING reference glasses for in situ microanalysis: New reference values for element concentrations and isotope ratios. *Geochemistry Geophysics Geosystems* 7.

Jóhannsdóttir, G. E., 2003. Gjóskulög í sjávarseti og jarðvegssniðum á Vestfjörðum. Unpublished BSc thesis, University of Iceland.

Jones, P. D., Ogilvie, A. E. J., Davies, T. D., Briffa, K. R., 2001. Unlocking the doors to the past: recent developments in climate and climate impact research in *History and Climate: Memories of the Future?*, 1-8.

Jowsey, P. C., 1966. An improved peat sampler. *New Phytologist* 65, 245-248.

Júlíusson, A. D., 2010. Signs of power: Manorial demesnes in medieval Iceland. *Viking and Medieval Scandinavia* 6, 1-29.

Kaland, S. H. H., 1982. Some economic aspects of the Orkneys in the Viking period. *Norwegian Archaeological Review* 15, 85-95.

Kaland, S. H. H., 1993. The settlement of Westness, Rousay, in: Batey, C.E., Jesch, J., Morris, C.D. (Eds.), *The Viking Age in Caithness, Orkney and the North Atlantic.* Edinburgh University Press, Edinburgh.

Karlsson, G., 1996. Plague without rats: The case of fifteenth-century Iceland. *Journal of Medieval History* 22, 263-284.

Karlsson, G., 2000. *Iceland's 1100 Years.* Hurst and Company, London.

Katla, Smithsonian Institution, Global Volcanism Project, `http://www.volcano.si.edu/world/volcano.cfm?vnum=1702-03=`, accessed 31 October, 2011.

Kawabata, E., Cronin, S.J., Bebbington, M.S., Moufti, M.R.H., El-Masry, N., Wang, T., 2015. Identifying multiple eruption phases from a compound tephra blanket: an example of the AD1256 Al-Madinah eruption, Saudi Arabia. *Bulletin of Volcanology* 77, 6.

Keatinge, T. H., Dickson, J. H., 1979. Mid-Flandrian Changes in Vegetation on Mainland Orkney. *New Phytologist* 82, 585-612.

Kirkbride, M. P., Dugmore, A. J., 2006. Responses of mountain ice caps in central Iceland to Holocene climate change. *Quaternary Science Reviews* 25, 1692-1707.

Kjartanson, G., 1967. Some new C^14 Datings in Iceland. *Náttúrufræðingurinn*, 141.

Knudsen, K L, Eiriksson, J, 2002. Application of tephrochronology to the timing and correlation of palaeoceanographic events recorded in Holocene and Late-Glacial shelf sediments off North Iceland. *Marine Geology* 191, 165-188.

Knudsen, K. L., Eiríksson, J., Jansen, E., Jiang, H., Rytter, F., Gudmundsdóttir, R. E., 2004. Palaeoceanographic changes off North Iceland through the last 1200 years: foraminifera, stable isotopes, diatoms and ice rafted debris. *Quaternary Science Reviews* 23, 2231-2246.

Korta, `http://ja.is/kort`, accessed 20 July, 2010.

Kristinsson, V., 1973. Population distribution and standard of living in Iceland. *Geoforum* 4, 53–62.

Kristjansdottir, G. B., Stoner, J. S., Jennings, A. E., Andrews, J. T., Gronvold, K., 2007. Geochemistry of Holocene cryptotephras from the North Iceland Shelf (MD99-2269): intercalibration with radiocarbon and palaeomagnetic chronostratigraphies. *The Holocene* 17, 155-176.

Krivogorskaya, Y., Perdikaris, S., McGovern, T. H., 2005. Fish bones and fishermen: the potential of zooarchaeology in the Westfjords *Archaeologica Islandica*, 1-31.

Kuehn, S., Foit, F., 2006. Correlation of widespread Holocene and Pleistocene tephra layers from Newberry Volcano, Oregon, USA, using glass compositions and numerical analysis. *Quaternary International* 148, 113-137.

Kuehn, S. C., Froese, D. G., Shane, P., 2011. The INTAV intercomparison of electron-beam microanalysis of glass by tephrochronology laboratories: Results and recommendations. *Quaternary International* 246, 19-47.

Kuzmin, Y. V, 2006. Chronology of the earliest pottery in East Asia : progress and pitfalls. *Antiquity* 80, 362–371.

Kvamme, T., Mangerud, J, Furnes, H., Ruddiman, W. F., 1989. Geochemistry of Pleistocene ash zones in cores from the North Atlantic. *Norsk Geologisk Tidskrift* 69, 251-272.

Kylander, M. E., Lind, E.M., Wastegard, S., Lowemark, L., 2011. Recommendations for using XRF core scanning as a tool in tephrochronology. The Holocene 22, 371–375.

Lacasse, C., 2001. Influence of climate variability on the atmospheric transport of Icelandic tephra in the subpolar North Atlantic. *Global and Planetary Change* 29, 31-55.

Lacasse, C., Garbe-Schonberg, C.-D., 2001. Explosive silicic volcanism in Iceland and the Jan Mayen area during the last 6 Ma: sources and timing of major eruptions. *Journal of Volcanology and Geothermal Research* 107, 113-147.

Lacasse, C., Sigurdsson, H, Carey, S., Paterne, M., Guichard, F., 1996. North Atlantic deep-sea sedimentation of Late Quaternary tephra from the Iceland hotspot. *Marine Geology* 129, 209-224.

Lacasse, C., Sigurdsson, H., Carey, S. N., Jóhannesson, H., Thomas, L. E., Rogers, N. W., 2006. Bimodal volcanism at the Katla subglacial caldera, Iceland: insight into the geochemistry and petrogenesis of rhyolitic magmas. *Bulletin of Volcanology* 69, 373-399.

Lackschewitz, K. S., Wallrabe-Adams, H.-J., 1997. Composition and origin of volcanic ash zones in Late Quaternary sediments from the Reykjanes Ridge: evidence for ash fallout and ice-rafting. *Marine Geology* 136, 209-224.

Lamb, H. H., 1977. *Climate*: *Past Present and Future*. Routledge.

Lamb, H. H., 1979. Climatic Variation and Changes in the Wind and Ocean Circulation: The Little Ice Age in the Northeast Atlantic. *Quaternary Research* 11, 1-20.

Lamb, H. H., 1982. *Climate, History, and the Modern World*. London: Routledge.

Lane, C. S., Andri, M., Cullen, V. L., Blockley, S. P. E., 2011. The occurrence of distal Icelandic and Italian tephra in the Lateglacial of Lake Bled , Slovenia. *Quaternary Science Reviews*, 1-6.

Lane, C. S., 2008. *Exploring the variability of microtephra deposits*: *chemical characterisation and discrimination methods*. Unpublished PhD thesis, University of Oxford.

Langdon, P. G., Barber, K. E., 2001. New Holocene tephras and a proxy climate record from a blanket mire in northern Skye, Scotland. *Journal of Quaternary Science* 16, 753-759.

Langdon, P. G., Barber, K. E., 2004. Snapshots in time: precise correlations of peat-based proxy climate records in Scotland using mid-Holocene tephras. *The Holocene* 14, 21-33.

Lanting, J. N. and van der Plicht, J. 1998 Reservoir effects and apparent ^{1}4C ages, *The Journal of Irish Archaeology* IX, 151-165.

Larsen, D. J., Miller, G. H., Geirsdóttir, Á., Thordarson, T., 2011. A 3000-year varved record of glacier activity and climate change from the proglacial lake Hvítárvatn, Iceland. *Quaternary Science Reviews* 30, 2715-2731.

Larsen, G., 1984. Recent volcanic history of the Veidivötn fissure swarm, southern Iceland - An approach to volcanic risk assessment. *Journal of Volcanology and Geothermal Research* 22, 33-58.

Larsen, G., 1992. Gjoskulagid ur Heklugosinu 1158. *Jardfraedafelag Islands*, 25-27.

Larsen, G., 2002. A brief overview of eruptions from ice-covered and ice-capped volcanic systems in Iceland during the past 11 centuries: frequency, periodicity and implications. *Geological Society, London, Special Publications* 202, 81-90.

Larsen, G., Dugmore, A. J., Newton, A. J., 1999. Geochemistry of historical age silicic tephras in Iceland. *The Holocene* 9, 463-471.

Larsen, G., Eiriksson, J., 2007. Late Quaternary terrestrial tephrochronology of Iceland – frequency of explosive eruptions, type and volume of tephra deposits. *Journal of Quaternary Science* 23, 109-120.

Larsen, G., Eiríksson, J., Knudsen, K. L., Heinemeier, J., 2002. Correlation of late Holocene terrestrial and marine tephra markers, north Iceland: implications for reservoir age changes. *Polar Research* 21, 283-290.

Larsen, G., Newton, A. J., Dugmore, A. J., Vilmundardottir, E. G., 2001. Geochemistry, dispersal, volumes and chronology of Holocene silicic tephra layers from the Katla volcanic system, Iceland. *Journal of Quaternary Science* 16, 119-132.

Lárusdóttir, B., 2006. Settlement Organization and Farm Abandonment: The Curious Landscape of Reykjahverfi, North-East Iceland in *People and Space in the Middle Ages*, 45-64.

Larúsdóttir, B., 2006. Settlement Organization and Farm Abandonment: The Curious Landscape of Reykjahverfi, North-East Iceland, in: *People and Space in the Middle Ages, 300-1300*. Brepols, 45-63.

Ledger, P. M. 2013. *Norse landnám and its impact on the vegetation of Vatnahverfi, Eastern Settlement, Greenland*, unpublished PhD thesis, University of Aberdeen.

Ledger, P. M., Edwards, K. J., Schofield, J. E. 2013. Shieling activity in the Norse Eastern Settlement: Palaeoenvironment of the 'Mountain Farm', Vatnahverfi, Greenland. *The Holocene* 23 (6), 810-822.

Ledger, P. M., Edwards, K. J., Schofield, J. E. 2014a. A multiple profile approach to the palynological reconstruction of Norse landscapes in Greenland's Eastern Settlement. *Quaternary Research* 82, 22-37.

Ledger, P. M., Edwards, K. J., Schofield, J. E. 2014b. Vatnahverfi: A Green and Pleasant Land? Palaeoecological Reconstructions of Environmental and Land-use Change. *Journal of the North Atlantic* 6, 29-46.

Ledger, P. M., Edwards, K. J., Schofield, J. E. 2015. Taphonomy or signal sensitivity in palaeoecological investigations of Norse landnám in Vatnahverfi, southern Greenland? *Boreas* 44:1, 197-215.

Ledger, P. M., Edwards, K. J., Schofield, J. E. 2017. Competing hypotheses, ordination and pollen preservation: Landscape impacts of Norse *landnám* in southern Greenland. *Review of Paleobotany and Palynology* 236, 1-11.

Lee, B., Bacon Shone, J., 2005. Application of discriminant function analysis and change-point problem in dating volcanic ashes. *Social Sciences Research Centre.*

Lillehammer, G., 2007. The Past in the Present. Landscape Perception, Archaeological Heritage and Marginal Farmland in Jaeren, South-western Norway. *Norwegian Archaeological Review* 40, 159-178.

Lineweaver, J. L., 1962. Oxygen outgassing caused by electron bombardment of glass. *Journal of Applied Physics* 34, 1786-1791.

Lloyd, J. M., Norddahl, H., Bentley, M. J., Newton, A. J., Tucker, O., Zong, Y., 2009. Lateglacial to Holocene relative sea-level changes in the Bjarkarlundur area near Reykholar, North West Iceland. *Journal of Quaternary Science* 24, 816-831.

Lowe, D. J., 2008. Globalization of tephrochronology: new views from Australasia. *Progress in Physical Geography* 32, 311-335.

Lowe, D. J., 2011. Tephrochronology and its application: A review. *Quaternary Geochronology* 6, 107-153.

Lowe, D. J., Hunt, J. B., 2001. A summary of terminology used in tephra-related studies in *Tephras*: *Chronology, Archaeology*, 17-22.

Lowe, D. J., Shane, P., Alloway, B. V., Newnham, R. M., 2008. Fingerprints and age models for widespread New Zealand tephra marker beds erupted since 30,000 years ago: a framework for NZ-INTIMATE. *Quaternary Science Reviews* 27, 95-126.

Lowe, J. J., Turney, C. S. M., 1997. Vedde ash layer discovered in a small lake basin on the Scottish mainland. *Journal of the Geological Society* 154, 605-612.

Lowe, J. J., Walker, M. J. C., Scott, E. M., Harkness, D. D., Bryant, C. J., Davies, S. M., 2004. A coherent high-precision radiocarbon chronology for the Late-glacial sequence at Sluggan Bog, Co. Antrim, Northern Ireland. *Journal of Quaternary Science* 19, 147-158.

Lund, J., 2013. Fragments of a conversion: handling bodies and objects in pagan and Christian Scandinavia AD 800–1100. *World Archaeology*, Volume 45, No. 1: 46-63.

Mahler, D. L. 2007. Sæteren ved Argisbrekka. Økonomiske forandringer på Færøerne i vikingetid og tidlig middelalder. Economic development during the Viking Age and Early Middle Ages on the Faroe Islands. *Annales Societatis Scientiarum Fœroensis Supplementum* 47. Faroe University Press, Tórshavn, Faroe Islands.

Mairs, K.-A., Church, M. J., Dugmore, A. J., Sveinbjarnardóttir, G., 2006. Degrees of success: evaluating the environmental impacts of long term settlement in South Iceland in *Dynamics of northern societies*: *proceedings of the SILA/NABO Conference on Arctic and North Atlantic Archaeology*. Aarhus University Press, Copenhagen, 365-373.

Malmberg, S. A., 1985. The water masses between Iceland and Greenland. *Journal of Marine Research Institute* 9, 127-140.

Mangerud, J, Lie, S. E., Furnes, H., Kristiansen, I. L., Lomo, L., 1984. A Younger Dryas ash bedn in western Norway, and its possible correlations with tephra in cores from the Norwegian Sea and the North Atlantic. *Quaternary Research* 21, 85-104.

Mann, M. E., 2007. Climate Over the Past Two Millennia. *Annual Review of Earth and Planetary Sciences* 35, 111-136.

Mardia, K. V., Kent, J. T., Bibby, J., 1989. *Multivariate Analysis*, 7th ed. Academic Press, Harcourt Brace Jovanovich, London.

Masse, G., Rowland, S., Sicre, M., Jacob, J., Jansen, E, Belt, S., 2008. Abrupt climate changes for Iceland during the last millennium: Evidence from high resolution sea ice reconstructions. *Earth and Planetary Science Letters* 269, 565-569.

McCormac, F. G., Bayliss, A., Baillie, M. G. L., Brown, D. M., 2004. Radiocarbon calibration in the Anglo-Saxon period. *Radiocarbon*, Vol. 46, No. 3, 1123-1125.

McGovern, T. H., 1990. The Archaeology Of The Norse North Atlantic. *Annual Review of Anthropology* 19, 331-351.

McGovern, T.H., 1999. Report of Cattle and Sheep Skulls Recovered from Hofstaðir, Mývatnssveit N Iceland. CUNY Northern Science and Education Center NORSEC Laboratory Report 55.

McGovern, T.H., 2001. Walrus Tusks and Bone From Aðalstræti 14-18, Reykjavík Iceland. CUNY Northern Science and Education Center NORSEC Report 55.

McGovern, T. H., Bigelow, G., Amorosi, T., Russell, D., 1988. Northern Islands, human error, and environmental degradation: A view of social and ecological change in the Medieval North Atlantic. *Human Ecology* 16, 225-270.

McGovern, T. H., Perdikaris, S., Einarsson, Á., Sidell, J., 2006. Coastal connections, local fishing, and sustainable egg harvesting: patterns of Viking Age inland wild resource use in Mývatn district, Northern Iceland. *Environmental Archaeology* 11, 187-205.

McGovern, T. H., Smiarowski, K., and Harrison, R., 2013. Hard Times at Hofstaðir? An Archaeofauna circa 1300 AD from Hofstaðir in Mývatnssveit, N Iceland. Hofstaðir 2011 Archaeofauna, NORSEC Lab Report 60.

McGovern, T. H., Vésteinsson, O., Friðriksson, A., Church, M., Lawson, I., Simpson, I. A., Einarsson, A., Dugmore, A. J., Cook, G. T., Perdikaris, S., Edwards, K. J., Thomson, A. M., Adderley, W. P., Newton, A., Lucas, G., Edvardsson, R. Aldred, O. Dunbar, E. 2007. Landscapes of settlement in northern Iceland: Historical ecology of human impact and climate fluctuation on the millennial scale. *American Anthropologist* 109, 27–51.

McKinzey, K. M., Olafsdottir, R., Dugmore, A. J., 2005. Perception, history and science: coherence or disparity in the timing of the Little Ice Age maximum in south-east Iceland? *Polar Record* 41, 319-334.

McNeely R., Dyke A.S., and Southon J.R., 2006. Canadian marine reservoir ages, preliminary data assessment, Open File 5049, Geological Survey Canada, 3.

Meara, R.H. 2012 *Geochemical fingerprinting of Icelandic silicic Holocene tephra layers*, unpublished PhD thesis, University of Edinburgh.

Met Office Historical Data, `http://www.metoffice.gov.uk/climate/uk/averages/regmapavge.html$#$nscotland`, accessed 28 February 2011.

Met Office Lerwick Data, `http://www.metoffice.gov.uk/climate/uk/stationdata/lerwickdata.txt`, accessed 20 January, 2012.

Met Office Wick Airport Data, `http://www.metoffice.gov.uk/climate/uk/stationdata/wickairportdata.txt`, accessed 20 January, 2012.

Metrich, N., Sigurdsson, H., Meyer, P. S., Devine, J. D., 1991. The 1783 Lakagigar eruption in Iceland: geochemistry, CO2 and sulfur degassing. *Contributions to Mineralogy and Petrology* 107, 435-447.

Milek, K. (ed.), 2007. *Vatnsfjordur 2006* Framvinduskýrslur/Interim Reports. Reykjavik.

Milek, K. (ed.), 2009. *Vatnsfjörður 2008* Framvinduskýrslur/Interim Reports. Reykjavík.

Milek, K. (ed.), 2010. *Vatnsfjörður 2009* Framvinduskýrslur/Interim Reports. Reykjavík.

Milek, K. (ed.), 2011. *Vatnsfjörður 2010* Framvinduskýrslur/Interim Reports. Reykjavík.

Milner, N., Barrett, J., Welsh, J., 2007. Marine resource intensification in Viking Age Europe: the molluscan evidence from Quoygrew, Orkney. *Journal of Archaeological Science* 34, 1461-1472.

Mitchell, I., 1999. *Scotland's mountains before the mountaineers.* Luath Press.

Mitchell, P., 2008. Practising archaeology at a time of climatic catastrophe. *Antiquity* 82, 1093-1103.

Mobilia, M. P., 2009. *Climate archives from a Viking Age site, Scotland: Seasonal temperature variability during the Medieval Warm Period.* Unpublished MSc thesis, University of North Carolina at Chapel Hill.

Morris, C., 1989. *The Birsay Bay Project Volume 1.* Department of Archaeology, University of Durham, Durham.

Morris, C., 1996. *The Birsay Bay Project Volume 2.* Department of Archaeology, University of Durham, Durham.

Morrocco, S. M., Ballantyne, C. K., Spencer, J. Q. G., Robinson, R. A. J., 2007. Age and significance of aeolian sediment reworking on high plateaux in the Scottish Highlands. *The Holocene* 17, 349-360.

Mortensen, A. K., Bigler, Matthias, Grönvold, K., Steffensen, Jörgen P., Johnsen, Sigfós J., 2005. Volcanic ash layers from the Last Glacial Termination in the NGRIP ice core. *Journal of Quaternary Science* 20, 209-219.

Myhre, B., 1993. The beginning of the Viking Age – some current archaeological problems, in: Faulkes, A., Perkins, R. (Eds.), *Viking Revaluations.* Viking Society for Northern Research, University College London, London, 182-204.

NABO, `http://www.nabohome.org/cgi_bin/explore.pl?seq=47`, accessed 5 December, 2011.

Newnham, R. M, Lowe, D. J, 1999. Testing the synchroneity of pollen signals using tephrostratigraphy. *Global and Planetary Change* 21, 113-128.

Newton, A. J., Dugmore, A. J., Gittings, B. M., 2007. Tephrabase: tephrochronology and the development of a centralised European database. *Journal of Quaternary Science* 22, 737-743.

Nicoll, K., 2004. Recent environmental change and prehistoric human activity in Egypt and Northern Sudan. *Quaternary Science Reviews* 23, 561-580.

Nielsen, C. H., Sigurdsson, H., 1981. Quantitative methods for electron microprobe analysis of sodium in natural and synthetic glasses. *American Mineralogist* 66, 547-552.

OxCal 4.2, 2016. https://c14.arch.ox.ac.uk/embed.php?File=oxcal.html, University of Oxford.

Ogilvie, A. E. J., 1984. The Past Climate and Sea-Ice Record from Iceland, Part 1: Data to A.D. 1780. *Climatic Change*. Springer Netherlands 6, 131-52.

Ogilvie, A. E. J., 1986. The climate of Iceland, 1701-1784. *Jökull* 36, 57-73.

Ogilvie, A. E. J., 1990. Climatic Changes in Iceland A.D. c. 865 to 1598. *Acta Archaeologica* 61, 233-251.

Ogilvie, A. E. J., 1995. Climate of Iceland from 1500. In: Bradley, Raymond S., Jones, Philip D. (Eds.), *Climate since AD 1500*. Routledge, 92-117.

Ogilvie, A. E. J., Jónsdóttir, I, 2000. Sea Ice , Climate , and Icelandic Fisheries in the Eighteenth and Nineteenth Centuries. *Fisheries* 53, 383-394.

Ogilvie, A. E. J., Jónsson, T., 2001. 'Little Ice Age' research: a perspective from Iceland. *Climatic Change* 48, 9-52.

Óladóttir, B. A., Larsen, G., Sigmarsson, O., 2011. Holocene volcanic activity at Grímsvötn, Bárdarbunga and Kverkfjöll subglacial centres beneath Vatnajökull, Iceland. *Bulletin of Volcanology* 73, 1187-1208.

Óladóttir, B. A., Larsen, G., Thordarsen, T., Sigmarsson, O., 2005. The Katla volcano S-Iceland: Holocene tephra stratigraphy and eruption frequency. *Jökull* 55, 53-74.

Óladóttir, B. A., Sigmarsson, O., Larsen, G., Devidal, J.-L., 2011. Provenance of basaltic tephra from Vatnajökull subglacial volcanoes, Iceland, as determined by major- and trace-element analyses. *The Holocene* 21, 1037-1048.

Óladóttir, B. A., Sigmarsson, O., Larsen, G., Thordarson, T., 2007. Katla volcano, Iceland: magma composition, dynamics and eruption frequency as recorded by Holocene tephra layers. *Bulletin of Volcanology* 70, 475-493.

Olsen, J., Björck, S., Leng, M. J., Gudmundsdóttir, E. R., Odgaard, B. V., Lutz, C. M., Kendrick, C. P. , Andersen, T. J., Seidenkrantz, M. S., 2010. Lacustrine evidence of Holocene environmental change from three Faroese lakes: a multiproxy XRF and stable isotope study. *Quaternary Science Reviews*, 29(19), 2764-2780.

Olsson, I.U., 1980. Content of 14C in marine mammals from northern Europe. *Radiocarbon* 22, 662-675.

Oram, R., Adderley, W.P., 2008. Lordship and Environmental Change in Central Highland Scotland. *Journal of the North Atlantic* 1, 74-84.

Outram, Z., Batt, C.M., 2010. Dating at Old Scatness. In: Dockrill, S. J., Bond, J. M., Brown, L. D., Turner, V. E., Bashford, D. J., Cussans, J. E. and Nicholson, R. A. (Eds.). *Excavations at Old Scatness, Shetland. Volume 1: The Pictish Village and Viking Settlement.* Lerwick: Shetland Heritage Publications. 99-130.

Owen, O., Dalland, M., 1999. *Scar: a Viking Boat Burial on Sanday, Orkney.* Phantassie: Tuckwell Press.

Owen, O., Lowe, C. 1999. *Kebister: The Four-thousand-year-old Story of One Shetland Township*, Society of Antiquaries of Scotland.

OxCal,

Pálson, H., Edwards, P. (translators), 2007. *The Book of Settlements: Landnámabók.* University of Manitoba Press.

Parker Pearson, M. 1982. Mortuary Practices, Society and Ideology: An Ethnoarchaeological Study. *Symbolic and Structural Archaeology*, I. Hodder (ed.). Cambridge: Cambridge University Press: 99–113.

Patterson, W. P., Dietrich, K. A., Holmden, C., Andrews, J. T., 2010. Two millennia of North Atlantic seasonality and implications for Norse colonies. *Proceedings of the National Academy of Science*, 1-5.

Pawlowsky-Glahn, V., Egozcue, J. J., 2006. Compositional data and their analysis: an introduction. *Geological Society, London, Special Publications* 264, 1-10.

Payne, R. J., Blackford, J. J., 2008. Extending the Late Holocene Tephrochronology of the Central Kenai Peninsula , Alaska. *Quaternary Research* 61, 243 – 254.

Payne, R. J., Gehrels, M., 2010. The formation of tephra layers in peatlands: An experimental approach. *Catena* 81, 12-23.

Payne, R. J., Kilfeather, A., Meer, J. van der, 2005. Experiments on the taphonomy of tephra in peat. *Suosuera (Finnish Peatland)* 56, 147-156.

Pearce, N. J. G., 2004. The application of ICP-MS methods to tephrochronological problems. *Applied Geochemistry* 19, 289-322.

Pearce, N. J. G., Denton, J. S., Perkins, W. T., Westgate, J. A., Alloway, B. V., 2007. Correlation and characterisation of individual glass shards from tephra deposits using trace element laser ablation ICP-MS analyses: current status and future potential. *Journal of Quaternary Science* 22, 721–736.

Perdikaris, S., McGovern, T. H., 2007. Cod Fish, Walrus, and Chieftains: Economic intensification in the Norse North Atlantic. *Studies in Human Ecology and Adaptation* 3, 193-216.

Pilcher, J. R., Bradley, R. S., Francus, P., Anderson, L., 2005. A Holocene tephra record from the Lofoten Islands, Arctic Norway. *Boreas* 34, 136-156.

Pilcher, J. R., Hall, V. A., 1992. Towards a tephrochronology for the Holocene of the north of Ireland. *The Holocene* 2, 255-259.

Pilcher, J. R., Hall, V. A., McCormac, F. G., 1995. Dates of Holocene Icelandic volcanic eruptions from tephra layers in Irish peats. *The Holocene* 5, 103-110.

Plunkett, G. M., Whitehouse, N. J., Hall, V. A., Brown, D. M., Baillie, M. G. L., 2004. A precisely-dated lake-level rise marked by diatomite formation in northeastern Ireland. *Journal of Quaternary Science* 19, 3-7.

Pollard, A. M., Blockley, S. P. E., Lane, C. S., 2006. Some numerical considerations in the geochemical analysis of distal microtephra. *Applied Geochemistry* 21, 1692-1714.

Pollard, A. M., Davoudi, H., Mostafapour, I., Valipour, H. R., Nashli, H. F. 2012. New Radiocarbon Chronology for the Late Neolithic to Iron Age in the Qazvin Plain, Iran. *The International Journal of the Humanities* Article 6, Volume 19, Issue 3, Summer 2012, Page 110-151.

Prestvik, T., 1980. Petrology of hybrid intermediate and silicic rocks from Öræfajökull, southeast Iceland. *Geologiska Foereningan i Stockholm.* Foerhandlingar 101, 299-307.

Principato, S. M., 2003. *The Late Quaternary History of Eastern Vestfirdir, NW Iceland.* Unpublished PhD thesis, University of Colorado.

Principato, S. M., 2008. Geomorphic evidence for Holocene glacial advances and sea level fluctuations on eastern Vestfirðir, northwest Iceland. *Boreas* 37, 132-145.

Principato, S. M., Geirsdóttir, Á., Jóhannsdóttir, G. E., Andrews, J. T., 2006. Late Quaternary glacial and deglacial history of eastern Vestfirdir, Iceland using cosmogenic isotope (^{3}6Cl) exposure ages and marine cores. *Journal of Quaternary Science* 21, 271-285.

Pyle, D., 1989. The thickness, volume and grainsize of tephra fall deposits. *Bulletin of Volcanology*, 1-15.

Pyne-O'Donnell, S. D. F., 2010. The taphonomy of Last Glacial-Interglacial Transition (LGIT) distal volcanic ash in small Scottish lakes. *Boreas* 40, 131-145.

Pyne-O'Donnell, S. D. F., Blockley, S. P. E., Turney, C. S. M., Lowe, J. J., 2008. Distal volcanic ash layers in the Lateglacial Interstadial (GI-1): problems of stratigraphic discrimination. *Quaternary Science Reviews* 27, 72-84.

Quillmann, U., Jennings, A., Andrews, J., 2010. Reconstructing Holocene palaeoclimate and palaeoceanography in Ìsafjarðardjúp, northwest Iceland, from two fjord records overprinted by relative sea-level and local hydrographic changes. *Journal of Quaternary Science* 25, 1144-1159.

Ranner, P. H., Allen, J. R. M., Huntley, B., 2005. A new early Holocene cryptotephra from northwest Scotland. *Journal of Quaternary Science* 20, 201-208.

Rea, H. A., Swindles, G. T., Roe, H. M., 2012. The Hekla 1947 tephra in the north of Ireland: regional distribution, concentration and geochemistry. *Journal of Quaternary Science*, advance copy.

Reed, S.J.B., 2005. *Electron Microprobe Analysis and Scanning Electron Microscopy in Geology.* Cambridge University Press.

Reimer, P.J., Baillie, M. G. L., Bard, E., Bayliss, A., Beck, J. W., Bertrand, C. J. H., Blackwell, P. G., Buck, C. E., Burr, G.S., Cutler, K. B., Damon, P. E., Edwards, R. L., Fairbanks, R. G., Friedrich, M., Guilderson, T. P., Hogg, A. G., Hughen, K. A., Kromer, B., McCormac, G., Manning, S., Ramsey, C. B., Reimer, R. W., Remmele, S., Southon, J. R., Stuiver, M., Talamo, S., Taylor, F. W., van der Plicht, J., Weyhenmeyer, C. E., 2004. IntCal04 terrestrial radiocarbon age calibration, 0–26 cal kyr BP. Radiocarbon 46 (3), 1029–1058.

Reimer, P., Bard, E., Bayliss, A., Beck, J., Blackwell, P., Bronk Ramsey, C., Buck, C., Cheng, H., Edwards, R., Friedrich, M., Grootes, P., Guilderson, T., Haflidason, H., Hajdas, I., Hatté, C., Heaton, T., Hoffmann, D., Hogg, A., Hughen, K., Kaiser, K., Kromer, B., Manning, S., Niu, M., Reimer, R., Richards, D., Scott, E., Southon, J., Staff, R., Turney, C., van der Plicht, J., 2013. IntCal13 and Marine13 Radiocarbon Age Calibration Curves 0–50,000 Years cal BP. Radiocarbon 55(4), 1869-1887.

Reimer, P. J., McCormac, F., Moore, J., McCormick, F., Murray, E.V. 2002 Marine radiocarbon reservoir corrections for the mid-to late Holocene in the eastern subpolar North Atlantic. *The Holocene*, 129-135.

Reimer, P. J., Reimer, R. W., 2001. A marine reservoir correction database and on-line interface. *Radiocarbon*, Vol 43, number 2A: 461-463.

Rhodes, E. J., Schwenninger, J.-L., 2007. Dose rates and radioisotope concentrations in the concrete calibration blocks at Oxford. *Ancient TL*, Volume 25, No. 1: 5-8.

Richards, M., Fuller, B., Molleson, T., 2006. Stable isotope palaeodietary study of humans and fauna from the multi-period (Iron Age, Viking and Late Medieval) site of Newark Bay, Orkney. *Journal of Archaeological Science* 33, 122-131.

Ritchie, A., 1994. *Viking Scotland.* Historic Scotland.

Roberts, R.G., 1997. Luminescence dating in archaeology: from origins to optical. *Radiation Measurements* 27, 819-892.

Roberts, S., Sigurvinsson, J., Westgate, J., Sandhu, A., 2007. Late Pliocene glaciation and landscape evolution of Vestfirðir, Northwest Iceland. *Quaternary Science Reviews* 26, 243-263.

Roesdahl, E., 1987. *The Vikings.* Penguin.

Ruddiman, W. F., Glover, L. K., 1972. Vertical mixing of ice-rafted volcanic ash in North Atlantic sediments. *Geological Society of America Bulletin* 83, 2817-2836.

Ruddiman, W. F., McIntyre, A., 1981. The North Atlantic Ocean during the last deglaciation. *Palaeogeography, Palaeoclimatology, Palaeoecology* 35, 145-214.

Sackmann, S. 1991 *Cultural knowledge in organizations*: *Exploring the collective mind.* Sage Publications.

Sayle, K., Cook, G. T., Ascough, P. H., Gestsdóttir, H., Hamilton, D., and McGovern, T. H., 2014. Utilization of ^{1}3C, ^{1}5N, and ^{3}4S Analyses to Understand ^{1}4C Dating Anomalies within a Late Viking Age Community in Northeast Iceland. *Radiocarbon* 56, 811–821.

Schofield, J. E., Edwards, K. J., 2011. Grazing impacts and woodland management in Eriksfjord: Betula, coprophilous fungi and the Norse settlement of Greenland. *Vegetation History and Archaeobotany*, 20(3), 181-197.

Schofield, J. E., Edwards, K. J., Christensen, C., 2008. Environmental impacts around the time of Norse *landnám* in the Qorlortoq valley, Eastern Settlement, Greenland *Journal of Archaeological Science* 35, 1643-1657.

Sejrup, H. P., Sjoholm, J., Furnes, H., Beyer, I., Eide, L., Jansen, E, Mangerud, J, 1989. Quaternary tephrochronology on the Iceland Plateau, north of Iceland. *Journal of Quaternary Science* 4, 109-114.

Selbekk, R., Tronnes, R., 2007. The 1362 AD Öræfajökull eruption, Iceland: Petrology and geochemistry of large-volume homogeneous rhyolite. *Journal of Volcanology and Geothermal Research* 160, 42-58.

Shane, P., 2005. Towards a comprehensive distal andesitic tephrostratigraphic framework for New Zealand based on eruptions from Egmont volcano. *Journal of Quaternary Science* 20, 45-57.

Shanks, M., Tilley, C. 1987. *Social Theory in Archaeology.* Oxford: Polity Press.

Shapley, M. D. and Finney, B. P. 2015. Lake morphometry controls the remobilization and long-term geochemical imprint of distal tephra deposition. *Journal of Paleolimnology* January.

Sharples, N., ed. 2012. *Late Iron Age farmstead in the Outer Hebrides : Excavations at Mound 1, Bornais, South Uist.* Oxbow Books.

Shaw, F. J., 1980. *The Northern and Western Islands of Scotland*: *Their economy and society in the seventeenth century.* John Donald, Edinburgh.

Sicre, M., Jacob, J., Ezat, U., Rousse, S., Kissel, C., Yiou, P., Eiriksson, J, Knudsen, K., Jansen, E, Turon, J., 2008. Decadal variability of sea surface temperatures off North Iceland over the last 2000 years. *Earth and Planetary Science Letters* 268, 137-142.

Sigmarsson, O., Condomines, M., Fourcade, S., 1992. A detailed Th, Sr and O isotope study of Hekla: differentiation processes in an Icelandic Volcano. *Contributions to Mineralogy and Petrology* 112, 20-34.

Sigmarsson, O., Vlastelic, I., Andreasen, R., Bindeman, I., Devidal, J.L., Moune, S., Keiding, J.K., Larsen, G., Höskuldsson, A., Thordarson, T.H., 2011. Remobilization of silicic intrusion by mafic magmas during the 2010 Eyjafjallajökull eruption. *Solid Earth* 2, 271–281.

Sigurdsson, H., Sparks, R. S. J., 1981. Petrology of rhyolitic and mixed magma ejecta from the 1875 eruption of Askja, Iceland. *Journal of Petrology* 22, 41-84.

Sigurgeirsson, M. Á., 2006. Discovery of the Hekla-1693 tephra at Vatnsfjördur in Milek (eds.), Vatnsfjördur Interim Field Report 2006, 78-79.

Simpson, I. A., 1997. Relict Properties of Anthropogenic Deep Top Soils as Indicators of Infield Management in Marwick, West Mainland, Orkney. *Journal of Archaeological Science* 24, 365-380.

Simpson, I. A, Adderley, W. P., 2002. Soil Limitations to Agrarian Land Production in Premodern Iceland *Human Ecology* 30, 423-443.

Simpson, I. A., Barrett, J. H., Milek, K. B., 2005. Interpreting the Viking Age to Medieval period transition in Norse Orkney through cultural soil and sediment analyses. *Geoarchaeology* 20, 355-377.

Simpson, I. A., Dugmore, A. J., Thomson, A., Vésteinsson, O., 2001. Crossing the thresholds: human ecology and historical patterns of landscape degradation. *Catena* 42, 175-192.

Simpson, I. A., Vésteinsson, O., Adderley, W., McGovern, T. H., 2003. Fuel resource utilisation in landscapes of settlement. *Journal of Archaeological Science* 30, 1401-1420.

Sjoholm, J., Sejrup, H. P., Furnes, H., 1991. Quaternary volcanic ash zones on the Iceland Plateau, southern Norwegian Sea. *Journal of Quaternary Research* 6, 159-173.

Skre, D., 2001. The social context of settlement in Norway in the first millennium AD. *Norwegian Archaeological Review* 34, 1-34.

Smit, B., Bray, J., Keddie, P., 1991. Identification of Marginal Agricultural Areas in Ontario, Canada. *Geoforum* 22, 333-346.

Smith, M. H., Arneborg, J., Smith, K. P. 2015. The 'Burgundian' hat from Herjolfsnes, Greenland: new discoveries, new dates. *Danish Journal of Archaeology*, 4:1, 21-32.

Snaefellsjokull, Smithsonian Institution, Global Volcanism Project `http://www.volcano.si.edu/world/volcano.cfm?vnum=1700-01=`, accessed 1 November, 2011.

Sommerville, A. A., Hansom, J. D., Housley, R. A., Sanderson, D. C. W., 2007. Optically stimulated luminescence (OSL) dating of coastal aeolian sand accumulation in Sanday, Orkney Islands, Scotland. *The Holocene* 17, 627-637.

South Uist, Bornish, Royal Commission on the Ancient and Historical Monuments of Scotland, `http://canmore.rcahms.gov.uk/en/site/108290/details/south+uist+bornish/`, accessed 23 July, 2017.

Sparks, R. S. J., 1981. Petrology of Rhyolitic and Mixed Magma Ejecta from the 1875 Eruption of Askja , Iceland. *Journal of Petrology* 22, 41-84.

Steinthorsson, S., Hardarson, B. S., Ellam, R. M., Larsen, G, 2000. Petrochemistry of the Gjálp-1996 subglacial eruption, Vatnajökull , SE Iceland. *Journal of Volcanology and Geothermal Research* 98, 79-90.

Stenseth, N. C., Ottersen, G., Hurrell, J. W., Mysterud, A., Lima, M., Chan, K.-S., Yoccoz, N. G., Adlandsvik, B., 2003. Review article. Studying climate effects on ecology through the use of climate indices: the North Atlantic Oscillation, El Niño

Southern Oscillation and beyond. *Proceedings. Biological sciences The Royal Society* 270, 2087-96.

Steward, J.H., 1977. *Evolution and Ecology: Essays on Social Transformation.* University of Illinois Press.

Stokes, S., David, J. L., Froggatt, P. C., 1992. Discriminant function analysis and correlation of late Quaternary rhyolitic tephra deposits from Taupo and Okataina volcanoes, New Zealand, using glass shard major element composition. *Quaternary International* 13, 103-117.

Stokes, S, Lowe, D., 1988. Discriminant function analysis of late Quaternary tephras from five volcanoes in New Zealand using glass shard major element chemistry. *Quaternary Research* 30, 270-283.

Stothers, R. B., 1996. The great dry fog of 1783. *Climatic Change* 32, 79-89.

Stothers, R. B., 1998. Far reach of the tenth century Eldgjá eruption, Iceland. *Climatic Change*, 715-726.

Stötter, J., Wastl, M., Caseldine, C., Häberle, T., 1999. Holocene palaeoclimatic reconstruction in northern Iceland: approaches and results. *Quaternary Science Reviews* 18, 457-474.

Streeter, R., Dugmore, A. J., Vésteinsson, O., 2012. Plague and landscape resilience in premodern Iceland. *Proceedings of the National Academy of Sciences of the United States of America* 109, 3664-9.

Stuiver, M. and Braziunas T. F. 1993. Modeling atmospheric ^{14}C influences and ^{14}C ages of marine samples to 10,000 BC. *Radiocarbon* 35, 137-189.

Stuiver M, Polach HA. 1977. Discussion: reporting of ^{14}C data. *Radiocarbon* 19(3): 355–63.

Stuiver, M. and Reimer, P. J., 1993. Extended ^{14}C data base and revised Calib 3.0 ^{14}C age calibration. *Radiocarbon* 35, 215-230.

Stummann Hansen, S. 2013. Toftanes. A Viking Age farmstead in the Faroe Islands: archaeology, environment and economy. *Acta Archaeologica* 84, no. 1.

Stylegar, F.-A., Grimm, O., 2005. Boathouses in Northern Europe and the North Atlantic. *International Journal of Nautical Archaeology* 34, 253-268.

Sutherland, D. G., Gordon, J. E., 1993. The Orkney Islands. In: Gordon, J. E., Sutherland, D.G. (Eds.), *Quaternary of Scotland.* Chapman and Hall, 69-82.

Suzuki, T., 1996. *Chemical analysis of volcanic glass by energy dispersive X-ray spectromery with JEOL JED-2001 and JSM-5200*: *analytical procedures and application.* Tokyo.

Sveinbjarndóttir, G., 1992. *Farm abandonment in Medieval and post-Medieval Iceland*: *an interdisciplinary study.* Oxbow Books.

Sveinbjarnardóttir, G., Mairs, K. A., Church, M. J., Dugmore, A. J., 2006. Settlement history, land holdings and landscape change, Eyjafjallahreppur, Iceland in *Dynamics of northern societies*: *proceedings of the SILA/NABO Conference on Arctic and North Atlantic Archaeology.* Aarhus University Press, Copenhagen, 323-333.

Sveinbjörnsdóttir, A., Heinemeier, J., Arneborg, J., Lynnerup, N., Olafsson, G., Zoëga, G. 2010. Dietary reconstruction and reservoir correction of 14C dates on bones from pagan and early Christian graves in Iceland. *Radiocarbon* 52, 682-696.

Swindles, G., 2010. Dating recent peat profiles using spheroidal carbonaceous particles (SCPs). *Mires and Peat* 7, 1-5.

Swindles, G. T., Galloway, J., Outram, Z., Turner, K., Schofield, J. E., Newton, A. J., Andrew, J., Church, M. J., Watson, E. J., Batt, C., Bond, J., Edwards, K. J., Turner, V., Bashford, D., 2013. Re-deposited cryptotephra layers in Holocene peats linked to anthropogenic activity. *The Holocene* 23 (10), 1493-1501.

Sylvester, A. G., 1975. History and surveillance of volcanic activity on Jan Mayen island. *Bulletin Volcanologique* 39, 313-335.

Taylor, A., 1995. North-South shifts of the Gulf Stream and their climatic connection with the abundance of zooplankton in the UK and its surrounding seas. *ICES Journal of Marine Science* 52, 711-721.

Thompson, R., Bradshaw, R., 1986. The distribution of ash in Icelandic lake sediments and the relative importance of mixing and erosion processes. *Journal of Quaternary Science* 1, 3-11.

Thomson, A. M., Simpson, I. A., 2006. Modeling Historic Rangeland Management and Grazing Pressures in Landscapes of Settlement. *Human Ecology* 35, 151-168.

Thordarson, T, Larsen, G, 2007. Volcanism in Iceland in historical time: Volcano types, eruption styles and eruptive history. *Journal of Geodynamics* 43, 118-152.

Tinner, W., Lotter, A. F., Ammann, B., Conedera, M., Hubschmid, P., Leeuwen, J. F. N. van, Wehrli, M., 2003. Climatic change and contemporaneous land-use phases north and south of the Alps 2300 BC to 800 AD. *Quaternary Science Reviews* 22, 1447-1460.

Tipping, R., 2007. Blanket peat in the Scottish Highlands: timing, cause, spread and the myth of environmental determinism. *Biodiversity and Conservation* 17, 2097-2113.

Tomlinson, E. L., Thordarson, T., Müller, W., Thirlwall, M., Menzies, M. A. 2010. Microanalysis of tephra by LA-ICP-MS — Strategies, advantages and limitations assessed using the Thorsmörk ignimbrite (Southern Iceland). *Chemical Geology* 279, 73-89.

Toolis, R., 2008. Excavation of medieval graves at St Thomas' Kirk, Hall of Rendall, Orkney. *Proceedings of the Society of Antiquaries of Scotland* (Vol. 138, 239-266). Society of Antiquaries of Scotland.

Torfajokull, Smithsonian Institution, Global Volcanism Program, `http://www.volcano.si.edu/world/volcano.cfm?vnum=1702-05=`, accessed 7 April, 2011.

Tulinius, T. H., 2005. The Westfjords. *Archaeologica Islandica* 4, 9-15.

Turner, V.E., Bond, J.M., and Larsen, A.C. 2013. *Viking Unst: Excavation and Survey in northern Shetland 2006-2010.* Lerwick: Shetland Heritage Publications.

Turney, C. S. M., Harkness, D. D., Lowe, J. J., 1997. The use of microtephra horizons to correlate Late-glacial lake sediment successions in Scotland. *Journal of Quaternary Science* 12, 525-531.

Turney, C. S. M., Lowe, J. J., Davies, S. M., Hall, V. A., Lowe, D. J., Wastegard, S., Hoek, W. Z., Alloway, B., SCOTAV, INTIMATE, 2004. Tephrochronology of Last Termination sequences in Europe: a protocal for improved analytical precision and

robust correlation procedures (a joint SCOTAV-INTIMATE proposal). *Journal of Quaternary Science* 19, 111-120.

Tweed, F. S., and Russell, A. J. 1999. Controls on the formation and sudden drainage of glacier-impounded lakes: implications for jökulhlaup characteristics. *Progress in Physical Geography* Vol. 23, No. 1, 79-110.

Vasey, D. E., 1991. Population, agriculture, and famine: Iceland, 1784-1785. *Human Ecology* 19, 323-350.

Vassamillet, L. F., Caldwell, V. E., 1969. Electron-probe microanalysis of alkali metals in glasses. *Journal of Applied Physics* 9 40, 1637-1640.

Vebæk, C. L. 1992. Vatnahverfi: an inland district of the Eastern settlement in Greenland. Meddelelser om Grønland, *Man and Society* 17, 1–132.

de la Vega Leinert, A. C., Keen, D. H., Jones, R. L., Wells, J. M., Smith, David E., 2000. Mid-Holocene environmental changes in the Bay of Skaill, Mainland Orkney, Scotland: an integrated geomorphological, sedimentological and stratigraphical study. *Journal of Quaternary Science* 15, 509-528.

Vésteinsson, O., 1998. Patterns of Settlement in Iceland. A Study in Prehistory, *Saga-Book of the Viking Society* 25, 1-29.

Vésteinsson, O., 2000. *The Christianization of Iceland.* Oxford University Press, Oxford.

Vésteinsson, O., 2002. *Archaeological investigations at Sveigakot 1998-2000.* FSÍ, Reykjavík.

Vésteinsson, O., 2004. Icelandic farmhouse excavations. Field methods and site choices. *Archaeologica Islandica* 3.

Vésteinsson, O., 2006. Communities of Dispersed Settlements: Social Organization at the Ground Level in Tenth- to Thirteenth-Century Iceland in *People and Space in the Middle Ages*, 87-114.

Vésteinsson, O. and McGovern, T.H., 2012. The peopling of Iceland. *Norwegian Archaeological Review*, vol. 45, No. 2, 206-218.

Vésteinsson, O., McGovern, T. H., Keller, C., 2002. Enduring Impacts: social and environmental aspects of Viking Age settlement in Iceland and Greenland. *Archaeologica Islandica* 2, 98-136.

Vickers, K., Bending, J., Buckland, P. C., Edwards, K. J., Hansen, S. S., Cook, G., 2005. Toftanes: The paleoecology of a Faroese Landnám farm. *Human Ecology*, 33(5), 685-710.

Visbeck, M. H., Hurrell, J. W., Polvani, L., Cullen, H., 2001. The North Atlantic Oscillation: past, present, and future. *Proceedings of the National Academy of the Sciences*, 12876-12877.

Unst, Sandwick, Royal Commission on the Ancient and Historical Monuments of Scotland, `http://canmore.rcahms.gov.uk/en/site/141/details/unst+sandwick`, accessed 18 October, 2013.

Wallace, B. L., 1990. L'anse aux Meadows: Gateway to Vinland. *Acta Archaeologica* 61, 166-197.

Wallace, B., 2003. The Norse in Newfoundland: L'anse aux Meadows and Vinland. *Newfoundland Studies* 19, 5-43.

Wallrabe-Adams, H.-J., Lackschewitz, K. S., 2003. Chemical composition, distribution, and origin of silicic volcanic ash layers in the Greenland-Iceland-Norwegian Sea: explosive volcanism from 10 to 300 ka as recorded in deep-sea sediment. *Marine Geology* 193, 273-293.

Wastegård, S., 2002. Early to middle Holocene silicic tephra horizons from the Katla volcanic system, Iceland: new results from the Faroe Islands. *Journal of Quaternary Science* 17, 723-730.

Wastegård, S., 2005. Late Quaternary tephrochronology of Sweden: a review. *Quaternary International* 130, 49-62.

Wastegård, S., Björck, S., Grauert, M., Hannon, G. E., 2001. The Mjáuvøtn tephra and other Holocene tephra horizons from the Faroe Islands: a link between the Icelandic source region, the Nordic Seas, and the European continent. *The Holocene* 11, 101-109.

Wastegård, S., Davies, S. M., 2009. An overview of distal tephrochronology in northern Europe during the last 1000 years. *Journal of Quaternary Science.*

Wastegård, S., Hall, V. A., Hannon, G. E., Bogaard, C. van den, Pilcher, J. R., Sigurgeirsson, M. Á., Hermanns-Auðardóttir, M., 2003. Rhyolitic tephra horizons in northwestern Europe and Iceland from the AD 700s-800s: a potential alternative for dating first human impact. *The Holocene* 13, 277-283.

Wastegård, S., Rasmussen, T. L., 2001. New tephra horizons from Oxygen Isotope Stage 5 in the North Atlantic: correlation potential for terrestrial, marine, and ice-core archives. *Quaternary Science Reviews* 20, 1587-1593.

Wastegård, S., Robertsdottir, B. G., Hannon, G. E., Hermanns-Audardottir, M., 2000a. Tephrochronology around the *landnám* tephra layer: the Asolfsstadir sequence, S. Iceland in *Iceland 2000*: *modern processes and past environments.* Keele University.

Wastegård, S., Turney, C. S. M., Lowe, J. J., Roberts, S. J., 2000b. New discoveries of the Vedde Ash in southern Sweden and Scotland. *Boreas* 29, 72-78.

Wastegård, S., Wohlfarth, B., Subetto, D. A., Sapelko, T. V., 2000c. Extending the known distribution of the Younger Dryas Vedde Ash into north western Russia. *Journal of Quaternary Science* 15, 581-586.

Whittle, A., Healy, F. and Bayliss, A. (eds.). 2011. *Gathering Time: Dating the Early Neolithic Enclosures of Southern Britain and Ireland.* Oxford: Oxbow.

Wickham-Jones, C. 2006 *Between the Wind and the Water: World Heritage Orkney*, Bollington: Windgather Press, 21-30.

Wikimedia, Orkney Islands UK Relief Location Map, `http://upload.wikimedia.org/wikipedia/commons/5/53/Orkney_Islands_UK_relief_location_map.jpg`, accessed 17 March, 2015.

Wilson, P., McGourty, J., Bateman, M.D., 2004. Mid- to late-Holocene coastal dune event stratigraphy for the north coast of Northern Ireland. *The Holocene* 14, 406-416.

Wood, R., 2015. From revolution to convention: The past, present and future of radiocarbon dating. *Journal of Archaeological Science.*

Wormald, C. P., 1982. Viking studies: whence and whither?, in: Farrell, R.T. (Ed.), *The Vikings*. Phillmore, London, pp. 128-53.

Yang, Q., Dixon, T.H., Myers, P.G., Bonin, J., Chambers, D., van den Broeke, M.R., 2016. Recent increases in Arctic freshwater flux affects Labrador Sea convection and Atlantic overturning circulation, *Nature Communications* 7.

Yukihara, E. G., and McKeever, S. W. 2011. *Optically stimulated luminescence: fundamentals and applications*. John Wiley and Sons.

Zedeno, M. N., 1997. Landscapes, Land Use, and the History of Territory Formation: An Example from the Puebloan Southwest. *Journal of Archaeological Method and Theory* 4, 67-103.

Zielinski, G. A., Germani, M. S., Larsen, G., Baillie, M. G. L., Whitlow, S., Twickler, M. S., Taylor, K., 1995. Evidence of the Eldgja (Iceland) eruption in the GISP2 Greenland ice core: relationship to eruption processes and climatic conditions in the tenth century. *The Holocene* 5, 129-140.

Zielinski, G. A., Mayewski, P. A., Meeker, L. D., Grönvold, K., Germani, M. S., Whitlow, S., Twickler, M. S., Taylor, K., 1997. Volcanic aerosol records and tephrochronology of the Summit, Greenland, ice cores. *Journal of Geophysical Research. American Geophysical Union*, 102.

Zillon, L. M., Wastegard, S., Snowball, I. F., 2002. Calendar year ages of three mid-Holocene tephra layers identified in varved lake sediments in west central Sweden. *Quaternary Science Reviews* 21, 1583-1591.

Zilmer, K., 2008. Scenes of island encounters in Icelandic sagas: reflections of cultural memory. *Viking and Medieval Scandinavia* 4, 227-248.

Zori, D., Byock, J., Erlendsson, E., Martin, S., Wake, T. Edwards, K.J., 2013. Feasting in Viking Age Iceland: sustaining a chiefly political economy in a marginal environment. *Antiquity*, 87(335), 150-165.

Þórarinsson, S., 1944. Tefrokronologiska studier pa Island. *Geografiska Annaler* XXVI, 1-217.

Þórarinsson, S., 1955a. Öskufall, svo að sporrœkt var, og Kötlugosið 1721. *Náttúrufraeðingurinn*, 87-98.

Þórarinsson, S., 1955b. Nákuðungslögin við Húnaflóa í ljósi nýrra aldursákvarðana. *Náttúrufraeðingurinn*, 172-186.

Þórarinsson, S., 1958. The Öraefajökull eruption of 1362. *Acta Naturalis Islandica* II, 1-96.

Þórarinsson, S., 1967. The Eruption of Hekla 1947-1948. *Visindafélag Islendinga.* Reykjavík.

Þórarinsson, S., 1967. The eruption of Hekla in historic times. *The eruption of Hekla 1947-48* 1, 1-183.

Þórarinsson, S., 1976. Course of events *The Eruption of Hekla 1947-1948* IV (1). Soc. Sci. Isl., Reykjavík, 1-47.

Þórarinsson, S., 1979. On the damage caused by volcanic eruptions with special reference to tephra and gases. *Volcanic activity and human ecology*, 125-140.

Þórarinsson, S., 1981. Greetings from Iceland: Ash-falls and volcanic aerosols in Scandinavia. *Geografiska Annaler* 63, 109- 118.

Þorgilsson, A. ca. 1067-1148. *Íslendingabók.* Siân Grønlie, trans., *Íslendingabók/The Book of the Icelanders; Kristni saga/The Story of the Conversion.* (Text Series, 18.) London: Viking Society for Northern Research, University College London, 2006.

A | *Unfiltered WDS-EPMA data*

All unfiltered WDS-EPMA data gathered as part of this thesis are presented below. They are grouped by date microprobed, and shown alongside the secondary standards used on each day. These standards are from Jochum et al. (2000; 2006). Two tables are presented because in some cases more elements were probed than others. 'No' indicates the order in which analyses were done on the day of microprobing.

Table A.1: Table 1 of all glass chemistry data from WDS-EPMA analysis, including secondary standards, arranged by dates.

Label	No	NaO_2	MgO	Al_2O_3	Si_2	K_2O	CaO	TiO_2	MnO	FeO
08-Sep-10										
g132_1	5	0.83	21.87	11.01	45.88	0.01	8.40	0.29	0.10	10.47
G132_1	281	0.82	22.22	11.05	45.36	0.04	8.35	0.33	0.28	10.43
g132_10	93	0.92	22.68	10.94	45.28	0.05	8.44	0.30	0.16	10.16
G132_10	218	0.90	22.67	11.01	45.27	0.06	8.29	0.29	0.09	10.16
g132_2	133	0.83	22.66	11.13	45.78	0.06	8.30	0.32	0.08	10.58
G132_2	282	0.82	22.24	11.29	45.74	0.05	8.41	0.31	0.15	10.04
g132_3	43	0.84	22.06	10.97	45.92	0.07	8.39	0.32	0.22	10.44
g132_4	13	0.95	22.00	11.30	46.00	0.03	8.35	0.28	0.12	10.26
g132_5	47	0.88	22.30	10.95	45.76	0.07	8.42	0.33	0.20	10.35
G132_5	179	0.94	22.51	11.17	45.54	0.04	8.44	0.27	0.18	10.23
g132_6	34	0.84	22.37	10.99	45.71	0.03	8.45	0.35	0.11	10.62
G132_6	180	0.86	22.35	10.96	45.60	0.05	8.43	0.27	0.18	10.13
g132_7	54	0.71	22.27	11.11	45.61	0.05	8.38	0.37	0.06	10.48
g132_8	20	0.86	21.89	11.16	45.71	0.05	8.44	0.27	0.18	10.27
g132_9	59	0.89	22.18	11.11	45.47	0.06	8.32	0.27	0.29	10.39
G132_9	219	0.82	22.84	10.89	44.98	0.08	8.33	0.23	0.10	10.18
		0.86	**22.32**	**11.07**	**45.60**	**0.05**	**8.38**	**0.30**	**0.16**	**10.32**
		0.06	**0.29**	**0.12**	**0.27**	**0.02**	**0.05**	**0.04**	**0.07**	**0.17**
sthl_1	177	4.56	1.94	18.00	63.44	1.31	5.44	0.75	0.04	4.47
sthl_10	234	4.62	1.86	17.92	63.52	1.37	5.21	0.65	0.06	4.35
sthl_2	178	4.66	1.92	18.10	63.29	1.27	5.12	0.70	0.10	4.41
sthl_5	270	4.66	1.96	17.82	63.47	1.24	5.28	0.69	0.12	4.63

Label	No	NaO_2	MgO	Al_2O_3	Si_2	K_2O	CaO	TiO_2	MnO	FeO	
sthl_6	272	4.58	1.93	17.86	63.58	1.38	5.26	0.72	0.07	4.25	
sthl_7	271	4.46	1.92	17.83	63.72	1.31	5.19	0.67	0.12	4.27	
sthl_9	233	4.70	1.99	18.13	63.55	1.26	5.23	0.61	0.16	4.52	
		4.60	**1.93**	**17.95**	**63.51**	**1.31**	**5.25**	**0.69**	**0.10**	**4.42**	
		0.08	**0.04**	**0.12**	**0.13**	**0.05**	**0.10**	**0.05**	**0.04**	**0.14**	
4309_1	257	3.11	1.04	24.25	55.30	0.46	10.42	0.36	0.33	3.83	99.09
4309_10	266	4.60	0.16	28.99	53.41	0.17	11.89	0.12	0.02	0.66	100.02
4309_11	267	0.38	14.43	2.66	50.48	0.01	17.84	1.11	0.33	12.40	99.64
4309_12	268	0.21	14.56	3.96	48.46	0.02	17.07	1.52	0.21	13.40	99.41
4309_13	269	5.39	0.48	15.98	63.43	3.69	2.38	0.59	0.19	5.40	97.52
4309_2	258	5.11	0.21	14.24	69.25	4.58	0.86	0.20	0.01	2.23	96.70
4309_3	259	0.30	13.97	2.17	49.64	0.04	14.48	1.41	0.43	16.71	99.14
4309_4	260	0.31	14.07	1.46	50.22	0.09	10.42	0.83	0.36	20.42	98.18
4309_5	261	0.32	15.47	2.91	50.98	0.00	19.20	0.94	0.21	9.17	99.21
4309_6	262	5.39	0.06	28.66	54.91	0.24	10.84	0.10	0.00	0.96	101.15
4309_7	263	4.73	0.03	28.76	53.89	0.24	11.32	0.12	0.01	1.01	100.11
4309_8	264	4.76	0.08	27.47	52.08	0.27	10.83	0.13	0.00	0.73	96.34
4309_9	265	4.71	0.15	28.37	52.86	0.13	11.51	0.09	0.03	0.73	98.59
4310_1	235	5.16	0.08	15.29	69.90	4.64	1.03	0.25	0.11	2.88	99.33
4310_10	244	0.01	0.00	0.08	101.01	0.00	0.00	0.01	0.03	0.05	101.20
4310_11	245	0.00	0.00	0.00	101.63	0.00	0.06	0.03	0.01	0.07	101.81
4310_12	246	5.21	0.09	15.16	69.97	4.72	1.03	0.22	0.14	2.90	99.45
4310_13	247	3.13	0.17	31.74	50.70	0.09	14.58	0.00	0.02	0.51	100.95
4310_14	248	2.79	0.18	32.11	50.70	0.06	15.25	0.05	0.00	0.50	101.65

Label	No	NaO_2	MgO	Al_2O_3	Si_2	K_2O	CaO	TiO_2	MnO	FeO	
4310_15	249	2.04	0.17	28.41	42.83	0.04	14.14	0.06	0.05	0.49	88.23
4310_16	250	0.09	0.02	0.02	101.11	0.01	0.02	0.01	0.00	0.00	101.29
4310_17	251	0.00	0.01	0.04	101.55	0.01	0.03	0.00	0.00	0.00	101.64
4310_18	252	4.55	0.37	14.48	58.34	3.30	2.08	0.48	0.20	4.41	88.21
4310_19	253	4.28	0.17	19.48	65.63	0.97	0.78	0.00	0.01	0.13	91.45
4310_2	236	5.30	0.08	15.47	69.85	4.58	1.04	0.26	0.16	3.33	100.06
4310_20	254	3.01	0.14	17.52	62.46	0.81	0.69	0.05	0.00	0.52	85.19
4310_21	255	2.33	1.16	13.72	55.87	4.19	4.07	0.96	0.22	7.30	89.82
4310_22	256	3.40	1.51	16.41	66.08	0.69	0.61	0.01	0.01	0.04	88.75
4310_3	237	4.46	0.06	12.95	60.70	4.04	0.94	0.18	0.14	2.53	86.01
4310_4	238	3.80	1.60	17.92	65.81	0.57	2.12	0.00	0.04	0.00	91.87
4310_5	239	0.64	0.14	21.02	62.41	0.24	0.91	0.05	0.00	0.08	85.48
4310_6	240	0.68	0.11	20.54	61.46	0.21	1.11	0.05	0.06	0.00	84.22
4310_7	241	2.59	0.96	11.62	47.21	3.34	3.33	0.78	0.19	6.35	76.36
4310_8	242	3.39	0.33	15.90	66.85	1.20	1.01	0.00	0.02	0.21	88.92
4310_9	243	0.00	0.00	0.07	100.68	0.00	0.00	0.00	0.00	0.07	100.82
4674_1	273	3.75	0.15	30.73	51.43	0.12	13.38	0.08	0.00	0.67	100.31
4674_2	130	5.52	0.55	15.46	62.15	3.57	2.37	0.58	0.24	5.09	95.53
4674_2	274	0.40	0.52	18.12	61.02	0.68	5.29	0.01	0.00	2.32	88.37
4674_3	275	2.96	1.22	12.54	47.11	0.97	4.19	0.93	0.27	7.16	77.35
4674_3	131	0.05	0.00	0.04	95.52	0.05	0.02	0.00	0.08	0.09	95.83
4674_4	276	3.58	1.85	15.49	59.73	1.34	5.36	1.39	0.40	10.12	99.25
4674_4	132	0.03	0.04	0.02	97.67	0.00	0.77	0.00	0.01	0.25	98.80
4674_5	277	3.53	1.87	15.21	59.05	1.37	5.12	1.26	0.20	9.81	97.41
4674_5	134	0.12	0.00	0.03	95.39	0.04	0.02	0.01	0.03	0.12	95.76
4674_6	278	3.64	1.90	14.69	57.17	1.43	5.15	1.43	0.21	9.93	95.55

Label	No	NaO_2	MgO	Al_2O_3	Si_2	K_2O	CaO	TiO_2	MnO	FeO	
4674_7	279	1.17	0.21	19.39	64.63	0.73	6.54	0.01	0.07	0.16	92.92
4674_8	280	4.68	0.48	13.67	54.95	2.85	1.81	1.10	0.13	4.77	84.45
4675_1	196	0.03	0.19	0.15	0.24	0.00	0.01	0.05	0.13	92.74	93.53
4675_10	205	0.49	0.04	0.00	93.59	0.09	0.07	0.02	0.00	0.05	94.35
4675_11	206	3.72	1.82	15.64	59.58	1.41	5.17	1.29	0.22	10.03	98.88
4675_12	207	3.88	1.81	15.40	59.05	1.48	5.43	1.32	0.35	10.02	98.74
4675_13	208	4.04	1.89	15.38	59.49	1.43	5.10	1.27	0.30	9.97	98.86
4675_14	209	4.00	0.14	29.61	51.54	0.16	13.11	0.11	0.06	0.73	99.45
4675_15	210	2.15	6.24	13.43	50.11	0.27	10.74	1.92	0.18	13.17	98.20
4675_16	211	2.12	6.43	13.59	50.06	0.23	10.60	1.87	0.22	13.36	98.48
4675_17	212	3.72	1.82	15.55	58.78	1.45	5.44	1.20	0.23	9.92	98.10
4675_18	213	3.62	1.89	14.97	57.84	1.46	5.20	1.28	0.37	9.68	96.30
4675_19	214	3.53	1.87	14.65	58.20	1.55	5.22	1.34	0.36	9.54	96.25
4675_2	197	3.78	0.13	11.20	53.70	3.13	0.37	0.17	0.02	2.10	74.59
4675_20	215	0.19	10.96	1.21	48.61	0.00	9.69	0.85	0.63	25.97	98.11
4675_21	216	3.36	0.18	30.69	50.44	0.09	13.91	0.06	0.00	0.72	99.44
4675_22	217	3.44	0.15	30.85	50.50	0.09	13.88	0.05	0.03	0.85	99.85
4675_3	198	4.70	0.05	12.37	58.14	3.74	0.91	0.26	0.09	2.66	82.93
4675_4	199	4.84	0.22	14.90	71.63	4.34	0.74	0.25	0.04	2.16	99.12
4675_5	200	5.59	0.07	15.41	70.11	4.33	1.01	0.23	0.18	2.78	99.71
4675_6	201	5.36	0.04	15.26	69.64	4.25	1.13	0.21	0.20	3.00	99.10
4675_7	202	3.50	1.75	14.75	57.30	1.39	5.14	1.18	0.25	9.33	94.59
4675_8	203	3.52	1.51	13.73	54.10	1.30	4.60	1.13	0.19	8.75	88.83
4675_9	204	3.83	1.84	15.25	58.95	1.44	5.08	1.25	0.25	9.41	97.31
4676_1	181	4.18	2.06	15.03	56.42	1.47	5.48	1.43	0.30	9.56	95.94
4676_10	190	3.49	0.00	12.37	31.01	0.41	3.14	0.02	0.00	0.34	50.78

Label	No	NaO_2	MgO	Al_2O_3	Si_2	K_2O	CaO	TiO_2	MnO	FeO	
4676_11	191	3.40	0.27	11.14	45.87	3.17	1.57	0.34	0.10	3.35	69.21
4676_12	192	0.02	1.19	1.90	0.39	0.00	0.09	21.28	0.44	66.53	91.83
4676_13	193	0.00	0.01	0.00	100.56	0.00	0.00	0.00	0.00	0.05	100.62
4676_14	194	0.02	0.00	0.00	98.94	0.01	0.02	0.00	0.00	0.03	99.00
4676_15	195	0.00	0.00	0.00	99.74	0.01	0.01	0.00	0.00	0.00	99.76
4676_2	182	3.46	1.81	13.66	52.41	1.32	4.93	1.33	0.17	9.22	88.30
4676_3	183	0.02	0.01	0.01	89.48	0.00	0.00	0.02	0.00	0.06	89.59
4676_4	184	1.66	0.16	28.01	41.13	0.03	13.85	0.05	0.06	0.47	85.41
4676_5	185	2.19	0.18	32.43	47.14	0.04	15.70	0.03	0.05	0.57	98.33
4676_6	186	4.00	1.48	11.70	46.04	1.26	3.58	1.05	0.14	7.56	76.80
4676_7	187	0.32	0.16	1.56	6.18	0.16	0.52	0.10	0.00	1.05	10.06
4676_8	188	3.05	0.16	22.93	39.35	0.10	10.47	0.00	0.10	0.39	76.55
4676_9	189	3.83	0.21	29.61	49.89	0.06	13.75	0.08	0.00	0.67	98.08
4677_10	108	1.00	5.15	13.11	50.91	0.48	9.32	3.11	0.28	14.76	98.11
4677_11	109	1.07	5.26	13.11	50.81	0.48	9.53	2.96	0.21	14.28	97.71
4677_12	110	0.22	0.00	0.09	84.40	0.08	0.07	0.00	0.00	0.05	84.91
4677_13	111	0.23	14.36	2.66	49.39	0.01	16.68	1.45	0.35	14.33	99.45
4677_14	112	3.40	1.94	15.45	59.55	1.37	5.23	1.35	0.27	9.70	98.26
4677_15	113	3.90	1.87	15.55	59.38	1.38	5.25	1.29	0.30	9.64	98.56
4677_16	114	3.77	1.80	15.13	59.21	1.45	5.39	1.24	0.27	9.55	97.81
4677_17	115	3.54	1.89	15.17	58.51	1.35	5.31	1.34	0.25	9.26	96.61
4677_18	116	0.01	0.00	0.05	0.21	0.00	0.01	0.03	0.00	0.08	0.40
4677_19	117	0.02	0.00	0.13	0.24	0.02	0.02	0.00	0.02	0.07	0.53
4677_2	100	0.08	0.00	0.00	93.78	0.00	0.01	0.02	0.00	0.09	93.98
4677_20	119	0.42	1.75	5.49	8.68	0.10	1.35	4.89	0.14	24.34	47.15
4677_21	120	0.00	0.00	0.00	94.29	0.00	0.01	0.00	0.00	0.02	94.32

Label	No	NaO_2	MgO	Al_2O_3	Si_2	K_2O	CaO	TiO_2	MnO	FeO	
4677_22	121	0.00	0.00	0.00	94.32	0.01	0.02	0.01	0.00	0.05	94.40
4677_23	122	4.92	0.69	14.71	64.51	4.52	2.51	0.83	0.27	6.17	99.13
4677_24	123	4.28	0.03	11.56	75.44	2.95	1.24	0.19	0.05	2.33	98.07
4677_25	125	4.74	0.06	27.61	53.81	0.23	10.39	0.12	0.00	0.90	97.87
4677_26	126	1.74	6.47	13.60	48.93	0.25	11.08	1.77	0.13	12.39	96.36
4677_27	127	3.85	1.75	15.63	59.72	1.50	5.49	1.26	0.24	9.18	98.62
4677_28	128	1.22	5.19	13.15	50.57	0.47	9.44	3.11	0.15	14.08	97.37
4677_29	129	0.01	0.00	0.02	0.24	0.00	0.01	0.03	0.00	0.00	0.32
4677_3	101	1.09	4.97	12.97	48.35	0.80	9.45	4.55	0.23	14.81	97.24
4677_4	102	0.11	0.05	0.02	86.47	0.02	0.98	0.00	0.03	0.01	87.70
4677_5	103	4.98	0.02	13.33	73.68	2.78	1.31	0.18	0.00	1.24	97.53
4677_6	104	0.03	0.00	0.02	94.47	0.03	0.01	0.00	0.00	0.01	94.57
4677_7	105	0.33	5.54	11.73	34.04	0.37	1.10	0.15	0.18	32.82	86.25
4677_8	106	0.23	5.14	11.20	33.06	0.28	1.21	0.15	0.21	33.71	85.20
4677_9	107	0.58	1.74	21.45	46.23	0.32	0.70	0.31	0.07	6.85	78.24
4679_10	11	3.16	0.22	31.29	50.90	0.06	14.20	0.01	0.04	0.55	100.43
4679_11	12	6.64	0.02	26.67	57.87	0.41	8.40	0.11	0.00	0.58	100.71
4679_12	14	6.60	0.05	27.00	58.11	0.43	8.74	0.11	0.06	0.62	101.71
4679_13	15	3.05	0.24	31.35	50.75	0.06	14.38	0.01	0.06	0.35	100.24
4679_14	16	3.01	0.27	31.21	51.10	0.06	14.15	0.07	0.01	0.50	100.37
4679_15	17	5.41	0.06	15.30	70.71	4.74	0.96	0.26	0.12	2.84	100.38
4679_16	18	5.28	0.06	15.34	70.71	4.68	0.99	0.24	0.15	2.77	100.22
4679_17	19	4.95	0.04	19.14	62.07	1.95	4.44	0.27	0.04	0.51	93.41
4679_18	21	0.99	0.56	6.29	26.09	0.56	1.94	0.51	0.17	3.56	40.68
4679_19	22	2.82	1.55	12.52	48.95	1.07	4.23	1.10	0.27	8.28	80.78
4679_2	1	5.39	0.47	16.25	65.05	3.76	2.36	0.57	0.20	5.18	99.23

Label	No	NaO_2	MgO	Al_2O_3	Si_2	K_2O	CaO	TiO_2	MnO	FeO	
4679_20	23	2.83	1.83	15.24	59.47	1.35	5.26	1.26	0.21	9.66	97.11
4679_21	24	3.28	0.24	30.83	50.50	0.06	14.39	0.09	0.00	0.45	99.82
4679_22	25	2.93	1.68	14.73	57.90	1.43	5.03	1.13	0.19	9.52	94.55
4679_23	26	3.44	1.83	15.54	59.44	1.42	5.26	1.26	0.17	9.57	97.94
4679_24	27	3.70	1.77	15.48	59.72	1.38	5.14	1.34	0.24	9.61	98.37
4679_25	28	3.47	1.85	15.36	59.60	1.39	5.36	1.34	0.26	9.50	98.13
4679_26	29	6.45	0.06	25.61	59.56	0.78	7.40	0.07	0.00	0.49	100.41
4679_27	30	4.19	0.09	29.09	52.94	0.20	12.08	0.20	0.00	0.81	99.60
4679_28	31	4.10	0.04	29.63	52.66	0.20	12.56	0.07	0.05	0.79	100.08
4679_29	32	4.43	2.09	14.72	59.93	1.38	5.24	1.28	0.36	10.11	99.54
4679_3	2	3.61	0.42	14.12	57.74	3.45	2.01	0.47	0.29	4.72	86.82
4679_30	33	5.05	0.04	28.13	55.00	0.29	10.79	0.14	0.00	0.69	100.15
4679_31	35	4.20	0.05	29.67	52.91	0.23	12.48	0.09	0.00	0.66	100.30
4679_32	36	2.98	0.22	31.51	50.51	0.04	14.67	0.04	0.01	0.64	100.61
4679_33	37	5.27	0.07	27.92	55.66	0.25	10.46	0.08	0.06	0.72	100.49
4679_34	39	4.27	1.69	16.51	59.32	1.27	5.62	1.21	0.22	8.38	98.49
4679_35	40	4.11	1.84	15.36	58.99	1.55	5.33	1.26	0.29	9.65	98.38
4679_36	41	1.45	6.77	13.95	50.53	0.22	11.46	1.73	0.29	12.59	99.00
4679_37	42	0.07	2.18	0.10	0.20	0.00	0.13	49.50	0.29	44.40	96.87
4679_38	44	0.31	13.42	2.76	50.45	0.00	18.71	1.13	0.25	12.13	99.16
4679_39	45	0.00	0.02	0.01	95.74	0.01	0.03	0.02	0.04	0.09	95.96
4679_4	3	2.70	0.48	16.03	65.41	3.86	2.22	0.54	0.22	5.33	96.79
4679_40	46	4.14	1.73	16.42	59.68	1.02	5.78	1.37	0.18	8.97	99.29
4679_41	48	0.39	5.01	12.92	48.17	0.77	9.66	4.62	0.18	14.98	96.68
4679_42	49	4.09	1.83	15.68	59.92	1.06	5.64	1.38	0.20	10.02	99.81
4679_43	50	3.35	1.82	15.40	59.60	1.54	5.25	1.31	0.23	9.53	98.03

Label	No	NaO_2	MgO	Al_2O_3	Si_2	K_2O	CaO	TiO_2	MnO	FeO	
4679_44	51	1.80	5.46	13.38	49.76	0.50	9.77	2.93	0.24	14.48	98.32
4679_45	52	4.45	1.60	14.24	61.09	1.63	4.61	1.06	0.28	10.07	99.01
4679_46	53	3.12	1.78	15.67	59.77	1.47	5.54	1.28	0.22	9.49	98.34
4679_47	55	3.73	1.77	15.48	59.98	1.56	5.30	1.27	0.25	9.40	98.75
4679_48	56	5.25	0.26	14.73	71.60	4.40	0.82	0.23	0.01	2.28	99.59
4679_5	4	3.67	1.45	16.49	60.12	1.36	5.46	1.12	0.26	8.51	98.43
4679_6	6	3.47	1.50	15.65	59.44	1.32	5.18	1.13	0.24	8.89	96.82
4679_7	7	2.94	1.78	15.84	60.13	1.47	5.27	1.29	0.28	9.64	98.63
4679_8	8	3.22	1.67	15.17	60.12	1.44	5.19	1.37	0.19	9.59	97.96
4679_9	9	2.97	0.23	31.59	50.85	0.06	14.56	0.03	0.00	0.58	100.88
4680_10	67	4.19	1.88	15.36	59.14	1.40	5.50	1.38	0.18	9.79	98.82
4680_11	68	4.19	1.85	15.39	59.43	1.49	5.22	1.29	0.26	9.15	98.26
4680_12	69	0.28	0.01	0.01	76.67	0.19	0.04	0.01	0.00	0.03	77.25
4680_13	70	2.58	1.06	13.17	53.11	1.37	3.80	0.87	0.15	7.16	83.26
4680_14	71	3.24	1.63	14.71	57.01	1.36	4.93	1.15	0.18	8.80	93.00
4680_15	72	3.47	0.06	24.00	43.17	0.16	9.94	0.08	0.00	0.59	81.46
4680_16	73	2.34	1.84	15.53	59.94	1.45	5.23	1.21	0.29	9.31	97.14
4680_17	74	4.19	0.51	14.44	57.53	1.52	3.55	0.59	0.10	5.73	88.17
4680_18	75	4.04	1.71	15.39	60.08	1.39	5.09	1.24	0.26	9.50	98.71
4680_19	76	4.64	0.34	15.71	59.65	1.60	4.41	1.17	0.00	4.56	92.07
4680_2	57	3.51	0.05	23.96	43.58	0.16	10.10	0.07	0.00	0.63	82.06
4680_20	77	0.24	14.61	2.71	50.12	0.00	17.96	1.17	0.21	10.36	97.37
4680_21	78	0.31	11.33	2.56	41.98	0.01	15.15	1.27	0.13	10.67	83.40
4680_22	79	3.45	1.77	15.03	58.48	1.29	5.06	1.29	0.26	9.57	96.20
4680_23	80	3.99	1.94	15.60	59.57	1.27	5.22	1.23	0.27	9.69	98.77
4680_24	81	2.96	1.77	15.41	59.48	1.41	5.28	1.30	0.39	9.75	97.75

Label	No	NaO_2	MgO	Al_2O_3	Si_2	K_2O	CaO	TiO_2	MnO	FeO	
4680_25	82	2.79	0.05	20.85	37.79	0.12	8.69	0.03	0.03	0.45	70.80
4680_26	83	2.34	1.75	15.28	59.54	1.34	5.29	1.25	0.23	9.44	96.46
4680_3	58	3.00	1.76	15.51	60.50	1.47	5.52	1.24	0.29	9.57	98.86
4680_4	60	2.56	1.81	15.47	59.89	1.50	5.26	1.29	0.16	9.13	97.07
4680_5	61	4.13	0.52	13.13	53.74	1.41	3.28	0.51	0.12	4.56	81.41
4680_6	62	2.67	1.18	12.27	46.91	1.00	4.16	0.92	0.17	7.10	76.40
4680_7	64	4.14	1.62	15.01	57.79	1.35	5.04	1.13	0.22	9.32	95.63
4680_8	65	3.62	1.13	13.41	55.29	1.46	3.90	0.84	0.20	7.38	87.24
4680_9	66	3.90	1.82	15.19	59.00	1.42	5.35	1.31	0.22	9.88	98.09
4681_10	160	5.62	0.08	14.65	67.93	4.20	1.00	0.32	0.15	2.93	96.87
4681_11	161	5.31	0.51	18.21	60.95	1.27	5.52	0.58	0.16	5.52	98.03
4681_12	162	1.77	6.63	13.85	49.53	0.24	11.01	1.90	0.27	12.45	97.65
4681_13	164	1.78	6.58	13.74	49.62	0.27	11.06	1.90	0.27	12.45	97.68
4681_14	165	3.92	1.83	15.18	58.31	1.21	5.04	1.33	0.20	8.93	95.95
4681_15	166	3.70	1.78	14.70	56.23	1.17	4.67	1.22	0.20	9.35	93.03
4681_16	167	5.56	0.07	14.84	68.36	4.56	1.02	0.25	0.23	2.64	97.53
4681_17	168	5.45	0.06	14.92	68.75	4.50	1.04	0.20	0.12	2.87	97.92
4681_18	169	4.94	1.06	14.22	66.29	2.82	2.75	1.18	0.16	5.54	98.96
4681_19	170	5.34	1.05	13.91	65.31	2.68	2.80	1.23	0.21	5.30	97.82
4681_2	150	4.65	1.17	13.95	65.52	2.56	2.96	1.30	0.24	5.90	98.24
4681_20	171	4.21	1.05	14.00	65.24	2.74	2.82	1.17	0.09	5.35	96.66
4681_21	172	3.86	1.88	15.62	58.36	1.42	5.45	1.22	0.24	8.92	96.97
4681_22	173	4.56	0.16	28.85	52.40	0.14	12.11	0.09	0.00	1.08	99.38
4681_23	174	2.96	0.09	14.98	69.56	4.70	1.07	0.25	0.14	3.32	97.07
4681_24	175	0.22	0.21	0.01	93.90	0.07	0.17	0.01	0.17	0.00	94.76
4681_25	176	3.96	0.15	28.59	52.00	0.14	12.28	0.10	0.06	0.93	98.22

Label	No	NaO_2	MgO	Al_2O_3	Si_2	K_2O	CaO	TiO_2	MnO	FeO	
4681_3	151	4.71	0.12	28.40	53.39	0.16	11.86	0.10	0.04	0.82	99.60
4681_4	152	7.51	0.02	23.71	61.53	0.69	5.80	0.00	0.10	0.28	99.64
4681_5	153	5.98	0.05	26.16	56.90	0.33	8.95	0.17	0.04	0.55	99.12
4681_6	155	5.53	0.07	27.44	54.84	0.24	10.16	0.10	0.00	0.51	98.89
4681_7	156	3.35	1.80	15.23	59.00	1.29	5.11	1.26	0.15	9.38	96.59
4681_8	157	5.86	0.50	15.97	64.02	3.58	2.46	0.60	0.21	5.08	98.29
4681_9	159	5.42	0.52	16.11	64.18	3.49	2.35	0.57	0.27	5.02	97.92
4682_10	92	4.66	0.53	16.77	67.44	3.18	0.52	0.01	0.00	0.05	93.16
4682_11	94	3.99	0.57	15.90	70.30	2.78	0.44	0.03	0.00	0.00	94.01
4682_12	95	3.45	0.84	16.14	64.15	3.84	0.92	0.00	0.00	0.08	89.41
4682_13	96	4.20	0.07	27.27	50.06	0.22	11.69	0.14	0.03	0.89	94.56
4682_14	97	6.79	0.37	20.50	58.13	3.10	1.84	0.07	0.01	0.02	90.82
4682_15	98	4.14	0.09	14.99	69.00	4.68	1.13	0.19	0.08	3.12	97.42
4682_16	99	3.87	0.09	15.08	69.45	4.70	1.08	0.24	0.08	3.06	97.65
4682_2	84	4.19	0.19	28.27	50.26	0.11	12.24	0.09	0.03	0.61	96.00
4682_3	85	5.36	0.45	16.40	65.27	3.78	2.26	0.52	0.20	5.18	99.41
4682_4	86	3.64	0.43	15.55	47.87	1.54	1.10	0.01	0.00	0.09	70.24
4682_5	87	2.58	0.43	16.69	54.94	1.82	1.21	0.03	0.10	0.01	77.83
4682_6	88	4.14	0.41	15.99	64.95	3.76	2.23	0.49	0.11	5.12	97.19
4682_7	89	5.44	0.21	14.62	65.11	4.25	1.25	0.58	0.16	3.71	95.33
4682_8	90	5.23	0.07	14.54	66.77	4.51	1.09	0.23	0.14	3.01	95.59
4682_9	91	5.32	0.10	14.93	68.70	4.53	1.08	0.20	0.14	3.05	98.05
4685_1	220	5.31	0.34	17.16	65.40	1.74	0.74	0.01	0.00	0.01	90.72
4685_10	229	5.93	0.06	19.04	63.28	1.96	0.89	0.05	0.01	0.14	91.35
4685_11	230	4.10	0.11	19.61	66.13	1.73	0.89	0.00	0.00	0.04	92.61
4685_12	231	0.30	15.00	2.08	51.22	0.00	19.23	0.98	0.24	10.72	99.78

Label	No	NaO_2	MgO	Al_2O_3	Si_2	K_2O	CaO	TiO_2	MnO	FeO	
4685_13	232	5.73	0.10	15.19	69.65	4.55	1.06	0.26	0.15	2.87	99.55
4685_2	221	0.00	0.00	0.03	0.27	0.01	0.03	0.00	0.00	0.00	0.33
4685_3	222	0.00	0.00	0.03	0.21	0.00	0.00	0.00	0.01	0.00	0.26
4685_4	223	5.76	0.06	19.64	62.29	2.17	0.99	0.00	0.00	0.00	90.92
4685_5	224	4.30	0.06	21.02	63.80	1.84	1.05	0.01	0.04	0.00	92.12
4685_6	225	3.10	0.25	20.77	64.54	1.68	1.12	0.00	0.00	0.00	91.45
4685_7	226	4.11	1.23	17.25	67.14	1.22	0.72	0.02	0.00	0.00	91.68
4685_8	227	5.44	0.07	14.96	68.26	4.57	1.10	0.24	0.15	3.19	97.99
4685_9	228	3.34	1.19	17.05	65.98	2.39	0.62	0.00	0.01	0.01	90.60
4766_10	143	11.37	0.04	19.51	68.24	0.13	0.09	0.04	0.06	0.01	99.50
4766_11	145	11.25	0.00	20.18	69.34	0.09	0.17	0.00	0.05	0.00	101.07
4766_12	146	0.00	0.00	0.00	100.43	0.00	0.02	0.00	0.00	0.05	100.50
4766_13	147	0.00	0.01	0.00	100.92	0.00	0.00	0.00	0.00	0.07	101.01
4766_14	149	0.00	0.02	0.00	101.45	0.01	0.02	0.00	0.00	0.03	101.53
4766_2	135	0.07	0.01	0.00	100.91	0.00	0.00	0.00	0.05	0.00	101.04
4766_3	136	0.07	0.01	0.00	100.33	0.00	0.01	0.00	0.05	0.02	100.49
4766_4	137	0.00	0.00	0.01	100.63	0.02	0.00	0.00	0.00	0.00	100.66
4766_5	138	0.08	0.05	0.99	97.97	0.32	0.00	0.16	0.08	0.83	100.49
4766_6	139	7.54	0.02	25.45	59.76	0.15	6.72	0.01	0.00	0.00	99.66
4766_7	140	3.76	1.35	15.30	61.56	3.01	4.43	0.99	0.14	7.86	98.39
4766_8	141	4.13	1.31	15.32	62.02	2.17	4.52	0.99	0.26	7.63	98.36
4766_9	142	4.33	1.62	15.50	59.97	1.81	4.88	1.08	0.23	9.04	98.48
09-Sep-10											
g132_1	34	0.83	22.20	11.01	45.82	0.06	8.49	0.28	0.11	10.33	
g132_2	33	0.81	22.15	11.12	45.63	0.04	8.37	0.32	0.15	10.49	

Label	No	NaO_2	MgO	Al_2O_3	Si_2	K_2O	CaO	TiO_2	MnO	FeO	
g132_3	3	0.87	21.89	11.24	45.82	0.06	8.53	0.31	0.10	10.12	
g132_4	4	0.93	21.89	11.06	45.23	0.07	8.29	0.31	0.16	10.00	
g132_5	66	0.88	21.89	11.34	45.91	0.08	8.56	0.30	0.00	10.08	
g132_6	67	0.84	22.01	11.19	45.52	0.06	8.30	0.28	0.13	10.37	
		0.86	**22.00**	**11.16**	**45.66**	**0.06**	**8.42**	**0.30**	**0.11**	**10.23**	
		0.04	**0.14**	**0.12**	**0.25**	**0.02**	**0.12**	**0.02**	**0.06**	**0.19**	
sthl_1	64	4.34	1.96	17.91	63.02	1.33	5.21	0.62	0.00	4.33	
sthl_2	65	4.82	1.94	18.07	62.93	1.36	5.19	0.74	0.04	4.45	
sthl_3	2	4.88	1.99	17.83	62.97	1.28	5.28	0.60	0.01	4.08	
sthl_4	1	4.51	1.94	18.00	63.24	1.32	5.31	0.75	0.06	4.63	
sthl_5	32	4.66	1.98	17.85	63.61	1.28	5.33	0.69	0.08	4.64	
sthl_6	31	4.66	1.96	17.78	63.48	1.32	5.30	0.70	0.06	4.60	
		4.65	**1.96**	**17.91**	**63.21**	**1.32**	**5.27**	**0.68**	**0.04**	**4.46**	
		0.20	**0.02**	**0.11**	**0.29**	**0.03**	**0.06**	**0.06**	**0.03**	**0.22**	
4682_1	5	4.27	0.96	19.61	59.31	2.37	0.98	0.04	0.03	0.18	87.74
4682_10	14	1.35	1.26	19.07	66.07	2.01	1.02	0.00	0.01	0.17	90.96
4682_11	15	1.87	1.19	19.02	62.68	2.12	1.05	0.00	0.00	0.11	88.05
4682_12	16	5.44	0.89	17.71	60.07	1.92	0.90	0.02	0.00	0.24	87.20
4682_13	17	2.85	0.85	14.01	48.67	1.25	0.53	0.04	0.00	0.29	68.50
4682_14	18	3.18	0.93	18.86	61.97	1.64	1.10	0.00	0.00	0.18	87.87
4682_15	19	3.59	1.64	18.03	62.29	3.23	0.67	0.03	0.00	0.09	89.57
4682_16	20	2.53	1.59	18.60	63.46	2.50	0.67	0.00	0.00	0.14	89.48
4682_17	21	3.67	0.55	15.28	62.28	3.48	0.96	0.00	0.02	0.14	86.38

Label	No	NaO_2	MgO	Al_2O_3	Si_2	K_2O	CaO	TiO_2	MnO	FeO	
4682_18	22	4.31	0.74	16.65	65.68	2.81	1.36	0.01	0.00	0.17	91.71
4682_19	23	5.28	0.10	14.87	68.22	4.64	0.96	0.31	0.02	2.79	97.20
4682_2	6	2.38	1.09	18.73	59.49	1.54	0.91	0.05	0.07	0.11	84.35
4682_20	24	5.18	0.09	15.18	69.42	4.68	1.09	0.22	0.20	3.24	99.30
4682_21	25	3.64	0.05	17.62	40.68	1.57	1.36	0.02	0.02	0.00	64.96
4682_22	26	2.78	1.65	14.88	59.31	1.99	1.56	0.06	0.08	1.25	83.55
4682_23	27	1.04	1.02	16.52	66.53	1.67	1.47	0.00	0.00	0.29	88.54
4682_24	28	0.30	14.72	2.36	50.84	0.00	19.18	0.89	0.18	11.33	99.80
4682_25	29	4.33	0.03	12.69	59.12	4.12	0.86	0.19	0.14	2.45	83.95
4682_26	30	5.25	0.08	14.35	65.38	4.41	0.98	0.24	0.14	2.84	93.67
4682_3	7	6.73	0.00	19.25	54.62	1.62	3.16	0.07	0.00	0.47	85.92
4682_4	8	6.31	0.02	26.58	56.25	0.47	8.62	0.07	0.00	0.71	99.05
4682_5	9	4.30	0.77	16.33	50.27	1.56	1.10	0.00	0.00	0.27	74.60
4682_6	10	3.28	1.19	17.97	61.68	2.95	0.93	0.00	0.00	0.16	88.14
4682_7	11	2.00	1.16	19.12	64.15	2.00	1.06	0.00	0.00	0.09	89.58
4682_8	12	0.26	13.51	2.90	47.94	0.00	18.61	0.90	0.21	9.04	93.38
4682_9	13	2.59	0.97	20.47	59.97	1.72	1.34	0.01	0.06	0.06	87.20
4765_1	36	0.21	0.02	0.04	100.47	0.08	0.02	0.01	0.00	0.00	100.84
4765_10	45	0.01	0.00	0.30	100.14	0.11	0.03	0.01	0.02	0.47	101.09
4765_11	46	0.08	0.00	0.00	102.10	0.03	0.01	0.01	0.00	0.05	102.29
4765_12	47	0.00	0.01	0.01	101.61	0.02	0.01	0.00	0.00	0.03	101.69
4765_13	48	0.01	0.00	0.00	101.66	0.00	0.00	0.00	0.00	0.09	101.76
4765_14	49	0.08	0.00	0.05	101.16	0.06	0.03	0.02	0.00	0.00	101.39
4765_15	50	11.36	0.03	19.94	69.35	0.02	0.00	0.01	0.00	0.00	100.71
4765_16	51	2.94	1.45	15.02	60.16	4.14	4.87	1.11	0.27	8.76	98.72
4765_17	52	3.38	1.68	15.01	59.84	3.00	4.90	1.16	0.19	9.51	98.67

Label	No	NaO_2	MgO	Al_2O_3	Si_2	K_2O	CaO	TiO_2	MnO	FeO	
4765_18	53	3.05	1.62	15.09	59.61	3.78	4.55	1.18	0.21	9.20	98.30
4765_19	54	3.59	1.61	15.55	60.10	2.71	5.11	1.16	0.14	8.38	98.34
4765_2	37	0.32	0.00	0.11	99.77	0.04	0.02	0.07	0.00	0.00	100.34
4765_20	55	0.00	0.00	0.00	101.28	0.00	0.02	0.00	0.00	0.05	101.34
4765_21	56	0.43	0.62	35.79	45.82	10.77	0.01	0.92	0.00	1.23	95.58
4765_22	57	0.42	0.57	35.92	45.79	10.64	0.00	0.91	0.02	1.24	95.52
4765_23	58	0.42	0.58	36.12	45.95	10.68	0.00	0.91	0.00	1.25	95.90
4765_24	59	0.45	0.55	36.21	45.83	10.59	0.00	0.88	0.07	1.15	95.73
4765_25	60	1.68	0.01	13.38	74.81	6.53	1.64	0.12	0.12	2.16	100.45
4765_26	61	0.25	0.00	18.74	65.06	16.44	0.00	0.03	0.06	0.02	100.61
4765_27	62	0.38	0.00	18.77	64.83	16.39	0.00	0.04	0.00	0.02	100.42
4765_28	63	0.21	0.00	18.68	65.40	16.50	0.00	0.00	0.02	0.08	100.90
4765_3	38	0.01	0.00	0.04	93.33	0.02	0.00	0.01	0.00	0.05	93.46
4765_4	39	0.24	0.01	0.06	100.78	0.04	0.04	0.00	0.01	0.04	101.23
4765_5	40	2.42	0.01	18.65	63.82	11.59	0.47	0.16	0.00	0.25	97.37
4765_6	41	2.14	0.00	13.05	73.84	7.32	1.27	0.09	0.00	2.01	99.73
4765_7	42	0.00	0.00	0.00	101.80	0.01	0.01	0.02	0.02	0.00	101.86
4765_8	43	0.05	0.00	0.02	101.01	0.02	0.00	0.00	0.02	0.00	101.13
4765_9	44	0.18	0.00	0.14	96.87	0.05	0.02	0.00	0.00	0.13	97.39
4767_1	35	4.03	1.35	15.06	60.14	2.02	4.58	1.04	0.20	8.57	96.99
05-Oct-10											
atho_1	4	4.06	0.10	12.32	75.07	2.65	1.72	0.22	0.12	3.32	
atho_10	45	4.26	0.12	12.31	75.10	2.66	1.72	0.30	0.07	3.22	
atho_2	5	4.37	0.08	12.21	74.60	2.68	1.80	0.28	0.13	3.16	
atho_3	202	4.38	0.08	12.25	75.02	2.74	1.72	0.29	0.11	3.23	

Label	No	NaO_2	MgO	Al_2O_3	Si_2	K_2O	CaO	TiO_2	MnO	FeO	
atho_4	200	4.20	0.11	12.43	74.38	2.76	1.74	0.25	0.12	3.30	
atho_5	201	4.42	0.10	12.18	74.76	2.62	1.70	0.20	0.07	3.36	
atho_6	44	4.27	0.09	12.20	75.01	2.63	1.73	0.22	0.07	3.25	
atho_7	46	4.38	0.09	12.25	74.92	2.67	1.76	0.25	0.09	3.37	
atho_8	48	4.26	0.10	12.14	75.15	2.74	1.77	0.28	0.07	3.32	
atho_9	47	4.63	0.10	12.21	74.86	2.65	1.71	0.34	0.09	3.29	
		4.32	**0.10**	**12.25**	**74.89**	**2.68**	**1.74**	**0.26**	**0.10**	**3.28**	
		0.15	**0.01**	**0.08**	**0.24**	**0.05**	**0.03**	**0.04**	**0.02**	**0.07**	
g132_1	168	0.86	22.74	10.98	45.10	0.02	8.39	0.31	0.10	10.47	
g132_10	3	0.83	22.51	11.03	45.27	0.05	8.45	0.33	0.12	10.26	
g132_2	169	0.79	22.63	10.93	45.01	0.05	8.50	0.27	0.16	10.40	
g132_3	170	0.85	22.52	10.95	44.98	0.02	8.62	0.27	0.12	10.15	
g132_4	171	0.87	22.42	10.73	44.91	0.04	8.51	0.31	0.20	10.11	
g132_5	172	0.81	22.45	11.08	45.00	0.01	8.54	0.28	0.15	10.08	
g132_6	1	0.79	22.62	10.95	45.31	0.02	8.25	0.29	0.06	9.96	
g132_7	2	0.75	22.61	11.07	45.17	0.01	8.40	0.34	0.18	10.14	
g132_8	198	0.84	22.56	10.92	45.12	0.04	8.62	0.35	0.17	10.36	
g132_9	199	0.73	22.35	10.96	45.17	0.06	8.46	0.28	0.18	10.22	
		0.81	**22.54**	**10.96**	**45.11**	**0.03**	**8.47**	**0.30**	**0.15**	**10.22**	
		0.05	**0.12**	**0.10**	**0.13**	**0.02**	**0.11**	**0.03**	**0.04**	**0.16**	
4676_1	138	4.10	1.97	15.03	58.10	1.33	5.85	1.41	0.28	9.84	97.90
4676_10	147	3.65	1.74	14.60	57.80	1.34	4.68	1.25	0.16	9.19	94.40
4676_11	148	4.36	0.28	29.17	52.43	0.08	12.91	0.09	0.00	0.77	100.07
4676_12	149	3.74	1.77	15.23	59.14	1.55	5.52	1.36	0.19	9.18	97.69

Label	No	NaO_2	MgO	Al_2O_3	Si_2	K_2O	CaO	TiO_2	MnO	FeO	
4676_13	150	5.83	0.51	15.79	63.89	3.13	2.41	0.57	0.17	5.05	97.35
4676_14	151	7.13	0.03	24.08	60.48	0.92	6.31	0.04	0.00	0.41	99.41
4676_15	152	6.45	0.24	19.22	63.10	2.84	3.58	0.34	0.15	2.86	98.78
4676_16	153	0.42	0.13	21.59	51.68	1.41	9.43	0.00	0.00	0.06	84.73
4676_17	154	5.56	0.06	14.78	68.52	4.56	0.99	0.25	0.19	2.82	97.73
4676_18	155	0.14	0.00	0.00	96.53	0.02	0.00	0.01	0.00	0.00	96.70
4676_19	156	4.99	1.20	15.39	61.40	1.51	4.69	0.81	0.30	7.40	97.68
4676_2	139	2.24	0.21	31.97	47.75	0.04	16.22	0.04	0.00	0.46	98.92
4676_3	140	0.07	0.00	0.00	97.51	0.09	0.01	0.05	0.00	0.00	97.73
4676_4	141	4.39	1.09	13.85	59.77	1.78	4.61	1.27	0.28	9.52	96.58
4676_5	142	5.14	0.23	13.59	69.78	2.29	2.38	0.32	0.10	3.70	97.54
4676_6	143	1.57	6.21	12.85	47.17	0.22	10.71	1.79	0.19	11.98	92.70
4676_7	144	0.02	0.00	0.00	99.33	0.09	0.00	0.00	0.04	0.00	99.48
4676_8	145	3.10	1.12	13.58	61.77	1.86	4.40	1.34	0.26	10.27	97.71
4676_9	146	2.47	0.18	32.36	49.00	0.05	16.04	0.04	0.00	0.57	100.70
4679_1	157	3.63	1.78	15.81	60.15	1.52	5.25	1.27	0.26	9.40	99.06
4679_10	166	2.85	1.76	15.64	60.11	1.54	5.39	1.41	0.24	9.37	98.30
4679_11	167	5.40	0.08	15.40	70.47	4.63	1.00	0.20	0.12	2.82	100.10
4679_2	158	4.70	0.11	29.43	54.22	0.22	12.16	0.12	0.00	0.73	101.69
4679_3	159	3.33	1.78	15.60	59.92	1.53	5.34	1.42	0.28	9.99	99.20
4679_4	160	6.15	0.02	27.02	57.80	0.39	9.05	0.10	0.00	0.56	101.09
4679_5	161	3.81	1.48	13.57	59.10	1.79	4.29	1.12	0.35	9.04	94.55
4679_6	162	4.13	1.85	15.45	59.69	1.51	5.40	1.39	0.27	9.42	99.11
4679_7	163	5.09	0.50	18.55	63.50	1.40	5.53	0.60	0.13	5.00	100.28
4679_8	164	3.95	1.74	15.71	60.13	1.50	5.34	1.36	0.20	9.26	99.18
4679_9	165	2.78	0.23	14.44	74.64	1.60	1.24	0.32	0.13	3.82	99.20

Label	No	NaO_2	MgO	Al_2O_3	Si_2	K_2O	CaO	TiO_2	MnO	FeO	
4685_1	128	6.72	0.12	19.26	63.17	0.96	1.21	0.01	0.05	0.00	91.49
4685_10	137	5.28	0.08	14.68	69.10	4.72	1.02	0.21	0.08	2.78	97.96
4685_2	129	5.35	0.50	15.23	61.27	3.56	2.32	0.57	0.27	4.92	93.98
4685_3	130	5.33	0.09	13.95	69.68	4.90	0.86	0.25	0.18	2.96	98.20
4685_4	131	0.29	14.50	2.03	50.75	0.00	19.38	1.04	0.22	10.54	98.74
4685_5	132	6.60	0.22	18.29	64.15	1.47	0.83	0.00	0.00	0.00	91.56
4685_6	133	4.76	1.46	16.02	64.89	1.00	0.64	0.00	0.01	0.00	88.79
4685_7	134	7.03	0.21	20.01	61.01	1.28	0.98	0.00	0.01	0.07	90.61
4685_8	135	3.93	0.08	29.68	50.31	0.15	13.43	0.06	0.00	1.08	98.72
4685_9	136	5.88	0.26	14.82	58.29	1.29	0.62	0.03	0.00	0.06	81.25
5163_1	89	3.88	1.90	15.13	58.87	1.48	5.24	1.39	0.23	9.55	97.68
5163_10	98	4.27	1.75	15.03	58.98	1.51	5.27	1.36	0.26	9.10	97.52
5163_11	99	4.56	1.72	15.76	59.87	1.46	5.35	1.24	0.15	9.48	99.59
5163_12	100	4.44	1.89	15.18	58.84	1.50	5.32	1.39	0.21	9.48	98.26
5163_13	101	4.18	1.85	15.06	59.23	1.59	5.36	1.29	0.28	9.43	98.27
5163_14	102	4.47	1.94	15.17	58.75	1.50	5.39	1.42	0.33	9.64	98.61
5163_15	103	4.27	1.94	15.40	58.80	1.47	5.54	1.24	0.24	9.27	98.17
5163_16	104	4.58	1.67	15.32	59.85	1.60	5.37	1.14	0.28	9.27	99.09
5163_17	105	4.70	1.64	15.29	60.26	1.51	5.18	1.19	0.37	9.04	99.19
5163_18	106	4.65	1.78	15.11	59.01	1.53	5.40	1.38	0.26	9.27	98.39
5163_19	107	4.44	1.87	15.21	58.75	1.47	5.50	1.44	0.23	9.47	98.37
5163_2	90	4.23	1.93	15.10	59.22	1.48	5.44	1.32	0.29	9.46	98.46
5163_20	108	4.36	1.82	15.13	59.22	1.52	5.37	1.39	0.33	9.78	98.92
5163_21	109	4.52	1.80	15.08	59.57	1.55	5.38	1.35	0.25	9.47	98.98
5163_22	110	4.45	1.83	15.07	59.01	1.50	5.43	1.34	0.31	9.55	98.48
5163_23	111	4.60	1.76	15.53	58.69	1.43	5.62	1.33	0.28	9.27	98.50

Label	No	NaO_2	MgO	Al_2O_3	Si_2	K_2O	CaO	TiO_2	MnO	FeO	
5163_24	112	4.32	1.82	15.06	58.64	1.52	5.47	1.35	0.26	9.44	97.89
5163_25	113	4.35	1.86	15.25	59.25	1.52	5.34	1.34	0.30	9.72	98.92
5163_26	114	4.52	1.82	15.20	59.55	1.52	5.29	1.41	0.31	9.42	99.04
5163_27	115	4.45	1.71	15.46	58.56	1.43	5.56	1.41	0.22	9.90	98.69
5163_28	116	4.19	1.92	14.76	59.25	1.65	5.21	1.37	0.25	9.22	97.82
5163_29	117	4.43	1.71	15.62	59.88	1.38	5.52	1.26	0.26	9.09	99.16
5163_3	91	4.18	1.65	15.29	59.64	1.56	5.35	1.17	0.19	8.98	98.01
5163_30	118	4.08	1.81	15.17	59.33	1.65	5.07	1.37	0.24	10.09	98.81
5163_31	119	4.36	1.39	15.93	60.10	1.44	5.26	1.16	0.20	7.42	97.26
5163_32	120	4.38	1.86	14.85	59.93	1.62	5.22	1.44	0.29	9.90	99.49
5163_33	121	4.33	1.80	15.21	59.35	1.61	5.37	1.32	0.30	9.64	98.92
5163_34	122	4.34	1.82	15.14	58.98	1.57	5.36	1.40	0.20	9.39	98.19
5163_35	123	4.26	2.11	15.17	59.29	1.40	5.66	1.28	0.21	9.77	99.15
5163_36	124	4.18	1.90	15.02	58.96	1.60	5.38	1.40	0.36	10.00	98.80
5163_37	125	3.98	2.93	14.41	58.28	1.39	5.91	1.32	0.26	10.70	99.18
5163_38	126	5.17	2.17	16.31	59.82	0.96	6.07	1.18	0.17	7.93	99.78
5163_39	127	4.45	1.80	15.31	58.81	1.56	5.35	1.27	0.25	9.69	98.48
5163_4	92	4.17	1.77	15.39	59.50	1.46	5.43	1.26	0.21	9.46	98.64
5163_5	93	4.37	1.82	15.32	58.77	1.53	5.32	1.35	0.23	9.50	98.21
5163_6	94	4.63	1.56	15.36	58.60	1.54	5.11	1.28	0.27	8.54	96.89
5163_7	95	4.41	1.91	15.30	59.01	1.51	5.41	1.35	0.20	9.47	98.57
5163_8	96	4.28	1.83	15.10	58.61	1.48	5.39	1.32	0.23	9.46	97.70
5163_9	97	4.43	1.86	15.06	58.82	1.50	5.27	1.29	0.27	9.62	98.12
5165_1	49	4.24	1.86	15.22	59.17	1.48	5.42	1.31	0.23	9.37	98.30
5165_10	58	4.32	1.85	15.53	59.74	1.46	5.41	1.29	0.21	9.45	99.26
5165_11	59	4.17	1.73	15.46	59.56	1.48	5.26	1.44	0.26	9.63	98.99

Label	No	NaO_2	MgO	Al_2O_3	Si_2	K_2O	CaO	TiO_2	MnO	FeO	
5165_12	60	4.12	1.88	15.42	59.17	1.52	5.40	1.39	0.26	9.38	98.55
5165_13	61	4.68	1.07	15.55	62.71	1.89	4.31	0.92	0.29	7.77	99.19
5165_14	62	4.93	1.05	15.66	63.16	1.83	4.40	0.91	0.27	8.11	100.32
5165_15	63	4.59	1.75	15.65	59.55	1.38	5.56	1.33	0.35	9.06	99.20
5165_16	64	4.19	1.88	15.33	58.86	1.47	5.49	1.34	0.30	9.90	98.75
5165_17	65	4.41	1.73	15.62	59.95	1.51	5.32	1.27	0.32	9.59	99.72
5165_18	66	4.26	1.72	15.48	60.09	1.56	5.18	1.26	0.35	9.67	99.55
5165_19	67	4.25	1.80	15.39	59.18	1.46	5.43	1.29	0.23	9.39	98.43
5165_2	50	4.01	1.76	15.62	59.80	1.52	5.38	1.36	0.27	9.67	99.38
5165_20	68	4.18	1.79	15.58	59.52	1.48	5.45	1.33	0.29	9.54	99.17
5165_21	69	3.95	1.84	15.60	59.67	1.57	5.49	1.36	0.24	9.59	99.30
5165_22	70	4.12	1.86	15.40	59.22	1.52	5.57	1.33	0.23	9.52	98.76
5165_23	71	4.16	1.88	15.37	59.46	1.52	5.34	1.32	0.26	9.68	98.98
5165_24	72	4.26	1.84	15.41	59.44	1.45	5.56	1.35	0.25	9.97	99.53
5165_25	73	4.52	1.75	15.64	59.51	1.60	5.36	1.29	0.25	9.38	99.30
5165_26	74	4.40	1.76	15.06	58.78	1.53	5.32	1.37	0.23	9.41	97.85
5165_27	75	3.53	1.76	15.47	59.04	1.53	5.55	1.29	0.31	9.80	98.28
5165_28	76	2.84	1.87	15.28	59.14	1.53	5.53	1.37	0.30	9.61	97.49
5165_29	77	4.12	1.25	15.56	62.25	1.77	4.55	1.03	0.27	8.07	98.85
5165_3	51	4.16	1.81	15.42	59.22	1.51	5.44	1.30	0.19	9.49	98.54
5165_30	78	4.62	1.07	15.55	62.90	1.78	4.53	0.88	0.27	8.04	99.63
5165_31	79	5.05	0.94	20.20	57.88	0.95	7.25	0.99	0.11	6.29	99.67
5165_32	80	4.53	1.15	19.44	57.78	1.05	7.27	1.07	0.12	6.56	98.97
5165_33	81	2.56	1.86	15.41	59.37	1.50	5.51	1.28	0.19	9.78	97.46
5165_34	82	4.18	1.82	15.38	59.33	1.57	5.43	1.29	0.26	9.56	98.82
5165_35	83	4.01	1.68	14.56	55.74	1.45	5.19	1.20	0.20	9.33	93.36

Label	No	NaO_2	MgO	Al_2O_3	Si_2	K_2O	CaO	TiO_2	MnO	FeO	
5165_36	84	4.28	1.84	15.39	59.77	1.44	5.31	1.33	0.26	9.36	98.97
5165_37	85	4.17	1.77	15.25	59.72	1.59	5.30	1.29	0.19	9.35	98.63
5165_38	86	4.42	1.78	15.45	59.47	1.56	5.37	1.30	0.25	9.69	99.28
5165_39	87	4.34	1.79	15.49	59.72	1.49	5.39	1.33	0.28	9.41	99.21
5165_4	52	4.47	1.69	16.17	59.55	1.46	5.71	1.30	0.19	9.11	99.67
5165_40	88	3.89	1.84	15.43	59.41	1.41	5.53	1.34	0.31	9.62	98.78
5165_41	173	2.43	6.21	13.57	50.04	0.26	10.76	1.92	0.27	12.79	98.24
5165_42	174	5.23	0.10	15.03	69.05	4.51	1.11	0.21	0.16	3.01	98.41
5165_43	175	0.60	0.00	4.50	2.34	0.37	1.01	0.57	1.51	39.69	50.60
5165_44	176	5.70	0.55	16.00	64.92	3.86	2.49	0.59	0.24	5.11	99.45
5165_45	177	0.29	14.88	4.37	49.61	0.03	19.50	1.57	0.21	8.87	99.32
5165_46	178	5.26	0.09	15.09	69.75	4.70	1.07	0.22	0.14	2.76	99.09
5165_47	179	5.09	0.21	14.64	70.96	4.60	0.84	0.25	0.12	2.10	98.81
5165_48	180	2.53	6.13	13.92	50.47	0.17	11.19	1.81	0.28	12.67	99.15
5165_49	181	2.82	6.12	13.93	50.53	0.19	11.14	1.93	0.19	12.66	99.52
5165_5	53	4.35	1.80	15.69	59.41	1.41	5.68	1.25	0.19	9.57	99.36
5165_50	182	3.20	4.29	13.30	49.24	0.94	8.72	4.38	0.19	14.49	98.76
5165_51	183	3.25	4.75	13.16	48.81	0.77	9.93	4.37	0.29	13.05	98.38
5165_52	184	3.63	0.06	30.75	51.87	0.17	13.46	0.01	0.00	0.80	100.75
5165_53	185	0.54	0.02	0.96	85.55	0.10	0.39	0.00	0.00	0.00	87.56
5165_54	186	5.10	0.10	15.32	69.58	4.70	1.07	0.26	0.12	2.75	99.01
5165_55	187	5.74	0.07	17.16	65.53	6.47	0.59	0.26	0.14	1.95	97.92
5165_56	188	6.75	0.22	19.76	64.23	2.56	3.65	0.32	0.11	2.40	100.01
5165_57	189	0.01	0.38	0.00	92.00	0.02	0.66	0.00	0.01	0.00	93.07
5165_58	190	0.72	0.03	1.99	3.33	0.12	1.02	0.08	0.01	55.84	63.15
5165_59	191	5.15	0.10	15.04	69.74	4.67	1.01	0.21	0.15	2.91	98.96

Label	No	NaO_2	MgO	Al_2O_3	Si_2	K_2O	CaO	TiO_2	MnO	FeO	
5165_6	54	4.21	1.80	15.31	59.87	1.58	5.28	1.36	0.27	9.21	98.89
5165_60	192	2.69	4.53	12.92	50.33	0.60	9.21	3.69	0.16	15.06	99.20
5165_61	193	5.20	0.07	15.11	69.62	4.77	1.05	0.28	0.20	3.11	99.42
5165_62	194	5.61	0.07	15.21	69.46	4.61	1.01	0.32	0.12	2.98	99.39
5165_63	195	5.18	0.10	27.82	55.39	0.08	10.77	0.09	0.00	0.83	100.25
5165_64	196	2.31	6.56	13.88	49.88	0.23	11.35	1.83	0.19	12.46	98.69
5165_65	197	3.41	1.80	13.92	58.91	1.56	5.17	1.54	0.28	9.89	96.49
5165_7	55	4.38	1.87	15.46	59.31	1.57	5.28	1.29	0.24	9.45	98.85
5165_8	56	5.17	0.87	21.64	57.77	0.84	7.99	0.81	0.09	5.37	100.55
5165_9	57	4.86	1.08	19.59	58.38	1.09	7.02	1.12	0.13	6.35	99.62
5166_1	6	0.84	0.34	3.14	12.60	0.30	1.03	0.29	0.07	2.00	20.61
5166_10	15	2.35	1.05	16.62	63.37	1.58	5.30	1.31	0.31	9.21	101.10
5166_11	16	4.59	1.54	14.60	56.75	1.66	4.92	1.35	0.20	8.50	94.11
5166_12	17	1.90	0.90	9.67	38.70	0.96	3.51	0.85	0.24	6.24	62.99
5166_13	18	3.52	1.59	15.27	57.96	1.39	5.24	1.33	0.29	8.99	95.59
5166_14	19	0.76	0.34	13.21	47.95	0.86	3.37	0.93	0.13	7.14	74.69
5166_15	20	3.29	1.55	14.80	57.19	1.61	5.50	1.33	0.26	9.71	95.22
5166_16	21	3.43	1.43	12.14	47.88	1.25	4.40	1.19	0.25	7.80	79.77
5166_17	22	3.15	1.00	8.31	31.82	1.10	3.14	0.92	0.14	6.12	55.69
5166_18	23	1.00	0.38	3.97	19.97	0.41	1.43	0.35	0.08	2.46	30.04
5166_19	24	1.73	0.66	7.64	30.45	0.78	2.69	0.65	0.13	4.62	49.34
5166_2	7	0.07	0.02	0.69	1.02	0.03	0.23	0.04	0.00	0.43	2.53
5166_20	25	1.18	0.73	7.78	30.94	0.69	2.72	0.62	0.08	4.71	49.46
5166_21	26	0.28	2.39	4.95	14.16	0.06	0.56	0.64	0.02	3.89	26.96
5166_22	27	5.41	1.52	15.36	58.94	1.86	4.92	1.37	0.26	8.33	97.97
5166_23	28	2.83	1.55	15.32	59.53	1.81	4.97	1.40	0.21	8.08	95.67

Label	No	NaO_2	MgO	Al_2O_3	Si_2	K_2O	CaO	TiO_2	MnO	FeO	
5166_24	29	4.33	1.76	15.05	58.79	1.53	5.05	1.33	0.31	8.84	96.99
5166_25	30	4.47	1.77	15.13	58.20	1.50	5.45	1.35	0.25	9.40	97.50
5166_26	31	3.70	1.58	15.24	59.39	1.65	5.11	1.31	0.26	8.82	97.06
5166_27	32	1.30	0.61	7.86	30.56	0.70	2.52	0.68	0.13	4.25	48.62
5166_28	33	0.31	0.64	3.27	10.09	0.15	0.61	0.28	0.05	1.95	17.35
5166_29	34	4.12	1.72	15.24	59.96	1.47	5.38	1.30	0.27	9.48	98.95
5166_3	8	0.06	0.00	0.70	2.82	0.04	0.17	0.01	0.01	0.25	4.08
5166_30	35	0.00	0.00	0.31	1.25	0.02	0.13	0.03	0.02	0.25	2.02
5166_31	36	0.33	0.11	2.11	9.45	0.23	0.63	0.15	0.03	1.09	14.13
5166_32	37	4.82	1.12	15.19	61.34	1.75	4.35	0.90	0.25	7.48	97.20
5166_33	38	4.58	1.08	15.33	62.20	1.84	4.35	0.95	0.32	7.51	98.16
5166_34	39	0.41	0.13	1.92	7.64	0.22	0.61	0.18	0.00	1.07	12.16
5166_35	40	4.48	1.90	15.09	58.37	1.52	5.33	1.39	0.29	9.80	98.15
5166_36	41	4.25	1.84	14.81	57.42	1.53	5.32	1.42	0.30	10.52	97.41
5166_37	42	4.56	1.82	14.73	56.62	1.59	5.24	1.49	0.26	9.48	95.78
5166_38	43	4.58	1.79	15.00	57.53	1.63	5.19	1.41	0.19	9.61	96.94
5166_4	9	0.01	0.00	0.09	0.22	0.00	0.04	0.01	0.01	0.04	0.42
5166_5	10	0.00	0.00	0.01	0.21	0.00	0.01	0.00	0.00	0.12	0.35
5166_6	11	3.00	1.06	10.94	42.93	1.18	4.01	1.04	0.19	6.79	71.14
5166_7	12	2.40	0.93	12.61	47.46	1.43	4.98	1.30	0.18	8.72	80.00
5166_8	13	1.00	0.42	4.49	18.11	0.47	1.50	0.42	0.10	2.72	29.22
5166_9	14	0.24	0.00	0.04	0.26	0.00	0.03	0.00	0.00	0.00	0.57
06-Oct-10											
atho_1	93	3.86	0.12	12.24	67.68	2.59	1.74	0.27	0.15	3.48	
atho_10	29	3.88	0.11	11.73	67.34	2.65	1.71	0.25	0.16	3.49	

Label	No	NaO_2	MgO	Al_2O_3	Si_2	K_2O	CaO	TiO_2	MnO	FeO	
atho_2	94	3.74	0.08	12.26	68.28	2.68	1.76	0.26	0.14	3.49	
atho_3	2	4.12	0.10	12.40	71.44	2.73	1.76	0.22	0.08	3.22	
atho_5	1	3.96	0.10	12.35	71.75	2.69	1.74	0.27	0.08	3.56	
atho_6	27	3.89	0.08	11.94	67.29	2.65	1.71	0.22	0.06	3.21	
atho_7	30	4.11	0.06	11.90	67.18	2.68	1.72	0.26	0.13	3.16	
atho_8	31	4.01	0.09	11.89	66.84	2.75	1.55	0.27	0.05	3.23	
atho_9	32	3.91	0.09	11.90	67.61	2.69	1.67	0.20	0.08	2.97	
g132_1	83	0.78	20.83	10.61	41.12	0.02	8.27	0.27	0.17	10.05	
g132_10	4	0.78	20.99	10.95	43.00	0.03	8.38	0.34	0.19	10.28	
g132_2	84	0.87	20.94	10.69	40.92	0.03	8.24	0.26	0.13	10.21	
g132_6	3	0.73	21.26	10.95	43.35	0.02	8.44	0.31	0.19	10.31	
g132_7	96	0.73	20.78	10.50	41.51	0.02	8.23	0.32	0.14	10.33	
g132_8	95	0.73	20.76	10.68	41.24	0.02	8.14	0.27	0.19	10.22	
g132_9	28	0.68	20.82	10.42	40.58	0.00	8.14	0.28	0.11	10.51	
4672_1	42	3.47	1.80	15.44	59.39	1.42	5.20	1.38	0.30	9.16	97.55
4672_10	51	5.57	0.05	27.66	56.61	0.40	9.83	0.09	0.03	0.66	100.88
4672_11	52	2.76	1.84	15.70	60.16	1.40	5.40	1.30	0.27	9.70	98.52
4672_12	53	3.54	1.78	15.74	60.19	1.38	5.43	1.31	0.20	9.34	98.91
4672_13	54	3.19	1.88	15.49	59.58	1.45	5.46	1.34	0.25	9.70	98.33
4672_14	55	5.22	0.10	28.13	55.80	0.20	10.58	0.14	0.00	0.60	100.77
4672_15	56	4.99	0.08	27.92	55.07	0.35	10.50	0.10	0.00	0.55	99.56

Label	No	NaO_2	MgO	Al_2O_3	Si_2	K_2O	CaO	TiO_2	MnO	FeO	
4672_16	57	3.80	1.65	14.98	60.97	1.58	5.04	1.30	0.28	9.42	99.02
4672_17	58	4.03	1.43	15.54	61.18	1.42	5.15	1.27	0.31	8.97	99.29
4672_18	59	0.75	2.50	19.39	41.95	0.53	0.77	2.11	0.02	10.67	78.68
4672_19	60	1.95	5.57	13.40	50.36	0.45	9.90	3.12	0.26	14.13	99.15
4672_2	43	3.16	1.89	15.43	59.69	1.56	5.36	1.41	0.25	9.17	97.92
4672_20	61	1.76	5.37	13.34	50.66	0.40	9.99	3.08	0.24	13.73	98.59
4672_21	62	3.90	1.83	15.36	59.47	1.36	5.45	1.31	0.28	9.08	98.03
4672_22	63	0.37	0.07	0.00	93.84	0.05	0.06	0.00	0.09	0.03	94.50
4672_23	64	0.96	0.21	17.76	60.59	0.86	6.72	0.00	0.00	0.63	87.73
4672_24	65	6.68	0.03	25.64	58.91	0.42	7.46	0.14	0.03	0.60	99.89
4672_25	66	0.37	0.02	0.00	93.19	0.05	0.03	0.00	0.00	0.04	93.69
4672_26	67	0.29	0.00	0.02	95.35	0.01	0.00	0.04	0.01	0.00	95.72
4672_27	68	0.24	15.14	3.39	51.13	0.02	20.03	1.01	0.18	8.44	99.57
4672_28	69	5.03	0.20	14.90	71.54	4.54	0.89	0.26	0.06	2.27	99.69
4672_29	70	3.50	1.73	15.49	60.43	1.43	5.10	1.26	0.21	8.92	98.07
4672_3	44	0.06	2.23	8.44	31.64	0.18	0.77	3.82	0.06	41.52	88.74
4672_30	71	3.71	0.01	10.89	72.68	3.13	0.69	0.11	0.08	1.62	92.91
4672_31	72	0.17	11.77	1.61	49.73	0.00	14.86	1.10	0.55	19.57	99.36
4672_32	73	3.74	0.07	30.85	51.42	0.17	13.61	0.10	0.00	0.79	100.75
4672_33	74	5.83	1.48	4.33	67.04	10.30	6.43	0.63	0.15	1.43	97.61
4672_34	75	4.64	0.04	29.13	54.23	0.27	11.56	0.12	0.02	0.85	100.85
4672_4	45	3.46	1.84	15.35	59.47	1.44	5.29	1.30	0.31	9.33	97.79
4672_5	46	1.85	8.35	12.49	50.34	0.15	15.44	0.68	0.21	8.08	97.59
4672_6	47	1.32	5.36	13.13	49.60	0.46	9.66	3.14	0.23	14.52	97.40
4672_7	48	3.24	1.73	14.71	56.61	1.27	4.41	1.27	0.31	9.08	92.63
4672_8	49	6.96	0.08	26.11	59.36	0.34	7.66	0.10	0.00	0.57	101.18

Label	No	NaO_2	MgO	Al_2O_3	Si_2	K_2O	CaO	TiO_2	MnO	FeO	
4672_9	50	0.24	14.07	2.04	51.10	0.00	17.24	1.17	0.29	12.98	99.12
4676_1	88	0.48	0.00	0.00	94.08	0.15	0.02	0.04	0.00	0.02	94.79
4676_2	89	0.17	1.43	0.73	5.33	0.18	0.08	47.08	0.40	42.66	98.06
4676_3	90	0.00	1.50	0.03	0.03	0.00	0.03	50.54	0.62	45.05	97.79
4676_4	91	5.72	0.54	16.12	64.72	3.72	2.40	0.57	0.18	4.99	98.96
4676_5	92	5.43	0.46	15.77	64.61	3.55	2.39	0.51	0.18	4.94	97.83
5155_1	17	3.34	0.05	16.14	34.32	0.15	5.69	0.07	0.04	0.64	60.45
5155_10	26	0.37	0.07	0.00	90.63	0.02	0.21	0.00	0.00	0.47	91.78
5155_2	18	1.60	0.15	15.31	73.03	0.96	5.49	0.04	0.00	0.08	96.66
5155_3	19	0.34	0.00	0.02	40.39	0.02	0.01	0.00	0.05	0.00	40.84
5155_4	20	2.28	0.10	20.37	35.95	0.08	8.78	0.08	0.00	0.43	68.06
5155_5	21	4.74	0.05	13.48	62.02	3.94	0.86	0.16	0.11	2.61	87.99
5155_6	22	5.70	0.09	14.66	67.32	4.27	0.97	0.24	0.15	2.79	96.18
5155_7	23	1.34	0.14	12.65	65.57	1.59	4.25	0.07	0.00	0.09	85.70
5155_8	24	1.08	0.29	13.34	68.40	1.37	4.43	0.00	0.00	0.06	88.96
5155_9	25	5.03	0.08	21.66	48.55	0.20	7.66	0.14	0.02	0.70	84.02
5158_1	33	3.88	1.80	15.20	59.00	1.46	5.29	1.30	0.19	9.75	97.86
5158_2	34	4.84	1.38	18.00	58.68	1.10	6.50	0.95	0.18	7.39	99.04
5158_3	35	4.10	1.87	15.27	59.61	1.56	5.44	1.31	0.20	9.53	98.90
5158_4	36	1.90	0.38	18.37	59.61	1.37	6.20	0.03	0.00	0.19	88.05
5158_5	37	3.01	1.77	15.18	59.14	1.45	5.15	1.42	0.29	9.89	97.31
5158_6	38	0.43	0.08	0.00	92.99	0.03	0.07	0.03	0.07	0.00	93.70
5158_7	39	0.47	0.00	0.02	90.50	0.13	0.02	0.00	0.02	0.09	91.25
5158_8	40	3.59	1.52	13.80	54.74	1.42	4.69	1.16	0.27	8.25	89.42
5158_9	41	3.78	1.44	13.68	53.32	1.37	4.46	1.04	0.21	8.32	87.62
5161_1	5	1.95	0.00	6.93	33.27	2.05	0.38	0.09	0.08	1.27	46.03

Label	No	NaO_2	MgO	Al_2O_3	Si_2	K_2O	CaO	TiO_2	MnO	FeO	
5161_10	14	2.74	0.03	8.65	41.31	2.62	0.63	0.09	0.05	1.81	57.93
5161_11	15	2.34	0.00	6.41	31.54	2.02	0.46	0.12	0.08	1.35	44.32
5161_12	16	1.89	0.01	5.53	26.85	1.63	0.39	0.08	0.02	1.13	37.52
5161_2	6	3.00	0.03	9.65	46.32	2.97	0.66	0.17	0.06	1.95	64.81
5161_3	7	2.53	0.02	8.07	38.75	2.38	0.58	0.13	0.02	1.58	54.07
5161_4	8	0.52	0.03	1.83	7.88	0.44	0.24	0.11	0.06	0.50	11.61
5161_5	9	3.30	0.04	10.19	49.05	3.24	0.72	0.16	0.10	2.01	68.80
5161_6	10	5.30	0.08	15.33	70.76	4.64	1.09	0.26	0.18	3.00	100.62
5161_7	11	4.57	0.05	12.85	61.35	4.01	0.87	0.21	0.08	2.55	86.54
5161_8	12	4.99	0.49	14.91	60.69	3.54	2.38	0.56	0.21	4.99	92.75
5161_9	13	3.90	0.40	11.97	49.08	2.69	1.74	0.48	0.19	3.73	74.19
5162_1	76	5.18	0.09	15.14	70.13	4.60	1.05	0.19	0.18	3.01	99.58
5162_2	77	3.71	0.04	9.95	46.80	2.93	0.60	0.15	0.12	2.03	66.35
5162_3	78	5.46	0.10	15.00	69.57	4.61	1.05	0.25	0.11	2.94	99.10
5162_4	79	4.81	0.46	13.73	54.65	3.15	2.00	0.46	0.19	4.28	83.72
5162_5	80	1.82	0.31	15.37	76.55	0.63	5.14	0.00	0.00	0.07	99.87
5162_6	81	3.57	0.02	11.61	77.68	3.75	0.90	0.22	0.07	2.17	99.98
5162_7	82	3.95	0.07	14.03	65.77	4.50	1.04	0.23	0.14	2.98	92.70
5191_1	85	0.43	0.00	0.00	95.43	0.03	0.00	0.04	0.00	0.00	95.93
5191_2	86	0.46	0.00	0.00	93.96	0.03	0.08	0.00	0.00	0.16	94.69
5191_3	87	0.58	3.53	18.64	50.93	0.47	0.83	0.48	0.10	4.10	79.67
07-Oct-10											
atho_1	6	3.96	0.10	12.29	75.60	2.75	1.70	0.20	0.06	3.22	
atho_2	5	3.98	0.10	12.23	74.90	2.77	1.81	0.26	0.03	3.30	
atho_3	4	3.99	0.10	12.20	75.46	2.70	1.74	0.22	0.07	3.31	

Label	No	NaO_2	MgO	Al_2O_3	Si_2	K_2O	CaO	TiO_2	MnO	FeO	
atho_4	91	3.15	0.10	12.11	75.70	2.77	1.75	0.21	0.10	3.14	
atho_5	92	4.09	0.10	12.27	75.05	2.74	1.72	0.17	0.06	3.16	
atho_6	93	4.13	0.10	12.35	75.44	2.79	1.72	0.24	0.10	3.10	
		3.88	**0.10**	**12.24**	**75.36**	**2.75**	**1.74**	**0.22**	**0.07**	**3.21**	
		0.37	**0.00**	**0.08**	**0.31**	**0.03**	**0.04**	**0.03**	**0.03**	**0.09**	
g132_1	3	0.85	22.03	11.00	45.69	0.01	8.45	0.31	0.02	10.39	
g132_2	2	0.84	22.22	10.94	45.73	0.05	8.62	0.32	0.26	10.27	
g132_3	1	0.93	21.98	10.87	45.80	0.05	8.48	0.29	0.21	10.34	
g132_4	94	0.80	22.17	10.76	45.39	0.04	8.45	0.32	0.16	10.11	
g132_5	95	0.74	22.06	10.74	45.46	0.04	8.33	0.35	0.15	10.36	
g132_6	96	0.85	22.28	10.90	45.38	0.03	8.39	0.26	0.15	10.36	
		0.84	**22.12**	**10.87**	**45.57**	**0.04**	**8.45**	**0.31**	**0.16**	**10.31**	
		0.06	**0.12**	**0.10**	**0.18**	**0.01**	**0.10**	**0.03**	**0.08**	**0.10**	
4310_1	64	7.00	0.04	24.80	59.51	0.44	7.50	0.10	0.05	0.64	100.08
4310_10	73	5.30	0.08	14.70	68.95	4.62	0.99	0.18	0.17	2.93	97.92
4310_11	74	5.41	0.09	14.76	69.07	4.62	1.01	0.17	0.15	2.74	98.02
4310_12	75	2.18	0.18	31.33	47.91	0.05	15.81	0.04	0.03	0.54	98.07
4310_13	76	5.09	0.07	14.81	68.91	4.82	1.03	0.23	0.13	2.85	97.95
4310_14	77	0.15	0.00	0.00	100.21	0.07	0.02	0.02	0.01	0.04	100.52
4310_15	78	5.73	0.51	15.99	64.44	3.81	2.35	0.58	0.26	5.08	98.75
4310_2	65	6.21	0.09	25.92	57.08	0.29	8.84	0.06	0.00	0.59	99.09
4310_3	66	4.25	0.31	17.56	64.97	1.75	0.62	0.03	0.00	0.00	89.49
4310_4	67	0.70	0.34	4.97	86.06	0.22	0.30	0.00	0.00	0.25	92.84

Label	No	NaO_2	MgO	Al_2O_3	Si_2	K_2O	CaO	TiO_2	MnO	FeO	
4310_5	68	0.29	14.26	2.38	50.51	0.01	19.33	0.85	0.22	9.02	96.88
4310_6	69	5.18	0.09	14.21	66.63	4.58	0.97	0.22	0.14	2.66	94.67
4310_7	70	5.72	0.36	15.29	64.59	0.84	0.73	0.04	0.04	0.12	87.72
4310_8	71	2.19	0.65	15.82	65.86	0.67	0.57	0.05	0.00	0.06	85.87
4310_9	72	3.67	1.47	16.02	67.27	0.75	0.53	0.03	0.00	0.05	89.79
4672_1	36	2.97	1.84	15.04	59.34	1.59	5.48	1.27	0.27	9.43	97.25
4672_10	45	4.11	0.03	26.91	50.11	0.28	11.06	0.09	0.00	0.76	93.36
4672_11	46	0.19	8.64	11.53	32.76	0.40	0.55	3.82	0.17	14.44	72.50
4672_12	47	3.80	1.86	14.42	60.38	1.48	5.28	1.24	0.20	9.41	98.05
4672_13	48	4.25	1.43	16.12	60.21	1.34	5.46	1.13	0.19	8.07	98.21
4672_14	49	0.56	2.44	18.93	41.25	0.48	0.77	2.19	0.01	10.45	77.07
4672_15	50	0.29	0.06	0.00	93.40	0.06	0.07	0.01	0.13	0.00	94.01
4672_16	51	0.09	0.00	0.04	87.17	0.04	0.03	0.00	0.02	0.07	87.45
4672_17	52	3.49	1.83	15.04	59.61	1.44	5.24	1.31	0.19	9.34	97.49
4672_18	53	0.24	11.52	1.57	48.81	0.00	14.26	1.05	0.52	19.53	97.51
4672_19	54	4.81	0.07	28.62	53.88	0.27	11.57	0.11	0.00	0.75	100.07
4672_2	37	3.32	1.89	15.06	58.55	1.47	5.48	1.37	0.30	9.32	96.75
4672_20	55	5.07	0.08	28.31	53.77	0.24	11.25	0.15	0.00	0.82	99.68
4672_21	56	0.25	15.42	1.99	51.48	0.00	20.47	0.80	0.17	8.40	98.98
4672_3	38	3.78	0.02	13.41	69.18	4.63	1.43	0.72	0.00	0.78	93.94
4672_4	39	3.59	1.76	14.57	57.27	1.44	5.05	1.24	0.35	9.16	94.43
4672_5	40	0.99	5.21	12.47	48.11	0.42	9.43	2.96	0.29	13.64	93.53
4672_6	41	0.40	0.18	12.73	71.11	1.12	4.19	0.00	0.01	0.03	89.78
4672_7	42	7.28	0.06	22.47	57.56	0.45	5.79	0.13	0.04	0.54	94.33
4672_8	43	0.27	14.10	2.79	49.28	0.02	16.99	1.52	0.25	12.37	97.59
4672_9	44	5.34	0.03	27.22	55.48	0.41	10.32	0.12	0.00	0.68	99.59

Label	No	NaO_2	MgO	Al_2O_3	Si_2	K_2O	CaO	TiO_2	MnO	FeO	
4765_1	79	0.16	0.00	0.01	94.58	0.03	0.03	0.03	0.01	0.00	94.84
4765_10	88	0.25	0.01	18.12	64.25	16.26	0.03	0.00	0.01	0.00	98.92
4765_11	89	1.90	0.03	11.81	67.69	6.36	1.04	0.10	0.10	1.81	90.85
4765_12	90	1.32	0.01	13.07	74.89	6.69	1.31	0.06	0.06	2.15	99.57
4765_2	80	0.02	0.00	0.00	101.26	0.01	0.00	0.00	0.00	0.06	101.36
4765_3	81	1.94	0.04	12.62	72.89	7.36	1.32	0.09	0.03	1.95	98.24
4765_4	82	0.16	0.00	0.02	100.63	0.01	0.05	0.02	0.05	0.03	100.97
4765_5	83	0.02	0.03	0.10	98.08	0.01	0.04	0.00	0.02	1.93	100.23
4765_6	84	0.01	0.05	0.34	98.65	0.11	0.05	0.00	0.01	1.70	100.91
4765_7	85	1.25	0.00	18.33	64.24	14.76	0.04	0.00	0.00	0.00	98.62
4765_8	86	0.13	0.00	0.00	101.81	0.01	0.00	0.00	0.00	0.01	101.95
4765_9	87	3.10	1.54	14.69	58.43	3.93	4.65	1.17	0.23	8.32	96.06
4766_1	57	0.00	0.02	0.01	101.69	0.00	0.01	0.00	0.00	0.00	101.73
4766_2	58	0.01	0.01	0.02	100.90	0.01	0.00	0.01	0.00	0.00	100.95
4766_3	59	0.00	0.01	0.00	101.24	0.00	0.00	0.04	0.02	0.05	101.36
4766_4	60	3.71	1.49	15.23	60.55	2.11	4.93	1.13	0.17	8.39	97.70
4766_5	61	3.54	1.47	14.33	57.37	2.93	4.55	1.10	0.22	7.75	93.27
4766_6	62	3.40	1.48	14.93	59.31	3.15	4.80	1.12	0.30	8.66	97.15
4766_7	63	3.66	1.55	15.21	60.04	2.91	4.83	1.11	0.25	8.47	98.03
5155_1	27	1.48	0.23	14.70	74.00	1.59	4.95	0.01	0.04	0.00	97.00
5155_2	28	1.31	0.25	13.57	69.18	1.90	4.19	0.00	0.03	0.04	90.46
5155_3	29	4.88	0.08	13.82	63.74	4.08	0.87	0.21	0.05	2.84	90.58
5155_4	30	5.06	0.10	14.11	66.34	4.24	0.96	0.17	0.15	2.90	94.03
5155_5	31	3.42	0.11	27.17	47.67	0.07	12.16	0.06	0.01	0.59	91.27
5155_6	32	1.98	0.03	14.94	74.51	1.10	5.19	0.00	0.00	0.08	97.81
5155_7	33	0.04	0.00	0.00	94.12	0.03	0.06	0.03	0.04	0.00	94.33

Label	No	NaO_2	MgO	Al_2O_3	Si_2	K_2O	CaO	TiO_2	MnO	FeO	
5155_8	34	1.41	0.21	14.44	69.57	0.81	5.11	0.03	0.06	0.01	91.66
5155_9	35	0.05	0.23	0.01	93.45	0.00	0.06	0.02	0.04	0.28	94.12
5158_1	7	3.36	1.59	14.67	56.39	1.46	4.77	1.25	0.22	8.27	91.96
5158_10	16	0.58	0.00	0.02	88.61	0.02	0.02	0.00	0.00	0.00	89.25
5158_11	17	3.39	1.59	14.55	56.58	1.44	4.96	1.10	0.27	8.82	92.70
5158_2	8	3.28	1.84	15.35	59.68	1.47	5.43	1.36	0.26	9.46	98.13
5158_3	9	3.88	1.82	15.60	58.58	1.50	5.31	1.33	0.31	9.55	97.87
5158_4	10	1.17	0.21	16.75	56.35	1.20	5.32	0.21	0.00	0.31	81.52
5158_5	11	3.46	1.59	13.54	53.28	1.30	4.24	1.20	0.25	7.99	86.86
5158_6	12	1.99	0.77	6.92	27.85	0.67	2.09	0.59	0.05	4.02	44.95
5158_7	13	2.90	1.26	11.14	43.98	1.06	3.64	0.95	0.16	6.55	71.64
5158_8	14	1.49	0.80	7.05	28.55	0.69	2.44	0.60	0.11	4.43	46.15
5158_9	15	3.74	1.32	13.75	53.30	1.40	4.28	1.09	0.18	7.62	86.69
5162_1	18	4.26	0.07	12.19	57.27	3.82	0.89	0.19	0.11	2.27	81.06
5162_2	19	4.50	0.07	13.45	62.71	4.15	0.97	0.23	0.12	2.48	88.67
5162_3	20	4.75	0.05	14.47	66.45	4.60	1.04	0.29	0.06	2.71	94.42
5162_4	21	4.92	0.01	12.47	78.61	1.52	1.39	0.27	0.00	0.42	99.60
5162_5	22	2.78	0.24	8.65	35.88	1.98	1.14	0.30	0.09	2.84	53.90
5162_6	23	0.02	0.00	0.01	91.30	0.06	0.03	0.01	0.00	0.00	91.43
5162_7	24	4.44	0.07	10.93	50.51	3.39	0.71	0.19	0.16	2.24	72.64
5162_8	25	3.45	0.00	11.71	77.10	4.00	0.93	0.28	0.06	2.19	99.72
5162_9	26	1.60	0.21	14.64	75.25	0.90	4.95	0.00	0.02	0.00	97.56
19-Apr-12 StHs6/80-G_6	118	4.23	2.00	17.39	62.37	1.30	5.25	0.81	0.07	4.34	

Label	No	NaO_2	MgO	Al_2O_3	Si_2	K_2O	CaO	TiO_2	MnO	FeO
StHs6/80-G_5	117	4.96	2.01	17.59	62.65	1.37	5.34	0.71	0.08	4.40
StHs6/80-G_4	62	4.91	1.89	17.42	62.49	1.32	5.24	0.73	0.05	4.29
StHs6/80-G_3	3	4.73	1.98	17.73	63.28	1.25	5.36	0.71	0.06	4.29
StHs6/80-G_2	2	4.63	1.94	17.78	63.41	1.28	5.21	0.71	0.06	4.63
StHs6/80-G_1	1	4.69	1.97	17.79	63.32	1.35	5.38	0.72	0.07	4.23
		4.69	**1.96**	**17.62**	**62.92**	**1.31**	**5.30**	**0.73**	**0.07**	**4.36**
		0.26	**0.04**	**0.18**	**0.47**	**0.04**	**0.07**	**0.04**	**0.01**	**0.14**
GOR132-G_6	122	0.84	22.59	10.87	45.49	0.04	8.38	0.27	0.16	9.99
GOR132-G_5	121	0.96	22.53	10.95	45.78	0.03	8.27	0.32	0.17	10.25
GOR132-G_4	64	0.81	22.52	10.95	45.11	0.02	8.51	0.28	0.16	10.34
GOR132-G_3	9	0.90	22.45	10.81	44.83	0.06	8.36	0.31	0.14	9.75
GOR132-G_2	8	0.75	22.53	10.69	45.52	0.04	8.51	0.38	0.08	9.99
GOR132-G_1	7	0.92	22.59	10.71	45.10	0.03	8.55	0.30	0.11	9.77
		0.86	**22.54**	**10.83**	**45.30**	**0.04**	**8.43**	**0.31**	**0.14**	**10.02**

Label	No	NaO_2	MgO	Al_2O_3	Si_2	K_2O	CaO	TiO_2	MnO	FeO	
		0.08	**0.05**	**0.11**	**0.35**	**0.01**	**0.11**	**0.04**	**0.03**	**0.24**	
ATHO-G_6	120	4.22	0.10	12.26	74.96	2.83	1.62	0.24	0.16	3.48	
ATHO-G_5	119	4.37	0.07	12.08	75.31	2.80	1.68	0.22	0.10	3.33	
ATHO-G_4	63	4.38	0.08	12.18	74.88	2.77	1.68	0.29	0.18	3.35	
ATHO-G_3	6	4.13	0.13	12.23	75.05	2.82	1.65	0.27	0.16	3.28	
ATHO-G_2	5	4.47	0.09	12.23	75.20	2.68	1.68	0.26	0.13	3.17	
ATHO-G_1	4	4.25	0.08	12.07	75.19	2.74	1.68	0.22	0.06	3.35	
		4.31	**0.09**	**12.18**	**75.10**	**2.77**	**1.67**	**0.25**	**0.13**	**3.33**	
		0.12	**0.02**	**0.08**	**0.16**	**0.06**	**0.03**	**0.03**	**0.05**	**0.10**	
5133_1	11	5.07	0.02	11.15	72.28	0.14	1.97	0.19	0.00	0.81	91.62
5133_10	20	4.78	0.06	11.16	78.27	0.45	1.57	0.21	0.06	2.78	99.34
5133_11	21	5.08	0.08	14.13	63.09	4.19	0.99	0.18	0.19	2.90	90.84
5133_12	22	4.74	0.00	12.53	75.34	0.97	1.82	0.19	0.02	0.79	96.40
5133_2	12	4.06	1.87	14.94	58.09	1.45	5.26	1.28	0.21	9.22	96.37
5133_3	13	3.96	1.90	14.93	57.75	1.51	5.38	1.35	0.24	9.33	96.35
5133_4	14	3.68	1.92	14.67	57.50	1.37	5.47	1.35	0.20	9.72	95.87
5133_5	15	3.95	1.82	15.09	58.96	1.42	5.06	1.32	0.27	8.96	96.86
5133_6	16	3.88	1.81	14.89	58.07	1.54	5.26	1.22	0.27	9.35	96.27

Label	No	NaO_2	MgO	Al_2O_3	Si_2	K_2O	CaO	TiO_2	MnO	FeO	
5133_7	17	5.54	0.53	15.68	63.83	3.76	2.28	0.64	0.24	5.32	97.83
5133_8	18	4.84	0.02	12.10	74.76	1.38	1.53	0.12	0.05	0.92	95.72
5133_9	19	0.38	2.19	20.83	47.42	0.35	0.35	0.83	0.15	2.88	75.38
5136_1	65	0.31	0.40	14.96	70.71	0.47	2.38	0.00	0.00	0.02	89.25
5136_10	74	5.57	0.10	14.50	67.36	3.78	0.99	0.24	0.14	2.87	95.56
5136_11	75	5.39	0.56	14.86	59.59	3.38	2.00	0.59	0.23	5.03	91.62
5136_12	76	4.70	0.10	12.70	58.31	3.62	0.78	0.21	0.07	2.37	82.87
5136_13	77	2.95	0.11	11.56	74.19	4.44	1.03	0.23	0.00	2.39	96.90
5136_2	66	5.89	0.50	15.93	63.70	3.18	2.36	0.65	0.17	4.99	97.37
5136_3	67	3.52	0.23	10.73	49.42	1.63	2.08	0.27	0.08	3.74	71.69
5136_4	68	3.53	0.18	11.03	65.47	3.12	1.66	0.29	0.02	2.68	87.96
5136_5	69	5.29	0.12	14.26	64.95	4.16	0.99	0.24	0.13	2.83	92.97
5136_6	70	4.15	0.01	12.74	72.28	2.86	1.24	0.11	0.08	2.12	95.59
5136_7	71	0.28	0.00	0.87	6.06	0.04	0.08	0.04	0.06	0.10	7.52
5136_8	72	4.88	0.44	15.54	62.47	3.25	2.19	0.58	0.22	4.87	94.43
5136_9	73	4.76	0.11	11.62	74.36	0.47	1.92	0.26	0.08	1.88	95.47
5142_1	38	2.98	1.69	15.22	59.44	1.47	4.97	1.25	0.25	9.02	96.29
5142_10	47	4.06	1.84	15.06	59.07	1.48	4.82	1.29	0.32	9.06	97.00
5142_11	48	3.95	1.77	15.04	59.02	1.47	5.35	1.33	0.19	9.63	97.74
5142_12	49	3.99	1.87	15.07	58.35	1.45	5.24	1.37	0.25	9.42	97.00
5142_13	50	3.54	1.81	14.80	57.34	1.42	5.23	1.24	0.22	9.25	94.86
5142_14	51	3.43	1.74	14.46	56.25	1.37	4.83	1.27	0.18	8.99	92.52
5142_15	52	3.50	1.89	15.00	58.80	1.34	5.04	1.33	0.31	9.60	96.79
5142_16	53	3.39	1.74	15.01	58.83	1.53	5.17	1.27	0.18	9.22	96.33
5142_17	54	3.44	2.17	14.57	58.23	1.38	5.34	1.42	0.14	10.17	96.86
5142_18	55	3.75	1.75	15.54	60.41	1.54	5.04	1.28	0.32	8.85	98.48

Label	No	NaO_2	MgO	Al_2O_3	Si_2	K_2O	CaO	TiO_2	MnO	FeO	
5142_19	56	3.46	1.85	14.92	59.01	1.27	5.35	1.33	0.24	9.58	97.00
5142_2	39	3.31	1.63	13.26	51.78	1.22	4.35	1.15	0.13	8.27	85.09
5142_20	57	3.98	1.89	15.08	59.10	1.44	5.17	1.33	0.23	9.07	97.28
5142_21	58	4.12	1.70	15.22	59.40	1.49	5.25	1.25	0.24	9.24	97.91
5142_22	59	4.21	1.80	14.98	58.72	1.52	4.85	1.19	0.28	9.12	96.67
5142_23	60	4.41	0.07	11.59	77.49	1.38	1.60	0.31	0.04	2.11	99.01
5142_24	61	5.19	0.04	13.12	76.64	0.94	1.92	0.18	0.05	0.88	98.97
5142_3	40	3.41	1.58	13.09	51.28	1.30	4.15	1.13	0.19	7.61	83.74
5142_4	41	4.01	1.41	15.09	59.06	1.44	4.51	1.06	0.22	8.77	95.57
5142_5	42	2.38	1.30	11.48	44.94	1.09	3.36	0.96	0.22	7.15	72.89
5142_6	43	3.81	0.01	11.88	75.59	3.58	1.17	0.24	0.07	1.84	98.20
5142_7	44	5.44	0.08	15.00	68.97	4.47	1.05	0.26	0.18	2.99	98.44
5142_8	45	3.87	1.89	15.22	59.23	1.49	5.04	1.34	0.15	9.55	97.78
5142_9	46	4.65	0.03	11.25	80.14	0.61	1.67	0.17	0.00	1.01	99.54
7094_1	10	0.13	0.00	0.02	0.20	0.01	0.01	0.01	0.02	0.00	0.40
7097_1	78	5.10	1.23	17.64	58.63	1.21	6.08	0.74	0.16	6.19	96.97
7097_10	87	4.31	1.64	15.39	57.86	1.37	5.30	1.19	0.22	8.67	95.95
7097_11	88	4.58	2.69	14.55	56.13	1.21	5.91	1.15	0.27	9.08	95.57
7097_12	89	4.16	1.77	14.09	55.33	1.44	4.80	1.30	0.15	8.80	91.83
7097_13	90	3.71	1.86	14.28	55.54	1.45	4.88	1.34	0.24	10.33	93.62
7097_14	91	3.62	1.90	13.32	53.55	1.30	4.90	1.20	0.21	9.82	89.82
7097_15	92	4.19	1.92	14.82	57.61	1.51	5.30	1.37	0.17	9.69	96.58
7097_16	93	4.02	1.68	14.11	55.17	1.30	5.07	1.25	0.14	8.42	91.16
7097_17	94	4.19	1.86	15.05	58.56	1.54	5.37	1.36	0.21	9.29	97.44
7097_18	95	4.05	1.72	14.49	56.43	1.46	4.96	1.24	0.09	8.78	93.21
7097_19	96	4.26	1.79	15.46	59.13	1.48	5.25	1.27	0.19	9.46	98.30

Label	No	NaO_2	MgO	Al_2O_3	Si_2	K_2O	CaO	TiO_2	MnO	FeO	
7097_2	79	4.36	1.81	13.85	54.64	1.40	4.95	1.22	0.29	8.88	91.40
7097_20	97	4.43	1.85	14.78	58.21	1.48	5.37	1.28	0.30	9.47	97.18
7097_21	98	4.13	1.44	15.54	60.79	1.66	4.95	1.08	0.20	9.10	98.89
7097_22	99	3.69	1.61	13.41	52.35	1.34	4.59	1.13	0.23	8.36	86.71
7097_3	80	4.16	1.94	15.19	58.75	1.54	5.14	1.24	0.13	9.53	97.62
7097_4	81	4.05	1.96	14.94	57.52	1.46	5.30	1.35	0.24	9.18	96.00
7097_5	82	4.15	1.76	14.29	54.78	1.49	5.04	1.30	0.19	8.84	91.84
7097_6	83	4.29	1.77	14.55	56.46	1.45	5.14	1.25	0.28	9.67	94.85
7097_7	84	4.30	1.74	14.90	57.93	1.64	5.13	1.23	0.28	9.04	96.20
7097_8	85	3.98	1.70	14.75	58.04	1.39	5.03	1.33	0.20	9.40	95.83
7097_9	86	4.31	1.72	14.75	58.26	1.55	5.02	1.31	0.23	9.09	96.23
7098_1	23	3.46	1.54	12.60	47.74	1.24	4.24	1.04	0.26	7.68	79.79
7098_10	32	4.14	1.72	15.08	59.53	1.63	5.05	1.29	0.21	8.75	97.39
7098_11	33	3.63	1.75	14.86	56.83	1.45	5.01	1.30	0.25	9.56	94.64
7098_12	34	2.82	1.74	15.10	59.79	1.62	5.17	1.20	0.22	8.97	96.62
7098_13	35	4.02	1.67	15.26	60.16	1.51	5.00	1.26	0.24	8.59	97.71
7098_14	36	4.31	1.72	15.67	59.11	1.48	4.78	1.23	0.21	9.04	97.56
7098_15	37	4.03	1.75	15.06	58.29	1.60	5.27	1.31	0.17	9.66	97.14
7098_2	24	4.21	1.64	16.08	56.55	1.32	5.21	1.13	0.19	8.63	94.95
7098_3	25	3.98	1.66	12.53	48.56	1.27	4.45	1.13	0.24	8.35	82.17
7098_4	26	4.35	1.69	14.89	58.69	1.67	5.15	1.20	0.25	9.00	96.90
7098_5	27	4.19	1.92	15.14	58.51	1.55	5.33	1.32	0.18	9.72	97.87
7098_6	28	4.64	1.86	15.24	58.37	1.55	5.22	1.32	0.23	9.32	97.75
7098_7	29	4.10	1.75	14.88	59.16	1.58	5.11	1.19	0.11	9.23	97.13
7098_8	30	2.78	0.97	8.63	34.22	0.92	2.81	0.71	0.18	5.12	56.34
7098_9	31	4.27	1.81	15.40	58.58	1.56	5.34	1.29	0.23	9.26	97.74

Label	No	NaO_2	MgO	Al_2O_3	Si_2	K_2O	CaO	TiO_2	MnO	FeO	
7099_1	100	4.23	1.81	14.33	55.29	1.44	4.94	1.22	0.21	8.66	92.13
7099_10	109	4.52	1.84	14.70	58.19	1.61	4.99	1.25	0.27	9.50	96.86
7099_11	110	4.35	1.97	14.46	56.95	1.59	5.33	1.40	0.23	9.60	95.87
7099_12	111	4.49	1.81	14.99	57.65	1.56	5.32	1.34	0.20	9.40	96.76
7099_13	112	3.63	1.80	14.35	56.59	1.42	4.99	1.27	0.24	9.33	93.61
7099_14	113	4.45	1.74	14.99	58.42	1.67	5.29	1.29	0.17	9.29	97.30
7099_15	114	4.52	1.54	14.89	59.88	1.34	5.09	1.22	0.21	8.46	97.15
7099_16	115	4.27	1.62	15.68	57.25	1.30	5.65	1.23	0.19	8.73	95.92
7099_17	116	4.96	1.43	15.22	60.47	1.33	4.87	1.07	0.17	7.94	97.47
7099_2	101	4.08	1.73	14.78	58.46	1.55	5.11	1.24	0.27	9.16	96.39
7099_3	102	3.69	1.94	13.58	53.62	1.36	4.85	1.24	0.25	8.82	89.36
7099_4	103	4.25	1.88	14.97	58.23	1.49	5.29	1.30	0.19	9.55	97.16
7099_5	104	3.55	1.42	11.80	45.78	1.12	3.99	0.99	0.20	7.25	76.11
7099_6	105	4.24	1.79	14.96	57.73	1.56	5.37	1.32	0.37	9.40	96.74
7099_7	106	4.44	1.87	14.39	55.52	1.41	5.11	1.29	0.33	9.58	93.95
7099_8	107	4.33	1.73	15.48	60.16	1.61	5.15	1.30	0.23	9.03	99.01
7099_9	108	3.77	1.53	15.64	56.80	1.24	5.47	1.13	0.16	7.57	93.33
20-Apr-12											
StHs6/80-G_6	115	4.62	1.95	17.66	63.23	1.33	5.22	0.76	0.03	4.61	
StHs6/80-G_5	114	4.71	1.91	17.65	63.54	1.31	5.34	0.75	0.11	4.59	
StHs6/80-G_4	65	4.72	1.96	17.93	63.42	1.32	5.33	0.71	0.09	4.47	
StHs6/80-G_3	64	4.36	1.98	17.71	63.45	1.36	5.30	0.70	0.02	4.24	

Label	No	NaO_2	MgO	Al_2O_3	Si_2	K_2O	CaO	TiO_2	MnO	FeO
StHs6/80-G_2	2	4.64	1.95	17.90	63.37	1.40	5.25	0.64	0.12	4.34
StHs6/80-G_1	1	4.76	1.91	17.99	63.60	1.32	5.27	0.74	0.11	4.14
		4.63	**1.94**	**17.81**	**63.43**	**1.34**	**5.29**	**0.72**	**0.08**	**4.40**
		0.14	**0.03**	**0.15**	**0.13**	**0.03**	**0.05**	**0.04**	**0.04**	**0.19**
GOR132-G_6	119	0.86	22.40	10.92	45.64	0.06	8.33	0.29	0.16	10.10
GOR132-G_5	118	0.85	22.31	10.84	45.76	0.03	8.43	0.27	0.09	10.30
GOR132-G_4	68	0.87	22.33	10.93	45.42	0.04	8.44	0.29	0.18	10.01
GOR132-G_3	69	0.78	22.30	11.04	45.51	0.01	8.43	0.32	0.14	10.37
GOR132-G_2	6	0.82	22.59	10.77	45.54	0.04	8.26	0.29	0.17	10.42
GOR132-G_1	5	0.86	22.52	11.12	45.87	0.00	8.63	0.31	0.10	10.32
		0.84	**22.41**	**10.94**	**45.62**	**0.03**	**8.42**	**0.30**	**0.14**	**10.25**
		0.03	**0.12**	**0.13**	**0.17**	**0.02**	**0.12**	**0.02**	**0.04**	**0.16**
ATHO-G_6	117	4.37	0.11	12.36	74.89	2.85	1.75	0.20	0.12	3.21
ATHO-G_5	116	4.19	0.08	12.13	75.23	2.73	1.67	0.24	0.09	3.32

Label	No	NaO_2	MgO	Al_2O_3	Si_2	K_2O	CaO	TiO_2	MnO	FeO	
ATHO-G_4	67	4.30	0.08	12.29	75.53	2.83	1.64	0.25	0.13	3.33	
ATHO-G_3	66	3.93	0.13	12.31	74.97	2.83	1.66	0.29	0.11	3.37	
ATHO-G_2	4	4.40	0.10	12.44	75.36	2.77	1.73	0.22	0.14	3.29	
ATHO-G_1	3	4.24	0.09	12.30	75.48	2.77	1.60	0.23	0.18	3.27	
		4.24	**0.10**	**12.31**	**75.24**	**2.80**	**1.67**	**0.24**	**0.13**	**3.30**	
		0.17	**0.02**	**0.10**	**0.27**	**0.05**	**0.06**	**0.03**	**0.03**	**0.05**	
5135_1	100	3.35	0.07	12.51	73.94	3.37	1.54	0.23	0.00	2.03	97.05
5135_10	109	4.27	1.72	14.76	58.33	1.43	4.88	1.27	0.21	8.87	95.75
5135_11	110	3.13	1.75	14.29	56.46	1.26	4.46	1.28	0.29	8.82	91.74
5135_12	111	3.18	1.86	15.13	59.47	1.33	5.37	1.25	0.31	9.42	97.31
5135_13	112	4.71	0.00	11.37	79.65	0.42	1.50	0.13	0.00	1.03	98.81
5135_14	113	5.28	0.04	12.03	75.72	1.94	1.30	0.21	0.08	1.40	97.99
5135_2	101	5.88	0.08	14.60	67.60	3.96	1.08	0.24	0.08	2.96	96.48
5135_3	102	5.21	0.00	11.18	80.03	0.50	1.38	0.13	0.00	0.42	98.85
5135_4	103	4.17	1.69	15.22	59.84	1.55	5.03	1.26	0.39	9.32	98.47
5135_5	104	4.41	1.77	15.41	59.90	1.53	5.13	1.21	0.30	8.97	98.62
5135_6	105	4.21	1.72	15.23	59.28	1.53	5.24	1.27	0.16	9.54	98.19
5135_7	106	5.16	0.03	12.23	79.44	0.51	1.68	0.23	0.09	1.17	100.53
5135_8	107	5.03	0.02	12.03	76.81	1.75	1.37	0.18	0.03	1.49	98.72
5135_9	108	3.38	1.75	14.89	59.03	1.48	5.02	1.28	0.29	9.28	96.40
5148_1	41	5.44	0.24	14.68	71.14	4.25	0.86	0.23	0.16	2.41	99.40

Label	No	NaO_2	MgO	Al_2O_3	Si_2	K_2O	CaO	TiO_2	MnO	FeO	
5148_10	50	5.62	0.08	14.89	69.30	4.76	1.06	0.21	0.08	3.10	99.11
5148_11	51	5.85	0.49	15.30	61.31	3.21	2.35	0.52	0.22	5.01	94.26
5148_12	52	5.50	0.08	14.80	68.46	4.40	1.07	0.22	0.18	2.81	97.52
5148_13	53	4.92	0.07	12.93	60.37	3.69	0.84	0.24	0.12	2.46	85.64
5148_14	54	3.94	0.10	14.99	69.14	4.64	1.03	0.24	0.12	3.02	97.23
5148_15	55	4.06	0.49	16.00	65.19	3.75	2.42	0.53	0.16	5.18	97.79
5148_16	56	5.36	0.03	14.07	76.69	0.40	2.44	0.16	0.04	0.60	99.79
5148_17	57	5.64	0.26	15.05	63.71	3.81	1.70	0.38	0.11	3.78	94.43
5148_18	58	3.81	0.11	14.69	69.26	4.55	1.08	0.28	0.13	3.00	96.92
5148_19	59	0.03	0.14	0.64	1.98	0.04	0.25	0.36	0.04	0.42	3.92
5148_2	42	5.08	0.21	14.68	70.94	4.46	0.89	0.25	0.10	2.09	98.69
5148_20	60	5.39	0.09	13.85	64.39	4.22	0.97	0.64	0.12	2.79	92.46
5148_21	61	5.41	0.08	13.31	61.98	4.19	1.05	0.23	0.08	2.59	88.94
5148_22	62	4.41	0.05	9.72	72.96	0.75	1.19	0.14	0.00	1.32	90.55
5148_23	63	4.83	0.09	12.76	75.92	1.19	2.18	0.26	0.06	2.04	99.34
5148_3	43	0.46	0.02	1.46	9.02	0.39	0.12	0.04	0.01	0.21	11.73
5148_4	44	5.46	0.23	14.63	70.80	4.47	0.81	0.23	0.12	2.39	99.15
5148_5	45	5.57	0.07	14.99	69.73	4.76	0.98	0.21	0.14	2.99	99.44
5148_6	46	5.48	0.06	13.49	77.47	0.45	2.22	0.21	0.00	0.79	100.19
5148_7	47	4.40	0.21	11.92	58.18	3.60	0.70	0.21	0.07	1.82	81.11
5148_8	48	5.52	0.09	14.74	68.30	4.64	1.01	0.21	0.03	3.04	97.58
5148_9	49	5.69	0.49	15.65	63.92	3.75	2.33	0.56	0.18	5.13	97.70
5149_1	30	3.03	1.67	14.53	56.69	1.22	4.09	1.32	0.17	8.60	91.30
5149_10	39	3.71	1.78	15.01	58.93	1.42	5.33	1.28	0.27	9.47	97.20
5149_11	40	3.71	1.81	15.26	59.68	1.36	5.20	1.35	0.19	9.31	97.87
5149_2	31	0.28	0.00	18.21	63.77	16.22	0.01	0.04	0.03	0.05	98.61

Label	No	NaO_2	MgO	Al_2O_3	Si_2	K_2O	CaO	TiO_2	MnO	FeO	
5149_3	32	0.31	0.00	18.13	63.65	16.36	0.02	0.00	0.00	0.02	98.48
5149_4	33	4.81	0.09	14.40	67.30	4.40	0.95	0.23	0.18	2.84	95.19
5149_5	34	0.36	1.11	15.53	45.33	0.40	0.46	0.67	0.07	4.47	68.38
5149_6	35	0.21	0.08	18.19	63.54	16.18	0.00	0.06	0.03	0.47	98.75
5149_7	36	4.53	0.07	11.84	57.03	3.79	0.77	0.20	0.07	2.11	80.41
5149_8	37	4.68	0.09	14.05	65.27	4.34	0.98	0.28	0.08	2.69	92.46
5149_9	38	0.17	0.02	18.41	63.90	16.40	0.03	0.03	0.03	0.18	99.16
5150_1	7	4.33	0.08	12.53	58.70	3.89	0.87	0.16	0.13	2.66	83.35
5150_10	16	4.56	0.25	12.20	72.79	1.40	2.10	0.29	0.10	3.70	97.39
5150_11	17	4.71	0.05	12.50	79.73	0.44	2.05	0.25	0.00	0.97	100.69
5150_12	18	4.91	0.07	11.64	79.53	0.74	1.41	0.19	0.05	0.91	99.45
5150_13	19	4.58	0.02	12.02	79.26	0.43	2.13	0.23	0.06	1.18	99.92
5150_14	20	6.40	0.00	17.92	68.92	0.38	3.49	0.13	0.00	0.64	97.89
5150_15	21	5.05	0.10	11.90	75.85	0.97	1.59	0.36	0.03	2.54	98.38
5150_16	22	4.42	0.02	11.57	80.68	0.18	1.88	0.20	0.03	1.31	100.29
5150_17	23	4.75	0.00	12.39	79.72	0.68	1.77	0.17	0.04	0.77	100.29
5150_18	24	4.47	0.05	10.85	80.25	0.66	1.35	0.19	0.00	1.29	99.12
5150_19	25	4.74	0.02	12.22	78.91	1.01	1.47	0.22	0.03	0.88	99.50
5150_2	8	7.24	0.02	23.42	61.45	0.31	5.96	0.06	0.03	0.37	98.85
5150_20	26	5.12	0.00	12.88	78.70	0.98	1.76	0.17	0.03	0.53	100.17
5150_3	9	4.88	0.04	12.38	78.66	0.21	1.81	0.24	0.06	0.94	99.22
5150_4	10	4.60	0.02	11.14	79.90	0.93	1.08	0.18	0.00	0.25	98.09
5150_5	11	4.95	0.02	11.77	78.18	0.28	1.85	0.33	0.00	2.13	99.50
5150_6	12	4.71	0.06	11.87	78.21	0.27	2.11	0.24	0.09	2.23	99.80
5150_7	13	5.86	0.03	15.77	73.68	1.49	2.69	0.14	0.03	0.47	100.17
5150_8	14	4.83	0.01	11.76	79.25	0.48	1.64	0.30	0.00	1.14	99.40

Label	No	NaO_2	MgO	Al_2O_3	Si_2	K_2O	CaO	TiO_2	MnO	FeO	
5150_9	15	4.59	0.19	11.46	79.87	0.56	1.37	0.17	0.07	1.95	100.23
7094_1	27	3.83	1.80	14.89	58.68	1.59	4.99	1.24	0.25	8.74	96.01
7094_2	28	2.32	1.10	8.58	33.82	0.80	3.05	0.77	0.14	6.03	56.60
7094_3	29	4.53	1.18	14.36	58.10	1.75	3.93	1.04	0.15	7.52	92.56
7095_1	70	4.31	1.55	13.42	52.84	1.33	4.71	1.23	0.21	8.54	88.14
7095_10	79	4.19	1.93	14.76	58.01	1.56	5.21	1.43	0.21	9.65	96.96
7095_11	80	4.65	1.86	14.83	58.33	1.65	5.21	1.33	0.33	8.76	96.93
7095_12	81	4.32	1.85	14.85	57.98	1.46	5.34	1.38	0.26	9.57	97.01
7095_13	82	4.54	1.79	14.68	57.69	1.55	5.10	1.27	0.35	9.19	96.17
7095_14	83	3.85	1.73	13.81	54.25	1.45	4.88	1.22	0.28	9.22	90.69
7095_15	84	4.54	1.85	14.84	58.34	1.55	5.14	1.26	0.23	9.11	96.86
7095_16	85	3.95	1.64	14.92	58.42	1.44	5.04	1.25	0.23	8.97	95.86
7095_17	86	4.09	1.86	15.21	59.48	1.51	5.27	1.32	0.25	9.35	98.34
7095_18	87	4.46	1.78	15.11	59.18	1.55	5.19	1.22	0.25	9.50	98.22
7095_19	88	3.38	1.83	13.46	53.02	1.45	4.79	1.21	0.28	9.04	88.45
7095_2	71	4.26	1.88	13.91	53.22	1.39	4.96	1.22	0.18	8.66	89.69
7095_20	89	4.34	1.83	14.89	58.25	1.57	5.19	1.28	0.23	9.61	97.21
7095_21	90	4.19	1.87	15.04	58.49	1.45	5.40	1.23	0.27	9.55	97.49
7095_22	91	4.48	1.77	15.06	58.23	1.56	5.35	1.34	0.28	9.19	97.27
7095_23	92	3.75	1.53	14.18	52.72	1.32	4.87	1.13	0.30	7.91	87.71
7095_24	93	3.74	0.10	17.95	37.97	0.19	6.55	0.09	0.01	0.95	67.54
7095_25	94	4.29	1.94	15.06	58.19	1.61	5.35	1.31	0.28	9.92	97.95
7095_26	95	4.22	1.92	15.09	57.10	1.46	5.49	1.26	0.24	9.44	96.23
7095_27	96	4.01	1.77	15.05	58.72	1.58	5.26	1.26	0.34	9.49	97.48
7095_28	97	4.42	1.84	14.84	57.89	1.55	5.27	1.35	0.28	9.51	96.96
7095_29	98	4.46	1.23	15.09	58.70	1.51	4.61	1.04	0.26	8.56	95.47

Label	No	NaO_2	MgO	Al_2O_3	Si_2	K_2O	CaO	TiO_2	MnO	FeO	
7095_3	72	3.12	1.32	9.89	38.45	1.02	3.36	0.87	0.15	6.38	64.56
7095_30	99	4.48	1.58	14.80	59.20	1.50	4.70	1.20	0.27	8.63	96.36
7095_4	73	4.02	1.75	14.29	54.88	1.42	4.98	1.16	0.21	9.27	91.99
7095_5	74	4.43	1.84	14.81	57.94	1.62	5.05	1.35	0.23	9.34	96.61
7095_6	75	4.26	1.83	14.94	57.45	1.48	5.22	1.27	0.28	9.40	96.12
7095_7	76	3.60	1.60	11.12	44.30	1.14	3.87	1.02	0.17	7.32	74.15
7095_8	77	4.38	1.76	14.80	56.51	1.44	5.15	1.22	0.24	9.20	94.70
7095_9	78	4.34	1.52	14.90	56.18	1.39	4.94	1.20	0.21	8.23	92.92

Table A.2: Table 1 of all glass chemistry data from WDS-EPMA analysis, including secondary standards, arranged by dates.

Label	No	NaO_2	MgO	Al_2O_3	Si_2	K_2O	CaO	TiO_2	MnO	FeO		
09-Jul-10												
g132_2	4	0.87	22.33	11.11	46.00	0.02	0.01	0.04	8.57	0.30	0.22	10.36
g132_4	26	0.88	22.11	11.07	46.02	0.05	0.01	0.03	8.17	0.30	0.13	10.07
g132_7	3	0.84	22.37	11.04	45.59	0.06	0.01	0.03	8.18	0.26	0.09	10.44
g132_8	27	1.07	22.37	10.90	45.83	0.10	0.00	0.03	9.21	0.28	0.09	10.65
		0.92	**22.30**	**11.03**	**45.86**	**0.06**	**0.01**	**0.03**	**8.53**	**0.28**	**0.13**	**10.38**
		0.11	**0.12**	**0.09**	**0.20**	**0.03**	**0.00**	**0.01**	**0.49**	**0.02**	**0.06**	**0.24**
sthl_1	29	4.52	1.95	17.54	63.73	0.13	0.02	1.24	5.56	0.70	0.14	4.55
sthl_3	28	4.74	1.97	18.07	64.01	0.21	0.02	1.25	5.11	0.69	0.15	4.59
sthl_4	1	4.27	1.87	17.83	63.16	0.14	0.03	1.20	5.36	0.77	0.07	4.24
sthl_5	2	4.53	1.95	17.85	63.79	0.23	0.02	1.25	5.63	0.74	0.00	4.59
		4.52	**1.94**	**17.82**	**63.67**	**0.18**	**0.03**	**1.23**	**5.42**	**0.72**	**0.09**	**4.49**
		0.19	**0.04**	**0.21**	**0.36**	**0.05**	**0.01**	**0.02**	**0.23**	**0.04**	**0.07**	**0.17**
4677_1	15	0.08	0.08	0.01	92.44	0.00	0.12	0.01	1.03	0.01	0.00	0.00	93.77
4677_10	23	0.02	0.00	0.00	0.16	0.02	1.29	0.00	0.01	0.00	0.00	0.03	1.52
4677_11	24	3.61	1.86	15.27	59.59	0.57	0.05	1.50	5.45	1.31	0.27	9.68	99.14
4677_12	25	2.56	1.86	15.21	59.95	0.64	0.06	1.43	5.32	1.30	0.32	9.56	98.21
4677_2	16	1.22	5.01	12.85	47.98	0.84	0.06	0.76	10.20	4.51	0.13	15.12	98.70
4677_3	17	1.08	4.85	12.76	48.03	0.85	0.06	0.75	10.08	4.63	0.21	14.78	98.07
4677_4	18	0.43	3.20	15.34	45.79	0.28	0.33	0.31	0.51	0.44	0.00	9.88	76.50
4677_5	19	1.19	4.88	12.86	48.23	0.82	0.05	0.80	9.25	4.58	0.31	15.05	98.02
4677_6	20	0.02	0.04	0.00	91.88	0.01	0.12	0.03	1.02	0.00	0.00	0.00	93.12

Label	No	NaO_2	MgO	Al_2O_3	Si_2	P	Cl	K_2O	CaO	TiO_2	MnO	FeO	
4677_7	21	0.01	0.05	0.02	92.01	0.00	0.10	0.03	0.97	0.00	0.00	0.00	93.18
4677_9	22	3.76	1.80	15.37	59.09	0.63	0.07	1.40	5.30	1.24	0.20	9.19	98.05
4680_1	5	3.85	1.81	15.50	59.41	0.62	0.05	1.52	5.59	1.37	0.39	9.53	99.65
4680_2	6	2.88	1.78	15.43	59.85	0.59	0.05	1.59	5.48	1.34	0.32	9.61	98.92
4680_3	7	3.99	1.99	15.35	60.00	0.68	0.03	1.34	5.24	1.49	0.20	9.45	99.74
4680_4	8	3.16	1.78	15.62	60.09	0.57	0.05	1.43	5.72	1.31	0.30	9.44	99.46
4680_5	9	2.67	1.76	15.64	60.68	0.54	0.06	1.43	5.56	1.27	0.35	9.51	99.48
4681_1	10	4.88	0.96	15.89	62.14	0.50	0.06	1.56	5.33	0.75	0.27	7.97	100.30
4681_2	11	4.63	0.40	26.60	54.81	0.11	0.01	0.16	12.07	0.24	0.04	1.59	100.65
4681_3	12	4.49	0.38	26.97	55.04	0.12	0.02	0.12	11.30	0.22	0.04	1.41	100.11
4681_4	13	4.68	0.36	27.26	55.19	0.14	0.01	0.14	11.04	0.23	0.03	1.45	100.54
4681_5	14	0.34	0.02	11.46	74.03	0.01	0.05	0.49	4.42	0.01	0.00	0.00	90.83
25-Feb-10													
sthl_7	73	4.70	2.02	17.84	63.46	0.17	0.01	1.33	5.29	0.76	0.10	4.47	
sthl_6	43	4.76	1.96	17.67	63.85	0.17	0.03	1.30	5.25	0.71	0.09	4.46	
sthl_5	41	4.31	2.02	17.56	63.81	0.15	0.04	1.30	5.25	0.68	0.02	4.35	
sthl_4	93	4.64	2.07	17.75	63.87	0.16	0.03	1.33	5.28	0.73	0.05	4.51	
sthl_3	92	4.68	2.03	17.92	63.65	0.20	0.01	1.32	5.23	0.76	0.07	4.27	
sthl_2	2	4.46	2.05	17.85	62.75	0.15	0.05	1.28	5.28	0.71	0.04	4.26	
sthl_1	1	4.65	2.02	18.13	62.77	0.17	0.03	1.35	5.25	0.69	0.10	4.42	
		4.60	**2.03**	**17.82**	**63.45**	**0.17**	**0.03**	**1.32**	**5.26**	**0.72**	**0.07**	**4.39**	
		0.16	**0.03**	**0.18**	**0.49**	**0.02**	**0.01**	**0.02**	**0.02**	**0.03**	**0.03**	**0.10**	
atho_5	42	4.18	0.10	12.22	75.49	0.02	0.05	2.77	1.72	0.28	0.14	3.28	
atho_4	4	3.90	0.11	12.25	75.84	0.00	0.04	2.78	1.66	0.25	0.07	3.60	

Label	No	NaO_2	MgO	Al_2O_3	Si_2	P	Cl	K_2O	CaO	TiO_2	MnO	FeO	
atho_3	95	4.43	0.10	12.12	75.70	0.02	0.05	2.76	1.74	0.29	0.10	3.35	
atho_2	3	4.18	0.10	12.25	76.13	0.01	0.06	2.75	1.70	0.31	0.11	3.53	
atho_1	94	4.14	0.09	12.31	76.06	0.02	0.05	2.73	1.73	0.27	0.02	3.43	
		4.17	**0.10**	**12.23**	**75.85**	**0.01**	**0.05**	**2.76**	**1.71**	**0.28**	**0.09**	**3.43**	
		0.19	**0.01**	**0.07**	**0.26**	**0.01**	**0.01**	**0.02**	**0.03**	**0.02**	**0.04**	**0.13**	
4308_1	32	4.31	1.80	14.77	57.88	0.57	0.05	1.56	5.22	1.20	0.30	9.21	96.87
4308_10	44	4.09	0.11	28.18	52.84	0.02	0.01	0.25	12.26	0.08	0.06	0.82	98.73
4308_11	45	0.22	16.11	2.39	52.17	0.00	0.02	0.00	20.32	0.73	0.18	7.37	99.50
4308_12	46	4.32	1.87	14.80	58.74	0.57	0.04	1.52	5.20	1.23	0.21	9.70	98.19
4308_13	47	5.21	0.09	14.16	66.82	0.03	0.26	4.47	1.06	0.27	0.02	2.82	95.22
4308_14	48	4.29	2.11	15.47	57.94	0.65	0.02	1.34	5.89	1.40	0.33	9.73	99.18
4308_15	49	4.61	1.62	16.27	58.27	0.61	0.03	1.34	6.00	1.32	0.28	8.82	99.18
4308_16	50	4.35	1.85	15.85	58.05	0.68	0.03	1.37	5.86	1.50	0.19	9.71	99.45
4308_17	51	4.21	0.08	29.25	51.90	0.00	0.01	0.16	12.98	0.06	0.09	0.77	99.51
4308_18	52	4.68	1.69	15.21	59.67	0.55	0.06	1.78	4.71	1.25	0.32	8.67	98.60
4308_19	53	4.32	1.77	15.01	59.65	0.55	0.05	1.74	4.78	1.27	0.37	8.72	98.24
4308_2	33	4.16	1.79	15.06	58.95	0.55	0.04	1.53	5.33	1.42	0.35	9.44	98.63
4308_20	54	4.21	1.92	14.86	58.07	0.56	0.06	1.54	5.38	1.28	0.25	9.42	97.55
4308_21	55	3.11	1.73	15.06	59.56	0.57	0.03	1.56	5.23	1.33	0.25	9.08	97.50
4308_22	56	4.45	1.88	15.09	59.09	0.58	0.05	1.54	5.24	1.31	0.29	9.64	99.16
4308_23	57	2.94	4.66	12.57	49.34	0.38	0.02	0.51	8.76	3.38	0.27	14.63	97.48
4308_24	58	3.83	0.21	29.36	51.69	0.01	0.00	0.09	13.26	0.09	0.04	0.57	99.16
4308_25	59	4.56	0.13	27.31	54.21	0.03	0.01	0.23	11.24	0.17	0.11	0.76	98.75
4308_26	60	4.33	1.96	14.86	58.67	0.61	0.03	1.53	5.39	1.32	0.36	9.67	98.73
4308_27	61	2.82	1.92	14.94	59.14	0.56	0.05	1.51	5.35	1.31	0.27	9.94	97.81

Label	No	NaO_2	MgO	Al_2O_3	Si_2	P	Cl	K_2O	CaO	TiO_2	MnO	FeO	
4308_28	62	3.83	1.69	15.34	59.74	0.50	0.05	1.74	4.72	1.31	0.17	8.86	97.95
4308_29	63	4.35	1.76	15.08	59.16	0.57	0.06	1.60	4.83	1.28	0.22	8.88	97.79
4308_3	34	4.00	2.12	14.56	58.40	0.55	0.04	1.52	5.24	1.29	0.21	10.02	97.96
4308_4	35	6.66	0.08	25.26	58.04	0.00	0.01	0.35	8.33	0.10	0.00	0.68	99.51
4308_5	36	0.76	1.91	16.27	60.99	0.03	0.00	1.02	4.07	0.00	0.06	0.03	85.13
4308_6	37	4.38	0.12	28.59	53.13	0.02	0.00	0.14	12.53	0.13	0.07	0.81	99.93
4308_7	38	1.97	9.91	9.82	51.89	0.00	0.03	0.10	16.92	0.74	0.07	8.04	99.49
4308_8	39	4.21	0.02	11.93	71.73	0.13	0.09	2.36	1.58	0.96	0.08	2.48	95.57
4308_9	40	0.25	14.65	2.25	51.45	0.01	0.02	0.00	19.82	0.85	0.20	9.77	99.27
4309_1	64	2.46	0.07	31.68	49.14	0.01	0.00	0.08	15.41	0.05	0.00	0.75	99.64
4309_10	74	2.25	6.62	13.33	49.55	0.17	0.03	0.23	11.18	1.75	0.14	12.60	97.83
4309_11	75	4.94	0.13	28.01	54.12	0.02	0.01	0.24	11.38	0.12	0.06	0.71	99.73
4309_12	76	0.00	2.12	0.06	0.02	0.01	0.02	0.01	0.04	49.31	0.44	45.85	97.87
4309_13	77	4.52	0.07	28.38	53.80	0.03	0.01	0.25	11.85	0.10	0.00	0.95	99.95
4309_14	78	5.44	0.06	26.80	54.24	0.05	0.02	0.36	10.33	0.09	0.01	0.74	98.14
4309_15	79	0.40	14.77	2.73	50.81	0.00	0.01	0.01	18.69	0.99	0.48	10.14	99.02
4309_16	80	4.33	0.13	27.99	52.95	0.02	0.02	0.20	12.25	0.07	0.00	0.75	98.70
4309_17	81	4.96	0.14	27.78	53.69	0.00	0.01	0.21	11.38	0.16	0.00	0.80	99.14
4309_18	82	0.06	2.01	0.08	1.11	0.00	0.02	0.00	0.02	48.08	0.56	45.11	97.06
4309_19	83	0.22	17.23	2.81	52.08	0.03	0.01	0.00	18.57	0.81	0.27	7.67	99.70
4309_2	65	3.07	0.10	31.32	49.95	0.00	0.00	0.10	14.86	0.06	0.05	0.68	100.20
4309_20	84	6.35	0.02	24.99	59.12	0.03	0.01	0.44	7.92	0.14	0.00	0.69	99.71
4309_21	85	3.12	4.82	12.60	47.44	0.59	0.06	0.74	9.53	4.66	0.38	14.76	98.70
4309_22	86	2.76	4.61	11.86	45.37	0.58	0.10	0.73	8.94	4.19	0.17	13.97	93.29
4309_23	87	4.47	0.07	28.10	52.74	0.00	0.01	0.22	12.25	0.14	0.07	0.89	98.96
4309_24	88	3.34	4.79	12.35	46.81	0.51	0.05	0.83	9.23	4.48	0.05	14.67	97.10

Label	No	NaO_2	MgO	Al_2O_3	Si_2	P	Cl	K_2O	CaO	TiO_2	MnO	FeO	
4309_25	89	4.94	0.05	27.76	54.62	0.01	0.00	0.31	10.98	0.09	0.00	0.80	99.56
4309_26	90	3.74	0.11	27.85	50.65	0.04	0.02	0.28	11.89	1.87	0.00	2.30	98.74
4309_27	91	7.65	0.04	24.24	60.55	0.02	0.01	0.63	6.36	0.06	0.03	0.54	100.13
4309_3	66	6.43	0.07	24.69	59.25	0.02	0.01	0.41	8.05	0.09	0.00	0.74	99.76
4309_4	67	7.21	0.05	24.53	60.33	0.02	0.01	0.60	6.92	0.07	0.02	0.46	100.21
4309_5	68	5.13	0.07	27.75	53.86	0.01	0.01	0.30	11.00	0.08	0.00	0.79	98.99
4309_6	69	4.43	0.03	28.74	53.24	0.03	0.01	0.25	11.87	0.10	0.00	0.70	99.40
4309_7	70	3.91	0.19	28.78	51.91	0.02	0.01	0.09	13.21	0.12	0.00	0.65	98.89
4309_8	71	2.84	5.66	12.82	48.94	0.33	0.02	0.48	10.14	2.87	0.18	14.01	98.29
4309_9	72	2.67	5.42	13.09	49.54	0.29	0.02	0.43	10.02	2.93	0.24	13.33	98.00
4310_1	5	2.65	5.45	12.81	49.35	0.34	0.02	0.42	9.84	3.06	0.20	14.20	98.34
4310_10	14	5.54	0.08	14.40	67.75	0.00	0.27	4.65	1.16	0.20	0.05	2.79	96.88
4310_11	15	0.35	12.73	3.31	48.95	0.03	0.00	0.00	18.42	1.92	0.29	13.42	99.43
4310_12	16	0.49	14.45	3.13	50.72	0.01	0.03	0.00	18.80	0.81	0.15	9.90	98.50
4310_13	17	4.45	0.06	27.56	50.59	0.03	0.05	0.22	11.56	0.15	0.04	0.92	95.63
4310_14	18	3.63	0.20	30.11	52.66	0.02	0.01	0.11	13.52	0.05	0.02	0.46	100.79
4310_15	19	0.37	13.30	2.24	50.65	0.01	0.00	0.00	18.31	1.32	0.19	13.12	99.51
4310_16	20	0.23	15.79	2.24	51.15	0.02	0.01	0.01	18.83	0.89	0.19	9.79	99.15
4310_17	21	4.50	0.07	28.96	52.88	0.03	0.01	0.20	11.97	0.09	0.10	0.76	99.58
4310_18	22	2.19	7.23	13.43	49.50	0.17	0.03	0.20	11.94	1.71	0.20	11.57	98.17
4310_19	23	2.10	7.07	13.71	49.25	0.19	0.00	0.19	11.93	1.77	0.13	11.71	98.04
4310_2	6	2.66	5.41	12.80	49.38	0.33	0.02	0.44	9.79	3.08	0.28	14.30	98.51
4310_20	24	4.21	0.29	27.83	53.76	0.03	0.00	0.17	11.79	0.23	0.05	1.32	99.68
4310_21	25	3.54	0.08	30.18	51.23	0.01	0.00	0.21	13.51	0.04	0.00	0.93	99.74
4310_22	26	3.35	0.06	26.63	44.91	0.03	0.08	0.19	12.55	0.07	0.00	0.77	88.64
4310_23	27	2.75	5.63	16.53	50.70	0.03	0.04	0.10	13.75	0.90	0.19	7.46	98.07

Label	No	NaO_2	MgO	Al_2O_3	Si_2	P	Cl	K_2O	CaO	TiO_2	MnO	FeO	
4310_24	28	4.82	0.20	27.68	54.53	0.04	0.02	0.18	11.45	0.15	0.00	1.09	100.17
4310_25	29	5.90	0.06	26.19	57.37	0.03	0.00	0.40	9.04	0.12	0.00	0.66	99.78
4310_26	30	5.12	0.10	26.63	54.33	0.04	0.05	0.28	9.70	0.13	0.00	0.88	97.26
4310_3	7	2.43	5.44	12.80	49.44	0.34	0.02	0.44	9.54	2.96	0.14	13.95	97.51
4310_4	8	2.14	7.26	13.93	49.72	0.17	0.01	0.17	11.97	1.68	0.17	11.17	98.39
4310_5	9	8.51	0.00	22.37	64.29	0.00	0.01	0.58	4.25	0.04	0.00	0.29	100.34
4310_6	10	3.28	0.21	30.26	51.51	0.01	0.01	0.10	13.75	0.05	0.01	0.56	99.77
4310_7	11	2.18	7.19	13.69	49.36	0.17	0.01	0.15	11.90	1.75	0.26	11.86	98.53
4310_8	12	3.68	0.22	29.58	51.66	0.03	0.01	0.09	13.53	0.05	0.00	0.54	99.40
4310_9	13	4.26	0.10	28.72	53.51	0.00	0.00	0.17	12.15	0.12	0.00	0.84	99.88
4311_1	31	0.00	0.00	0.05	0.03	0.02	0.11	0.00	0.01	0.00	0.00	0.06	0.28
28-Feb-11													
atho_1	31	4.20	0.09	12.45	75.60	0.00	0.03	2.67	1.69	0.23	0.07	3.32	
atho_2	53	4.14	0.08	12.14	76.06	0.02	0.02	2.67	1.66	0.28	0.14	3.32	
atho_3	8	4.24	0.09	12.34	75.44	0.01	0.02	2.76	1.63	0.25	0.12	3.30	
atho_4	32	4.30	0.08	12.10	75.74	0.04	0.02	2.73	1.63	0.23	0.13	3.23	
atho_5	9	3.94	0.10	12.40	75.38	0.03	0.03	2.64	1.64	0.30	0.13	3.30	
		4.17	**0.09**	**12.29**	**75.64**	**0.02**	**0.02**	**2.69**	**1.65**	**0.26**	**0.12**	**3.29**	
		0.14	**0.01**	**0.16**	**0.27**	**0.01**	**0.01**	**0.05**	**0.02**	**0.03**	**0.03**	**0.03**	
g132_1	1	0.86	23.10	11.76	44.16	0.04	0.01	0.03	8.46	0.27	0.16	9.65	
g132_1	10	0.78	22.12	10.98	46.00	0.06	0.00	0.04	8.27	0.30	0.22	10.00	
g132_2	2	0.86	22.96	11.85	44.15	0.05	0.00	0.01	8.28	0.31	0.19	10.15	
g132_2	11	0.74	22.22	10.99	45.89	0.06	0.00	0.03	8.51	0.32	0.13	10.17	
g132_3	12	0.75	22.22	10.82	46.07	0.03	0.01	0.05	8.44	0.29	0.13	10.11	

Label	No	NaO_2	MgO	Al_2O_3	Si_2	P	Cl	K_2O	CaO	TiO_2	MnO	FeO	
g132_4	13	0.90	22.14	11.14	45.96	0.03	0.00	0.03	8.47	0.30	0.19	10.23	
g132_5	14	0.71	21.98	11.00	45.92	0.01	0.00	0.03	8.34	0.31	0.19	10.05	
g132_6	15	0.81	21.99	10.97	45.64	0.04	0.00	0.03	8.44	0.32	0.19	10.39	
g132_7	54	0.83	22.43	10.78	46.02	0.03	0.00	0.04	8.33	0.29	0.14	10.09	
g132_8	55	0.72	22.16	10.93	45.72	0.01	0.02	0.03	8.46	0.32	0.11	10.26	
		0.80	**22.33**	**11.12**	**45.55**	**0.04**	**0.00**	**0.03**	**8.40**	**0.30**	**0.17**	**10.11**	
		0.07	**0.39**	**0.37**	**0.75**	**0.02**	**0.01**	**0.01**	**0.09**	**0.02**	**0.04**	**0.20**	
sthl_1	47	4.80	2.00	17.30	63.38	0.18	0.01	1.33	5.35	0.76	0.07	4.43	
sthl_2	42	4.72	1.92	17.27	64.02	0.19	0.00	1.25	5.15	0.78	0.07	4.37	
sthl_3	3	4.51	1.91	17.72	63.88	0.18	0.01	1.27	5.40	0.70	0.06	4.48	
sthl_4	4	4.53	1.91	17.90	63.55	0.17	0.01	1.28	5.25	0.67	0.05	4.29	
sthl_5	5	4.77	1.97	17.85	63.60	0.17	0.03	1.30	5.32	0.69	0.03	4.42	
sthl_6	6	4.55	1.90	17.93	63.70	0.19	0.01	1.32	5.14	0.69	0.12	4.18	
sthl_7	7	4.40	1.84	17.74	63.47	0.17	0.03	1.29	5.27	0.72	0.04	4.58	
		4.61	**1.92**	**17.67**	**63.66**	**0.18**	**0.01**	**1.29**	**5.27**	**0.72**	**0.06**	**4.39**	
		0.15	**0.05**	**0.28**	**0.23**	**0.01**	**0.01**	**0.03**	**0.10**	**0.04**	**0.03**	**0.13**	
4682_1	43	4.46	0.65	16.03	67.04	0.02	0.02	2.92	0.52	0.02	0.02	0.00	91.69
4682_2	44	5.72	0.08	14.42	68.08	0.03	0.29	4.72	1.19	0.27	0.12	2.99	97.92
4682_3	45	5.84	0.47	15.82	64.97	0.13	0.22	3.78	2.26	0.54	0.18	4.96	99.17
4682_4	46	3.66	0.55	15.03	69.63	0.01	0.02	3.20	0.39	0.00	0.03	0.04	92.55
4685_1	48	4.65	0.52	15.61	63.25	0.11	0.20	3.79	2.42	0.54	0.24	5.12	96.48
4685_2	49	4.06	0.08	14.06	70.00	0.03	0.31	5.10	0.84	0.23	0.10	2.81	97.62
4685_3	50	5.98	0.07	17.15	62.74	0.00	0.03	1.84	0.88	0.00	0.00	0.06	88.74
4685_4	51	4.11	1.19	16.09	65.30	0.03	0.01	1.00	0.68	0.02	0.01	0.05	88.49

Label	No	NaO_2	MgO	Al_2O_3	Si_2	P	Cl	K_2O	CaO	TiO_2	MnO	FeO	
4685_5	52	3.95	0.08	27.78	50.86	0.03	0.01	0.15	13.15	0.05	0.00	0.85	96.92
5161_1	33	5.20	0.09	14.90	69.89	0.04	0.29	4.67	1.03	0.21	0.11	2.94	99.36
5161_2	34	5.44	0.09	15.14	70.09	0.02	0.31	4.70	0.98	0.27	0.07	2.94	100.06
5161_3	35	5.42	0.09	14.97	70.04	0.01	0.29	4.73	1.05	0.20	0.11	3.04	99.97
5161_4	36	5.24	0.07	14.78	70.03	0.01	0.31	4.66	1.07	0.22	0.19	3.03	99.61
5161_5	37	5.53	0.10	14.79	70.13	0.02	0.27	4.73	1.05	0.28	0.17	3.00	100.08
5161_6	38	5.38	0.06	14.83	69.89	0.01	0.30	4.55	1.06	0.22	0.20	2.82	99.32
5165_1	39	3.99	1.79	14.86	59.11	0.54	0.05	1.53	5.33	1.36	0.27	9.77	98.59
5165_2	40	3.17	1.81	14.92	59.91	0.60	0.06	1.55	5.30	1.25	0.26	9.05	97.87
5165_3	41	4.42	1.40	14.70	61.78	0.52	0.07	1.69	4.72	1.10	0.18	7.84	98.44
5165_1	16	3.96	1.76	15.58	59.99	0.58	0.07	1.52	5.26	1.29	0.29	9.29	99.59
5165_10	25	4.35	1.80	15.29	60.12	0.54	0.04	1.53	5.29	1.35	0.26	9.59	100.15
5165_11	26	4.07	1.80	15.52	60.35	0.58	0.06	1.47	5.35	1.31	0.28	9.12	99.92
5165_12	27	4.00	1.83	15.35	60.11	0.58	0.05	1.53	5.34	1.31	0.25	9.79	100.14
5165_13	28	3.97	1.84	15.28	59.98	0.59	0.05	1.54	5.21	1.32	0.27	9.17	99.20
5165_14	29	4.15	1.91	15.40	60.13	0.62	0.04	1.49	5.22	1.30	0.29	9.63	100.18
5165_15	30	3.27	1.89	15.79	60.11	0.57	0.06	1.42	5.46	1.29	0.26	9.09	99.21
5165_2	17	4.01	1.59	15.63	60.49	0.53	0.05	1.59	5.17	1.27	0.34	9.14	99.80
5165_3	18	1.55	0.07	24.99	57.74	0.03	0.00	1.53	4.27	0.03	0.02	0.27	90.50
5165_4	19	4.69	1.69	15.69	60.52	0.61	0.04	1.53	5.32	1.33	0.21	8.80	100.44
5165_5	20	3.76	1.86	15.45	59.98	0.59	0.05	1.42	5.27	1.36	0.26	9.48	99.48
5165_6	21	4.13	1.81	15.60	60.25	0.56	0.03	1.62	5.27	1.34	0.28	9.45	100.35
5165_7	22	4.42	1.74	15.24	59.57	0.60	0.04	1.53	5.25	1.37	0.25	9.35	99.35
5165_8	23	4.00	1.80	15.48	60.24	0.63	0.05	1.53	5.28	1.45	0.21	9.33	99.99
5165_9	24	4.07	1.67	15.60	60.62	0.54	0.04	1.62	5.26	1.30	0.27	8.95	99.92

B | *Filtered WDS-EPMA data*

WDS-EPMA data from samples in this dissertation have been filtered, as discussed in Section 5.4.1. Although summary tables are presented in Section 6.3, below the data is given in full. In Appendix A, the full unfiltered data set is presented with secondary standards.

Table B.1: Filtered glass chemistry data from WDS-EPMA analysis, arranged by OxT-number.

Label	SiO_2	TiO_2	Al_2O_3	FeO	MnO	MgO	CaO	Na_2O	K_2O	Total
4308	57.88	1.20	14.77	9.21	0.30	1.80	5.22	4.31	1.56	96.25
4308	57.94	1.40	15.47	9.73	0.33	2.11	5.89	4.29	1.34	98.51
4308	58.05	1.50	15.85	9.71	0.19	1.85	5.86	4.35	1.37	98.74
4308	58.07	1.28	14.86	9.42	0.25	1.92	5.38	4.21	1.54	96.92
4308	58.27	1.32	16.27	8.82	0.28	1.62	6.00	4.61	1.34	98.53
4308	58.40	1.29	14.56	10.02	0.21	2.12	5.24	4.00	1.52	97.37
4308	58.67	1.32	14.86	9.67	0.36	1.96	5.39	4.33	1.53	98.08
4308	58.74	1.23	14.80	9.70	0.21	1.87	5.20	4.32	1.52	97.59
4308	58.95	1.42	15.06	9.44	0.35	1.79	5.33	4.16	1.53	98.04
4308	59.09	1.31	15.09	9.64	0.29	1.88	5.24	4.45	1.54	98.52
4308	59.14	1.31	14.94	9.94	0.27	1.92	5.35	2.82	1.51	97.19
4308	59.16	1.28	15.08	8.88	0.22	1.76	4.83	4.35	1.60	97.16
4308	59.56	1.33	15.06	9.08	0.25	1.73	5.23	3.11	1.56	96.90
4308	59.65	1.27	15.01	8.72	0.37	1.77	4.78	4.32	1.74	97.63
4308	59.67	1.25	15.21	8.67	0.32	1.69	4.71	4.68	1.78	98.00
4308	59.74	1.31	15.34	8.86	0.17	1.69	4.72	3.83	1.74	97.40
4308	71.73	0.96	11.93	2.48	0.08	0.02	1.58	4.21	2.36	95.35
4309	46.81	4.48	12.35	14.67	0.05	4.79	9.23	3.34	0.83	96.54
4309	47.44	4.66	12.60	14.76	0.38	4.82	9.53	3.12	0.74	98.06
4309	48.94	2.87	12.82	14.01	0.18	5.66	10.14	2.84	0.48	97.94
4309	49.54	2.93	13.09	13.33	0.24	5.42	10.02	2.67	0.43	97.69
4310	49.25	1.77	13.71	11.71	0.13	7.07	11.93	2.10	0.19	97.84
4310	49.35	3.06	12.81	14.20	0.20	5.45	9.84	2.65	0.42	97.98
4310	49.36	1.75	13.69	11.86	0.26	7.19	11.90	2.18	0.15	98.35
4310	49.38	3.08	12.80	14.30	0.28	5.41	9.79	2.66	0.44	98.15

Label	SiO_2	TiO_2	Al_2O_3	FeO	MnO	MgO	CaO	Na_2O	K_2O	Total
4310	49.44	2.96	12.80	13.95	0.14	5.44	9.54	2.43	0.44	97.15
4310	49.50	1.71	13.43	11.57	0.20	7.23	11.94	2.19	0.20	97.97
4310	49.72	1.68	13.93	11.17	0.17	7.26	11.97	2.14	0.17	98.21
4310	50.70	0.90	16.53	7.46	0.19	5.63	13.75	2.75	0.10	98.01
4310	64.44	0.58	15.99	5.08	0.26	0.51	2.35	5.73	3.81	98.75
4310	68.91	0.23	14.81	2.85	0.13	0.07	1.03	5.09	4.82	97.95
4310	68.95	0.18	14.70	2.93	0.17	0.08	0.99	5.30	4.62	97.92
4310	69.07	0.17	14.76	2.74	0.15	0.09	1.01	5.41	4.62	98.02
4310	69.90	0.25	15.29	2.88	0.11	0.08	1.03	5.16	4.64	99.33
4310	69.97	0.22	15.16	2.90	0.14	0.09	1.03	5.21	4.72	99.45
4672	53.77	0.15	28.31	0.82	0.00	0.08	11.25	5.07	0.24	99.68
4672	55.48	0.12	27.22	0.68	0.00	0.03	10.32	5.34	0.41	99.59
4672	58.55	1.37	15.06	9.32	0.30	1.89	5.48	3.32	1.47	96.75
4672	59.34	1.27	15.04	9.43	0.27	1.84	5.48	2.97	1.59	97.25
4672	59.61	1.31	15.04	9.34	0.19	1.83	5.24	3.49	1.44	97.49
4672	60.21	1.13	16.12	8.07	0.19	1.43	5.46	4.25	1.34	98.21
4672	60.38	1.24	14.42	9.41	0.20	1.86	5.28	3.80	1.48	98.05
4672	59.39	1.38	15.44	9.16	0.30	1.80	5.20	3.47	1.42	97.55
4672	59.47	1.31	15.36	9.08	0.28	1.83	5.45	3.90	1.36	98.03
4672	59.47	1.30	15.35	9.33	0.31	1.84	5.29	3.46	1.44	97.79
4672	59.58	1.34	15.49	9.70	0.25	1.88	5.46	3.19	1.45	98.33
4672	59.69	1.41	15.43	9.17	0.25	1.89	5.36	3.16	1.56	97.92
4672	60.16	1.30	15.70	9.70	0.27	1.84	5.40	2.76	1.40	98.52
4672	60.19	1.31	15.74	9.34	0.20	1.78	5.43	3.54	1.38	98.91
4672	60.43	1.26	15.49	8.92	0.21	1.73	5.10	3.50	1.43	98.07
4672	60.97	1.30	14.98	9.42	0.28	1.65	5.04	3.80	1.58	99.02

Label	SiO_2	TiO_2	Al_2O_3	FeO	MnO	MgO	CaO	Na_2O	K_2O	Total
4672	61.18	1.27	15.54	8.97	0.31	1.43	5.15	4.03	1.42	99.29
4674	57.17	1.43	14.69	9.93	0.21	1.90	5.15	3.64	1.43	95.55
4674	59.05	1.26	15.21	9.81	0.20	1.87	5.12	3.53	1.37	97.41
4674	59.73	1.39	15.49	10.12	0.40	1.85	5.36	3.58	1.34	99.25
4674	62.15	0.58	15.46	5.09	0.24	0.55	2.37	5.52	3.57	95.53
4675	50.06	1.87	13.59	13.36	0.22	6.43	10.60	2.12	0.23	98.48
4675	50.11	1.92	13.43	13.17	0.18	6.24	10.74	2.15	0.27	98.20
4675	57.84	1.28	14.97	9.68	0.37	1.89	5.20	3.62	1.46	96.30
4675	58.20	1.34	14.65	9.54	0.36	1.87	5.22	3.53	1.55	96.25
4675	58.43	1.17	14.69	8.32	0.23	1.54	4.65	3.10	3.93	96.06
4675	58.78	1.20	15.55	9.92	0.23	1.82	5.44	3.72	1.45	98.10
4675	58.95	1.25	15.25	9.41	0.25	1.84	5.08	3.83	1.44	97.31
4675	59.05	1.32	15.40	10.02	0.35	1.81	5.43	3.88	1.48	98.74
4675	59.49	1.27	15.38	9.97	0.30	1.89	5.10	4.04	1.43	98.86
4675	59.58	1.29	15.64	10.03	0.22	1.82	5.17	3.72	1.41	98.88
4675	69.64	0.21	15.26	3.00	0.20	0.04	1.13	5.36	4.25	99.10
4675	70.11	0.23	15.41	2.78	0.18	0.07	1.01	5.59	4.33	99.71
4675	71.63	0.25	14.90	2.16	0.04	0.22	0.74	4.84	4.34	99.12
4676	58.10	1.41	15.03	9.84	0.28	1.97	5.85	4.10	1.33	97.90
4676	59.14	1.36	15.23	9.18	0.19	1.77	5.52	3.74	1.55	97.69
4676	59.77	1.27	13.85	9.52	0.28	1.09	4.61	4.39	1.78	96.58
4676	61.40	0.81	15.39	7.40	0.30	1.20	4.69	4.99	1.51	97.68
4676	61.77	1.34	13.58	10.27	0.26	1.12	4.40	3.10	1.86	97.71
4676	63.89	0.57	15.79	5.05	0.17	0.51	2.41	5.83	3.13	97.35
4676	68.52	0.25	14.78	2.82	0.19	0.06	0.99	5.56	4.56	97.73
4676	69.78	0.32	13.59	3.70	0.10	0.23	2.38	5.14	2.29	97.54

Label	SiO_2	TiO_2	Al_2O_3	FeO	MnO	MgO	CaO	Na_2O	K_2O	Total
4676	56.42	1.43	15.03	9.56	0.30	2.06	5.48	4.18	1.47	95.94
4677	47.98	4.51	12.85	15.12	0.13	5.01	10.20	1.22	0.76	98.70
4677	48.03	4.63	12.76	14.78	0.21	4.85	10.08	1.08	0.75	98.07
4677	48.23	4.58	12.86	15.05	0.31	4.88	9.25	1.19	0.80	98.02
4677	48.35	4.55	12.97	14.81	0.23	4.97	9.45	1.09	0.80	97.24
4677	48.93	1.77	13.60	12.39	0.13	6.47	11.08	1.74	0.25	96.36
4677	50.57	3.11	13.15	14.08	0.15	5.19	9.44	1.22	0.47	97.37
4677	50.81	2.96	13.11	14.28	0.21	5.26	9.53	1.07	0.48	97.71
4677	50.91	3.11	13.11	14.76	0.28	5.15	9.32	1.00	0.48	98.11
4677	58.51	1.34	15.17	9.26	0.25	1.89	5.31	3.54	1.35	96.61
4677	59.09	1.24	15.37	9.19	0.20	1.80	5.30	3.76	1.40	98.05
4677	59.21	1.24	15.13	9.55	0.27	1.80	5.39	3.77	1.45	97.81
4677	59.38	1.29	15.55	9.64	0.30	1.87	5.25	3.90	1.38	98.56
4677	59.55	1.35	15.45	9.70	0.27	1.94	5.23	3.40	1.37	98.26
4677	59.59	1.31	15.27	9.68	0.27	1.86	5.45	3.61	1.50	99.14
4677	59.72	1.26	15.63	9.18	0.24	1.75	5.49	3.85	1.50	98.62
4677	59.95	1.30	15.21	9.56	0.32	1.86	5.32	2.56	1.43	98.21
4679	48.17	4.62	12.92	14.98	0.18	5.01	9.66	0.39	0.77	96.68
4679	49.76	2.93	13.38	14.48	0.24	5.46	9.77	1.80	0.50	98.32
4679	50.53	1.73	13.95	12.59	0.29	6.77	11.46	1.45	0.22	99.00
4679	58.99	1.26	15.36	9.65	0.29	1.84	5.33	4.11	1.55	98.38
4679	59.32	1.21	16.51	8.38	0.22	1.69	5.62	4.27	1.27	98.49
4679	59.44	1.13	15.65	8.89	0.24	1.50	5.18	3.47	1.32	96.82
4679	59.44	1.26	15.54	9.57	0.17	1.83	5.26	3.44	1.42	97.94
4679	59.47	1.26	15.24	9.66	0.21	1.83	5.26	2.83	1.35	97.11
4679	59.60	1.31	15.40	9.53	0.23	1.82	5.25	3.35	1.54	98.03

Label	SiO_2	TiO_2	Al_2O_3	FeO	MnO	MgO	CaO	Na_2O	K_2O	Total
4679	59.60	1.34	15.36	9.50	0.26	1.85	5.36	3.47	1.39	98.13
4679	59.68	1.37	16.42	8.97	0.18	1.73	5.78	4.14	1.02	99.29
4679	59.69	1.39	15.45	9.42	0.27	1.85	5.40	4.13	1.51	99.11
4679	59.72	1.34	15.48	9.61	0.24	1.77	5.14	3.70	1.38	98.37
4679	59.77	1.28	15.67	9.49	0.22	1.78	5.54	3.12	1.47	98.34
4679	59.92	1.42	15.60	9.99	0.28	1.78	5.34	3.33	1.53	99.20
4679	59.92	1.38	15.68	10.02	0.20	1.83	5.64	4.09	1.06	99.81
4679	59.93	1.28	14.72	10.11	0.36	2.09	5.24	4.43	1.38	99.54
4679	59.98	1.27	15.48	9.40	0.25	1.77	5.30	3.73	1.56	98.75
4679	60.11	1.41	15.64	9.37	0.24	1.76	5.39	2.85	1.54	98.30
4679	60.12	1.12	16.49	8.51	0.26	1.45	5.46	3.67	1.36	98.43
4679	60.12	1.37	15.17	9.59	0.19	1.67	5.19	3.22	1.44	97.96
4679	60.13	1.29	15.84	9.64	0.28	1.78	5.27	2.94	1.47	98.63
4679	60.13	1.36	15.71	9.26	0.20	1.74	5.34	3.95	1.50	99.18
4679	60.15	1.27	15.81	9.40	0.26	1.78	5.25	3.63	1.52	99.06
4679	61.09	1.06	14.24	10.07	0.28	1.60	4.61	4.45	1.63	99.01
4679	65.05	0.57	16.25	5.18	0.20	0.47	2.36	5.39	3.76	99.23
4679	65.41	0.54	16.03	5.33	0.22	0.48	2.22	2.70	3.86	96.79
4679	71.60	0.23	14.73	2.28	0.01	0.26	0.82	5.25	4.40	99.59
4679	74.64	0.32	14.44	3.82	0.13	0.23	1.24	2.78	1.60	99.20
4680	57.79	1.13	15.01	9.32	0.22	1.62	5.04	4.14	1.35	95.63
4680	58.48	1.29	15.03	9.57	0.26	1.77	5.06	3.45	1.29	96.20
4680	59.00	1.31	15.19	9.88	0.22	1.82	5.35	3.90	1.42	98.09
4680	59.14	1.38	15.36	9.79	0.18	1.88	5.50	4.19	1.40	98.82
4680	59.41	1.37	15.50	9.53	0.39	1.81	5.59	3.85	1.52	99.65
4680	59.43	1.29	15.39	9.15	0.26	1.85	5.22	4.19	1.49	98.26

Label	SiO_2	TiO_2	Al_2O_3	FeO	MnO	MgO	CaO	Na_2O	K_2O	Total
4680	59.48	1.30	15.41	9.75	0.39	1.77	5.28	2.96	1.41	97.75
4680	59.54	1.25	15.28	9.44	0.23	1.75	5.29	2.34	1.34	96.46
4680	59.57	1.23	15.60	9.69	0.27	1.94	5.22	3.99	1.27	98.77
4680	59.85	1.34	15.43	9.61	0.32	1.78	5.48	2.88	1.59	98.92
4680	59.89	1.29	15.47	9.13	0.16	1.81	5.26	2.56	1.50	97.07
4680	59.94	1.21	15.53	9.31	0.29	1.84	5.23	2.34	1.45	97.14
4680	60.00	1.49	15.35	9.45	0.20	1.99	5.24	3.99	1.34	99.74
4680	60.08	1.24	15.39	9.50	0.26	1.71	5.09	4.04	1.39	98.71
4680	60.09	1.31	15.62	9.44	0.30	1.78	5.72	3.16	1.43	99.46
4680	60.50	1.24	15.51	9.57	0.29	1.76	5.52	3.00	1.47	98.86
4680	60.68	1.27	15.64	9.51	0.35	1.76	5.56	2.67	1.43	99.48
4681	49.53	1.90	13.85	12.45	0.27	6.63	11.01	1.77	0.24	97.65
4681	49.62	1.90	13.74	12.45	0.27	6.58	11.06	1.78	0.27	97.68
4681	58.31	1.33	15.18	8.93	0.20	1.83	5.04	3.92	1.21	95.95
4681	58.36	1.22	15.62	8.92	0.24	1.88	5.45	3.86	1.42	96.97
4681	59.00	1.26	15.23	9.38	0.15	1.80	5.11	3.35	1.29	96.59
4681	60.95	0.58	18.21	5.52	0.16	0.51	5.52	5.31	1.27	98.03
4681	64.02	0.60	15.97	5.08	0.21	0.50	2.46	5.86	3.58	98.29
4681	64.18	0.57	16.11	5.02	0.27	0.52	2.35	5.42	3.49	97.92
4681	65.24	1.17	14.00	5.35	0.09	1.05	2.82	4.21	2.74	96.66
4681	65.31	1.23	13.91	5.30	0.21	1.05	2.80	5.34	2.68	97.82
4681	65.52	1.30	13.95	5.90	0.24	1.17	2.96	4.65	2.56	98.24
4681	66.29	1.18	14.22	5.54	0.16	1.06	2.75	4.94	2.82	98.96
4681	67.93	0.32	14.65	2.93	0.15	0.08	1.00	5.62	4.20	96.87
4681	68.36	0.25	14.84	2.64	0.23	0.07	1.02	5.56	4.56	97.53
4681	68.75	0.20	14.92	2.87	0.12	0.06	1.04	5.45	4.50	97.92

Label	SiO_2	TiO_2	Al_2O_3	FeO	MnO	MgO	CaO	Na_2O	K_2O	Total
4681	69.56	0.25	14.98	3.32	0.14	0.09	1.07	2.96	4.70	97.07
4682	64.95	0.49	15.99	5.12	0.11	0.41	2.23	4.14	3.76	97.19
4682	65.11	0.58	14.62	3.71	0.16	0.21	1.25	5.44	4.25	95.33
4682	65.27	0.52	16.40	5.18	0.20	0.45	2.26	5.36	3.78	99.41
4682	66.77	0.23	14.54	3.01	0.14	0.07	1.09	5.23	4.51	95.59
4682	68.22	0.31	14.87	2.79	0.02	0.10	0.96	5.28	4.64	97.20
4682	68.70	0.20	14.93	3.05	0.14	0.10	1.08	5.32	4.53	98.05
4682	69.00	0.19	14.99	3.12	0.08	0.09	1.13	4.14	4.68	97.42
4682	69.42	0.22	15.18	3.24	0.20	0.09	1.09	5.18	4.68	99.30
4682	69.45	0.24	15.08	3.06	0.08	0.09	1.08	3.87	4.70	97.65
4682	68.08	0.27	14.42	2.99	0.12	0.08	1.19	5.72	4.72	97.60
4682	64.97	0.54	15.82	4.96	0.18	0.47	2.26	5.84	3.78	98.82
4685	68.26	0.24	14.96	3.19	0.15	0.07	1.10	5.44	4.57	97.99
4685	69.10	0.21	14.68	2.78	0.08	0.08	1.02	5.28	4.72	97.96
4685	69.65	0.26	15.19	2.87	0.15	0.10	1.06	5.73	4.55	99.55
4685	69.68	0.25	13.95	2.96	0.18	0.09	0.86	5.33	4.90	98.20
4685	63.25	0.54	15.61	5.12	0.24	0.52	2.42	4.65	3.79	96.16
4685	70.00	0.23	14.06	2.81	0.10	0.08	0.84	4.06	5.10	97.29
4765	72.89	0.09	12.62	1.95	0.03	0.04	1.32	1.94	7.36	98.24
4765	74.89	0.06	13.07	2.15	0.06	0.01	1.31	1.32	6.69	99.57
4765	59.61	1.18	15.09	9.20	0.21	1.62	4.55	3.05	3.78	98.30
4765	59.84	1.16	15.01	9.51	0.19	1.68	4.90	3.38	3.00	98.67
4765	60.10	1.16	15.55	8.38	0.14	1.61	5.11	3.59	2.71	98.34
4765	60.16	1.11	15.02	8.76	0.27	1.45	4.87	2.94	4.14	98.72
4766	59.31	1.12	14.93	8.66	0.30	1.48	4.80	3.40	3.15	97.15
4766	59.97	1.08	15.50	9.04	0.23	1.62	4.88	4.33	1.81	98.48

Label	SiO_2	TiO_2	Al_2O_3	FeO	MnO	MgO	CaO	Na_2O	K_2O	Total
4766	60.04	1.11	15.21	8.47	0.25	1.55	4.83	3.66	2.91	98.03
4766	60.55	1.13	15.23	8.39	0.17	1.49	4.93	3.71	2.11	97.70
4766	61.56	0.99	15.30	7.86	0.14	1.35	4.43	3.76	3.01	98.39
4766	62.02	0.99	15.32	7.63	0.26	1.31	4.52	4.13	2.17	98.36
4767	60.14	1.04	15.06	8.57	0.20	1.35	4.58	4.03	2.02	96.99
5163	58.28	1.32	14.41	10.70	0.26	2.93	5.91	3.98	1.39	99.18
5163	58.56	1.41	15.46	9.90	0.22	1.71	5.56	4.45	1.43	98.69
5163	58.60	1.28	15.36	8.54	0.27	1.56	5.11	4.63	1.54	96.89
5163	58.61	1.32	15.10	9.46	0.23	1.83	5.39	4.28	1.48	97.70
5163	58.64	1.35	15.06	9.44	0.26	1.82	5.47	4.32	1.52	97.89
5163	58.69	1.33	15.53	9.27	0.28	1.76	5.62	4.60	1.43	98.50
5163	58.75	1.42	15.17	9.64	0.33	1.94	5.39	4.47	1.50	98.61
5163	58.75	1.44	15.21	9.47	0.23	1.87	5.50	4.44	1.47	98.37
5163	58.77	1.35	15.32	9.50	0.23	1.82	5.32	4.37	1.53	98.21
5163	58.80	1.24	15.40	9.27	0.24	1.94	5.54	4.27	1.47	98.17
5163	58.81	1.27	15.31	9.69	0.25	1.80	5.35	4.45	1.56	98.48
5163	58.82	1.29	15.06	9.62	0.27	1.86	5.27	4.43	1.50	98.12
5163	58.84	1.39	15.18	9.48	0.21	1.89	5.32	4.44	1.50	98.26
5163	58.87	1.39	15.13	9.55	0.23	1.90	5.24	3.88	1.48	97.68
5163	58.96	1.40	15.02	10.00	0.36	1.90	5.38	4.18	1.60	98.80
5163	58.98	1.36	15.03	9.10	0.26	1.75	5.27	4.27	1.51	97.52
5163	58.98	1.40	15.14	9.39	0.20	1.82	5.36	4.34	1.57	98.19
5163	59.01	1.34	15.07	9.55	0.31	1.83	5.43	4.45	1.50	98.48
5163	59.01	1.35	15.30	9.47	0.20	1.91	5.41	4.41	1.51	98.57
5163	59.01	1.38	15.11	9.27	0.26	1.78	5.40	4.65	1.53	98.39
5163	59.22	1.39	15.13	9.78	0.33	1.82	5.37	4.36	1.52	98.92

Label	SiO_2	TiO_2	Al_2O_3	FeO	MnO	MgO	CaO	Na_2O	K_2O	Total
5163	59.22	1.32	15.10	9.46	0.29	1.93	5.44	4.23	1.48	98.46
5163	59.23	1.29	15.06	9.43	0.28	1.85	5.36	4.18	1.59	98.27
5163	59.25	1.34	15.25	9.72	0.30	1.86	5.34	4.35	1.52	98.92
5163	59.25	1.37	14.76	9.22	0.25	1.92	5.21	4.19	1.65	97.82
5163	59.29	1.28	15.17	9.77	0.21	2.11	5.66	4.26	1.40	99.15
5163	59.33	1.37	15.17	10.09	0.24	1.81	5.07	4.08	1.65	98.81
5163	59.35	1.32	15.21	9.64	0.30	1.80	5.37	4.33	1.61	98.92
5163	59.50	1.26	15.39	9.46	0.21	1.77	5.43	4.17	1.46	98.64
5163	59.55	1.41	15.20	9.42	0.31	1.82	5.29	4.52	1.52	99.04
5163	59.57	1.35	15.08	9.47	0.25	1.80	5.38	4.52	1.55	98.98
5163	59.64	1.17	15.29	8.98	0.19	1.65	5.35	4.18	1.56	98.01
5163	59.82	1.18	16.31	7.93	0.17	2.17	6.07	5.17	0.96	99.78
5163	59.85	1.14	15.32	9.27	0.28	1.67	5.37	4.58	1.60	99.09
5163	59.87	1.24	15.76	9.48	0.15	1.72	5.35	4.56	1.46	99.59
5163	59.88	1.26	15.62	9.09	0.26	1.71	5.52	4.43	1.38	99.16
5163	59.93	1.44	14.85	9.90	0.29	1.86	5.22	4.38	1.62	99.49
5163	60.10	1.16	15.93	7.42	0.20	1.39	5.26	4.36	1.44	97.26
5163	60.26	1.19	15.29	9.04	0.37	1.64	5.18	4.70	1.51	99.19
5163	59.11	1.36	14.86	9.77	0.27	1.79	5.33	3.99	1.53	97.99
5163	59.91	1.25	14.92	9.05	0.26	1.81	5.30	3.17	1.55	97.22
5163	61.78	1.10	14.70	7.84	0.18	1.40	4.72	4.42	1.69	97.85
5165	48.81	4.37	13.16	13.05	0.29	4.75	9.93	3.25	0.77	98.38
5165	49.24	4.38	13.30	14.49	0.19	4.29	8.72	3.20	0.94	98.76
5165	49.88	1.83	13.88	12.46	0.19	6.56	11.35	2.31	0.23	98.69
5165	50.04	1.92	13.57	12.79	0.27	6.21	10.76	2.43	0.26	98.24
5165	50.33	3.69	12.92	15.06	0.16	4.53	9.21	2.69	0.60	99.20

Label	SiO_2	TiO_2	Al_2O_3	FeO	MnO	MgO	CaO	Na_2O	K_2O	Total
5165	50.47	1.81	13.92	12.67	0.28	6.13	11.19	2.53	0.17	99.15
5165	50.53	1.93	13.93	12.66	0.19	6.12	11.14	2.82	0.19	99.52
5165	58.78	1.37	15.06	9.41	0.23	1.76	5.32	4.40	1.53	97.85
5165	58.86	1.34	15.33	9.90	0.30	1.88	5.49	4.19	1.47	98.75
5165	58.91	1.54	13.92	9.89	0.28	1.80	5.17	3.41	1.56	96.49
5165	59.04	1.29	15.47	9.80	0.31	1.76	5.55	3.53	1.53	98.28
5165	59.14	1.37	15.28	9.61	0.30	1.87	5.53	2.84	1.53	97.49
5165	59.17	1.31	15.22	9.37	0.23	1.86	5.42	4.24	1.48	98.30
5165	59.17	1.39	15.42	9.38	0.26	1.88	5.40	4.12	1.52	98.55
5165	59.18	1.29	15.39	9.39	0.23	1.80	5.43	4.25	1.46	98.43
5165	59.22	1.33	15.40	9.52	0.23	1.86	5.57	4.12	1.52	98.76
5165	59.22	1.30	15.42	9.49	0.19	1.81	5.44	4.16	1.51	98.54
5165	59.31	1.29	15.46	9.45	0.24	1.87	5.28	4.38	1.57	98.85
5165	59.33	1.29	15.38	9.56	0.26	1.82	5.43	4.18	1.57	98.82
5165	59.37	1.28	15.41	9.78	0.19	1.86	5.51	2.56	1.50	97.46
5165	59.41	1.34	15.43	9.62	0.31	1.84	5.53	3.89	1.41	98.78
5165	59.41	1.25	15.69	9.57	0.19	1.80	5.68	4.35	1.41	99.36
5165	59.44	1.35	15.41	9.97	0.25	1.84	5.56	4.26	1.45	99.53
5165	59.46	1.32	15.37	9.68	0.26	1.88	5.34	4.16	1.52	98.98
5165	59.47	1.30	15.45	9.69	0.25	1.78	5.37	4.42	1.56	99.28
5165	59.51	1.29	15.64	9.38	0.25	1.75	5.36	4.52	1.60	99.30
5165	59.52	1.33	15.58	9.54	0.29	1.79	5.45	4.18	1.48	99.17
5165	59.55	1.33	15.65	9.06	0.35	1.75	5.56	4.59	1.38	99.20
5165	59.55	1.30	16.17	9.11	0.19	1.69	5.71	4.47	1.46	99.67
5165	59.56	1.44	15.46	9.63	0.26	1.73	5.26	4.17	1.48	98.99
5165	59.67	1.36	15.60	9.59	0.24	1.84	5.49	3.95	1.57	99.30

Label	SiO_2	TiO_2	Al_2O_3	FeO	MnO	MgO	CaO	Na_2O	K_2O	Total
5165	59.72	1.33	15.49	9.41	0.28	1.79	5.39	4.34	1.49	99.21
5165	59.72	1.29	15.25	9.35	0.19	1.77	5.30	4.17	1.59	98.63
5165	59.74	1.29	15.53	9.45	0.21	1.85	5.41	4.32	1.46	99.26
5165	59.77	1.33	15.39	9.36	0.26	1.84	5.31	4.28	1.44	98.97
5165	59.80	1.36	15.62	9.67	0.27	1.76	5.38	4.01	1.52	99.38
5165	59.87	1.36	15.31	9.21	0.27	1.80	5.28	4.21	1.58	98.89
5165	59.95	1.27	15.62	9.59	0.32	1.73	5.32	4.41	1.51	99.72
5165	60.09	1.26	15.48	9.67	0.35	1.72	5.18	4.26	1.56	99.55
5165	62.25	1.03	15.56	8.07	0.27	1.25	4.55	4.12	1.77	98.85
5165	62.71	0.92	15.55	7.77	0.29	1.07	4.31	4.68	1.89	99.19
5165	62.90	0.88	15.55	8.04	0.27	1.07	4.53	4.62	1.78	99.63
5165	64.92	0.59	16.00	5.11	0.24	0.55	2.49	5.70	3.86	99.45
5165	69.05	0.21	15.03	3.01	0.16	0.10	1.11	5.23	4.51	98.41
5165	69.46	0.32	15.21	2.98	0.12	0.07	1.01	5.61	4.61	99.39
5165	69.58	0.26	15.32	2.75	0.12	0.10	1.07	5.10	4.70	99.01
5165	69.62	0.28	15.11	3.11	0.20	0.07	1.05	5.20	4.77	99.42
5165	69.74	0.21	15.04	2.91	0.15	0.10	1.01	5.15	4.67	98.96
5165	69.75	0.22	15.09	2.76	0.14	0.09	1.07	5.26	4.70	99.09
5165	70.96	0.25	14.64	2.10	0.12	0.21	0.84	5.09	4.60	98.81
5165	59.99	1.29	15.58	9.29	0.29	1.76	5.26	3.96	1.52	98.94
5165	60.35	1.31	15.52	9.12	0.28	1.80	5.35	4.07	1.47	99.28
5165	59.98	1.32	15.28	9.17	0.27	1.84	5.21	3.97	1.54	98.56
5165	60.11	1.29	15.79	9.09	0.26	1.89	5.46	3.27	1.42	98.58
5165	60.49	1.27	15.63	9.14	0.34	1.59	5.17	4.01	1.59	99.22
5165	59.98	1.36	15.45	9.48	0.26	1.86	5.27	3.76	1.42	98.84
5165	59.57	1.37	15.24	9.35	0.25	1.74	5.25	4.42	1.53	98.71

Label	SiO_2	TiO_2	Al_2O_3	FeO	MnO	MgO	CaO	Na_2O	K_2O	Total
5165	60.24	1.45	15.48	9.33	0.21	1.80	5.28	4.00	1.53	99.30
5165	60.62	1.30	15.60	8.95	0.27	1.67	5.26	4.07	1.62	99.35
5166	56.62	1.49	14.73	9.48	0.26	1.82	5.24	4.56	1.59	95.78
5166	56.75	1.35	14.60	8.50	0.20	1.54	4.92	4.59	1.66	94.11
5166	57.19	1.33	14.80	9.71	0.26	1.55	5.50	3.29	1.61	95.22
5166	57.42	1.42	14.81	10.52	0.30	1.84	5.32	4.25	1.53	97.41
5166	57.53	1.41	15.00	9.61	0.19	1.79	5.19	4.58	1.63	96.94
5166	57.96	1.33	15.27	8.99	0.29	1.59	5.24	3.52	1.39	95.59
5166	58.20	1.35	15.13	9.40	0.25	1.77	5.45	4.47	1.50	97.50
5166	58.37	1.39	15.09	9.80	0.29	1.90	5.33	4.48	1.52	98.15
5166	58.79	1.33	15.05	8.84	0.31	1.76	5.05	4.33	1.53	96.99
5166	58.94	1.37	15.36	8.33	0.26	1.52	4.92	5.41	1.86	97.97
5166	59.39	1.31	15.24	8.82	0.26	1.58	5.11	3.70	1.65	97.06
5166	59.53	1.40	15.32	8.08	0.21	1.55	4.97	2.83	1.81	95.67
5166	59.96	1.30	15.24	9.48	0.27	1.72	5.38	4.12	1.47	98.95
5166	61.34	0.90	15.19	7.48	0.25	1.12	4.35	4.82	1.75	97.20
5166	62.20	0.95	15.33	7.51	0.32	1.08	4.35	4.58	1.84	98.16
5133	57.50	1.35	14.67	9.72	0.20	1.92	5.47	3.68	1.37	95.87
5133	57.75	1.35	14.93	9.33	0.24	1.90	5.38	3.96	1.51	96.35
5133	58.07	1.22	14.89	9.35	0.27	1.81	5.26	3.88	1.54	96.27
5133	58.09	1.28	14.94	9.22	0.21	1.87	5.26	4.06	1.45	96.37
5133	58.96	1.32	15.09	8.96	0.27	1.82	5.06	3.95	1.42	96.86
5133	74.76	0.12	12.10	0.92	0.05	0.02	1.53	4.84	1.38	95.72
5133	75.34	0.19	12.53	0.79	0.02	0.00	1.82	4.74	0.97	96.40
5133	78.27	0.21	11.16	2.78	0.06	0.06	1.57	4.78	0.45	99.34
5135	58.33	1.27	14.76	8.87	0.21	1.72	4.88	4.27	1.43	95.75

Label	SiO_2	TiO_2	Al_2O_3	FeO	MnO	MgO	CaO	Na_2O	K_2O	Total
5135	59.03	1.28	14.89	9.28	0.29	1.75	5.02	3.38	1.48	96.40
5135	59.28	1.27	15.23	9.54	0.16	1.72	5.24	4.21	1.53	98.19
5135	59.47	1.25	15.13	9.42	0.31	1.86	5.37	3.18	1.33	97.31
5135	59.84	1.26	15.22	9.32	0.39	1.69	5.03	4.17	1.55	98.47
5135	59.90	1.21	15.41	8.97	0.30	1.77	5.13	4.41	1.53	98.62
5135	67.60	0.24	14.60	2.96	0.08	0.08	1.08	5.88	3.96	96.48
5135	73.94	0.23	12.51	2.03	0.00	0.07	1.54	3.35	3.37	97.05
5135	75.72	0.21	12.03	1.40	0.08	0.04	1.30	5.28	1.94	97.99
5135	76.81	0.18	12.03	1.49	0.03	0.02	1.37	5.03	1.75	98.72
5135	79.65	0.13	11.37	1.03	0.00	0.00	1.50	4.71	0.42	98.81
5135	80.03	0.13	11.18	0.42	0.00	0.00	1.38	5.21	0.50	98.85
5136	62.47	0.58	15.54	4.87	0.22	0.44	2.19	4.88	3.25	94.43
5136	63.70	0.65	15.93	4.99	0.17	0.50	2.36	5.89	3.18	97.37
5136	67.36	0.24	14.50	2.87	0.14	0.10	0.99	5.57	3.78	95.56
5136	72.28	0.11	12.74	2.12	0.08	0.01	1.24	4.15	2.86	95.59
5136	74.19	0.23	11.56	2.39	0.00	0.11	1.03	2.95	4.44	96.90
5136	74.36	0.26	11.62	1.88	0.08	0.11	1.92	4.76	0.47	95.47
5142	58.23	1.42	14.57	10.17	0.14	2.17	5.34	3.44	1.38	96.86
5142	58.35	1.37	15.07	9.42	0.25	1.87	5.24	3.99	1.45	97.00
5142	58.72	1.19	14.98	9.12	0.28	1.80	4.85	4.21	1.52	96.67
5142	58.80	1.33	15.00	9.60	0.31	1.89	5.04	3.50	1.34	96.79
5142	58.83	1.27	15.01	9.22	0.18	1.74	5.17	3.39	1.53	96.33
5142	59.01	1.33	14.92	9.58	0.24	1.85	5.35	3.46	1.27	97.00
5142	59.02	1.33	15.04	9.63	0.19	1.77	5.35	3.95	1.47	97.74
5142	59.06	1.06	15.09	8.77	0.22	1.41	4.51	4.01	1.44	95.57
5142	59.07	1.29	15.06	9.06	0.32	1.84	4.82	4.06	1.48	97.00

Label	SiO_2	TiO_2	Al_2O_3	FeO	MnO	MgO	CaO	Na_2O	K_2O	Total
5142	59.10	1.33	15.08	9.07	0.23	1.89	5.17	3.98	1.44	97.28
5142	59.23	1.34	15.22	9.55	0.15	1.89	5.04	3.87	1.49	97.78
5142	59.40	1.25	15.22	9.24	0.24	1.70	5.25	4.12	1.49	97.91
5142	59.44	1.25	15.22	9.02	0.25	1.69	4.97	2.98	1.47	96.29
5142	60.41	1.28	15.54	8.85	0.32	1.75	5.04	3.75	1.54	98.48
5148	68.30	0.21	14.74	3.04	0.03	0.09	1.01	5.52	4.64	97.58
5148	68.46	0.22	14.80	2.81	0.18	0.08	1.07	5.50	4.40	97.52
5148	69.14	0.24	14.99	3.02	0.12	0.10	1.03	3.94	4.64	97.23
5148	69.26	0.28	14.69	3.00	0.13	0.11	1.08	3.81	4.55	96.92
5148	69.30	0.21	14.89	3.10	0.08	0.08	1.06	5.62	4.76	99.11
5148	69.73	0.21	14.99	2.99	0.14	0.07	0.98	5.57	4.76	99.44
5148	70.80	0.23	14.63	2.39	0.12	0.23	0.81	5.46	4.47	99.15
5148	70.94	0.25	14.68	2.09	0.10	0.21	0.89	5.08	4.46	98.69
5148	71.14	0.23	14.68	2.41	0.16	0.24	0.86	5.44	4.25	99.40
5149	58.93	1.28	15.01	9.47	0.27	1.78	5.33	3.71	1.42	97.20
5149	59.68	1.35	15.26	9.31	0.19	1.81	5.20	3.71	1.36	97.87
5150	78.18	0.33	11.77	2.13	0.00	0.02	1.85	4.95	0.28	99.50
5150	78.21	0.24	11.87	2.23	0.09	0.06	2.11	4.71	0.27	99.80
5150	78.66	0.24	12.38	0.94	0.06	0.04	1.81	4.88	0.21	99.22
5150	78.91	0.22	12.22	0.88	0.03	0.02	1.47	4.74	1.01	99.50
5150	79.25	0.30	11.76	1.14	0.00	0.01	1.64	4.83	0.48	99.40
5150	79.26	0.23	12.02	1.18	0.06	0.02	2.13	4.58	0.43	99.92
5150	79.53	0.19	11.64	0.91	0.05	0.07	1.41	4.91	0.74	99.45
5150	79.90	0.18	11.14	0.25	0.00	0.02	1.08	4.60	0.93	98.09
5150	80.25	0.19	10.85	1.29	0.00	0.05	1.35	4.47	0.66	99.12
7094	58.68	1.24	14.89	8.74	0.25	1.80	4.99	3.83	1.59	96.01

Label	SiO_2	TiO_2	Al_2O_3	FeO	MnO	MgO	CaO	Na_2O	K_2O	Total
7095	57.10	1.26	15.09	9.44	0.24	1.92	5.49	4.22	1.46	96.23
7095	57.45	1.27	14.94	9.40	0.28	1.83	5.22	4.26	1.48	96.12
7095	57.69	1.27	14.68	9.19	0.35	1.79	5.10	4.54	1.55	96.17
7095	57.89	1.35	14.84	9.51	0.28	1.84	5.27	4.42	1.55	96.96
7095	57.94	1.35	14.81	9.34	0.23	1.84	5.05	4.43	1.62	96.61
7095	57.98	1.38	14.85	9.57	0.26	1.85	5.34	4.32	1.46	97.01
7095	58.01	1.43	14.76	9.65	0.21	1.93	5.21	4.19	1.56	96.96
7095	58.19	1.31	15.06	9.92	0.28	1.94	5.35	4.29	1.61	97.95
7095	58.23	1.34	15.06	9.19	0.28	1.77	5.35	4.48	1.56	97.27
7095	58.25	1.28	14.89	9.61	0.23	1.83	5.19	4.34	1.57	97.21
7095	58.33	1.33	14.83	8.76	0.33	1.86	5.21	4.65	1.65	96.93
7095	58.34	1.26	14.84	9.11	0.23	1.85	5.14	4.54	1.55	96.86
7095	58.42	1.25	14.92	8.97	0.23	1.64	5.04	3.95	1.44	95.86
7095	58.49	1.23	15.04	9.55	0.27	1.87	5.40	4.19	1.45	97.49
7095	58.70	1.04	15.09	8.56	0.26	1.23	4.61	4.46	1.51	95.47
7095	58.72	1.26	15.05	9.49	0.34	1.77	5.26	4.01	1.58	97.48
7095	59.18	1.22	15.11	9.50	0.25	1.78	5.19	4.46	1.55	98.22
7095	59.20	1.20	14.80	8.63	0.27	1.58	4.70	4.48	1.50	96.36
7095	59.48	1.32	15.21	9.35	0.25	1.86	5.27	4.09	1.51	98.34
7097	56.13	1.15	14.55	9.08	0.27	2.69	5.91	4.58	1.21	95.57
7097	57.52	1.35	14.94	9.18	0.24	1.96	5.30	4.05	1.46	96.00
7097	57.61	1.37	14.82	9.69	0.17	1.92	5.30	4.19	1.51	96.58
7097	57.86	1.19	15.39	8.67	0.22	1.64	5.30	4.31	1.37	95.95
7097	57.93	1.23	14.90	9.04	0.28	1.74	5.13	4.30	1.64	96.20
7097	58.04	1.33	14.75	9.40	0.20	1.70	5.03	3.98	1.39	95.83
7097	58.21	1.28	14.78	9.47	0.30	1.85	5.37	4.43	1.48	97.18

Label	SiO_2	TiO_2	Al_2O_3	FeO	MnO	MgO	CaO	Na_2O	K_2O	Total
7097	58.26	1.31	14.75	9.09	0.23	1.72	5.02	4.31	1.55	96.23
7097	58.56	1.36	15.05	9.29	0.21	1.86	5.37	4.19	1.54	97.44
7097	58.63	0.74	17.64	6.19	0.16	1.23	6.08	5.10	1.21	96.97
7097	58.75	1.24	15.19	9.53	0.13	1.94	5.14	4.16	1.54	97.62
7097	59.13	1.27	15.46	9.46	0.19	1.79	5.25	4.26	1.48	98.30
7097	60.79	1.08	15.54	9.10	0.20	1.44	4.95	4.13	1.66	98.89
7098	58.29	1.31	15.06	9.66	0.17	1.75	5.27	4.03	1.60	97.14
7098	58.37	1.32	15.24	9.32	0.23	1.86	5.22	4.64	1.55	97.75
7098	58.51	1.32	15.14	9.72	0.18	1.92	5.33	4.19	1.55	97.87
7098	58.58	1.29	15.40	9.26	0.23	1.81	5.34	4.27	1.56	97.74
7098	58.69	1.20	14.89	9.00	0.25	1.69	5.15	4.35	1.67	96.90
7098	59.11	1.23	15.67	9.04	0.21	1.72	4.78	4.31	1.48	97.56
7098	59.16	1.19	14.88	9.23	0.11	1.75	5.11	4.10	1.58	97.13
7098	59.53	1.29	15.08	8.75	0.21	1.72	5.05	4.14	1.63	97.39
7098	59.79	1.20	15.10	8.97	0.22	1.74	5.17	2.82	1.62	96.62
7098	60.16	1.26	15.26	8.59	0.24	1.67	5.00	4.02	1.51	97.71
7099	56.95	1.40	14.46	9.60	0.23	1.97	5.33	4.35	1.59	95.87
7099	57.25	1.23	15.68	8.73	0.19	1.62	5.65	4.27	1.30	95.92
7099	57.65	1.34	14.99	9.40	0.20	1.81	5.32	4.49	1.56	96.76
7099	57.73	1.32	14.96	9.40	0.37	1.79	5.37	4.24	1.56	96.74
7099	58.19	1.25	14.70	9.50	0.27	1.84	4.99	4.52	1.61	96.86
7099	58.23	1.30	14.97	9.55	0.19	1.88	5.29	4.25	1.49	97.16
7099	58.42	1.29	14.99	9.29	0.17	1.74	5.29	4.45	1.67	97.30
7099	58.46	1.24	14.78	9.16	0.27	1.73	5.11	4.08	1.55	96.39
7099	59.88	1.22	14.89	8.46	0.21	1.54	5.09	4.52	1.34	97.15
7099	60.16	1.30	15.48	9.03	0.23	1.73	5.15	4.33	1.61	99.01

Label	SiO_2	TiO_2	Al_2O_3	FeO	MnO	MgO	CaO	Na_2O	K_2O	Total
7099	60.47	1.07	15.22	7.94	0.17	1.43	4.87	4.96	1.33	97.47

C | *Database of known geochemistry*

Table C.1: Table of all geochemical data for Icelandic eruptions from published sources. Citations are in Table 3.1.

System	Year	SiO2	TiO2	Al2O3	FeO	MnO	MgO	CaO	Na2O	K2O	Total
Hekla 3	ca. 1000 BC	72.39	0.23	13.62	3.09	0.13	0.13	2.14	4.26	2.65	98.64
Hekla 3	ca. 1000 BC	72.35	0.19	13.88	2.96	0.07	0.13	2.12	4.22	2.35	98.27
Hekla 3	ca. 1000 BC	68.63	0.44	14.70	5.14	0.17	0.34	3.14	4.28	2.07	98.91
Hekla 3	ca. 1000 BC	68.11	0.34	14.56	5.31	0.17	0.33	3.09	4.09	2.20	98.20
Hekla 3	ca. 1000 BC	67.08	0.45	14.69	5.65	0.16	0.42	3.35	4.22	2.09	98.11
Hekla 3	ca. 1000 BC	66.90	0.38	14.27	4.82	0.17	0.35	2.84	3.80	2.00	95.53
Hekla 3	ca. 1000 BC	66.76	0.58	14.95	6.25	0.12	0.58	3.60	4.08	2.00	98.92

Hekla 3	ca. 1000 BC	65.38	0.66	14.66	6.85	0.18	0.58	3.34	3.81	1.88	97.34
Hekla 3	ca. 1000 BC	65.22	0.67	14.91	7.61	0.24	0.72	4.02	4.23	1.75	99.37
Hekla 3	ca. 1000 BC	64.59	0.66	14.66	7.74	0.25	0.70	3.96	3.77	1.82	98.15
Hekla 3	ca. 1000 BC	64.28	0.55	14.40	6.40	0.21	0.58	3.79	3.89	1.77	95.87
Hekla 3	ca. 1000 BC	63.79	0.76	14.81	7.07	0.20	0.74	4.07	3.75	1.72	96.91
Hekla 3	ca. 1000 BC	63.74	0.63	14.95	7.02	0.20	0.77	3.99	3.84	1.70	96.84
Hekla 3	ca. 1000 BC	63.58	0.81	15.06	7.53	0.20	0.83	4.26	4.27	1.39	97.93
Hekla 3	ca. 1000 BC	62.05	0.76	14.36	7.78	0.21	0.81	4.47	3.49	1.69	95.62
Snaefellsjokull	+- or - 200	76.75	0.10	12.30	1.70	0.02	0.07	0.66	3.34	4.30	99.24
Snaefellsjokull	+- or - 200	75.59	0.12	12.46	1.48	0.03	0.09	0.65	3.40	4.07	97.89
Snaefellsjokull	+- or - 200	74.67	0.04	12.22	1.59	0.01	0.12	0.71	2.92	3.90	96.18

Snaefellsjokull	+ or - 200	74.46	0.12	12.22	1.71	0.00	0.13	0.72	3.05	4.37	96.78
Snaefellsjokull	+ or - 200	74.41	0.12	12.27	1.47	0.05	0.06	0.73	3.89	3.71	96.71
Snaefellsjokull	+ or - 200	74.35	0.13	12.21	1.55	0.04	0.05	0.71	3.16	3.92	96.12
Snaefellsjokull	+ or - 200	74.04	0.11	12.27	1.51	0.00	0.06	0.60	4.06	3.77	96.42
Snaefellsjokull	+ or - 200	73.96	0.10	12.23	1.54	0.06	0.07	0.72	3.66	4.16	96.50
Snaefellsjokull	+ or - 200	73.87	0.17	11.83	1.76	0.03	0.05	0.76	3.98	3.94	96.39
Snaefellsjokull	+ or - 200	73.84	0.17	12.37	1.63	0.06	0.07	0.83	3.61	4.32	96.90
Snaefellsjokull	+ or - 200	73.64	0.12	12.42	1.60	0.04	0.13	0.74	4.03	3.69	96.41
Snaefellsjokull	+ or - 200	73.54	0.15	12.53	1.54	0.05	0.07	0.78	3.53	3.99	96.18
Snaefellsjokull	+ or - 200	73.43	0.12	12.37	1.66	0.03	0.07	0.71	4.07	3.70	96.16
Snaefellsjokull	+ or - 200	73.30	0.20	11.98	1.53	0.07	0.11	0.63	4.30	3.68	95.80
Snaefellsjokull	+ or - 200	71.44	0.27	13.14	3.86	0.14	0.21	1.15	4.86	3.48	98.55
Torfajokull	870 + or - 2	46.88	2.06	13.69	12.35	0.19	6.16	10.84	2.60	0.24	95.01
Torfajokull	870 + or - 2	47.19	1.99	13.42	12.45	0.20	6.71	11.30	2.57	0.20	96.03

Torfajokull	870 + or - 2	47.59	2.04	14.33	10.77	0.17	7.42	11.79	2.32	0.23	96.66
Torfajokull	870 + or - 2	47.61	2.02	13.35	11.92	0.20	6.54	10.91	2.54	0.24	95.33
Torfajokull	870 + or - 2	47.61	1.99	12.18	12.88	0.18	5.97	10.83	1.84	0.24	93.72
Torfajokull	870 + or - 2	47.65	2.06	14.48	10.80	0.18	7.34	12.07	2.31	0.31	97.20
Torfajokull	870 + or - 2	47.82	4.42	13.00	14.01	0.18	4.87	9.26	3.26	0.84	97.66
Torfajokull	870 + or - 2	47.91	1.84	13.38	12.56	0.17	6.52	11.08	2.68	0.24	96.38
Torfajokull	870 + or - 2	47.95	1.78	13.31	12.47	0.22	6.49	11.18	2.55	0.21	96.16
Torfajokull	870 + or - 2	48.20	1.73	13.81	11.24	0.25	7.64	12.29	2.27	0.17	97.60
Torfajokull	870 + or - 2	48.32	2.08	12.67	13.31	0.25	6.29	11.39	2.73	0.17	97.21
Torfajokull	870 + or - 2	48.33	2.04	13.16	13.18	0.25	6.53	10.62	2.69	0.25	97.05

Torfajokull	870 + or - 2	48.35	1.93	13.78	12.19	0.19	6.72	11.06	2.47	0.22	96.91
Torfajokull	870 + or - 2	48.42	1.86	13.19	12.30	0.22	6.26	11.03	2.44	0.21	95.93
Torfajokull	870 + or - 2	48.50	1.81	13.15	12.57	0.21	6.22	11.18	2.54	0.24	96.42
Torfajokull	870 + or - 2	48.50	4.14	12.91	13.51	0.17	4.23	8.51	3.52	0.85	96.34
Torfajokull	870 + or - 2	48.53	1.93	12.68	12.95	0.26	5.94	10.98	2.67	0.24	96.18
Torfajokull	870 + or - 2	48.58	1.92	13.38	12.33	0.20	6.53	11.13	2.58	0.26	96.91
Torfajokull	870 + or - 2	48.61	1.90	13.31	12.36	0.32	6.51	10.86	2.64	0.20	96.71
Torfajokull	870 + or - 2	48.63	2.00	13.12	11.90	0.25	6.71	10.92	2.44	0.31	96.28
Torfajokull	870 + or - 2	48.67	1.89	13.46	11.99	0.16	6.64	10.98	2.70	0.21	96.70
Torfajokull	870 + or - 2	48.67	1.92	13.51	12.30	0.20	6.44	11.34	2.59	0.21	97.18

Torfajokull	870 + or - 2	48.68	1.44	13.83	12.10	0.28	5.45	11.58	2.47	0.30	96.13
Torfajokull	870 + or - 2	48.70	1.85	13.30	12.22	0.20	6.56	11.46	2.44	0.23	96.96
Torfajokull	870 + or - 2	48.72	1.94	12.92	12.67	0.22	6.04	11.00	2.45	0.23	96.19
Torfajokull	870 + or - 2	48.74	1.98	13.81	12.11	0.21	6.78	11.23	2.59	0.21	97.66
Torfajokull	870 + or - 2	48.74	1.79	13.45	12.36	0.17	6.58	11.73	2.49	0.18	97.49
Torfajokull	870 + or - 2	48.76	1.99	13.60	10.79	0.18	7.20	12.02	2.65	0.27	97.46
Torfajokull	870 + or - 2	48.76	1.84	13.04	12.37	0.23	6.32	10.92	2.47	0.22	96.17
Torfajokull	870 + or - 2	48.77	1.99	13.20	11.77	0.24	6.01	10.11	2.97	0.33	95.39
Torfajokull	870 + or - 2	48.78	1.83	13.32	12.46	0.24	7.32	11.02	2.66	0.21	97.84
Torfajokull	870 + or - 2	48.79	1.75	13.53	11.78	0.21	6.75	11.43	2.46	0.19	96.89

Torfajokull	870 + or - 2	48.82	2.34	12.53	13.42	0.26	5.94	10.86	2.53	0.30	97.00
Torfajokull	870 + or - 2	48.86	1.73	13.46	11.52	0.21	6.69	11.25	2.59	0.18	96.49
Torfajokull	870 + or - 2	48.86	1.95	13.22	11.82	0.18	6.49	10.79	2.57	0.24	96.12
Torfajokull	870 + or - 2	48.88	1.88	13.37	12.29	0.23	6.35	11.25	2.47	0.17	96.89
Torfajokull	870 + or - 2	48.91	2.12	12.71	13.64	0.18	6.01	10.92	2.49	0.25	97.23
Torfajokull	870 + or - 2	48.93	2.58	12.62	13.65	0.30	5.15	9.23	2.87	0.37	95.70
Torfajokull	870 + or - 2	48.96	1.97	13.67	13.19	0.20	6.24	10.77	2.75	0.27	98.02
Torfajokull	870 + or - 2	48.96	2.73	13.68	13.14	0.27	5.72	9.87	3.20	0.41	97.98
Torfajokull	870 + or - 2	49.03	1.77	13.23	12.61	0.22	6.78	11.11	2.73	0.29	97.77
Torfajokull	870 + or - 2	49.11	1.81	13.77	12.39	0.24	6.57	11.47	2.39	0.19	97.94

Torfajokull	870 + or - 2	49.16	1.84	13.76	12.48	0.19	6.47	11.22	2.52	0.25	97.89
Torfajokull	870 + or - 2	49.18	2.07	13.04	12.58	0.18	6.45	10.19	2.58	0.28	96.55
Torfajokull	870 + or - 2	49.19	3.11	13.40	13.68	0.21	5.65	9.97	2.66	0.44	98.31
Torfajokull	870 + or - 2	49.23	1.84	13.39	12.50	0.16	6.17	11.43	2.38	0.25	97.35
Torfajokull	870 + or - 2	49.27	1.94	13.00	12.40	0.21	6.67	11.30	2.41	0.30	97.50
Torfajokull	870 + or - 2	49.29	2.04	13.59	12.75	0.24	6.48	11.34	2.62	0.28	98.63
Torfajokull	870 + or - 2	49.29	1.94	13.39	12.52	0.26	6.62	11.77	2.24	0.19	98.22
Torfajokull	870 + or - 2	49.31	2.02	13.97	11.21	0.21	7.22	11.86	2.49	0.27	98.56
Torfajokull	870 + or - 2	49.31	1.73	13.36	12.47	0.29	6.35	11.25	2.39	0.28	97.43
Torfajokull	870 + or - 2	49.32	1.80	13.85	12.41	0.24	6.72	11.57	2.23	0.22	98.36

Torfajokull	870 + or - 2	49.35	1.93	13.47	12.20	0.26	5.65	10.05	2.85	0.34	96.10
Torfajokull	870 + or - 2	49.37	1.74	13.52	12.29	0.22	6.74	11.37	2.39	0.20	97.84
Torfajokull	870 + or - 2	49.39	1.84	13.68	13.14	0.23	6.26	11.01	2.55	0.32	98.42
Torfajokull	870 + or - 2	49.48	1.69	13.47	11.81	0.20	7.18	11.89	2.11	0.19	98.02
Torfajokull	870 + or - 2	49.49	2.08	13.12	13.30	0.26	6.02	11.16	2.72	0.24	98.39
Torfajokull	870 + or - 2	49.52	1.98	13.55	12.45	0.15	6.71	11.41	2.61	0.20	98.58
Torfajokull	870 + or - 2	49.54	2.03	13.32	12.51	0.18	6.37	10.84	2.72	0.19	97.70
Torfajokull	870 + or - 2	49.56	1.96	13.00	12.59	0.20	6.12	10.24	2.70	0.28	96.65
Torfajokull	870 + or - 2	49.57	1.89	13.04	12.77	0.21	5.90	9.95	2.82	0.26	96.41
Torfajokull	870 + or - 2	49.57	1.78	13.29	11.99	0.25	6.55	11.45	2.52	0.25	97.65

Torfajokull	870 + or - 2	49.59	1.89	13.77	12.02	0.21	6.95	11.53	2.41	0.17	98.54
Torfajokull	870 + or - 2	49.64	1.93	13.56	12.61	0.19	6.70	11.22	2.37	0.21	98.43
Torfajokull	870 + or - 2	49.73	1.87	13.19	12.28	0.22	6.56	11.52	2.61	0.23	98.21
Torfajokull	870 + or - 2	49.73	2.18	13.49	12.93	0.27	6.04	11.09	2.67	0.22	98.62
Torfajokull	870 + or - 2	49.78	1.98	13.17	13.09	0.19	6.21	10.66	2.55	0.25	97.88
Torfajokull	870 + or - 2	49.79	1.90	13.05	12.76	0.26	6.30	10.63	2.74	0.28	97.71
Torfajokull	870 + or - 2	49.80	1.74	13.56	11.85	0.17	6.66	11.45	2.46	0.22	97.91
Torfajokull	870 + or - 2	49.85	1.83	13.58	12.40	0.20	6.48	11.15	2.64	0.30	98.43
Torfajokull	870 + or - 2	49.90	1.86	13.50	12.46	0.24	6.43	11.37	2.67	0.28	98.71
Torfajokull	870 + or - 2	50.05	2.01	13.64	12.81	0.19	6.49	11.09	2.46	0.29	99.03

Torfajokull	870 + or - 2	50.09	1.77	13.85	12.04	0.11	6.55	11.57	2.70	0.24	98.92
Torfajokull	870 + or - 2	50.11	1.90	12.98	12.53	0.13	6.66	10.97	2.54	0.27	98.09
Torfajokull	870 + or - 2	50.17	2.89	12.89	13.39	0.22	5.51	9.67	2.98	0.45	98.17
Torfajokull	870 + or - 2	50.26	1.81	13.56	12.32	0.23	6.48	11.37	2.35	0.19	98.57
Torfajokull	870 + or - 2	50.31	2.06	13.09	13.02	0.20	6.01	10.25	2.68	0.33	97.95
Torfajokull	870 + or - 2	50.37	1.99	13.30	12.45	0.23	5.91	10.65	2.85	0.27	98.02
Torfajokull	870 + or - 2	50.39	1.89	13.17	12.81	0.21	6.28	10.52	2.82	0.28	98.37
Torfajokull	870 + or - 2	50.43	2.53	13.46	13.02	0.21	5.45	9.82	3.06	0.41	98.39
Torfajokull	870 + or - 2	50.60	1.84	13.17	12.17	0.25	6.36	10.63	2.63	0.30	97.95
Torfajokull	870 + or - 2	50.65	2.17	13.39	12.68	0.25	5.97	10.27	2.82	0.36	98.56

Torfajokull	870 + or - 2	50.75	1.81	13.67	12.42	0.23	6.69	11.22	2.51	0.30	99.60
Torfajokull	870 + or - 2	50.82	1.98	13.29	12.65	0.19	6.08	10.02	2.52	0.33	97.88
Torfajokull	870 + or - 2	64.95	1.31	13.50	7.31	0.15	1.60	4.62	3.63	2.00	99.07
Torfajokull	870 + or - 2	69.54	0.23	14.41	2.26	0.08	0.21	0.91	4.72	4.50	96.86
Torfajokull	870 + or - 2	69.76	0.24	14.34	2.36	0.05	0.24	0.95	4.94	4.59	97.47
Torfajokull	870 + or - 2	69.91	0.22	14.19	2.22	0.09	0.24	0.95	4.78	4.64	97.24
Torfajokull	870 + or - 2	70.03	0.24	13.88	2.25	0.05	0.18	0.81	4.80	4.56	96.80
Torfajokull	870 + or - 2	70.28	0.18	14.38	2.38	0.10	0.27	0.82	4.81	4.70	97.92
Torfajokull	870 + or - 2	70.45	0.23	14.46	2.32	0.09	0.26	0.97	4.89	4.45	98.12
Torfajokull	870 + or - 2	70.50	0.23	14.27	2.30	0.13	0.21	0.79	5.10	4.54	98.07

Torfajokull	870 + or - 2	70.54	0.29	14.77	2.41	0.12	0.29	0.83	4.60	4.78	98.63
Torfajokull	870 + or - 2	70.72	0.31	14.59	2.27	0.09	0.27	0.85	4.61	4.58	98.29
Torfajokull	870 + or - 2	70.77	0.31	14.67	2.22	0.14	0.26	0.91	4.43	4.51	98.22
Torfajokull	870 + or - 2	70.97	0.26	13.74	2.56	0.11	0.21	0.98	4.46	4.88	98.17
Torfajokull	870 + or - 2	71.13	0.24	14.67	2.16	0.09	0.31	0.86	4.44	4.81	98.71
Torfajokull	870 + or - 2	71.16	0.19	14.16	2.37	0.02	0.21	0.83	5.33	4.59	98.86
Torfajokull	870 + or - 2	71.30	0.23	14.19	2.32	0.07	0.18	0.89	4.88	4.44	98.50
Torfajokull	870 + or - 2	71.34	0.26	14.75	2.20	0.00	0.27	0.96	4.73	4.86	99.37
Torfajokull	870 + or - 2	71.50	0.23	14.49	2.27	0.06	0.22	0.91	4.93	4.63	99.24
Torfajokull	870 + or - 2	71.52	0.34	14.80	2.21	0.14	0.26	0.88	4.79	4.81	99.75

Torfajokull	870 + or - 2	71.60	0.28	14.40	2.43	0.10	0.20	0.88	4.99	4.74	99.62
Torfajokull	870 + or - 2	71.75	0.22	14.85	2.22	0.07	0.26	0.92	5.12	4.52	99.93
Torfajokull	870 + or - 2	71.82	0.25	14.80	2.49	0.09	0.24	0.83	4.47	4.67	99.66
Torfajokull	870 + or - 2	71.83	0.28	14.66	2.42	0.14	0.29	0.93	4.56	4.70	99.81
Torfajokull	870 + or - 2	71.89	0.25	14.69	2.45	0.00	0.28	0.82	4.62	4.56	99.56
Torfajokull	870 + or - 2	72.10	0.18	14.36	2.34	0.13	0.22	0.89	4.93	4.57	99.72
Torfajokull	870 + or - 2	74.43	0.07	13.01	2.00	0.02	0.01	1.32	2.24	2.85	95.95
Eldgja	935	45.30	4.53	11.45	15.47	0.23	6.19	10.90	2.68	0.66	97.41
Eldgja	935	45.74	4.77	12.17	15.78	0.25	5.29	10.17	2.82	0.65	97.64
Eldgja	935	46.39	4.49	12.51	15.55	0.22	5.53	10.39	2.79	0.76	98.63
Eldgja	935	46.79	4.67	12.48	14.90	0.21	4.89	9.43	3.39	0.84	97.60
Eldgja	935	46.97	4.65	12.53	15.02	0.21	5.08	9.55	3.15	0.85	98.01
Eldgja	935	47.06	4.72	12.60	14.69	0.26	4.96	9.44	3.15	0.86	97.74
Eldgja	935	47.16	4.71	12.38	14.65	0.22	4.92	9.47	3.25	0.68	97.44
Eldgja	935	47.22	4.70	12.46	14.69	0.32	4.82	9.31	3.31	0.87	97.70
Eldgja	935	47.22	4.74	12.53	14.92	0.25	4.91	9.39	3.23	0.83	98.02

Eldgja	935	48.78	2.61	12.37	14.37	0.22	5.91	10.30	2.65	0.44	97.65
Eldgja	935	49.12	2.57	12.96	14.08	0.25	5.57	9.69	2.79	0.42	97.45
Eldgja	935	49.47	2.33	13.13	13.59	0.29	6.13	10.54	2.79	0.35	98.62
Hekla	1104	46.00	4.68	12.43	14.21	0.25	5.00	9.79	2.69	0.89	95.94
Hekla	1104	48.43	1.95	12.91	13.09	0.16	6.21	10.60	2.71	0.24	96.30
Hekla	1104	48.54	1.77	13.58	12.51	0.24	6.37	11.68	2.34	0.23	97.26
Hekla	1104	48.84	2.16	13.22	12.80	0.20	6.45	10.92	2.61	0.30	97.50
Hekla	1104	49.89	2.96	13.19	13.12	0.21	5.49	10.21	2.83	0.47	98.37
Hekla	1104	50.74	2.05	13.24	12.84	0.19	6.03	10.61	2.42	0.27	98.39
Hekla	1104	70.23	0.19	13.86	3.28	0.03	0.17	1.84	4.59	2.71	96.90
Hekla	1104	70.36	0.19	13.58	3.02	0.13	0.13	1.82	4.58	2.68	96.49
Hekla	1104	70.59	0.23	13.88	3.06	0.11	0.12	2.02	4.40	2.76	97.17
Hekla	1104	70.65	0.24	13.73	3.06	0.12	0.12	1.85	4.87	2.73	97.37
Hekla	1104	70.69	0.17	14.12	3.19	0.11	0.08	1.85	4.55	2.57	97.33
Hekla	1104	70.72	0.22	13.79	3.21	0.14	0.19	1.96	4.45	2.58	97.26
Hekla	1104	70.78	0.18	13.91	3.09	0.09	0.14	1.85	4.28	2.72	97.04
Hekla	1104	70.79	0.22	13.38	3.26	0.16	0.12	1.79	4.42	3.21	97.35
Hekla	1104	70.79	0.19	14.30	3.05	0.15	0.14	1.92	4.55	2.59	97.68
Hekla	1104	70.81	0.17	14.01	3.25	0.14	0.15	1.94	4.03	2.68	97.18
Hekla	1104	70.82	0.26	13.60	3.21	0.11	0.15	1.90	4.76	2.65	97.46
Hekla	1104	70.97	0.21	13.79	3.24	0.13	0.16	1.92	4.70	2.65	97.77
Hekla	1104	70.99	0.22	13.99	3.12	0.13	0.15	1.94	4.50	2.92	97.96
Hekla	1104	71.01	0.22	13.88	3.27	0.09	0.13	1.91	4.57	2.65	97.73
Hekla	1104	71.15	0.18	13.77	3.22	0.06	0.10	1.85	4.17	2.79	97.29
Hekla	1104	71.18	0.23	14.10	3.30	0.10	0.10	1.79	4.84	2.75	98.39
Hekla	1104	71.24	0.26	13.74	3.28	0.12	0.16	1.95	4.62	2.64	98.01
Hekla	1104	71.25	0.18	13.70	3.10	0.10	0.12	1.98	4.51	2.69	97.63
Hekla	1104	71.27	0.17	13.41	3.26	0.10	0.13	1.91	4.54	2.73	97.52
Hekla	1104	71.28	0.21	13.66	3.19	0.06	0.14	1.75	4.34	2.91	97.54
Hekla	1104	71.30	0.20	13.74	3.30	0.12	0.17	1.86	4.64	2.61	97.94

Hekla	1104	71.32	0.19	14.05	3.12	0.09	0.14	1.85	4.25	2.91	97.92
Hekla	1104	71.32	0.18	14.08	2.99	0.17	0.11	1.92	4.57	2.63	97.97
Hekla	1104	71.40	0.17	13.85	3.28	0.08	0.12	1.98	4.11	2.65	97.64
Hekla	1104	71.43	0.28	14.13	3.22	0.19	0.12	1.87	4.58	2.61	98.43
Hekla	1104	71.47	0.21	13.80	3.31	0.15	0.14	1.74	4.92	2.61	98.35
Hekla	1104	71.49	0.25	13.64	3.20	0.09	0.14	1.78	4.39	2.78	97.76
Hekla	1104	71.51	0.22	13.81	3.11	0.09	0.12	2.05	4.94	2.71	98.56
Hekla	1104	71.65	0.18	13.51	3.15	0.06	0.10	1.82	3.99	2.75	97.21
Hekla	1104	71.71	0.22	14.54	2.92	0.13	0.14	2.15	5.01	2.52	99.34
Hekla	1104	71.74	0.19	14.22	3.15	0.11	0.15	1.93	4.75	2.66	98.90
Hekla	1104	71.75	0.26	13.36	3.23	0.10	0.18	1.72	4.75	2.92	98.27
Hekla	1104	71.81	0.17	14.02	3.07	0.10	0.13	1.86	4.21	2.57	97.94
Hekla	1104	71.81	0.21	13.84	3.36	0.08	0.16	1.94	4.48	2.64	98.52
Hekla	1104	71.83	0.14	13.92	3.11	0.11	0.10	1.99	4.37	2.69	98.26
Hekla	1104	71.86	0.22	13.98	3.08	0.08	0.14	2.05	4.65	2.47	98.53
Hekla	1104	71.91	0.24	13.47	3.21	0.12	0.14	1.90	4.57	2.70	98.26
Hekla	1104	71.97	0.21	13.94	3.24	0.13	0.13	1.98	4.56	2.67	98.83
Hekla	1104	71.99	0.20	13.74	3.21	0.11	0.11	2.03	4.40	2.64	98.43
Hekla	1104	72.00	0.16	13.84	3.09	0.05	0.08	1.75	4.30	2.66	97.93
Hekla	1104	72.02	0.13	13.35	3.16	0.11	0.13	1.77	4.63	2.87	98.17
Hekla	1104	72.04	0.22	13.62	3.10	0.13	0.12	1.78	4.53	2.88	98.42
Hekla	1104	72.04	0.23	14.03	3.04	0.11	0.17	1.88	4.61	2.60	98.71
Hekla	1104	72.05	0.23	14.26	3.14	0.10	0.13	1.97	4.26	2.84	98.98
Hekla	1104	72.11	0.19	14.39	3.34	0.11	0.16	1.91	4.16	2.51	98.88
Hekla	1104	72.13	0.21	13.60	3.18	0.11	0.15	1.96	4.32	2.81	98.47
Hekla	1104	72.23	0.13	13.98	3.27	0.08	0.13	1.94	4.24	2.68	98.68
Hekla	1104	72.24	0.25	13.98	3.00	0.06	0.09	1.82	4.22	2.74	98.40
Hekla	1104	72.27	0.17	14.05	3.10	0.09	0.18	1.97	4.41	2.72	98.96
Hekla	1104	72.29	0.19	13.70	2.97	0.04	0.10	1.94	3.56	2.70	97.49
Hekla	1104	72.29	0.27	13.75	3.13	0.08	0.10	1.97	4.70	2.76	99.05

Hekla	1104	72.36	0.23	13.97	3.06	0.17	0.15	1.85	4.68	2.81	99.28
Hekla	1104	72.39	0.22	13.51	3.40	0.11	0.16	1.89	4.01	2.57	98.26
Hekla	1104	72.39	0.18	14.75	3.15	0.11	0.10	2.07	4.48	2.70	99.93
Hekla	1104	72.45	0.14	14.01	3.36	0.12	0.14	1.78	4.15	2.81	98.96
Hekla	1104	72.47	0.21	13.87	3.25	0.11	0.12	1.87	4.18	2.60	98.68
Hekla	1104	72.51	0.15	14.19	3.28	0.10	0.13	2.05	4.77	2.68	99.86
Hekla	1104	72.52	0.21	13.70	3.27	0.13	0.12	1.82	4.41	2.77	98.95
Hekla	1104	72.62	0.15	13.85	3.31	0.16	0.17	1.91	4.34	2.68	99.19
Hekla	1104	72.65	0.18	13.80	3.12	0.07	0.10	1.93	4.19	2.60	98.64
Hekla	1104	72.68	0.17	14.03	3.22	0.13	0.13	1.99	4.19	2.57	99.11
Hekla	1104	72.71	0.23	14.16	3.27	0.07	0.13	2.01	4.48	2.69	99.75
Hekla	1104	72.84	0.21	14.36	3.18	0.09	0.11	1.88	4.06	2.80	99.53
Hekla	1104	72.85	0.21	13.92	3.12	0.08	0.11	2.03	4.30	2.67	99.29
Hekla	1104	72.88	0.23	14.02	3.04	0.13	0.13	2.08	4.00	2.73	99.24
Hekla	1104	72.88	0.23	13.63	3.33	0.10	0.14	1.79	5.02	2.87	99.99
Hekla	1104	72.90	0.23	13.80	3.08	0.05	0.11	1.93	4.40	2.81	99.31
Hekla	1104	72.91	0.18	14.43	3.08	0.04	0.09	1.98	4.60	2.43	99.74
Hekla	1104	72.95	0.21	14.10	3.18	0.08	0.14	1.89	4.22	2.69	99.46
Hekla	1104	73.01	0.12	13.94	3.23	0.14	0.13	1.98	3.98	2.73	99.26
Hekla	1104	73.01	0.22	13.84	2.84	0.11	0.12	1.97	5.00	2.84	99.95
Hekla	1104	73.03	0.22	14.12	3.12	0.10	0.16	1.81	4.40	2.56	99.52
Hekla	1104	73.18	0.29	13.90	3.21	0.14	0.15	1.85	4.14	2.84	99.70
Hekla	1104	73.18	0.20	14.23	3.03	0.13	0.10	1.83	4.47	2.70	99.87
Hekla	1104	73.26	0.17	13.91	3.22	0.12	0.13	2.03	4.56	2.50	99.90
Hekla	1104	73.28	0.16	14.10	3.25	0.10	0.09	1.84	4.39	2.65	99.86
Hekla	1104	73.32	0.19	14.10	3.23	0.14	0.10	1.86	4.25	2.74	99.93
Hekla	1104	73.63	0.19	13.89	3.16	0.14	0.11	1.67	4.50	2.65	99.94
Hekla	1158	66.36	0.46	14.02	5.68	0.22	0.43	2.89	4.40	2.26	96.72
Hekla	1158	66.98	0.55	14.41	5.57	0.18	0.52	3.19	4.89	2.28	98.57
Hekla	1158	67.07	0.51	14.40	5.96	0.28	0.41	3.25	4.83	2.19	98.90

Hekla	1158	67.32	0.50	14.29	5.75	0.20	0.45	3.27	4.87	2.31	98.96
Hekla	1158	67.48	0.47	14.32	5.72	0.18	0.39	3.00	4.78	2.18	98.52
Hekla	1158	67.48	0.44	14.88	5.58	0.14	0.44	3.15	4.16	2.20	98.47
Hekla	1158	67.49	0.52	14.20	5.43	0.21	0.41	3.03	4.48	2.45	98.22
Hekla	1158	67.52	0.38	14.42	5.63	0.20	0.46	3.02	4.18	2.12	97.93
Hekla	1158	67.62	0.40	13.99	6.13	0.14	0.49	3.04	4.06	2.15	98.02
Hekla	1158	67.70	0.55	14.51	5.72	0.17	0.50	3.19	4.53	2.28	99.15
Hekla	1158	67.75	0.50	14.47	5.77	0.20	0.50	3.22	4.69	2.18	99.28
Hekla	1158	68.22	0.52	14.71	5.56	0.23	0.45	3.02	4.89	2.31	99.91
Hekla	1300	56.45	1.46	14.35	9.57	0.24	2.15	5.60	4.24	1.43	95.49
Hekla	1300	56.75	1.48	14.40	9.69	0.24	2.15	5.60	4.12	1.49	95.92
Hekla	1300	56.97	1.25	15.59	8.46	0.20	1.60	5.73	4.76	1.41	95.97
Hekla	1300	57.07	1.38	15.09	9.77	0.22	2.10	5.32	4.09	1.50	96.54
Hekla	1300	57.42	1.15	15.01	9.09	0.24	1.44	4.75	4.53	1.76	95.39
Hekla	1300	57.42	1.44	14.98	9.34	0.30	2.02	5.25	4.18	1.48	96.41
Hekla	1300	57.43	1.37	15.36	9.60	0.24	2.16	6.03	4.34	1.33	97.86
Hekla	1300	57.75	1.39	15.53	9.38	0.23	1.87	5.77	3.64	1.40	96.96
Hekla	1300	57.77	1.12	15.23	8.65	0.25	1.44	4.84	4.50	1.61	95.41
Hekla	1300	57.85	1.35	16.83	7.75	0.21	1.60	6.21	4.05	1.32	97.17
Hekla	1300	57.85	1.56	15.20	10.38	0.23	2.02	5.76	3.54	1.51	98.05
Hekla	1300	57.95	1.45	15.64	9.33	0.22	2.08	5.86	4.48	1.52	98.53
Hekla	1300	58.00	1.42	15.41	9.87	0.21	2.12	5.37	4.27	1.50	98.17
Hekla	1300	58.08	1.53	14.64	9.53	0.30	2.13	5.42	4.43	1.62	97.68
Hekla	1300	58.10	1.63	15.63	9.53	0.28	2.03	5.55	4.45	1.46	98.66
Hekla	1300	58.42	1.36	16.43	8.95	0.15	1.90	5.81	4.38	1.32	98.72
Hekla	1300	58.47	1.21	15.36	9.47	0.27	1.58	4.88	4.38	1.55	97.17
Hekla	1300	58.56	1.28	16.40	8.61	0.24	1.74	5.99	4.22	1.18	98.22
Hekla	1300	58.60	1.10	14.75	8.98	0.25	1.69	4.94	4.33	1.54	96.18
Hekla	1300	58.64	1.47	15.04	9.39	0.19	2.06	5.65	4.30	1.43	98.17
Hekla	1300	58.68	1.15	15.33	9.42	0.20	1.62	4.91	4.27	1.58	97.16

Hekla	1300	58.69	1.09	15.00	9.15	0.24	1.57	5.08	4.42	1.59	96.83
Hekla	1300	58.77	1.14	14.53	9.73	0.26	2.11	4.72	4.24	1.54	97.04
Hekla	1300	58.79	1.30	14.60	9.07	0.27	1.62	4.91	4.06	1.57	96.19
Hekla	1300	58.93	1.37	14.61	9.81	0.21	2.07	5.49	4.32	1.52	98.33
Hekla	1300	59.04	1.34	14.91	9.33	0.26	1.62	5.06	4.31	1.60	97.47
Hekla	1300	59.49	1.47	15.21	8.31	0.22	1.87	5.04	4.27	1.72	97.60
Hekla	1300	59.50	1.59	15.21	10.24	0.29	2.05	5.88	3.62	1.49	99.87
Hekla	1300	59.64	1.07	15.10	8.59	0.24	1.41	4.76	4.24	1.92	96.97
Hekla	1300	59.70	1.23	15.24	9.29	0.25	1.54	5.27	4.33	1.64	98.49
Hekla	1300	59.81	1.18	14.99	9.23	0.21	1.68	5.09	4.16	1.60	97.95
Hekla	1300	59.85	1.12	14.87	9.20	0.25	1.63	4.85	4.29	1.42	97.48
Hekla	1300	59.91	1.16	15.02	8.55	0.26	1.55	4.77	4.28	1.72	97.22
Hekla	1300	59.94	1.11	14.93	9.43	0.28	1.60	4.99	4.43	1.38	98.09
Hekla	1300	59.96	1.25	14.74	8.71	0.27	1.60	4.87	4.38	1.74	97.52
Hekla	1300	60.01	1.21	15.30	9.37	0.32	1.58	1.20	4.06	1.58	94.63
Hekla	1300	60.02	1.53	14.19	10.59	0.24	1.79	5.12	4.13	1.80	99.41
Hekla	1300	60.45	1.15	15.26	9.13	0.22	1.63	4.96	3.96	1.60	98.36
Hekla	1300	60.71	1.28	14.70	8.08	0.28	1.28	4.30	4.56	1.74	96.93
Hekla	1300	60.87	1.15	15.26	9.34	0.20	1.59	5.05	3.92	1.54	98.92
Hekla	1300	59.00	1.10	14.85	9.42	0.24	1.56	5.00	4.31	1.65	97.13
Hekla	1300	59.07	1.05	14.64	8.87	0.26	1.44	4.90	4.57	1.63	96.43
Hekla	1300	59.49	1.19	15.27	9.42	0.30	1.62	4.83	4.46	1.73	98.31
Hekla	1300	59.74	1.05	14.74	8.75	0.23	1.51	4.85	4.45	1.78	97.10
Hekla	1300	59.88	1.11	14.89	9.10	0.23	1.50	4.83	4.43	1.71	97.68
Hekla	1300	61.62	0.89	14.78	8.81	0.30	1.08	4.54	4.72	1.88	98.62
Katla	1357	47.65	4.46	13.72	11.89	0.28	3.76	8.96	2.45	0.78	93.95
Oraefajokull	1362	67.81	0.26	14.04	3.35		0.04	1.07	5.63	3.72	95.92
Oraefajokull	1362	68.24	0.27	13.68	3.21		0.01	0.99	5.61	3.81	95.82
Oraefajokull	1362	68.54	0.25	13.91	3.45		0.03	1.09	5.52	3.60	96.39
Oraefajokull	1362	69.00	0.24	13.31	3.07		0.03	1.06	5.00	3.58	95.29

Oraefajokull	1362	69.14	0.26	13.38	3.17		0.00	0.98	4.93	3.76	95.62
Oraefajokull	1362	69.47	0.23	13.10	3.08		0.05	0.98	4.93	3.21	95.05
Oraefajokull	1362	69.91	0.28	13.20	3.20		0.04	1.00	5.66	3.38	96.67
Oraefajokull	1362	70.11	0.32	13.36	3.23		0.07	1.00	5.54	3.45	97.08
Oraefajokull	1362	70.34	0.25	13.41	3.22		0.02	1.02	5.24	3.43	96.93
Oraefajokull	1362	70.36	0.26	12.06	3.27		0.02	1.00	4.91	3.19	95.07
Oraefajokull	1362	70.46	0.24	12.80	3.13	0.11	0.03	0.96	5.47	3.38	96.58
Oraefajokull	1362	70.47	0.22	12.91	3.02	0.05	0.06	0.98	5.50	3.49	96.70
Oraefajokull	1362	70.49	0.24	12.86	3.23	0.11	0.05	1.06	5.81	3.23	97.08
Oraefajokull	1362	70.53	0.25	13.01	3.12		0.00	0.97	4.11	3.51	95.50
Oraefajokull	1362	70.62	0.22	12.92	3.09	0.07	0.03	0.93	5.54	3.44	96.86
Oraefajokull	1362	70.66	0.23	13.30	3.05		0.05	0.81	4.81	3.61	96.52
Oraefajokull	1362	70.69	0.26	13.27	3.21		0.00	1.09	4.56	3.19	96.27
Oraefajokull	1362	70.88	0.20	13.99	3.05		0.15	1.86	4.84	2.71	97.68
Oraefajokull	1362	70.95	0.22	13.52	3.20		0.00	0.93	5.43	3.37	97.62
Oraefajokull	1362	71.02	0.22	13.22	3.07	0.08	0.04	0.96	5.40	3.18	97.19
Oraefajokull	1362	71.04	0.25	13.26	3.05	0.12	0.01	1.04	5.42	3.46	97.65
Oraefajokull	1362	71.07	0.29	13.41	3.08		0.00	1.03	4.13	3.33	96.34
Oraefajokull	1362	71.07	0.24	13.13	3.07		0.04	0.87	4.62	3.70	96.74
Oraefajokull	1362	71.18	0.21	13.25	3.02	0.07	0.05	1.09	5.55	3.54	97.96
Oraefajokull	1362	71.21	0.23	13.20	3.18		0.06	1.00	4.90	3.30	97.08
Oraefajokull	1362	71.25	0.23	13.07	3.14	0.11	0.04	0.89	5.67	3.20	97.60
Oraefajokull	1362	71.32	0.23	12.81	3.08	0.12	0.03	1.04	5.47	3.28	97.38
Oraefajokull	1362	71.51	0.29	13.50	3.14		0.04	0.95	4.62	3.27	97.32
Oraefajokull	1362	71.66	0.25	13.34	3.07		0.03	0.95	5.01	3.82	98.13
Oraefajokull	1362	71.66	0.31	13.62	3.19		0.02	0.98	5.25	3.40	98.43
Oraefajokull	1362	71.68	0.28	13.28	2.95		0.00	0.92	5.38	3.44	97.93
Oraefajokull	1362	71.85	0.22	13.37	3.25	0.09	0.05	0.90	5.30	3.43	98.46
Oraefajokull	1362	71.87	0.16	13.49	3.28	0.10	0.02	0.99	5.61	3.44	98.96
Oraefajokull	1362	71.92	0.24	13.51	3.09		0.03	0.87	4.86	3.75	98.27

Oraefajokull	1362	72.05	0.21	12.98	2.99	0.07	0.00	0.90	5.69	3.50	98.39
Oraefajokull	1362	72.07	0.22	13.43	3.26	0.19	0.01	1.05	5.46	3.52	99.21
Oraefajokull	1362	72.13	0.21	13.43	3.10		0.00	0.89	4.93	3.61	98.30
Oraefajokull	1362	72.25	0.31	12.73	3.30		0.01	1.01	5.38	3.20	98.19
Oraefajokull	1362	72.27	0.27	13.57	3.11		0.00	0.91	4.90	3.02	98.05
Oraefajokull	1362	72.28	0.30	13.52	3.16		0.00	1.01	5.56	3.48	99.31
Oraefajokull	1362	72.32	0.22	13.10	3.08	0.08	0.03	0.99	5.64	3.37	98.83
Oraefajokull	1362	72.33	0.24	13.37	3.25		0.05	1.00	5.24	3.31	98.79
Oraefajokull	1362	72.35	0.27	13.61	3.19		0.00	1.00	4.84	3.49	98.75
Oraefajokull	1362	72.36	0.21	13.60	3.16	0.12	0.05	0.95	5.73	3.31	99.49
Oraefajokull	1362	72.49	0.30	13.69	3.26		0.06	1.00	5.17	3.22	99.19
Oraefajokull	1362	72.50	0.26	13.36	2.95		0.04	0.81	5.69	3.33	98.94
Oraefajokull	1362	72.55	0.29	14.09	1.55		0.42	1.90	4.10	3.01	97.91
Oraefajokull	1362	72.56	0.23	13.63	3.14		0.04	0.98	5.13	3.19	98.90
Oraefajokull	1362	72.60	0.26	13.62	3.25		0.04	1.01	5.13	3.64	99.55
Oraefajokull	1362	72.62	0.25	13.61	3.13		0.04	1.08	5.12	3.40	99.25
Oraefajokull	1362	72.71	0.27	13.46	3.13		0.04	1.03	5.13	3.53	99.30
Oraefajokull	1362	72.71	0.26	13.89	3.06		0.04	0.98	5.32	3.51	99.77
Oraefajokull	1362	72.73	0.33	13.10	3.34		0.03	1.01	5.16	3.25	98.95
Oraefajokull	1362	72.74	0.24	13.59	3.19		0.00	1.06	5.28	3.54	99.64
Oraefajokull	1362	72.76	0.23	13.55	3.17		0.03	0.89	5.03	3.78	99.44
Oraefajokull	1362	72.86	0.25	13.33	3.00		0.00	0.99	5.20	3.48	99.11
Oraefajokull	1362	72.88	0.31	13.80	3.23		0.00	1.00	4.99	3.66	99.87
Oraefajokull	1362	72.94	0.27	13.56	3.03		0.04	0.96	5.61	3.45	99.86
Oraefajokull	1362	73.01	0.26	13.42	3.17		0.00	0.94	5.38	3.46	99.64
Oraefajokull	1362	73.10	0.33	13.44	3.43		0.02	1.06	5.08	3.31	99.77
Oraefajokull	1362	73.12	0.26	13.81	2.96		0.04	0.84	4.77	3.66	99.46
Oraefajokull	1362	73.19	0.27	13.40	3.00		0.00	0.96	5.28	3.55	99.65
Oraefajokull	1362	73.21	0.29	13.13	3.32		0.01	0.99	5.27	3.29	99.51
Oraefajokull	1362	73.39	0.27	13.88	3.28		0.05	0.97	4.45	3.26	99.55

Oraefajokull	1362	73.39	0.31	13.51	3.36		0.05	0.95	4.78	3.30	99.65
Oraefajokull	1362	73.44	0.29	12.88	3.26		0.04	1.01	5.10	3.28	99.30
Veidivotn	1477	49.63	1.87	13.56	12.48	0.24	6.52	11.33	2.51	0.23	98.38
Veidivotn	1477	49.84	1.92	13.50	12.51	0.23	6.39	11.47	2.40	0.23	98.48
Veidivotn	1477	49.65	1.91	13.46	12.34	0.24	6.35	11.48	2.39	0.24	98.06
Veidivotn	1477	49.86	1.87	13.55	12.56	0.20	6.57	11.50	2.45	0.23	98.79
Veidivotn	1477	49.44	1.84	13.52	12.44	0.26	6.54	11.42	2.46	0.24	98.16
Veidivotn	1477	49.64	1.88	13.49	12.32	0.23	6.54	11.56	2.49	0.22	98.36
Veidivotn	1477	50.32	1.83	13.96	12.32	0.21	6.60	11.43	2.46	0.23	99.36
Veidivotn	1477	50.16	1.84	13.79	12.62	0.24	6.68	11.52	2.47	0.24	99.56
Veidivotn	1477	50.30	1.84	13.84	12.65	0.19	6.54	11.46	2.43	0.24	99.49
Veidivotn	1477	50.00	1.86	13.85	12.81	0.24	6.68	11.55	2.49	0.24	99.72
Veidivotn	1477	50.60	1.87	13.90	12.59	0.20	6.70	11.56	2.46	0.23	100.11
Veidivotn	1477	50.33	1.87	13.87	12.75	0.22	6.58	11.42	2.48	0.25	99.77
Veidivotn	1477	49.55	1.86	13.77	12.84	0.24	6.64	11.58	2.46	0.22	99.15
Veidivotn	1477	50.09	1.88	13.72	12.79	0.19	6.53	11.37	2.50	0.22	99.29
Veidivotn	1477	50.38	1.89	13.86	12.56	0.21	6.59	11.50	2.40	0.25	99.63
Veidivotn	1477	50.34	1.90	13.84	12.70	0.22	6.59	11.47	2.47	0.22	99.76
Veidivotn	1477	50.40	1.90	13.87	12.51	0.23	6.60	11.39	2.41	0.23	99.54
Veidivotn	1477	49.87	1.91	13.75	13.01	0.22	6.49	11.42	2.45	0.22	99.33
Veidivotn	1477	50.17	1.92	13.78	12.84	0.20	6.59	11.52	2.56	0.25	99.82
Veidivotn	1477	50.14	1.95	13.82	12.78	0.20	6.55	11.38	2.47	0.26	99.54
Veidivotn	1477	50.29	1.96	13.85	13.08	0.18	6.32	11.17	2.42	0.26	99.54
Veidivotn	1477	50.06	2.68	13.51	14.38	0.26	6.03	9.95	2.80	0.33	100.00
Veidivotn	1477	49.67	2.91	12.93	14.47	0.24	5.44	9.99	2.80	0.40	98.84
Veidivotn	1477	49.87	3.23	12.64	15.84	0.26	4.79	9.75	2.49	0.47	99.34
Veidivotn	1477	51.68	2.52	13.24	14.24	0.25	4.58	8.51	2.96	0.60	98.59
Veidivotn	1477	49.73	1.58	13.37	10.68	0.19	7.25	12.25	2.21	0.16	97.43
Veidivotn	1477	50.67	1.79	13.50	12.53	0.22	6.36	11.29	2.44	0.24	99.03
Veidivotn	1477	49.60	1.83	13.70	12.67	0.21	6.57	11.39	2.60	0.27	98.83

Veidivotn	1477	49.76	1.85	13.48	12.67	0.23	6.30	11.31	2.64	0.23	98.46
Veidivotn	1477	49.28	1.86	13.26	12.52	0.22	6.32	11.37	2.56	0.26	97.66
Veidivotn	1477	49.46	1.89	13.72	12.87	0.22	6.28	11.29	2.45	0.25	98.42
Veidivotn	1477	49.36	1.89	13.12	13.11	0.24	6.52	11.33	2.31	0.21	98.09
Veidivotn	1477	50.19	1.91	13.37	12.49	0.22	6.36	11.28	2.71	0.25	98.77
Veidivotn	1477	50.38	1.91	13.33	12.42	0.22	6.43	11.32	2.40	0.25	98.66
Veidivotn	1477	49.57	1.91	13.76	12.71	0.21	6.51	11.31	2.44	0.21	98.65
Veidivotn	1477	49.36	1.92	13.68	12.69	0.23	6.47	11.16	2.57	0.26	98.34
Veidivotn	1477	50.02	1.92	13.11	12.72	0.23	6.50	11.11	2.55	0.22	98.40
Veidivotn	1477	49.72	1.93	12.84	12.93	0.22	6.52	11.39	2.45	0.25	98.26
Veidivotn	1477	49.24	1.93	13.81	12.68	0.22	6.32	11.36	2.57	0.28	98.41
Veidivotn	1477	46.83	3.84	13.15	14.61	0.26	6.03	10.66	2.66	0.50	98.54
Hekla	1510	57.59	1.33	14.78	9.59	0.26	1.99	5.33	4.05	1.49	96.41
Hekla	1510	59.68	0.93	15.30	7.55	0.18	0.91	4.70	5.01	1.85	96.11
Hekla	1510	60.01	0.99	13.36	8.49	0.26	1.75	4.58	4.47	1.75	95.66
Hekla	1510	60.39	0.55	17.43	5.36	0.20	0.81	5.86	5.56	1.18	97.34
Hekla	1510	60.64	0.89	15.11	7.53	0.24	1.20	4.46	4.23	1.69	95.99
Hekla	1510	60.77	1.57	16.53	7.89	0.20	0.89	5.48	5.25	1.36	99.94
Hekla	1510	60.79	0.94	14.84	7.61	0.22	1.27	4.31	4.25	1.68	95.91
Hekla	1510	60.79	1.01	15.08	7.60	0.22	1.25	4.59	4.55	1.82	96.91
Hekla	1510	60.90	0.88	14.30	7.53	0.18	1.19	4.30	4.11	1.68	95.07
Hekla	1510	61.23	0.89	14.69	7.72	0.20	1.17	4.28	4.42	1.69	96.29
Hekla	1510	61.29	0.88	15.13	8.40	0.29	1.17	4.26	4.60	1.74	97.76
Hekla	1510	61.51	0.96	14.82	8.11	0.26	1.25	4.70	4.25	1.62	97.48
Hekla	1510	61.55	0.90	15.07	7.69	0.25	1.24	4.49	4.36	1.70	97.25
Hekla	1510	61.64	1.01	16.74	7.93		1.33	4.48	4.62	1.67	99.42
Hekla	1510	61.72	0.96	14.93	7.86	0.26	1.25	4.74	4.57	1.68	97.97
Hekla	1510	61.78	0.92	15.06	6.85	0.19	0.85	4.19	4.38	1.69	95.91
Hekla	1510	61.78	0.97	16.47	7.79		1.30	4.38	4.44	1.63	98.76
Hekla	1510	61.80	0.89	16.70	6.62		1.01	4.68	4.51	1.63	97.84

Hekla	1510	61.85	1.02	15.92	7.76		1.25	4.57	4.46	1.69	98.52
Hekla	1510	61.90	1.02	15.63	7.83		1.33	4.42	5.17	1.65	98.95
Hekla	1510	61.93	0.87	15.19	7.69	0.19	1.16	4.39	3.89	1.75	97.06
Hekla	1510	61.95	0.93	14.88	8.08	0.12	1.30	4.46	4.34	1.68	97.74
Hekla	1510	61.95	0.93	15.13	7.87	0.21	1.26	4.55	4.73	1.74	98.37
Hekla	1510	61.98	0.99	15.18	7.98	0.24	1.34	4.55	4.28	1.77	98.31
Hekla	1510	62.13	0.96	14.84	7.58	0.29	1.34	4.36	4.68	1.75	97.93
Hekla	1510	62.16	0.92	15.11	8.52	0.30	1.17	4.47	4.45	1.73	98.83
Hekla	1510	62.17	0.86	15.30	8.39	0.24	1.22	4.41	4.43	1.67	98.69
Hekla	1510	62.17	0.95	15.16	8.87	0.23	1.13	4.58	4.59	1.76	99.44
Hekla	1510	62.19	1.01	16.13	7.99		1.26	4.51	4.14	2.85	100.08
Hekla	1510	62.21	0.94	14.96	7.56	0.22	1.19	4.18	4.08	1.77	97.11
Hekla	1510	62.29	0.95	15.17	7.45	0.30	1.25	4.54	4.42	1.71	98.08
Hekla	1510	62.34	0.91	15.12	7.86	0.26	1.26	4.47	4.52	1.65	98.39
Hekla	1510	62.34	0.97	14.95	7.81	0.22	1.42	4.55	4.52	1.70	98.48
Hekla	1510	62.37	0.84	15.00	8.14	0.29	1.69	5.26	4.23	1.40	99.22
Hekla	1510	62.53	1.03	14.83	8.03	0.25	1.30	4.45	4.28	1.61	98.31
Hekla	1510	62.59	0.81	15.09	8.49	0.27	1.33	4.76	4.81	1.63	99.78
Hekla	1510	62.68	0.77	15.01	7.76	0.26	1.32	4.46	4.69	1.78	98.73
Hekla	1510	62.70	1.03	15.57	7.60	0.25	1.32	4.46	4.63	1.59	99.15
Hekla	1510	62.76	0.98	15.25	7.91	0.20	1.37	4.75	4.53	1.74	99.49
Hekla	1510	62.82	0.97	15.40	8.04	0.22	1.29	4.46	4.58	1.79	99.57
Hekla	1510	62.84	1.01	15.03	7.89	0.21	1.36	4.55	4.45	1.76	99.10
Hekla	1510	63.02	0.94	15.17	8.14	0.22	1.47	4.70	3.74	1.75	99.15
Hekla	1510	63.05	0.94	15.12	7.65	0.27	1.33	4.75	4.43	1.82	99.36
Hekla	1510	63.05	0.97	15.44	7.89	0.24	1.39	4.28	4.50	1.69	99.45
Hekla	1510	63.30	1.01	15.25	8.51	0.21	1.27	4.44	4.08	1.63	99.70
Hekla	1510	63.33	0.89	14.70	8.42	0.21	1.36	4.48	4.33	1.68	99.40
Hekla	1510	63.42	0.93	15.15	8.00	0.22	1.29	4.44	4.55	1.75	99.75
Hekla	1510	63.44	1.02	15.24	7.86	0.21	1.34	4.69	4.21	1.77	99.78

Hekla	1510	63.54	0.88	15.15	7.43	0.20	1.29	4.61	4.38	1.87	99.35
Hekla	1510	63.61	0.95	15.11	7.53	0.23	1.25	4.65	4.18	1.66	99.17
Hekla	1510	63.61	1.07	15.56	7.65	0.23	1.19	4.21	4.48	1.83	99.83
Hekla	1510	63.66	0.92	15.27	8.12	0.20	1.26	4.42	4.17	1.70	99.72
Hekla	1510	63.71	0.98	15.26	7.94	0.22	1.37	4.43	4.06	1.71	99.68
Hekla	1510	63.84	0.83	14.88	8.03	0.28	1.03	4.32	4.70	1.79	99.70
Hekla	1510	63.99	1.01	15.23	7.35	0.21	1.31	4.34	4.25	1.69	99.38
Hekla	1510	64.20	1.04	14.49	7.99	0.22	1.21	4.36	4.33	1.72	99.56
Hekla	1510	71.49	0.26	14.51	3.25		0.13	1.93	4.57	1.68	97.82
Hekla	1510	72.85	0.25	15.09	0.98		0.13	1.91	4.35	1.65	97.21
Hekla	1693	57.64	1.30	14.93	9.71	0.25	1.95	5.28	4.33	1.53	96.92
Hekla	1693	57.81	1.38	15.14	9.82	0.29	1.97	5.41	4.26	1.59	97.67
Hekla	1693	57.87	1.35	15.08	9.78	0.30	1.96	5.43	4.51	1.55	97.83
Hekla	1693	57.98	1.32	15.08	9.56	0.32	1.93	5.33	4.35	1.54	97.41
Hekla	1693	58.07	1.37	15.01	10.00	0.32	1.92	5.32	4.39	1.50	97.90
Hekla	1693	58.18	1.32	14.96	9.64	0.21	1.88	5.27	4.37	1.45	97.28
Hekla	1693	58.24	1.36	15.04	10.01	0.30	1.98	5.35	4.39	1.58	98.25
Hekla	1693	58.27	1.33	14.99	9.79	0.26	1.97	5.31	4.48	1.58	97.98
Hekla	1693	58.42	1.34	15.23	9.71	0.27	1.95	5.42	4.45	1.58	98.37
Hekla	1693	58.74	1.29	15.17	9.43	0.27	1.89	5.33	4.48	1.51	98.11
Katla	1721	49.10	4.52	13.42	14.28	0.23	5.00	9.86	3.01	0.73	100.15
Katla	1721	48.04	1.90	13.93	12.26	0.18	6.86	12.08	2.19	0.24	97.68
Katla	1721	47.13	2.56	15.77	11.99	0.16	7.07	11.43	1.92	0.55	98.58
Katla	1721	63.49	0.93	15.78	6.86	0.31	1.33	4.53	2.32	1.68	97.23
Katla	1721	49.41	1.68	13.37	12.45	0.24	6.45	12.15	2.48	0.17	98.40
Katla	1721	47.58	4.00	12.62	14.28	0.25	5.01	10.15	2.59	0.67	97.15
Katla	1721	67.97	1.05	13.97	5.69	0.22	1.00	2.97	1.46	2.41	96.74
Katla	1721	75.76	0.11	11.89	2.85	0.05	0.00	0.42	0.96	1.11	93.15
Katla	1721	46.88	4.45	12.41	14.68	0.24	4.98	9.65	2.75	0.52	96.56
Katla	1721	48.32	1.28	14.90	10.35	0.23	8.25	13.74	1.95	0.05	99.07

Katla	1721	49.79	1.87	13.64	12.07	0.19	6.79	12.91	2.37	0.18	99.81
Katla	1721	56.69	1.63	14.78	10.71	0.30	1.43	6.78	5.09	1.34	98.75
Katla	1721	56.31	1.13	12.76	13.42	0.26	3.09	6.40	4.66	0.80	98.83
Katla	1721	47.00	4.60	12.35	15.17	0.27	4.96	9.66	3.20	0.67	97.89
Katla	1721	47.07	4.64	12.38	14.61	0.24	4.95	9.68	3.12	0.69	97.39
Katla	1721	46.88	4.65	12.25	15.05	0.26	4.83	9.67	3.01	0.65	97.25
Katla	1721	46.88	4.71	12.45	14.97	0.21	4.98	9.71	3.04	0.68	97.63
Katla	1721	46.82	4.63	12.21	14.85	0.24	4.88	9.63	3.12	0.71	97.10
Katla	1721	46.69	4.77	12.47	14.96	0.22	5.00	9.74	3.17	0.69	97.72
Katla	1721	47.05	4.72	12.52	14.57	0.21	4.91	9.59	3.01	0.68	97.26
Katla	1721	47.40	4.81	12.46	15.52	0.24	4.60	9.40	3.14	0.69	98.26
Katla	1721	46.78	4.68	12.31	15.10	0.25	4.96	9.64	3.10	0.71	97.54
Katla	1721	46.66	4.68	12.43	15.03	0.27	4.89	9.74	3.06	0.68	97.43
Katla	1721	47.26	4.63	13.03	14.66	0.24	4.73	9.65	3.05	0.71	97.96
Katla	1721	46.39	4.65	13.06	14.63	0.25	4.95	9.73	2.93	0.70	97.28
Katla	1721	47.71	4.37	13.79	14.53	0.23	4.53	9.77	3.16	0.69	98.77
Katla	1721	48.12	4.37	13.26	14.66	0.23	4.76	9.37	2.98	0.89	98.63
Katla	1721	48.60	4.39	13.02	13.93	0.23	4.67	9.20	3.14	0.87	98.05
Katla	1721	46.95	4.41	12.68	14.46	0.24	4.85	9.21	3.13	0.81	96.75
Katla	1721	47.71	4.45	13.05	14.58	0.23	4.84	9.43	3.04	0.82	98.15
Katla	1721	47.87	4.47	12.94	14.66	0.23	4.63	9.31	3.23	0.85	98.20
Katla	1721	47.59	4.51	12.86	14.22	0.24	4.88	9.21	3.24	0.83	97.58
Katla	1721	47.08	4.51	12.91	14.84	0.24	4.71	9.40	3.05	0.90	97.64
Katla	1721	47.31	4.53	12.49	14.83	0.23	4.80	9.15	3.08	0.82	97.23
Katla	1721	47.10	4.54	12.93	14.75	0.22	4.84	9.37	3.13	0.88	97.76
Katla	1721	47.70	4.65	12.88	14.54	0.22	4.74	9.43	3.12	0.91	98.19
Katla	1721	49.18	4.30	13.83	14.07	0.27	4.36	9.61	3.26	0.87	99.77
Katla	1721	47.56	4.41	14.29	14.37	0.18	4.72	9.33	3.09	0.84	98.78
Katla	1721	47.70	4.43	13.28	14.54	0.22	4.87	9.51	3.11	0.85	98.51
Katla	1721	47.91	4.43	13.18	14.45	0.22	4.81	9.48	3.01	0.81	98.30

Katla	1721	47.72	4.43	13.07	14.50	0.21	4.87	9.49	3.01	0.84	98.14
Katla	1721	47.94	4.46	13.14	14.44	0.22	4.82	9.49	2.99	0.83	98.34
Katla	1721	48.14	4.51	13.28	14.66	0.19	4.76	9.66	3.16	0.85	99.21
Katla	1721	48.23	4.50	13.27	14.43	0.21	4.87	9.60	3.04	0.83	98.98
Katla	1721	47.80	4.48	13.11	14.60	0.17	4.86	9.45	3.10	0.84	98.41
Katla	1721	48.27	4.49	13.10	14.37	0.18	4.75	9.53	3.06	0.83	98.58
Katla	1721	48.02	4.50	13.25	14.67	0.21	4.91	9.47	2.92	0.80	98.75
Katla	1721	47.57	4.48	13.04	14.56	0.21	4.85	9.40	3.12	0.86	98.08
Katla	1721	47.86	4.51	13.31	14.61	0.23	4.84	9.54	3.12	0.86	98.87
Katla	1721	47.81	4.51	13.19	14.52	0.21	4.80	9.53	3.02	0.82	98.41
Katla	1721	47.99	4.55	13.19	14.75	0.24	4.89	9.45	3.06	0.86	98.97
Katla	1721	47.72	4.52	13.20	14.31	0.25	4.84	9.54	3.01	0.85	98.24
Katla	1721	48.23	4.60	13.27	14.95	0.24	4.93	9.65	3.03	0.82	99.72
Katla	1721	48.01	4.54	13.21	14.21	0.21	4.81	9.51	2.99	0.85	98.32
Katla	1721	47.44	4.53	13.05	14.29	0.22	4.84	9.57	3.10	0.85	97.89
Oraefajokull	1727	56.92	1.51	13.83	12.76	0.39	1.37	5.08	4.71	1.50	98.07
Oraefajokull	1727	56.97	1.56	13.73	12.34	0.31	1.29	5.21	4.80	1.56	97.77
Oraefajokull	1727	57.45	1.45	13.80	12.72	0.33	1.36	5.11	4.67	1.58	98.47
Oraefajokull	1727	57.47	1.94	12.52	14.13	0.49	1.63	5.25	4.00	1.84	99.27
Oraefajokull	1727	57.62	1.67	14.00	13.11	0.34	1.44	5.20	4.57	1.67	99.62
Oraefajokull	1727	57.67	1.72	13.39	13.09	0.33	1.56	5.27	4.07	1.76	98.86
Oraefajokull	1727	57.72	1.59	14.05	12.14	0.40	1.32	5.10	3.37	1.56	97.25
Oraefajokull	1727	57.72	1.72	13.50	13.63	0.43	1.30	5.51	4.67	1.37	99.85
Oraefajokull	1727	57.80	1.58	13.90	12.83	0.44	1.40	5.29	4.57	1.62	99.43
Oraefajokull	1727	57.83	1.58	14.03	12.71	0.34	1.34	5.14	4.83	1.59	99.39
Oraefajokull	1727	57.84	1.55	13.42	12.43	0.38	1.47	5.37	4.53	1.73	98.72
Oraefajokull	1727	57.93	1.71	13.15	13.04	0.39	1.49	5.06	4.36	1.75	98.88
Oraefajokull	1727	57.94	1.50	13.26	12.24	0.31	1.32	5.30	4.55	1.66	98.08
Oraefajokull	1727	58.00	1.35	14.71	11.99	0.36	1.15	5.53	5.15	1.52	99.76
Oraefajokull	1727	58.03	1.76	13.43	12.97	0.40	1.45	5.24	4.30	1.59	99.17

Oraefajokull	1727	58.43	1.70	13.86	12.18	0.26	1.40	5.12	4.03	1.73	98.71
Oraefajokull	1727	58.50	1.65	13.60	12.68	0.37	1.44	5.20	4.25	1.59	99.28
Oraefajokull	1727	58.60	1.70	13.28	12.66	0.37	1.19	5.10	4.21	1.55	98.66
Oraefajokull	1727	59.98	1.46	13.93	11.75	0.34	1.13	4.83	4.26	1.73	99.41
Hekla	1766	60.10	1.13	15.07	9.08	0.25	1.58	5.03	4.42	1.46	98.12
Hekla	1766	60.27	1.14	15.02	9.69	0.30	1.69	5.13	4.35	1.50	99.09
Hekla	1766	58.11	1.44	15.14	10.37	0.25	2.13	5.77	4.22	1.29	98.72
Hekla	1766	60.32	1.13	14.97	9.13	0.26	1.54	4.99	4.41	1.48	98.23
Hekla	1766	59.70	1.17	14.99	9.46	0.27	1.58	5.20	4.34	1.46	98.18
Hekla	1766	60.92	1.05	15.19	8.88	0.25	1.45	5.14	4.49	1.49	98.84
Hekla	1766	60.11	1.11	14.99	9.13	0.27	1.48	5.06	4.34	1.49	97.98
Laki	1783	50.32	1.71	13.90	12.32	0.26	7.03	11.88	2.53	0.19	100.14
Laki	1783	48.88	2.44	13.88	13.31	0.27	6.34	11.60	2.55	0.28	99.55
Laki	1783	49.51	2.66	13.52	13.78	0.23	5.99	10.74	2.54	0.34	99.31
Laki	1783	50.42	3.06	13.19	14.62	0.27	5.23	9.89	2.77	0.47	99.92
Laki	1783	50.44	3.20	13.03	14.44	0.23	5.20	9.90	2.92	0.47	99.83
Laki	1783	50.48	3.11	12.98	14.57	0.26	5.10	10.04	2.62	0.49	99.65
Laki	1783	50.30	3.18	12.81	15.00	0.22	4.99	9.95	2.91	0.49	99.85
Laki	1783	49.45	3.14	13.07	14.53	0.24	5.19	10.02	2.83	0.49	98.96
Laki	1783	50.70	2.99	13.19	14.79	0.24	5.46	10.07	2.74	0.45	100.63
Laki	1783	50.09	3.63	11.72	16.31	0.41	4.61	9.47	2.72	0.42	99.38
Eyjafjoll	1821	68.31	0.35	13.79	4.38	0.15	0.12	1.00	6.04	3.50	97.64
Eyjafjoll	1821	68.37	0.38	13.95	4.51	0.14	0.14	1.18	6.42	3.34	98.43
Eyjafjoll	1821	68.43	0.38	14.47	4.39	0.18	0.14	1.10	6.62	3.57	99.28
Eyjafjoll	1821	68.55	0.35	14.28	4.32	0.13	0.14	1.13	6.38	3.56	98.84
Eyjafjoll	1821	68.60	0.41	13.77	4.59	0.12	0.16	1.27	6.12	3.55	98.59
Eyjafjoll	1821	68.64	0.38	14.12	4.41	0.18	0.11	1.17	6.18	3.54	98.73
Eyjafjoll	1821	68.79	0.32	14.63	3.94	0.11	0.12	1.11	7.06	3.15	99.23
Eyjafjoll	1821	68.94	0.35	14.06	4.81	0.18	0.16	1.32	6.41	3.31	99.54
Eyjafjoll	1821	69.02	0.31	14.67	3.79	0.10	0.08	1.04	6.44	3.25	98.70

Eyjafjoll	1821	69.03	0.36	14.20	4.06	0.14	0.15	1.05	6.42	3.93	99.34
Eyjafjoll	1821	69.04	0.37	14.38	4.39	0.13	0.08	1.08	3.53	3.54	96.54
Eyjafjoll	1821	69.08	0.30	13.83	4.35	0.15	0.21	1.27	5.89	3.50	98.58
Eyjafjoll	1821	69.12	0.45	13.64	4.53	0.18	0.19	1.36	6.20	3.34	99.01
Eyjafjoll	1821	69.30	0.30	14.03	4.10	0.12	0.10	0.80	6.21	3.69	98.65
Eyjafjoll	1821	69.38	0.37	13.88	4.18	0.15	0.11	1.14	5.59	3.61	98.41
Eyjafjoll	1821	69.64	0.38	13.87	3.97	0.17	0.09	0.77	6.84	3.58	99.31
Eyjafjoll	1821	69.68	0.34	14.14	4.46	0.21	0.17	1.12	6.14	3.47	99.73
Eyjafjoll	1821	69.99	0.43	14.06	4.39	0.17	0.09	1.18	5.89	3.41	99.61
Eyjafjoll	1821	70.13	0.45	14.20	3.75	0.09	0.05	0.77	6.68	3.45	99.57
Eyjafjoll	1821	70.49	0.31	14.07	4.38	0.13	0.10	1.14	5.68	3.64	99.94
Hekla	1845	58.30	1.03	15.58	8.90	0.27	2.53	5.75	4.24	1.08	97.68
Hekla	1845	59.85	0.97	14.99	8.33	0.21	1.62	4.77	4.29	1.50	96.53
Hekla	1845	60.19	1.10	15.13	8.39	0.27	1.61	5.05	4.41	1.49	97.64
Hekla	1845	60.32	1.10	15.14	9.00	0.37	1.70	5.12	4.41	1.53	98.69
Hekla	1845	60.37	1.17	15.41	8.59	0.23	1.69	4.86	4.18	1.59	98.09
Hekla	1845	60.79	0.99	14.99	8.13	0.24	1.40	4.62	4.03	1.86	97.05
Hekla	1845	60.93	1.03	15.15	8.73	0.29	1.72	5.27	4.31	1.66	99.09
Hekla	1845	62.60	0.79	13.96	9.07	0.31	0.84	4.25	4.80	1.35	97.97
Hekla	1845	63.45	0.67	14.79	8.65	0.55	0.71	4.33	5.07	1.51	99.73
Hekla	1845	66.15	0.31	15.03	5.56	0.21	0.53	3.25	4.39	1.86	97.29
Askja	1875	68.88	0.93	14.98	3.57		0.77	2.59	3.59	2.31	97.62
Askja	1875	70.94	0.96	13.23	3.92		0.81	2.71	3.77	2.30	98.64
Askja	1875	71.02	0.81	12.37	3.63		0.71	2.54	3.34	2.35	96.77
Askja	1875	71.33	0.88	12.72	3.55	0.11	0.70	2.57	3.56	2.36	97.78
Askja	1875	71.35	0.84	12.20	3.44	0.10	0.64	2.39	3.35	2.57	96.88
Askja	1875	71.50	0.76	12.25	3.47	0.10	0.71	2.33	3.64	2.22	96.98
Askja	1875	71.61	0.90	12.69	3.93		0.70	2.44	3.49	2.35	98.11
Askja	1875	71.83	0.69	12.58	3.43	0.13	0.67	2.31	3.23	2.34	97.21
Askja	1875	71.88	0.92	12.85	3.83		0.74	2.59	3.59	2.43	98.83

Askja	1875	71.93	0.82	12.48	3.43	0.07	0.58	2.23	3.16	2.51	97.21
Askja	1875	71.94	0.93	12.58	3.40		0.71	2.51	3.51	2.39	97.97
Askja	1875	72.00	0.96	12.86	3.76		0.87	3.00	4.16	2.25	99.86
Askja	1875	72.04	0.79	12.08	3.34	0.09	0.66	2.43	3.35	2.37	97.15
Askja	1875	72.07	0.83	12.30	2.88	0.08	0.53	1.97	3.53	2.56	96.75
Askja	1875	72.14	0.79	12.66	3.23	0.10	0.63	2.29	3.53	2.46	97.83
Askja	1875	72.19	0.84	12.32	3.30	0.14	0.61	2.36	3.58	2.62	97.96
Askja	1875	72.20	0.80	12.52	3.40	0.11	0.69	2.35	3.40	2.32	97.79
Askja	1875	72.20	0.72	12.50	3.30	0.18	0.67	2.30	3.60	2.24	97.71
Askja	1875	72.21	0.77	12.69	3.42	0.09	0.65	2.30	3.18	2.38	97.69
Askja	1875	72.24	0.74	12.16	3.06	0.10	0.62	2.33	3.05	2.56	96.86
Askja	1875	72.30	0.86	12.60	3.77		0.73	2.39	3.48	2.49	98.62
Askja	1875	72.55	0.75	12.26	3.23	0.08	0.58	2.12	3.30	2.54	97.41
Askja	1875	72.55	0.87	12.94	3.86		0.74	2.50	3.44	2.37	99.27
Askja	1875	72.61	0.70	12.33	3.17	0.16	0.65	2.38	3.45	2.44	97.89
Askja	1875	72.73	0.83	12.47	2.93	0.12	0.60	2.32	3.27	2.45	97.72
Askja	1875	72.79	0.85	13.03	3.75		0.79	2.71	3.73	2.33	99.98
Askja	1875	72.84	0.80	12.36	3.10	0.09	0.59	2.09	3.28	2.48	97.63
Askja	1875	72.90	0.89	12.61	3.76		0.75	2.42	3.48	2.20	99.01
Askja	1875	73.09	0.86	12.59	3.82		0.69	2.53	3.63	2.39	99.60
Askja	1875	73.17	0.82	12.66	3.69		0.65	2.26	3.20	2.55	99.00
Askja	1875	73.25	0.85	12.57	4.07		0.78	2.38	3.46	2.37	99.73
Askja	1875	73.33	0.85	12.58	3.92		0.72	2.29	3.48	2.42	99.59
Askja	1875	73.52	0.85	12.85	3.72		0.64	2.30	3.34	2.51	99.73
Askja	1875	73.56	0.81	12.60	3.95		0.69	2.02	3.45	2.34	99.42
Askja	1875	73.78	0.82	12.64	3.34	0.13	0.68	2.40	3.38	2.38	99.55
? MOR-T2	ca. AD 1400	61.03	0.45	17.07	3.58	0.23	0.34	0.63	6.49	5.29	95.11

? T2	MOR-	ca. AD 1400	61.42	0.41	16.69	3.48	0.27	0.27	0.76	6.78	5.40	95.48
? T2	MOR-	ca. AD 1400	61.85	0.39	16.53	3.36	0.27	0.24	0.75	6.40	5.45	95.24
? T2	MOR-	ca. AD 1400	61.99	0.47	16.84	3.71	0.28	0.30	0.58	6.78	5.52	96.47
? T2	MOR-	ca. AD 1400	62.07	0.47	17.25	3.70	0.24	0.33	0.61	6.77	5.58	97.02
? T2	MOR-	ca. AD 1400	62.20	0.43	16.81	3.61	0.37	0.34	0.70	5.54	5.58	95.58
? T2	MOR-	ca. AD 1400	62.32	0.90	16.94	3.34	0.18	0.30	0.83	6.59	5.40	96.80
? T2	MOR-	ca. AD 1400	62.41	0.75	16.84	3.37	0.25	0.31	0.68	6.91	5.38	96.90
? T2	MOR-	ca. AD 1400	62.45	0.44	16.84	3.40	0.21	0.35	1.27	6.19	5.54	96.69
? T2	MOR-	ca. AD 1400	62.45	0.43	17.00	3.45	0.28	0.28	1.41	6.97	5.18	97.45
? T2	MOR-	ca. AD 1400	62.62	0.46	16.89	3.50	0.16	0.33	0.70	6.91	5.55	97.12

? T2	MOR-	ca. AD 1400	62.77	0.42	16.99	3.40	0.30	0.32	0.74	7.00	5.81	97.75
? T2	MOR-	ca. AD 1400	62.80	0.43	17.12	3.48	0.25	0.30	0.76	6.60	5.49	97.23
? T2	MOR-	ca. AD 1400	62.84	0.49	17.39	3.41	0.27	0.31	0.75	6.77	5.27	97.50
? T2	MOR-	ca. AD 1400	63.00	0.43	16.99	3.46	0.24	0.29	0.69	6.83	5.37	97.30
? T2	MOR-	ca. AD 1400	63.05	0.44	16.87	3.51	0.22	0.29	0.67	6.94	5.75	97.74
? T2	MOR-	ca. AD 1400	63.08	0.48	17.34	3.35	0.28	0.31	0.76	5.42	5.63	96.65
? T2	MOR-	ca. AD 1400	63.16	0.53	17.29	3.43	0.27	0.31	0.72	6.79	6.19	98.69
? T2	MOR-	ca. AD 1400	63.30	0.46	17.30	3.64	0.20	0.32	0.74	6.86	5.47	98.29
? T2	MOR-	ca. AD 1400	63.30	0.45	17.21	3.46	0.20	0.34	0.72	6.72	5.36	97.76
? T2	MOR-	ca. AD 1400	63.32	0.47	17.23	3.47	0.22	0.31	0.66	6.87	5.57	98.12

? T2	MOR-	ca. AD 1400	63.46	0.44	17.44	3.43	0.28	0.29	0.67	7.01	5.42	98.44
? T2	MOR-	ca. AD 1400	63.55	0.34	17.17	3.39	0.23	0.30	0.84	6.72	5.52	98.06
? T2	MOR-	ca. AD 1400	63.71	0.51	17.39	3.37	0.26	0.33	0.81	6.86	5.65	98.89
? T2	MOR-	ca. AD 1400	63.72	0.36	17.10	3.39	0.30	0.28	0.76	6.68	5.38	97.97
? T2	MOR-	ca. AD 1400	63.75	0.42	17.27	3.33	0.19	0.36	0.75	6.94	6.10	99.11
? T2	MOR-	ca. AD 1400	63.86	0.44	17.21	3.52	0.25	0.33	0.76	7.08	5.44	98.89
Hekla		1947	69.93	0.35	13.43	4.77	0.11	0.16	1.19	5.18	3.35	98.47
Hekla		1947	69.61	0.38	13.51	4.67	0.11	0.14	1.10	5.46	3.46	98.44
Hekla		1947	63.60	1.01	15.35	8.16	0.18	1.24	4.39	4.16	1.76	99.85
Hekla		1947	62.98	1.00	15.24	7.70	0.20	1.13	4.29	4.66	1.78	98.98
Hekla		1947	62.51	0.88	15.30	8.09	0.20	1.14	4.54	4.77	1.65	99.08
Hekla		1947	62.13	0.88	15.04	8.24	0.20	1.17	4.54	4.21	1.71	98.12
Hekla		1947	62.01	0.91	15.28	7.99	0.20	1.32	4.40	4.26	1.77	98.14
Hekla		1947	63.91	1.03	15.12	7.80	0.21	1.25	4.17	4.18	1.66	99.33
Hekla		1947	61.93	0.87	14.71	7.84	0.21	1.23	4.27	4.78	1.81	97.65
Hekla		1947	63.34	0.98	14.96	7.46	0.22	1.23	4.30	4.27	1.75	98.51
Hekla		1947	62.58	1.00	14.74	7.89	0.22	1.19	4.19	4.62	1.76	98.19
Hekla		1947	61.03	0.92	15.11	8.12	0.22	1.31	4.52	4.59	1.66	97.48

Hekla	1947	60.89	0.97	14.77	7.93	0.22	1.24	4.55	4.81	1.77	97.15
Hekla	1947	62.51	0.98	15.68	7.52	0.23	1.19	4.18	4.77	1.71	98.77
Hekla	1947	62.47	0.90	15.30	8.13	0.23	1.19	4.39	4.32	1.77	98.70
Hekla	1947	62.97	0.92	15.34	7.72	0.24	1.25	4.42	4.83	1.88	99.57
Hekla	1947	62.14	0.96	15.02	7.88	0.24	1.18	4.28	3.95	1.73	97.38
Hekla	1947	59.09	1.15	15.19	8.98	0.24	1.71	4.99	4.52	1.69	97.56
Hekla	1947	60.07	1.33	15.13	8.63	0.26	1.73	5.15	2.88	1.61	96.79
Hekla	1947	62.56	1.03	15.13	8.12	0.27	1.36	4.66	4.25	1.71	99.09
Hekla	1980	54.70	2.08	14.70	11.90	0.27	2.89	7.09	4.00	1.19	98.82
Hekla	1980	55.10	2.00	14.70	11.80	0.23	2.84	7.07	4.02	1.15	98.91
Hekla	1980	54.60	1.91	14.70	11.40	0.24	2.87	7.12	3.98	1.19	98.01
Hekla	1980	54.50	1.91	14.60	11.70	0.22	2.90	7.09	1.16	1.16	95.24
Hekla	1980	55.60	2.01	14.60	12.10	0.24	2.88	7.20	1.16	1.16	96.95
Hekla	1980	55.30	1.89	14.50	12.00	0.23	2.93	7.08	1.18	1.18	96.29
Hekla	1980	55.40	1.97	14.40	11.80	0.20	2.86	7.04	1.13	1.13	95.93

D | *R code*

Below is the R code for calculating the Mahalanobis distance of probe data (e.g. OxT-xxxx) from the calibration set (proximal eruption data, from Appendix C). The method is discussed in Section 5.4.

```
> probeID <- function(cal,idfile){
+ id <- unique(cal$ID)
+ cal <- cal[!is.na(cal[,6]),]
+ size <- length(id)
+ cal.m <- t(t(cal[cal$ID == id[1],2:10]) - colMeans(cal[cal$ID == id[1],2:10]))
+ for (j in 2:size){cal.m <- rbind(cal.m,t(t(cal[cal$ID == id[j],2:10]) - colMeans
    (cal[cal$ID == id[j],2:10])))}
+ C <- cov(cal.m)
+ Cinv <- solve(C)
+ MD <- matrix(c(1:((size+1)^2)),nrow = (size + 1))*0
+ for (i in 1:(size -1)){
+    for (j in (i+1):size){
+    Md <- (colMeans(cal[cal$ID == id[i],2:10]) - colMeans(cal[cal$ID == id[j
    ],2:10]))\%*\%Cinv\%*\%(colMeans(cal[cal$ID == id[i],2:10]) - colMeans(cal[
    cal$ID == id[j],2:10]))
+ MD[i,j] <- Md
+     }
+ }
+ idm <- colMeans(idfile[2:10])
+ for (i in 1:size){
+   idmat <- (colMeans(cal[cal$ID == id[i],2:10]) - idm)\%*\%Cinv\%*\%(colMeans(
    cal[cal$ID == id[i],2:10]) - idm)
+ MD[i,size+1] <- idmat
+ }
+ MDmat <- MD + t(MD)
+ try <- cmdscale(MDmat)
+ plot(try[1:size,], xlab = "x", ylab = "y", main = "Relationship of Probe (red)
    to calibration data (black)", xlim = c(min(try[,1]), max(try[,1])), ylim = c(
    min(try[,2]),max(try[,2])))
+ points(try[(size+1),1],try[size+1,2],col = "red")
+ identify(try)
+ close <- MDmat[,(size + 1)]
+ names(close) <- id
+ close <- sort(close)
+ close <- close[2:(size + 1)]
+ close
+ }
> cal <- read.csv("C:/Users/Jamie/Desktop/Calibdata.csv",header = T)
> id <- unique(cal$ID)
> probe <- read.csv("C:/Users/Jamie/Desktop/probe.csv",header = T)
> pro5135 <- probe[probe[,1]=="5135",]
> pro5135
      ID    SiO2   TiO2   Al2O3    FeO    MnO    MgO    CaO   Na2O    K2O
```

```
233 5135 58.3309 1.2669 14.7584 8.8707 0.2126 1.7206 4.8835 4.2694 1.4349
234 5135 59.0319 1.2803 14.8868 9.2769 0.2881 1.7531 5.0178 3.3794 1.4816
235 5135 59.2767 1.2660 15.2348 9.5424 0.1612 1.7232 5.2444 4.2096 1.5339
236 5135 59.4677 1.2474 15.1336 9.4199 0.3108 1.8581 5.3671 3.1843 1.3257
237 5135 59.8378 1.2562 15.2205 9.3228 0.3879 1.6942 5.0252 4.1699 1.5508
238 5135 59.8971 1.2084 15.4073 8.9740 0.3018 1.7686 5.1264 4.4071 1.5289
> out5135 <- probeID(cal,pro5135)
> out5135
     H1300      H1766      H1693      H1845      H1947      H1510      O1727
  3.905909   4.142377   5.149240   7.337330  10.447107  11.051372  57.994854
        H3      H1980      H1158      H1104      E1821      A1875      O1362
 59.163432  66.719622  76.051447 201.766213 248.537005 272.528901 283.239033
    Bas871      L1783      V1477     Snae200      Rhy871      K1721       E395
393.260283 394.892855 404.902410 424.699324 446.318766 480.236843 503.656059
    MOR-T2
867.867313
> pro5149 <- probe[probe[,1]=="5149",]
> pro5149
      ID    SiO2   TiO2   Al2O3    FeO    MnO    MgO    CaO   Na2O     K2O
266 5149 58.9250 1.2826 15.0095 9.4706 0.2671 1.7838 5.3317 3.7113  1.4191
267 5149 59.6801 1.3496 15.2590 9.3146 0.1869 1.8126 5.2015 3.7069  1.3623
268 5149 63.5384 0.0582 18.1948 0.4705 0.0300 0.0755 0.0004 0.2052 16.1775
269 5149 63.6521 0.0000 18.1322 0.0218 0.0000 0.0000 0.0150 0.3067 16.3562
270 5149 63.7677 0.0424 18.2110 0.0532 0.0300 0.0000 0.0058 0.2809 16.2224
271 5149 63.8983 0.0279 18.4054 0.1819 0.0300 0.0158 0.0296 0.1711 16.4047
> out5149 <- probeID(cal,pro5149)
> out5149
  MOR-T2   Rhy871  Snae200    E1821    O1362    H1104    H1158    H1300
2247.487 3199.792 4024.774 4098.618 4381.469 4786.799 4812.922 4856.811
   H1693    H1947    O1727    H1510       H3    H1980    H1845    H1766
4899.414 4906.538 4946.294 4949.201 4957.323 5020.541 5037.212 5053.367
   A1875    K1721   Bas871    V1477     E395    L1783
5242.591 5940.604 6010.993 6023.041 6029.911 6051.026
> pro5150 <- probe[probe[,1]=="5150",]
> pro5150
      ID    SiO2   TiO2   Al2O3    FeO    MnO    MgO    CaO   Na2O    K2O
272 5150 78.1777 0.3265 11.7738 2.1305 0.0000 0.0181 1.8524 4.9466 0.2764
273 5150 78.2075 0.2394 11.8740 2.2337 0.0940 0.0588 2.1071 4.7147 0.2721
274 5150 78.6598 0.2389 12.3794 0.9443 0.0562 0.0422 1.8148 4.8770 0.2099
275 5150 78.9061 0.2228 12.2246 0.8805 0.0276 0.0224 1.4728 4.7393 1.0072
276 5150 79.2472 0.2994 11.7646 1.1357 0.0000 0.0080 1.6421 4.8276 0.4774
277 5150 79.2636 0.2312 12.0230 1.1831 0.0647 0.0190 2.1335 4.5770 0.4271
278 5150 79.5347 0.1949 11.6357 0.9130 0.0458 0.0680 1.4098 4.9108 0.7378
279 5150 79.8997 0.1750 11.1365 0.2518 0.0000 0.0170 1.0805 4.5991 0.9306
280 5150 80.2489 0.1949 10.8532 1.2914 0.0000 0.0533 1.3485 4.4711 0.6635
> out5150 <- probeID(cal,pro5150)
> out5150
    A1875     H1104        H3     H1158     O1362     H1510     H1947   Snae200
 347.9977  491.5868  591.6724  600.9863  660.8463  732.7446  748.4401  749.8844
    H1845     H1766     H1300     E1821     H1693     H1980     O1727     Rhy871
 755.8288  822.8417  843.5620  854.2819  911.0393 1080.3298 1090.1438 1196.3958
   Bas871     V1477     L1783     K1721      E395    MOR-T2
1279.3989 1314.0773 1329.6398 1442.0012 1453.6747 2369.4800
>
```

E | *East Mound radiocarbon, OSL, and stratigraphic diagrams*

Table E.1: Radiocarbon dates from the East Mound (Griffiths forthcoming).

Lab ID	Context	Context Description	Material Dated	δ^{13}C	δ^{15}N	C:N	Radiocarbon age (BP)	Calibrated date (95% confidence)
SUERC-17858	2035	Trench 5: Dump of stones and domestic debris. Silty sand.	carbonized grain: barley	-23.4	-	-	895 ±35	cal AD 1030–1220
SUERC-17859	2040	Trench 5: Domestic refuse within hearth deposit in corner of square structure. Ash and charcoal rich - hearth deposits/rakings (sandy silt with clay).	carbonized grain: barley	-23.2	-	-	950 ±35	cal AD 1010–1170
SUERC-17860	2043	Trench 5: Small, single, primary dump of domestic debris.	branch charcoal with bark: Salix sp.	-27.0	-	-	915 ±35	cal AD 1020–1220
SUERC-17861	2056	Trench 5: Deposit of domestic refuse. Firm clayey silt.	charcoal: Corylus sp.	-27.3	-	-	965 ±35	cal AD 1010–1160
SUERC-17862	2106	Trench 5: Deposit of domestic refuse. Dark organic silty sand. Overlying levelling of earlier wall and covered by windblown sand.	charcoal: Betula sp.	-26.3	-	-	920 ±35	cal AD 1020–1220
SUERC-17866	2111	Trench 5: Dump of domestic refuse.	carbonized grain: barley	-29.7	-	-	885 ±35	cal AD 1030–1230

SUERC-17867	2115	Trench 5: Domestic refuse within floor deposit in corner of square structure. Brown silty sand with charcoal inclusions, bone and shell. Includes hearth debris and general trample. Contained near complete Viking bone comb and other significant finds.	carbonized grain: barley	-24.7	-	-	905 ±35	cal AD 1020–1220
SUERC-17868	2078	Trench 5: Dumped domestic refuse. Manganese stained silty sand.	carbonized grain: barley	-22.5	-	-	1000 ±35	cal AD 980–1150
SUERC-17869	2092	Trench 5: Domestic refuse within yard surface deposit. Silty sand with ash lenses. Contains bone, shell and several artefacts.	carbonized grain: barley	-22.9	-	-	900 ±35	cal AD 1020–1220
SUERC-24701	2077	Trench 5: Domestic refuse deposit. Silty sand with yellow clay lenses. Rich in shell, animal and fish bone.	carbonized grain: barley	-21.5	-	-	1160 ±35	cal AD 770–980

SUERC-24702	2016	Trench 5: Internal domestic refuse deposit in Structure 1, concentrated in SE corner. Dark, highly organic sandy silt, rich in ash and charcoal (hearth debris), fishbone and shell. Contained Viking/Late Norse steatite sherds and iron objects.	charcoal: Salix sp.	-24.6	-	-	990 ±35	cal AD 980–1160
SUERC-24703	2095	Trench 5: Domestic dump. Dark charcoal-rich silty sand, containing shell, animal and fish bone and steatite sherds.	carbonized grain: barley	-24.3	-	-	1065 ±30	cal AD 890–1030
SUERC-24704	2109	Trench 5: Turf/organic material in secondary working area. Thin, distinct manganese-stained sandy clay rich in carbonised grain.	carbonized grain: barley	-22.9	-	-	1000 ±35	cal AD 980–1150
SUERC-24705	2080	Trench 5: Domestic refuse debris in floor trample. Silty sand with yellow clay spreads and lenses. Rich in domestic debris.	carbonized grain: barley	-22.4	-	-	975 ±35	cal AD 990–1160

SUERC-24706	2148	Trench 5: Upper fill of drain. Sandy silt with occasional charcoal. Sealed by flagging [2132] and above windblown sand layer (2149) indicating time when drain out of use.	charcoal: Salix sp.	-25.9	-	-	1015 ±35	cal AD 970–1120
SUERC-24710	2156	Trench 5: Ash and charcoal concentration in dump in byre end of Area 3 long hall structure. Rich in charcoal, ash, shell, animal and fish bone. Also contains iron objects, a fine whetstone, worked bone, and a whalebone gaming piece.	charcoal: Salix sp.	-24.5	-	-	1000 ±35	cal AD 980–1150
SUERC-24711	2160	Trench 5: Bedding/levelling layer for floor surface in N-S structure in Area 1. Charcoal-rich silty sand.	charcoal: Salix sp.	-25.3	-	-	915 ±35	cal AD 1020–1220

SUERC-24712	2164	Trench 5: Domestic refuse deposit in byre within organic layer with ash spread as antiseptic and pitted with hoof-marks. Dark very silty sand rich in charcoal, peat ash lenses and Fuel Ash Slag. Context contained worked stone, quern fragment, steatite and copper alloy fragments as well as much shell, animal and fish bone.	carbonized grain: barley	-24.5	-	-	1000 ±35	cal AD 980–1150
SUERC-24713	2152	Trench 5: Layer in a dump of shells, charcoal, burnt clay and peat ash. Dark silty sand with charcoal and patches of burnt turf and peat ash. . Rich in shell, animal and fish bone; contained steatite, iron objects and worked bone objects including comb pieces.	charcoal: Salix sp.	-26.5	-	-	1035 ±35	cal AD 900–1040

SUERC-24714	2146	Trench 5. Organic occupation deposit in domestic end of long structure. Dark sandy silt with clay, charcoal and peat-ash lenses. Contained many iron objects and Viking-Norse domestic artefacts including a fine whetstone, quern and whalebone object.	carbonized grain: barley	-24.3	-	-	1035 ±35	cal AD 900–1040
SUERC-24715	2105	Trench 5: Metal working deposit. Yellow clay with patches of heavily burnt material and ash: at least 10% charcoal and high content of fuel ash slag, clinker and slag. Contained many iron objects/ fragments and worked bone artefacts.	roundwood charcoal with bark: Salix sp.	-25.4	-	-	1010 ±35	cal AD 970–1150
SUERC-24716	2105	Trench 5: Metal working deposit. Yellow clay with patches of heavily burnt material and ash: at least 10% charcoal and high content of fuel ash slag, clinker and slag. Contained many iron objects/ fragments and worked bone artefacts.	roundwood charcoal with bark: Salix sp.	-25.9	-	-	1050 ±35	cal AD 890–1030

SUERC-24720	2178	Trench 5: Discrete dump compressed into surface of metalworking area. Possibly a dump from cleaning or refurbishment of hearth. Heat-affected red, sandy clay rich in charcoal.	charcoal: Salix sp.	-26.4	-	-	940 ±35	cal AD 1020–1190
SUERC-33699	2202	Trench 5: Metalworking hearth.	roundwood charcoal with bark: Salix sp.	-28.5	-	-	925 ±30	cal AD 1020–1190
SUERC-33700	2240	Trench 5: Rake-out from bowl hearth in metalworking area. Friable black silt with lenses of silty sand; extremely charcoal rich with occasional small pieces of burnt clay. The bowl had been clay lined, surrounded and partly lined with stones.	roundwood charcoal with bark: Salix sp.	-25.9	-	-	955 ±30	cal AD 1010–1160
SUERC-33701	2269	Trench 5: Fill of small metalworking hearth [2281] in metal working area. Black silty clay, with very abundant visible charcoal, burnt clay and fuel ash slag.	charcoal with bark and outer rings: Salix sp.	-24.9	-	-	970 ±30	cal AD 1010–1160

SUERC-33702	2301	Trench 5: Square hearth in longhouse. Rich in fuel ash slag, peat ash, charcoal and burnt clay. Possible tuyere in base, hammerscale, slag and small furnace bottom.	carbonized grain: barley	-26.1	-	-	975 ±30	cal AD 1010–1160
SUERC-33706	2263	Trench 5: Domestic refuse debris in longhouse floor. Compact dark blackish brown sandy clay with clear areas orangey pink peat ash; patches of black and grey greasy clay; frequent charcoal.	carbonized grain: barley	-25.7	-	-	965 ±30	cal AD 1010–1160
SUERC-33707	2264	Trench 5: Domestic refuse debris in longhouse floor. Dark blackish brown slightly sandy silt with patches of orangey pinkish black sandy clay and abundant charcoal.	carbonized grain: barley	-25.2	-	-	1005 ±30	cal AD 980–1120
SUERC-33708	2265	Trench 5: Domestic refuse debris in longhouse floor. Friable dark greyish brown sandy (20%) silt - silty clay; concentrations of charcoal; lenses white-orange peat ash.	carbonized grain: barley	-22.4	-	-	975 ±30	cal AD 1010–1160

SUERC-33709	2285	Trench 5: Hearth fill in longhouse.	carbonized grain: barley	-24.3	-	-	950 ±30	cal AD 1020–1170
SUERC-33710	2300	Trench 5: Cooking pit in longhouse floor. Ashy, humic sandy clay with peat-ash concentrations and flecks and concentrations of charcoal.	carbonized grain: barley	-22.7	-	-	985 ±30	cal AD 990–1160
SUERC-33711	2304	Trench 5: Main sub-square hearth in longhouse. Crumbly ashy deposits, red burnt clay, black silty clay and sticky grey clay, with firm peat ash lenses, charcoal concentrations and abundant FAS.	carbonized grain: barley	-23.6	-	-	940 ±30	cal AD 1020–1170
SUERC-33712	2271	Trench 5: Dark sandy silt deposit with peat ash lenses in corner of 'stalling area'.	carbonized grain: barley	-25.2	-	-	960 ±30	cal AD 1010–1160
SUERC-33716	2277	Trench 5: Concentration of charcoal in sub-circular depression in the stalling area of longhouse. Highly organic sandy silt.	carbonized grain: barley	-23.0	-	-	940 ±30	cal AD 1020–1170

SUERC-33717	2225	Trench 5: Compact dark brown organic deposit in domestic end of longhouse. Sandy silt with large lenses of peat ash, concentrations of charcoal, grey 'kitchen grease' clay and yellow clay.	roundwood charcoal: Salix sp.	-26.1	-	-	940 ±30	cal AD 1020–1170
SUERC-33718	2273	Trench 5: Layer built up of hearth rakings in byre. Compact, dark brownish slightly sandy silt - slightly sandy clay; large peat ash lenses; abundant charcoal concentrations and burnt clay.	carbonized grain: barley	-26.5	-	-	1025 ±30	cal AD 970–1040
SUERC-33719	2290	Trench 5: Fill of circular cooking pit. Burnt stone around centre; possible lining clay and greasy grey cooking residues. Contains well-preserved oat grains used in cooking activity/grain drying. Friable-compact, burnt orangey clay, pinkish orange peat ash, dark brownish black silt and greasy greyish black silty clay, with abundant charcoal concentrations.	carbonized grain: oat	-24.0	-	-	920 ±30	cal AD 1020–1210

SUERC-33720	2305	Trench 5: Peat ash and charcoal rich sandy silt deposit in longhouse.	carbonized grain: barley	-23.1	-	-	990 ±30	cal AD 990–1160
SUERC-33721	2288	Trench 5: Single peat ash midden dump. Compact, dark brownish black clayey silt with nearly 50% context pinkish orange lenses of peat ash and abundant charcoal concentrations.	roundwood charcoal: Salix sp.	-27.0	-	-	975 ±30	cal AD 1010–1160
SUERC-33722	2231	Trench 5: Peat ash hearth in early structure. Compact light brownish pink clayey silt; with abundant charcoal concentrations.	carbonized grain: barley	-24.6	-	-	965 ±30	cal AD 1010–1160
SUERC-47146	2205	Trench 5: Fill of pit with the remains of a dismantled metal working hearth. Sandy silt with burnt clay, mammal and fish bones, shells and fuel ash slag. Includes an articulated cow element.	articulated animal bone: cow phalange	-22.2	5.3	3.3	941 ±39	cal AD 1010–1190
SUERC-47147	2221	Trench 5: Small deposit above western longhouse roof tumble. Silty sand with very occasional charcoal and small collection of animal bone.	articulated animal bone: pig calcaneum	-21.9	8.3	3.2	1033 ±39	cal AD 900–1040

SUERC-47148	2294	Trench 5: Fill of metal working hearth. Very finely-laminated. Clay and ash-rich silty sand with abundant charcoal.	articulated animal bone: mouse	-21.3	-	-	999 ±39	cal AD 980–1160
SUERC-47149	2219	Trench 5: Deposit in post-abandonment layers over byre. Silty sand with concentrations of charcoal.	roundwood charcoal with bark: Salix sp.	-27.6	-	-	1013 ±39	cal AD 970–1150
SUERC-47150	2229	Trench 5: Matrix in rough stone surface. Silty sand with concentrations of charcoal.	carbonized grain: barley	-24.7	-	-	887 ±39	cal AD 1030–1250
SUERC-47151	2236	Trench 5: Midden deposit. Sandy silt with abundant peat ash and many concentrations of charcoal; fish and animal bone.	charcoal: Salix sp.	-26.3	-	-	990 ±39	cal AD 980–1160
SUERC-47155	2275	Trench 5: Hearth-related deposit. Sandy silt with frequent charcoal concentrations and clay.	carbonized grain: barley	-24.1	-	-	957 ±39	cal AD 1010–1170
SUERC-47156	2276	Trench 5: Silt with concentrations of charcoal covering flagstone path in longhouse.	charcoal: Corylus	-27.4	-	-	1024 ±39	cal AD 900–1120

Table E.2: OSL dates from the East Mound (Griffiths forthcoming).

Field code	**Laboratory code**	**Context**	**OSL age estimate (years before 2007)**	**OSL date (BC/AD)**
SG06-20	X3099	2001	185 ± 130	AD1690 - 1820
SG06-21	X3100	2001	170 ± 45	AD1790 - 1835
SG06-22	X3101	2032	620 ± 125	AD1260 - 1385
SG06-23	X3102	2047	1065 ± 95	AD845 - 940

F | *Orkney, Highlands, and Western Isles Published Chronological Information*

Table F.1: Table of all local (Orcadian and selected Highlands and Western Isles) chronological data from published sources, chosen based on the criteria in Section 5.5. Due to local marine reservoir effects (e.g. Barrett et al. 2000), radiocarbon dates are shown calibrated (using OxCal and IntCal09) (Bronk Ramsay 2012; Reimer et al. 2009). This data is presented graphically in Figure 8.6 and a map of all locations is shown in Figure 8.5.

Date	Location	Type	Event	Method	Citation
ca. 4.7 and 3.8 ka	Skara Brae	Neolithic archaeology	Neolithic settlement of Skara Brae	14C	Leinert et al. 2000; Ashmore, 1998
ca. 7 ka to the present	Wick Valley	landscape feature	sea level rise of approx. 4 m	14C	Dawson and Smith 1997; Leinert et al. 2000 cite this as comparable to understudied Orkney
ca. 5 ka	Bay of Skaill	landscape feature	sand deposition and formation of the Bay	14C (non-AMS)	Keatinge and Dickson 1979
ca. 6.1 and 5 ka	Bay of Skaill	landscape feature	machair formation/-dune erosion/sand movement	14C	Leinert et al. 2000
ca. 5.2 and 4.9 ka	Bay of Skaill	landscape feature	final woodland decline	14C	Leinert et al. 2000; Keatinge and Dickson 1979
782-995 cal AD	Quoygrew	Viking/Medieval farm mound	earliest date from archaeology at site	14C	Simpson et al. 2005

Date	Location	Type	Event	Method	Citation
1004-1262 cal AD	Quoygrew	Viking, Medieval farm mound	near base of fish midden	14C	Simpson et al. 2005
1256-1400 cal AD	Quoygrew	Viking, Medieval farm mound	soil overlaying farm mound	14C	Simpson et al. 2005
1015-1219 cal AD	Marwick	Viking, Medieval, later township	topsoils thought to be from Viking period	14C	Simpson 1997
AD 1480-1550	Bay of Lopness	landscape feature	Increased aeolian sand activity	OSL	Somerville et al. 2007
976-1184 cal AD	Pool	Viking, medieval, later coastal settlement	flax, linseed appearance at Pool	14C (non-AMS)	Bond and Hunter 1987
716-990 cal AD	Pool	Viking, medieval, later coastal settlement	flax, linseed appearance at Pool	14C (non-AMS)	Bond and Hunter 1987
660-875 cal AD	Pool	Viking, medieval, later coastal settlement	flax, linseed appearance at Pool	14C (non-AMS)	Bond and Hunter 1987
uncertain – pre-995	Brough of Deerness, Newark Bay, Birsay	Viking churches	conversation to Christianity in Orkney	14C review	Barrett et al. 2000

Date	Location	Type	Event	Method	Citation
11th-12th centuries	Orkney	trend	fishing intensifies	14C	Barrett et al. 1997; Barrett et al. 2000b; Barrett et al. 2001
within the interval AD 1550-1700	Western Isles	landscape feature	storminess/aeolian deposition	OSL	Morocco et al. 2007
1000-900 cal BP	Dunadd	medieval royal occupation	reverse in trend of declining woodland taxa and open ground; very close to end of royal occupation period as known from documentary sources	14C	Housley et al. 2009
Hekla 1947	Dunadd	medieval royal occupation	found on site	tephrochronology	Housley et al. 2009
Hekla 1510	Dunadd	medieval royal occupation	found on site	tephrochronology	Housley et al. 2009
1300-1350	Highland Scotland	medieval landscape	Authors propose that feuds, raiding, and aggressive territorial expansion in the Highlands were caused in part by a climatic downtown that put pressure on fodder and crop production	historical sources coupled with environmental proxies	Oram and Adderley 2008

Date	Location	Type	Event	Method	Citation
13th -15th centuries	Bornish, South Uist	Viking/medieval farmstead	Author proposes that changes in limpet size indicate a second stage of collection intensification	14C	Sharples 2005
10-13th c	Quoygrew	Viking/Medieval farm mound	stratified middens containing primarily limpets	14C and artefactual	Milner et al 2007
11-12th c	Quoygrew	Viking/Medieval farm mound	intensification of limpet harvesting	14C and artefactual	Milner et al 2007
AD 959-1249	Brough of Deerness	Viking church	foundation of church	14C	Barrett and Slater 2009
9th-11th century	Viking Orkney	Viking Orkney	Orkney prior to the sagas	14C and historical sources	Barrett 2000

G | *Linear Interpolation Code*

Shown below is the code, written in Python, for determining the percentage of marine diet from radiocarbon dates on bone using linear interpolation between two points as described in Section 9.2.1. The example shown is from Greenland, with example δ^{13}C values for individual dates in brackets after "vpdb" and the boundary values for linear interpolation in the line below that (-21‰ and -12.5‰ is used for Greenland). For Iceland, they were -20.7‰ and -13.3‰. For Orkney, Shetland, the Faroe Islands, and the Western Isles, they were -21‰ and -13‰.

```
> def percent_lerp(start, end, x):
     >return ((x-start) / (end-start)) * 100.0

> vpdb = [-15.9, -14.8, -16.2, -16.2, -15.4, -14.1, -15.2]

> print([round(percent_lerp(-21, -12.5, v)) for v in vpdb])
```